E. BREITMAIER
W. VOELTER

^{13}C NMR SPECTROSCOPY

5

Monographs
in Modern Chemistry

E. Breitmaier / W. Voelter
^{13}C NMR Spectroscopy

Monographs in Modern Chemistry

Series Editor: Hans F. Ebel

Vol. 1: F. Kohler
The Liquid State

Vol. 2: H. Meier
Organic Semiconductors

Vol. 3: C. Reichardt
Solvent Effects in
Organic Chemistry

Vol. 4: G. Ertl/J. Küppers
Low Energy Electrons
and Surface Chemistry

Vol. 5: E. Breitmaier/W. Voelter
^{13}C NMR Spectroscopy

Vol. 6: D. O. Hummel (Editor)
Polymer Spectroscopy

Vol. 7: D. Ginsburg
Propellanes

Vol. 8: G.M.J.Schmidt et al.
Solid State Photochemistry

Vol. 9: G. Henrici-Olivé/S. Olivé
Coordination and Catalysis

Vol. 10: H. Strehlow/W. Knoche
Fundamentals
of Chemical Relaxation

The series is to be continued

E. BREITMAIER
W. VOELTER

^{13}C NMR SPECTROSCOPY

Methods and Applications in Organic Chemistry

2nd Edition

Verlag Chemie
Weinheim · New York · 1978

Prof. Dr. Eberhard Breitmaier
Institut für Organische Chemie und Biochemie
der Universität Bonn
Gerhard-Domagk-Straße 1
D-5300 Bonn

Prof. Dr. Wolfgang Voelter
Institut für Organische Chemie
der Universität Tübingen
Auf der Morgenstelle 18
D-7400 Tübingen

This book contains 93 figures and 114 tables.

CIP-Kurztitelaufnahme der Deutschen Bibliothek

Breitmaier, Eberhard
[C NMR spectroscopy]
13C NMR spectroscopy: methods and applications/
E. Breitmaier; W. Voelter. – 2. ed. – Weinheim,
New York: Verlag Chemie, 1978.
(Monographs in modern chemistry; Vol. 5)
ISBN 3-527-25780-2 (Weinheim)
ISBN 0-09573-004-9 (New York)
NE: Voelter, Wolfgang:

© Verlag Chemie GmbH, D-6940 Weinheim, 1974, 1978
All rights reserved (including those of translation into foreign languages). No part of this book may be reproduced in any form – by photoprint, microfilm, or any other means – nor transmitted or translated into a machine language without written permission from the publishers.

Registered names, trademarks, etc. used in this book, even without specific indication thereof, are not to be considered unprotected by law.

Printed by Dr. Alexander Krebs, D-6944 Hemsbach
Bookbinder: Josef Spinner, D-7583 Ottersweier

Printed in West-Germany

Foreword

Physical methods have had a revolutionary effect on the conduct of organic chemical teaching and research. In retrospect, the most important new physical method for organic chemists introduced during the 1940's was infrared spectroscopy, during the 1950's proton nuclear magnetic resonance spectroscopy and during the last decade, without question, mass spectrometry. If organic chemists were asked to speculate about the most important physical method of the 1970's, then it is likely that many of them, including myself, will suggest ^{13}C NMR spectroscopy. If this should prove correct, then it is clearly important that books with major emphasis on organic chemical applications of such a technique be available and, while the following book by Breitmaier and Voelter is not the first one, it is certainly the most up-to-date one in that field. It provides in one place not only the appropriate background about theoretical and instrumental aspects but, most importantly, covers in very considerable detail those organic compounds which have already been scrutinized by this technique. I suspect that experts in the field as well as students and research workers who are only starting to become familiar with ^{13}C NMR will find the book of great value and it is with great pleasure that I express our collective appreciation to the authors for it.

Stanford, California
July, 1973

Carl Djerassi

Preface to the First Edition

The carbon skeletons of organic molecules are of central interest in organic chemistry. For this reason, carbon is potentially the most informative NMR probe for the study of organic compounds. Unfortunately, the natural abundance of ^{13}C, the only magnetic isotope of carbon, is not more than 1.1%. Moreover, ^{13}C is a much less sensitive NMR probe than ^{1}H at the same magnetic field strength due to its nuclear properties. Finally, conventional NMR spectroscopy, usually involving continuous wave frequency sweep techniques, is itself an insensitive method. Thus, it is understandable that only a few chemists were engaged in the measurement of ^{13}C NMR structural parameters before 1970, although the first ^{13}C NMR signals were observed in 1957.

The sensitivity of NMR spectroscopy was improved significantly in the late 1960's by signal accumulation, double resonance techniques, and, above all, by the application of the principle of multichannel excitation, which resulted in the development of pulsed and Fourier transform techniques. Commercial NMR spectrometers devised for such methods have been available since 1968, and in the past three years, pulse Fourier transform ^{13}C NMR spectroscopy has become a routine method for structural elucidation in organic chemistry, now competing with proton NMR.

It was our intention to provide in this monograph an account of these developments, with special emphasis on pulsed and Fourier transform techniques. The early methods of indirect observation of ^{13}C NMR are referred to only in passing, as these techniques will probably not gain general significance in routine ^{13}C NMR. The text consists of five chapters. A concise introduction is given in Chapter 1 to acquaint students and newcomers to the field with the terminology and basic principles of NMR, in particular ^{13}C NMR, and to lay the basis for an understanding of Chapter 2, which deals mainly with pulsed and Fourier transform methods and double resonance techniques. Chapter 3 provides a survey of the correlations between the structures of organic molecules and ^{13}C NMR parameters such as chemical shifts, coupling constants, and spin-lattice relaxation times. Structural assignments for organic molecules and natural compounds are reviewed in Chapters 4 and 5. Chapter 5 also serves to illustrate the potential of ^{13}C NMR for the solution of biochemical problems.

The monograph is meant to be a concise introduction and reference source rather than a comprehensive text completely covering the flood of literature which has already accumulated. However, we did attempt to take the ^{13}C NMR literature into account up to early 1973, particularly emphasizing more recent work. All ^{13}C chemical shift values are reported using the δ scale relative to tetramethylsilane (TMS). Mr. G. Haas converted data referenced to other standards to the TMS scale, and we gratefully acknowledge his work. Although this convention is not always used, we have assigned positive signs to upfield shifts (shielded with respect to TMS) and negative signs to downfield shifts (deshielded with respect to TMS) throughout this book.

We express our gratitude to the Deutsche Forschungsgemeinschaft, Bonn – Bad Godesberg, Germany, for providing our department with an NMR spectrometer equipped for pulsed and Fourier transform NMR. Most of the illustrations used in this monograph were recorded with this instrument. The permission of professors Ernst Bayer and Eugen Müller to use this spectrometer, as well as their interest in our work, is gratefully acknowledged. We are also grateful to Mr. T. Keller and Drs. V. Formacek, R. Price and Ch. Tänzer of Bruker Physik AG, Karlsruhe-Forchheim, Germany, for many stimulating discussions. Dr. Harry Smith of the Max-Planck-

Institut für Medizinische Forschung, Heidelberg, Germany, reviewed our manuscript and improved our English. We wish to thank him for his work and his useful comments. We are especially grateful to Dr. Heide Voelter for typing and proofreading parts of the manuscript. Finally, we acknowledge the permission of Academic Press and the American Chemical Society to adapt copyrighted material for Figs. 2.14, 2.19, 2.22, 3.11, and 3.12.

Tübingen (Germany), in February 1974 Eberhard Breitmaier Wolfgang Voelter

Preface to the Second Edition

The progress made in carbon-13 NMR spectroscopy during the past five years, particularly in instrumentation, has warranted due publication of a revised and updated edition of this monograph. The section dealing with the Bloch equations in chapter 1 has been shortened, leaving only the relevant information required for an understanding of chapter 2; further, the literature references are now summarized at the end of the text. Chapter 2 now contains an updated review of instrumental techniques useful as aids in assignment. In chapter 3, the survey of carbon chemical shifts has been thoroughly revised, and a review of carbon-13 spin-lattice relaxation times taken from Angew. Chem. Internat. Edit. *14*, 149 (1975) has been included. New data have been incorporated in chapter 4, taking into consideration those classes of compounds which were not investigated before publication of the first edition. A new paragraph dealing with empirical carbon shift increments and their use has been added. Finally, some new data and spectra have been incorporated in chapter 5. The signs of the chemical shifts have been reversed so as to bring them into line with the currently adopted notation. At the same time errors found in the first edition have been eliminated. Some helpful criticisms and suggestions, particularly those quoted in book reviews by J. W. Emsley, H. Günther, R. Radeglia, E. W. Randall and D. Ziessow, are gratefully acknowledged. Finally, E. B. would like to thank Mrs. Erika Ochterbeck, Bonn, for her assistance in preparing the manuscripts and in proofreading, and Dr. Rolf Sievers, Bonn, for making available his compound indexing computer program. We hope that this second edition of the monograph will prove to be a valuable work of reference for all concerned with the application of carbon-13 NMR spectroscopy.

Bonn and Tübingen, January 1978 Eberhard Breitmaier Wolfgang Voelter

Contents

1. Introduction to NMR . . . 1

1.1. Nuclear Magnetism . . . 1

1.2. Nuclear Precession . . . 2

1.3. Nuclear Magnetic Energy Levels . . . 2

1.4. Nuclear Magnetic Resonance . . . 3

1.5. Relaxation . . . 4
1.5.1. The Equilibrium of Nuclear Spins in the H_0 Field . . . 4
1.5.2. Spin-Lattice Relaxation . . . 5
1.5.3. Spin-Spin Relaxation . . . 5
1.5.4. Saturation . . . 6

1.6. The Magnetization Vectors . . . 6

1.7. The Bloch Equations . . . 7
1.7.1. The Motion of the Magnetization Vectors in a Fixed Coordinate System . . . 7
1.7.2. The Motion of the Magnetization Vectors in the Rotating Coordinate System . . . 8
1.7.3. NMR in the Rotating Frame of Reference . . . 9
1.7.4. Relaxation in the Rotating Frame of Reference . . . 11

1.8. NMR Spectra . . . 11
1.8.1. Nuclear Induction . . . 11
1.8.2. Absorption and Dispersion Spectra . . . 12
1.8.3. Magnitude Spectra . . . 13

1.9. Chemical Shift . . . 13
1.9.1. Shielding of Nuclei in Atoms and Molecules . . . 13
1.9.2. Calibration of NMR Spectra . . . 14
1.9.3. The Reference Standard . . . 15

1.10. Spin-Spin Coupling . . . 15
1.10.1. Multiplicity of Signals . . . 15
1.10.2. Coupling Constants . . . 16
1.10.3. Comparison between Chemical Shifts and Coupling Constants . . . 16
1.10.4. The Origin of Spin-Spin Coupling . . . 16

2. Instrumental Methods of ^{13}C NMR . . . 19

2.1. The Sensitivity of ^{13}C NMR . . . 19

2.2. Methods of Sensitivity Enhancement in ^{13}C NMR . . . 19

2.3. Continuous Wave NMR Spectroscopy . . . 19

2.4. Pulsed NMR Spectroscopy . . . 20
2.4.1. Free Induction Decay (FID) . . . 20
2.4.2. Pulse Interferograms . . . 22

2.5. Pulse Fourier Transform (PFT) NMR Spectroscopy . . . 22
2.5.1. FID Signal and NMR Spectrum as Fourier Transforms . . . 22
2.5.2. Acquisition of Pulse Interferograms for Fourier Transformation . . . 24

2.5.2.1. Digitization 24
2.5.2.2. Dwell Time and Pulse Interval 25
2.5.2.3. Filtering of Frequencies Outside of the Spectral Width 25
2.5.3. Optimization of Pulse Interferograms for Fourier Transformation 26
2.5.3.1. Adjustment of Pulse Frequency 26
2.5.3.2. Adjustment of Pulse Width 27
2.5.4. Data Transformation and Subsequent Manipulations 27
2.5.4.1. Fourier Transformation 27
2.5.4.2. Phase Correction 29
2.5.4.3. Computation of Magnitude Spectra 30
2.5.5. Controlling Signal to Noise and Resolution in PFT NMR 30
2.5.5.1. Signal to Noise Improvement by Digital Filtering 30
2.5.5.2. Number of FID Data Points and Resolution 30
2.5.6. Spin-Lattice Relaxation and Signal to Noise in PFT NMR 33
2.5.7. Comparison between CW and PFT 33

2.6. Double Resonance Techniques used in ^{13}C NMR as Assignment Aids 36
2.6.1. The Basic Concept of Spin Decoupling 36
2.6.2. Proton Broad Band Decoupling in ^{13}C NMR 37
2.6.3. The Nuclear Overhauser Effect in $^{13}\mathrm{C}\{^{1}\mathrm{H}\}$ NMR 39
2.6.4. Quenching Nuclear Overhauser Effects in $^{13}\mathrm{C}\{^{1}\mathrm{H}\}$ NMR 40
2.6.5. Proton Off-Resonance Decoupling 42
2.6.6. Pulsed Proton Broadband Decoupling 43
2.6.6.1. Measurement of NOE Enhanced Coupled ^{13}C NMR Spectra 43
2.6.6.2. Measurement of Proton Decoupled ^{13}C NMR Spectra with Suppressed NOE 43
2.6.6.3. Measurement of Nuclear Overhauser Enhancements 43
2.6.7. Selective Proton Decoupling 48

2.7. Measurement of ^{13}C Relaxation Times 48
2.7.1. Spin-Lattice Relaxation Times 48
2.7.1.1. The Inversion-Recovery or 180°, τ, 90° Method 48
2.7.1.2. Saturation Recovery Method 52
2.7.1.3. Progressive Saturation or 90°, τ,... Method 53
2.7.2. Spin-Spin Relaxation Times 55
2.7.2.1. CPMGSE Experiments 55
2.7.2.2. Spin-Locking Fourier Transform Experiments 57

2.8. Instrumentation 59
2.8.1. The Magnet 60
2.8.2. The Stabilization Channel (Lock) 63
2.8.3. The Observation Channel 64
2.8.4. The Decoupling Channel 65
2.8.5. The Sample 65

3. ^{13}C NMR Spectral Parameters and Structural Properties 67

3.1. Chemical Shifts 67
3.1.1. A Comparison of ^{13}C and ^{1}H Shifts 67
3.1.2. Referencing ^{13}C Chemical Shifts 68
3.1.3. A Survey of ^{13}C Chemical Shifts 68
3.1.3.1. Carbon Hybridization 71

3.1.3.2. Electronegativity 71
3.1.3.3. Crowding of Alkyl Groups and Substituents 71
3.1.3.4. Unshared Electron Pairs at Carbon 72
3.1.3.5. Electron Deficiency at Carbon 72
3.1.3.6. Mesomeric Effects 72
3.1.3.7. Conjugation 73
3.1.3.8. Steric Interactions 74
3.1.3.9. Electric Fields of Charged Substituents 75
3.1.3.10. Anisotropic Intramolecular Magnetic Fields 76
3.1.3.11. Heavy Atoms 76
3.1.3.12. Isotope Effect 76
3.1.3.13. Intramolecular Hydrogen Bridging 76
3.1.3.14. Substituent Increments and Functional Group Shifts 77
3.1.4. Medium Shifts 77
3.1.4.1. Dilution Shifts 77
3.1.4.2. Solvent Shifts 77
3.1.4.3. pH Shifts 80
3.1.5. Isotropic Shifts 82
3.1.6. Intramolecular Mobility and Temperature Dependence of ^{13}C Chemical Shifts and Line Widths 85
3.1.6.1. Introduction 85
3.1.6.2. The Temperature Dependence of ^{13}C NMR Spectra 89

3.2. ^{13}C Coupling Constants 92
3.2.1. Basic Theoretical Considerations 92
3.2.2. Carbon-Proton Coupling 93
3.2.2.1. One-Bond Coupling (J_{CH}) 93
3.2.2.2. Two-Bond Coupling ($^2J_{CH}$) 98
3.2.2.3. Three-Bond Coupling ($^3J_{CH}$) 98
3.2.3. Carbon-Deuterium Coupling 100
3.2.4. Carbon-Carbon Coupling 102
3.2.5. Coupling between Carbon and Heteronuclei X (X $\neq$ C, H, D) 106

3.3. Spin-Lattice Relaxation Times 110
3.3.1. Mechanisms of ^{13}C Spin-Lattice Relaxation 110
3.3.1.1. Relaxation Resulting from Chemical Shift Anisotropy (CSA Mechanism) 110
3.3.1.2. Relaxation by Scalar Coupling (SC Mechanism) 110
3.3.1.3. Relaxation by Spin Rotation (SR Mechanism) 111
3.3.1.4. Relaxation by Internuclear Dipole-Dipole Interaction (DD Mechanism) 111
3.3.1.5. Electron Spin-Nucleus Interactions and Consequences 112
3.3.2. Influence of Molecular Motion on Dipole-Dipole Relaxation 113
3.3.3. Information Content of ^{13}C Spin-Lattice Relaxation Times 115
3.3.3.1. Degree of Alkylation and Substitution of C Atoms 115
3.3.3.2. Molecular Size and Relaxation Mechanisms 115
3.3.3.3. Anisotropy of Molecular Motion 116
3.3.3.4. Internal Molecular Motion 119
3.3.3.5. Association and Solvation of Molecules and Ions 124
3.3.3.6. Determination of Quadrupole Relaxation Times and Coupling Constants from ^{13}C Spin-Lattice Relaxation Times 126
3.3.4. Medium and Temperature Effects 127
3.3.5. Outlook 129

4. ^{13}C NMR Spectroscopy of Organic Compounds . . . 131
4.1. Saturated Hydrocarbons . . . 131
4.2. Alkenes . . . 137
4.3. Alkynes and Allenes . . . 141
4.4. Haloorganic Compounds . . . 142
4.5. Alcohols . . . 153
4.6. Ethers . . . 155
4.7. Carbonyl Compounds . . . 159
4.7.1. Ketones, Aldehydes . . . 159
4.7.2. Quinones . . . 171
4.7.3. Carboxylic Acids . . . 171
4.8. Aliphatic Organonitrogen Compounds . . . 177
4.8.1. Amines . . . 177
4.8.2. Alkylcyanides, Isocyanides, Isocyanates, and Isothiocyanates . . . 177
4.8.3. Nitro Compounds and Nitrosamines . . . 179
4.9. Aliphatic Organosulfur Compounds . . . 181
4.10. Aromatic Compounds . . . 183
4.10.1. Benzene and Derivatives . . . 183
4.10.2. Fused Aromatic Rings . . . 184
4.10.3. Coupling Constants . . . 189
4.10.4. ^{13}C Enriched Aromatic Compounds, Mechanistic Studies . . . 192
4.10.5. Hydroaromatic Compounds . . . 196
4.11. Heterocyclic Compounds . . . 196
4.12. Carbocations . . . 205
4.13. Substituent Increments, Summary and Practical Use . . . 205
4.13.1. Substituted Alkanes . . . 208
4.13.2. Substituted Cyclohexanes and Bicyclo[2.2.2]heptanes . . . 209
4.13.3. Substituted Alkenes . . . 211
4.13.4. Substituted Benzenes . . . 212
4.13.5. Substituted Pyridines . . . 215
4.13.6. Nitrogen Increments in Fused Heterocycles . . . 215

5. ^{13}C NMR Spectroscopy of Natural Products . . . 219
5.1. Terpenes . . . 219
5.2. Steroids . . . 225
5.2.1. Androstanes, Pregnanes and Estranes . . . 227
5.2.2. Cholestanes . . . 229
5.2.3. Steroid Alkaloids . . . 230
5.3. Alkaloids . . . 240
5.3.1. Nicotine . . . 240
5.3.2. Gelsemine and Derivatives . . . 240
5.3.3. Arenaïne . . . 241
5.3.4. Piperine and Derivatives . . . 242

5.3.5. Amaryllidaceae Alkaloids . . . 243

5.4. Carbohydrates . . . 247
5.4.1. Aldohexoses and Aldopentoses . . . 248
5.4.2. Di- and Polysaccharides . . . 258
5.4.3. Polyols . . . 260
5.4.4. Inositols . . . 263

5.5. Nucleosides and Nucleotides . . . 264
5.5.1. Assignment of the Purine Resonances . . . 264
5.5.2. Assignment of the Pyrimidine Resonances . . . 265
5.5.3. Assignment of the Isoalloxazine Resonances . . . 265
5.5.4. Assignment of the Sugar and Polyol Carbon Atoms . . . 266
5.5.5. Correlations of ^{13}C Chemical Shifts with Other Physicochemical Parameters . . . 269

5.6. Amino Acids . . . 273
5.6.1. ^{13}C Chemical Shifts of Amino Acids . . . 273
5.6.2. pH Dependence of the ^{13}C Chemical Shift Values of Amino Acids . . . 282
5.6.3. Prediction of Carbon Shifts and their Correlation with Other Physicochemical Parameters . . . 282

5.7. Peptides . . . 283
5.7.1. Oligopeptides . . . 283
5.7.2. Polypeptides and Proteins . . . 284
5.7.3. Conformational Effects . . . 286

5.8. Porphyrins . . . 287

5.9. Elucidation of Biosynthetic Pathways . . . 289
5.9.1. Radicinin . . . 289
5.9.2. Asperlin . . . 290
5.9.3. Sterigmatocystin . . . 290
5.9.4. Virescenosides . . . 290
5.9.5. Methyl Palmitoleate . . . 292
5.9.6. Sepedonin . . . 292
5.9.7. Antibiotic X-537 A . . . 293
5.9.8. Cephalosporin . . . 293
5.9.9. Prodigiosin . . . 295

5.10. Appendix . . . 296

6. References . . . 301

Subject Index . . . 310

Compound Index . . . 315

Author Index . . . 333

1. Introduction to NMR

1.1. Nuclear Magnetism

When placed in a static magnetic field H_0, a nucleus may undergo nuclear magnetic resonance (NMR) [1–5] if it possesses an angular momentum p. This angular momentum is referred to as nuclear spin. The component of p in the direction of H_0 (Fig. 1.1), denoted as p_0, can only take on half-integral or integral multiples m of $h/2\pi$:

$$p_0 = m\frac{h}{2\pi}; \; m = \pm n\frac{1}{2}; \; n = 0,1,2,\ldots \tag{1.1}$$

The values of m, the spin quantum number, are further limited by the total spin quantum number I:

$$m = I, I-1, \ldots, -I\,. \tag{1.1a}$$

I is a constant characteristic of the ground state of every nucleus.

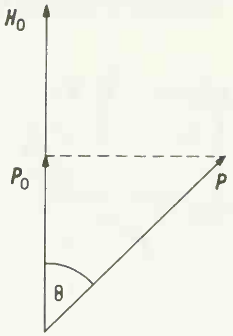

Fig. 1.1. Component p_0 of the torque p in the direction of the H_0 field.

According to an empirical rule, the magnitude of I depends on wether the atomic number z and the mass number a of an atom ${}^a_zX$ are both even, both odd or mixed (Table 1.1).

Table 1.1. Atomic Number z, Mass Number a, and Spin Quantum Number I of Selected Nuclei.

z	a	I	${}^a_zX$
even	even	0	${}^{12}_{6}C$, ${}^{16}_{8}O$
odd	odd	$\frac{1}{2}, \frac{3}{2}, \frac{5}{2}, \ldots$	${}^{1}_{1}H$, ${}^{15}_{7}N$, ${}^{19}_{9}F$, ${}^{31}_{15}P$
even	odd	$\frac{1}{2}, \frac{3}{2}, \frac{5}{2}, \ldots$	${}^{13}_{6}C$, ${}^{17}_{8}O$
odd	even	1, 2, 3, …	${}^{2}_{1}H$, ${}^{14}_{7}N$

Nuclei with total spin quantum number $I \neq 0$ interact with magnetic fields due to their magnetic moment μ. Its magnitude μ is related to the spin p by eq. (1.2).

$$\mu = \gamma p\,. \tag{1.2}$$

A constant γ, called the gyromagnetic ratio, characterizes each nucleus. In keeping with eqs. (1.1) and (1.2), the component of $\boldsymbol{\mu}$ in the direction of $\boldsymbol{H}_0$, μ_0, is also quantized.

$$\mu \cos \Theta = \mu_0 = \gamma I \frac{h}{2\pi}. \tag{1.3}$$

Table 1.1 shows that the nucleus of major interest in organic chemistry, ^{12}C, does not have a nuclear spin and cannot be used as an NMR nucleus. In contrast, its isotope ^{13}C, whose natural abundance is only 1.1%, has a nuclear spin of $\frac{1}{2}$.

1.2. Nuclear Precession

When exposed to a static magnetic field $\boldsymbol{H}_0$, a spinning nucleus behaves like a gyroscope in a gravitational field. As illustrated by Fig. 1.2, the spin axis – which coincides with the magnetic moment vector $\boldsymbol{\mu}$ – precesses about $\boldsymbol{H}_0$. The frequency of precession, ν_0, is known as the Larmor frequency of the observed nucleus.

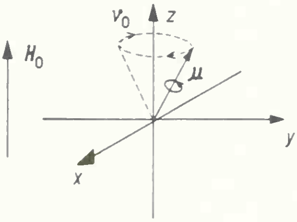

Fig. 1.2. Larmor precession of a spinning nucleus in a static magnetic field.

In contrast to bar magnets, the magnetic moments of spinning nuclei do not align in the direction of $\boldsymbol{H}_0$, no matter how strong this field is. Instead, the Larmor precession is accelerated by increasing the strength H_0 of the field vector $\boldsymbol{H}_0$:

$$\nu_0 \propto H_0. \tag{1.4}$$

1.3. Nuclear Magnetic Energy Levels

The energy of a magnetic moment $\boldsymbol{\mu}$ in a field $\boldsymbol{H}_0$ is given by the product of H_0 and μ_0. Thus, from eq. (1.3),

$$E = -\mu_0 H_0 = -\gamma \frac{h}{2\pi} I H_0. \tag{1.5}$$

Following quantum mechanical rules, a nucleus with total spin quantum number I may occupy $(2I + 1)$ different energy levels when placed in a magnetic field. For nuclei with $I = \frac{1}{2}$, e.g. ^{1}H, ^{13}C, ^{15}N, ^{19}F, ^{31}P, two spin alignments relative to $\boldsymbol{H}_0$ arise (Fig. 1.3): these are symbolized by $+\frac{1}{2}$ and $-\frac{1}{2}$.

Precession of the nuclear spins about H_0 is energetically favored (Fig. 1.3(b)) since the component of their magnetic moment vector μ in the direction of H_0 reinforces the magnetic field (Fig. 1.3(a)).

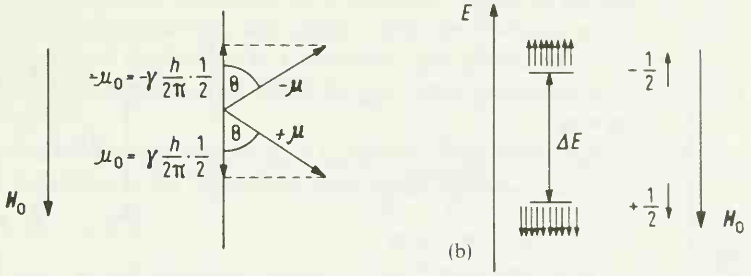
$-\mu_0 = -\gamma \frac{h}{2\pi} \cdot \frac{1}{2}$
$\mu_0 = \gamma \frac{h}{2\pi} \cdot \frac{1}{2}$
θ
θ
$-\mu$
$+\mu$
H_0
(a)
E
ΔE
$-\frac{1}{2}$
$+\frac{1}{2}$
H_0
(b)

Fig. 1.3. Alignment of nuclear spins with $I = 1/2$ in the magnetic field H_0 (a); corresponding energy levels and spin populations (b).

The energies $E_{+1/2}$ and $E_{-1/2}$ and the energy difference ΔE between the two levels are derived from eq. (1.5):

$$E_{+1/2} = -\mu_0 H_0 = -\gamma \frac{h}{4\pi} H_0 \, .$$

$$E_{-1/2} = \mu_0 H_0 = \gamma \frac{h}{4\pi} H_0 \, . \tag{1.6}$$

$$\Delta E = E_{-1/2} - E_{+1/2} = 2\mu_0 H_0 = \gamma \frac{h}{2\pi} H_0 \, . \tag{1.7}$$

1.4. Nuclear Magnetic Resonance

ΔE in eq. (1.7) and Fig. 1.3(b) is the difference between the energies of precession along and opposite to H_0. Using eq. (1.7), the Larmor precession frequency ν_0 of nuclei with $I = \frac{1}{2}$ can be calculated, recalling that ΔE also equals $h\nu_0$:

$$\nu_0 = \frac{\gamma}{2\pi} H_0 \, . \tag{1.8}$$

For a field strength of 21.3 kilogauss, the Larmor frequency of ^{13}C is in the order of 22 to 23 MHz, much lower than that of ^1H (90 MHz). This is in the radio-frequency (rf) range.

An alternating magnetic field H_1 with frequency ν_1 irradiating an ensemble of nuclear spins precessing in the static field H_0 may overcome the energy difference ΔE if it meets two conditions: The vector of the alternating field H_1 must rotate in the plane of precession with the Larmor frequency ν_0 of the nuclei to be observed (Fig. 1.4(a)).

$$\nu_1 = \nu_0 \, . \tag{1.9}$$

As a result, the spins originally precessing with H_0 flip over, and now precess against H_0. Absorption of energy ΔE from H_1 takes place (nuclear magnetic resonance).

In order to observe NMR, a sample containing nuclear spins (*e.g.* ^1H, ^{13}C) is placed in a static magnetic field H_0. An alternating field H_1 with radio-frequency ν_1 is applied perpendicularly to

H_0. Usually, ν_1 is increased or decreased slowly and continuously during observation (frequency sweep). When ν_1 matches the Larmor frequency of the nucleus to be observed (eq. (1.9)), an absorption signal is recorded in the receiver of the NMR spectrometer (Fig. 1.4(b)).

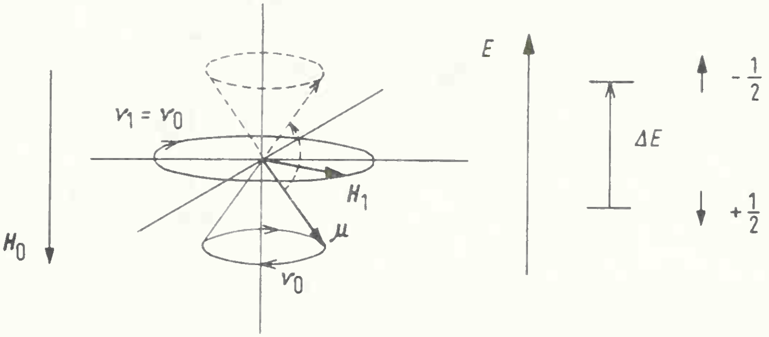

Fig. 1.4. (a) Action of a radiofrequency field H_1 on a nucleus precessing about H_0 direction.

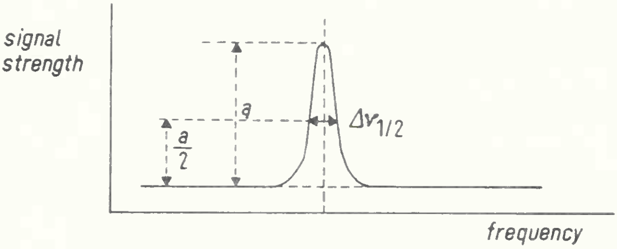

Fig. 1.4. (b) NMR signal ($\Delta\nu_{1/2}$ is the half-maximum intensity width).

Continuous irradiation by the radio-frequency H_1 would soon cause all nuclei to precess against H_0, and no further absorption of energy would occur, if there were no processes at work to restore the energetically favored orientation of the spins. In fact, energy absorption from radiofrequency fields due to NMR is observed for long periods if the rf power is not too high. The processes responsible are referred to as relaxation.

1.5. Relaxation

1.5.1. The Equilibrium of Nuclear Spins in the H_0 Field

At equilibrium, the nuclear magnetic energy levels are populated according to a Boltzmann distribution which favors the lower state. For the two orientations relative to H_0 of nuclei with $I = \frac{1}{2}$, the spin populations may be symbolized by N_+ and N_- (Fig. 1.3(b)). The distribution N_+/N_- can be expressed by the Boltzmann factor, recalling that $\Delta E = 2\mu_0 H_0$:

$$\frac{N_+}{N_-} = e^{\frac{\Delta E}{kT}} \approx 1 + \frac{\Delta E}{kT} = 1 + \frac{2\mu_0 H_0}{kT}. \tag{1.10}$$

At room temperature, $\Delta E = 2\mu_0 H_0$ is much less than 4.2 Joule, even at the highest field strengths now achievable. As a result, the term $\frac{2\mu_0 H_0}{kT}$ is very small and $\frac{N_+}{N_-}$ is not much greater than 1.

1.5.2. Spin-Lattice Relaxation

At resonance, the rf field H_1 causes a spin transfer from the lower to the upper level. The equilibrium distribution of the spins in the static field H_0 is disturbed. Following any disruption, the nuclear spins relax to the equilibrium with their surroundings (the "lattice"), which, of course, includes H_0. This relaxation is assumed to be a first-order rate process with a rate constant $1/T_1$ characterizing each kind of nuclei. T_1 is called the spin-lattice relaxation time. It covers a range of about 10^{-4} to 10^4 s.

For liquids with rapid intermolecular motion, T_1 is a measure of the life-time of a nucleus in a particular spin state. According to the Heisenberg uncertainty relation,

$$\Delta E \, \Delta t = h \, \Delta \nu_{1/2} T_1 \gtrapprox h \,, \tag{1.11}$$

the minimum width $\Delta \nu_{1/2}$ at half maximum intensity of an NMR signal (Fig. 1.4(b)) can be estimated by eq. (1.12):

$$\Delta \nu_{1/2} \gtrapprox \frac{1}{T_1} \,. \tag{1.12}$$

1.5.3. Spin-Spin Relaxation

In solids and liquids with slowly tumbling molecules internuclear dipole-dipole interactions may become important. Furthermore, energy quanta $\Delta E = 2\mu_0 H_0$ are exchanged between nuclei to a certain degree. Both factors tend to shorten the life-times of all spin states, again leading to line broadening. This second type of first-order relaxation process, called spin-spin relaxation and characterized by the time constant $1/T_2$, competes with spin-lattice relaxation. T_2 is referred to as the spin-spin relaxation time.

Since spin-spin relaxation reduces the life-time of a nucleus in a particular spin state to $T_2 \leqq T_1$, the half maximum intensity linewidth is expressed more precisely by eq. (1.13), which accounts for spin-spin relaxation.

$$\Delta \nu_{1/2} = \text{const.} \frac{1}{T_2} \,. \tag{1.13}$$

The observed linewidth of an NMR signal depends additionally on the field inhomogeneity ΔH_0, whose contribution to $\Delta \nu_{1/2}$ arises from eq. (1.8):

$$\Delta \nu_{1/2(\text{inhom.})} = \frac{\gamma \, \Delta H_0}{2\pi} = \text{const.} \frac{\gamma \, \Delta H_0}{2} \,. \tag{1.14}$$

By adding eqs. (1.13) and (1.14) one obtains the observed half maximum intensity linewidth $\Delta \nu_{1/2(\text{obs.})}$:

$$\Delta \nu_{1/2(\text{obs.})} = \Delta \nu_{1/2} + \Delta \nu_{1/2(\text{inhom.})} = \text{const.} \left(\frac{1}{T_2} + \frac{\gamma \, \Delta H_0}{2} \right) . \tag{1.15}$$

Spin-lattice relaxation of nuclei (*e.g.* ^{1}H, ^{13}C) in a molecule may be accelerated

a) by interaction with adjacent nuclei having spin 1 or greater (*e.g.* ^{2}H, ^{14}N): the electric quadrupole moments of such nuclei result in additional magnetic fields in the tumbling molecule;

b) by interaction with unpaired electrons in paramagnetic compounds (radicals, some metal chelates).

Spin-spin relaxation of nuclei is accelerated when they participate in a dipolar bond ($O-{}^1H$, $N-{}^1H$, ${}^{13}C-{}^1H$). Spin-spin relaxation involving dipole-dipole interaction is very effective in solids and viscous liquids with slow molecular motion since the magnetic fields caused by slowly tumbling dipoles change very slowly.

All these interactions cause considerable line broadening, making the observation of NMR signals rather difficult in some cases (*e.g.* in paramagnetic compounds). Briefly summarized, T_2 affects NMR signal linewidths, but not the energy level population as does T_1.

1.5.4. Saturation

If the radio-frequency power is too high, relaxation cannot compete with the disruption of the equilibrium of spins. The population difference between the nuclear magnetic energy levels decreases to zero and so does the intensity of the absorption signal (saturation).

1.6. The Magnetization Vectors

The Boltzmann factor $\frac{2\mu_0 H_0}{kT}$ only slightly favors the lower spin state. It is more realistic therefore to study the influence of magnetic fields on an assembly of a large number of identical nuclei than on one spinning nucleus.

For an assembly of identical nuclei with $I = \frac{1}{2}$, two orientations with respect to $\boldsymbol{H}_0$ are possible for each nucleus. Due to the favoring of the lower state with spin alignment more nearly parallel to $\boldsymbol{H}_0$, more nuclei precess about the direction of $\boldsymbol{H}_0$, defined as the $+z$ direction (Fig. 1.5). A net macroscopic magnetization $\boldsymbol{M}_0$ along the $+z$ axis arises as shown in Fig. 1.5(a). This orientation of the magnetization vector $\boldsymbol{M}_0$ parallel to $\boldsymbol{H}_0$ is characteristic of equilibrium of the spin ensemble. Upon disturbance of equilibrium by and rf field $\boldsymbol{H}_1$ with the proper frequency ν_1, the magnetic moment vectors $\boldsymbol{\mu}$ are forced to precess in phase (Fig. 1.5(b)). The resultant magnetization vector $\boldsymbol{M}$ is no longer parallel to $\boldsymbol{H}_0$ (Fig. 1.5(b)), and is now composed of three components along the

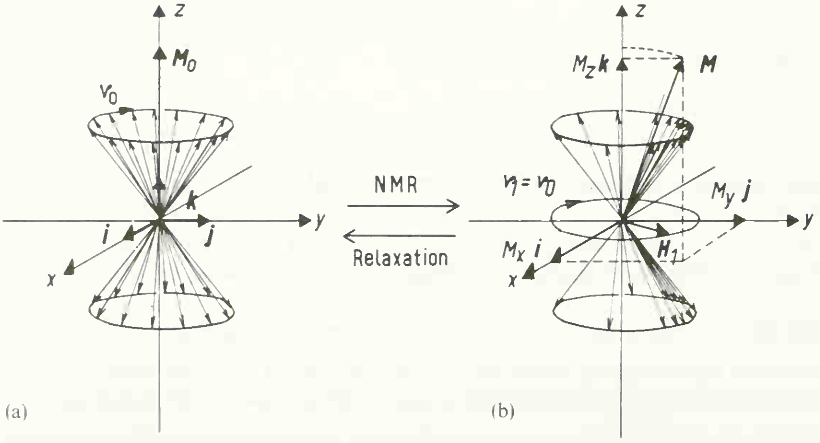

Fig. 1.5. The vectors of magnetization (a) in equilibrium, (b) at resonance ($\nu_1 = \nu_0$).

axes x, y, and z. These components are related to $\boldsymbol{M}$ by eq. (1.16), using the unit vectors $\boldsymbol{i}, \boldsymbol{j}$, and $\boldsymbol{k}$ along x, y, and z as illustrated in Fig. 1.5(b).

$$\boldsymbol{M} = M_x \boldsymbol{i} + M_y \boldsymbol{j} + M_z \boldsymbol{k} . \tag{1.16}$$

$M_z \boldsymbol{k}$ is the longitudinal magnetization along the z axis; $M_x \boldsymbol{i}$ and $M_y \boldsymbol{j}$ make up the transverse magnetization in the xy plane.

Relaxation can be described in terms of the magnetization vector components. At resonance, the equilibrium magnetization M_0 parallel to $\boldsymbol{H}_0$ decreases to M_z due to the transitions between the nuclear magnetic energy levels caused by the alternating field $\boldsymbol{H}_1$. Following resonance, the equilibrium of the nuclear spins with their lattice and with each other is restored by relaxation.

By spin-lattice relaxation, the longitudinal magnetization M_z increases to its equilibrium value M_0 (longitudinal relaxation). T_1 is therefore often called the longitudinal relaxation time.

By spin-spin relaxation, the nuclei relax to equilibrium among themselves (*i.e.* precession occurs without phase coherence). The vectors dephase (Fig. 1.5(b) → Fig. 1.5(a)), and the components of transverse magnetization, M_x and M_y, decay to zero as a result (transverse relaxation). The spin-spin relaxation time T_2 is thus also referred to as the phase memory time or the transverse relaxation time.

Longitudinal and transverse relaxation have been assumed by Bloch et al. [6] to be first-order rate processes. Following this assumption, the increase of M_z to M_0 and the decay of M_x and M_y to zero are expressed by eqs. (1.17) in terms of spin-lattice and spin-spin relaxation time, T_1 and T_2.

$$\frac{\mathrm{d}M_z}{\mathrm{d}t} = -\frac{M_z - M_0}{T_1}, \tag{1.17a}$$

$$\frac{\mathrm{d}M_x}{\mathrm{d}t} = -\frac{M_x}{T_2}, \tag{1.17b}$$

$$\frac{\mathrm{d}M_y}{\mathrm{d}t} = -\frac{M_y}{T_2}. \tag{1.17c}$$

1.7. The Bloch Equations

1.7.1. The Motion of the Magnetization Vectors in a Fixed Coordinate System

Upon irradiation with the rf field $\boldsymbol{H}_1$ at resonance,

$$\nu_1 = \nu_0$$

transitions between the nuclear magnetic energy levels occur. The nuclear spins change their directions relative to $\boldsymbol{H}_0$: The direction of the nuclear spin $\boldsymbol{p}$ is now time dependent. Following the equation of motion of a spin $\boldsymbol{p}$ in a magnetic field $\boldsymbol{H}$, this time dependence is given by the vector product of the magnetic moment $\boldsymbol{\mu}$ due to the spin $\boldsymbol{p}$ and the total field $\boldsymbol{H}$ resulting from the static field $\boldsymbol{H}_0$ and the rf field $\boldsymbol{H}_1$.

$$\frac{\mathrm{d}\boldsymbol{p}}{\mathrm{d}t} = \boldsymbol{\mu} \times \boldsymbol{H} . \tag{1.18}$$

By multiplying eq. (1.18) with the gyromagnetic ratio γ one obtains the time dependence of the magnetic moment $\boldsymbol{\mu}$, remembering that $\boldsymbol{\mu} = \gamma \boldsymbol{p}$:

$$\frac{\mathrm{d}\boldsymbol{\mu}}{\mathrm{d}t} = \gamma \boldsymbol{\mu} \times \boldsymbol{H} . \tag{1.19}$$

For an assembly of nuclei with magnetic moment $\boldsymbol{\mu}$ the resultant vector sum is the magnetization vector $\boldsymbol{M}$. Its time dependence is also given by eq. (1.19).

$$\frac{\mathrm{d}\boldsymbol{M}}{\mathrm{d}t} = \gamma \boldsymbol{M} \times \boldsymbol{H} . \tag{1.20}$$

1.7.2. The Motion of the Magnetization Vector in the Rotating Coordinate System

In the eyes of a distant observer using a fixed coordinate system, a meteorite falling in the gravitational field of the earth describes a parabolic path. An observer "standing" on earth uses the rotating frame of reference of the earth. For him, the complicated path of the falling meteorite simplifies to a straight vertical line.

Correspondingly, the path of the magnetization vector $\boldsymbol{M}$ subjected to magnetic fields is simplified in a coordinate system rotating at the angular velocity $\omega_1 = 2\pi\nu_1$ of the alternating field $\boldsymbol{H}_1$. In this case, the directions of the unit vectors $\boldsymbol{i}$, $\boldsymbol{j}$, and $\boldsymbol{k}$ change (they rotate), whereas their magnitudes remain constant. Due to the time dependence of the unit vectors, the derivative $\frac{\mathrm{d}\boldsymbol{M}}{\mathrm{d}t}$ of the magnetization vector,

$$\boldsymbol{M} = M_x \boldsymbol{i} + M_y \boldsymbol{j} + M_z \boldsymbol{k} ,$$

with respect to time is obtained using the product rule of differentiation:

$$\begin{aligned} \frac{\mathrm{d}\boldsymbol{M}}{\mathrm{d}t} &= \frac{\partial M_x}{\partial t}\boldsymbol{i} + M_x \frac{\partial \boldsymbol{i}}{\partial t} + \frac{\partial M_y}{\partial t}\boldsymbol{j} + M_y \frac{\partial \boldsymbol{j}}{\partial t} + \frac{\partial M_z}{\partial t}\boldsymbol{k} + M_z \frac{\partial \boldsymbol{k}}{\partial t} \\ &= \frac{\partial M_x}{\partial t}\boldsymbol{i} + \frac{\partial M_y}{\partial t}\boldsymbol{j} + \frac{\partial M_z}{\partial t}\boldsymbol{k} + M_x \frac{\partial \boldsymbol{i}}{\partial t} + M_y \frac{\partial \boldsymbol{j}}{\partial t} + M_z \frac{\partial \boldsymbol{k}}{\partial t} . \end{aligned} \tag{1.21}$$

Looking at eq. (1.21), the time dependence of the magnetization vector $\boldsymbol{M}$ results from two contributions. One is the partial time derivate of $\boldsymbol{M}$ in the rotating coordinate system:

$$\left(\frac{\partial \boldsymbol{M}}{\partial t}\right)_{\mathrm{rot}} = \frac{\partial M_x}{\partial t}\boldsymbol{i} + \frac{\partial M_y}{\partial t}\boldsymbol{j} + \frac{\partial M_z}{\partial t}\boldsymbol{k} . \tag{1.22}$$

The other arises from the rotation of the unit vectors $\boldsymbol{i}$, $\boldsymbol{j}$, and $\boldsymbol{k}$ with angular velocity ω. Since the time derivatives of the unit vectors are the vector products of $\boldsymbol{\omega}$ and $\boldsymbol{i}$, $\boldsymbol{j}$, and $\boldsymbol{k}$, respectively,

$$\frac{\partial \boldsymbol{i}}{\partial t} = \boldsymbol{\omega} \times \boldsymbol{i} ; \quad \frac{\partial \boldsymbol{j}}{\partial t} = \boldsymbol{\omega} \times \boldsymbol{j} ; \quad \frac{\partial \boldsymbol{k}}{\partial t} = \boldsymbol{\omega} \times \boldsymbol{k} , \tag{1.23}$$

the second term simplifies as follows:

$$\begin{aligned} M_x \frac{\partial \boldsymbol{i}}{\partial t} + M_y \frac{\partial \boldsymbol{j}}{\partial t} + M_z \frac{\partial \boldsymbol{k}}{\partial t} &= M_x \boldsymbol{\omega} \times \boldsymbol{i} + M_y \boldsymbol{\omega} \times \boldsymbol{j} + M_z \boldsymbol{\omega} \times \boldsymbol{k} \\ &= \boldsymbol{\omega} \times (M_x \boldsymbol{i} + M_y \boldsymbol{j} + M_z \boldsymbol{k}) \\ &= \boldsymbol{\omega} \times \boldsymbol{M} . \end{aligned} \tag{1.24}$$

Using eqs. (1.22; 1.24), and recalling eq. (1.20), the time derivative of $\boldsymbol{M}$ is

$$\frac{\mathrm{d}\boldsymbol{M}}{\mathrm{d}t} = \left(\frac{\partial \boldsymbol{M}}{\partial t}\right)_{\mathrm{rot}} + \boldsymbol{\omega} \times \boldsymbol{M} = \gamma \boldsymbol{M} \times \boldsymbol{H} . \tag{1.25}$$

From this relation, the time derivative of $\boldsymbol{M}$ in the rotating frame of reference can be calculated:

$$\left(\frac{\partial \boldsymbol{M}}{\partial t}\right)_{\mathrm{rot}} = \gamma \boldsymbol{M} \times \boldsymbol{H} - \boldsymbol{\omega} \times \boldsymbol{M} = \gamma\left(\boldsymbol{M} \times \boldsymbol{H} - \frac{\boldsymbol{\omega} \times \boldsymbol{M}}{\gamma}\right). \tag{1.26}$$

With $\boldsymbol{\omega} \times \boldsymbol{M} = -\boldsymbol{M} \times \boldsymbol{\omega}$, eq. (1.26) changes to

$$\left(\frac{\partial \boldsymbol{M}}{\partial t}\right)_{\mathrm{rot}} = \gamma \boldsymbol{M} \times \left(\boldsymbol{H} + \frac{\boldsymbol{\omega}}{\gamma}\right). \tag{1.27}$$

Since only terms with identical dimensions are allowed to be added, $\boldsymbol{\omega}/\gamma$ must have the dimension of a magnetic field. Thus, in the rotating frame of reference, the effective field $\boldsymbol{H}_{\mathrm{eff}}$ experienced by $\boldsymbol{M}$ differs from $\boldsymbol{H}$ by a term $\boldsymbol{\omega}/\gamma$ arising from rotation,

$$\boldsymbol{H}_{\mathrm{eff}} = \boldsymbol{H} + \frac{\boldsymbol{\omega}}{\gamma}, \tag{1.28}$$

and eq. (1.29) replaces eq. (1.27):

$$\left(\frac{\partial \boldsymbol{M}}{\partial t}\right)_{\mathrm{rot}} = \gamma \boldsymbol{M} \times \boldsymbol{H}_{\mathrm{eff}} . \tag{1.29}$$

Eq. (1.19) described the precession of $\boldsymbol{M}$ about the total magnetic field $\boldsymbol{H}$ using a coordinate system with fixed axes x, y, and z. Correspondingly, eq. (1.29) describes the magnetization vector $\boldsymbol{M}$ as it precesses about the effective field $\boldsymbol{H}_{\mathrm{eff}}$ [7] in a coordinate system rotating with frequency $\omega = 2\pi\nu$ about the z axis and symbolized as the x', y', z' frame of reference with the rotating unit vectors $\boldsymbol{i}'$, $\boldsymbol{j}'$, and $\boldsymbol{k}'$.

1.7.3. NMR in the Rotating Frame of Reference

In the absence of $\boldsymbol{H}_1$, the vector $\boldsymbol{M}$ keeps its equilibrium value and position $\boldsymbol{M}_0$ in the z direction. $\boldsymbol{M}$ is thus time-invariant in the rotating frame of reference, so that

$$\left(\frac{\partial \boldsymbol{M}}{\partial t}\right)_{\mathrm{rot}} = \gamma \boldsymbol{M} \times \boldsymbol{H}_{\mathrm{eff}} = 0 \tag{1.30}$$

and consequently

$$\boldsymbol{H}_{\mathrm{eff}} = 0 , \tag{1.31}$$

since

$$\boldsymbol{M} = \boldsymbol{M}_0 \neq 0 .$$

If the frame rotates at the Larmor frequency $\omega_0 = 2\pi\nu_0$, the rotational field term of eq. (1.28) reaches ω_0/γ. Since the effective field is zero, the Larmor equation (1.8a) is obtained:

$$H_{\text{eff}} = \left(H_0 + \frac{\omega_0}{\gamma}\right) k' = 0\,, \quad \text{so that} \quad \omega_0 k' = -\gamma H_0 k'\,. \tag{1.8a}$$

This means further that the rotational field ω/γ opposes $H_0 k'$ in the rotating frame of reference (Fig. 1.6(a)), finally cancelling $H_0 k'$ when the coordinate system rotates at Larmor frequency ω_0.

If an rf field H_1 with $\omega_1 = 2\pi\nu_1$ is applied perpendicularly to H_0 along the x' axis, the effective field H_{eff} in the frame of reference rotating at ω_1 is obtained from Fig. 1.6(a):

$$H_{\text{eff}} = \left(H_0 + \frac{\omega_1}{\gamma}\right) k' + H_1 i'\,. \tag{1.32}$$

If the frame of reference rotates at the radiofrequency ν_1 matching the Larmor frequency ν_0 (NMR), the term $\left(H_0 + \frac{\omega_1}{\gamma}\right) k'$ becomes zero according to eq. (1.8a). The remaining effective field at resonance is now

$$H_{\text{eff(res.)}} = H_1 i'\,, \tag{1.33}$$

so that eq. (1.29) changes to (1.34):

$$\left(\frac{\partial M}{\partial t}\right)_{\text{rot}} = \gamma M \times H_1 i'\,. \tag{1.34}$$

This relation tells us that, at resonance, the magnetization vector M precesses about the field vector $H_1 i'$ of the radio-frequency (Fig. 1.6(b)).

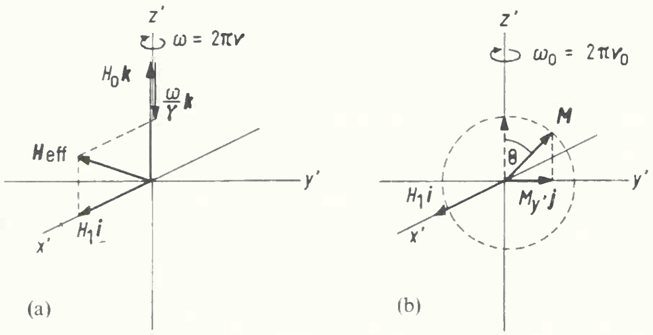

Fig. 1.6. The effective field in the rotating frame (a) off resonance ($\omega \neq \omega_0$), (b) on resonance ($\omega = \omega_0$).

Since the coordinate system and H_1 are choosen to rotate at the same frequency, H_1 can be assigned along the rotating x' axis. According to eq. (1.34), the magnetization vector M precesses about the x' axis (Fig. 1.6(b)). The precession frequency ω_1 of M about x' also follows the Larmor equation:

$$\omega_1 = \gamma H_1\,. \tag{1.8b}$$

Thus, an rf field H_1, applied at resonance for t_p seconds, causes the vector M to precess about the x' axis by an angle Θ (Fig. 1.6(b)):

$$\Theta = \omega_1 t_p = \gamma H_1 t_p \text{ (radians)}\,. \tag{1.35}$$

1.7.4. Relaxation in the Rotating Frame of Reference

If only $\boldsymbol{H}_0$ is applied, the nuclear moments precess without any phase coherence. No resultant component of the magnetization in the $x'y'$ plane is observed and M_z equals M_0 (Fig. 1.7(a)).
A radio-frequency H_1 applied perpendicularly to $\boldsymbol{H}_0$ forces the nuclei to precess in phase, tipping the vector $\boldsymbol{M}_0$ by an angle Θ toward the y' axis (Fig. 1.7(b)). A transverse magnetization $M_{y'}\boldsymbol{j}$ in the $x'y'$ plane arises and the magnitude of the longitudinal magnetization $M_{z'}$ decreases (Fig. 1.7(b)). Restoring equilibrium, the nuclei exchange energy with each other (spin-spin relaxation). They dephase, causing $M_{y'}\boldsymbol{j}'$ to spread out in components in the $x'y'$ plane and, finally, to decay to zero with time constant $1/T_2$ (Fig. 1.7(c,d)). Dephasing may be accelerated due to field inhomogeneities so that

$$(1/T_2^*)_{(\text{inhom.})} > 1/T_2 \,.$$

Moreover, the nuclear moments lose energy to their surroundings (spin-lattice relaxation), causing $M_z\boldsymbol{k}'$ to increase to $\boldsymbol{M}_0$ (Fig. 1.7(d) → Fig. 1.7(a)).
The decay of the magnitude of transverse magnetization, $M_{y'}$, due to spin-spin relaxation (T_2) or due to field inhomogeneities (T_2^*) may be faster but cannot be slower than the spin-lattice relaxation (T_1):

$$T_2^* \leqq T_2 \leqq T_1 \,. \tag{1.36}$$

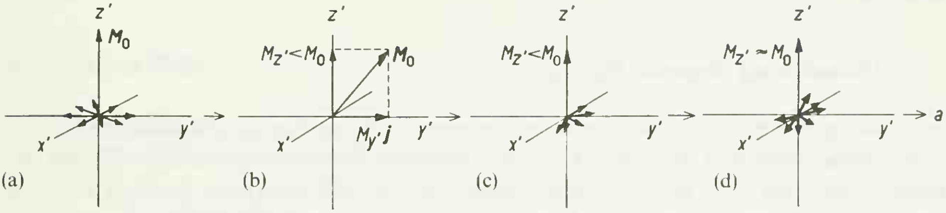

Fig. 1.7. Relaxation.

1.8. NMR Spectra

1.8.1. Nuclear Induction

At resonance, the magnetization vector $\boldsymbol{M}$ precesses about the vector $H_1\boldsymbol{i}'$ of the alternating field according to eq. (1.34). As a result, a component of transverse magnetization $M_{y'}\boldsymbol{j}$ rotates in the $x'y'$ plane at the Larmor frequency ν_0. If a receiver coil is placed in the $x'y'$ plane, the rotating magnetic vector $M_{y'}\boldsymbol{j}$ induces an electromotive force measurable as an inductance current. This process is called nuclear induction [5, 8]. The orientation of the coil axis will affect the phase relative to $H_1\boldsymbol{i}'$ but not the magnitude of the induction current.
In the rotating frame of reference, the field vector $H_1\boldsymbol{i}'$ of the rf field, rotating at angular velocity ω_1 in phase with the rotating x axis (x'), is used as the reference. The transverse magnetization $M_x\boldsymbol{i} + M_y\boldsymbol{j}$ in the fixed coordinate system is then resolved in two components $\boldsymbol{u}$ and $\boldsymbol{v}$ in the

rotating frame of reference: ***u*** rotates in phase, ***v*** rotates 90° or $\pi/2$ out of phase with $H_1 \boldsymbol{i}'$ (Fig. 1.8).

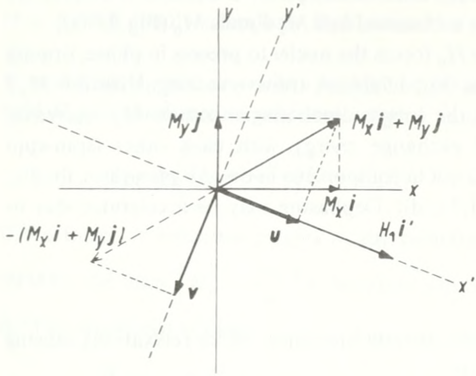

Fig. 1.8. The components ***u*** and ***v*** of transverse magnetization in the rotating frame.

Following eq. (1.34), the magnetization vector ***M*** is rotated toward the y' axis by the oscillation of $H_1 \boldsymbol{i}'$ in phase with the x' axis of the rotating frame of reference. In agreement with the Lenz rule of induction, the current $I_{\text{ind.}}$ due to the induced EMF opposes the inducing magnetization. At resonance, the magnetization vector rotates 90° = $\pi/2$ behind $H_1 \boldsymbol{i}'$ (Fig. 1.6). The maximum induction current, however, is observed 90° = $\pi/2$ ahead of phase relative to $H_1 \boldsymbol{i}'$ in the ***v*** direction.

1.8.2. Absorption and Dispersion Spectra

Maximum induction current due to resonance between rf field and Larmor precession corresponds to maximum absorption of energy. Thus, the plot of the induction current in ***v*** direction ($\pi/2$ ahead of the vector $H_1 \boldsymbol{i}'$) as a function of frequency is the NMR absorption spectrum, called the v mode. The absorption curve has a Lorentzian shape as shown in Fig. 1.9(a).

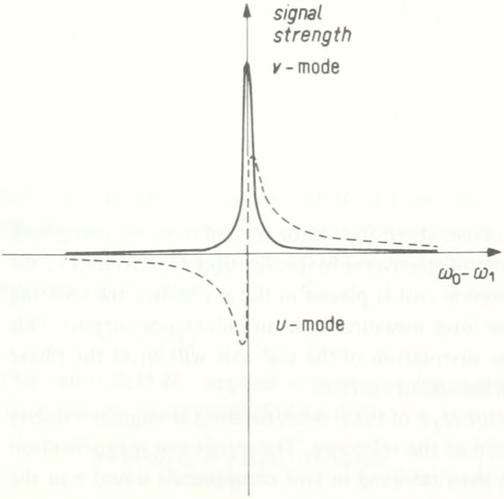

Fig. 1.9. Absorption (v, ———) and dispersion (u, – – –) spectrum.

Before and after resonance, there are magnetization components of opposite sign 180° out of phase and in phase ($+u$ and $-u$ direction) with the rf field $H_1 i'$ (Fig. 1.8). At resonance, there is no magnetization in the u direction. If the receiver coil obtains the inductance current in phase with $H_1 i'$ (the u direction), a dispersion curve (Fig. 1.9(b)) results, called the u mode. When the absorption or out of phase spectrum (v) reaches its maximum ($I_{\text{ind.}}(\omega) = \text{max.}$) the dispersion or in phase spectrum (u) goes through zero and changes its sign as illustrated in Fig. 1.9.

1.8.3. Magnitude Spectra

If NMR spectra are computed by Fourier transformation of pulse interferograms (Chapter 2), complex quantities are used during computation. Real and imaginary components $v(\omega)$ and $\mathrm{i}u(\omega)$ of the NMR spectrum are obtained as a result. Magnitude or power spectra $P(\omega)$ can be computed from the real and imaginary part as follows:

$$P(\omega) = \sqrt{[v(\omega)]^2 + [\mathrm{i}u(\omega)]^2} \tag{1.37}$$

If the real part $v(\omega)$ of the NMR spectrum is computed in the absorption (v) mode, the imaginary part is usually displayed in the dispersion (u) mode. The magnitude spectrum is therefore related to the v and u mode as indicated in eq. (1.37).

1.9. Chemical Shift

1.9.1. Shielding of Nuclei in Atoms and Molecules

The Larmor frequency of a "free" nuclear spin is given by the Larmor equation:

$$\nu_0 = \frac{\gamma}{2\pi} H_0 \left(I = \frac{1}{2}\right). \tag{1.8}$$

In atoms and molecules, a nucleus i is shielded by electrons. It does not experience the static field H_0 applied but an individual field H_i, arising from superposition of the H_0 field and an additional field $H_{\text{ind.i}}$ induced by the shielding electrons:

$$H_\mathrm{i} = H_0 - H_{\text{ind.i}}. \tag{1.38}$$

The strength of $H_{\text{ind.i}}$ induced by the electrons is proportional to the strength of the applied field H_0.

$$H_{\text{ind.i}} = \sigma_\mathrm{i} H_0 . \tag{1.39}$$

The factor σ_i [9] is called the magnetic shielding constant for the nucleus i, and characterizes the chemical environment of that nucleus. The effective field experienced by the nucleus i follows from eqs. (1.38, 1.39):

$$H_\mathrm{i} = H_0(1 - \sigma_\mathrm{i}). \tag{1.40}$$

Thus, the nucleus i precesses at the Larmor frequency

$$\nu_{0_i} = \frac{\gamma}{2\pi} H_0 (1 - \sigma_i) \tag{1.8c}$$

when exposed to the static magnetic field $\boldsymbol{H}_0$.

Eq. (1.8c) tells us that nuclei having different chemical environments precess at different Larmor frequencies. The shift of Larmor frequencies due to chemical nonequivalence of nuclei in molecules is called the chemical shift.

For n chemically non-equivalent nuclei in a molecule, n absorption signals are observed in the NMR spectrum due to n different Larmor frequencies. For example, acetone has two kinds of chemically non-equivalent ^{13}C nuclei, one carbonyl nucleus and two methyl nuclei. Two signals are observed in the ^{13}C NMR spectrum as shown in Fig. 1.10 (a). The signal intensity is proportional to the number of equivalent nuclei of a particular type giving rise to the considered signal. In acetone, for instance (Fig. 1.10 (a)), the ratio of signal intensities is equal to the ratio of the numbers of chemically non-equivalent ^{13}C nuclei:

$$n_{CO} : n_{CH_3} = 1:2\,.$$

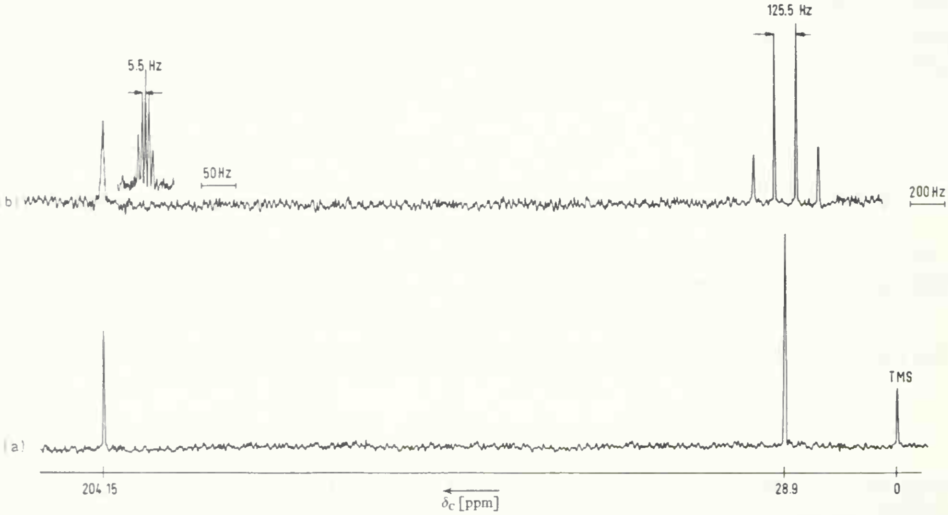

Fig. 1.10. Natural abundance ^{13}C NMR spectrum of acetone, neat liquid, (a) decoupled, 512 scans, (b) coupled, 4096 scans; swept radiofrequency 22.628 MHz corresponding to field strength of 21.3 Kilogauss; the frequency differences relative to tetramethylsilane (TMS) are $\Delta\nu_{CH_3} = 655$ Hz and $\Delta\nu_{CO} = 4632$ Hz; the values according to eq. (1.43) are therefore $\delta_{CH_3} = \frac{655}{22.628} \cdot 10^{-6} = 28.9$ ppm and $\delta_{CO} = \frac{4632}{22.628} \cdot 10^{-6} = 204.15$ ppm.

1.9.2. Calibration of NMR Spectra

In order to measure chemical shifts, the absorption signal of a reference compound R appearing at frequency ν_{0R} is assigned the shift zero. The chemical shift (or Larmor frequency) of chemically equivalent nuclei of a sample having their signal at frequency ν_{0S} may then be measured as the frequency difference $\Delta\nu_S$ in Hertz (Fig. 1.10 (b), legend).

$$\Delta\nu_S = \nu_{0S} - \nu_{0R} \quad [\mathrm{Hz}] . \tag{1.41}$$

According to the Larmor equation (1.8), chemical shifts can be related to field differences ΔH_S, measurable in millitesla.

$$\Delta H_S = H_S - H_R \quad [\mathrm{mT}] . \tag{1.42}$$

Also because of the Larmor equation (1.8), the frequency or field differences $\Delta\nu_S$ or ΔH_S are proportional to the swept radio-frequency ν_1 (in MHz) or the field strength of H_0 (in T). Therefore, chemical shifts $\Delta\nu_S$ (or ΔH_S) obtained at different radio-frequencies ν_1 (or field strengths H_0) have to be adjusted to the same radio-frequency (or field) before comparison. In order to get chemical shift values which are independent of the frequency or field strength used, the δ scale of chemical shifts is introduced. δ values are obtained by dividing the frequency differences $\Delta\nu_S$ (in Hz) by the frequency ν_1 used (in MHz $= 10^6$ Hz).

$$\delta_S = \frac{\nu_{0S} - \nu_{0R}}{\nu_1} 10^{-6} . \tag{1.43}$$

Because $\Delta\nu_S$ between nuclei of the same type is very small (several Hz) compared to ν_1 (several MHz), the shifts on the δ scale are given in ppm (parts per million $=$ units of 10^{-6}). Examples for the calculation of δ values in ppm are given for the ^{13}C chemical shifts of acetone in the legend of Fig. 1.10 (a).

1.9.3. The Reference Standard

A common reference compound used for calibrating ^1H and ^{13}C NMR spectra is tetramethylsilane (TMS), $Si(CH_3)_4$. In the ΔH scale (eq. (1.42)), the carbon-13 signal due to the four equivalent methyl groups of TMS appears at very high field strength relative to the signals of other carbons in organic compounds (Fig. 1.10 (a)). The same applies to the proton signal of TMS, the common reference for ^1H NMR spectra [1 – 5].

Signals with small $\delta_S(\Delta\nu_S, \Delta H_S)$ relative to TMS are said to appear at high field. The corresponding nuclei are strongly shielded; σ_i of eq. (1.40) is small. Signals with large δ_S are said to be at low field. Their nuclei are weakly shielded ("deshielded"); the amount of σ_i in eq. (1.40) is small.

The reference compound can be added to the sample solution (internal reference) or kept separate from the sample in a sealed capillary (external reference, Fig. 2.32). If an external reference is necessary, a correction term accounting for the difference between the bulk susceptibilities of reference (χ_R) and sample solution (χ_S) must be added to the observed shift, $\delta_{\mathrm{obs.}}$:

$$\delta_{\mathrm{corrected}} = \delta_{\mathrm{obs.}} + \frac{2\pi}{3}(\chi_R - \chi_S) . \tag{1.44}$$

1.10. Spin-Spin Coupling

1.10.1. Multiplicity of Signals

The ^{13}C NMR spectrum of acetone shown in Fig. 1.10 (a) was obtained by proton decoupling. For the two non-equivalent nuclei two sharp singlets are observed. If proton decoupling is not applied, a proton coupled ^{13}C spectrum is obtained, and both ^{13}C signals of acetone split into multiplets as shown in Fig. 1.10 (b). A large quartet is found for the methyl carbons, which are each directly bonded to three protons with $I_H = \frac{1}{2}$. The signal of the carbonyl carbon atom, which is separated from six hydrogen atoms by two bonds, splits into a narrow septet.

A system containing n equivalent nuclei X with total spin quantum number I_X and m equivalent nuclei A with I_A is said to be of type A_mX_n if the chemical shift difference of X and A is large. The number of lines in the NMR spectrum of each of both nuclei follows the multiplicity rule (1.45).

$$\left.\begin{array}{ll} 2nI_X + 1 & \text{for nucleus A} \\ 2mI_A + 1 & \text{for nucleus X} \end{array}\right\} \tag{1.45}$$

The ^{13}C NMR spectrum of a methyl group, representing an AX_3 system, is a quartet according to eq. (1.45), since $I_X = \frac{1}{2}$ and $n = 3$. The ^1H NMR spectrum of a methyl group, however, is a doublet because one ^{13}C nucleus is adjacent to three equivalent protons, so that $I_A = \frac{1}{2}$ for ^{13}C and $m = 1$. Due to the low natural abundance of ^{13}C the doublets arising from coupling of carbon-13 with protons are usually lost in the noise of ^1H NMR spectra.

1.10.2. Coupling Constants

The multiplet lines in the ^{13}C spectrum of acetone are equidistant. The distance (quoted in Hz) between any two neighboring lines is termed the coupling constant. The coupling constant of an A_mX_n system is given the symbol J_{AX}.

In the ^{13}C NMR spectrum of acetone (Fig. 1.10 (b)), the coupling constant is 125.5 Hz for the methyl signal and 5.5 Hz for the carbonyl signal. This illustrates that the magnitude of the coupling constant J_{AX} decreases with the increasing number of bonds separating the nuclei A and X. If A and X are more than 4 to 5 bonds apart, the multiplet structure of the A and X spectrum cannot be resolved.

1.10.3. Comparison between Chemical Shifts and Coupling Constants

Chemical shifts depend on the strength of the applied magnetic field H_0 according to eq. (1.8c) when measured on the frequency scale. Coupling constants remain constant when the strength of the magnetic field H_0 changes.

Because of intramolecular mobility (rotations, inversions) and intermolecular interactions, chemicals shifts depend on temperature, solvent, and concentration. Coupling constants, however, for the most part do not depend on these conditions.

1.10.4. The Origin of Spin-Spin Coupling [10]

The magnitude of $^{13}C-^1H$ coupling constants depends on the hybridization of the carbon atom (sp^3, sp^2, sp) coupled to the proton. This is indicative of a mechanism of spin-spin coupling involving the bonding electrons as is illustrated in Fig. 1.11 for a group AX with nuclei A and X, each with a total spin quantum number of $I = \frac{1}{2}$.

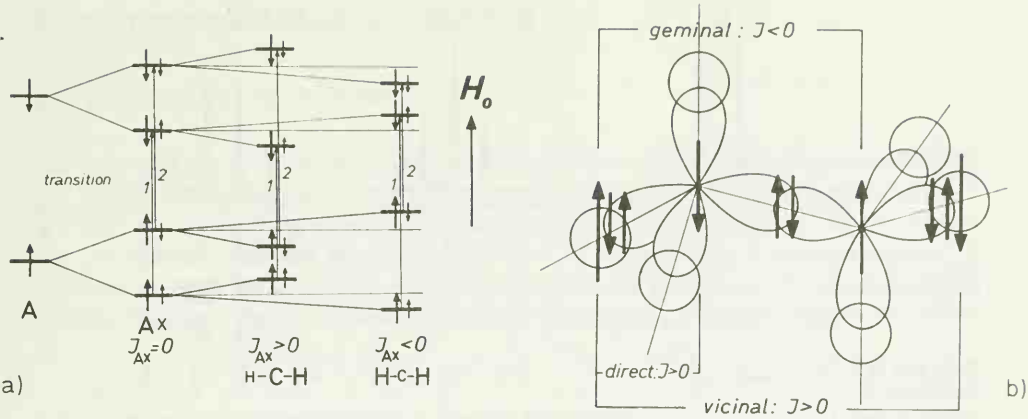

Fig. 1.11. Energy levels of an AX spin system (a) and interaction of the nuclear spins A and X with $I = 1/2$, involving the bonding electrons (ethane molecular orbital model).

The multiplets arise from splitting of nuclear energy levels: Those of nucleus A split due to the additional magnetic field caused by the nucleus X precessing with or against H_0 when $I_X = \frac{1}{2}$. Precession of X with H_0 is more stable (Fig. 1.11(a)). – For nucleus A, only transitions with $I_A = \pm 1$ and $I_X = 0$ are allowed (Fig. 1.11(a)) due to quantum mechanical rules. Therefore, only two transitions are possible for A, both of them requiring the same amount of energy. No splitting arises yet ($J_{AX} = 0$, Fig. 1.11(a)), and other influcences must be taken in account.

Additionally, spin-correlation by the way of bonding electrons plays a role as can be rationalized in Fig. 1.11 (b), recalling the Pauli principle. In the more stable state, any spin, including the spins of both bonding electrons occupying the bonding molecular orbital, is antiparallel to an adjacent one (Fig. 1.11 (b)). Thus, for nuclei separated by *one* and *three* bonds (*direct* and *vicinal* coupling) a stabilization occurs for *antiparallel* precession, and J_{AX} is defined to be *positive* ($J_{AX} > 0$, Fig. 1.11 (a)). The stabilization energy corresponds to a frequency of $\frac{1}{4} J_{AX}$ as can be seen from Fig. 1.11 (a). The *parallel* precession of A and X, on the other side, is *destabilized* by the same amount of energy. Two transitions of *different* frequencies take place, and the A signal splits into a dublet as a result.

For *geminal* nuclei A and X, the Pauli principle favours a *parallel* precession (Fig. 1.11 (b)). A stabilization-destabilization pattern opposite to the directly bonded and vicinal nuclei arises (Fig. 1.11(a)), and the coupling constant is defined to be *negative* ($J_{AX} < 0$). There are experimental techniques to determine the relative sign of coupling constants [5].

Often, more than one nucleus X with $I_X = \frac{1}{2}$, each with spin aligned with or opposed to H_0, couples with nucleus A. This is the case in CH_2 and CH_3 groups, representing AX_2 and AX_3 systems. In this case, all possible spin configurations of the X nuclei relative to H_0 must be considered, as illustrated in Fig. 1.12. Thus, a total spin characterizes each spin configuration relative to H_0. Each total spin has a particular weight arising from the number of spin configurations producing that total spin. The multiplicity of the signal A is given by the number of unequal total spins of the coupling nuclei X, and the multiplicity rule (1.45) is obtained.

The intensities of the multiplet lines arise from the number of spin configurations belonging to each total spin (Fig. 1.12). For n coupling nuclei X the intensity ratios are equal to the n^{th} binominal coefficients (Table 1.3).

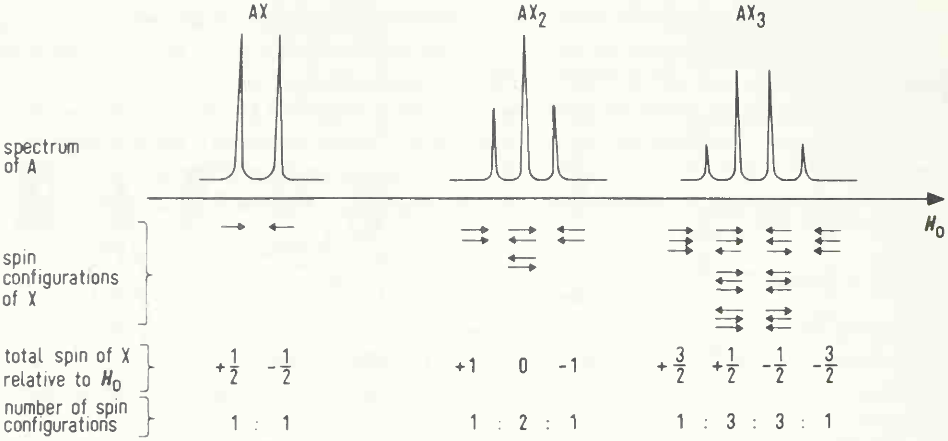

Fig. 1.12. Multiplicity and multiplet line intensities of the A signals in AX, AX_2, and AX_3 systems.

Table 1.2. Multiplicity of Signal A due to Coupling with Nuclei X ($I_X = \frac{1}{2}$).

System	Multiplicity
AX (CH)	$2 = 2 \cdot 1 \cdot \frac{1}{2} + 1$
AX_2 (CH_2)	$3 = 2 \cdot 2 \cdot \frac{1}{2} + 1$
AX_3 (CH_3)	$4 = 2 \cdot 3 \cdot \frac{1}{2} + 1$
AX_n	$2nI_X + 1$

Table 1.3. Multiplet Line Intensity Ratios of Signal A due to Coupling with *n* equivalent Nuclei X ($I_X = \frac{1}{2}$).

$n = 0$	1
1	1 1
2	1 2 1
3	1 3 3 1
4	1 4 6 4 1
5	1 5 10 10 5 1

The analysis of multiplets by means of the multiplicity rules given above applies to systems where chemical shift differences between nuclei A and X in the frequency scale are large compared to the coupling constant J_{AX}. This is expected for carbon-13-proton multiplets, as the difference in Larmor frequencies between protons (about 90 MHz at 2.13 Tesla) and carbon-13 nuclei (about 22.6 MHz at 2.13 Tesla) is on the order of several MHz; the coupling constants, however, are between 0 and 300 Hz. Natural abundance ^{13}C NMR spectra should therefore be easily analyzed following the multiplicity rules (1.45). But, as large one-bond ^{13}C-^{1}H couplings are involved, some energy levels may approach each other so that they mix. As a result, spectra of higher than first order are frequently observed for longer range couplings. The analysis of these spectra may require quantum mechanical calculations [5], computer simulation of spectra [12] or proton decoupling experiments as outlined in section 2.6.

2. Instrumental Methods of ^{13}C NMR

2.1. The Sensitivity of ^{13}C NMR

The main difficulty in ^{13}C NMR is the low natural abundance of the carbon-13 nucleus (1.108 %) and its low gyromagnetic ratio γ, which yields a much smaller Boltzmann exponent $2\gamma p_0 H_0/kT$ than that of protons. Low natural abundance and small gyromagnetic ratio are the reasons why ^{13}C NMR is much less sensitive (1.59 %) than ^{1}H NMR (100 %). A common measure of sensitivity in NMR is the signal to noise ratio of a reference sample, *e.g.* 1 % ethyl benzene in deuteriochloroform. Several methods are available for *improving the signal: noise in* ^{13}*C NMR.*

2.2. Methods of Sensitivity Enhancement in ^{13}C NMR

The number of ^{13}C nuclei in the homogeneity range of the magnet can be increased by ^{13}*C enrichment* of the compound to be measured. Further, the *sample concentration* at a given volume or the *sample volume* at a given concentration can be *increased;* the former is limited by limited solubility, the latter by the air gap of the magnet.

In keeping with the Boltzmann equation, the sensitivity of ^{13}C NMR can be slightly increased by *lowering the sample temperature.* Care must be taken with temperature dependent spectra.

The Boltzmann exponent can be also increased by *increasing the magnetic field strength.* Fields of up to 8.5 Tesla having the necessarily high homogeneity are now attainable in superconducting solenoids cooled with liquid helium.

The signal strength increases with the *rf power* as long as relaxation effects are adequate to restore equilibrium. The method is therefore limited by saturation.

Accumulation of spectra in a digital computer involving averaging of noise is known as the CAT method (computer averaged transients). The signal : noise ratio, $S:N$, increases with the number of accumulated scans n according to eq. (2.1).

$$(S:N)_n = (S:N)_1 \sqrt{n}\,. \tag{2.1}$$

The most economical and efficient method of sensitivity enhancement in ^{13}C NMR of organic molecules is the *pulse Fourier transform* technique *(PFT)* in combination with *decoupling methods* such as proton broad band and off-resonance decoupling. These methods will be described in the following sections.

2.3. Continuous Wave NMR Spectroscopy

In the conventional NMR experiment, a radio-frequency field is applied continuously to a sample in a magnetic field. The radio-frequency power must be kept low to avoid saturation. An NMR spectrum is obtained by sweeping the rf field through the range of Larmor frequencies of the observed nucleus. The nuclear induction current (Section 1.8.1) is amplified and recorded as a function of frequency. This method, which yields the frequency domain spectrum $f(\omega)$, is known as the steady-state absorption or continuous wave (CW) NMR spectroscopy [1 – 3].

2.4. Pulsed NMR Spectroscopy

2.4.1. Free Induction Decay

In pulsed NMR experiments, the sample is irradiated by short intense rf pulses. In keeping with eq. (1.35), an rf pulse of width t_p seconds (Fig. 2.1 (a)) rotates the vector of magnetization by an angle of $\Theta = \omega_1 t_p$ rad (Fig. 2.1 (b)). A transverse component of magnetization, M'_y, results. The magnitude of M'_y is given by eq. (2.2),

$$M'_y = M_0 \sin \omega_1 t_p\,, \tag{2.2}$$

as can be seen in Fig. 1.6 (b).

Following the rf pulse, the transverse magnetization M'_y decays exponentially to zero *via* spin-spin relaxation with time constant $1/T_2$ (Fig. 2.1 (c)).

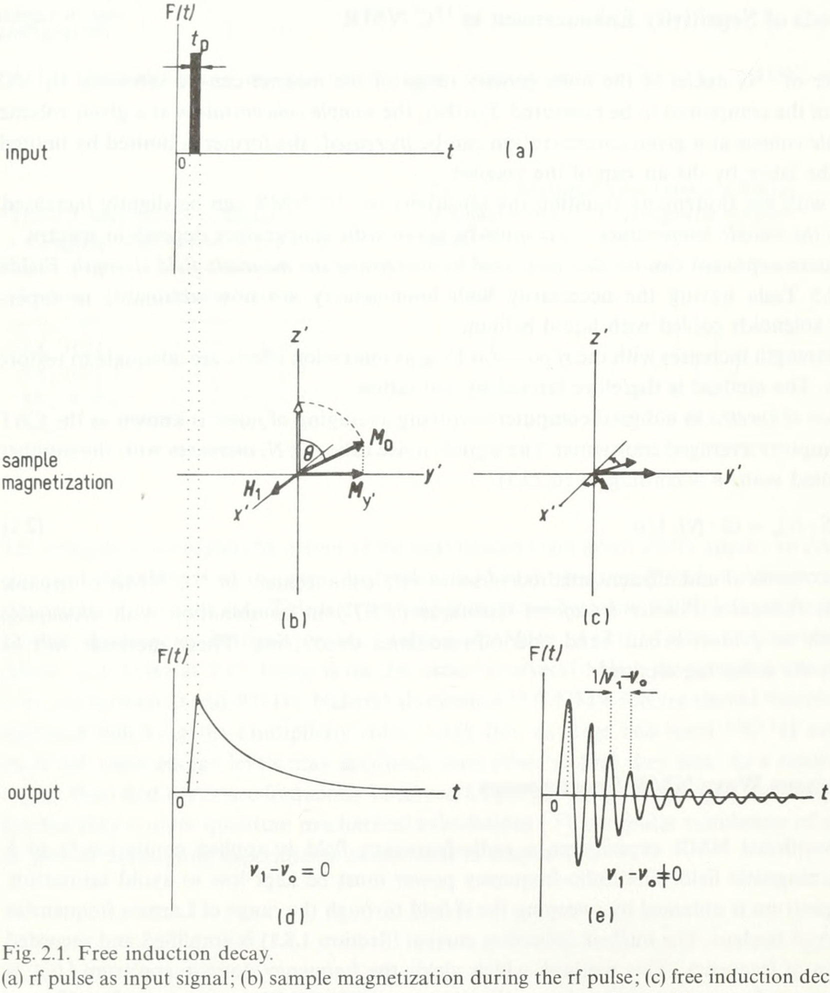
F/t/
t_p
input
0
t
(a)
z'
M_0
θ
sample magnetization
H_1
$M_{y'}$
y'
x'
(b)
z'
y'
x'
(c)
F/t/
output
0
t
$\nu_1 - \nu_o = 0$
(d)
F/t/
$1/\nu_1 - \nu_o$
0
t
$\nu_1 - \nu_o \neq 0$
(e)

Fig. 2.1. Free induction decay.
(a) rf pulse as input signal; (b) sample magnetization during the rf pulse; (c) free induction decay following the rf pulse; (d) output signal for rf at resonance; (e) output signal for rf off resonance.

At resonance, the magnetization M_y' always has a phase shift of $\pi/2$ relative to the rf field H_1 in the rotating frame of reference (Fig. 1.8). This is due to the experimental arrangement and is not affected by pulsing. Thus, a nuclear induction current stemming from the decay of M_y' is built up in the receiver coil following the rf pulse (Fig. 2.1 (d)).

If the rf differs from the Larmor frequency of the nuclei to be investigated (off-resonance), the transverse magnetization M_y' is rotating relative to the frame of reference after the pulse has ended. M_y' and H_1 periodically rephase and dephase. Their interference is observed in the receiver coil as a decaying beat pattern (Fig. 2.1 (e)) analogous to the wiggles of CW high resolution NMR spectra. The spacing between two beat peaks is the reciprocal of the difference between the frequency of the pulse and the Larmor frequency, $1/(\nu_1 - \nu_0)$ (Fig. 2.1 (e)).

The time domain function $F(t)$ arising from the freely relaxing spins following an rf pulse is called the free induction decay (FID) signal or the transverse relaxation function [7].

Due to chemical shielding, each nucleus may resonate within a range of Larmor frequencies, $2\pi\Delta = \omega_0 - \omega$, depending on its chemical environment. In order to rotate all nuclear spins within that range by the same angle Θ, the strength of the rf pulse must meet the requirement

$$\gamma H_1 \gg 2\pi\Delta \,. \tag{2.3}$$

Furthermore, the pulse width must be much shorter than the relaxation times,

$$t_p \ll T_1, T_2 \,, \tag{2.4}$$

so that relaxation is negligible during the pulse.

According to eq. (2.2), the FID signal initiated by an rf pulse increases with the pulse width t_p, reaching a maximum for $\omega_1 t_p = \pi/2$, a 90° pulse, and decreasing to zero for $\omega_1 t_p = \pi$, a 180° pulse. Pulse widths can thus be adjusted for 90° pulses by maximizing the FID signals.

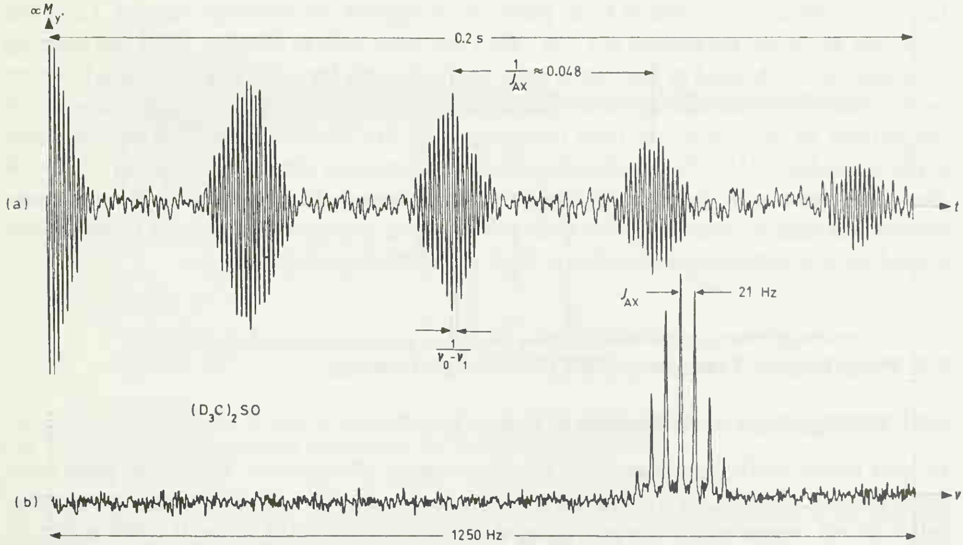

Fig. 2.2. (a) FID signal of hexadeuteriodimethylsulfoxide; neat liquid; natural ^{13}C abundance; 22.63 MHz; 30 °C; pulse width: 10 μs for about 30° as pulse angle; observation time: 0.8 s; 0.2 s of the decay are shown; 2048 accumulated scans;

(b) Fourier transform of (a); recorded width: 1250 Hz; the distance between two beat maxima in (a) is about 0.048 s; this corresponds to a carbon-deuterium coupling constant of about 21 Hz.

2.4.2. Pulse Interferograms

For a liquid sample containing identical nuclei, the transverse magnetization M'_y arises from one Larmor frequency, which is actually the maximum of a very small frequency distribution caused by spin-spin relaxation and slight field inhomogeneities. The FID signal $\mathrm{F}(t)$ of this sample decays exponentially according to eq. (2.5), in keeping with the differential equations (1.17) describing transverse relaxation. F(0) is the amplitude of the FID signal at the time the pulse has stopped. For short pulses ($t_p \ll T_2$), the pulse width is negligible and F(0) approximates the FID amplitude at time zero.

$$\mathrm{F}(t) = \mathrm{F}(0)\mathrm{e}^{-t/T_2}\,. \tag{2.5}$$

If a sample contains equivalent nuclei A (^{13}C) subject to spin-spin coupling with nuclei X (^{1}H), the transverse magnetization arises from two or more Larmor frequencies, depending on the multiplicity. The corresponding magnetization vectors periodically rephase and dephase with the field vector H_1 as in the off-resonance case with one Larmor frequency (Section 2.4.1). The FID signal is thus modulated by the frequency of the coupling constant J_{AX} [7, 13] as illustrated in Fig. 2.2(a) for hexadeuteriodimethylsulfoxide.

Similarly, in a sample containing two non-equivalent nuclei A_1 and A_2, the transverse magnetization results from two components due to two Larmor frequencies. In this case, the FID signal is modulated by the chemical shift difference of Larmor frequencies, $\Delta\nu = \nu_1 - \nu_2$. This modulation is illustrated in Fig. 2.3(a) by the FID signal of a sample of 1-^{13}C–D-glucose after mutarotation. The product mixture of mutarotation contains α- and β-glucopyranose with differently shielded glycosidic carbons separated in the ^{13}C NMR spectrum by 87.5 Hz.

FID signals caused by rf pulses and modulated due to spin-spin coupling and chemically shifted Larmor frequencies are referred to as pulse interferograms. As illustrated in Figs. 2.2(a) and 2.3(a), the structural parameters of a CW NMR spectrum such as chemical shifts and coupling constants can be obtained by analysis of pulse interferograms. Most organic molecules, however, contain more than two non-equivalent nuclei; additionally, spin-spin coupling may complicate the patterns. As an example, the pulse interferogram in Fig. 2.3(a) changes to the pattern shown in Fig. 2.4(a) due to ^{13}C–^{1}H coupling if proton decoupling is not applied while pulsing 1-^{13}C–D-glucose. In these cases, visual analysis of pulse interferograms becomes difficult. Fourier transformation is used to obtain chemical shifts and coupling constants. Examples of Fourier transformed pulse interferograms are given in Figs. 2.2(b), 2.3(b), and 2.4(b).

2.5. Pulse Fourier Transform (PFT) NMR Spectroscopy

2.5.1. FID Signal and NMR Spectrum as Fourier Transforms

In most pulsed NMR experiments, the rf field is applied off-resonance. Modulated pulse interferograms (Fig. 2.1(d), 2.2(a), 2.3(a), and 2.4(a)) arise because the vectors of transverse magnetization do not precess with a constant phase shift of $\pi/2$ relative to the vector H_1. This is demonstrated in Fig. 2.5. The transverse magnetization is then a resultant of two components, $v(t)$, with a phase shift of $\pi/2$ relative to H_1 and $u(t)$ in phase with H_1:

$$\begin{aligned} v(t) &= M_0 \sin\Theta \cos\omega t \\ u(t) &= M_0 \sin\Theta \sin\omega t\,. \end{aligned} \tag{2.6}$$

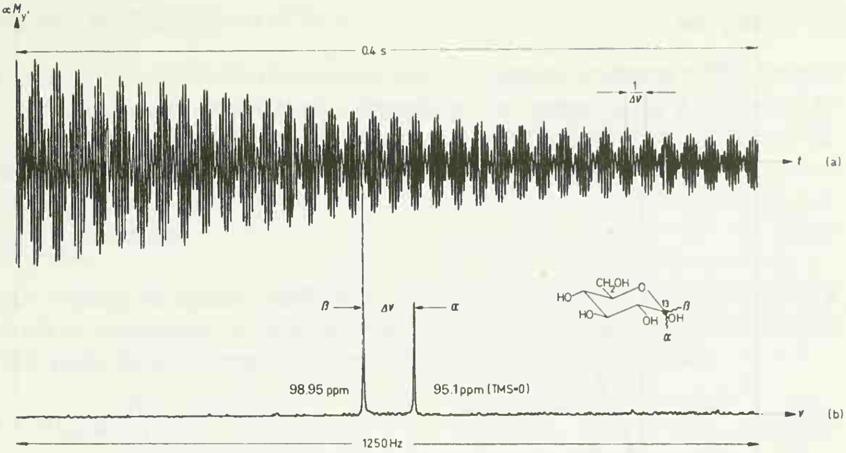

Fig. 2.3. (a) FID signal of mutarotated 1-^{13}C-D-glucose (60% ^{13}C); 22.63 MHz; 50 mg/ml deuterium-oxide; proton decoupled; 30 °C; pulse width adjusted for maximum signal (12 μs); observation time: 0.4 s; 32 accumulated scans;
(b) Fourier transform of (a); observed width: 1250 Hz; the distance between two beat maxima in (a) is about 0.0115 s; this corresponds to a chemical shift difference of about 87.5 Hz or 3.85 ppm at 22.63 MHz.

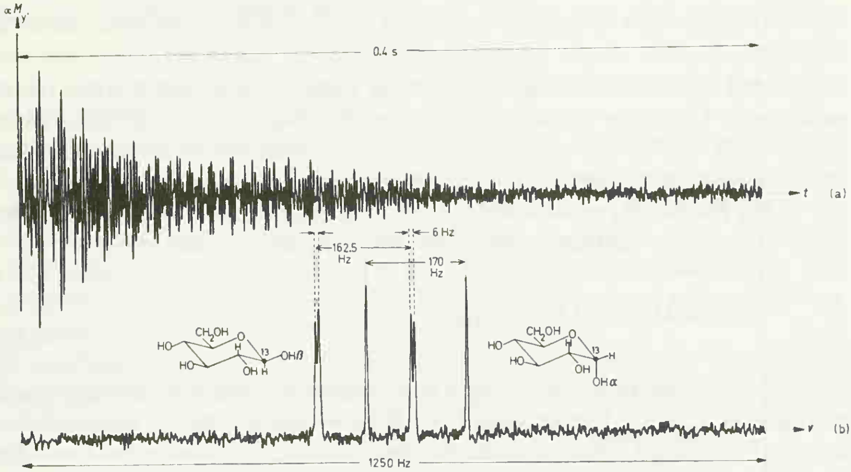

Fig. 2.4. (a) FID signal of mutarotated 1-^{13}C-D-glucose (60% ^{13}C); same sample and conditions as in Fig. 2.3, however without proton decoupling; (b) Fourier transform of (a).

In mathematical treatments of FID and NMR signals, F(t) and f(ω), it is convenient to use complex quantities. The time domain signal is then defined by eq. (2.7).

$$\mathrm{F}(t) = v(t) + \mathrm{i}\,u(t) \quad \text{where} \quad \mathrm{i} = \pm\sqrt{-1}\,. \tag{2.7}$$

Combining eq. (2.6) and (2.7) yields

$$\mathrm{F}(t) = M_0 \sin\Theta\,(\cos\omega t + \mathrm{i}\sin\omega t) \tag{2.8}$$

or, recalling that

$$e^{i\omega t} = \cos \omega t + i \sin \omega t\,, \tag{2.9}$$

$$F(t) = M_0 \sin \Theta e^{i\omega t}\,. \tag{2.10}$$

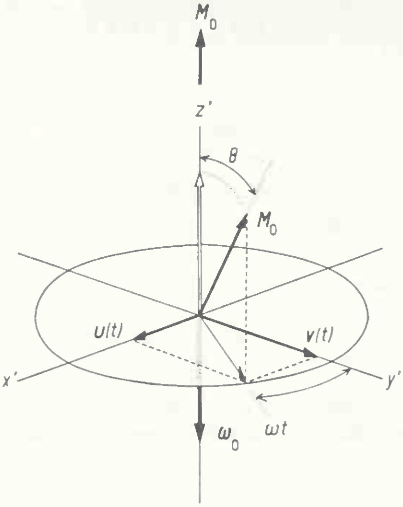

Fig. 2.5. The components $v(t)$ and $u(t)$ of the transverse magnetization in the rotating frame of reference for the off-resonance case ($\omega_1 - \omega_0 = \omega \neq 0$).

Since NMR spectra are not sequences of lines representing discrete Larmor frequencies but sequences of Lorentzian frequency distributions f(ω) (Fig. 1.9), eq. (2.10) must be replaced by eq. (2.11): $M_0 \sin \Theta e^{i\omega t}$ is multiplied by the frequency function f(ω), where ω represents the difference between the frequency ω_1 and the Larmor frequency distribution $\omega_0 + \Delta\omega$, $\omega = \omega_1 - (\omega_0 + \Delta\omega)$. Further, $M_0 \sin \Theta f(\omega) e^{i\omega t}$ must be integrated over the Larmor frequency distribution. Given a Lorentzian line shape as in Fig. 1.9, the limits of integration are ± ∞:

$$F(t) = M_0 \sin \Theta \int_{-\infty}^{+\infty} f(\omega) e^{i\omega t} \, d\omega\,. \tag{2.11}$$

Eq. (2.11) can be solved by developing it as a complex series of sines and cosines according to relation (2.9). This is a Fourier series [14]. Thus, we can say that an exponential in the time domain, F(t), and a Lorentzian in the frequency domain, f(ω), are Fourier transforms of each other [15–17].

2.5.2. Acquisition of Pulse Interferograms for Fourier Transformation

2.5.2.1. Digitization

Fourier transformations of pulse interferograms are normally performed in digital computers. Consequently, the FID analog signal must pass an analog to digital converter. The pulse interferogram is then recorded digitally as a series of several thousand (N) data points. Adjusted to the memory structure of digital computers, N is usually a power of 2, *e.g.* $2^{12} = 4096$ or 4"K".

2.5.2.2. Dwell Time and Pulse Interval

The sampling time during which FID data points must be collected in order to obtain the true NMR spectrum after Fourier transformation depends on the spectral width Δ. According to information theory [18], the sweep time per data point, called the dwell time t_{dw}, must satisfy the minimum given by the Nyquist equation (2.12).

$$t_{\mathrm{dw}} \leqq \frac{1}{2\Delta} \quad \text{s/point}\,. \tag{2.12}$$

Following this relation, the spectral width of $\Delta = 5\,\mathrm{kHz}$ often used in ^{13}C NMR requires a dwell time of 100 μs. Multiplying the dwell time with the number of data points N to be collected during the FID yields the time τ required for recording the interferogram digitally.

$$\tau = N t_{\mathrm{dw}} \leqq \frac{N}{2\Delta}\,. \tag{2.13}$$

When several pulse interferograms must be accumulated in order to improve the signal : noise ratio, τ is the minimum repetition time between two pulses or the minimum pulse interval.

2.5.2.3. Filtering of Frequencies Outside of the Spectral Width

Sometimes, Larmor frequencies not included in Δ contribute to the FID signal. This is the case particularly when only partial spectra are desired. All frequencies outside of the spectral width given by eq. (2.12) at a certain dwell time are "folded back" within the range Δ of the Fourier transformed FID. This is also true for high and low frequency noise.

Folding back of frequencies is illustrated in Fig. 2.6 for three sine waves arising from the frequencies Δ, $\Delta + \nu$, and $\Delta - \nu$. During the dwell time t_{dw}, the frequency Δ is sampled twice per cycle according to eq. (2.12). The lower frequency, $\Delta - \nu$, is sampled more, the higher one, $\Delta + \nu$, less than twice per cycle. The digital values of lower and higher frequency, however, are exactly equal (Fig. 2.6), so that both frequencies, $\Delta + \nu$, and $\Delta - \nu$, are undistinguishable digitally. After Fourier transformation, the higher frequency $\Delta + \nu$ behaves as if it had been being folded back onto the frequency $\Delta - \nu$.

In order to avoid folding back in PFT NMR spectra, frequency components higher than Δ must be filtered before digitization.

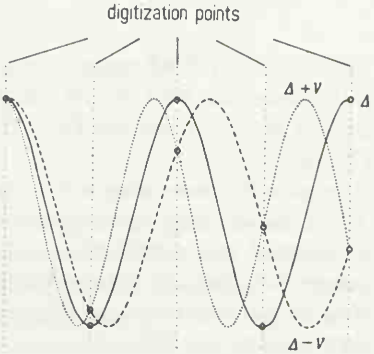

Fig. 2.6. "Folding back": At a sampling time given by the spectral width Δ (Hz) and the number of data points N, $\tau = N/2\Delta$, two frequencies higher and lower than Δ, $\Delta + \nu$ and $\Delta - \nu$, have identical digital values. The higher frequency is folded back on the lower one on Fourier transformation.

2.5.3. Optimization of Pulse Interferograms for Fourier Transformation

2.5.3.1. Adjustment of Pulse Frequency

The frequency of the rf pulse must be outside of the Larmor frequency range to be observed as indicated in Fig. 2.7. This requirement is due to the experimental arrangement, which measures frequency differences relative to the rf field using phase sensitive detectors. Positive and negative frequencies relative to the irradiating frequency cannot be distinguished in the FID. Fourier transformation of an interferogram obtained by an rf pulse of frequency ν_1' which is within the spectral width Δ yields a distorted NMR spectrum in which the frequencies on both sides of the irradiating pulse overlap.

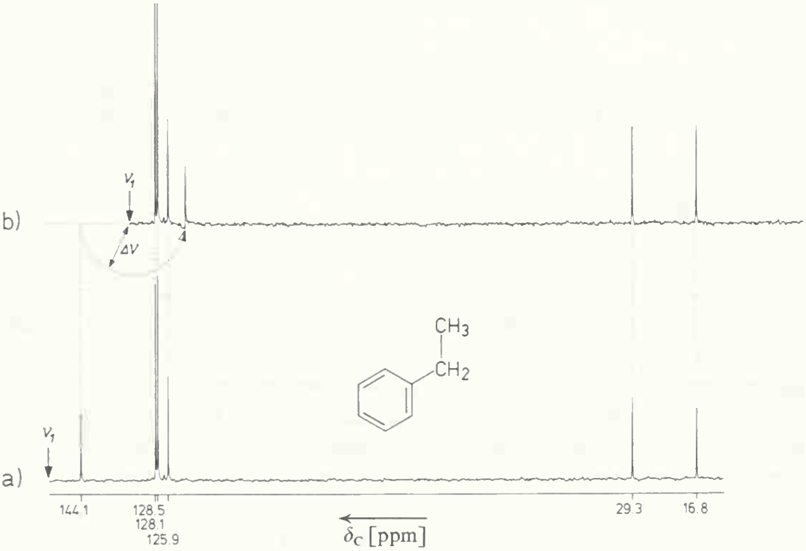

Fig. 2.7. Correct adjustment of the pulse frequency offset ν_1 (a) and maladjustment (b). In (b) the signal at 144.1 ppm is folded to $\delta < 125$ ppm. Sample: 90% ethylbenzene in hexadeuteriobenzene at 20 MHz; single scan experiments with 90° pulses.

For routine PFT NMR measurements, the pulse frequency is adjusted by changing the frequency of the transmitter until the CW spectrum of a reference sample with signals at both ends of the spectral width (*e.g.* acetone, Fig. 1.10) is reproduced exactly by Fourier transformation of the FID signal.

If the pulse frequency offset is chosen in the center of the Larmor frequency range Δ, both halves $\Delta/2$ of the spectrum are sampled simultaneously and folded into each other. Folding can be corrected by a modification of the Fourier transformation software and hardware. Simultaneous sampling and folding of both halves, however, makes up a signal: noise enhancement of up to $\sqrt{2}$ (about 40%) as illustrated in Fig. 2.14. This is the concept of *d*igital *q*uadrature *d*etection (DQD or QD).

2.5.3.2. Adjustment of Pulse Width

For a maximum FID signal the pulse width t_p must be adjusted for a 90° pulse according to eq. (2.2), so that $\gamma H_1 t_p = \pi/2$. This is usually achieved by displaying the pulse interferogram of a reference sample on an oscilloscope and changing the pulse width t_p until the maximum FID signals is observed. For further examination, the 90° pulse width found in this manner is doubled (180° pulse), and no signal should be observed for a correct adjustment. More conveniently, the 90° pulse can be determined by a computer controlled series of PFT spectra with varying pulse width as is illustrated in Fig. 2.8 for the ^{13}C-^{1}H quartet of methanol.

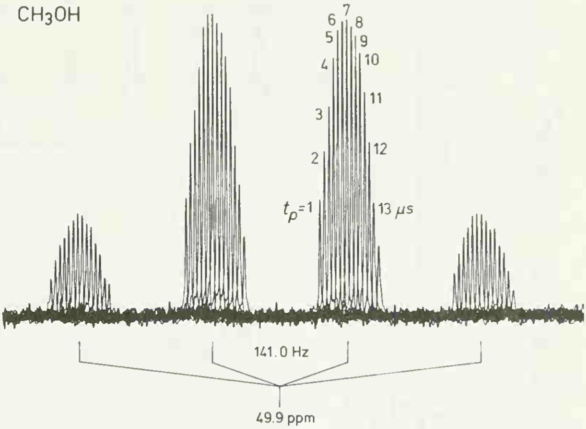

Fig. 2.8. Adjustment of the 90° pulse width; sample: methanol, 80 Vol. % in deuterium oxide at 30°C and 20 MHz; computer controlled experiment with variable pulse width. The 90° pulse width is found to be 7 μs.

In order to rotate the magnetization vectors of all nuclear spins within the range of Larmor frequencies to be observed, the pulse must not only be adjusted for 90°, so that $\gamma H_1 t_p = \pi/2$ (eq. 1.41)), but must also be very strong, so that $\gamma H_1 \gg 2\pi\Delta$ (eq. (2.3)). These requirements give the relation between pulse width and spectral width:

$$t_p \ll \frac{1}{4\Delta} . \qquad (2.14)$$

Maximum FID signal for a large spectral width (*e.g.* $\Delta = 5$ kHz for ^{13}C) thus requires very short rf pulses (*e.g.* $t_p \ll 1/4 \cdot 5 \cdot 10^3 = 50\,\mu s$ for ^{13}C). Usually, square wave bursts of about 5 μs width are used in PFT ^{13}C NMR.

2.5.4. Data Transformation and Subsequent Manipulations

2.5.4.1. Fourier Transformation

Routine Fourier transformations of pulse interferograms are achieved in digital computers with a memory size of 4 – 64 K. According to eq. (2.9), a Fourier series of sines and cosines from eq. (2.11) is developed and transformation is computed for all data points of the FID signal. The transformation program makes use of the Cooley-Tukey algorithm [19, 20] which requires a minimum of time consuming multiplications and efficiently uses the computer memory. This computation is called the fast Fourier transformation (FFT) and requires less than one min for transforming an 8 K interferogram, depending on the speed of the computer.

The solution of eq. (2.11) is a complex function. FFT computation therefore yields both real and imaginary PFT NMR spectra, $v(\omega)$ and $i\,u(\omega)$, which are related to the absorption and dispersion modes of CW spectra. The two parts of the complex spectrum are usually stored in

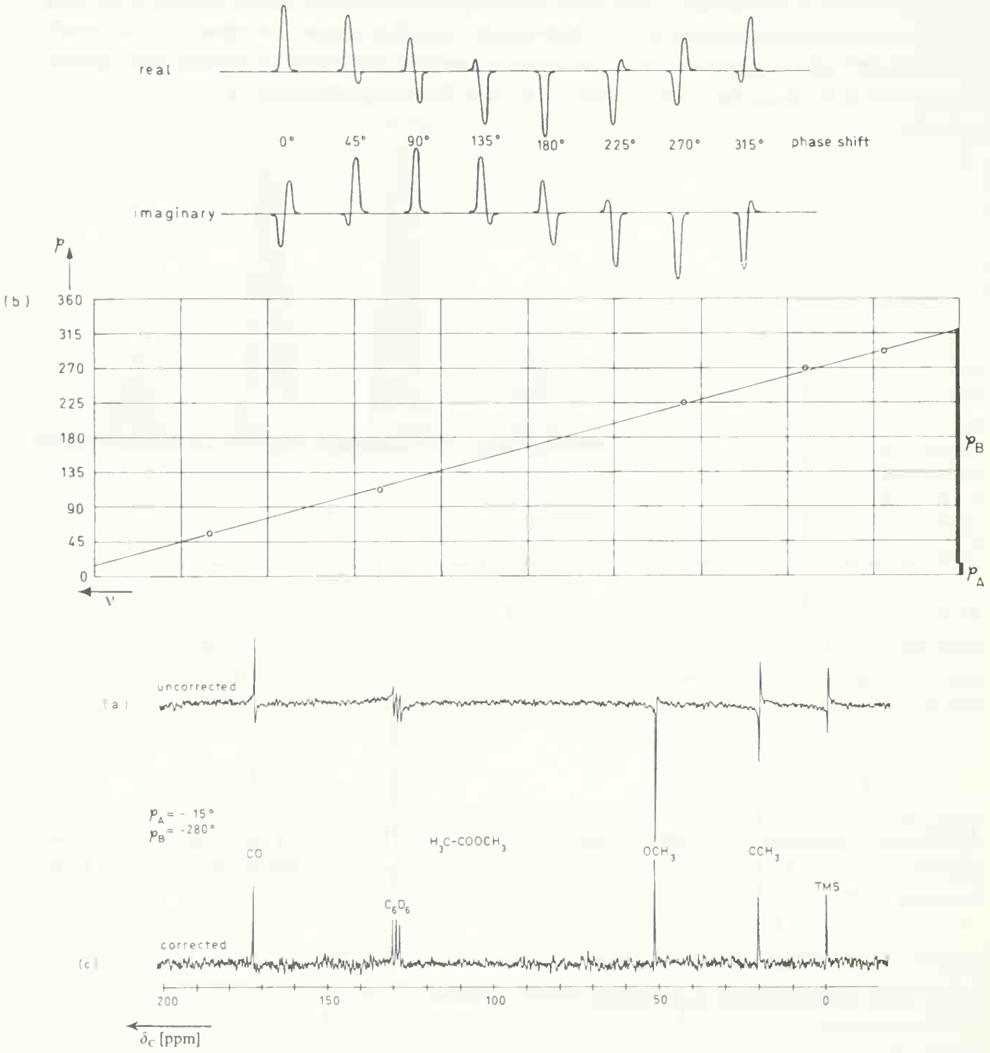

Fig. 2.9. (a, c) 22.63 MHz PFT $^{13}C\{^1H\}$ NMR spectrum of methyl acetate (20%) in hexadeuteriobenzene (75%) and tetramethylsilane (5%); 256 accumulated pulse interferograms;

(a) real part before phase correction;

(b) phase correction according to eq. (2.15), achieved by using the phase shifts indicated above; extrapolation of the linear plot $\varphi(\nu)$ yields $\varphi_A = +15°$ and $\varphi_B = +280°$; for correction, the signs have to be changed, thus $\varphi_A = -15°$ and $\varphi_B = -280°$;

(c) real part after phase correction according to (b).

different blocks of the memory and can be displayed on an oscilloscope to aid in further data manipulations.

2.5.4.2. Phase Correction

The real and imaginary spectra obtained by Fourier transformation of FID signals are usually mixtures of the absorption and dispersion modes as shown in Fig. 2.9(a). These phase errors

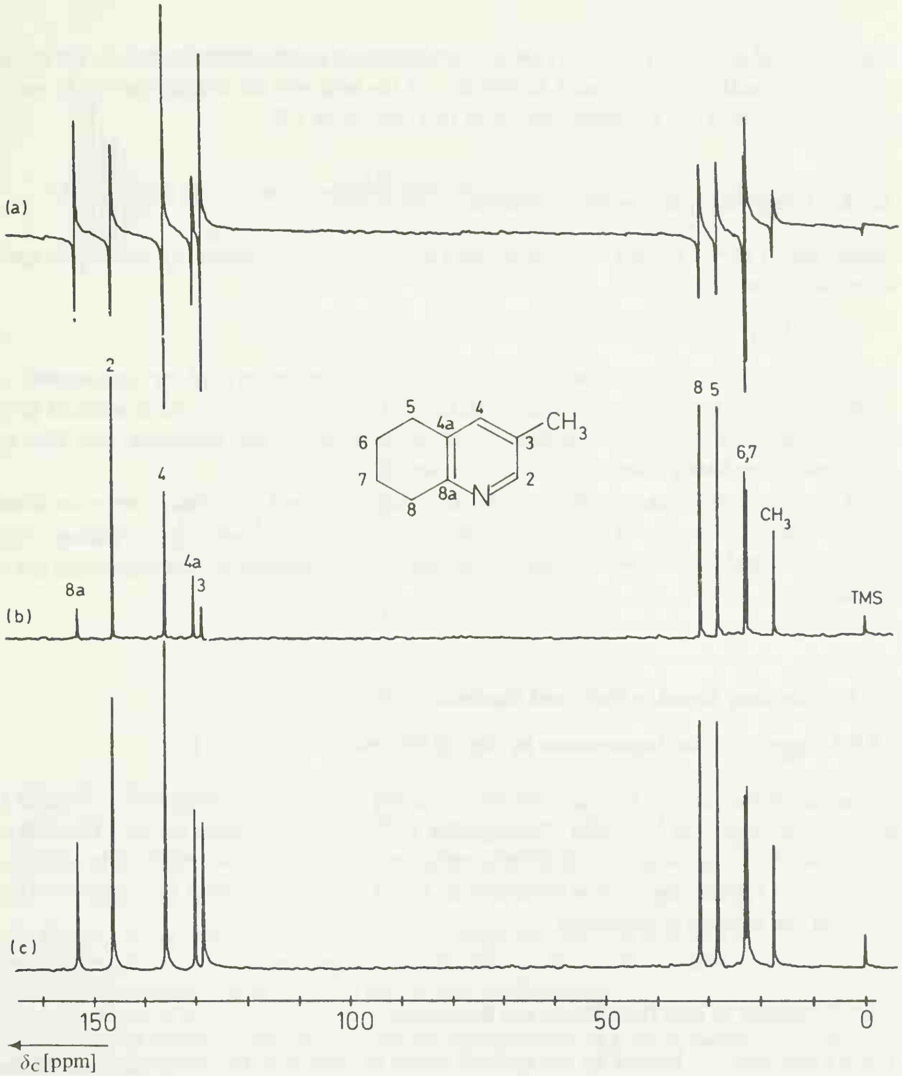

Fig. 2.10. 22.63 MHz PFT ^{13}C NMR spectra of 3-methyl-5,6,7,8-tetrahydroquinoline; 200 mg/ml deuteriochloroform; proton decoupled; 512 accumulated pulse interferograms; pulse width: 10 μs; pulse interval: 0.4 s;
(a) dispersion ($i \cdot u$) mode, phase corrected; (b) absorption (v) mode, phase corrected;
(c) magnitude ($\sqrt{v^2 + u^2}$) spectrum.

mainly arise from frequency independent maladjustments of the phase detector and from frequency dependent influences such as the finite length of rf pulses, delays in the start of data acquisition, and phase shifts induced by filtering frequencies outside the spectral width Δ.
One method of phase correction assumes a linear dependence of the phase φ on the frequency as in eq. (2.15); φ_A is the phase at frequency difference zero, φ_B is the phase shift across the total spectral width from zero to Δ Hz.

$$\varphi = \varphi_A + \varphi_B \nu . \tag{2.15}$$

Fig. 2.9(b,c) illustrates a phase correction. For correcting phase, either the real or the imaginary part of the spectrum can be used. Correction of the real part for absorption mode yields the dispersion mode in the imaginary part and *vice versa* (Fig. 2.9).

2.5.4.3. Computation of Magnitude Spectra

Magnitude or power spectra can be computed from the real and imaginary parts of the spectrum according to eq. (1.37).

$$\mathrm{P}(\nu) = \sqrt{[v(\nu)]^2 + [u(\nu)]^2} . \tag{1.43}$$

Due to the quadratic form of eq. (1.37), the magnitude spectrum is phase independent, and a manipulated signal : noise improvement relative to the pure u and v mode is attained (Fig. 2.9). If only magnitude information is desired, phase correction is not necessary, and P(ν) can be computed immediately after Fourier transformation.
Weak lines are sometimes more easily localized in dispersion and magnitude spectra, as illustrated in Fig. 2.10 (b, c). The signals of dispersion and magnitude spectra suffer from "tailing" (Fig. 2.10 (b, c)), and a weak line closely spaced to a strong one may be lost or distorted in the tail of the strong signal.

2.5.5. Controlling Signal to Noise and Resolution in PFT NMR

2.5.5.1. Signal to Noise Improvement by Digital Filtering

The signal : noise ratio or alternatively the resolution of the interferogram and its Fourier transform can be improved by digital filtering. This involves multiplication of the FID with an exponential $e^{\pm at}$ [21]. Negative values of at enhance the signal: noise ratio while causing some artificial line broadening. This is illustrated in Fig. 2.11. Positive values of at improve the resolution at the expense of sensitivity.

2.5.5.2. Number of FID Data Points and Resolution

For a dwell time t_{dw} limited by the spectral width according to eq. (2.12), the resolution $d\nu$ of a PFT NMR spectrum depends on the number N of data points constituting the digitized FID signal to be transformed:

$$d\nu = \frac{1}{N t_{dw}} = \frac{2\Delta}{N} \mathrm{Hz} . \tag{2.16}$$

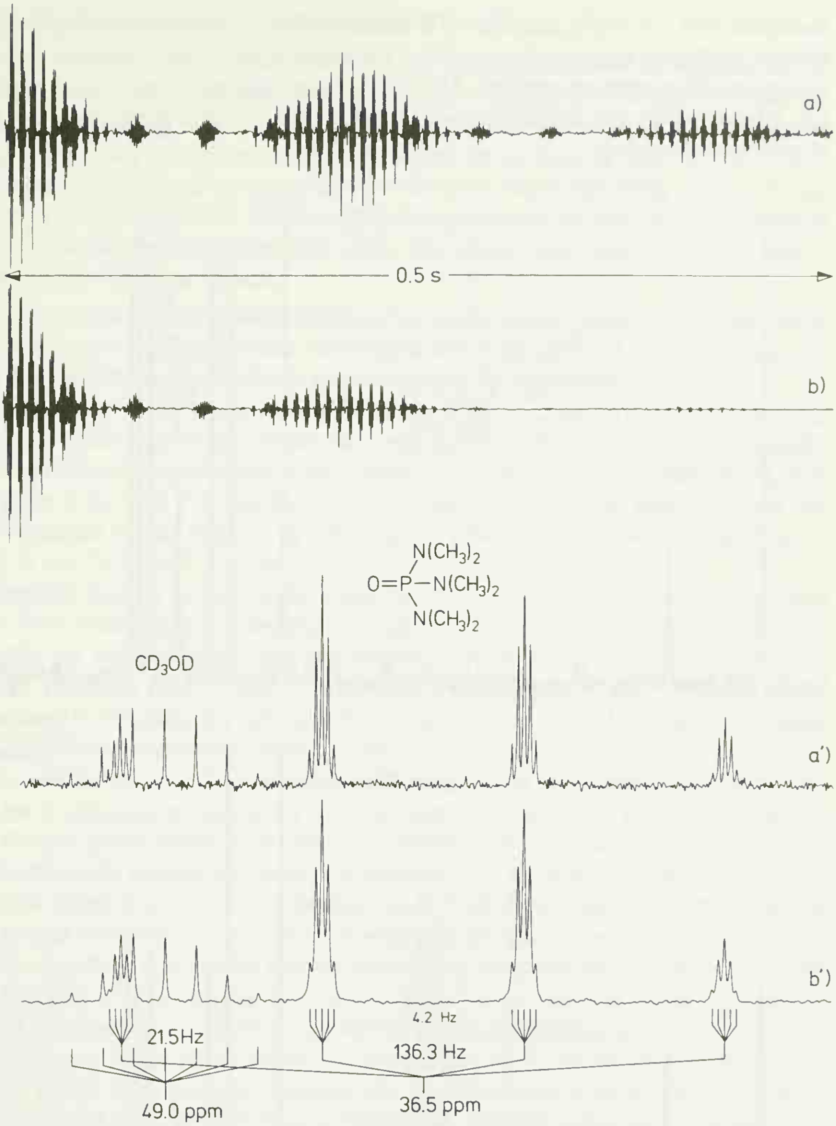

Fig. 2.11. Signal: noise enhancement by exponential multiplication on cost of resolution; sample: hexamethylphosphoramide (70%) in tetradeuteriomethanol (30%) at 30 °C and 15.08 MHz; coupled:
(a) 5000 accumulated interferograms without exponential multiplication;
(a′) Fourier transform of (a);
(b) 5000 accumulated interferograms with exponential multiplication for a line broadening of 1 Hz;
(b′) Fourier transform of (b).

If an 8 K interferogram (8192 points) is transformed, the resolution is $d\nu = 1.22$ Hz for a spectral width of 5 kHz. In the Fourier transform of a 2 K interferogram (2048 points) resolution is reduced to $d\nu = 4.88$ Hz. This is illustrated by Fig. 2.12, which shows the proton broad band decoupled PFT ^{13}C NMR spectrum of D-galactose. This carbohydrate with six non-equivalent carbons undergoes mutarotation in water. The equilibrium mixture contains two anomers so that twelve ^{13}C signals are expected. All 12 signals are observed in the Fourier transform of the 8 K interferogram; the spectrum arising from the 2 K interferogram, however, shows only 10 well resolved signals.

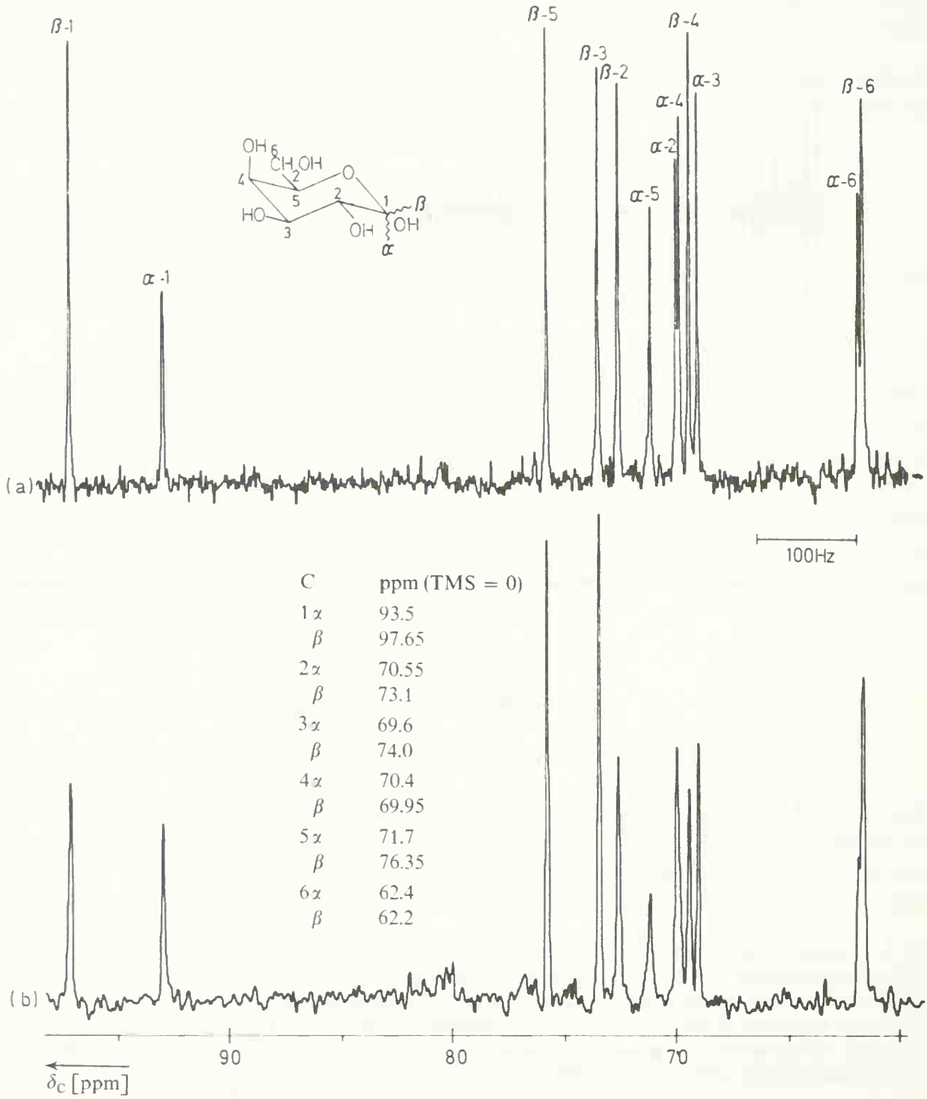

C	ppm (TMS = 0)
1α	93.5
β	97.65
2α	70.55
β	73.1
3α	69.6
β	74.0
4α	70.4
β	69.95
5α	71.7
β	76.35
6α	62.4
β	62.2

Fig. 2.12. Phase corrected 22.63 MHz PFT ^{13}C NMR spectrum of mutarotated D-galactose; 100 mg/ml deuteriumoxide; 30 °C; proton decoupled; 512 accumulated pulse interferograms;
(a) obtained from an 8 K interferogram (pulse interval: 0.8 s);
(b) obtained from a 2 K interferogram (pulse interval: 0.2 s).

2.5.6. Spin-Lattice Relaxation and Signal to Noise in PFT NMR

For signal : noise improvement of weak samples, pulse interferograms are accumulated by the CAT method before Fourier transformation. According to eq. (2.13), the minimum repetition time of an 8 K ^{13}C interferogram at a spectral width of 5 kHz is $\tau = 0.82$ s. Spin-lattice relaxation times of some ^{13}C nuclei such as quaternary ^{13}C atoms are as large as 100 s, so that $T_1 \gg \tau$. These nuclei cannot relax within the pulse interval τ. Using the Bloch equations, it can be shown, that a stationary state is reached in this case [22]; the equilibrium magnetization is attenuated and the signal strength depends on the ratio $\tau/2T_1$. The signal : noise ratio of the FID and its Fourier transform decreases as a result.

An obvious way to avoid signal : noise attenuation for slowly relaxing carbons is to add a delay time to the pulse interval. This delay time should be at least in the order of $3T_1$. However, accumulation of pulse interferograms becomes time consuming by this method.

A more practicable way [17] is to decrease the flip angle of $\boldsymbol{M}_0$ to a value of $\Theta < 90°$ by reducing the pulse width. Restoration of the equilibrium magnetization then requires shorter periods. However, the transverse magnetization is also decreased by reducing Θ according to eq. (2.2). The signal : noise of the total FID and its Fourier transform decreases. The best way to use this method is to optimize the flip angle Θ by adjusting the pulse width for optimum signal : noise of all signals in the PFT NMR spectrum.

The third method involves a three pulse sequence, $90° - \tau - 180° - \tau - 90°$ with a repetition time of t_r s. This pulse sequence refocuses the magnetization vector $\boldsymbol{M}_0$ into its equilibrium position within the repetition time, thus representing a pulse driven relaxation acceleration. The technique, known as DEFT NMR [23, 24] (driven equilibrium Fourier transform NMR) can be understood by following the behavior of the magnetization vector $\boldsymbol{M}_0$ under the influence of the pulse sequence in the rotating frame of reference (Fig. 2.13(a – e)).

Starting with equilibrium of nuclear spins (a), a 90° pulse rotates the magnetization vector $\boldsymbol{M}_0$ by 90° (b). Due to spin-spin relaxation, the spins dephase in (c), causing an FID signal. The 180° pulse turns the spin system towards the negative y' axis (d). The spins then refocuse, because the sign of dephasing in (c) remains the same. The inverted FID signal is produced as seen in (g) and a spin echo arises in (e) which may dephase again. Following a subsequent 90° pulse, the spin system returns to equilibrium (a). The pulse sequence can then be repeated for accumulation of FID signals. Fig. 2.13 (g) illustrates a driven equilibrium interferogram in comparison to the FID signal following a 90° pulse (Fig. 2.13 (f)); reduction in signal : noise is shown to be less for the sequenced FID than for the single 90° pulse FID during accumulation.

The repetition time t_r of the pulse sequence is independent of T_1, which may be different for non-equivalent nuclei. The optimum repetition time has been found to be $t_r = 4\tau$ [22]. DEFT NMR requires careful adjustment of pulse widths for 90° and 180° pulses and (computer controlled) pulse programming for accurate timing between pulses and pulse sequences. Other methods for improving signal : noise using other pulse sequences and spin echo trains have been described [22, 25]. DEFT NMR, however, appears to be the most efficient method so far as long as T_1 and T_2 are of the same order of magnitude.

2.5.7. Comparison between CW and PFT

As any time domain function F(t), a square wave rf pulse of width t_p can be approximated by a Fourier series of sines and cosines with frequencies $n/2t_p$ ($n = 1, 2, 3, 4, 5, \ldots$) [14, 7]. An rf pulse of

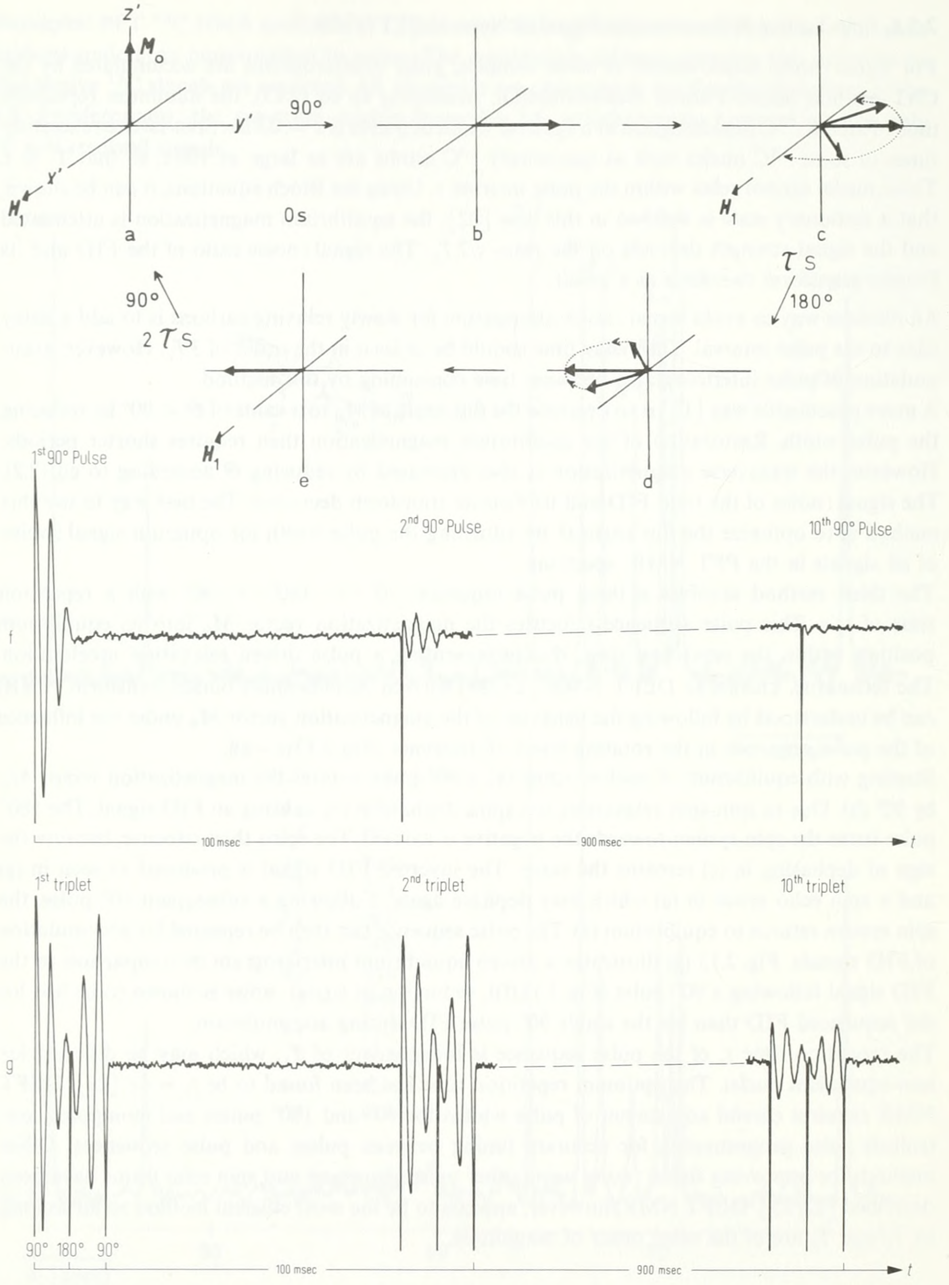
z'
M$_o$
y'
x'
H$_1$
90°
0s
a
b
c
H$_1$
τ S
180°
90°
2 τ S
H$_1$
e
d
1st 90° Pulse
2nd 90° Pulse
10th 90° Pulse
f
100 msec
900 msec
t
1st triplet
2nd triplet
10th triplet
g
90° 180° 90°
100 msec
900 msec
t

Fig. 2.13. Driven equilibrium FID; (a) – (b) – (c) – (d) – (e) – (a): the sample magnetization following a 90°, τ, 180°, τ, 90° pulse sequence; (f) and (g): comparison between the FID signals following repetitive 90° pulses and those following repetitive 90°, τ, 180°, τ 90° pulse sequences; example: ^{13}C FID of ^{13}enriched carbon tetrachloride, $^{13}CCl_4$.
(f) and (g) recorded by B. Knüttel, Bruker Physik AG, Karlsruhe-Forchheim, Germany.

width t_p thus simulates a multifrequency transmitter of frequency range $\Delta = 1/4t_p$ (eq. (2.14)). Following this consideration, an rf pulse of 250 µs simultaneously rotates the M_0 vectors of all Larmor frequencies within a range of at least $\Delta = 1$ kHz. It simulates at least 1000 simultaneously stimulating transmitters, the resolution in the Fourier transform depending on the number of FID data points (eq. (2.16)), not the stimulation time t_p.

During the 250 µs needed to stimulate the Larmor frequencies within a range of 1 kHz by a single rf pulse, only $0.5 \cdot 10^{-6}$ of a 1 kHz scan is stimulated in a CW experiment using a 500 s/1 kHz sweep. A more realistic comparison accounts for the time required for Fourier transformation: NMR information at a spectral width of 1 kHz can be obtained

(1) in 10–25 s by Fourier transformation of a 2 K interferogram,
(2) in 500 s by a CW experiment, using a sweep of 1 kHz/500 s.

Furthermore, in the 500 s required for sweeping a 1 kHz spectrum, at least 1000 2 K interferograms can be accumulated before being Fourier transformed. The signal : noise of the PFT NMR spectrum is thus increased by a factor of $10\sqrt{10}$ according to eq. (2.1).

In summary, PFT NMR is much more sensitive for equivalent measuring times and much less time consuming for equivalent signal : noise ratios in comparison to CW NMR. For illustration, the proton decoupled ^{13}C NMR spectra of quinoline, obtained from one CW scan and one pulse, respectively, are compared in Fig. 2.14. A further signal:noice enhancement of up to 40% arises from application of the QD technique outlined in section 2.5.3.1 (Fig. 2.14 (c)).

In requiring less measuring time and producing higher sensitivity in comparison to CW, PFT NMR follows the Fellgett principle [26, 27]: The signal : noise of any spectroscopic experiment increases if simultaneous multichannel excitation is applied. In the PFT technique, rf pulses simulate multichannel transmitters. If m transmitters stimulate simultaneously, the enhancement factor relative to one channel excitation ($m = 1$) is the square root of m (eq. (2.17), [26, 27]).

$$(S:N)_m = (S:N)_1 \sqrt{m} . \tag{2.17}$$

The minimum number of simultaneously exciting channels m required for resolving a spectrum of width Δ at a resolution $\mathrm{d}\nu$, limited by natural line width and field inhomogeneity, is

$$m = \frac{\Delta}{\mathrm{d}\nu} . \tag{2.18}$$

In addition, the resolution of a PFT NMR spectrum is governed by eq. (2.16), *i.e.*

$$\mathrm{d}\nu = \frac{2\Delta}{N} . \tag{2.16}$$

The number of simultaneously stimulating channels simulated by an rf pulse is therefore

$$m = \frac{N}{2} , \tag{2.19}$$

which depends only on the computer memory size and yields an enhancement factor of $\sqrt{N/2}$ according to eq. (2.17). Thus, according to the Fellgett principle, a PFT NMR spectrum obtained from an 8 K interferogram is expected to show a signal : noise enhancement factor of $\sqrt{4096} = 64$ relative to a CW spectrum of equal width, resolution, and measuring time.

Due to its greatly enhanced sensitivity in comparison to CW NMR, the PFT method has made ^{13}C NMR into a routine method of structure analysis for all molecules having the natural ^{13}C

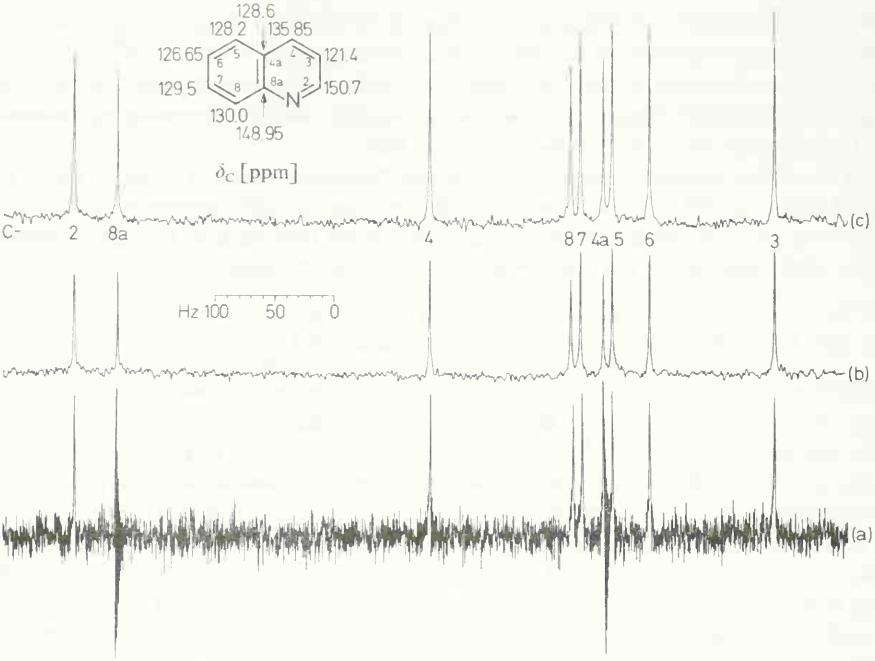

Fig. 2.14. 22.63 MHz $^{13}C\{^1H\}$ NMR spectrum of quinoline (70%) in hexadeuterioacetone (30%) at 25 °C; single scan experiments;
(a) CW spectrum; sweep: 1 Hz/s; spectral width: 1000 Hz; measuring time: 1000 s;
(b) PFT spectrum, obtained from one 90° pulse interferogram after Fourier transformation and phase correction;
(c) PFT spectrum, obtained as in (b), however using the quadrature detection technique.
The measuring and calculation time (Fourier transformation and phase correction for the 8 K interferogram/4 K spectrum) was less than 100 s in (b) and (c).

abundance of 1.1 %. Additionally, phase corrected PFT NMR spectra contain all spectral details without the lineskewing and ringing observed in CW spectra. Finally, short lived molecules can be measured by PFT NMR, and sensitivity enhancement by accumulation of interferograms before Fourier transformation requires much less time than the accumulation of CW NMR spectra due to the small time required for acquisition of FID signals.

2.6. Double Resonance Techniques used in ^{13}C NMR as Assignment Aids

2.6.1. The Basic Concept of Spin Decoupling

As was illustrated for the methyl and carbonyl signals in the ^{13}C NMR spectrum of acetone (Fig. 1.10), $^{13}C-^1H$ spin-spin coupling vanishes when proton broad band decoupling is applied. Proton broad band decoupling is the most important decoupling technique used in routine

^{13}C NMR, simplifying ^{13}C$-^{1}$H multiplet systems to spectra of up to z singlet lines for z non-equivalent ^{13}C nuclei of a sample.

Spin decoupling or nuclear magnetic double resonance (NMDR) is achieved by irradiating an ensemble of nuclei not only with a radio-frequency H_1 at resonance with the nuclei to be observed but additionally with a second alternating field H_2 at resonance with the nuclei to be decoupled (*e.g.* ^{1}H). Decoupling experiments can be carried out to convert homonuclear (^{1}H$-^{1}$H, ^{19}F$-^{19}$F) or heteronuclear multiplets (^{19}F$-^{1}$H, ^{13}C$-^{1}$H) into singlets. NMDR spectra are often symbolized by putting the nuclei to be decoupled between brackets beside the nuclei to be observed: A{X}. Proton decoupled ^{13}C NMR experiments are thus referred to as ^{13}C{^{1}H} NMR spectra.

Collapsing of spin multiplets AX$_n$ (Fig. 1.10(b) → Fig. 1.10(a)) by NMDR can be explained using a frame of reference rotating at the angular velocity $\omega_2 = 2\pi\nu_2$ of the irradiating radiofrequency H_2. The effective field, which causes precession of the magnetization vectors, is then given by eq. (1.32).

$$H_{\text{eff}} = H_0 + \frac{\omega_2}{\gamma} + H_2\,. \tag{1.32}$$

If H_2 is applied at resonance with the nuclei X to be decoupled, ω_2/γ cancels H_0 so that $H_{\text{eff}} = H_2$ according to eq. (1.33). As a result, the magnetization vectors of the irradiated nuclei X precess perpendicular to H_0. Now, the irradiated nuclei X have their spins quantized perpendicularly to H_0 while the spins of the observed nuclei A are still quantized along H_0. Since the observed coupling between nuclei A and X is the scalar product of the spin quantizations I_{A} and I_{X} [28–30], the observed coupling is related to the angle α enclosed by the spin quantizations I_{A} and I_{X}.

$$J_{\text{AX(obs)}} \propto \cos\alpha\,. \tag{2.20}$$

The observed splitting $J_{\text{AX(obs)}}$ is equal to the coupling constant J_{AX} when both spins A and X are quantized in the same direction ($\alpha = 0°$, $\cos\alpha = 1$, NMR, coupled). Coupling between A and X collapses ($J_{\text{AX(obs)}} = 0$), however, when the spins A and X are quantized perpendicularly to each other ($\alpha = 90°$, $\cos\alpha = 0$, NMDR, decoupled).

Another explanation of spin decoupling assumes that the perturbing field H_2 induces rapid transitions between the spin levels of the irradiated nuclei X. The lifetime t_x of X in its spin states is then short compared to the reciprocal coupling constant, so that the condition for spin-spin coupling,

$$t_x \geqq \frac{1}{J_{\text{AX}}} \tag{2.21}$$

is not met anymore and no coupling is observed [28, 29]. Decoupling of A$_m$X$_n$ systems cannot be considered as to arise from saturation of the transitions of one nucleus since decoupling fields are much stronger than saturating fields (see eq. (2.22)).

2.6.2. Proton Broad Band Decoupling in ^{13}C NMR

In a ^{13}C{^{1}H} experiment, a ^{13}C$-^{1}$H multiplet can be selectively decoupled by an H_2 field whose frequency matches the Larmor frequency of the coupling protons. In routine ^{13}C NMR, however, usually all ^{13}C$-^{1}$H multiplets are decoupled for sensitivity and simplicity reasons. This is achieved when the decoupling field H_2 covers the range of all proton Larmor frequencies. For the protons in organic compounds in a magnetic field H_0 of 2.3 Tesla this is at least 1 kHz at about 90 MHz. Decoupling fields with large frequency ranges can be realized either by a very large rf power H_2 so that

$$\frac{\gamma_X H_2}{2\pi} \geqq \Delta_X = 1\ \text{kHz for } {}^1\text{H} . \tag{2.22}$$

or by modulation of the decoupling frequency by an audio-frequency [31] or white noise [32]. Modulation of the decoupling frequency distributes the rf power among the center band (*e.g.* 90 MHz) and numerous sidebands (*e.g.* 90 MHz ± 10, ± 20, ± 30, ± 40, ± 50 Hz etc.), with the spacing given by the modulation frequency (*e.g.* 10 Hz). Decoupling frequency bands of several kHz width are attainable by noise modulation. This is much greater than the range of the normal frequency distribution for protons according to eq. (2.22).

Double resonance techniques using large, noise modulated frequency bands are referred to as broad band or noise decoupling. Decoupling frequency bands covering the range of all proton Larmor frequencies cause all $^{13}C-^{1}H$ multiplets to collapse. Examples of PFT $^{13}C\{^{1}H\}$ spectra obtained by high power broad band decoupling are shown in Figs. 1.10 (a), 2.3 (b), 2.7, 2.9, 2.10, 2.12, and 2.14. Low power proton noise decoupling broadens the signals of proton coupled carbons, leaving only non-coupled ones with significant signal : noise. This is an aid in assigning quaternary carbons as shown in Fig. 2.15 for colchicine.

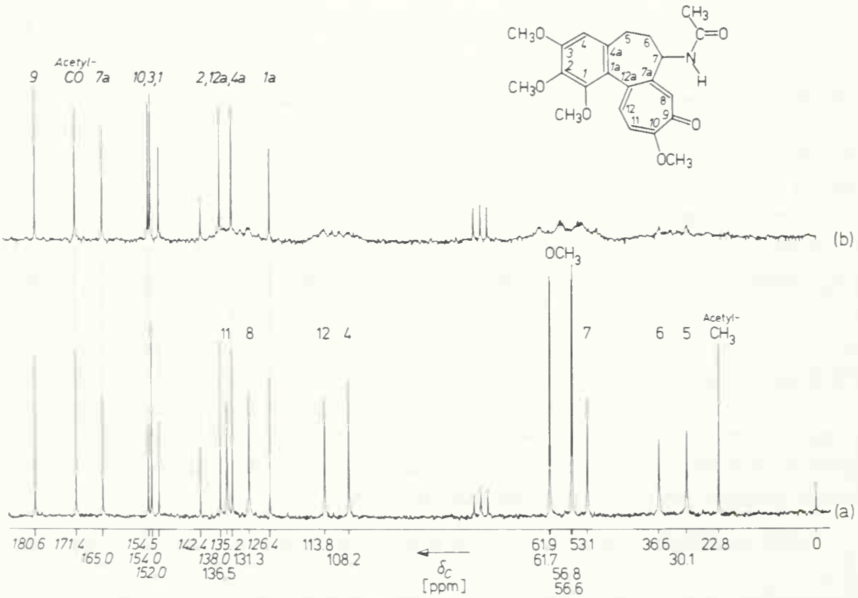

Fig. 2.15. Proton decoupled ^{13}C NMR spectra of colchicine, 150 mg in 1 ml deuteriochloroform, 20 MHz, 25 °C, 2000 scans;
(a) high power noise decoupled, ^{1}H decoupling frequency at 4 ppm;
(b) low power noise decoupled, ^{1}H decoupling frequency at 14 ppm, for localization of quaternary carbons *(italic type)* in the spectrum.

2.6.3. The Nuclear Overhauser Effect in $^{13}C\{^1H\}$ NMR

Decoupling increases the sensitivity of NMR measurements because the intensities of all multiplet lines in a coupled spectrum are accumulated in one singlet signal in the decoupled spectrum. Thus the ^{13}C signal intensity in a $^{13}C\{^1H\}$ experiment on formic acid should be twice the intensity of one doublet line in the coupled ^{13}C spectrum. However, as demonstrated in Fig. 2.16, the intensity of the ^{13}C signal of formic acid increases much more than twice upon proton decoupling [33]. This additional sensitivity enhancement achieved during decoupling is attributed to the nuclear Overhauser effect (NOE) [34].

The nuclear Overhauser effect observed in $^{13}C\{^1H\}$ experiments arises from an intramolecular dipole-dipole relaxation mechanism. Any nucleus with spin is a magnetic dipole. Two such nuclei A and X (*e.g.* ^{13}C and ^1H) in a molecule having intermolecular and intramolecular mobility (translations, vibrations, rotations) give rise to fluctuating magnetic fields. Energy transfers between A and X may occur *via* these fluctuating fields. In an A{X} experiment, the transitions of nuclei X are irradiated while the resonance of nuclei A is observed. Since the irradiating field is very strong (eq. (2.22)), the homonuclear relaxation processes are not adequate to restore the equilibrium population of the nuclei X: The nuclei X transfer their energy to the nuclei A *via* internuclear dipole-dipole interaction. The nuclei A, receiving these transferred amounts of energy, behave as if they had been irradiated themselves and relax. By way of this additional heteronuclear relaxation processes of the nuclei A, induced by double resonance, the population of the lower A level increases. As a result, the intensity of the A signal is enhanced.

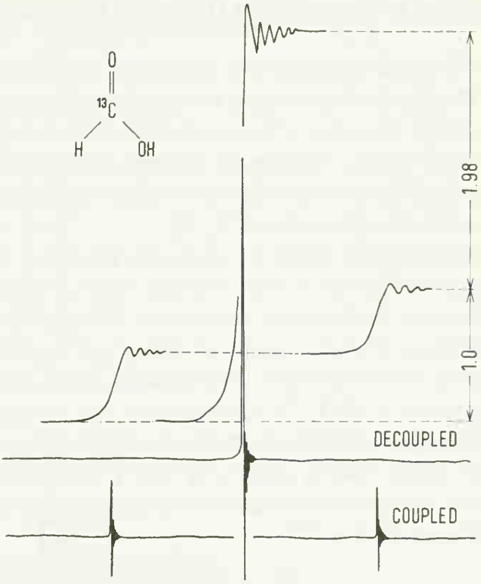

Fig. 2.16. Nuclear Overhauser effect observed on proton broad band decoupling of ^{13}C enriched formic acid [33]. (Reproduced by permission of the copyright owner from K.F. Kuhlmann and D. M. Grant, J. Amer. Chem. Soc. *90*, 7355 (1968).)

The maximum NOE enhancement factor f_A (X) observable for the A signal in an A{X} experiment mainly depends on the gyromagnetic ratios of A and X if the A nuclei are predominantly relaxed by an intramolecular dipole-dipole mechanism during irradiation of the X nuclei [34].

$$f_A(X) = \frac{\gamma_X}{2\gamma_A}. \qquad (2.23)$$

Using the gyromagnetic ratios of ^{13}C and ^{1}H, $\gamma_{^{13}C} = 6.726$ and $\gamma_{^{1}H} = 26.752$ rad s^{-1} $gauss^{-1}$, the maximum NOE enhancement factor observable in $^{13}C\{^{1}H\}$ spectra is almost 2 in good agreement with measurements (Fig. 2.16) [33].

$$f_{^{13}C}(^{1}H) = 1.988 \quad [34].$$

In summary, NOE sensitivity enhancements are attained in heteronuclear NMDR when the nucleus with low γ is observed while the nucleus with high γ is decoupled. On the other hand, negligible enhancement of ^{1}H NMR sensitivity can be expected from $^{1}H\{^{13}C\}$ experiments, the enhancement factor being only $f_{^{1}H}(^{13}C) = 0.126$ [34].

2.6.4. Quenching Nuclear Overhauser Effects in $^{13}C\{^{1}H\}$ NMR

^{13}C signal intensities are affected to varying extends in $^{13}C\{^{1}H\}$ NMR spectra due to NOE. The signals of quaternary carbons are weak, those of coupled carbons (CH, CH_2, CH_3) are very strong. The ratio of non-equivalent carbons cannot be determined by integration of $^{13}C\{^{1}H\}$ NMR spectra. This can be achieved, however, by adding small amounts of paramagnetic compounds such as *tert*-butyl nitroxide, cobalt(II)-acetate, copper(II)- and iron(III)-acetylacetonate to the sample solution [37, 38].

Paramagnetic additives accelerate relaxation by way of dipole-dipole interaction between unpaired electrons and magnetic nuclei. The internuclear $^{13}C-^{1}H$ dipole-dipole mechanism does not predominate anymore in ^{13}C and ^{1}H relaxation during $^{13}C\{^{1}H\}$ experiments in the presence of paramagnetic additives, and nuclear Overhauser effects are reduced. Signal intensities are decontrasted. Additionally, signal : noise enhancements for slowly relaxing nuclei are achieved in PFT ^{13}C measurements due to acceleration of relaxation. Paramagnetic additives in sample solutions are in this sense experimental alternatives to the signal : noise improvement of slowly relaxing carbons by DEFT (Section 2.5.6) [38]. Pseudo-contact and contact shifts as well as line broadenings are negligible as long as the concentrations of the paramagnetic substances are low [38].

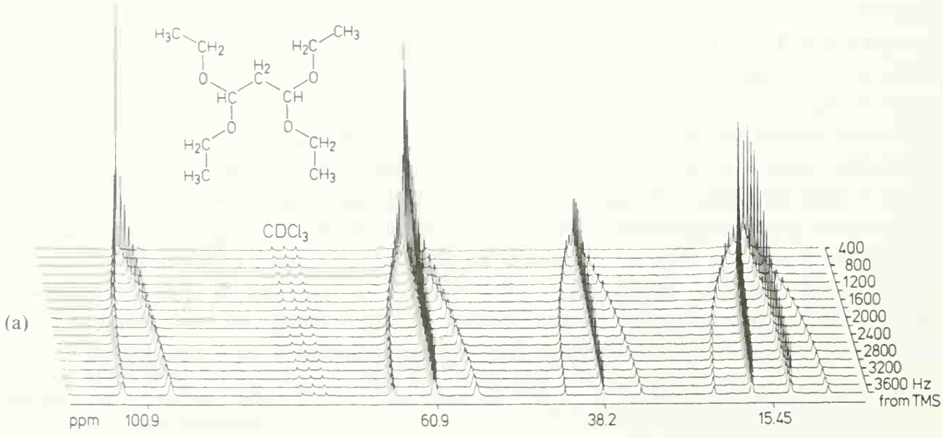

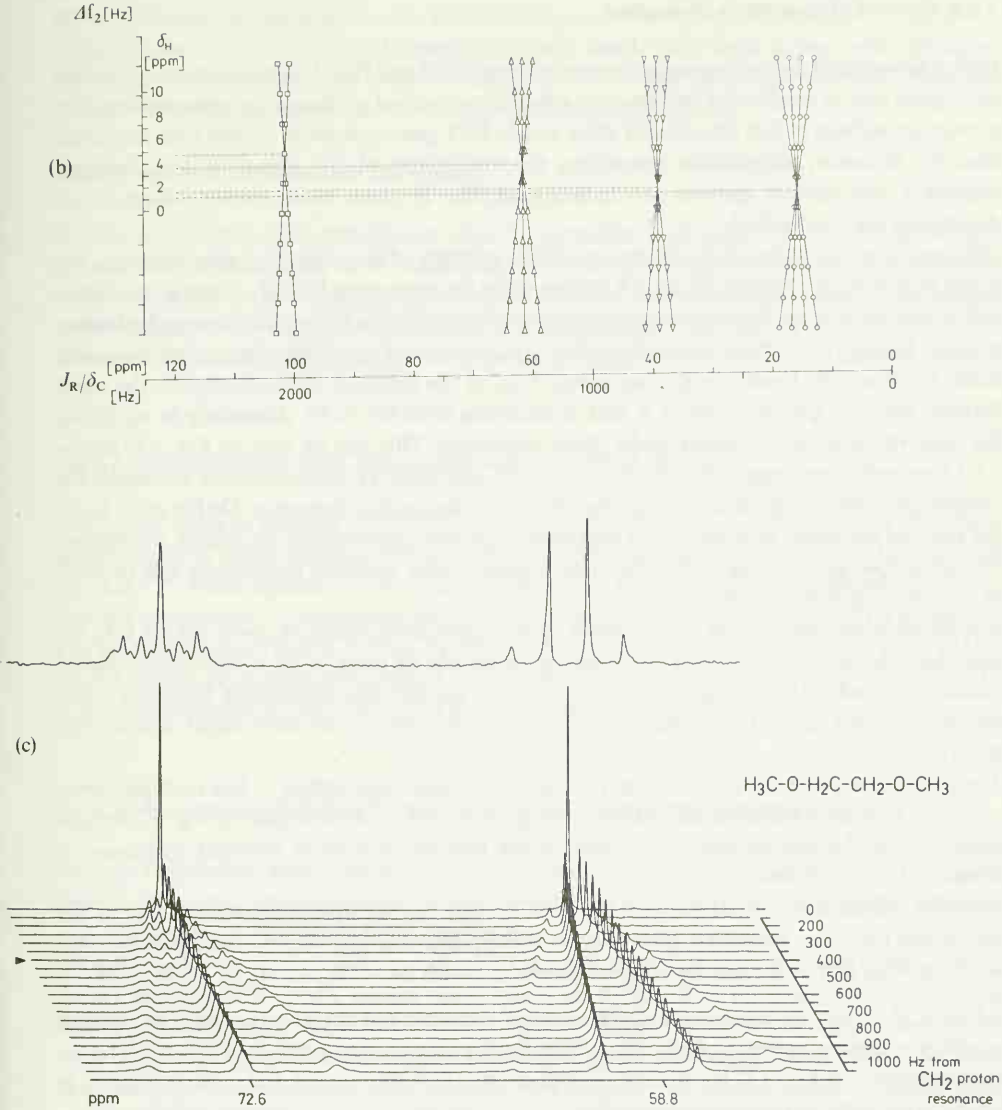

Fig. 2.17. Series of stacked proton off-resonance decoupled ^{13}C NMR spectra with varying frequency offset Δf_2.

(a) The residual C–H splittings of 1,1,3,3-tetraethoxypropane (50 Vol. % in deuteriochloroform, 25 °C, 20 MHz, 500 scans/experiment) asymptotically approach the coupling constants J_{CH} with increasing offset from the TMS proton resonance.

(b) A J_R *versus* Δf_2 plot in the ppm or Hz scale for offsets between – and +1 KHz from TMS gives the chemical shifts of directly coupled ^1H and ^{13}C nuclei.

(c) Residual splittings of higher order are observed for the triplet at 72.6 ppm of 1,2-dimethoxyethane (50 Vol. % in hexadeuterioacetone, 25 °C, 15.08 MHz, 500 scans/experiment).

2.6.5. Proton Off-Resonance Decoupling

Proton broad band decoupling simplifies and sensitizes CW and PFT ^{13}C NMR spectra. Further, the signals due to quaternary carbons can often be recognized in decoupled spectra since they are weaker because of lack Overhauser effect and, in PFT spectra, because of their long relaxation time T_1. However, information concerning the multiplicity of ^{13}C signals is lost. Primary, secondary and tertiary carbons are indistinguishable. In these cases, proton off-resonance decoupling may be applied.

Off-resonance decoupling is based on eq. (2.20): splitting of magnitude smaller than J_{AX} but larger than 0 Hz is observed for an AX system when the perturbing field H_2 is not at resonance with the nuclei X to be decoupled. In this case the effective field in the rotating frame of reference is given by eq. (1.32). With increasing offset $\Delta f_2 = \Delta \nu_2 - \Delta \nu_{0X}$ of the decoupling frequency band $\Delta \nu_2$ from the Larmor frequency range $\Delta \nu_{0X}$ of the nuclei X to be decoupled, the angle between the spin quantizations of A and X decreases from 90° to 0°. According to eq. (2.20), the observed coupling increases under these conditions. This can be seen in Fig. 2.17 (a) for 1,1,3,3-tetraethoxypropane. The residual $^{13}C-^{1}H$ splittings J_R asymptotically approach the coupling constant J_{CH} with increasing offset Δf_2 of the decoupling frequency. On the other hand, the residual couplings decrease as the decoupling frequency approaches the proton resonances, smaller couplings vanishing first. Additionally, signal : noise increases successively due to NOE as complete decoupling comes closer.

For off-resonance decoupling of ^{13}C NMR spectra, frequency offsets of about 0.5 – 1 kHz are used. In order to avoid complete collapsing of multiplets by large, noise modulated frequency bands, non-modulated decoupling fields are usually applied. The decoupling frequency offset can be adjusted until the multiplets are so narrow that no or only slight overlapping occurs.

The practical use and the advantage of proton-off-resonance decoupling – less multiplet overcrowding and more signal : noise relative to coupled spectra – is illustrated in Fig. 5.2 for epiandrosterone. An unequivocal assignment of the number of directly attached hydrogens is achievable for all carbons.

However, off-resonance multiplets are distortet in that the multiplet lines on the side of the decoupling frequency are weaker than those on the opposite side. Further, off-resonance splittings of higher than first order may be observed in systems such as $-CH_2-CH_2-$, $-\underset{|}{C}H-CH_2-$, $-CH{=}CH-$, *etc.*, as soon as the C – H residual coupling and the H – H vicinal or geminal coupling constants approach each other. This can be seen for the methylene triplet of 1,2-dimethoxyethane in Fig. 2.17 (c). For off-resonance offsets smaller than 1 KHz, the intensities of higher order splittings successively increase.

The residual coupling J_R of an individual carbon with the carbon-proton coupling constant J_{CH} is a linear function of the decoupling frequency offset Δf_2 from the protons attached to that carbon, provided the constant decoupling power $\gamma H_2/2\pi$ is sufficiently strong and the offset is not too large:

$$J_R = \frac{2\pi J_{CH}}{\gamma H_2} \Delta f_2 = \text{const.} \cdot \Delta f_2 \tag{2.24}$$

This linear relation is an additional aid in assigning ^{13}C and ^{1}H shifts. After recording a series of off-resonance decoupled spectra with varying frequency offsets Δf_2 but with the same decoupling power, the residual splittings can be plotted *versus* the decoupling frequencies. For an $n + 1$ multiplet due to n protons, $n + 1$ straight lines will result. They focus in one point, giving as coordinates the chemical shifts of both coupling nuclei (C and H) as shown in Fig. 2.17 (b) for another off-resonance spectra series of 1,1,3,3-tetraethoxypropane.

2.6.6. Pulsed Proton Broadband Decoupling

Proton decoupling begins immediately after the decoupler is switched on. The changes of spin populations responsible for NOE enhancements, however, are spin-lattice relaxation processes requiring considerably more time (up to some minutes). Correspondingly, proton decoupling stops instantly if the decoupler is switched off, but the NOE decreases slowly *via* spin-lattice relaxation. This is the basic concept of the pulsed decoupling techniques discussed in the following.

2.6.6.1. Measurement of NOE Enhanced Coupled ^{13}C NMR Spectra

The signal : noise of coupled ^{13}C NMR spectra is much lower than that of proton decoupled ones because of signal splitting and lack of nuclear Overhauser enhancement. NOE enhanced coupled ^{13}C NMR spectra can be measured, however, by switching on the proton decoupler between subsequent ^{13}C transmitter pulses an switching it off during pulsing and FID aquisition. The timing is outlined in Fig. 2.18 (a). By this technique, referred to as alternately pulsed $^{13}C\{^1H\}$ double resonance or gated decoupling [35, 36], signal : noise enhancements of up to 2 (eq. 2.23!) may be achieved, as can be clearly seen by comparing Figs. 2.18 (b) and (c).

2.6.6.2. Measurement of Proton Decoupled ^{13}C NMR Spectra with Suppressed NOE

Nuclear Overhauser enhancements and spin-lattice relaxation times are individual for each carbon. As a result, signal intensities cannot be evaluated from PFT ^{13}C NMR spectra obtained with continuous proton broad band decoupling.

If the decoupler is switched on only during FID acquisition as shown in the timing of Fig. 2.19 (a), proton decoupled ^{13}C NMR spectra with suppressed NOE will be obtained. This technique is known as inverse gated decoupling. Additionally, relaxation effects on the signal intensity are reduced by waiting between subsequent transmitter pulses sufficiently long ($3\ T_{1\,\max}$) in order to permit relaxation to the "slowest" carbon (with $T_{1\,\max}$) of the sample molecule. Quantitative evaluation of proton decoupled ^{13}C NMR spectra is then possible as is illustrated in Fig. 2.19 (c) for the tautomers of acetylacetone.

2.6.6.3. Measurement of Nuclear Overhauser Enhancements

The measurement of nuclear Overhauser enhancement factors η_C is necessary sometimes as these data provide information about relaxation mechanisms and the distance of protons to quaternary carbons. However, η_C cannot always be obtained as shown in Fig. 2.16 for the very simple case of formic acid. For larger molecules, integration of coupled spectra suffers from bad signal :

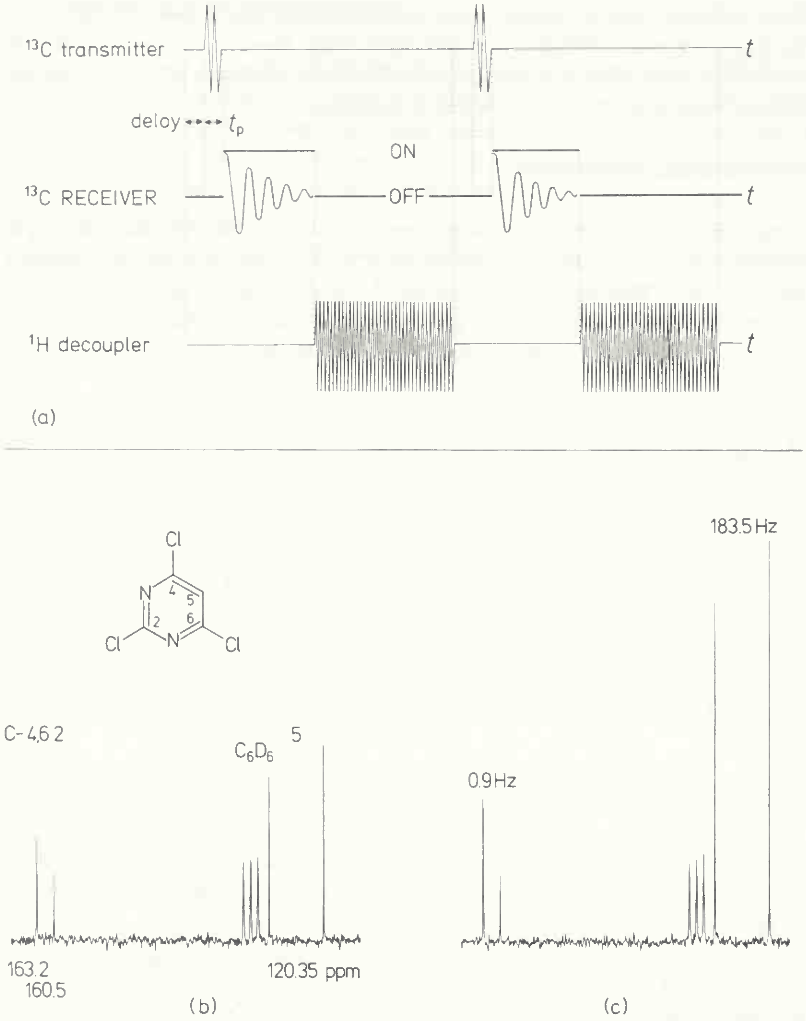

Fig. 2.18. Measurement of NOE enhanced coupled ^{13}C NMR spectra; sample: 2,4,6-trichloropyrimidine, 75 Vol. % in hexadeuteriobenzene, 25 °C, 20 MHz;
(a) timing of the alternating transmitter and decoupler pulses for gated decoupling;
(b) single resonance spectrum (decoupler off, delay between subsequent transmitter pulses: 10 s, 50 scans);
(c) gated decoupled spectrum, obtained with the pulse timing of (a) (delay between subsequent transmitter pulses: 10 s, 50 scans, noise normalized to the level obtained in (b)).

noise and multiplet overcrowding as is illustrated for menthol in Fig. 2.20(b). In these cases, a modification of the inverse gated decoupling technique can be applied: The signal intensity is measured once with long decoupling time, *i.e.* $3\ T_{1\,\mathrm{max.}}$, accounting for the "slowest" carbon. In the second experiment, the decoupler is switched on only during FID acquisition as outlined in the timing of Fig. 2.20(a). For long decoupling times, the signal intensity I_1 benefits from the full NOE enhancement. In the second experiment with short decoupling time, practically no NOE enhancement builds up and a weaker signal with intensity $I_2 < I_1$ is recorded. The intensity ratio I_1/I_2 is then the NOE factor η_C. The measurement can be averaged from a series of experiments as is shown in Fig. 2.20(b) for the carbons of menthol with an η_C of about 2.

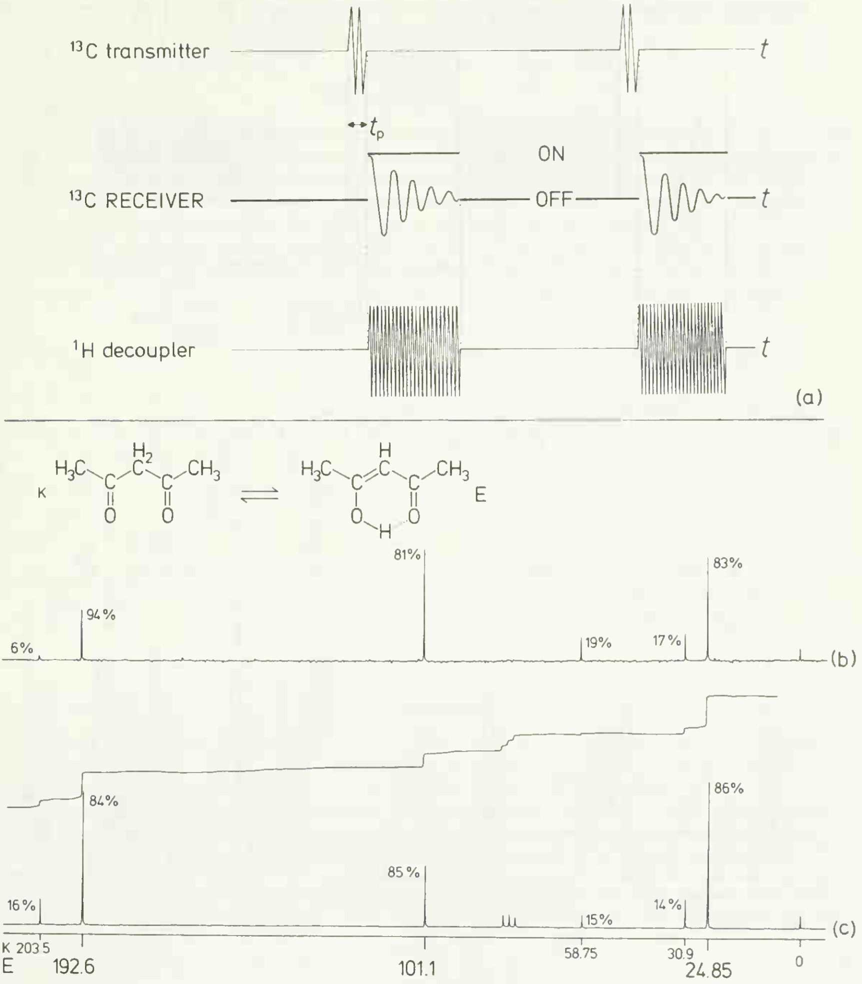

Fig. 2.19. Quantitative evaluation of ^{13}C NMR spectra with suppressed NOE; sample: acetylacetone, 50 Vol. % in deuteriochloroform, 25 °C, 20 MHz;
(a) timing of the decoupler and transmitter pulses for inverse gated decoupling;
(b) ^{13}C NMR spectrum obtained with normal proton noise decoupling and without delay between subsequent 90° transmitter pulses, 200 scans;
(c) ^{13}C NMR spectrum obtained by inverse gated decoupling as outlined in (a); delay time between subsequent 90° transmitter pulses: 60 s; 200 scans.
Note that acetylacetone was found to be 85% enolized by integration of its ^{1}H NMR spectrum in deuteriochloroform.

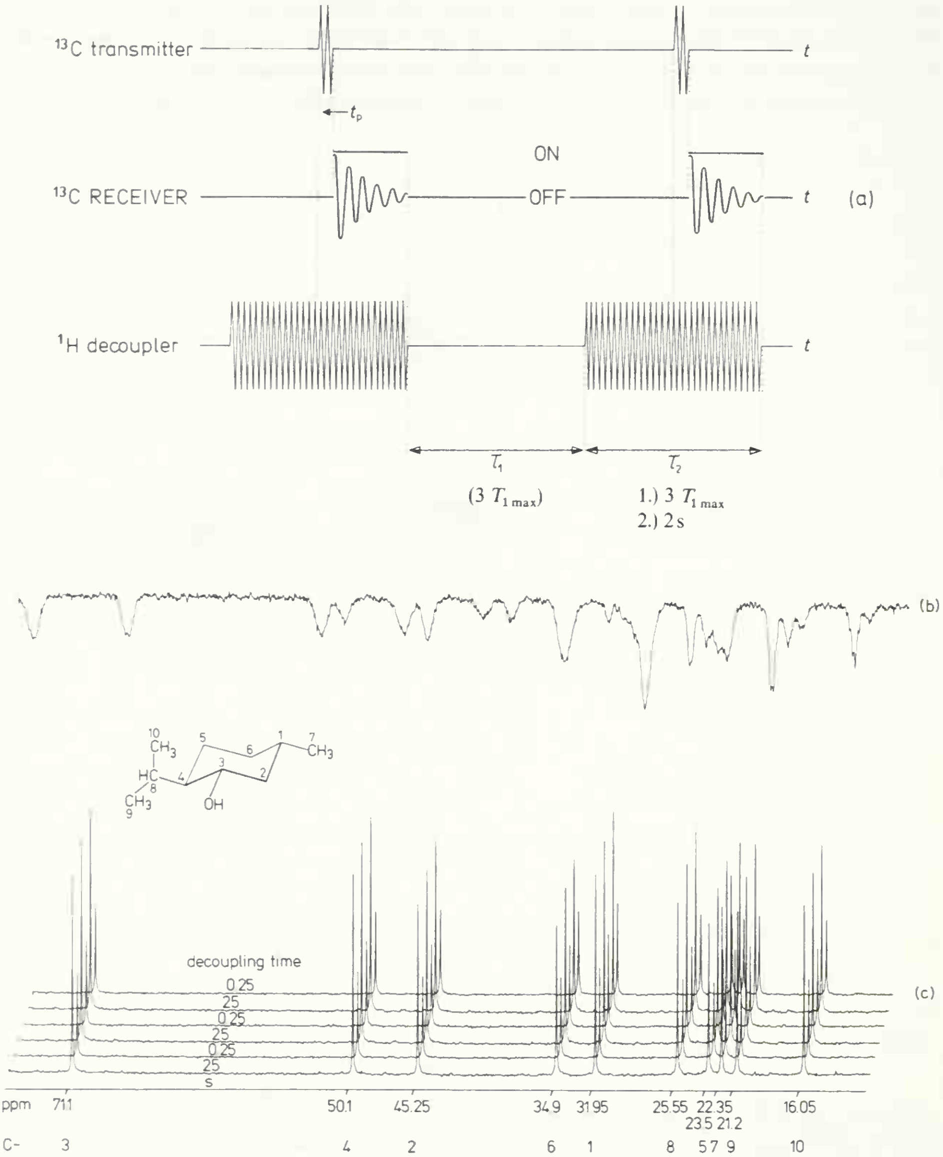

Fig. 2.20. Measurement of NOE enhancement factors by pulsed proton decoupling; sample: menthol, 200 mg in 1 ml of deuteriochloroform, 25 °C, 20 MHz;

(a) timing of decoupler and transmitter pulses for repetitive experiments with long and short decoupling times (3 $T_{1\,\mathrm{max}}$ and some ms, respectively); note that decoupling also takes place during FID acquisition; thus, τ_2 in (a) is the total decoupling time;

(b) coupled ^{13}C NMR spectrum of menthol, 500 scans;

(c) computer controlled series of six ^{13}C experiments according to the timing (a) with alternating long (25 s) and short decoupling times (250 ms), 100 scans/experiment.

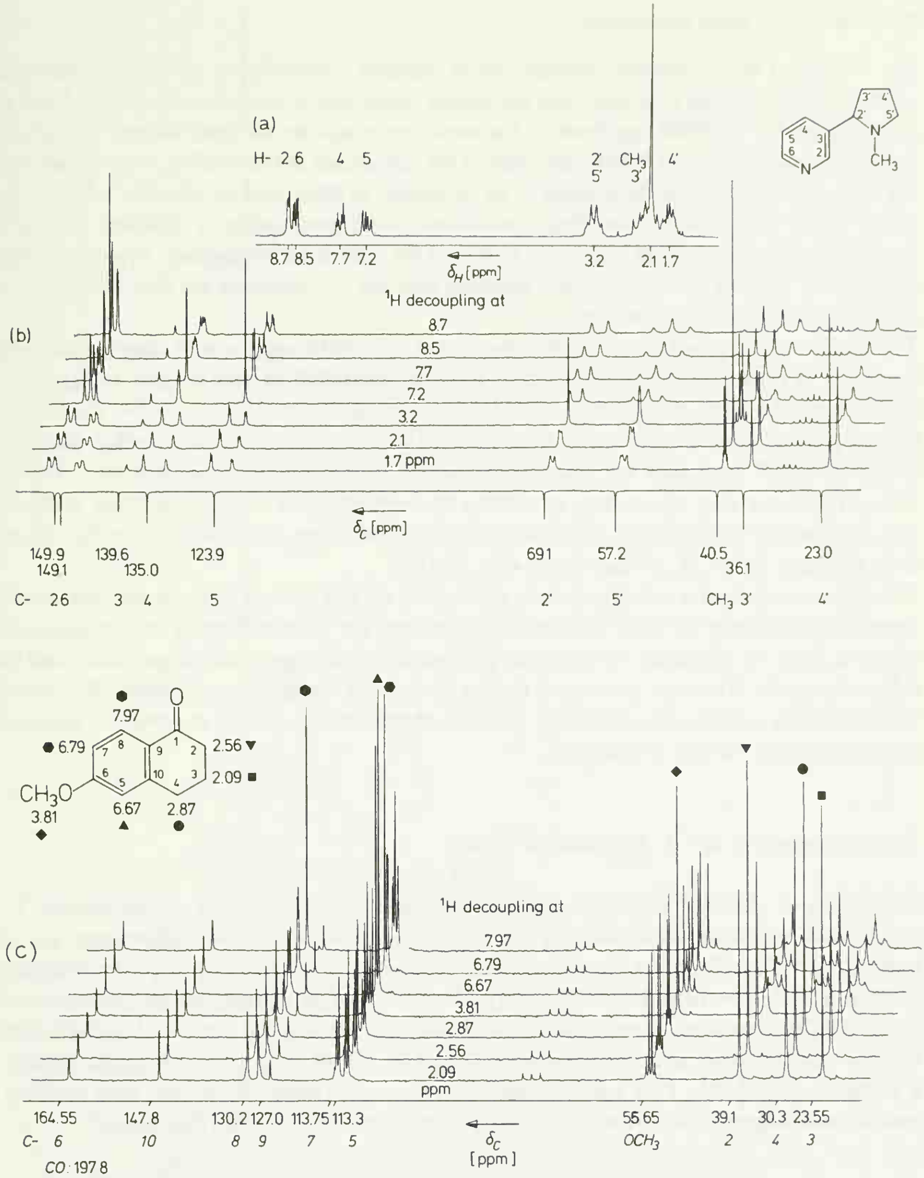

Fig. 2.21. Selective proton decoupling;

(a) ^1H PFT NMR spectrum of nicotine, 50 Vol.% in hexadeuterioacetone, 25 °C, 80 MHz, indicating the assigned ^1H resonances to be decoupled;

(b) automatically recorded series of selectively proton decoupled ^{13}C NMR spectra of nicotine, sample (a), 20 MHz, 500 scans/experiment; a proton broadband decoupled spectrum (bottom) is recorded for comparison with inverted phase;

(c) automatically recorded series of selectively proton decoupled 20 MHz ^{13}C NMR spectra of 6-methoxy-α-tetralone, 200 mg in 1 ml of deuteriochloroform, 500 scans/experiment; the decoupling frequency offsets are calculated from the known proton chemical shifts relative to the offset determined for TMS.

2.6.7. Selective Proton Decoupling

The ^{13}C signal of an individual carbon can be assigned unequivocally by selective decoupling of the protons attached to it, provided the proton resonance is unequivocally assigned and well separated in the ^{1}H NMR spectrum of the same compound in the same solvent. For selective proton decoupling, the ^{1}H NMR spectrum of the compound is recorded in order to determine the Larmor frequencies of the protons to be decoupled as illustrated for nicotine in Fig. 2.21(a). These values are set the decoupling frequencies. Noise modulation is switched off and the decoupling power is reduced relative to that used for wide band decoupling. Typical values are adjusted for $\gamma H_2/2\pi \approx 400 \pm 100$ Hz, ensuring that the ^{13}C satellites are also touched by the decoupling frequency distribution.

The stacked series of selectively proton decoupled ^{13}C NMR spectra with varying decoupling frequency is conveniently recorded fully computer controlled as can be seen for nicotine in Fig. 2.21(b). The series clearly shows that ^{13}C signals, *e.g.* those of C-2, C-6, C-4, C-5 and C-4′, are unequivocally assigned if the protons attached to these carbons do not overlap with others in the ^{1}H NMR spectrum. For overlapping proton resonances (*e.g.* the pairs H-2′, H-5′ and H-3′, CH_3) more than one carbon is affected by decoupling, of course, and other assignment aids such as the off-resonance multiplicities have to be taken into account (*e.g.* for the pairs C-2′, C-5′ and C-3′, CH_3 of nicotine in Fig. 2.21(b)).

The offsets necessary for selective proton decoupling do not have to be measured, provided the decoupling frequency of TMS protons is known and the proton shifts of the compound are available from the literature. In this case, the decoupling frequency offsets are calculated from the proton shifts. This was performed for the protons of 6-methoxy-α-tetralone. The result of the decoupling experiments with these values is shown in Fig. 2.21(c). A complete assignment of all protonated carbons is achieved.

2.7. Measurement of ^{13}C Relaxation Times

In addition to chemical shifts and coupling constants, relaxation times – particularly T_1 – are gaining increasing significance in ^{13}C NMR as molecular mobility parameters and aids in assigning ^{13}C NMR spectra. Several methods for measuring spin-lattice and spin-spin relaxation times T_1 and T_2 have been described [7, 13]. Many of those only permit selective determination of T_1 or T_2 for one kind of nuclei in simple molecules. For organic structural analysis, simultaneous determination and comparison of T_1 and T_2 for all non-equivalent nuclei present in a molecule is desirable. PFT methods meeting these requirements exist, and hold promise as routine measurements of T_1 and T_2. Some of these methods are described below.

2.7.1. Spin-Lattice Relaxation Times

2.7.1.1. The Inversion-Recovery or 180°, τ, 90° Method

Spin-lattice relaxation times T_1 of individual nuclei (^{13}C, ^{1}H) present in a molecule can be obtained by Fourier transformation of the FID signal following a 180°, τ, 90° pulse sequence. The technique is referred to as inversion-recovery method [39, 40] or partially relaxed NMR spectroscopy [41]; it can be explained by follwing the pulse driven motion of the magnetization vector M_0 in the rotating frame of reference with the axes x', y', z' (Fig. 2.22).

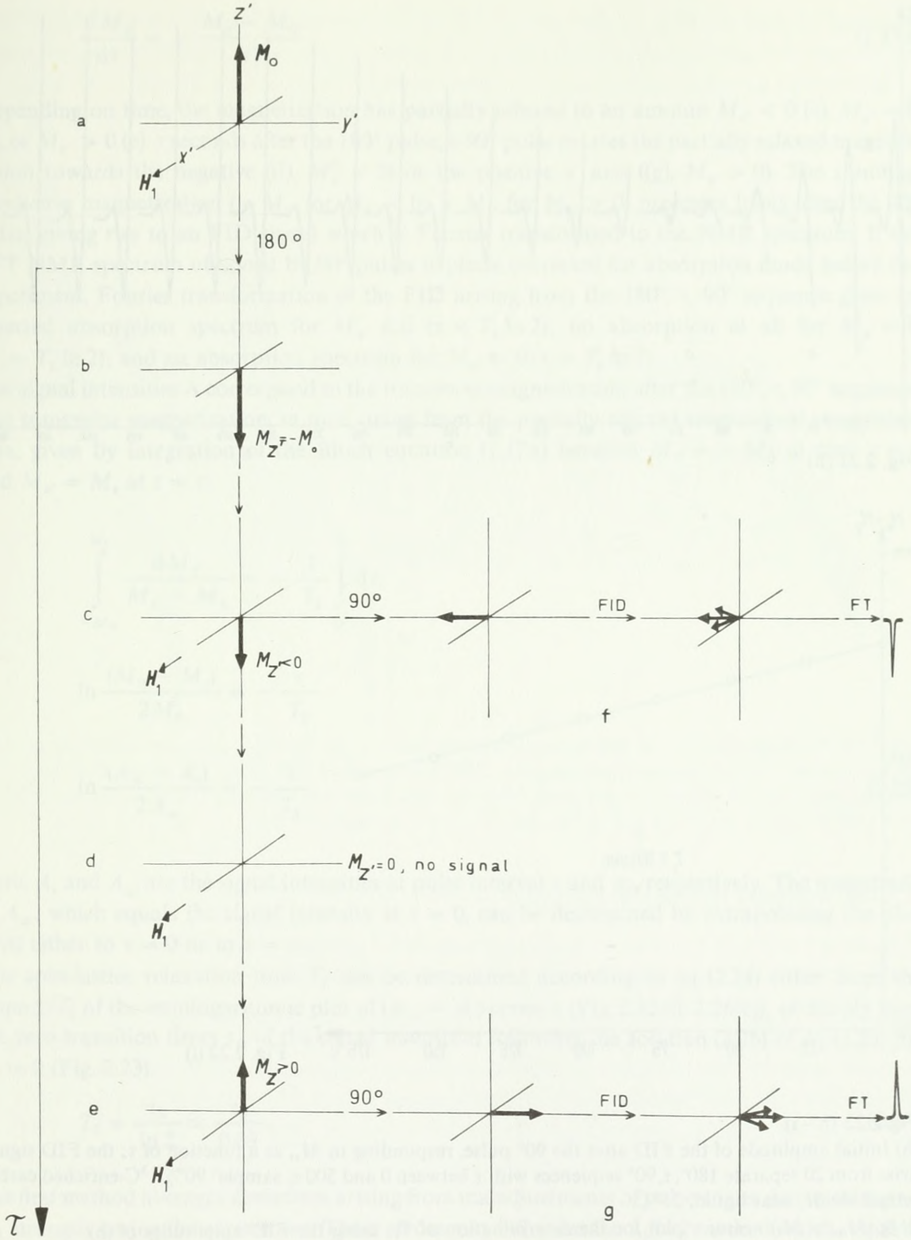
z'
M₀
a
y'
x'
H₁
180°
b
M_z' = -M₀
90°
FID
FT
c
M_z' < 0
H₁
f
d
M_z' = 0, no signal
H₁
M_z' > 0
90°
FID
FT
e
H₁
g
τ

Fig. 2.22. (a) – (g) Pulse driven motion of the magnetization vector M_0 in the rotating frame of reference during an inversion-recovery experiment for the measurement of T_1;

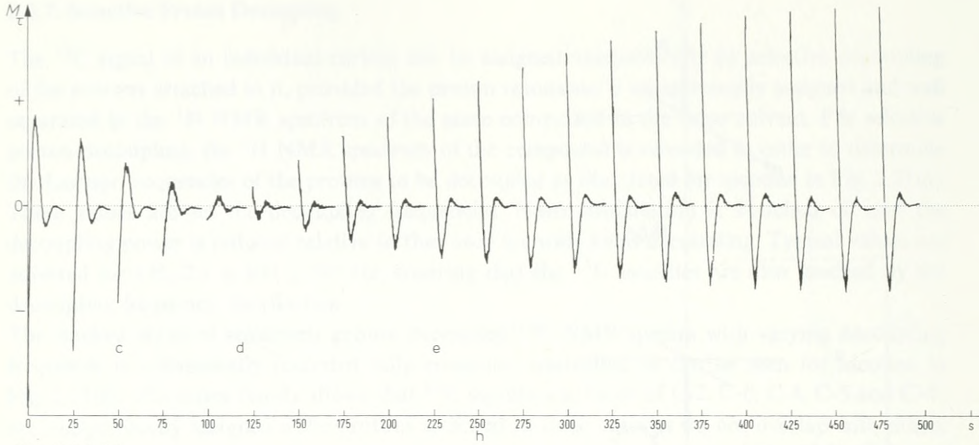

Fig. 2.22 (h)

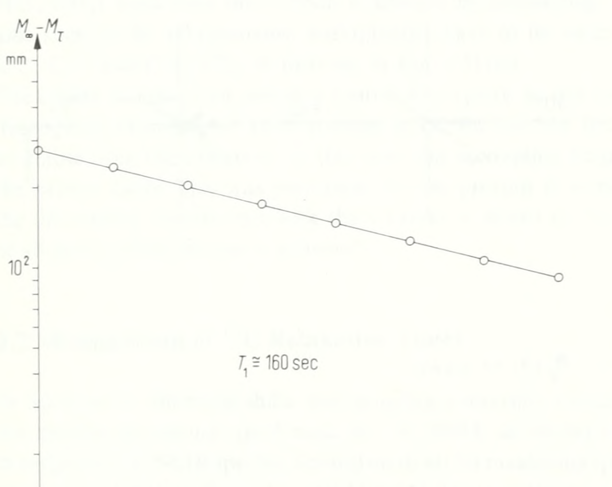

Fig. 2.22 (i)

Fig. 2.22 (h – i).
(h) Initial amplitude of the FID after the 90° pulse, responding to M_τ, as a function of τ; the FID signals arise from 20 separate 180°, τ, 90° sequences with τ between 0 and 500 s; sample: 90% ^{13}C-enriched carbon tetrachloride, neat liquid, 25 °C.
(i) lg ($M_\infty - M_\tau$) *versus* τ plot for the determination of T_1, using the FID amplitudes of (h).
(h) recorded by B. Knüttel, Bruker Physik AG, Karlsruhe-Forchheim, Germany.

Starting at equilibrium (a), a 180° pulse along the x' axis inverts the magnetization vector ($\boldsymbol{M}_0 \rightarrow -\boldsymbol{M}_0$) (b). By subsequent longitudinal relaxation, the longitudinal magnetization $\boldsymbol{M}_{z'}$ reequilibrates, going from $-\boldsymbol{M}_0$ through zero to $+\boldsymbol{M}_0$, following the Bloch equation (1.17 a).

$$\frac{\mathrm{d}M_z}{\mathrm{d}t} = -\frac{M_z - M_0}{T_1}. \qquad (1.17\,\mathrm{a})$$

Depending on time, the magnetization has partially relaxed to an amount $M_{z'} < 0$ (c), $M_{z'} = 0$ (d), or $M_{z'} > 0$ (e). τ seconds after the 180° pulse, a 90° pulse rotates the partially relaxed magnetization towards the negative ((f), $M_{z'} < 0$) or the positive y' axis ((g), $M_{z'} > 0$). The resulting transverse magnetization ($-M_{y'}$ for $M_{z'} < 0$; $+M_{y'}$ for $M_{z'} > 0$) precesses freely after the 90° pulse, giving rise to an FID signal which is Fourier transformed to the NMR spectrum. If the PFT NMR spectrum obtained by 90° pulses is phase corrected for absorption mode before the experiment, Fourier transformation of the FID arising from the 180°, τ, 90° sequence gives an inverted absorption spectrum for $M_{z'} < 0$ ($\tau < T_1 \ln 2$); no absorption at all for $M_{z'} = 0$ ($\tau_0 = T_1 \ln 2$); and an absorption spectrum for $M_{z'} > 0$ ($\tau > T_1 \ln 2$).

The signal intensities A correspond to the transverse magnetization after the 180°, τ, 90° sequence. The transverse magnetization, in turn, arises from the partially relaxed longitudinal magnetization, given by integration of the Bloch equation (1.17a) between $M_{z'} = -M_0$ at time $t = 0$ and $M_{z'} = M_\tau$ at $t = \tau$:

$$\int\limits_{-M_0}^{M_\tau} \frac{\mathrm{d}M_{z'}}{M_{z'} - M_0} = -\frac{1}{T_1}\int\limits_0^{\tau} \mathrm{d}t$$

or

$$\ln\frac{(M_0 - M_\tau)}{2M_0} = -\frac{\tau}{T_1}$$

or

$$\ln\frac{(A_\infty - A_\tau)}{2A_\infty} = -\frac{\tau}{T_1}. \qquad (2.25)$$

Here, A_τ and A_∞ are the signal intensities at pulse interval τ and ∞, respectively. The magnitude of A_∞, which equals the signal intensity at $\tau = 0$, can be determined by extrapolating the plot $A_\tau(\tau)$ either to $\tau = 0$ or to $\tau = \infty$.

The spin-lattice relaxation time T_1 can be determined according to eq. (2.24) either from the slope $1/T_1$ of the semilogarithmic plot of $(A_\infty - A_\tau)$ *versus* τ (Fig. 2.22 (i). 2.26(c)), or simply from the zero transition times τ_0 of the signal intensities following the solution (2.26) of eq. (2.25) for $A_\tau = 0$ (Fig. 2.23).

$$T_1 = \frac{\tau_0}{\ln 2} \approx \frac{\tau_0}{0.69}. \qquad (2.26)$$

The first method averages deviations arising from maladjustments of pulse angles due to changing H_1 strength during the experiment. These errors may influence the $\tau_0/\ln 2$ method which requires a good signal : noise and small pulse interval steps for an accurate determination of the zero transitions.

The measurement of T_1 in ^{13}C{^{1}H} NMR is illustrated for the ^{13}C nuclei of diphenylether in Fig. 2.23. If accumulation of the FID signals is required for signal : noise improvement, the waiting period between two subsequent sequences should be at least 3 T_1 (180°, τ, 90°, $-3\,T_1$, $-$180°, τ, 90°, $-3\,T_1$, $-\cdots$), T_1 accounting for the slowest relaxing nucleus in the molecule. In this case, the experiment may require several hours, and it is advantageous when pulse sequencing, waiting periods, accumulations, Fourier transformation, phase correction and stacked recording of the spectra $A_\tau(\nu, \tau)$ are completely computer controlled.

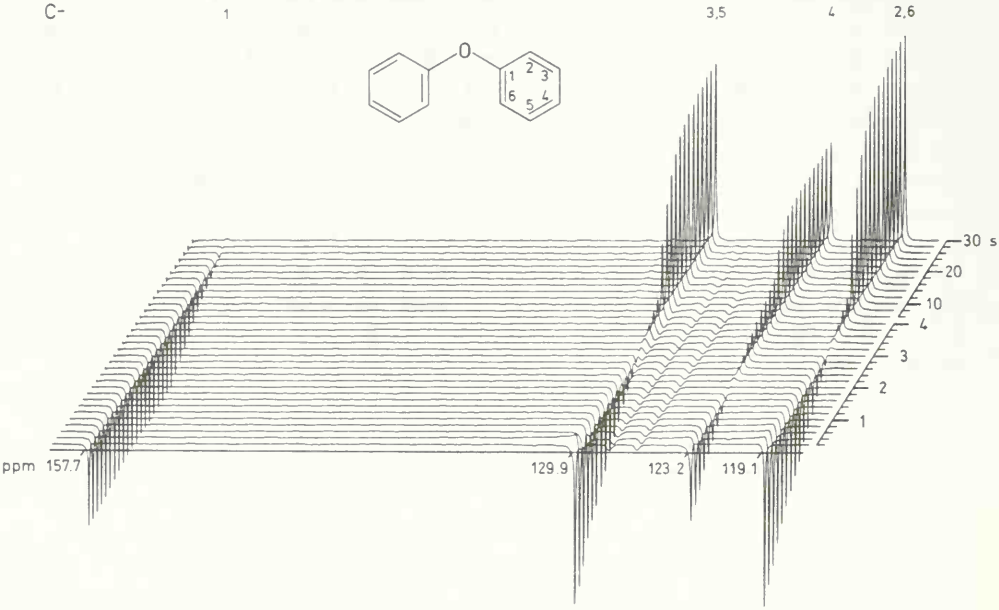

Fig. 2.23. Determination of ^{13}C spin-lattice relaxation times by the inversion-recovery technique; sample: diphenylether, 75% in hexadeuteriobenzene, 25 °C, degassed, 15.08 MHz, 10 scans/experiment. T_1, conveniently but not accurately obtained from the zero transition times τ_0 according to eq. (2.26), is 40.5 s for C-1, 4.6 s for C-2,6 and C-3,5, and 2.9 s for C-4, respectively.

2.7.1.2. Saturation Recovery Method [43]

Spin-lattice relaxation of nuclear spins may also be initiated by a perturbing 90° pulse along x' which rotates the magnetization to the $x'y'$ plane (Fig. 2.24(a) → (b)). The resultant transverse magnetization is then dispersed by a field gradient pulse (the *homospoil pulse*) along the z' axis. This ensures that a second 90° pulse applied along x' after τ s monitors only the partially relaxed magnetization M_τ (Fig. 2.24(d) → (e)) without the contribution of the residual transverse magnetization built up by the first 90° pulse. The subsequent FID is Fourier transformed to the NMR signal with amplitude A_τ responding to the partially relaxed magnetization M_τ. – As known from the inversion recovery techniques, waiting periods of $3\,T_{1\,\mathrm{max.}}$ permitting relaxation to the slowest carbon of the molecule have to be programmed between subsequent pulse sequences when several FID's must be accumulated for a sufficient signal:noise ratio.

A stacked set of saturation recovery spectra is given in Fig. 2.25 which shows that the signal intensity approaches an equilibrium value A_∞ responding to the fully relaxed magnetization M_0. The intensity A_τ as a function of τ is the integral of the Bloch equation (1.17a) between $M_{z'} = M_\tau$ and M_0, or in terms of intensities, from A_τ at time τ to A_∞ at time ∞:

$$\ln \frac{A_\infty - A_\tau}{A_\infty} = -\frac{\tau}{T_1}. \qquad (2.27)$$

Thus, T_1 is obtained as the reciprocal slope of a semilogarithmic $(A_\infty - A_\tau)$ *versus* τ plot. Fig. 2.25(b) illustrates an example of a convenient graphical evaluation also including the lg → ln conversion necessary when decadic semilogarithmic paper is used.

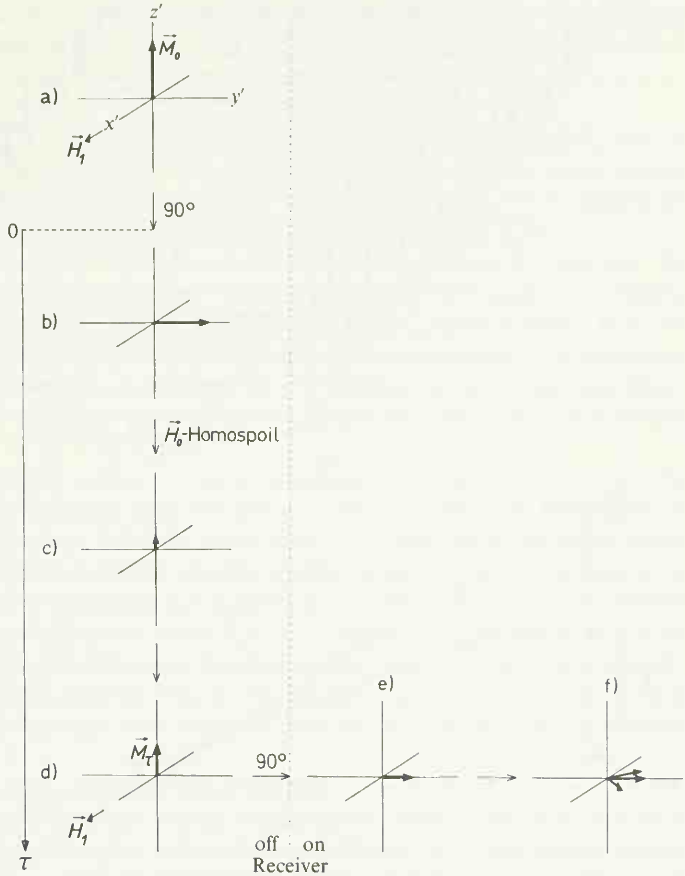

Fig. 2.24. Motion of the magnetization vector during a saturation-recovery experiment; the first 90° pulse rotates the magnetization vector M_0 to the $x'y'$ plane (a → b) where the resultant transverse magnetization is dispersed by a field gradient pulse *(Homospoil)*; after τ s (d), a second 90° pulse monitors the partially relaxed magnetization M_τ (d → f), and the resultant FID signal is Fourier transformed to the NMR signal with amplitude A_τ.
(Reproduced by permission of the copyright owner from E. Breitmaier and G. Bauer: ^{13}C-NMR-Spektroskopie, eine Arbeitsanleitung mit Übungen. Georg Thieme Verlag, Stuttgart, 1977.)

2.7.1.3. Progressive Saturation or 90°, τ, ... Method

^{13}C spin-lattice relaxation times of individual nuclei can also be measured by PFT $^{13}C\{^1H\}$ experiments using a 90°, τ, 90°, τ, ... pulse train and noise modulation of the proton decoupling frequency. This method is known as progressive saturation [43] and based on the following concept.

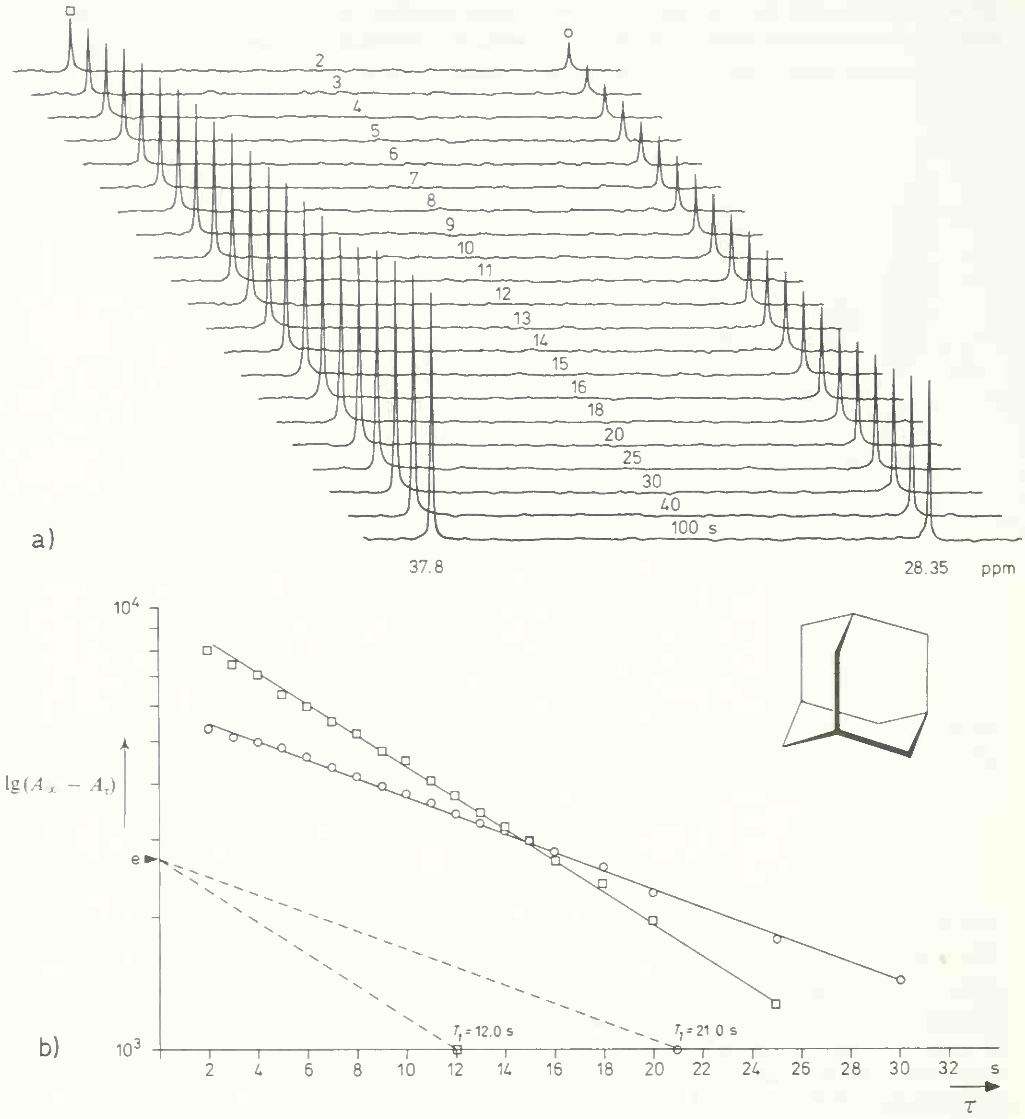

Fig. 2.25. Measurement of ^{13}C spin-lattice relaxation times by saturation-recovery:
(a) stacked set of saturation-recovery spectra; sample: adamantane, saturated solution in deuteriochloroform, 25 °C, 25 MHz, 50 scans/experiment (*i. e.* $(90°, \textit{Homospoil}, \tau, 90°)_{25}$);
(b) graphic evaluation of the intensities taken from spectra set (a); T_1 is 12.0 s for CH_2 and 21.0 s for CH.
(Reproduced by permission of the copyright owner from E. Breitmaier and G. Bauer: ^{13}C-NMR-Spektroskopie, eine Arbeitsanleitung mit Übungen. Georg Thieme Verlag, Stuttgart 1977.)

Recalling Section 2.5.6, the pulse interval τ of a $90°, \tau, 90°, \tau, \ldots$ sequence used for accumulation of FID signals in PFT ^{13}C NMR is often short compared to ^{13}C spin-lattice relaxation. After several 90° pulses, a steady state magnetization $M_0' < M_0$ is established [22]; the signal intensity in the Fourier transform of the FID is attenuated. Using subsequent 90° pulse trains with increasing intervals τ, the steady state magnetization M'_0 approaches the relaxed magnetization M_0. The 90° pulse train successively rotates the M'_0 vectors towards the y' axis, giving rise to transverse magnetizations which yield a train of FID signals subject to be accumulated and Fourier transformed. In the PFT spectrum obtained for each τ, the signal intensity A_τ corresponds to the steady state magnetization M'_0. The intensity A_τ as a function of τ is the integral of the Bloch equation (1.17a) between $M_{z'} = M'_0$ and M_0, or, in terms of intensities, from A_τ at $t = \tau$ to A_∞ at $t = \infty$.

According to eq. (2.27), T_1 is obtained as the reciprocal slope of the semilogarithmic plot of $(A_\infty - A_\tau)$ *versus* τ (Fig. 2.26(c)). The equilibrium intensity A_∞ corresponding to the relaxed magnetization M_0 is approximated by recording a PFT spectrum arising from a 90° pulse train with an interval of at least $\tau = 3T_1$, T_1 accounting for the slowest relaxing nucleus.

Progressive saturation measurement of T_1 is restricted to nuclei with $T_1 > T_2$. Otherwise, the transverse magnetization remaining along the y' axis after the interval τ is rotated to the negative z' axis by the following 90° pulse. The resulting signal attenuation would invalidate eq. (2.27). The requirement $T_1 > T_2$ is realized in $^{13}C\{^1H\}$ NMR when noise modulation of the decoupling field is applied: $^{13}C\{^1H\}$ spin-echo experiments on ^{13}C enriched methyl iodide involving a $90°,\tau,180°$ pulse sequence show that proton noise decoupling accelerates the free induction decay, T_2 being decreased to $T_2^* \ll T_1, T_2$ [44].

T_1 measurements by progressive saturation can be completely computer controlled. First, the sequence $90°,\tau,\ldots$ is repeated several times for each τ without acquiring the FID signals in order to establish the steady state. Then, the steady state FID signals are accumulated until a certain signal : noise is reached. Following Fourier transformation and phase correction, the PFT NMR spectrum for each τ is recorded. Automatic stacking of the spectra can be programmed so that the three dimensional representation of $A_\tau(v,\tau)$ is obtained as shown in Fig. 2.26(b) for propynol [43]. Fig. 26(c) compares the results obtained from inversion-recovery and progressive saturation measurements. Both methods yield almost identical slopes and T_1 values [43]. Thus, the progressive saturation technique does not suffer from serious systematic errors provided $T_1 > T_2$.

The $180°,\tau,90°$ method is more general, not being restricted to nuclei with $T_1 > T_2$ or $T_1 > T_2^*$. However, long accumulation times due to long waiting periods between the pulse sequences are required for nuclei with small signal : noise and long T_1 such as ^{13}C. These waiting periods are not necessary in the $90°,\tau,\ldots$ method. Therefore, progressive saturation is more advantageous for measuring ^{13}C spin-lattice relaxation times of slowly relaxing carbons when proton noise decoupling can be applied.

2.7.2. Spin-Spin Relaxation Times

2.7.2.1. CPMGSE Experiments

Spin-Spin relaxation times are obtained from spin-echo experiments [7, 44–46] using $90°,\tau,180°$ pulse sequences as known from the DEFT method discussed in Section 2.5.6. T_2 values without serious errors due to maladjustment or changes of pulse angles are obtained by a pulse train of sequence $90°,\tau,180°,3\tau,180°,5\tau,180°,7\tau,\ldots$ The initial 90° pulse is applied along the x' axis of the rotating frame. All subsequent 180° pulses are phase shifted by 90° relative to the 90° pulse, thus being applied along the y' axis of the rotating frame of reference. The method was developed

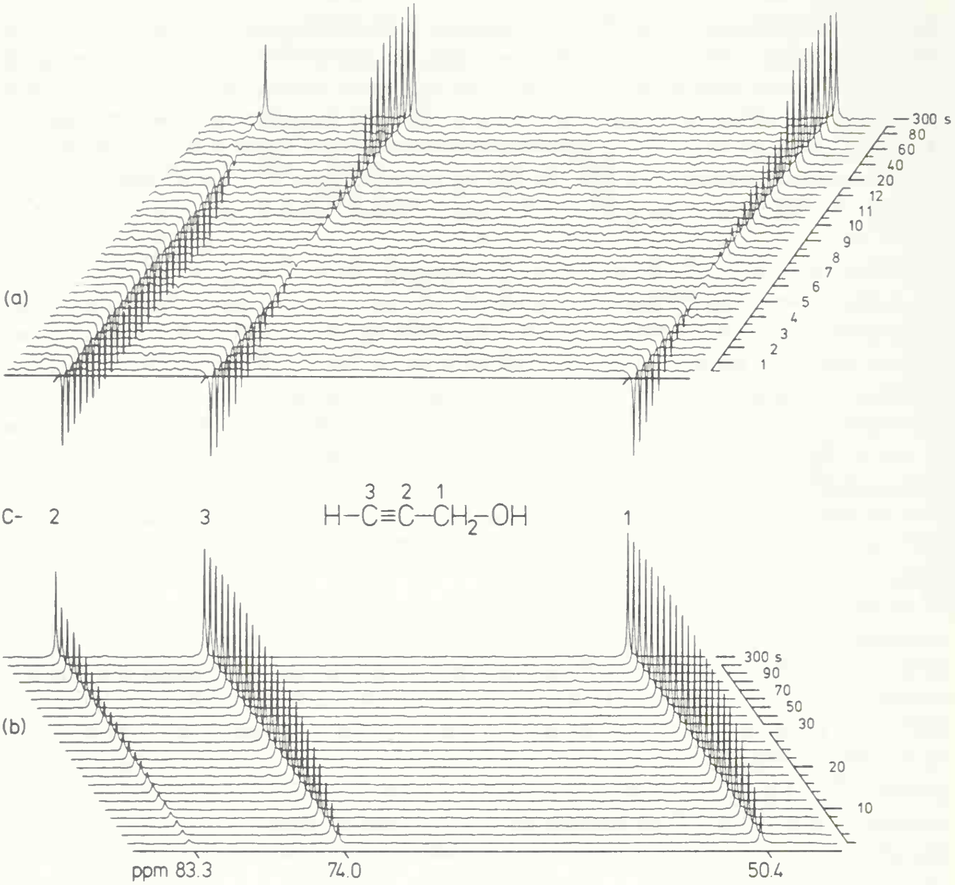

Fig. 2.26a, b.

by Carr, Purcell, Meiboom, and Gill [45, 46] and is referred to as CPMG spin-echo or CPMGSE technique.

The concept of CPMGSE becomes reasonable by following the pulse driven motion of the magnetization vector M_0 in a frame of reference rotating for clarity slower than the smallest Larmor frequency of the nuclei to be observed (Fig. 2.27). An initial 90° pulse applied along x' rotates M_0 to y' (a), giving rise to an FID signal in the receiver due to transverse relaxation: The nuclear spins dephase with different angular velocity, some slower (⌒➝), some faster (⌒⌒➝), due to different local fields in the sample mainly caused by inhomogeneous H_0. In this situation (b), reached after τ s, a 180° pulse along y' rotates the spins 180° about y' (c). Since the direction of dephasing does not change after the 180° pulse, the spins rephase to a spin-echo in (d) after 2τ s. An echo FID is obtained which culminates in (e), followed by renewed dephasing (b). Another 180° pulse at time 3τ restricts dephasing, rotating the spins about y' (c) and causing another spin-echo (d). Thus, a $90°, \tau, 180°, 3\tau, 180°, 5\tau, 180°, 7\tau, \ldots$ pulse train generates a train of echo FID signals spaced at $2\tau, 4\tau, 6\tau, \ldots$ as illustrated in Fig. 2.28 for the ^{13}C resonance of ^{13}C enriched carbon tetrachloride, $^{13}CCl_4$. The phase of the echo signals does not change as all echos are along the

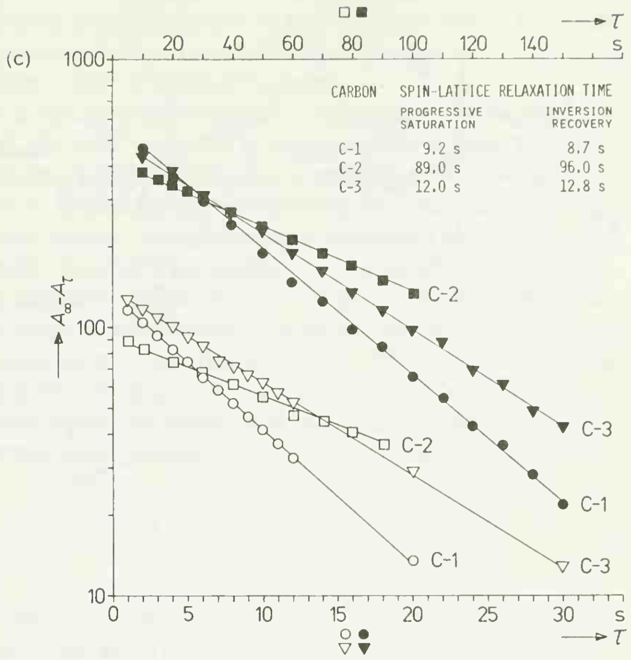

Fig. 2.26. Determination of ${}^{13}C$ spin-lattice relaxation times by inversion-recovery (a), progressive saturation (b), and comparative evaluation of the intensities (c), values from (a) with full, from (b) with empty characters, abszissa on top for C-2, abszissa on bottom for C-1 and C-3); sample: propynol, 75 Vol.% in hexadeuterioacetone, 25 °C, not degassed, 15.08 MHz, 10 scans/experiment in (a), 100 scans/experiment in (b).

positive y' axis. If the 180° pulses are applied in phase with the initial 90° pulse, the phase of subsequent echo signals alternates [7, 45] since rephasing alternately occurs in the positive and negative y' axis.

The echo amplitude decays with time. This decay is faster than transverse relaxation since dephasing of nuclei is accelerated by varying local fields at different places in the sample due to inhomogeneous H_0, and since diffusion of nuclei within the sample from one homogeneity range to another may take place. The echo amplitude $A_{t(\mathrm{echo})}$ therefore does not decay as a simple exponential. The decay rather follows eq. (2.28), the term $\mathrm{f}(t)$ accounting for inhomogeneity and diffusion.

$$A_{t(\mathrm{echo})} = \text{const.}\left[\mathrm{e}^{-t/T_2} - \mathrm{f}(t)\right]. \tag{2.28}$$

T_2 of the observed nucleus is obtained as the reciprocal slope of the semilogarithmic plot $A_{t(\mathrm{echo})}$ *versus* t for small values of t since $\mathrm{f}(t)$ can be neglected when t approaches zero.

2.7.2.2. Spin-Locking Fourier Transform Experiments

CPMGSE experiments are restricted to compounds containing one ${}^{13}C$ nucleus as is the case in carbon disulfide or compounds containing one ${}^{13}C$ carbon at high concentration (*e.g.* ${}^{12}CH_3-{}^{13}COOH$) so that only one resonance is detectable with significant signal : noise. If more chemically shifted or coupled ${}^{13}C$ nuclei are present in a molecule, the FID echo signals

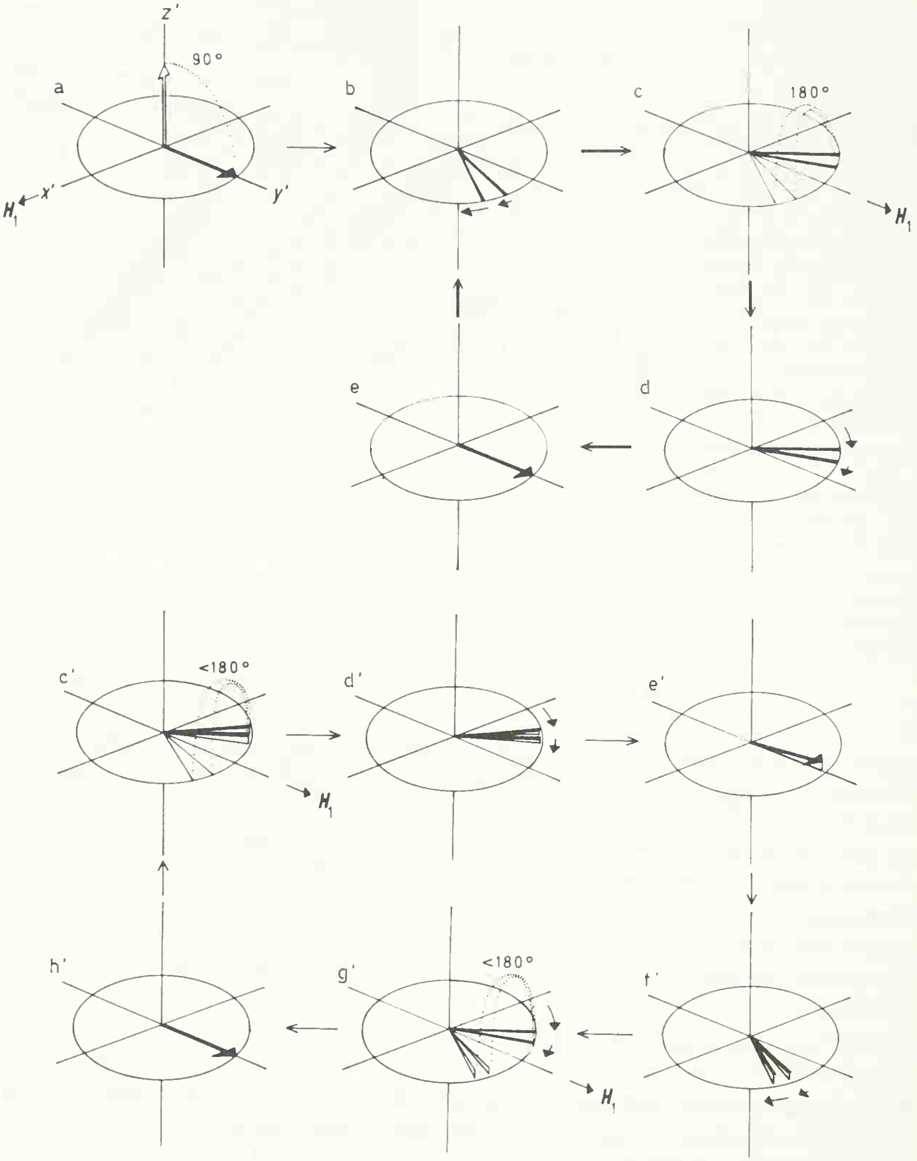

Fig. 2.27. Motion of the magnetization vector M_0 driven by a 90°, τ, 180°, 3τ, 180°, 5τ, ... pulse train during a CPMGSE experiment.

In (a)–(e), the 180° pulses are supposed to be exactly adjusted. In practice, this is usually not the case. The Figs. (c')–(h') account for such maladjustments: If the pulse angles are slightly smaller than 180°, the first 180° pulse causes the spins to rephase above the x', y' plane (e'). As a result, the measurable component of transverse magnetization in the x', y' plane is slightly reduced, and so is the amplitude of the first echo and all subsequent odd echoes. The second 180° pulse maladjusted like the first one, is just large enough to refocuse the spins exactly in the x', y' plane (h'). Therefore, the second echo and all subsequent even echoes have the correct amplitude.

are modulated. In this case, the Fourier transformation of an FID signal somewhere in the echo train must be computed in order to obtain the T_2 of individual nuclei. Spin-locking Fourier transform experiments are a modification of the CPMGSE-FT concept.

If a CPMG pulse train is applied at very small pulse intervals τ, dephasing of the magnetization vectors away from y' is restricted. The spins are forced to precess almost in phase with the y' axis of the rotating frame ("spin-locking") [47]. This situation is approached when the 90° pulse along x' is followed by an rf field H_1 applied along y' continuously for t seconds. During this period t, the magnetization is aligned along y', decaying at a rate determined by the spin-lattice relaxation time in the rotating frame, $T_{1(\mathrm{rot})}$ [47]. For liquids, $T_{1(\mathrm{rot})}$ practically equals the spin-spin relaxation time T_2. When the continuous rf field is switched off after t s, the freely developing transverse magnetization gives rise to an FID signal which is Fourier transformed. Each individual line in the resulting PFT NMR spectrum has decayed to a fraction $e^{-t/T_{1(\mathrm{rot})}}$ of the equilibrium intensity A_0; A_0 is measurable by a PFT NMR experiment applying 90° pulses along x' to the totally relaxed spins. Since spin-locking largely reduces field inhomogeneity and diffusion influences on transverse relaxation, the signal intensity decay $A_t(t)$ can be approximated by an exponential.

$$A_t = A_0 e^{-t/T_{1(\mathrm{rot})}} = A_0 e^{-t/T_2}. \tag{2.29}$$

In analogy to the methods described for measuring T_1, T_2 is the reciprocal slope of a semilogarithmic plot of $(A_t - A_0)$ *versus* t, when the experiment is repeated for a series of different t.

The spin-locking FT method is illustrated in Fig. 2.29 for *o*-dichlorobenzene in a $^{13}C\{^1H\}$ experiment avoiding noise modulation of the decoupling frequency during application of the CW field [47]. The results are compared in Fig. 2.29 with T_1 measurements in order to demonstrate the relation between T_1 and T_2 in liquids: $T_1 \geqq T_2$.

2.8. Instrumentation

An NMR spectrometer capable of PFT measurements is a combination of a CW circuit such as found in conventional NMR spectrometers [1–5], a computer controllable pulse generator, and a small digital computer of core memory size 8–20 K. Fig. 2.30 outlines this experimental arrangement. The units necessary for CW experiments are connected by solid lines. Those additionally required for PFT spectroscopy are connected by dotted lines.

Besides a strong magnet, modern NMR spectrometers consist of at least two rf channels: one for field/frequency stabilization and one for each nucleus to be observed. One additional channel is required for each nucleus to be decoupled. $^{13}C\{^1H\}$ experiments thus require three channels: one for observing ^{13}C NMR (H_1); one for proton decoupling (H_2); one for field/frequency stabilization (H_0, mostly operating at deuterium Larmor frequency). The observing and decoupling frequencies, ν_1 and ν_2, must be synchronized and phase-locked. This is achieved by deriving both from one master oscillator. The stabilization frequency ν_0 is usually derived from the same master oscillator in order to compensate for variations in the observing and decoupling frequency.

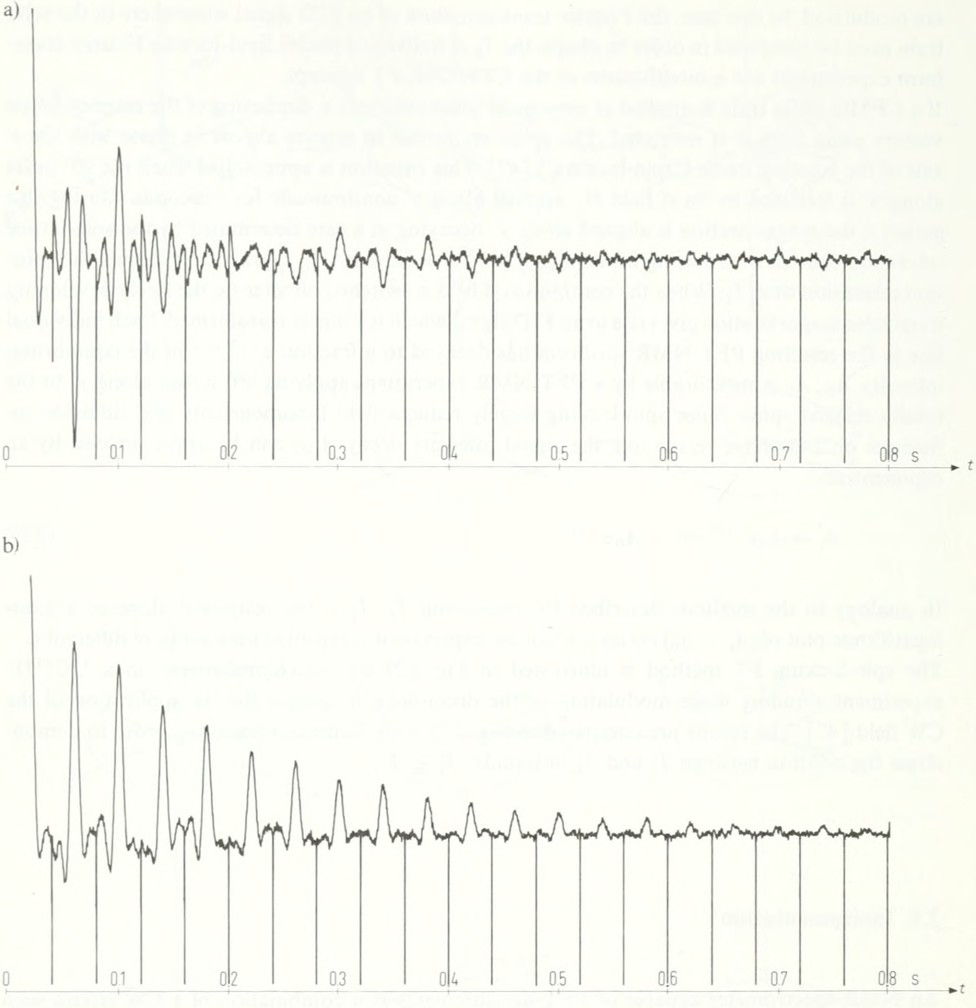

Fig. 2.28 a, b.

2.8.1. The Magnet

According to the Larmor equation (1.8), the strength of the magnetic field, H_0, determines the Larmor frequency of any nucleus as shown in Fig. 2.31. Magnetic fields between 1 and 3 Tesla and having the required homogeneity and stability are attainable by electromagnets. Commercially available instruments include magnets of 2.114 and 2.35 Tesla (1 Tesla = 10 kilogauss). For these fields, the range of Larmor frequencies of nuclei interesting in organic structure analysis can be obtained from Fig. 2.31, *e.g.*:

2.114 Tesla: ^{13}C: 22.63 MHz; ^{1}H: 90 MHz; ^{2}H: 13.82 MHz.
2.35 Tesla: ^{13}C: 25.2 MHz; ^{1}H: 100 MHz; ^{2}H: 15.3 MHz.

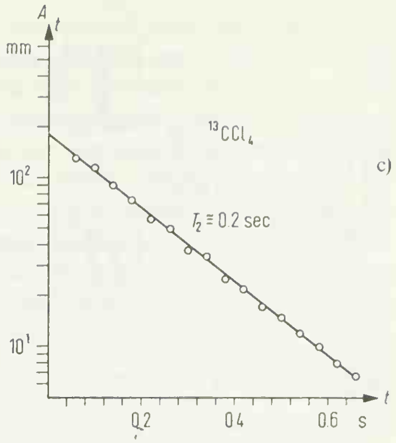

Fig. 2.28. Spin-echo trains for the determination of the ^{13}C spin-spin relaxation time T_2 of carbon tetrachloride; neat liquid sample, 90% ^{13}C enriched; 25 °C;

(a) Carr-Purcell sequence: the 180° pulses are applied in phase with the initial 90° pulse; the phase of subsequent echo signals alternates;

(b) Carr-Purchell-Meiboom-Gill sequence: the 180° pulses are applied perpendicularly to the initial 90° pulse; subsequent echoes have the same phase;

(c) Semilogarithmic plot A_t *versus* t (data from Fig. (b)) for the determination of T_2. (a) and (b) by B. Knüttel, Bruker Physik AG, Karlsruhe-Forchheim, Germany.

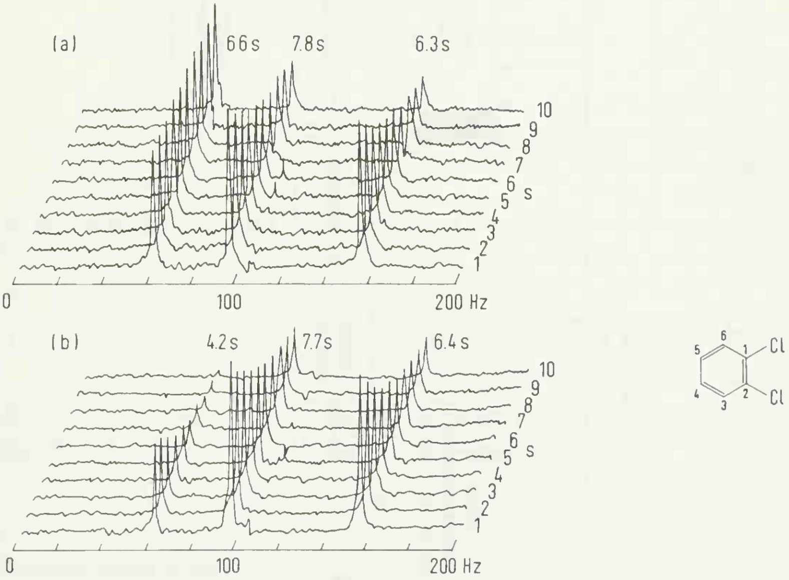

Fig. 2.29. Relaxation times of ^{13}C nuclei in *o*-dichlorobenzene [47] by $^{13}C\{^1H\}$ NMR.

(a) Spin-lattice relaxation times by an inversion-recovery experiment (the differences of signal amplitudes, $(A_\infty - A_\tau)$, are plotted *versus* δ and τ);

(b) Spin-spin relaxation times by a spin-locking FT experiment. (Reproduced by permission of the copyright owner from R. Freeman and H. D. W. Hill, J. Chem. Phys. *55*, 1985 (1971).)

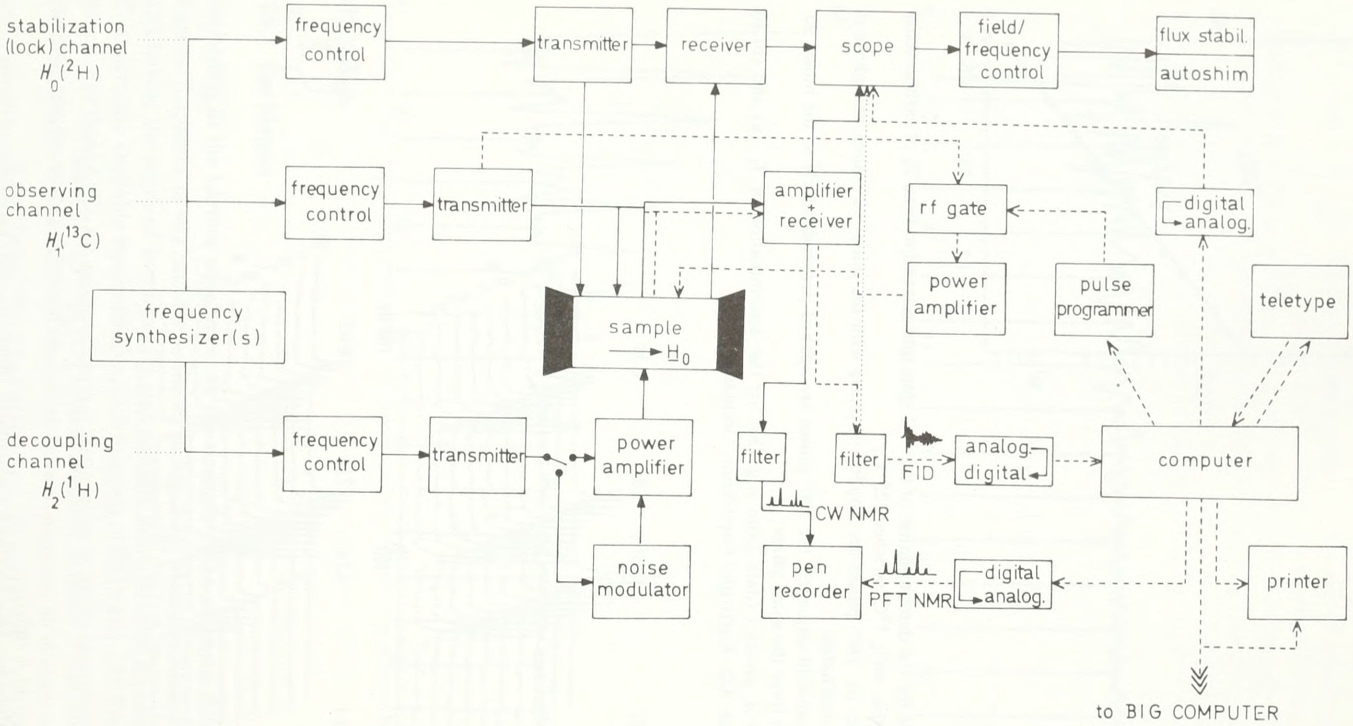
stabilization
(lock) channel
$H_0(^2H)$
observing
channel
$H_1(^{13}C)$
decoupling
channel
$H_2(^1H)$
frequency synthesizer(s)
frequency control
frequency control
frequency control
transmitter
transmitter
transmitter
receiver
scope
field/frequency control
flux stabil.
autoshim
amplifier + receiver
rf gate
power amplifier
pulse programmer
digital analog.
teletype
sample
$\underline{H}_0$
power amplifier
noise modulator
filter
filter
FID
analog. digital
computer
CW NMR
pen recorder
PFT NMR
digital analog.
printer
to BIG COMPUTER

Fig. 2.30. Schematic diagram of an NMR spectrometer, operating at CW (solid connections) as well as PFT (dotted connections), and also equiped for double resonance.

The stronger the magnetic field H_0, the better the line separation of chemically shifted nuclei in the frequency scale according to eq. (1.8c). Since coupling constants remain unaffected by the magnetic field strength, multiplet overlapping decreases with increasing field strength, and homonuclear couplings ($^1H-^1H$, $^{19}F-^{19}F$, $^{13}C-^{13}C$) become small compared to chemical shift differences in Hz. Thus, the homonuclear multiplets also approach A_mX_n systems (Section 1.10.4), assignable by following the multiplicity rule (1.45). Moreover, the population of the lower spin level increases with increasing field according to eq. (1.10), leading to a corresponding increase in the sensitivity of the NMR experiment. In conclusion, analysis of homo- and heteronuclear coupled NMR spectra becomes much easier and sensitivity is increased by high-field NMR. High-field NMR is realized in superconducting solenoids giving rise to magnetic fields of 5 – 10 Tesla. The range of Larmor frequencies for common nuclei at these fields also follows from Fig. 2.31:

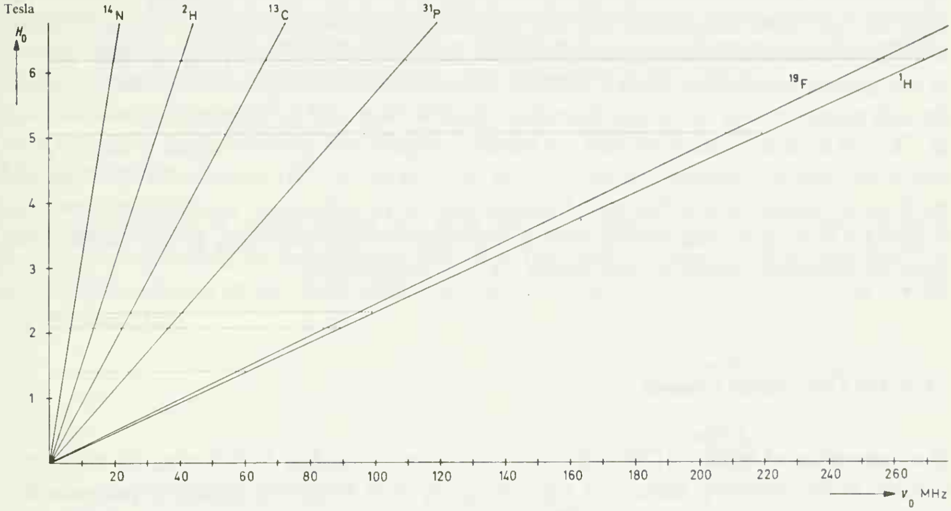

Fig. 2.31. Magnetic field strength and Larmor frequency range of some nuclei interesting for organic structure analysis.

5.06 Tesla: ^{13}C: 55.45 MHz; ^1H: 220 MHz; ^2H: 33.65 MHz.
6.18 Tesla: ^{13}C: 67.88 MHz; ^1H: 270 MHz; ^2H: 41.46 MHz.

2.8.2. The Stabilization Channel (Lock)

"CATing" of CW spectra, coherent accumulation of FID signals, and multipulse experiments necessary for measuring relaxation times require field/frequency stabilization, *i.e.* the ratio of magnetic field strength to transmitter frequency must be held constant. This is usually accomplished by electronically "locking on" to a strong, narrow signal and compensating any tendency for the signal to drift – caused by small field or frequency variations – with corresponding changes in the field strength.

Following eq. (1.8) and Fig. 2.31, the field/frequency ratio must not necessarily be stabilized for the nuclei to be observed (homonuclear lock). It can also be adjusted for any other nucleus (heteronuclear lock).

The homogeneity of the static field H_0 is optimized by changing the currents in shim coils placed in the air gap of the magnet until maximum signal and ringing is reached (optimum signal : noise and resolution). The current in the y gradient shim coils can be automatically controlled for maximum signal and homogeneity (autoshim) during the long measuring periods required for CAT experiments or FID signal accumulations of weak samples. Computer controlled autoshim of the y^2 gradient is also possible.

Homonuclear stabilization causes a strong interference beat in the NMR spectrum stemming from the lock signal. This interference may lead to computer memory overflow during spectrum or FID accumulation before the sample signals have reached significant signal : noise. In view of the inherent insensitivity of the ^{13}C NMR experiment, a heteronuclear lock is usually chosen for such measurements. An intense deuterium signal is often used for heteronuclear stabilization in ^{13}C NMR, as deuterated solvents are readily available and cause no signal at all (D_2O) or only weak narrow multiplets due to $^{13}C-^{2}H$ coupling in $^{13}C\{^{1}H\}$ experiments. Alternatively, the fluorine resonance of a fluorinated sample additive or solvent (*e.g.* hexafluorobenzene) can be used for locking, fluorine being a more sensitive nucleus than deuterium. Proton stabilization, however, obviously cannot be used during $^{13}C\{^{1}H\}$ experiments.

2.8.3. The Observation Channel

The observation of NMR by CW techniques [1–5] can be recalled by following the solid connections in the observing channel of Fig. 2.30, going from frequency control to pen recorder. Similarly, the operating concept of PFT NMR can be recognized by following the dotted connections in Fig. 2.30, going from pulse programmer *via* sample and computer to pen recorder.

The computer controllable pulse programmer generates dc pulses. These pulses gate the rf input signal of the H_1 transmitter, adjusted to the spectral width Δ according to Fig. 2.7 by the frequency control. The widths of the resulting rf pulses are adjustable for 90° or 180° by maximizing or minimizing FID signals displayed on a scope. In addition, various pulse sequences can be programmed. The rf pulses are amplified and fed to the tuned circuit of transmitter coil and receiver. The FID output signal is filtered, amplified, and digitized. Before performing the Fourier transformation, the accumulated FID signal can be observed on a scope in order to determine if the signal : noise is satisfactory.

After the Fourier transformation, the effects on the spectrum of data manipulations such as phase adjustments can be observed on a scope before giving final calculating commands. Communication with the computer is generally *via* teletype, which can also serve as paper tape reader/puncher. Light pen control *via* oscilloscope is also possible.

The PFT NMR spectrum can then be plotted in analog form by a pen recorder controlled by the computer. If the computer core memory allows, additional subroutines may be stored which automatically compute signal intensities and positions (in ppm values relative to some standard or in Hz) and outputs them to the teletype or line printer.

The data can be fed into a larger computer. Using a bank of chemical shift data and coupling constants of several thousand compounds, stored on magnetic tapes, and the appropriate software, structural assignments by the computer are possible [48].

2.8.4. The Decoupling Channel

According to eq. (2.22), the rf power of decoupling fields H_2 is much stronger than that of observing fields H_1. Therefore, the rf transmitter power of the decoupling channel must be amplified before being fed to the transmitter coil. For decoupling of large Larmor frequency ranges, wide frequency bands must be generated by modulation with white noise of adjustable band width ($\lessapprox 30\,\mathrm{kHz}$). For broad band decoupling, H_2 is amplified and noise modulated; off-resonance decoupling in $^{13}C\{^1H\}$ experiments is mostly achieved without noise modulation. In order to obtain coupling constants without sacrificing NOE signal: noise enhancements, H_1 and H_2 can be gated alternately by the pulse generator as outlined in Section 2.6.6.

2.8.5. The Sample

The sample solution is usually placed in a glass tube of diameter 5, 8, 10, or 15 mm, which is rotated perpendicularly to the magnetic field H_0. This trick averages the magnetic field for each sample molecule so that homogeneity is improved within the sample and sharper signals are obtained [49].

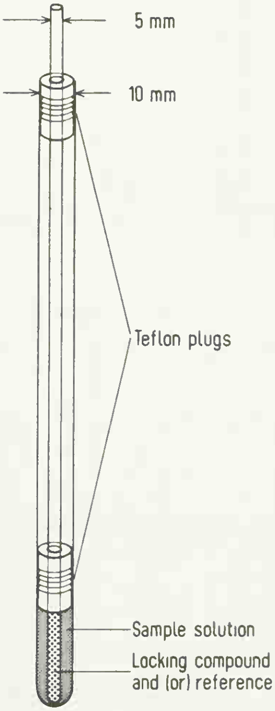

Fig. 2.32. Coaxially centered sample tubes for external lock or reference.

For ^{13}C experiments, the sample is usually prepared by dissolving the compound to be investigated in a deuterated solvent which is usually required for field/frequency stabilization. For calibration, a small amount of a reference compound (*e.g.* carbon disulfide or tetramethylsilane) is added to the sample.

If the reference compound does not dissolve in the sample solution it can be used externally in a capillary coaxially centered in the sample tube by teflon plugs as illustrated in Fig. 2.32. This is also advantageous if the reference signal causes or suffers from solvent shifts. The use of external references requires susceptibility corrections of chemical shifts according to eq. (1.44), with reference to volume susceptibility tables (*e.g.* in ref. [2]). The deuterated locking compound can also be used externally, for instance because of solubility reasons, if deuterium/hydrogen exchange is to be expected, or if the pH dependences of chemical shifts are to be measured. In order to obtain relaxation times accurately by multipulse experiments, the samples should be degassed, particularly to remove dissolved oxygen. The sample insert temperature can be registered thermoelectrically and adjusted for low or high temperatures by a stream of cooled or heated nitrogen gas. High rf powers used for decoupling considerably increase the insert temperature so that cooling is required for sensitivity reasons (eq. (1.10)) and in order to protect sample and insert.

3. ^{13}C NMR Spectral Parameters and Structural Properties

3.1. Chemical Shifts

3.1.1. A Comparison of ^{13}C and ^{1}H Shifts

Magnetic field strengths used in ^{13}C NMR at present usually are between 2 and 2.5 Tesla, corresponding to ^{13}C Larmor frequencies between 20 and 25 MHz (Fig. 2.31). The range Δ of ^{13}C chemical shifts of all organic compounds measured so far and including reactive intermediates such as carbonium ions approaches 400 ppm or 10 kHz at 25 MHz. The average ^{13}C line widths $\Delta \nu_{1/2}$ now attainable are about 1 Hz, *i.e.* on the same order as those observed in ^{1}H NMR.

In order to observe efficient structural resolution, chemical shifts must provide a high spectral width to line width ratio $\Delta : \Delta \nu_{1/2}$. This ratio is about 10 kHz : 1 Hz or 10^4 for ^{13}C at 25 MHz, or one power of ten higher than that observed in ^{1}H NMR at the same field and 100 MHz with $\Delta \nu_{1/2} = 1$ Hz and $\Delta = 1$ kHz. A comparison of signal separation in ^{1}H and ^{13}C NMR at the same magnetic field strength is given in Fig. 3.1.

Together with the large number of correlations now available between ^{13}C chemical shifts and structures, its high $\Delta : \Delta \nu_{1/2}$ ratio makes ^{13}C the NMR nucleus of choice for structural analysis of organic compounds using chemical shifts. Furthermore, ^{13}C chemical shifts provide more direct information concerning the carbon skeleton than do proton shifts, and ^{13}C NMR spectra are often more easily assignable than homonuclear coupled ^{1}H NMR spectra. This is not only

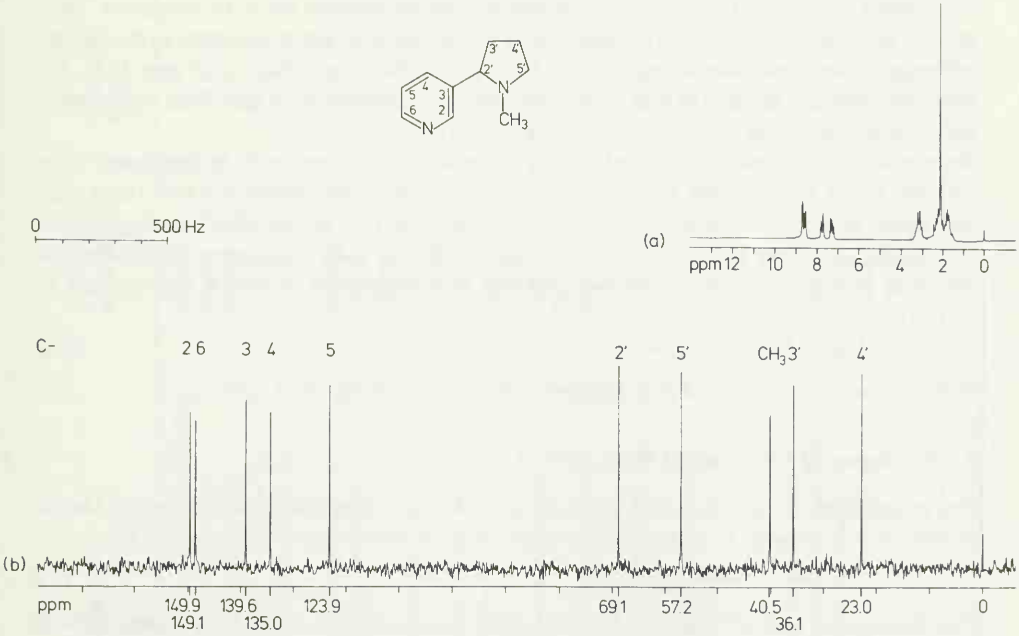

Fig. 3.1. Nicotine, 75 Vol.% in hexadeuterioacetone at 25 °C;
(a) 80 MHz ^{1}H NMR spectrum;
(b) 20 MHz ^{13}C NMR spectrum, proton broadband decoupled.
Both spectra have been recorded at the same magnetic field strength with identical frequency scales.

due to the spectrum simplification and sensitivity enhancement by broad band or off-resonance proton decoupling in ^{13}C NMR, but also to the low natural abundance of ^{13}C, which assures that complicating homonuclear $^{13}C-^{13}C$ couplings are lost in the noise as long as ^{13}C enriched compounds are not measured.

3.1.2. Referencing ^{13}C Chemical Shifts

Any heteronuclear or homonuclear signal of a solvent or an added reference substance can be used for referencing ^{13}C shifts. For example, ^{13}C shifts can be directly measured relative to a deuterium signal of the deuterated solvent usually required for field/frequency stabilization. However, homonuclear shift references such as the ^{13}C signals of tetramethylsilane (TMS), carbon disulfide, benzene, cyclohexane, 1,4-dioxane or the easily localizable multiplet signals of deuterated solvents (Fig. 2.18) are predominantly applied in ^{13}C NMR.

For ^{13}C shift/structure correlations and for tabulations of ppm values one generally accepted reference should be used. Carbon disulfide, which appears in the low field region of ^{13}C spectra, was widely used in the literature [50a, b]. But there is a trend toward the proton shift reference TMS in ^{13}C NMR, particularly because of some parallel behaviors in ^1H and ^{13}C shifts.

Neither CS_2 nor TMS are ideal standards. The ^{13}C signal of CS_2 and carbonyl carbons overlap, as do the ^{13}C signals of cyclopropane and some methyl carbons with TMS (Fig. 3.3). Furthermore, the ^{13}C resonance of TMS has been shown to suffer from medium shifts on the order of ± 0.1 to ± 1.5 ppm in common NMR solvents even at infinite dilution [51]. This must be considered if ^{13}C shifts relative to TMS of one compound in different solvents are to be compared. There are two alternative methods to overcome this problem: one is to use cyclohexane as the internal reference; cyclohexane was shown to have ^{13}C solvent shifts lower than ± 0.5 ppm [51]. The other alternative is to use TMS as an external reference (Sections 1.9.3 and 2.8.5) and to make bulk susceptibility shift corrections according to eq. (1.50).

Since medium shifts may be expected for any resonance, the solvent must be mentioned when ^{13}C shift values are tabulated. In this work, all ^{13}C shifts are given relative to TMS. Those shifts that where originally reported relative to other references (*e.g.* carbon disulfide, δ_{CS_2}, or 1,4-dioxane, $\delta_{C_4H_8O_2}$), have been converted into shifts relative to TMS (δ_{TMS}) using the known shift difference between common reference substances as illustrated in Table 3.1 and outlined by eq. (3.1):

$$\delta_{TMS} = 192.5 + \delta_{CS_2} = 67.6 + \delta_{C_4H_8O_2} = \cdots \tag{3.1}$$

However, conversion errors due to medium shifts may be as high as 1 ppm.

3.1.3. A Survey of ^{13}C Chemical Shifts [50a–k]

The magnetic shielding constant σ_i (eq. 1.39) arises from all chemical influences on the Larmor frequency of a nucleus. It is described in terms of three additive contributions (eq. 3.2):

$$\sigma_i = \sigma^{dia} + \sigma^{para} + \sigma^{N}. \tag{3.2}$$

The diamagnetic term σ^{dia} accounts for local electronic circulations around the nucleus induced by the applied field H_0. According to the Lenz rule, the resultant intramolecular field opposes H_0 so that the nucleus will be shielded. As known from the Lamb formula 3.3 [9],

$$\sigma^{dia} \propto r^{-1}, \tag{3.3}$$

Table 3.1. ^{13}C Data of Common Deuterated Solvents and of Their ^{1}H Isotopes.

Compound	C – D Signal multiplicity	C – D Coupling constants [Hz]	^{13}C Shifts [ppm]	isotopic ^{1}H Compound	
				^{13}C Shift [ppm]	C – H Coupling constant [Hz]
Dideuteriomethylenchloride	Quintet	27	53.1	53.8	177.5
Deuteriochloroform	Triplet	32	77.0 ± 0.5	78.0 ± 0.5	210.5
Deuteriobromoform	Triplet	31.5	10.2	10.3	205
Trideuterionitromethane	Septet	23.5	60.5	61.1	146.5
Trideuterioacetonitrile	Septet	21	1.3	1.7	117.4
	*)	< 1	118.2	118.2	< 5
Tetradeuteriomethanol	Septet	21.5	49.0	49.9	141
Hexadeuterioethanol	Septet	19.5	15.8	16.9	127
	Quintet	22	55.4	56.3	140.5
Decadeuteriodiethylether	Septet	19	13.4	14.5	127
	Quintet	21	64.3	65.3	142
Octadeuterio-1,4-dioxane	Quintet	22	66.5	67.6	146
Octadeuteriotetrahydrofuran	Quintet	20.5	25.2	26.2	132
	Quintet	22	67.4	68.2	137
Hexadeuterioacetone	Septet	20	29.8	30.7	126
	*)	< 1	206.5	206.7	7.5
Hexadeuteriodimethylsulfoxide	Septet	21	39.7	40.9	137
Tetradeuterioacetic acid	Septet	20	20.0	20.9	129
	*)	< 1	178.4	178.8	7.5
Heptadeuteriodimethylformamide	Septet	21	30.1	30.9	138
	Septet	21	35.2	36.0	138
	Triplet	30	167.7	167.9	188
Octadecadeuteriohexamethylphosphoramide	Septet	21	35.8	36.9	129.5
Dodecadeuteriocyclohexane	Quintet	19	26.4	27.8	126
Hexadeuteriobenzene	Triplet	24	128.0 ± 0.5	128.5 ± 0.5	161
Pentadeuteriopyridine	Triplet (3,5)	25	123.5	124.2	166
	Triplet (4)	24.5	135.5	136.2	163
	Triplet (2,6)	27.5	149.2	149.7	177

*) long-range multiplet, not resolved.

the diamagnetic term decreases with distance r between nucleus and circulating electrons. Thus, s electrons will cause a stronger shielding than p electrons ($r_s : r_p = 1 : \sqrt{3}$!), and for atoms with s electrons only such as hydrogen, σ^{dia} is the dominant shielding term.

The contribution σ^N is referred to as the neighbour anisotropy effect. This term accounts for the fields arising from electronic circulations around the atoms surrounding the observed nucleus. It depends on the nature of the neighbour atoms and on molecular geometry. – Sometimes, a medium term must be added in eq. (3.2), correcting for solvent and pH effects.

For nuclei other than hydrogen such as ^{13}C, the paramagnetic shielding term σ^{para} predominates. It opposes σ^{dia} and deshields therefore. According to eq. 3.4 derived by Karplus and Pople [52],

$$\sigma^{para} = -\frac{e^2 h^2}{m^2 c^2} \Delta E^{-1} \, r_{2p}^{-3} \left[Q_{AA} + \sum Q_{AX}\right] \tag{3.4}$$

the paramagnetic term increases with a decreasing mean electronic excitation energy ΔE and with the inverse cube r_{2p}^{-3} of the distance between a 2p electron and the nucleus. It further depends on the number of electrons occupying the p orbital (Q_{AA}) and multiple bond contributions ($\sum Q_{AX}$). Both is summarized in the $[Q_{AA} + \sum Q_{AX}]$ factor also known as the charge density bond order matrix in the MO formalism.

The connection between ^{13}C shielding and electronic excitation agrees with the fact that carbonyl compounds are most deshielded ($\delta_c > 170$ ppm, $n \rightarrow \pi^*$ transitions with $\Delta E \approx 7$ eV) when compared with alkenes and aromatic compounds ($\delta_c \approx 100-150$ ppm, $\pi \rightarrow \pi^*$ transitions with $\Delta E \approx 8$ eV) and alkanes ($\delta_c < 50$ ppm, $\sigma \rightarrow \sigma^*$ transitions with $\Delta E \approx 10$ eV).

Fig. 3.2 reflects the dependence of σ^{para} on r_{2p}^{-3}: The ^{13}C shifts of non-benzenoid aromatic ions correlate linearly with the π electron density relative to benzene ($Q_\pi = 1$) [53]. In the negative ions, for example, an increased π electron density at the carbons causes electronic repulsion. As a result, the bonding orbitals expand, r increases, σ^{para} decreases and the carbons are more shielded. The upfield shift of 160 ppm per additional π-electron as found in Fig. 3.2 illustrates that the large ^{13}C chemical shift range can be mainly attributed to the r_{2p}^{-3} dependence of σ^{para}.

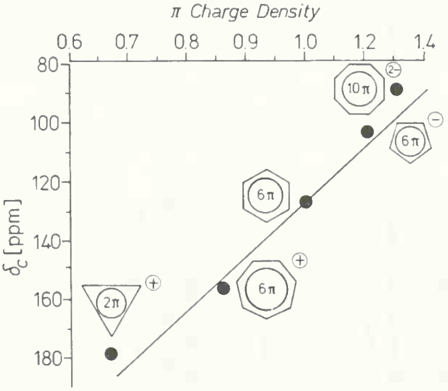

Fig. 3.2. π-Electron Density *versus* ^{13}C Chemical Shift of Ring Carbons in Benzene and Non-Benzenoid Monocyclic Aromatic Ions [53].

Generally, ^{13}C chemical shifts correlate with some typical properties of carbon within its molecular environment discussed in the following.

3.1.3.1. Carbon Hybridization

The hybridization of a carbon determines to a great extent the range within which its ^{13}C signal is found. As illustrated in Fig. 3.3, sp^3 carbons resonate at highest field, followed by sp carbons, while sp^2 hybridized centers are shifted farthest to low field. The hybridization effect in ^{13}C NMR thus parallels the effect observed in ^1H NMR. The ^{13}C resonances of sp^3 carbons are found between -20 and 100 ppm relative to TMS; sp carbons resonate from 70 to 110 ppm; the low field sp^2 carbon signals occur at 120 to 240 ppm in organic compounds.

3.1.3.2. Electronegativity [50]

A correlation of ^{13}C chemical shifts with substituent electronegativities is found for the α carbons in many classes of compounds as is illustrated for the halohexanes in Table 3.2.

Table 3.2. ^{13}C Shift Increments $Z = \delta_{RX} - \delta_{RH}$ [ppm] Induced in Hexane by Halogenation of a Terminal Hydrogen.

	$\overset{\alpha}{X-CH_2}$	$\overset{\beta}{CH_2}$	$\overset{\gamma}{CH_2}$	$\overset{\delta}{CH_2}$	$\overset{\varepsilon}{CH_2}$	$\overset{>\varepsilon}{CH_3}$
X=H	δ = 14.2	23.1	32.2	32.2	23.1	14.2
X=J	Z = −7.2	10.9	−1.5	−0.9	0.0	0.0
X=Br	Z = 19.7	10.2	−3.8	−0.7	0.0	0.0
X=Cl	Z = 31.0	10.0	−5.1	−0.5	0.0	0.0
X=F	Z = 70.1	7.8	−6.8	0.0	0.0	0.0

This is explained in terms of increasing electron withdrawal from the α carbon orbitals with increasing electronegativity of the substituent. Correspondingly, a larger r^{-3} in eq. (3.4) and hence a deshielding occurs.

The bond polarization due to electronegative substituents should propagate along the carbon chain and decrease with the inverse cube of the distance. Much smaller inductive effects are thus expected in β and γ position. Table 3.2 shows, however, that the observed β and γ effects do not correlate at all with substituent electronegativities and other influences must be involved therefore.

3.1.3.3. Crowding of Alkyl Groups and Substituents [50, 63]

Increasing crowding of alkyl groups or electron withdrawing substituents at a carbon causes a successive downfield shift of its ^{13}C resonance (Table 3.3). Similarly, crowding of shielding heteroatoms such as iodine successively reinforces upfield shifts (Table 3.3).

Table 3.3. ^{13}C Chemical Shifts δ_C [ppm] of Halogenated and Alkylated Methane Derivatives.

−2.3	23.8	52.8	77.7	95.5	X = Cl
CH_4	CH_3X	CH_2X_2	CHX_3	CX_4	
	−21.8	−55.1	−141.0	−292.5	X = I

	5.7 CH_3R
	15.4 CH_2R_2
	24.3 CHR_3
R = CH_3	31.4 CR_4

3.1.3.4. Unshared Electron Pairs at Carbon

An unshared electron pair at a terminal carbon causes a downfield shift of its ^{13}C resonance. A comparison of carbon dioxide with carbon monoxide and nitrile with cyanide anion and isocyanide [54] illustrates this:

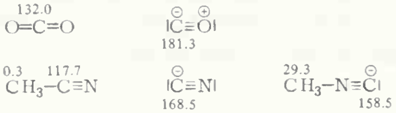

On the other side, odd numbered carbons in conjugated dienyl anions are shielded [55]:

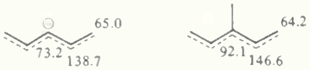

This was explained by MO approximations in terms of a change of the charge density bond order term in eq. (3.4).

3.1.3.5. Electron Deficiency at Carbon

Electron deficiency at a carbon causes drastic deshielding. This is observed for the sp^2 carbons typical of carbocations [56]. In such systems, the sp^2 ^{13}C chemical shift range may approach 400 ppm relative to TMS. If the positive charge is dispersed in a carbocation, *e.g.* by resonance, the electron deficient carbon will be more shielded. The following comparison of *t*-butyl-, dimethylhydroxy- and dimethylphenyl-carbenium ion illustrates this:

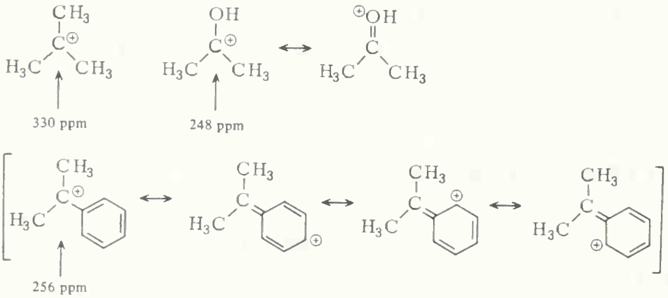

Downfield shifts due to electron deficiency are observed for carbene metal complexes [57a] and for the sp carbons of metal carbonyls [57b].

3.1.3.6. Mesomeric Effects

The ^{13}C chemical shifts of benzenoid carbons largely depend on the mesomeric interaction between substituent und benzene ring. Electron releasing substituents (*e.g.* $-\bar{N}H_2$, $-\bar{O}H$) will increase the electron density at the *o*- and *p* carbons relative to benzene (128.5 ppm), while slight electron deficiencies will be induced by electron withdrawing groups (*e.g.* $-NO_2$, $-CN$).

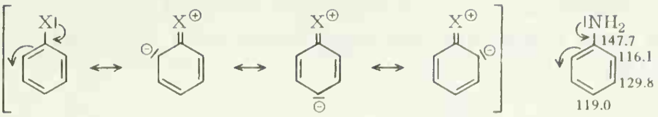

Aniline

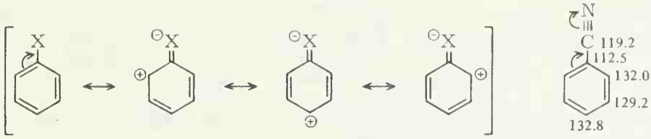

Benzonitrile

These formulae explain that the *o*- and *p* carbons of monosubstituted benzenes are shielded by electron releasing substituents but deshielded by electron acceptors while the *m* carbons remain almost unaffected by both kinds of substituents [50].

Inductive and electric field effects of the substituents may overlap to the *o*-mesomeric effects. But the *m* and *p* shifts of monosubstituted benzenes mostly follow the pattern discussed above.

Conversely, ^{13}C chemical shifts may reflect the contribution of polar species to the bonding state of a molecule. As an example, the methylene sp^2 carbon shielding in diazomethane and ketene indicates that the carbanionic polar states of both molecules are significant [58].

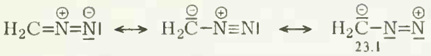

$$H_2C{=}\overset{\oplus}{N}{=}\overset{\ominus}{\underline{N}}| \longleftrightarrow H_2\overset{\ominus}{\underline{C}}-\overset{\oplus}{N}{\equiv}N| \longleftrightarrow H_2\underset{23.1}{\overset{\ominus}{\underline{C}}}-\underline{N}{=}\overset{\oplus}{\underline{N}}$$

Diazomethane

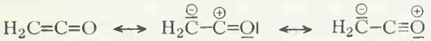

$$H_2C{=}C{=}O \longleftrightarrow H_2\overset{\ominus}{\underline{C}}-\overset{\oplus}{C}{=}\underline{O}| \longleftrightarrow H_2\underset{2.5}{\overset{\ominus}{\underline{C}}}-\underset{194.0}{C}{\equiv}\overset{\oplus}{\underline{O}}$$

Ketene

In α,β-unsaturated carbonyl compounds, a distinct deshielding of the β-olefinic carbon clearly responds to the polarized state:

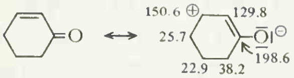

2-Cyclohexenone

3.1.3.7. Conjugation

The decrease of bonding order arising from delocalization of multiple bonds in conjugated systems results in a shielding of the central carbon atoms. This can be clearly seen by comparison of the pairs 1-butene/1,3-butadiene and *cis*-3-octene/*cis*-*cis*-3,5-octadiene:

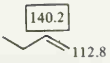

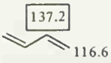

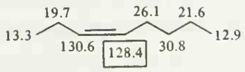

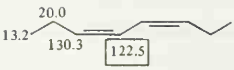

In a similar manner, carbonyl carbons in α,β-unsaturated aldehydes, ketones and carboxylic acids are shielded by about 10 ppm when compared with those of corresponding saturated carbonyl compounds [50]:

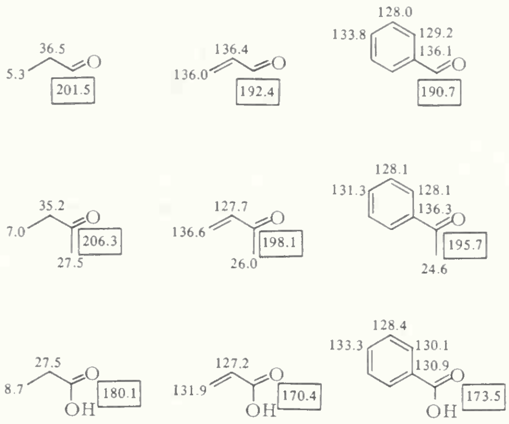
36.5
5.3
O
201.5
136.4
136.0
O
192.4
128.0
133.8
129.2
136.1
O
190.7
35.2
7.0
O
206.3
27.5
127.7
136.6
O
198.1
26.0
128.1
131.3
128.1
136.3
O
195.7
24.6
27.5
8.7
O
180.1
OH
127.2
131.9
O
170.4
OH
128.4
133.3
130.1
130.9
O
173.5
OH

3.1.3.8. Steric Interactions

Steric interactions, mostly arising from touching or overlapping of Van der Waals radii of closely spaced hydrogens usually causes a shielding of the carbons attached to these hydrogens. The steric perturbation of the C – H bond involved causes the charge to drift towards carbon; the bonding orbitals at carbon expand and a shielding will arise according to eq. (3.4) [59]:

In saturated open-chain and cyclic systems [64 – 66], the steric effect on carbon shielding is observed when two hydrogenated carbons are *γ-gauche* relative to each other. In mobile open-chain alkanes with *gauche* rotamer populations of approximately 30%, shieldings of about −2 ppm are observed for the γ carbon when a methyl group is introduced in the α position. Other substituents (*e.g.* the halogens in table 3.2) cause γ effects of up to −7 ppm.

According to a simple model developed by Grant [59], the steric shift δ_{St} depends on the proton-proton repulsive force $F_{HH}(r_{HH})$, which is a function of the proton-proton distance r_{HH}, but also on the angle Θ between the H – H axis and the perturbed C – H bond:

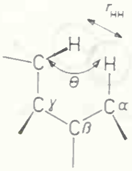
r_{HH}
H
C
H
Θ
Cγ
Cα
Cβ

$$\delta_{St} = \text{const.}\ F_{HH}(r_{HH}) \cos \Theta \qquad (3.5)$$

Eq. (3.5) shows that the sign of δ_{St} may change with Θ. In conclusion, steric interactions are not generally associated with upfield shifts.

Typical *γ-gauche* effects are observed in conformationally rigid systems such as methylcyclohexanes and methylnorbornanes [50, 64], *e.g.*:

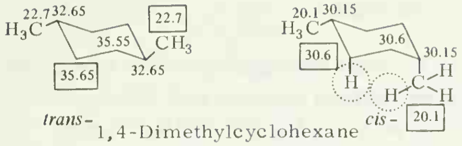
22.7
32.65
H_3C
35.55
35.65
32.65
22.7
CH_3
20.1
30.15
H_3C
30.6
30.6
30.15
H
C
H
H
H
20.1

trans- 1,4-Dimethylcyclohexane *cis*-

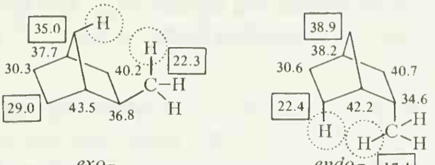
35.0
H
37.7
H
30.3
40.2
22.3
C–H
29.0
43.5
36.8
H
38.9
38.2
30.6
40.7
22.4
42.2
34.6
H
H
C
H
H
17.4

exo- 2-Methylnorbornane *endo*-

Another example of sterically induced upfield shifts is the $\delta_{trans} > \delta_{cis}$ relation characteristic of the carbons α to the double bond in *cis*- and *trans*-alkenes [50, 67], *e.g.*:

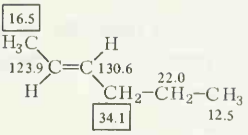
16.5
H_3C
H
123.9
C=C
130.6
22.0
H
CH_2–CH_2–CH_3
34.1
12.5

(E)-2-Hexene

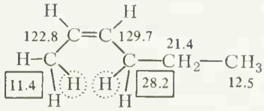
H
H
122.8
C=C
129.7
21.4
H–C
C
CH_2—CH_3
11.4
H
H
28.2
12.5
H
H

(Z)-2-Hexene

In conjugated systems, steric repulsion between alkyl groups may oppose conjugation and cancel the upfield shift characteristic of the conjugated state. This can be seen for a series of acetophenones and a relation between the torsion angle Φ of phenyl- and carbonyl bonding plane becomes obvious [50c], *e.g.*:

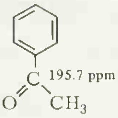
C
195.7 ppm
O
CH_3

$\Phi = 0°$

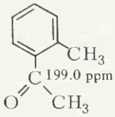
CH_3
C
199.0 ppm
O
CH_3

$\Phi \approx 28°$

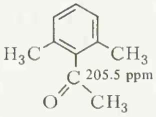
H_3C
CH_3
C
205.5 ppm
O
CH_3

$\Phi \approx 50°$

3.1.3.9. Electric Fields of Charged Substituents

Electric fields originating from charged substituents may also contribute to carbon shielding. The *o* carbons in nitrobenzene are an example; they are expected to be deshielded according to the mesomeric effect of the nitro group as outlined in section 3.1.3.6. In fact, a shielding of −5.3 ppm relative to the benzene carbons is observed. This can partially be explained by the intramolecular electric field of the nitro group which causes the charge of the *o* C−H bond to move towards the *o* carbon. A shielding for the latter will be the result.

Intramolecular electric fields also contribute to the pH induced shifts [61] discussed for basic and acidic groups in section 3.1.4.3.

3.1.3.10. Anisotropic Intramolecular Magnetic Fields

The neighbor anisotropy term σ^N of eq. (3.2) plays an important role in proton shielding, permitting for example a distinct differentiation between aromatic and olefinic protons due to the ring current effect. However, this contribution is small in ^{13}C NMR (<2 ppm). A comparison of the methyl carbon shieldings in methylcyclohexene and toluene shows that the ring current effect often cannot be clearly separated from other shielding contributions:

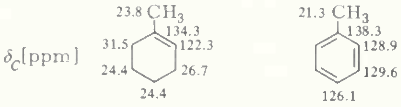

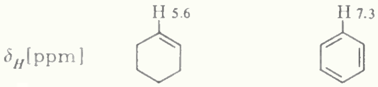

A small ring current was described for 1,4-dodecamethylene benzene [60]. The most shielded methylene carbons of this *ansa* compound shift upfield by 0.7 ppm relative to those in cyclopentadecane:

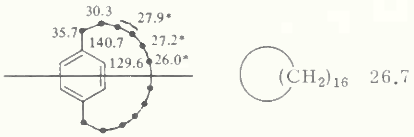

*Assignments interchangeable

3.1.3.11. Heavy Atoms

Tables 3.2 and 3.3 illustrated for iodine that heavy atom substitution causes a significant upfield shift of the substituted carbon. This is attributed to increased diamagnetic shielding caused by the large number of electrons introduced by heavy atoms.

3.1.3.12. Isotope Effect

Upfield shifts may also arise from substitution of an atom (*e.g.* ^1H) by its heavier isotope (*e.g.* ^2H). The upfield shift follows from a lower potential energy of the ground state, hence an increased ΔE in eq. (3.4), and a reduction of bond distance. Both influences will decrease the paramagnetic shielding term. Deuterium isotope shifts depend on the degree of deuteration and reach values of up to 1.5 ppm (Table 3.1).

3.1.3.13. Intramolecular Hydrogen Bridging

Intramolecular hydrogen bridging, *e.g.* in salicylaldehyde or *o*-hydroxyacetophenone involves the non-bonding electron of the carbonyl oxygen. As a result, the carbonyl carbon will be more positivated [50] so that a deshielding is observed:

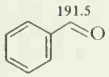

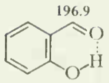

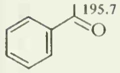

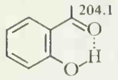

In a similar manner, intermolecular hydrogen bridges will cause a deshielding as is found for chloroform in pyridine (Table 3.4). If the hydrogen bridges are broken, *e.g.* by solvation in diluted solutions in non polar solvents (*e.g.* carbon tetrachloride or cyclohexane) upfield shifts have to be expected (Table 3.4).

3.1.3.14. Substituent Increments and Functional Group Shifts

Empirical additive substituent increments obtained by analysis of substituted alkanes, alkenes, cycloalkanes, aromatic and heteroaromatic compounds have proved to be useful for the prediction of ^{13}C chemical shifts. These substituent increments will be tabulated for the various classes of organic compounds in chapter 4.13.

Many functional groups containing carbon resonate within characteristic shift ranges. A selection of these shift ranges are outlined in Fig. 3.3 which also simply summarizes some previously discussed substituent effects on aliphatic carbon shiedling. Both a parallel and a significant difference to proton shift trends can be observed here. As in ^{1}H NMR, cyclopropane carbons are more deshielded than the ring carbons of other alicycles. In contrast to proton shifts, however, the ^{13}C signals of aromatic ring carbons overlap with the sp^{2} carbon signals of alkenes. This stems from the fact that the induced field attributed to the cyclic delocalization of π electrons in aromates [2–5] weakens the H_0 field in the center and strengthens it at the periphery of the ring, but does not significantly influence the ring carbons themselves.

3.1.4. Medium Shifts

3.1.4.1. Dilution Shifts

Dilution shifts of ^{13}C signals may reach a magnitude of several ppm. The ^{13}C resonance of methyl iodide dissolved in cyclohexane [68a] or tetramethylsilane [68b] shifts upfield by about 7 ppm upon dilution. Much smaller upfield dilution shift (0.5 ppm) are observed for the ^{13}C signal of chloroform in cyclohexane [69]. A constant shift independent of further dilution may be reached at lower concentrations. In this case, the solution behaves as if it were infinitely diluted in terms of chemical shifts. This was reported for substituted benzenes in trifluoroacetic acid at a solute concentration of 10 to 15 mol% [70].

3.1.4.2. Solvent Shifts

Solvent shifts of ^{13}C signals are often larger than those observed in ^{1}H NMR. Downfield shifts are found for both the ^{13}C and ^{1}H signal of chloroform in going from non-polar solvents such as cyclohexane or carbon tetrachloride to mediums susceptible to hydrogen bonding such as pyridine or hexamethylphosphoramide [69] (Table 3.4). The ^{13}C solvent shift range of chloro-

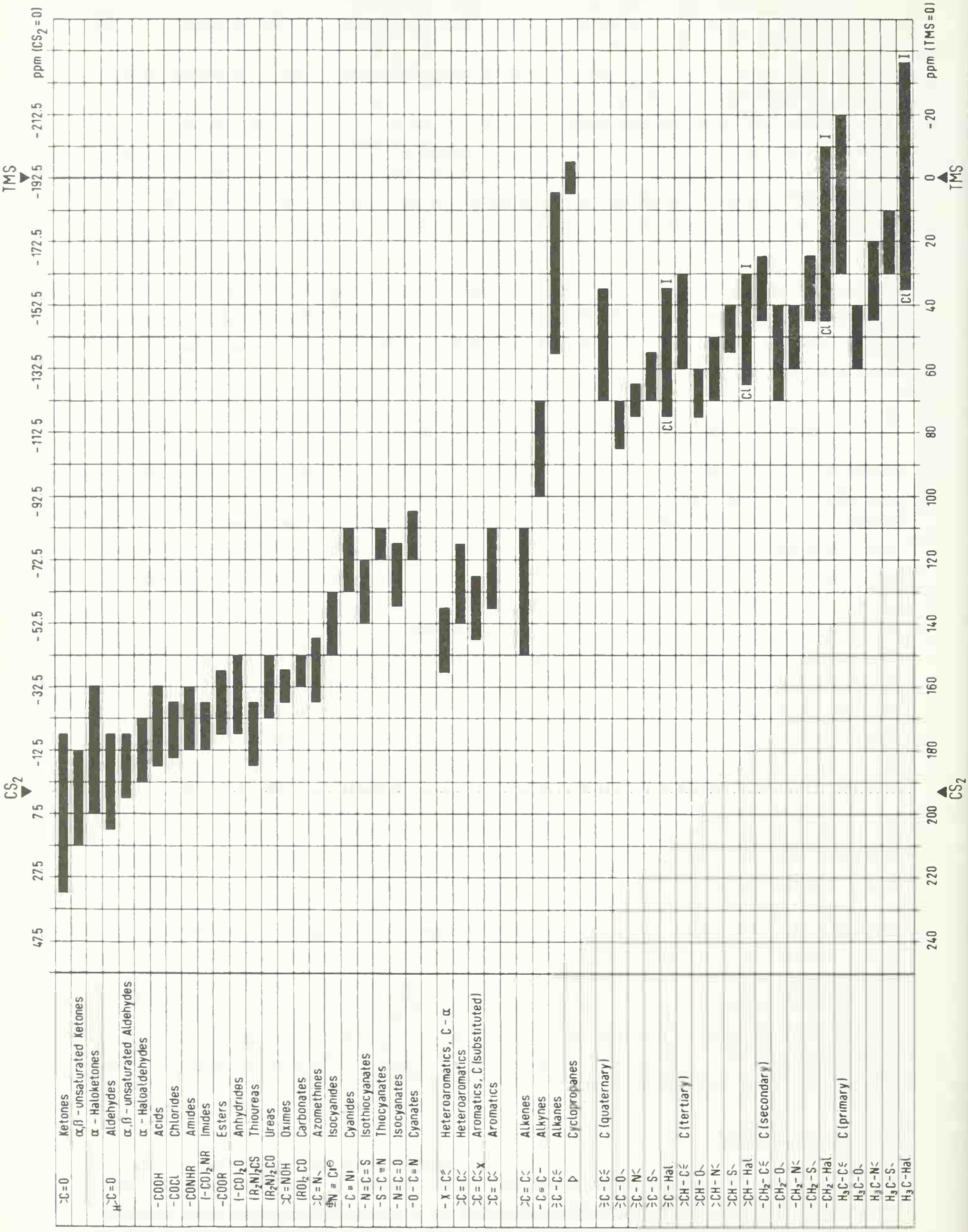

Fig. 3.3. ^{13}C Chemical shift ranges in organic compounds.

Table 3.4. Solvent ^{13}C and ^{1}H Shifts of Chloroform and $^{13}C-^{1}H$ One Bond Coupling Constants [69] (internal reference: cyclohexane; mole fraction of $CHCl_3$: 0.16; temperature: 45 – 50 °C).

Solvent	δ_C ppm	δ_H ppm	$J_{^{13}C-^{1}H}$ Hz
Cyclohexane	0.00	0.000	208.1
Carbon tetrachloride	0.20	0.120	208.4
Neat[a]	0.37	0.147	209.5
Benzene[b]	0.47	−0.747	210.6
Acetic acid	1.02	0.400	–
Nitromethane	1.12	0.382	213.6
Nitrobenzene	1.12	0.410	–
Diethyl ether	1.24	0.605	213.7
Methanol	1.35	0.611	214.3
Acetonitrile[b]	1.63	0.445	214.6
Acetone	1.76	0.812	215.6
Triethylamine	1.85	0.967	214.2
Dimethylformamide	2.55	1.182	217.4
Pyridine	2.63	1.282	215.0
Hexamethylphosphoramide	4.24	1.995	–

[a] with 10% cyclohexane as internal reference;

[b] shifts and coupling constants do not follow the linear correlation found for the other solvents.

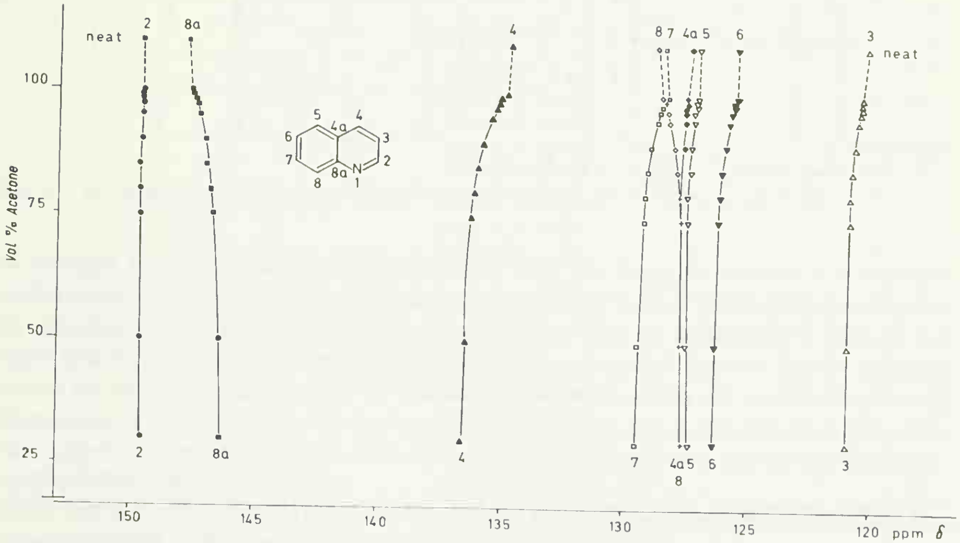

Fig. 3.4. ^{13}C chemical shifts of quinoline in the system acetone-water-quinoline with varying water concentration at 25 °C [71].

form is more than 4 ppm, which is about twice as much as that found for the proton signal of that compound (Table 3.4).

Using the data shown in Table 3.4, a linear plot of ^{13}C *versus* ^{1}H solvent shifts is obtained [69]. Moreover, ^{13}C solvent shifts correlate linearly with the one bond carbon-13-proton coupling constants [69]. This is attributed to changes in the average distance of bonding electrons in the C–H bond of chloroform due to intermolecular association [69]. Since much smaller solvent shifts of the carbon tetrachloride ^{13}C resonance are found [69], interactions between chlorine and the solvent can be disregarded. Thus, having a C–H bond, chloroform appears to associate with polar solvents by hydrogen bonding. Hydrogen bonding between polar solvents and basic substituents in aromatic compounds also generates downfield shifts of the aromatic ring carbons [70].

In solutions of dipolar compounds in water, hydrogen bonding is the most important kind of intermolecular interaction; downfield shifts of the ^{13}C signals are to be expected. In the system acetone-water-quinoline, most of the quinoline carbon signals (C-2 to C-7) follow this pattern on increasing the water concentration, C-2 showing the smallest influence. The carbon nuclei C-8 and C-8a, however, shift to higher field [71] as shown in Fig. 3.4. Thus, medium shifts may be different in magnitude and direction for non-equivalent nuclei. Closely spaced signals may then invert their sequence or coalesce. Both effects are observed in following the ^{13}C resonances of C-4a, C-7, and C-8 of quinoline on addition of water in Fig. 3.4.

3.1.4.3. pH Shifts

Protonation of amines, carboxylate anions and α-aminocarboxylic acids causes considerable upfield shifts particulary in β position of the protonated group [61, 72–75]:

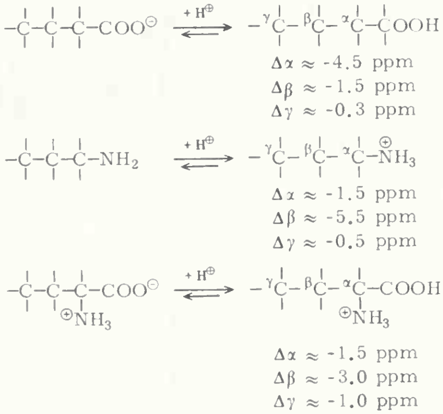

$$-C-C-C-COO^{\ominus} \xrightleftharpoons{+H^{\oplus}} -{}^{\gamma}C-{}^{\beta}C-{}^{\alpha}C-COOH$$

$\Delta\alpha \approx -4.5$ ppm
$\Delta\beta \approx -1.5$ ppm
$\Delta\gamma \approx -0.3$ ppm

$$-C-C-C-NH_2 \xrightleftharpoons{+H^{\oplus}} -{}^{\gamma}C-{}^{\beta}C-{}^{\alpha}C-\overset{\oplus}{N}H_3$$

$\Delta\alpha \approx -1.5$ ppm
$\Delta\beta \approx -5.5$ ppm
$\Delta\gamma \approx -0.5$ ppm

$$-C-C-\underset{{}^{\oplus}NH_3}{C}-COO^{\ominus} \xrightleftharpoons{+H^{\oplus}} -{}^{\gamma}C-{}^{\beta}C-{}^{\alpha}\underset{{}^{\oplus}NH_3}{C}-COOH$$

$\Delta\alpha \approx -1.5$ ppm
$\Delta\beta \approx -3.0$ ppm
$\Delta\gamma \approx -1.0$ ppm

The upfield protonation shifts particulary for C-β are mainly attributed to the electric field E of the charged group and its gradient $\frac{\partial E}{\partial r}$ at the site of the observed carbon [61a–c], while in α and γ position the contributions of inductive and steric effects will be more relevant. A model was developed [61c] in order to estimate and separate the contributions E and $\frac{\partial E}{\partial r}$ to the shielding constant. Under the simplifying assumption of a uniform electric field, no net charge will be induced at a carbon of undistorted tetrahedral bond symmetry, *e.g.* at the quaterny carbon of neopentylamine. In conclusion, the incremental protonation shift Δ_β upon perturbation of the tetrahedral bonding symmetry (*e.g.* in ethylamine) is caused by the field gradient $\frac{\partial E}{\partial r}$ [61c]. The difference of protonation shifts (about 3.4 ppm) can thus be considered as a measure for the electric field of $-\overset{\oplus}{N}H_3$ [61b]:

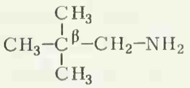

$$CH_3-\overset{CH_3}{\underset{CH_3}{C^{\beta}}}-CH_2-NH_2$$

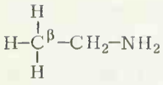

$$H-\overset{H}{\underset{H}{C^{\beta}}}-CH_2-NH_2$$

$$\Delta = \delta_{\beta_{R-\overset{\oplus}{N}H_3}} - \delta_{\beta_{R-NH_2}} \approx -5.2 \qquad \Delta' \approx -1.8; \qquad \Delta-\Delta' \approx 3.4\ \text{ppm}$$

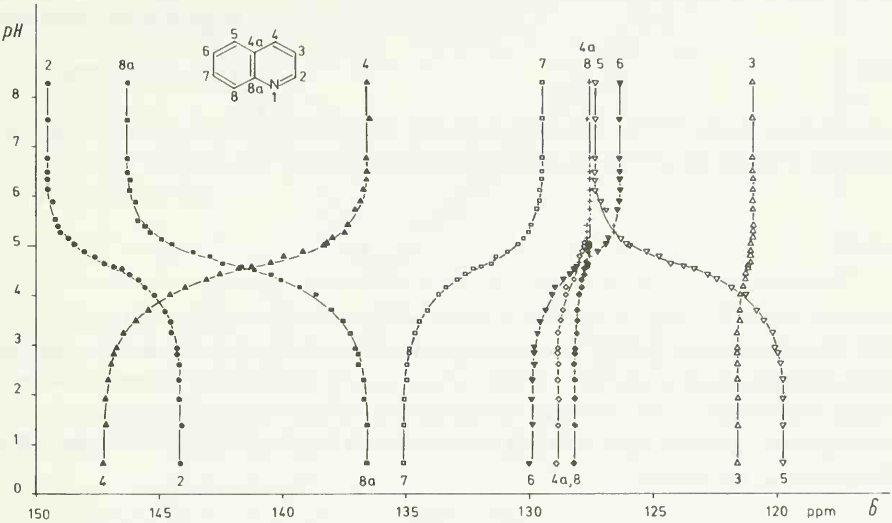

Fig. 3.5. pH dependence of quinoline ^{13}C shifts in water-acetone (70:30 Vol%) at 25 °C [71].

In nitrogen heteroaromatics, upfield protonation shifts are found for carbons α to nitrogen while those in β and γ position are deshielded on protonation [71, 76, 77]. This is shown in Fig. 3.5 for quinoline [71]. The protonation shifts for C-β and C-γ can be rationalized in terms of the cannonical formulae of protonated pyridine [50d] while the upfield shifts for C-α are probably due to the lower π character of the N–C-α bond. The curves in Fig. 3.5 representing the pH dependence of ^{13}C shifts resemble titration curves. pK values and, in the case of amino acids, the isoelectric points pI can be obtained from the point of inflection of the δ *versus* pH plot for each individual carbon [61, 71, 75].

According to the Henderson-Hasselbach equation (3.6), an accurate approximation of the pK value is obtained from a semilogarithmic plot

$$\text{of } \frac{\delta_{\max} - \delta}{\delta - \delta_{\min}} \textit{ versus } \text{pH}$$

for values of δ near the point of inflection:

$$\text{pH} = \text{pK} + \log \frac{\delta_{\max} - \delta}{\delta - \delta_{\min}} \quad [78, 79]. \tag{3.6}$$

δ_{max} and δ_{min} are the maximum and minimum shifts of the carbon atom, corresponding to the pH invariant segments of the δ *versus* pH plot (*e.g.* $\delta_{max} = 147.2$ ppm at pH < 2.0; $\delta_{min} = 136.6$ ppm at pH > 6.5 for C-4 of quinoline in Fig. 3.5). Henderson-Hasselbach plots are illustrated in Fig. 3.6 for C-4 and C-5 of quinoline, using the data shown in Fig. 3.5.

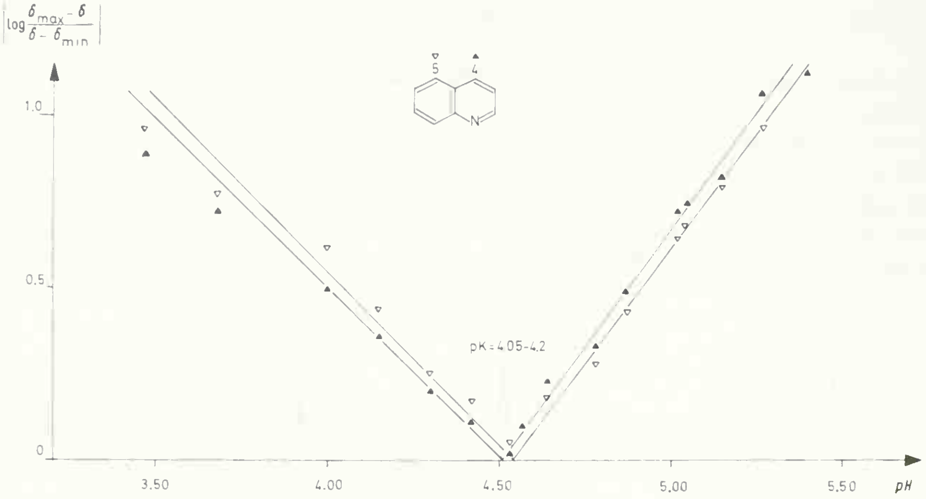

Fig. 3.6. Amount of $\log \frac{\delta_{max} - \delta}{\delta - \delta_{min}}$ *versus* pH plot for pK determination of quinoline, using the data shown for C-4 and C-5 in Fig. 3.5.

Alternatively, chemical shifts δ at pH values near pK can be calculated with eq. (3.2) if pK, δ_{max}, and δ_{min} are known.

3.1.5. Isotropic Shifts

In addition to line broadening due to accelerated relaxation, paramagnetic salts and chelates give rise to isotropic shifts when added to samples containing molecules with groups susceptible to coordination with metal ions, *e.g.* $-OH$, $-NH_2$, $-SH$, $-COOH$, $>C=O$. The isotropic shift Δ_i of a nucleus i in a sample S is the difference between chemical shifts measured before and after addition of the paramagnetic shift reagent SR [80]:

$$\delta_{i(S+SR)} - \delta_{i(S)} = \Delta_i \,. \tag{3.7}$$

Δ_i arises from two contributions:

$$\Delta_i = \Delta_i^{dipolar} + \Delta_i^{contact} \tag{3.7a}$$

The pseudo-contact term $\Delta_i^{dipolar}$ is due to the valence electrons of the shift reagent SR; they cause an additional intramolecular field in the adduct S+SR, shielding or deshielding the nuclei i in the molecule S. The Fermi contact term $\Delta_i^{contact}$ accounts for interaction between the nuclei i and the field of the unpaired electrons of the paramagnetic additive SR which may be delocalized within the adduct S+SR [80].

The net effect of a shift reagent is an expansion of the NMR spectrum. The magnitude of the isotropic shift increases with the concentration of the paramagnetic additive; coupling constants remain practically unaffected. Shift reagents thus simulate to some degree high-field NMR. However, whereas NMR spectra are expanded linearly and without changes of δ values by raising the magnetic field strength, shift reagents change δ and sometimes signal sequences since the magnitude of the isotropic shift Δ_i depends on the distance r_i of nucleus i from the paramagnetic metal ion in the adduct S+SR [80].

Since the unpaired 4f electrons in lanthanoid ions occupy orbitals of extremely low radial extension, the Fermi contact term $\Delta_i^{\text{contact}}$ is small for lanthanoid shift reagents, and pseudo-contact shifts $\Delta_i^{\text{dipolar}}$ predominate. Moreover, the influence of unpaired electrons in lanthanoid additives on relaxation of sample nuclei is so small, that practically no line broadening is observed. The pseudo-contact term $\Delta_i^{\text{dipolar}}$ of nucleus i is a function of the polar coordinates r_i, ϑ_i, and φ_i of i, with the paramagnetic ion at the origin (Fig. 3.7(a)) [80].

$$\Delta_i^{\text{dipolar}} = \mathrm{f}(r_i, \vartheta_i, \varphi_i)\,. \tag{3.8}$$

Crudely approximated, the magnitude of the pseudo-contact shift $\Delta_i^{\text{dipolar}}$, which predominates in lanthanoid shift reagents, decreases with increasing distance r_i between the observed nucleus i and the paramagnetic ion:

$$\Delta_i^{\text{dipolar}} \propto \frac{1}{r_i^3}\,. \tag{3.8a}$$

For expanding NMR spectra of aqueous sample solutions, lanthanoid salts such as the chlorides, nitrates, or perchlorates of europium and praseodym are used [80]. In organic solvents, tris-(β-diketonato)-europium(III) chelates *(1)* are usually applied [80]. Chiral europium(III) chelates such as tris-(3-*tert*-butylhydroxymethylen)-d-camphorato-europium(III) *(2)* separate the signals of enantiomers in the NMR spectra of racemate solutions [80].

(1)

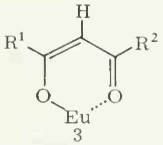

(2)

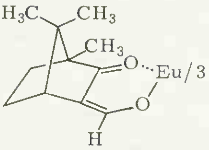

Lanthanoid shift reagents can aid in signal assignments in $^{13}C\{^1H\}$ experiments, as was reported for the $^{13}C\{^1H\}$ NMR spectra of ribose-5-phosphate [81], using europium chloride in aqueous solution, and in the case of isoborneol [82], isotropic shifts being induced by tris-(dipivaloyl-methanato)-europium(III) (*1*, $R^1 = R^2 =$ *tert*-butyl). As shown for isoborneol in Fig. 3.7(b), proton and carbon shifts do not differ significantly in their order of magnitude [80]. Plotting the isotropic shifts Δ_i observed for camphor *versus* the molar ratio between shift reagent and sample, [SR]/[S] [83], as illustrated in Fig. 3.7(c), demonstrates three characteristics:

(1) The plot $\Delta_i = \mathrm{f}([\mathrm{SR}]/[\mathrm{S}])$ is not linear, but may be approximated by a straight line at small concentrations of the shift reagent.

(2) In accordance with the proportionality (3.8a), the magnitude of the pseudo-contact shift, which predominates for lanthanoid shift reagents, decreases with the distance of nucleus i from the paramagnetic ion. Thus, C-9 of camphor is shifted more than C-10 on addition of the europium chelate. Often, the crude approach (3.8a) is a valuable assignment aid.

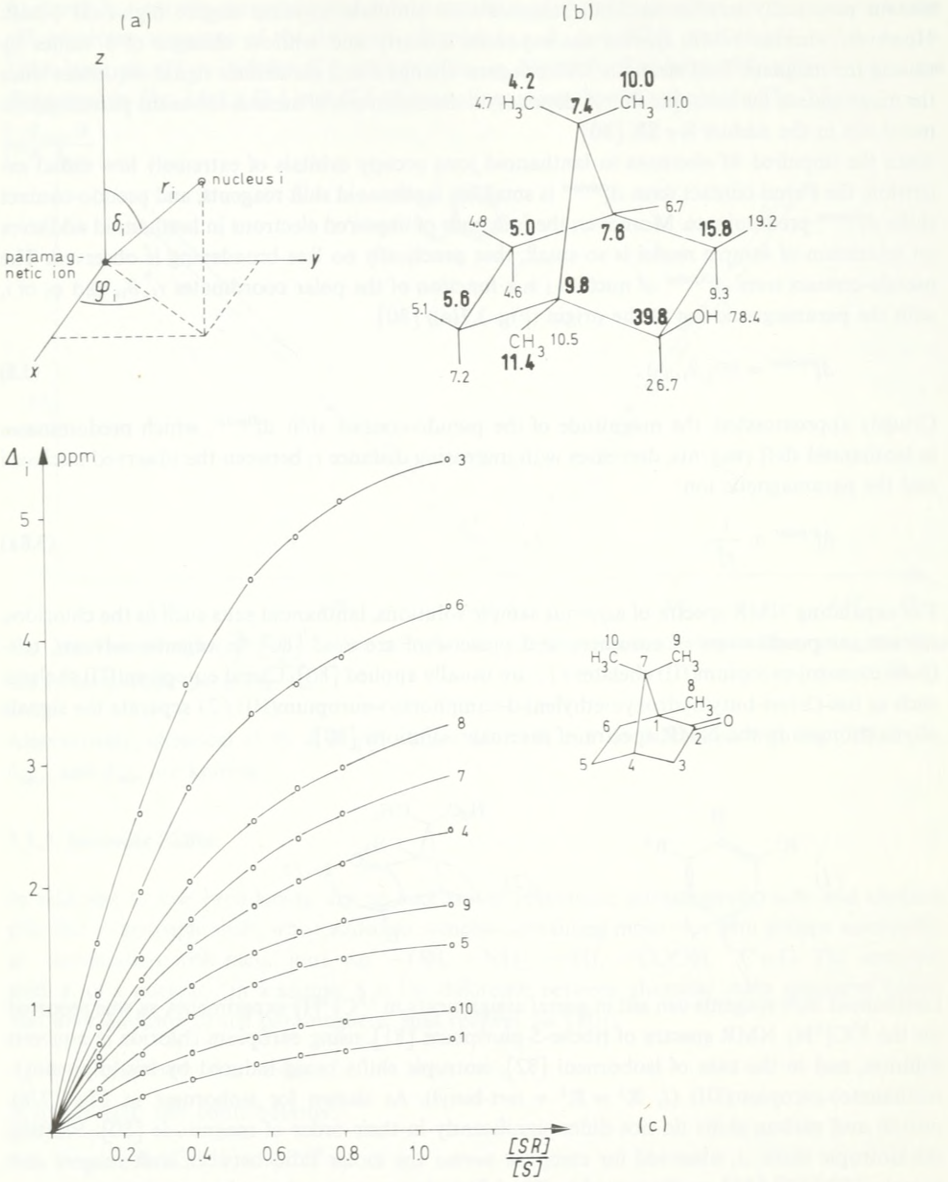

Fig. 3.7. (a) Polar coordinates r_i, ϑ_i, and φ_i of a nucleus i relative to a paramagnetic ion.
(b) Proton (small numbers) and carbon-13 (large numbers) isotropic shifts Δ_i of isoborneol in ppm; shift reagent: tris-(dipivaloylmethanato-)-europium(III) (**2**, $R^1 = R^2 = t$-butyl); molar ratio [SR]/[S] = 1 [80, 82].
(c) Carbon-13 isotropic shift of camphor as a function of the molar ratio [SR]/[S] of shift reagent and sample [83]; shift reagent: tris-[4,4,4-trifluoro-(2-thienyl)-1,3-butanedionato]-europium(III) (**1**, R^1 = trifluoromethyl, R^2 = thienyl).

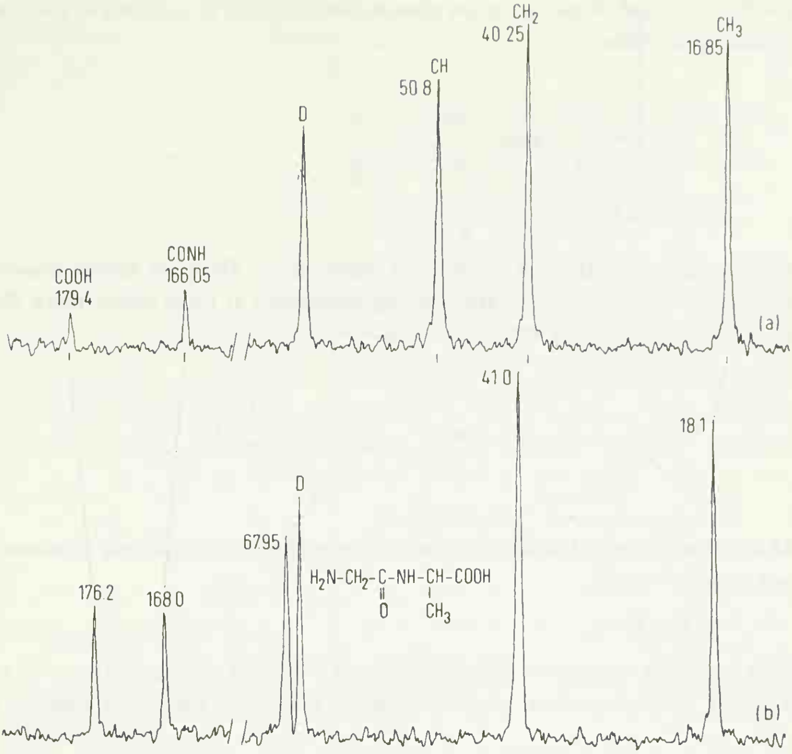

Fig. 3.8. 22.63 MHz PFT $^{13}C\{^{1}H\}$ NMR spectrum of glycylalanine; 0.3 M in deuterium oxide; pH = 3.4; 25 °C; 2048 accumulated pulse interferograms; pulse width: 5 μs; pulse interval: 0.4 s; magnitude; internal reference: D = 1,4-dioxane;
(a) without, (b) with praseodym perchlorate ([SR]/[S] = 0.86).

(3) Carbonyl compounds (*e.g.* camphor in Fig. 3.7(c)) show smaller isotropic shifts than comparable alcohols (*e.g.* isoborneol in Fig. 3.7(b)).

In aqueous oligopeptide solutions, C_α in the C-terminal amino acid shifts drastically downfield, whereas the carboxyl signal of this residue suffers an upfield shift [83]. Fig. 3.8 illustrates this for glycylalanine [83].

3.1.6. Intramolecular Mobility and the Temperature Dependence of ^{13}C Chemical Shifts and Line Widths

3.1.6.1. Introduction

Many molecules show intramolecular mobility: Rotations of groups about σ bonds or inversions of cycloaliphatic rings are representative phenomena. A well known example is N,N-dimethylformamide, which exists as a mixture of *cis* and *trans* isomers due to the partial π character of the N – CO bond: Rotation of the dimethylamino group is restricted at room temperature but occurs upon heating.

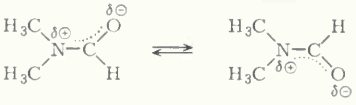

(*1A*) (*1B*)

Another example is the ring inversion of cyclohexanes. These are usually non-resolvable equilibrium mixtures of rapidly interconverting conformers at room temperature, the configuration of substituents changing from axial to equatorial.

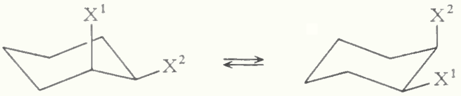

(*2A*) (*2B*)

As a generalization, intramolecular mobility may give rise to equilibria of isomerization between two species A and B:

$$A \rightleftarrows B .$$

Such equilibria depend on the temperature T (°K) and the free enthalpy of activation $\Delta G^{\neq}$ (Fig. 3.9). The rate constant k_r of isomerization is given by the Eyring equation (3.5) [84]:

$$k_r = \frac{kT}{h} e^{-\Delta G^{\neq}/RT} . \tag{3.9}$$

Eq. (3.9) arises from the absolute rate theory and can be expressed in the following logarithmic form, using the numeric values of the Boltzmann constant k, the gas constant R, the Planck constant h, and log e [85].

$$\Delta G^{\neq} = 4.57\, T \left(10.32 + \log \frac{T}{k_r} \right) \cdot 4.19 \text{ kJ/mole} \quad (1 \text{ kcal/mole} = 4.19 \text{ kJ/mole}). \tag{3.9a}$$

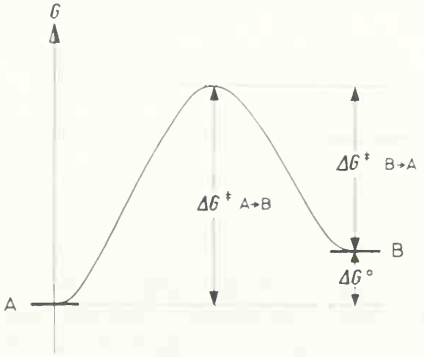

Fig. 3.9. The free enthalpy barrier of an intramolecular rotation or inversion A ⇄ B; ΔG^0 is zero if A and B are degenerate in energy.

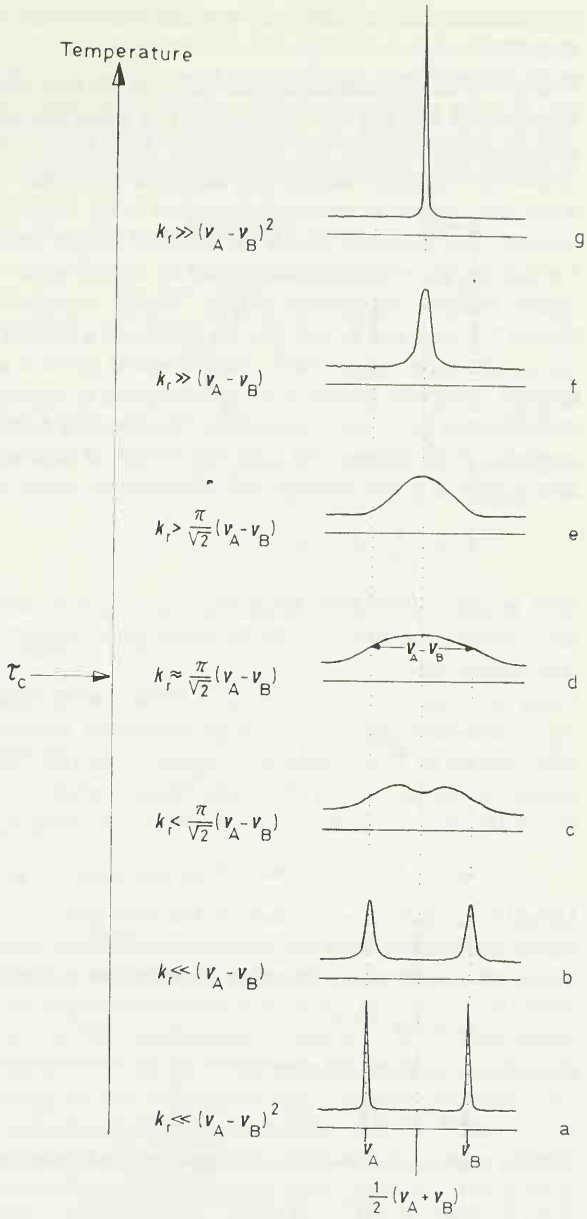
Temperature
$k_r \gg (\nu_A - \nu_B)^2$
g
$k_r \gg (\nu_A - \nu_B)$
f
$k_r > \frac{\pi}{\sqrt{2}}(\nu_A - \nu_B)$
e
τ_c
$\nu_A - \nu_B$
$k_r \approx \frac{\pi}{\sqrt{2}}(\nu_A - \nu_B)$
d
$k_r < \frac{\pi}{\sqrt{2}}(\nu_A - \nu_B)$
c
$k_r \ll (\nu_A - \nu_B)$
b
$k_r \ll (\nu_A - \nu_B)^2$
a
ν_A
ν_B
$\frac{1}{2}(\nu_A + \nu_B)$

Fig. 3.10. Temperature dependence of chemical shifts and line shapes due to intramolecular mobility.

In an NMR experiment, A and B have two separated signals for the same nucleus when the following conditions are met.

(1) The nucleus has different chemical environments in A and B.

(2) The chemical shift difference $\nu_A - \nu_B$ of the nucleus in A and B is large relative to its line width $\Delta\nu_{1/2}$ ($(\nu_A - \nu_B) \gg \Delta\nu_{1/2}$), contributions of relaxation and field inhomogeneities to $\Delta\nu_{1/2}$ being small.

(3) Interconversion between A and B occurs so slowly that k_r is very small relative to the chemical shift difference.

Due to the third condition and the fact that the rate constant k_r is a function of temperature according to eq. (3.9), the NMR spectra of molecules susceptible to interconversions due to intramolecular mobility are temperature dependent. This behavior, which is discussed more detailed in standard texts (*e.g.* [5]) and reviews [84, 85], is illustrated in Fig. 3.10.

If the rate constant is very small compared to the chemical shift difference $\nu_A - \nu_B$ at low temperature, two separated signals are observed for the corresponding nucleus in A and B (Fig. 3.10(a)); the line widths are determined by the spin-spin relaxation time and the field inhomogeneity, being on the order of 1 Hz in $^{13}C\{^1H\}$ experiments. As the temperature increases, the lifetime $1/k_r$ of A and B, and thus the lifetime of a nucleus in a particular spin state, is reduced due to increasing k_r. As a result, the line widths of the A and B signals increase (Fig. 3.10(b,c)), recalling Sections 1.5.2 and 1.5.3. Furthermore, k_r approaches the magnitude of the chemical shift difference ($\nu_A - \nu_B$). Consequently, the signals of A and B approach each other (Fig. 3.10(c)), coalescing at the temperature T_c in Fig. 3.10(d). At the coalescence temperature T_c, the rate constant is related to the chemical shift difference by eq.(3.10).

$$k_r = \frac{\pi}{\sqrt{2}}(\nu_A - \nu_B)\,. \tag{3.10}$$

As k_r becomes successively larger than ($\nu_A - \nu_B$) with increasing temperature, the line width of the averaged signal decreases, finally reaching the "natural" line width $\Delta\nu_{1/2}$ at a high temperature (Fig. 3.10(e,f,g)).

Using the temperature dependence of NMR spectra, thermodynamic data of interconversions due to intramolecular mobility can be determined. If the coalescence temperature is known, the rate constant at T_c is calculated according to eq. (3.6). Often, T_c and ($\nu_A - \nu_B$) are not known exactly. In this case, k_r can be roughly approximated by measuring the half maximum intensity line widths $\Delta\nu_{1/2(T_c)}$ at temperatures near T_c and using eq. (3.11) [84, 85].

$$k_r \cong 2\Delta\nu_{1/2(T_c)} \quad (\text{near } T_c)\,. \tag{3.11}$$

Using the k_r values thus obtained, the free enthalpies $\Delta G^{\ddagger}_{T_c}$ of rotation or inversion can be determined according to eq. (3.9a). Other thermodynamic parameters of intramolecular mobility are the energy of activation, ΔE_a from the Arrhenius equation (3.12).

$$k_r = A\,e^{-\Delta E_a/RT}\,, \tag{3.12}$$

the enthalpy of activation, ΔH^{+},

$$\Delta H^{+} = \Delta E_a - RT\,, \tag{3.13}$$

and the entropy of activation, ΔS^{+}, given by the Gibbs-Helmholtz equation (3.10),

$$\Delta G^{+} = \Delta H^{+} - T\,\Delta S^{+} \tag{3.14}$$

The calculation of these data requires the temperature dependence of k_r [84]; the energy of activation can then be obtained as the slope of a log k_r *versus* $1/T$ plot according to eq. (3.12). However, the measurement of $k_r = f(T)$ is more difficult and includes more errors than the determination of k_r at or near T_c by using eqs. (3.10) and (3.11) [84, 85].

For this reason it is usually preferable to determine the numerically more accurate free enthalpy of activation, $\Delta G^{\ddagger}_{T_c}$, from the temperature dependent NMR spectra according to eq. (3.9a).

If energies of activation are required, a convenient and accurate way to obtain rate constants k_r as functions of temperature is to calculate line shapes for different values of k_r. The experimentally obtained line shapes at T (°K) are compared with the calculated ones. The best fitting pairs of experimental and computer simulated lineshapes give corresponding pairs of rate constant and temperature, so that $k_r = f(1/T)$ can be plotted for the determination of ΔE_a. This is illustrated in Fig. 3.11 for the methyl resonance of N,N-dimethyltrichloroacetamide [86].

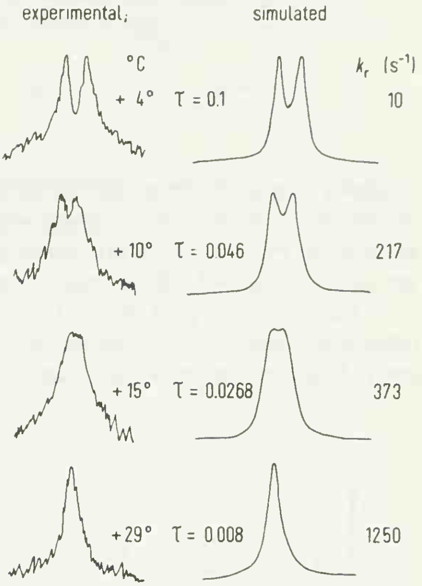

Fig. 3.11. Experimental and computer simulated methyl ^{13}C signal shapes (22.63 MHz) of N,N-dimethyltrichloroacetamide at various temperatures (measured) fitted to rate constants (simulated) [86]. (Reproduced by permission of the copyright owner from Ref. [86].)

3.1.6.2. The Temperature Dependence of ^{13}C NMR Spectra

Studies of intramolecular mobility using ^{1}H NMR often suffer from small shift differences between rotational and inversional isomers as well as from unresolved splitting due to homonuclear spin-spin coupling. Because of the large spectral width to line width ratio in ^{13}C{^{1}H} NMR (Section 3.1.1), temperature dependent ^{13}C{^{1}H} experiments should provide a larger signal separation for rotational and inversional isomers than ^{1}H NMR while eliminating the complications of homonuclear spin-spin coupling, at least in samples with naturally abundant ^{13}C. Indeed, this has been reported for the inversion of several cycloaliphatic rings [87–90].

The high-field 251 MHz ^{1}H NMR spectrum of cyclononane (Fig. 3.12(a)) changes from a single line at room temperature to two broad overlapping signals about 30 Hz apart at −160°C [87]. At the same field strength H_0, and within the same range of temperatures, the PFT ^{13}C{^{1}H} NMR spectrum changes from a single resonance to two widely spaced signals of intensity ratio 2 : 1, the shift difference being 570 Hz or about 9 ppm at 63.1 MHz (Fig. 3.12(b)) [87]. From temperatures near coalescence (about 120°K for ^{1}H and 140°K for ^{13}C) an inversion barrier of about 25 kJ/mole is obtained [87].

Cyclononane prefers a twist boat-chair (TBC) conformation (see references cited in [87]) with two classes of CH$_2$ groups differing in symmetry (• and ·). At room temperature, a rapid inversion between two enantiomeric TBC forms probably occurs, involving an intermediate boat-chair form: An averaged spectrum having one signal as in Fig. 3.10(g) is observed (Fig. 3.12) [87]. At very low temperature, this inversion is frozen, and two signals are observed for the non-equivalent nuclei (three • and six ·), those lying on C_2 axes (•) appearing at lower field.

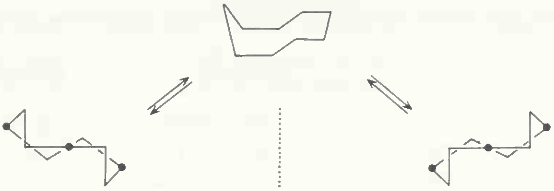

Similarly, ring inversion of methyl cyclohexanes [88], dimethylcyclohexanes [89], and *cis*-decalin [90] is more easily examined with $^{13}C\{^{1}H\}$ experiments than with ^{1}H NMR. As an example, the PFT $^{13}C\{^{1}H\}$ NMR spectra of *cis*-1,2-dimethylcyclohexane at various temperatures are shown in Fig. 3.13 [89]. At high temperatures, *i.e.* $T = 250\,^{\circ}K$, sharp, averaged ^{13}C signals for C-1,2, C-3,6, C-4,5, and the axial and equatorial methyl carbons are observed. This was attributed to a fast ring inversion between two chair forms of equal potential energy, the methyl groups rapidly exchanging axial and equatorial configuration: $k_r \gg (\nu_{eq} - \nu_{ax})$. As the temperature

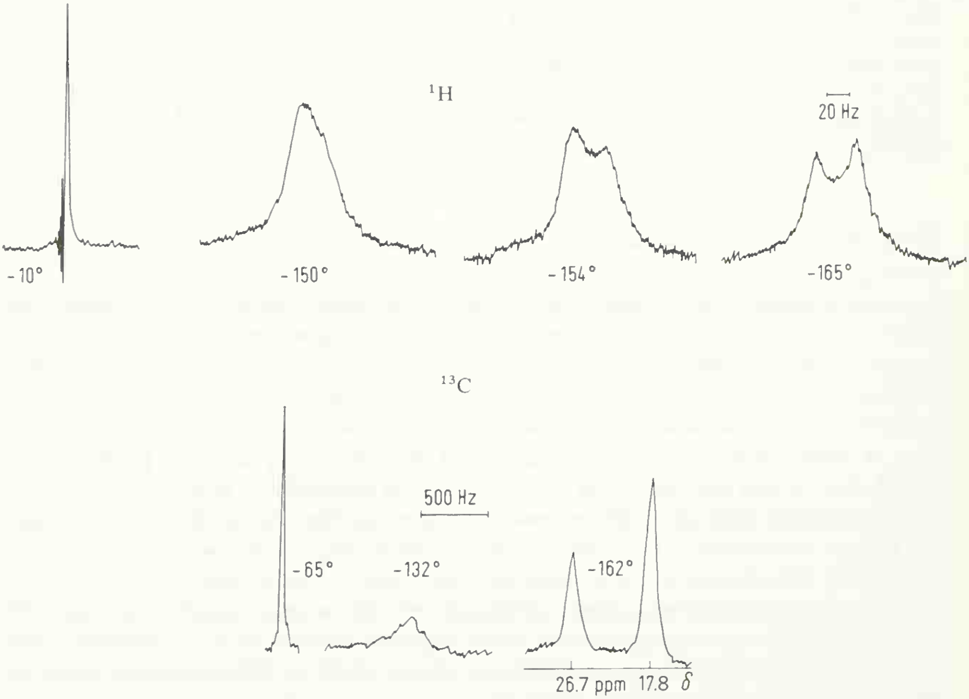

Fig. 3.12. Temperature dependent ^{1}H- and PFT $^{13}C\{^{1}H\}$ NMR spectra of cyclononane [87]. 251 MHz for ^{1}H and 63.1 MHz for ^{13}C.

decreases, the line widths of the averaged signals increase, as was the case in going from (g) to (a) in Fig. 3.10. At 158 °K, a single signal is obtained for each carbon (Fig. 3.13). Using the line widths near the coalescence point ($T_c \approx 220$ °K), the free enthalpy barrier of inversion is found to be $\Delta G^{\ddagger}_{220} \approx$ 41.4 kJ/mole for *cis*-1,2-dimethylcyclohexane and $\Delta G^{\ddagger}_{220} \approx$ 38.9 kJ/mole for the *cis*-1,4-isomer [89], which agrees well with values known from ^{1}H NMR.

Intramolecular rotations in carbonic acid amides have been thoroughly investigated by ^{1}H NMR [85]. The thermodynamic data of rotation in N,N-dimethyltrichloroacetamide as obtained by ^{1}H and ^{13}C{^{1}H} NMR agree quite well (^{1}H: $\Delta G^{\ddagger}_{294} = 76.5$ kJ/mole; ^{13}C: $\Delta G^{\ddagger}_{288} = 73.6$ kJ/mole) [86].

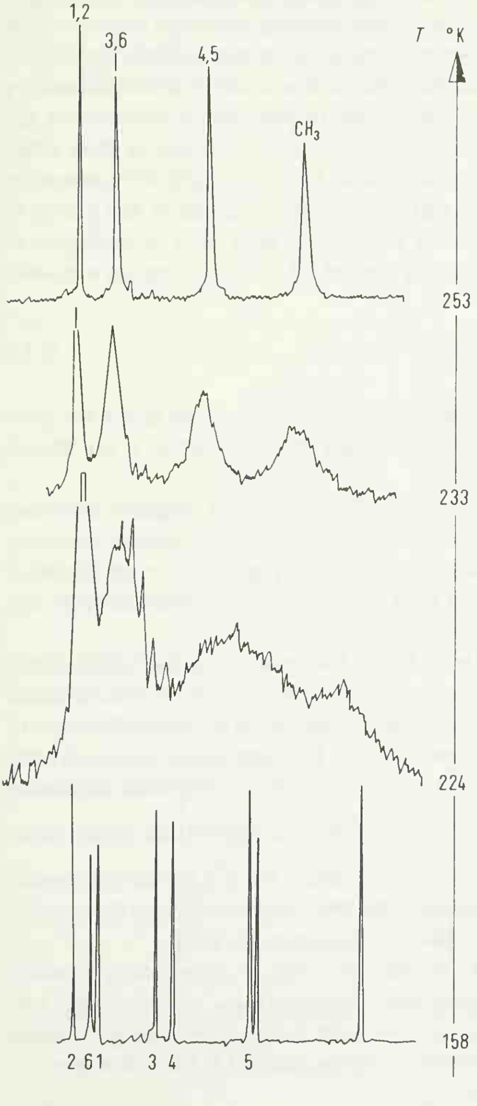

Temperature °C	Carbon	δ_C [ppm]
−100	1	33.45
	2	35.5
	3	28.7
	4	27.3
	5	21.0
	6	34.05
	1-CH_3(ax)	11.75
	2-CH_3(eq)	20.3
40	1,2	35.05
	3,6	32.05
	4,5	24.2
	1,2-CH_3	16.25

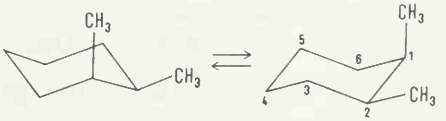

Fig. 3.13. Temperature dependent 22.63 MHz PFT ^{13}C{^{1}H} NMR spectra of *cis*-1,2-dimethylcyclohexane [89].

Any interconversion in a sample may give rise to temperature dependent NMR spectra. For example, the ^{13}C NMR spectrum of dimeric cyclopentadienyl iron dicarbonyl is temperature dependent [91]. This was attributed to intermolecular exchanges of carbonyls and interconversion between *cis* and *trans* complexes.

3.2. ^{13}C Coupling Constants

3.2.1. Basic Theoretical Considerations

The mechanism assumed to predominate in nuclear spin-spin coupling was outlined for an AX group in Section 1.10.4: The spin of nucleus A polarizes the bonding electrons of atom A in the molecule AX; spin correlation between the electrons in the AX bond affects the spin of nucleus X. It is therefore reasonable to assume that at least one-bond coupling constants depend on the angular and radial distribution of the bonding electrons occupying molecular orbitals. The angular distribution of bonding electrons is expressed in terms of the s character of hybrid orbitals making up the bond, *e.g.* 0.25, 0.33, and 0.5 for sp^3, sp^2, and sp orbitals, respectively. In valence bond and molecular orbital approximations, the charge bond-order matrix $P_{s_C s_X}$ accounts for these hybridization parameters [92]. The radial distribution of valence electrons might be expressed in terms of bond polarity. More precisely, this radial part is related to the carbon 2s and proton 1s orbital densities (for A = ^{13}C and X = ^{1}H), denoted as $s_C^2(0)$ and $s_H^2(0)$ [92]. According to an MO treatment of one-bond coupling constants, directly bonded ^{13}C$-$X constants are expressed by eq. (3.15).

$$J_{\mathrm{CX}} = \left(\frac{4}{3}\right)^2 h\,\mu_\beta\,\gamma_{\mathrm{C}}\,\gamma_{\mathrm{X}}\,P^2_{s_C s_X}\,s_{\mathrm{C}}^2(0)\,s_{\mathrm{X}}^2(0)\,(\Delta E_e)^{-1}\,. \qquad (3.15)$$

In this equation, ΔE_e is the approximated electronic excitation energy; γ_C and γ_X are the gyromagnetic ratios of the coupled nuclei, ^{13}C and X; μ_β is the Bohr magneton, h the Planck constant.

In this form, eq. (3.15) yields only positive ^{13}C$-$X couplings; however, negative one-bond couplings (*e.g.* $J_{\mathrm{C^{19}F}}$) are also observed [92]. Moreover, interpretation of carbon one-bond coupling constants in terms of carbon s character or hybridization (Fig. 3.14) assumes the factor $s_C^2(0)s_X^2(0)(\Delta E_e)^{-1}$ to be constant. In fact, ΔE_e and $s_C^2(0)$ are found to vary considerably in substituted methanes [93, 94].

Another more successful MO approach, referred to as INDO (intermediate neglect of differential overlap), avoids the average electronic energy approximation [92]. Its concept is a self-consistent field perturbation calculation. The INDO approach permits computation of one-bond carbon-13 coupling constants. The results obtained for J_{CH} agree well with the experimental data for hydrocarbons and molecules with $-$F, $-$OR, $-$NR$_3$ as substituents, but not for those containing 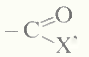 $-\mathrm{C}\!\begin{smallmatrix}\nearrow\mathrm{O}\\ \searrow\mathrm{X}\end{smallmatrix}$, $-$NO$_2$, or $-$CN. Qualitatively good agreement between computed and experimental carbon couplings are also achieved with INDO for carbon-carbon, but not for carbon-fluorine and carbon-nitrogen-15 coupling constants. Nevertheless, the INDO approach yields the negative sign of some ^{13}C$-^{19}$F coupling constants as is observed experimentally [92].

For structural elucidation by means of carbon-13 coupling constants, an empirical approach is often sufficient: Carbon-13 one-bond coupling constants, particularly J_{CH} values, crudely correlate with carbon hybridization and bond polarity. The latter is largely affected by electron withdrawing heteroatoms or substituents. These relations will be outlined in the following.

3.2.2. Carbon-Proton Coupling

3.2.2.1. One-Bond Coupling (J_{CH})

One-bond carbon-proton coupling constants J_{CH} range from 120 to 320 Hz (Fig. 3.14). There are two structural features that increase carbon-proton coupling constants. These are 1) increasing s character of the carbon hybrid orbital making up the C–H bond; 2) electron withdrawing substituents at the coupling carbon and an increased degree of substitution with such groups.

For closely analogous representatives of sp^3, sp^2, and sp carbons such as the series ethane, ethylene, acetylene, or methylamine, formaldimine, hydrogen cyanide, J_{CH} increases linearly with carbon s character as shown in Fig. 3.14. The J_{CH} ranges for the three types of carbon

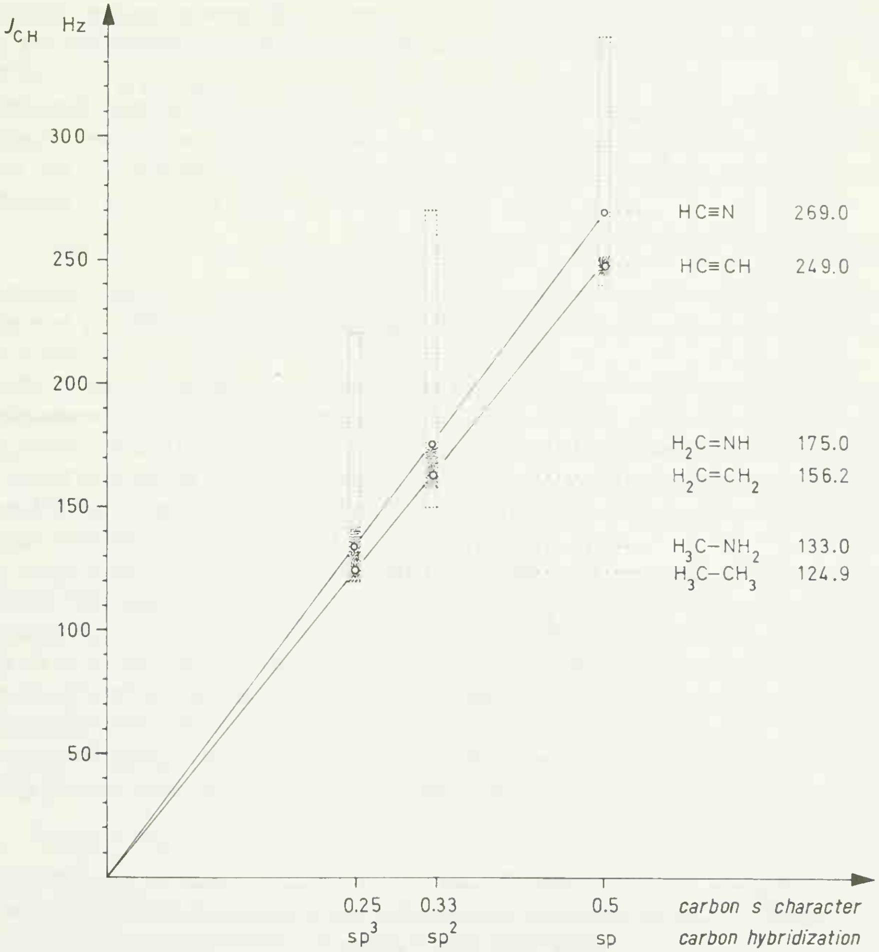

Fig. 3.14. Ranges of one-bond carbon-13-proton coupling constants for sp^3, sp^2, and sp carbons (dotted rectangles) and linear correlation between J_{CH} and carbon *s* character of comparable compounds (coupling constants from Ref. [92]).

hybridization are narrow and do not overlap, provided that only one heteroatom or substituent is attached to the coupling carbon (Fig. 3.14). Thus, sp^3 carbons in CH_3X compounds or $-CH_2X$ groups have J_{CH} values between 120 and 150 Hz (Tables 3.2, 3.4). In the series ethane, methyl-

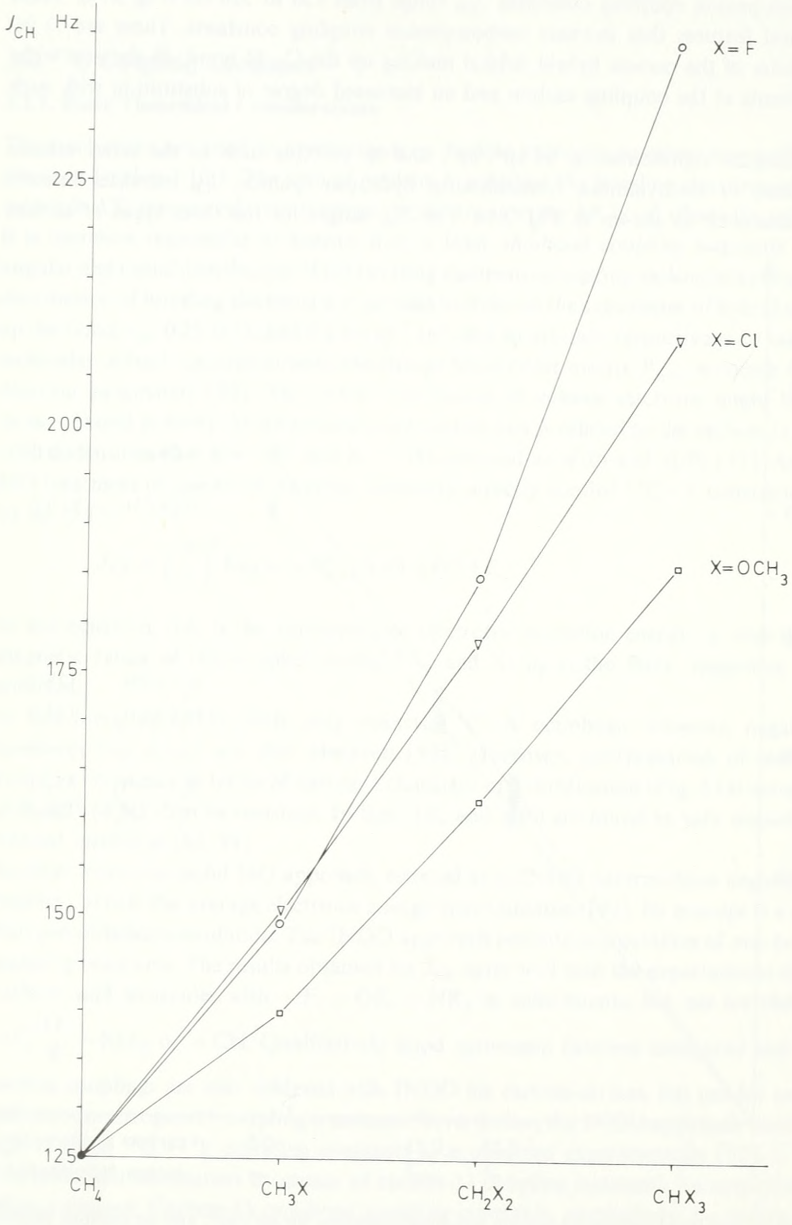

Fig. 3.15. One-bond coupling constants, J_{CH}, of methane derivatives as a function of the degree of substitution with electron withdrawing substituents.

amine, methanol (Table 3.5), the methyl coupling J_{CH} increases with increasing electron withdrawal by the substituent at the methyl carbon. For $=CH_2$ carbons of terminal vinyl compounds and for benzenoid $\gtrdot$CH carbons, one-bond couplings between 150 and 170 Hz are observed. Influences of a substituent, a heteroatom, conjugation or cumulation of π bonds are within the same range (Tables 3.6, 3.7). Much smaller J_{CH} values (25 – 75 Hz) are reported for the sp^2 carbons of open-chain carbenium ions [52] since dynamic effects cause an averaging with the two bond coupling constant $^2J_{CH}$ in this case. A one-bond coupling constant of 250 Hz ± 5 is characteristic of the terminal sp carbon of an ethynyl group (Table 3.6, bottom).

The range of J_{CH} expands considerably if more than one electron withdrawing substituent is found at the coupling carbon. This trend is exemplified in a series of formaldehyde derivatives (Table 3.6) and in di- and trisubstituted methanes, CH_2X_2, and CHX_3 (Table 3.5). Whereas methyl iodide, bromide, chloride, and fluoride show almost equal J_{CH} values of about 150 Hz, the coupling constants increase almost linearly for each additional substituent at the methyl carbon, but individually for each kind of substituent. Fig. 3.15 illustrates this for X = F, Cl, and OCH_3.

For substituted methanes of type CHXYZ, the Coupling constant J_{CHXYZ} can be approximated by adding the coupling constant of methane, J_{CH_4}, and the empirical increments, j, according to eq. (3.16). The j parameters include j_X, j_Y, j_Z for the substituents [95] and j_{XY}, j_{XZ}, j_{YZ} for pair combinations of substituents [96].

$$J_{CHXYZ} = J_{CH_4} + j_X + j_Y + j_Z + j_{XY} + j_{XZ} + j_{YZ}\,. \qquad (3.16)$$

The one-bond coupling constants J_{CH} of cycloaliphatic rings such as cyclohexane or heteroalicyclics such as 1,4-dioxane are almost equal to those found for comparable open-chain compounds (Table 3.7).

In strongly strained systems such as cyclopropane or cyclopropene, very large coupling constants J_{CH} are measured (Table 3.7). This is attributed to the high s character of the ring carbon hybrid orbitals, cyclopropane (161 Hz) having olefinic character, and cyclopropene (220 Hz) being more closely related to an alkyne [2, 97, 98]. Similarly, the three-membered heteroalicyclic compounds aziridine (172 Hz), oxirane (175.5 Hz), and thiirane (170.5 Hz) show much larger J_{CH} values than their higher membered homologues [99].

The J_{CH} values reported for *cis*- and *trans* isomers of alkenes and azomethenes differ as shown in Table 3.6. The larger coupling constant, found for the acetaldoxime isomer with a proton configuration *trans* to the hydroxyl group, is attributed to the lone electron pair at nitrogen which is *cis* to the proton [100]. In alkenes, crowding of alkyl groups such as methyl or *tert*-butyl at the sp^2 carbons reduces one-bond C – H coupling constants of the olefinic carbons by 5 – 10 Hz [101] (Table 3.6).

The one-bond coupling constants of halo- and pseudohalobenzenes, $X-C_6H_5$ (X = halogen, CN, NO_2) decrease with the distance from the substituent X in the order

$$J_{CH(2,6)} > J_{CH(3,5)} > J_{CH(4)}\,,$$

fluorobenzene being an exception, as shown in Table 3.7. Methyl coupling constants J_{CH} of substituted toluenes, *t*-butylbenzenes, N,N-dimethylanilines, and anisols are reported to correlate linearly with the Hammet substituent constants in each series [103].

The one-bond coupling constants J_{CH} of pyridine ring carbons behave similarly to those of substituted benzenes (Table 3.7). In azoles, J_{CH} increases with the number of nitrogen atoms in the five-membered ring (Table 3.7).

One-bond coupling constants J_{CH} may suffer from slight solvent influences. Table 3.4 shows this behavior for chloroform, whose carbon-proton coupling increases with the polarity of the medium when measured in different solvents, being 208 Hz in cyclohexane and 215 Hz in pyridine [69]. This is attributed to association between chloroform and solvents susceptible to hydrogen bonding.

Table 3.5. One-Bond Coupling Constants J_{CH} of Methane Derivatives HCH_2X (Left Side) and $HCHX_2$ or HCX_3 (Right Side); Data from Ref. [92].

Compound	Formula	J_{CH} (Hz)	Compound	Formula	J_{CH} (Hz)
Methane	HCH_3	125.0			
Ethane	HCH_2CH_3	124.9			
			Propane	$HCH(CH_3)_2$	119.4
			t-Butane	$HC(CH_3)_3$	114.2
Propene	$HCH_2CH=CH_2$	122.4			
Toluene	$HCH_2C_6H_5$	129.4			
Propyne	$HCH_2C\equiv CH$	132.0			
Methyl iodide	HCH_2I	151.1			
Methyl bromide	HCH_2Br	151.5			
Methyl chloride	HCH_2Cl	150.0			
			Dichloromethane	$HCHCl_2$	178.0
			Chloroform	$HCCl_3$	209.0
Methyl fluoride	HCH_2F	149.1			
			Difluoromethane	$HCHF_2$	184.5
			Trifluoromethane	HCF_3	239.1
Methylamine	HCH_2NH_2	133.0			
Methanol	HCH_2OH	141.0			
			Ethanol	$HCH(OH)CH_3$	140.3
				HCH_2CH_2OH	126.9
			2-Propanol	$HC(OH)(CH_3)_2$	142.8
				$(HCH_2)_2CHOH$	126.9
Dimethyl ether	HCH_2OCH_3	140.0			
			Formaldehyde dimethylacetal	$HCH(OCH_3)_2$	161.8
			Methyl orthoformate	$HC(OCH_3)_3$	186.0
Acetic acid	HCH_2COOH	130.0			
			Malonic acid	$HCH(COOH)_2$	132.0
Acetonitrile	HCH_2CN	136.1			
			Malodinitrile	$HCH(CN)_2$	145.2
Nitromethane	HCH_2NO_2	146.0			
			Dinitromethane	$HCH(NO_2)_2$	169.4
Fluoroacetonitrile	$HCHFCN$	166.0			
			Difluoroacetonitrile	HCF_2CN	205.5

Table 3.6. One-Bond Coupling Constants J_{CH} of sp^2 and sp Carbons.

Class	Compound	Formula	J_{CH} (Hz)	Ref.
sp^2	Ethylene	$H_2C=CH_2$	156.2	[92]
	Vinyl fluoride	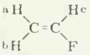	159.2 (a) 162.2 (b) 200.2 (c)	[92]
	Trimethylethylene	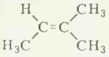	148.4	[101]
	1,1-Di-*t*-butylethylene	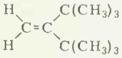	151.9	[101]
	Tri-*t*-butylethylene	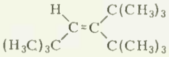	143.3	[101]
	Methylenecyclobutane	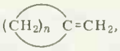 $n = 3$	154.9	[101]
	Methylenecyclopentane	$n = 4$	154.2	[101]
	Methylenecyclohexane	$n = 5$	153.5	[101]
	Methylenecycloheptane	$n = 6$	153.4	[101]
	Allene	$H_2C=C=CH_2$	168.2	[92]
	cis-Stilbene	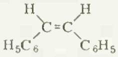	155.0	[102]
	trans-Stilbene	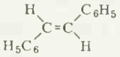	151.0	[102]
	cis-Diazastilbene *)	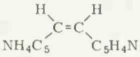	159.0	[102]
	trans-Diazastilbene *)	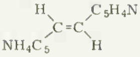	157.0	[102]
	Acetaldoxime	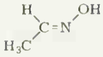	163.0	[92]
		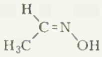	177.0	[92]
	Formaldehyde	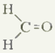	172.0	[92]
	Acetaldehyde	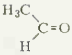	172.4	[92]
	Formamide	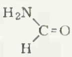	188.3	[92]
	N,N-Dimethylformamide	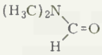	191.2	[92]
	Formate anion in aq. sol.	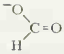	194.8	[92]
	Formic acid	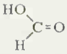	222.0	[92]
	Methyl formate	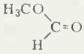	226.2	[92]
	Formyl fluoride	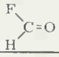	267.0	[92]

*) *cis*- and *trans*-Di-α-pyridylethylene.

Table 3.6 (Continued).

Class	Compound	Formula	J_{CH} (Hz)	Ref
sp	Acetylene	$HC{\equiv}CH$	249.0	[92]
	Propyne	$HC{\equiv}C{-}CH_3$	248.0	[92]
	2-Propyn-1-ol	$HC{\equiv}C{-}CH_2OH$	248.0	[92]
	Phenylacetylene	$HC{\equiv}C{-}C_6H_5$	251.0	[92]
	Hydrogen cyanide	$HC{\equiv}N$	269.0	[92]

3.2.2.2. Two-Bond Coupling ($^2J_{CH}$)

Two-bond carbon-proton coupling constants reported so far and denoted as $^2J_{CH}$ range from -5 to 60 Hz (Table 3.8) [103]. They follow an overall pattern similar to that found for carbon-proton one-bond coupling, also being related to carbon hybridization: Increasing s character of the hybrid orbitals not only at the coupling carbon but also at that bearing the coupling proton appears to increase the two-bond coupling constant $^2J_{CH}$. This trend is observed in comparing the $^2J_{CH}$ values of 1-phenoxy-1-propyne ($-$C(sp)$-$C(sp)$-$C(sp^3)$-$H(s)) and phenoxyacetylene ($-$C(sp)$-$C(sp)$-$H(s)) as illustrated in Table 3.8. Electron withdrawal at the coupling carbon by heteroatoms or substituents also increases $^2J_{CH}$. This is found by comparison of the values listed for acetylene and phenoxyacetylene or of those reported for acetaldehyde and its mono-, di-, and trichlorinated derivative (Table 3.8).

A significant difference between $^2J_{CH}$ values was observed for the *cis*- and *trans* isomers of 1,2-dichloroethylene, 16 Hz being measured for *cis*, and 0.8 Hz for *trans* [103]. In β-D-glucose with *trans* configuration of the hydroxyl groups at C-1 and C-2, a two-bond coupling of $^2J_{CH} = 6$ Hz between C-1 and the axial proton attached to C-2 was found. A much smaller C-1$-$H-2 coupling, less than 1 Hz, was measured for the α anomer containing the hydroxyl groups in 1,2-position *cis* to each other (Fig. 2.4(b)) [102]. The complex ion $[HRh(CN)_5]^-$ has a $^2J_{CH}$ of 56.2 Hz for the *trans* and 5.7 Hz for the *cis* configuration of the coupling proton [106].

3.2.2.3. Three-Bond Coupling ($^3J_{CH}$)

In aliphatic compounds, *vicinal* C$-$H couplings $^3J_{CH}$ are related to the dihedral angle Φ similar to $^3J_{HH}$ ($J_{trans} > J_{gauche}$, Table 3.9). Karplus curves have been calculated [50h]. Because of large deviations due to substituents and their relative geometry, configurational assignments from $^3J_{CH}$ are difficult. More successfully, the relation $J_{trans} > J_{cis}$ (Table 3.9) can be applied for alkenes, provided the couplings are well resolved.

Three bond couplings $^3J_{CH}$ of benzene carbons with the ring protons (*m* couplings) are larger than *o* and *p* C$-$H couplings. The typical ranges are given in Table 3.9 and provide useful aids in assigning benzenoid carbon signals in strong samples. For example, carbons without coupling protons in the *m* positions can often be recognized in coupled spectra by lacking long-range splittings because *o* and *p* couplings (<4 Hz) frequently cannot be resolved.

Similar to benzene, relatively large three-bond C$-$H couplings are measured in pyridine [50d] and five membered heterocycles [105] (Table 3.9). If the coupling nuclei C and H enclose nitrogen as in pyridine (Table 3.9) or pyrimidine [50i] values of up to 12 Hz are typical for $^3J_{CH}$.

Table 3.7. One-Bond Coupling Constants J_{CH} of some Alicyclic and Aromatic Carbons.

Compound	Structure	J_{CH} (Hz)	Ref.
Cyclopropane		161	[97]
Cyclobutane		136	[97]
Cyclopentane		131	[97]
Cyclohexane		127	[97]
Tetrahydrofuran		149 (a) 133 (b)	[102]
1,4-Dioxane	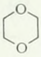	145	[102]
Cyclopropene (sp^2)		220	[98]
Benzene	X = H	159	[92]
Fluorobenzene	X = F	155 (2,6) 163 (3,5) 161 (4)	[92]
Bromobenzene	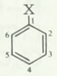 X = Br	171 (2,6) 164 (3,5) 161 (4)	[102]
Benzonitrile	X = CN	173 (2,6) 166 (3,5) 163 (4)	[102]
Nitrobenzene	$X = NO_2$	171 (2,6) 167 (3,5) 163 (4)	[102]
Mesitylene	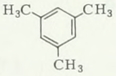	154	[92]
Pyridine	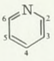	170 (2,6) 163 (3,5) 152 (4)	[92]
2,4,6-Trimethylpyridine	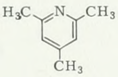 H_3C N CH_3 CH_3	158.5	[92]
Pyrrole	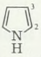	170 (3) 182 (2)	[105]
Pyrazole	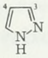	178 (4) 190 (3)	[105]
Imidazole	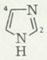	199 (4) 208 (2)	[105]
1,2,3-Triazole	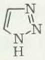	205	[105]
1,2,4-Triazole	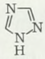	208	[105]
Tetrazole	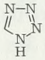	216	[105]

Table 3.8. Two-Bond Coupling Constants $^2J_{CH}$ of Selected Organic Compounds*).

Compound	Formula*)	$^2J_{CH}$ (Hz)	Ref.
Ethane	$H_3\mathbf{C}-C\mathbf{H}_3$	−4.5	[103]
1,2-Dichloroethane	$ClH_2\mathbf{C}-C\mathbf{H}_2Cl$	−3.4	[103]
1,1,2,2-Tetrachloroethane	$Cl_2H\mathbf{C}-C\mathbf{H}Cl_2$	1.2	[103]
Ethylene	$H_2\mathbf{C}=C\mathbf{H}_2$	−2.4	[103]
1,2-Dichloroethylene, *trans*	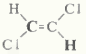	0.8	[103]
1,2-Dichloroethylene, *cis*	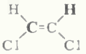	16.0	[103]
Methylenecyclopentane	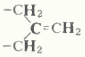	4.2	[101]
Methylenecyclohexane		5.2	[101]
Methylenecycloheptane		5.5	[101]
Acetone	$(C\mathbf{H}_3)_2\mathbf{C}=O$	5.5	[102]
3-Aminoacrolein	$H_2N-CH=C\mathbf{H}-\mathbf{C}H=O$	6.0	[102]
Acetaldehyde	$H_3\mathbf{C}-C\mathbf{H}=O$	26.7	[104]
2-Ethylbutyraldehyde	$(C_2H_5)_2\mathbf{C}H-C\mathbf{H}=O$	22.1	[104]
Acrolein	$H_2C=\mathbf{C}H-C\mathbf{H}=O$	26.9	[104]
3-Aminoacrolein	$H_2N-CH=\mathbf{C}H-C\mathbf{H}=O$	20.0	[102]
Propynal	$H-C\equiv\mathbf{C}-C\mathbf{H}=O$	33.2	[104]
Chloroacetaldehyde	$Cl\mathbf{C}H_2-C\mathbf{H}=O$	32.5	[104]
Dichloroacetaldehyde	$Cl_2\mathbf{C}H-C\mathbf{H}=O$	35.3	[104]
Trichloroacetaldehyde	$Cl_3\mathbf{C}-C\mathbf{H}=O$	46.3	[104]
Acetylene	$H-\mathbf{C}\equiv C-\mathbf{H}$	49.3	[103]
Phenoxyacetylene	$C_6H_5O-\mathbf{C}\equiv C-\mathbf{H}$	61.0	[103]
1-Phenoxy-1-propyne	$C_6H_5O-C\equiv\mathbf{C}-C\mathbf{H}_3$	10.8	[103]
Typical values:	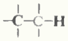	$^2J_{CH} = 1-6$	
	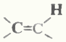	$^2J_{CH} = 1-16$	
	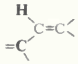	$^2J_{CH} = 8$	
	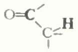	$^2J_{CH} = 5-8$	
	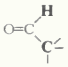	$^2J_{CH} = 20-25$	
	$-\mathbf{C}\equiv C-\mathbf{H}$	$^2J_{CH} \geqq 40$	

---

*) The coupling nuclei are printed in bold type.

3.2.3. Carbon-Deuterium Coupling

Carbon-proton and carbon-deuterium coupling constants are related to each other by eq. (3.15a) which follows not only from eq. (3.15) but also from Ramsay's theory [5, 10].

$$J_{CH}/J_{CD} = \gamma_H/\gamma_D = 6.51 \tag{3.15a}$$

Table 3.9. Typical Three-Bond Coupling Constants in Aliphatic Compounds (a), and Long-Range Couplings in Benzene Derivatives (b), Pyridine (c), and Five-Membered Heteroaromatics (d) [105].

(a)

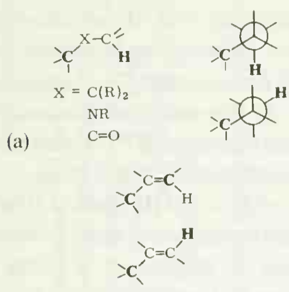

$^3J_{CH} \approx 0$ (gauche-)

$^3J_{CH} = 5-7$ (trans-)

$^3J_{CH} \geqq 12$ (cis-)

$^3J_{CH} \geqq 18$ (trans-)

(b)

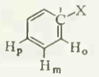

$^2J_{CHo} = 1-4$
$^3J_{CHm} = 7-10$
$^4J_{CHp} = 0.5-2$

(c)

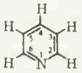

$^2J_{C\text{-}2,H\text{-}3} = 2$
$^3J_{C\text{-}2,H\text{-}4} = 7$
$^3J_{C\text{-}2,H\text{-}6} = 12$
$^2J_{C\text{-}3,H\text{-}2} = 7$
$^2J_{C\text{-}3,H\text{-}4} = 2$
$^3J_{C\text{-}3,H\text{-}5} = 6$
$^3J_{C\text{-}4,H\text{-}2} = 4$

(d) Compound	Structure	C	Long-Range Coupling Constants (Hz) $^2J_{CH\text{-}2}$	$^2J_{CH\text{-}3}$	$^{2,3}J_{CH\text{-}4}$	$^{3,4}J_{CH\text{-}5}$
Pyrrole	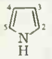	2	–	7.6	7.6	7.6
		3	7.8	–	4.6	7.8
Furan	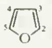	2	–	7.0	10.8	7.0
		3	14.0	–	4.0	5.8
Thiophene	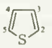	2	–	7.35	10.0	5.15
		3	4.7	–	5.9	9.5
Selenophene	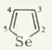	2	–	7.0	10.0	3.5
		3	4.5	–	6.0	10.4
Pyrazole	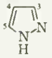	3	–	–	6.5; 7.5	
		4	–	9.5	–	9.5
Imidazole	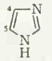	2	–	–	9.4	9.4
		4	7.3	–	–	13.0
1,2,4-Triazole	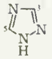	3,5	–	–	–	9.4

As can be seen in Table 3.1 for commonly used deuterated solvents, deviations of J_{CH}/J_{CD} from the ratio γ_H/γ_D are rare and small so that J_{CH} and J_{CD} are essentially the same measurement. To conclude, all relations found for J_{CH} can also be found for $_{CD}$. The signal multiplicities, however, are different (3 for CD, 5 for CD_2 and 7 for CD_3, respectively) because of different spin quantum numbers ($I_D = 1$; $I_H = \frac{1}{2}$).

Carbon-Deuterium multiplets are weak or even lost in the noise of proton decoupled ^{13}C NMR spectra, particularly in a larger molecule. A practical use of this fact leads to the unequivocal assignment of specificly deuterated carbons by comparison with the spectrum of the fully protonated compound. This method is advantageous if other assignment techniques such as proton decoupling fail due to equal multiplicities, non-resolved couplings, higher order splittings or multiplet overcrowding. Typical examples are given in ref. [107].

3.2.4. Carbon-Carbon Coupling

Homonuclear carbon multiplets are usually lost in the noise when ^{13}C NMR spectra of samples with naturally abundant ^{13}C are recorded. Only in strong solutions or neat liquid samples of small molecules C–C multiplets can be observed as weak satellites in $^{13}C\{^1H\}$ experiments [109a]. Otherwise, ^{13}C enriched compounds must be synthesized. However, as illustrated for uniformly ^{13}C enriched and mutarotated D-glucose in Fig. 3.16(b), homonuclear C–C coupling may give rise to $^{13}C\{^1H\}$ NMR spectra of higher than first order. In this case, complete assignments are not as straightforward as in spectra obtained from samples with natural ^{13}C abundance (Fig. 3.16(a)), and high-field NMR might be helpful for a more detailed analysis (Fig. 3.16(c)).

The one-bond coupling constants J_{CC} tabulated so far cover a span of 30 to 180 Hz (Table 3.10(a)). They increase with increasing s character of the hybrid orbitals contributing to the bond between the coupling carbon nuclei. A rough correlation between J_{CC} and the product $s_1 \cdot s_2$ of the s characters of the interacting carbon hybrid orbitals (C-1, C-2), *i.e.* the "s" bond order of the C–C bond, is observed (Table 3.10(a); Fig. 3.17).

Calculated carbon-carbon couplings J_{CC} obtained with the INDO approach agree qualitatively with the experimental data of open-chain hydrocarbons. Considerable deviations are found for molecules containing electron withdrawing substituents and for aromatic compounds [92].

Some empirical relations are deducible by inspection of the experimental data. Electron withdrawal increases J_{CC}. However, the effects are weaker than those in $^{13}C-^1H$ coupling. Nevertheless, the parallel behavior of J_{CH} and J_{CC} toward hybridization and electron withdrawal reflects in a linear correlation between J_{CH} in compounds of the type XYZCH and J_{CC} in compounds of the type $XYZCCH_3$ [109a].

An increase of J_{CC} of only 2.5 to 3 Hz is found in going from ethane to ethanol, or from *t*-butylamine to *t*-butanol (Table 3.10(a)). Homonuclear carbon couplings of sp^3-sp^2 type in carbonyl compounds increase more significantly with the electron withdrawal, *e.g.* in going from aldehydes or ketones ($J_{CC} \approx 40$ Hz) to comparable carboxylic acid derivatives ($J_{CC} \approx 50$ Hz) (Table 3.10(a)).

In substituted benzenes and in pyridine, couplings between adjacent carbons, not including the substituted atom, differ by about 2 Hz. Differences of J_{CC} on the same order are reported for the C-1–C-2 couplings of α- and β-D-glucose (Fig. 3.16(b)), the β-anomer with an equatorial hydroxyl group at C-1 showing the larger homonuclear coupling [108].

It has been suggested that because the carbon orbitals forming the C–H bonds have more s character in cyclopropane than in normal hydrocarbons, the orbitals forming the cyclopropane C–C bonds must have more p character [99, 109a]. The small 1–2-couplings (10–15 Hz) for the cyclopropane ring carbons and the large 1-α couplings (44-78 Hz) in substituted cyclopropanes appear to provide evidence for this assumption.

One-bond and longer-range homonuclear ^{13}C coupling constants in benzenes, which are monosubstituted by various ^{13}C enriched substituents ($-CH_3$, $-CH_2OH$, $-CH_2Cl$, $-COOH$, $-COOCH_3$, $-COCl$, $-CN$, symbolized as C-7), decrease in the following order [109b]:

$$J_{1,7} \gg {}^3J_{3,7} > {}^2J_{2,7} > {}^4J_{4,7}$$

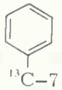

Two- and three-bond carbon-carbon coupling constants of selected organic compounds are listed in Table 3.10(b). They have been interpreted in terms of the Fermi-contact mechanism as they correlate with proton-proton and carbon-proton coupling constants in comparable bonding situations [109a].

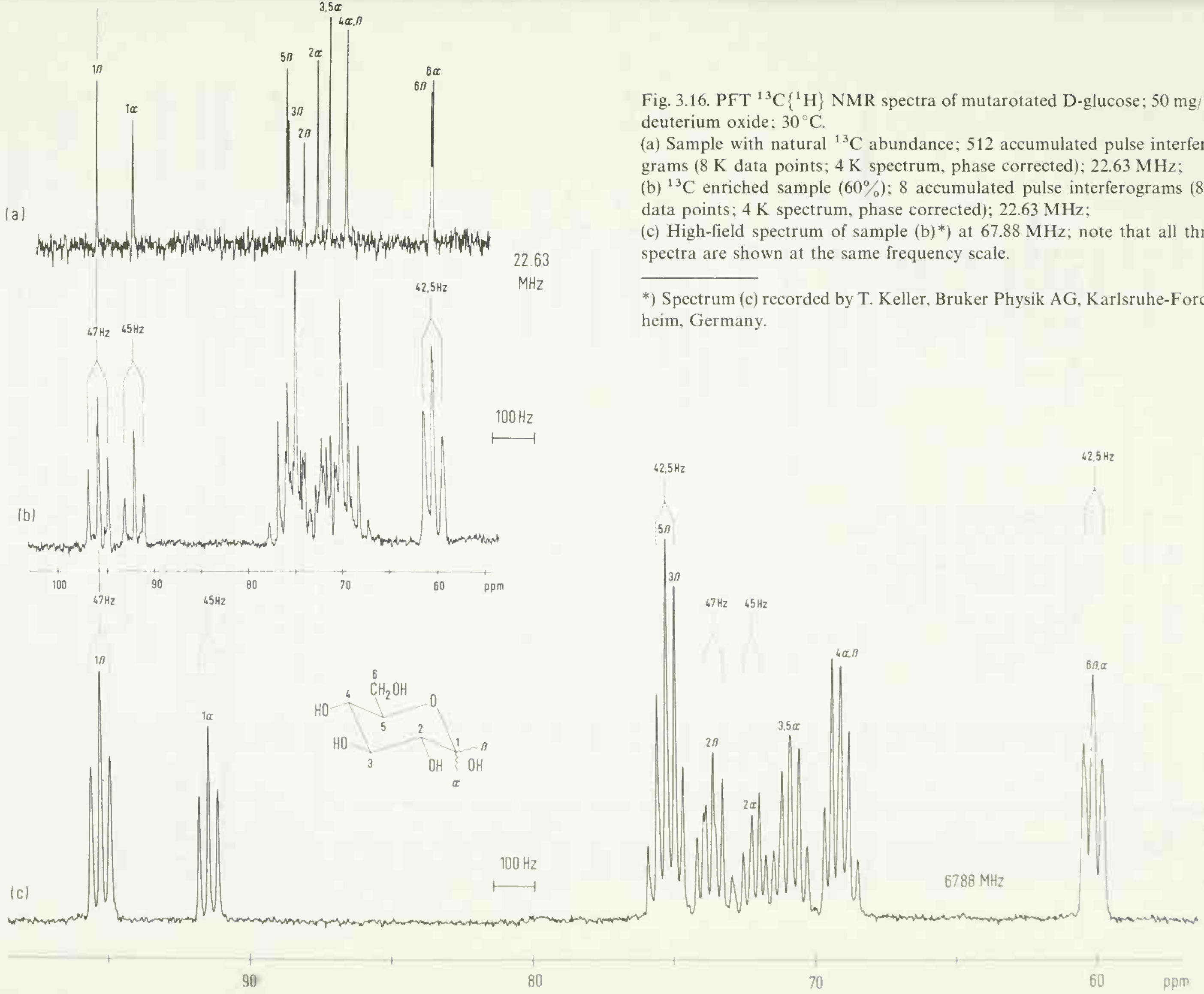

Fig. 3.16. PFT $^{13}C\{^{1}H\}$ NMR spectra of mutarotated D-glucose; 50 mg/ml deuterium oxide; 30 °C.
(a) Sample with natural ^{13}C abundance; 512 accumulated pulse interferograms (8 K data points; 4 K spectrum, phase corrected); 22.63 MHz;
(b) ^{13}C enriched sample (60%); 8 accumulated pulse interferograms (8 K data points; 4 K spectrum, phase corrected); 22.63 MHz;
(c) High-field spectrum of sample (b)*) at 67.88 MHz; note that all three spectra are shown at the same frequency scale.

---

*) Spectrum (c) recorded by T. Keller, Bruker Physik AG, Karlsruhe-Forchheim, Germany.

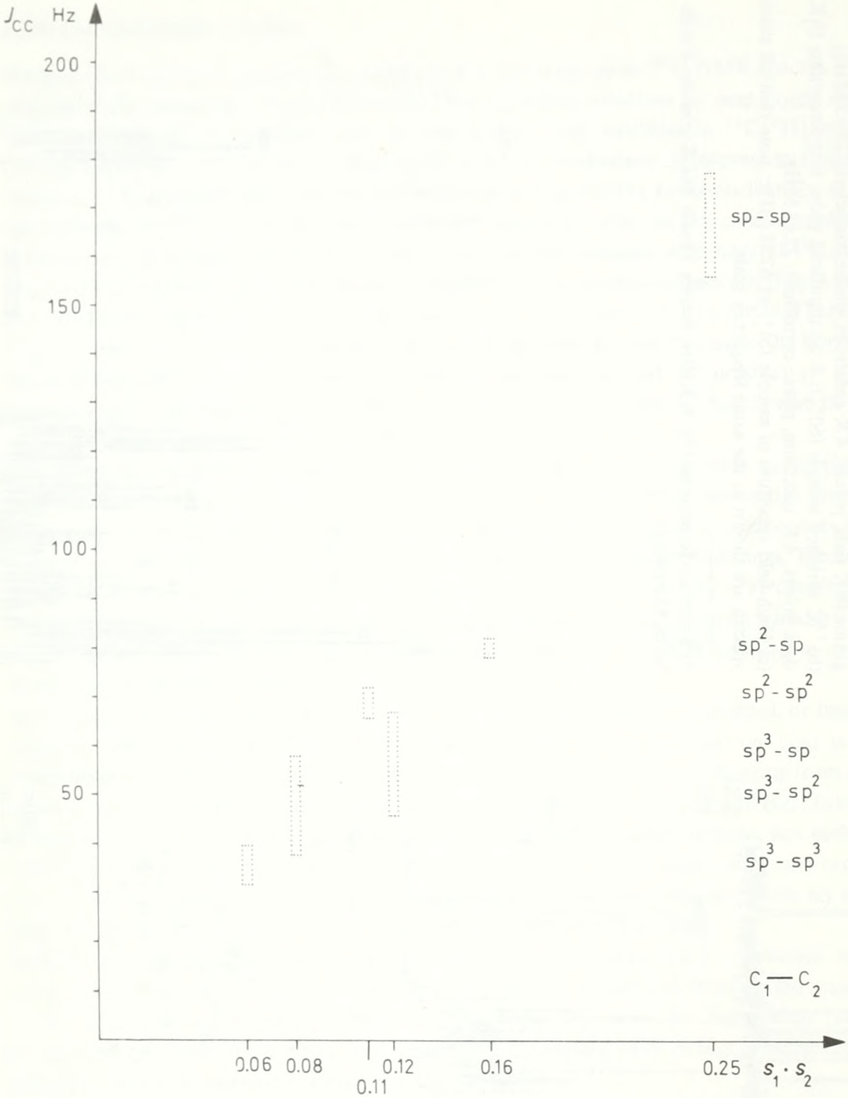

Fig. 3.17. Homonuclear carbon one-bond coupling constants observed for the six possible combinations of carbon nuclei in organic compounds; the ranges of J_{CC} are represented as dependant on the product of s characters, $s_1 \cdot s_2$, of the coupling nuclei.

Table 3.10(a). One-Bond Carbon-Carbon Coupling Constants J_{CC}. *)

Class	Compound	Formula	J_{CC} (Hz)	Ref
sp^3-sp^3	Ethane	$\mathbf{H_3C}-\mathbf{CH_3}$	34.6	[92]
	2-Methylpropane	$\mathbf{H_3C}-\mathbf{CH}(CH_3)_2$	36.9	[92]
	Ethylbenzene	$\mathbf{H_3C}-\mathbf{CH_2}-C_6H_5$	34.0	[92]
	Propionitrile	$\mathbf{H_3C}-\mathbf{CH_2}-CN$	33.0	[92]
	1-Propanol	$\mathbf{H_3C}-\mathbf{CH_2}-CH_2OH$	34.2	[92]
		$H_3C-\mathbf{CH_2}-\mathbf{CH_2}OH$	37.8	[92]
	Ethanol	$\mathbf{H_3C}-\mathbf{CH_2}OH$	37.7	[92]
	2-Propanol	$(\mathbf{H_3C})_2\mathbf{C}HOH$	38.4	[109a]
	t-Butylamine	$(\mathbf{H_3C})_3\mathbf{C}NH_2$	37.1	[92]
	t-Butanol	$(\mathbf{H_3C})_3\mathbf{C}OH$	39.5	[92]
Cyclopropanes	Methylcyclopropane	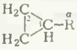 R = CH_3	44.0 (1 – α)	[109a]
	Dicyclopropylketone	R = 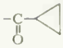	54.0 (1 – α)	[109a]
			10.2 (1 – 2)	[109a]
	Cyclopropanecarboxylic acid	R = $COOH$	72.5 (1 – α)	[109a]
			10.0 (1 – 2)	[109a]
	Cyclopropyl cyanide	R = CN	77.9 (1 – α)	[109a]
			10.9 (1 – 2)	[109a]
	Cyclopropyl iodide	R = I	12.9 (1 – 2)	[109a]
	Cyclopropyl bromide	R = Br	13.3 (1 – 2)	[109a]
	Cyclopropyl chloride	R = Cl	13.9 (1 – 2)	[109a]
sp^3-sp^2	2-Butanone	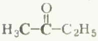 $\mathbf{H_3C}-\mathbf{C}(=O)-C_2H_5$	38.4	[92]
	Acetaldehyde	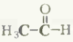 $\mathbf{H_3C}-\mathbf{C}(=O)-H$	39.4	[92]
	Acetone	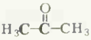 $\mathbf{H_3C}-\mathbf{C}(=O)-CH_3$	40.1	[92]
	3-Pentanone	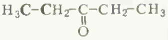 $\mathbf{H_3C}-\mathbf{CH_2}-C(=O)-CH_2-CH_3$	35.7	[109a]
		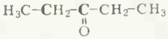 $H_3C-\mathbf{CH_2}-\mathbf{C}(=O)-CH_2-CH_3$	39.7	[109a]
	Acetophenone	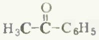 $\mathbf{H_3C}-\mathbf{C}(=O)-C_6H_5$	43.3	[92]
	Acetate anion (aq.)	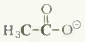 $\mathbf{H_3C}-\mathbf{C}(=O)-O^{\ominus}$	51.6	[92]
	N,N-Dimethylacetamide	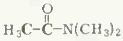 $\mathbf{H_3C}-\mathbf{C}(=O)-N(CH_3)_2$	52.2	[92]
	Acetic acid	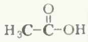 $\mathbf{H_3C}-\mathbf{C}(=O)-OH$	56.7	[92]
	Ethyl acetate	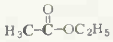 $\mathbf{H_3C}-\mathbf{C}(=O)-OC_2H_5$	58.8	[92]
sp^3-sp	*t*-Butyl cyanide	$(H_3C)_3\mathbf{C}-\mathbf{C}\equiv N$	52.0	[92]
	iso-Propyl cyanide	$(H_3C)_2\mathbf{CH}-\mathbf{C}\equiv N$	54.8	[92]
	Propionitrile	$H_3C-\mathbf{CH_2}-\mathbf{C}\equiv N$	55.2	[92]
	Acetonitrile	$\mathbf{H_3C}-\mathbf{C}\equiv N$	56.5	[92]
	Propyne	$\mathbf{H_3C}-\mathbf{C}\equiv C-H$	67.4	[109a]
sp^2-sp^2 alkenic	Ethylene	$\mathbf{H_2C}=\mathbf{CH_2}$	67.6	[92]
	Acrylic acid	$\mathbf{H_2C}=\mathbf{CH}-COOH$	70.4	[92]
	Acrylonitrile	$\mathbf{H_2C}=\mathbf{CH}-CN$	70.6	[92]
	Styrene	$\mathbf{H_2C}=\mathbf{CH}-C_6H_5$	70.0 ± 3	[92]

---

*) The coupling carbons are printed in bold type.

Table 3.10(a) (Continued).

Class	Compound	Formula		J_{CC} (Hz)	Ref.
sp^2-sp^2 aromatic	Benzene	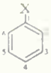	X = H	57.0	[92]
	Nitrobenzene		$X = NO_2$	55.4 (1 – 2) 56.3 (2 – 3) 55.8 (3 – 4)	[92]
	Iodobenzene		X = I	60.4 (1 – 2) 53.4 (2 – 3) 58.0 (3 – 4)	[109 a]
	Anisole		$X = OCH_3$	58.2 (2 – 3) 56.0 (3 – 4)	[109 a]
	Aniline		$X = NH_2$	61.3 (1 – 2) 58.1 (2 – 3) 56.6 (3 – 4)	[92]
	Pyridine	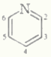		53.8 (2 – 3) 56.2 (3 – 4)	[92]
	Thiophene		X = S	64.2	[109 a]
	Pyrrole		X = NH	65.9	[109 a]
	Furan		X = O	69.1	[109 a]
sp^2-sp	Benzonitrile	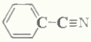		80.3	[92]
	1,1-Dimethylallene	$(H_3C)_2C=C=CH_2$		99.5	[109 a]
sp-sp	Phenylethynyl cyanide	$C_6H_5-C\equiv C-C\equiv N$		155.8	[92]
	Acetylene	$H-C\equiv C-H$		171.5	[92]
	Phenylacetylene	$C_6H_5-C\equiv C-H$		175.9	[92]

Table 3.10(b). Longer-Range Carbon-Carbon Coupling Constants $^2J_{CC}$ and $^3J_{CC}$; Data from Ref. [109a].

Compound		Formula		$^2J_{CC}$ (Hz)
Propyne		$H_3C-C\equiv C-H$		11.8
2-Butanone		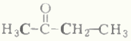 $H_3C-\overset{O}{\overset{\Vert}{C}}-CH_2-CH_3$		15.2
Cyclobutanone		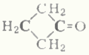		9.5
Cyclobutyl bromide		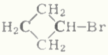		9.0
				$^3J_{CC}$ (Hz)
Pyridine	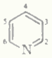		2 – 5	13.95
Aniline	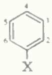	$X = NH_2$	2 – 5	7.9
Iodobenzene		X = I	2 – 5	8.6
Nitrobenzene		$X = NO_2$	2 – 5	7.6

3.2.5. Coupling between Carbon and Heteronuclei X (X ≠ C, H, D)

Couplings between carbon and heteronuclei X (X ≠ C, H) may lead to an observable splitting of the ^{13}C signals in $^{13}C\{^1H\}$ experiments. A knowledge of the magnitudes of heteronuclear coupling constants J_{CX} helps to assign signals in $^{13}C\{^1H\}$ NMR spectra.

The largest heteronuclear carbon couplings known so far are the J_{CHg} data of organomercury compounds. They may approach the order of 2 kHz for one-bond and 100 Hz for longer-range couplings (Table 3.11(a,b), [109, 110]). Carbon-13-nitrogen-15 coupling constants are at the other extreme, their magnitude ranging from 0 – 20 Hz [111 – 115]. These splittings are directly observable in $^{13}C\{^{1}H\}$ experiments on ^{15}N enriched samples.

The relative sign of one-bond coupling constants may be negative, as is the case for all J_{CF} data (Table 3.13, [92]). Variable signs, depending on the types of compounds, are observed for J_{CP} and J_{CN} (Tables 3.11, 3.12): A small negative J_{CP} is measured for triphenylphosphine with trivalent phosphorus, and a larger positive one for tetramethylphosphonium salts (Table 3.8(a)); negative one-bond C – N couplings are reported for nitriles (Table 3.12) due to $\gamma_N < 0$ according to eq. (3.15).

Table 3.11(a). One-Bond Coupling Constants J_{CX} in Methyl Derivatives $X(CH_3)_n$ of Heteroatoms; Data from Ref. [110] if not otherwise indicated.

Hetero-atom X	Compound $X(CH_3)_n$	J_{CX} (Hz)	Ref.
^{1}H	HCH_3	125.0	
^{13}C	$C(CH_3)_4$	36.9	
^{14}N	$^{\oplus}N(CH_3)_4$	10.0	
^{15}N	$^{\oplus}N(CH_3)_4$	5.8	[112]
^{19}F	FCH_3	– 157.5	
^{29}Si	$Si(CH_3)_4$	– 52.0	
$^{31}P(III)$	$P(CH_3)_3$	– 13.6	
	$^{\oplus}P(CH_3)_4$	55.5	
$^{31}P(V)$	$OP(CH_3)(OCH_3)_2$	141.5 5.0 ($^{2}J_{CP}$)	[102]
^{77}Se	$Se(CH_3)_2$	– 62.0	
	$^{\oplus}Se(CH_3)_3$	– 50.0	
^{113}Cd	$Cd(CH_3)_2$	– 537.0	
^{119}Sn	$Sn(CH_3)_4$	– 340.0	
^{125}Te	$Te(CH_3)_2$	162.0	
^{199}Hg	$Hg(CH_3)_2$	687.4	
	$O_2NOHgCH_3$	1800.0	
^{207}Pb	$Pb(CH_3)_2$	395.0	

Table 3.11(b). One-Bond and Longer-Range Couplings, J_{CX} and $^{2}J_{CX}$, $^{3}J_{CX}$, $^{4}J_{CX}$, of Selected Phenyl Derivatives $X(C_6H_5)_n$; Data from Ref. [110].

Hetero-atom X	Compound $X(C_6H_5)_n$	J_{CX} (Hz)	$^{2}J_{CX}$ (Hz)	$^{3}J_{CX}$ (Hz)	$^{4}J_{CX}$ (Hz)
^{1}H	HC_6H_5	157.5	1.0	7.4	– 1.1
^{11}B	$^{\ominus}B(C_6H_5)_4$	49.5	–	2.6	–
^{19}F	FC_6H_5	– 245.3	21.0	7.7	3.3
^{31}P	$P(C_6H_5)_3$	12.4	19.6	6.7	0.0
	$^{\oplus}P(C_6H_5)_4$	88.4	10.9	12.8	2.9
^{199}Hg	$Hg(C_6H_5)_2$	1186.0	88.0	101.6	17.8

An approximate correlation between J_{CN} and carbon and nitrogen s charcter is deducible from the limited amount of experimental data available (Table 3.12, [111]). However, couplings between carbon and many heteronuclei, *e.g.* the J_{CF} data shown in Table 3.13, do not depend simply on carbon s character as is the case for J_{CH} and J_{CC}. Nevertheless, electron withdrawal at

Table 3.12. Carbon-13-Nitrogen: 15 Coupling Constants of Selected Organic Compounds. *)

Compound	Formula	J_{CN} (Hz)		Ref.
Methylamine	$H_3\mathbf{C}-\mathbf{N}H_2$	7.0		[111]
Methylammonium ion	$H_3\mathbf{C}-\overset{\oplus}{\mathbf{N}}H_3$	< 8.0		[111]
Tetramethylammonium ion	$\overset{\oplus}{\mathbf{N}}(\mathbf{C}H_3)_4$	5.8		[112]
Tetraethylammonium ion	$\overset{\oplus}{\mathbf{N}}(\mathbf{C}H_2CH_3)_4$	4.0		[112]
Glycine	$H_3\overset{\oplus}{\mathbf{N}}-\mathbf{C}H_2-COO^{\ominus}$	6.2		[113]
	$H_2\mathbf{N}-\mathbf{C}H_2-COO^{\ominus}$	4.9		[113]
DL-Alanine	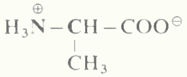 $H_3\overset{\oplus}{\mathbf{N}}-\underset{\displaystyle CH_3}{\underset{\vert}{\mathbf{C}H}}-COO^{\ominus}$	5.6		[113]
Dimethylnitrosamine	$(H_3\mathbf{C})_2N-{}^{15}\mathbf{N}O$	7.5 C_{anti} 1.4 C_{syn}	($^2J_{CN}$)	[113]
1,1-Dimethylhydrazine	$(H_3\mathbf{C})_2N-{}^{15}\mathbf{N}H_2$	< 1.0	($^2J_{CN}$)	[113]
trans-N-Methylbenzaldimine	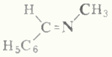	< 3.0		[111]
	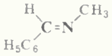	7.1		[111]
Acetamide	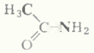	9.5	($^2J_{CN}$)	[111, 113]
	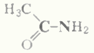	< 15.0		[113]
Acetanilide	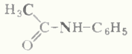	9.3		[113]
	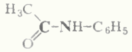	13.0		[113]
N,N-Dimethylformamide	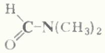	13.4		[113]
Pyridine	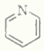	0.44	(J_{CN})	[113]
		2.4	($^2J_{CN}$)	[113]
		3.6	($^3J_{CN}$)	[113]
Pyridinium ion	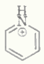	12.0	(J_{CN})	[113]
		2.1	($^2J_{CN}$)	[113]
		5.3	($^3J_{CN}$)	[113]
Cyanide anion	$^{\ominus}\mathbf{C}\equiv\mathbf{N}$	± 5.9		[92]
Acetonitrile	$H_3C-\mathbf{C}\equiv\mathbf{N}$	−17.5		[114]
	$H_3\mathbf{C}-C\equiv\mathbf{N}$	3.0	($^2J_{CN}$)	[114]
Propionitrile	$H_5C_2-\mathbf{C}\equiv\mathbf{N}$	−16.4		[92]
t-Butyl cyanide	$(H_3C)_3C-\mathbf{C}\equiv\mathbf{N}$	−15.4		[92]
	$H_3\mathbf{C}-\overset{\oplus}{\mathbf{N}}\equiv\overset{\ominus}{C}$	−10.6		[115]
Methyl isothiocyanate	$H_3\mathbf{C}-\mathbf{N}=C=S$	13.4		[111]

*) The coupling nuclei are printed in bold type.

the coupling carbon often increases J_{CX}. This trend is obvious when the J_{CF} values of mono-, di-, and trifluoroethanol, or those of mono- and trifluoroacetic acid are compared (Table 3.13). Relatively large longer-range C–X splittings are found not only for X = mercury (Table 3.11(b)), but also for fluorine, phosphorus(III,V) and nitrogen-15.

Table 3.13. Carbon-Fluorine Coupling Constants of Selected Organic Compounds; Data from Ref. [92] if not otherwise indicated

Compound	Formula	$-J_{CF}$ (Hz)	Ref.
Fluoromethane	FCH_3	157.5	
Difluoromethane	$FCFH_2$	234.8	
Trifluoromethane	FCF_2H	274.3	
Tetrafluoromethane	FCF_3	259.2	
1,1,1-Trifluoroethane	FCF_2CH_3	271.0	
Benzyl fluoride	$FCH_2C_6H_5$	165.0	
t-Butyl fluoride	$FC(CH_3)_3$	167.0	
2-Fluoroethanol	FCH_2CH_2OH	167.0	
2,2-Difluoroethanol	$FCFHCH_2OH$	240.5	
2,2,2-Trifluoroethanol	FCF_2CH_2OH	278.0	
Hexafluorodiethyl ether	FCF_2OCF_3	265.0	
Trifluoroacetone	$FCF_2C(O)CH_3$	289.0	
Hexafluoroacetone hydrate	$(FCF_2)_2C(OH)_2$	285.5	[102]
		$^2J_{CF}$: 34.0	[102]
Monofluoroacetic acid	FCH_2COOH	181.0	
Trifluoroacetic acid	FCF_2COOH	283.2	
		$^2J_{CF}$: 44.0	[102]
p-Fluoroanisole	$p\text{-}FC_6H_4OCH_3$	237.0	
p-Fluorotoluene	$p\text{-}FC_6H_4CH_3$	241.0	
Fluorobenzene	FC_6H_5	244.0	
p-Trifluoromethylfluorobenzene	$p\text{-}FC_6H_4CF_3$	252.0	
p-Fluoroacetophenone	$p\text{-}FC_6H_4C(O)CH_3$	253.0	
p-Nitrofluorobenzene	$p\text{-}FC_6H_4NO_2$	257.0	
1,1-Difluoroethylene	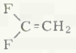 $F_2C{=}CH_2$	287.0	
Fluorophosgene	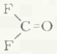 $F_2C{=}O$	308.4	
Acetyl fluoride	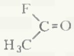 $F(H_3C)C{=}O$	353.0	
Formyl fluoride	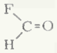 $F(H)C{=}O$	369.0	

The magnitudes of two-bond carbon-fluorine couplings $^2J_{CF}$ in trifluoroacetic acid and hexafluoroacetone hydrate are 44 and 34 Hz, respectively (Table 3.13). Five-bond couplings of more than 20 Hz are reported for 1,4,8-trimethyl-5-fluorophenanthrene derivatives; their magnitudes decrease on saturation of the 9,10 bond in the phenanthrene moiety [116]. These large five-bond splittings provide evidence that a through-space mechanism might be operative in carbon-13 coupling [116].

In alkyl phosphonates, one-bond coupling constants J_{CP} range from 125 to 165 Hz; negative two-bond couplings between 6 and 7 Hz and positive three-bond splittings of about 5 to 6 Hz are observed [117]. Four-membered cyclic phosphines such as 2,2,3,4,4-pentamethylphosphetanes show two-bond coupling constants $^2J_{CP}$ which are larger (25 Hz) for *trans* and smaller (5 Hz) for *cis* configuration of the exocyclic substituent X (X = $-Cl$, $-CH_3$, $-C_6H_5$) at phosphorus [118]. A similar stereospecifity of carbon-phosphorus three-bond coupling has been reported for nucleotides [119]. Two- and three-bond coupling constants in this class of compounds cover the range of 1 to 10 Hz. These longer-range splittings are valuable aids for assigning the ^{13}C signals of pyranose, furanose and polyalcoholic carbons near phosphorus in nucleotides. An illustrative example is the assignment achieved for C-5′ and C-4′ of ribose and ribitol in the enzyme cofactor flavin adenine dinucleotide due to carbon-phosphorus long-range coupling [120].

Relations between longer-range carbon-nitrogen-15 coupling constants were reported for dimethylnitrosamine and pyridine [113]. The methyl group *anti* to the oxygen in dimethylnitrosamine shows a larger two-bond coupling $^2J_{CN}$ than that with *syn* configuration (Table 3.12). A considerable increase of J_{CN} and $^3J_{CN}$ in pyridine is found on protonation at nitrogen.

3.3. Spin-Lattice Relaxation Times

3.3.1. Mechanisms of ^{13}C Spin-Lattice Relaxation [7,121]

In spin-lattice relaxation, the excited nuclei transfer their excitation energy to their environment. They do so *via* interaction of their magnetic vectors with fluctuating local fields of sufficient strength and a fluctuation frequency of the order of the Larmor frequency of the nuclear spin type. Depending upon the atomic and electronic environment of a nucleus in a molecule and the motion of that molecule, there are five potential mechanisms contributing to spin-lattice relaxation of the nucleus.

3.3.1.1. Relaxation Resulting from Chemical Shift Anisotropy (CSA Mechanism)

The magnetic shielding of a nucleus arising from the surrounding electrons can be anisotropic, *e.g.* in derivates of benzene, acetylene, and carbonyl compounds (chemical shift anisotropy). The shielding constant σ then possesses spatially oriented components, which can change with time if the molecule moves relative to the field H_0. There arise fluctuating local fields which permit spin-lattice relaxation of the anisotropically shielded nucleus. A contribution of the CSA mechanism is apparent from a proportionality of the T_1 values measured to the square of the magnetic field strength H_0 applied. This contribution is usually negligible for the ^{13}C nuclei of organic molecules.

3.3.1.2. Relaxation by Scalar Coupling (SC Mechanism)

The spins of two proximate nuclei A and X in a molecule undergo coupling, *i.e.* the signals of A and X are split, but only if the lifetime of these nuclei in their nuclear magnetic energy levels (Fig. 1.3) is sufficiently large (scalar coupling).

If nucleus X relaxes very much faster than nucleus A then no signal splitting is observed. However, the fast relaxation of X generates fluctuating fields which in turn contribute to the relaxation of nucleus A. Quadrupole nuclei having $I \geqslant 1$, *i.e.* nuclei whose charge distribution is not spherically symmetrical, relax so rapidly, for instance, that they accelerate the relaxation of neighboring nuclei. The contribution of the SC mechanism, which can be recognized from a frequency and temperature dependence of T_1 is particularly large when the coupling nuclei precess with similar Larmor frequencies. This applies to ^{13}C and the quadrupole ^{79}Br. As a consequence ^{13}C nuclei bound to Br relax relatively fast ($CHCl_3$: $T_1 = 32.4$ s; $CHBr_3$: $T_1 = 1.65$ s).

3.3.1.3. Relaxation by Spin Rotation (SR Mechanism)

If a molecule or molecular segment rotates, then the magnetic vectors of the bonding electron spins will also rotate. This gives rise to fluctuating local fields which can contribute to spin-lattice relaxation of the nuclei of a rotating molecule or a rotating alkyl group. This SR mechanism plays an important role in small symmetrical molecules (methane, cyclopropane) or in small segments of larger molecules (methyl groups). If the ^{13}C nuclei are not protonated (as in CS_2), spin rotation can even become the predominant relaxation mechanism. In such cases T_1 is found to decrease significantly with increasing temperature.

3.3.1.4. Relaxation by Internuclear Dipole-Dipole Interaction (DD Mechanism)

Each nuclear spin generates a local magnetic field upon molecular motion. If two magnetic nuclei such as ^{13}C and ^{1}H are linked by a bond, then each of the nuclei will experience not only the external field $\boldsymbol{H}_0$, but also the local field of the other nuclear spin (internuclear dipole-dipole interaction). Now molecular motion is very rapid in liquids. Rotations of C–H bonds are correspondingly fast in dissolved organic molecules, and the orientations of ^{1}H and ^{13}C relative to $\boldsymbol{H}_0$ will be constantly changing. The resulting constantly imposed magnetic reorientation of the two nuclear spins generates fluctuating local fields which contribute to the relaxation of the nuclei. Most of the ^{13}C nuclei in organic molecules, especially those linked to hydrogen (CH, CH_2, CH_3) are relaxed predominantly by internuclear dipole-dipole interaction.

T_1 values of ^{13}C are usually measured with proton noise decoupling. Thus, just one signal, not a multiplet, and consequently only one T_1 value results for each C atom of a molecule. During this decoupling, the protons transfer their excitation energy to the "lattice" primarily by internuclear DD interaction with ^{13}C and consequently forced ^{13}C relaxation. As a result, the population of the energetically more favorable ^{13}C spin states (Fig. 1.3) increases, and the ^{13}C signal intensities are enhanced on proton-decoupling more than would be expected from the multiplet intensities in the spectra recorded without decoupling (nuclear Overhauser enhancement, NOE [34]).

If ^{13}C relaxation proceeds exclusively by the DD mechanism, the NOE factor η_C, indicating the enhancement of the ^{13}C signal intensity on decoupling, is determined by the gyromagnetic ratios of ^{1}H and ^{13}C according to eq. (3.17) [34].

$$\eta_C = \frac{\gamma_H}{2\gamma_C} = 1.988 \qquad (3.17)$$

NOE factors of this magnitude are indeed measured for numerous ^{13}C signals of organic molecules, especially for signals of CH and CH_2 carbon atoms, as shown for formic acid in Fig. 2.16 [33].

NOE factors smaller than 1.988 indicate participation of other mechanisms in the spin-lattice relaxation of protonated ^{13}C nuclei. The percentage contribution of the DD mechanism can be ascertained from the measured NOE factor according to eq. (3.18).

$$\% \text{ DD} = \frac{\eta_C}{1.988} \times 100 \qquad (3.18)$$

Accordingly, the time constant $T_{1(DD)}$ of the DD mechanism can be calculated from the measured η_C and T_1 values [eq. (3.19)].

$$T_{1(DD)} = T_1 \frac{1.988}{\eta_C} \qquad (3.19)$$

Since the relaxation rates $1/T_1$ on cooperation of several relaxation mechanisms can be assumed to be additive, as shown in eq. (3.20),

$$\frac{1}{T_1} = \frac{1}{T_{1(DD)}} + \frac{1}{T_{1(SR)}} + \frac{1}{T_{1(SC)}} + \frac{1}{T_{1(CSA)}} + \cdots \qquad (3.20)$$

the measured T_1 value and the value of $T_{1(DD)}$, accessible from the NOE factor η_C *via* eq. (3.19), can be used to calculate the time constant of a second relaxation mechanism, provided that no further mechanisms are operative. For instance, in benzene the DD mechanism is accompanied only by the SR mechanism. Benzene contains no quadrupole nucleus, and the contribution of the CSA mechanism to ^{13}C relaxation of liquid benzene is so small that the T_1 value can be shown to be independent of the magnetic field strength [123]. Then $T_{1(DD)}$ and $T_{1(SR)}$ can be determined from the experimental values of T_1 and η_C according to Scheme 3.1 [121, 124–126].

Experimental data: Spin-lattice relaxation time $T_1 = 29.3$ s
NOE factor $\eta_C = 1.6$

Percentage of DD relaxation:

$\%$ DD $= \eta_C \times 100/1.988 = 80\%$

Contribution of DD mechanism:

$T_{1(DD)} = T_1 \times 1.988/\eta_C = 29.3 \times 1.988/1.6 = 36.4$ s

Contribution of SR mechanism:

from $\frac{1}{T_1} = \frac{1}{T_{1(DD)}} + \frac{1}{T_{1(SR)}}$

it follows

$$T_{1(SR)} = \frac{T_1 T_{1(DD)}}{T_{1(DD)} - T_1} = \frac{29.3 \times 36.4}{36.4 - 29.3} = 150 \text{ s}$$

Scheme 3.1. Determination of $T_{1(DD)}$ and $T_{1(SR)}$ from T_1 and η_C measured for benzene.

3.3.1.5. Electron Spin-Nucleus Interactions and Consequences

During molecular motion, unpaired electrons generate much stronger fluctuating local fields than the nuclear spins, owing to their considerably larger magnetic moment. As a result, relaxation in the presence of unpaired electrons is dominated by electron spin-nucleus dipole-dipole interactions analogous to internuclear dipole-dipole interactions, especially for non-protonated

^{13}C nuclei. Thus smaller T_1 values are observed for paramagnetic compounds themselves, or in their presence, *e.g.* in solvents containing oxygen. Paramagnetic contaminants, including the oxygen nearly always dissolved in liquids, must therefore be removed if characteristic and reproducible T_1 values are to be measured.

Acceleration of relaxation of a nuclear spin by paramagnetic compounds is the greater the slower the nucleus relaxes. For example, the non-protonated carbon nuclei of phenylacetylene in a normally prepared sample (20% in $(CD_3)_2CO$ as solvent) display T_1 values lower by a factor of two (numbers in parentheses)*) than those for a degassed, *i.e.* largely oxygen-free, solution [125]. In contrast, the faster-relaxing protonated carbon atoms (T_1 < 20 s) are affected much less.

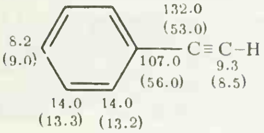

Phenylacetylene

The pronounced relaxation acceleration observed for slowly relaxing nuclei in the presence of paramagnetic compounds is exploited in Fourier transform ^{13}C NMR spectroscopy. On use of the fast pulse sequences that are frequently necessary, the spin-lattice relaxation of "slow" ^{13}C nuclei can no longer follow excitation and the pertinent ^{13}C signals have low intensities. In such cases, addition of small amounts of relaxation accelerators such as radicals or transition metal salts to the sample amplify these signals [127].

It ist quite reasonable that a paramagnetic central ion should accelerate the relaxation of the C atoms of a ligand, and that the magnitude of the acceleration should depend upon the distance between the ion and the C atom being observed.

In such cases, T_1 measurements provide information about the distances between the paramagnetic ion and the ligand. Thus the spin-lattice relaxation times of the ^{13}C nuclei in α- and β-methyl D-glucopyranoside become selectively smaller on binding to the Mn^{2+} complex of the protein concanavalin A [128]. The experimental T_1 values show that the two glucopyranoside anomers retain their C1 chair conformation, but adopt different orientations on binding to the protein complex [128]. The non-reducing end of the α-anomer (C-3, C-4) approaches the Mn^{2+} ion most closely (average separation approx. 1 nm) [128].

3.3.2. Influence of Molecular Motion on Dipole-Dipole Relaxation

The majority of ^{13}C NMR measurements are performed with solutions or liquid samples with proton decoupling. Under these conditions, the ^{13}C spin-lattice relaxation times T_1 depend mainly upon the speed of molecular motion relative to ^{13}C Larmor precession. The overall tumbling of molecules in liquids cannot easily be resolved into components such as rotation, vibration, or translation. In order to derive a useful relation with the spin-lattice relaxation, the average time required by a molecule between two reorientations is taken as a measure of molecular motion. This time is referred to the unit circle, *i.e.* divided by 2π, and then designated the effective molecular correlation time τ_C [7, 122, 129–131]. If the molecules are rotating or vibrating, one revolution or vibration per second (1 Hz) is equal to 2π rad/s. τ_C then corresponds to the average time required by the molecules to rotate through 1 radian.

---

*) Unless otherwise stated, the T_1 values in the formulae are quoted in s.

Only those molecular motions whose "frequencies" lie in the region of the ^{13}C Larmor precession lead to rapid ^{13}C dipolar relaxation. The ^{13}C nuclei are known to precess with a frequency of $\nu_0 \approx 2.26 \times 10^7$ Hz or $\omega_0 = 2\pi\,\nu_0 \approx 1.42 \times 10^8$ rad/s at a field strength of $H_0 \approx 2.1$ Tesla. Most effective DD relaxation then becomes possible owing to molecular motions having correlation times of

$$\tau_C \approx \frac{1}{1.42 \times 10^8} \approx 7 \times 10^{-9}\ \text{s/rad}.$$

The correlation function $T_1 = f(\tau_C)$ shown in Fig. 3.18 gives a minimum for such motion; however, this is true only for a field strength of 2.1 Tesla. At higher fields the minimum lies at shorter correlation times, *i.e.* the fastest DD relaxation requires even faster motion (Fig. 3.18).
Very slow molecular motion ($\tau_C > 10^{-9}$ s/rad at $H_0 \approx 2.1$ Tesla) leads to an increase in T_1, while T_2 decreases (Fig. 3.18). The signals then broaden (line width at half-maximum intensity $\Delta\nu_{1/2} \sim 1/T_2$). Therefore the more sluggish macromolecules usually give poorly resolved ^{13}C NMR spectra having a bandlike structure.

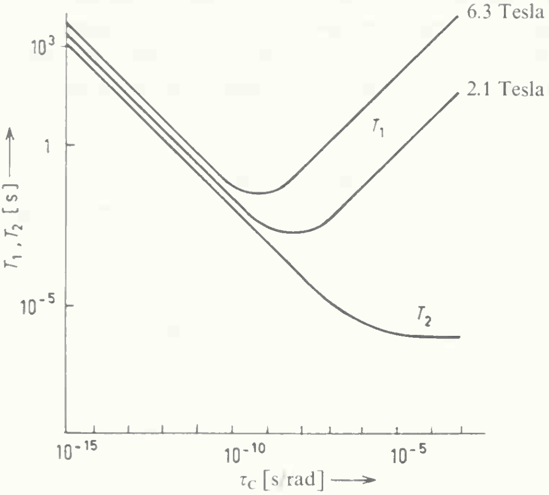

Fig. 3.18. Relation between the relaxation times T_1 and T_2 and the effective correlation time τ_C. In stronger magnetic fields the T_1 minimum shifts towards smaller correlation times, *i.e.* higher "frequencies" of molecular motion.

If the viscosity is sufficiently low, small and medium-sized molecules tumble very fast. The "frequencies" of their motion often even exceed the Larmor frequency $\omega_0 = 2\pi\,\nu_0$, and the correlation time consequently becomes shorter than the value $\tau_{C(\min)}$ leading to the most effective DD relaxation ($\omega_0\,\tau_C \ll 1$). This situation corresponds to the declining branch of the correlation function (Fig. 3.18): T_1 and T_2 increase, are approximately equal, and the signals become sharper owing to $\Delta\nu_{1/2} \sim 1/T_2$ *(motional narrowing)*. Under these circumstances the dipolar relaxation time $T_{1(DD)}$ of a ^{13}C nucleus is shown in eq. (3.21) to be inversely proportional to the number N of directly adjacent protons and to the effective correlation time τ_C [122, 129–131].

$$\frac{1}{T_{1(DD)}} = \hbar^2\,\gamma_C^2\,\gamma_H^2\,r_{CH}^{-6}\,N\,\tau_C \tag{3.21}$$

$\hbar \equiv h/2\pi$; h is Planck's constant; γ_C and γ_H are the gyromagnetic ratios of ^{13}C and ^{1}H respectively; r_{CH} is C–H internuclear distance, usually about 0.109 nm.

3.3.3. Information Content of ^{13}C Spin-Lattice Relaxation Times

3.3.3.1. Degree of Alkylation and Substitution of C Atoms

Within rigid molecules the correlation time τ_C is equal for all carbon atoms. Moreover, the C−H bond lengths in nearly all organic compounds are approximately 0.109 nm, except for acetylenes ($r_{CH} \approx 0.106$ nm). Under these conditions, the spin-lattice relaxation time T_1 of a ^{13}C nucleus relaxing by the DD mechanism is shown by eq. (3.22) to depend solely upon the number N of directly bonded H atoms:

$$T_{1(DD)} = \text{const.}/N. \tag{3.22}$$

Neglecting the methyl carbons, which do not belong to the rigid skeleton of a molecule owing to internal rotation of the CH_3 groups (Section 3.3.4.), the T_1 values for the CH and CH_2 groups of the same molecule give a ratio of 2:1; quaternary C atoms having $N = 0$ relax much more slowly:

$$T_{1(C)} \gg T_{1(CH)} > T_{1(CH_2)} \text{ and } T_{1(CH)}:T_{1(CH_2)} = 2:1. \tag{3.23}$$

This relation (3.23) can be demonstrated for simple rigid molecules, *e.g.* for adamantane having $T_{1(CH)} = 17.0$ s and $T_{1(CH_2)} = 7.8$ s [132*)]. It is a valuable aid in the assignment of the ^{13}C NMR spectra of large molecules, particularly when signal crowding precludes clear distinction between singlets, doublets, and triplets in coupled or proton off-resonance decoupled ^{13}C NMR spectra.

3.3.3.2. Molecular Size and Relaxation Mechanisms

The T_1 values of the ^{13}C nuclei generally decrease with increasing molecular size if the molecules are rigid. Thus values in the ms or ns range are observed for the ^{13}C nuclei of the rigid backbone of macromolecules. Medium size molecules ($C_{10}-C_{50}$) typically show T_1 values between 0.1 s and 20 s. For very small molecules of high symmetry (dumbbells, tetrahedra, pyramids, small regular polyhedra), however, values of up to 100 s and beyond are possible. This applies, *e.g.* to methane derivatives except for bromides (effective SC relaxation, *cf.* Section 3.3.1.2.), especially when the molecule contains no H atoms ($^{13}CCl_4$: $T_1 \approx 160$ s). The reason is that the ^{13}C nuclei of very mobile small molecules relax partly, and sometimes even predominantly, by the less effective spin-rotation mechanism. The considerable contribution of spin rotation to ^{13}C spin-lattice relaxation has already been demonstrated for benzene (Section 3.3.1.4.).

The relation between molecular size, T_1, and the relaxation mechanisms is apparent from the homologous series of the cycloalkanes. T_1 and NOE data as well as the contributions of the DD and SR mechanisms accessible from these experimental values *via* eqs. (3.19) and (3.20) are listed in Table 3.14. The ^{13}C nuclei of cyclopropane relax almost as fast by spin-rotation as by the DD mechanism ($T_{1(SR)} \approx T_{1(DD)}$). However, in cyclobutane the DD mechanism predominates ($T_{1(DD)} < T_{1(SR)}$), and the carbon atoms of cyclohexane and its higher homologs relax exclusively by the DD mechanism ($T_{1(DD)} \ll T_{1(SR)}$) [133]. The $T_{1(DD)}$ values themselves decrease fairly regularly with increasing ring size (Table 3.14).

---

*) See also Fig. 2.25 and compare the results.

Table 3.14. Spin-lattice relaxation times T_1 and NOE factors η_C of the ^{13}C nuclei of cycloalkanes containing n carbon atoms [133].

n	T_1 [s]	η_C	DD [%]	$T_{1(DD)}$ [s]	$T_{1(SR)}$ [s]
3	36.7	1.0	50.2	72.2	74.6
4	35.7	1.4	70.5	50.7	121
5	29.2	1.52	76.5	38.2	124
6	19.6	1.9	95.5	20.5	447
7	16.2	1.96	98.5	16.4	> 1000
8	10.3	2.0	100	10.3	> 1000
10	4.7	2.0	100	4.7	> 1000

3.3.3.3. Anisotropy of Molecular Motion

Eq. (3.21) discussed in Section 3.3.2. is only valid if the motion of the molecules under study has no preferential orientation, *i.e.* is not anisotropic. Strictly speaking, this applies only for approximately spherical bodies such as adamantane. Even an ellipsoidal molecule like *trans*-decalin performs anisotropic motion in solution: it will preferentially undergo rotation and translation such that it displaces as few as possible of the other molecules present. This anisotropic rotation during translation is accounted for by the three diagonal components R_1, R_2, and R_3 of the rotational diffusion tensor. If the principal axes of this tensor coincide with those of the moment of inertia – as can frequently be assumed in practice – then R_1, R_2, and R_3 indicate the speed at which the molecule rotates about its three principal axes.

The connection between anisotropic molecular motion and nuclear relaxation was derived by *Woessner* as early as 1962 [134]. Accordingly, the dipole-dipole relaxation time of a carbon nucleus is a function of the diagonal components R_1, R_2, and R_3 of the rotational diffusion tensor and the cosines λ, μ, and ν of the angles assumed by the C–H bonds relative to the principal axes of this tensor.

$$1/T_{1(DD)} = f(R_1, R_2, R_3, \lambda, \mu, \nu) \tag{3.24}$$

If the position of the principal axes of the rotational diffusion tensor were known with respect to the molecular coordinates, then the motion of the molecule could be calculated from the measured relaxation times. With simple molecules, however, it is possible to interpret the T_1 values qualitatively in the sense of an anisotropic motion.

Thus the C–H nuclei in the *para* position of monosubstituted benzene derivatives relax faster than those in the *ortho* or *meta* positions (Table 3.15 [125]). The reason for this behavior lies in a preferred rotation about the molecular axis passing through the substituent X and the *p*-carbon. In this motion, the *para* C–H bond does not change its direction relative to the field H_0; fluctuating local fields can only arise at the *p*-C nucleus by rotations of the molecule perpendicular to the preferred axis. However, these less preferred rotations still have sufficiently large frequencies to effectively relax the *p*-C atom. The preferred rotation itself continuously changes the orientation of the *ortho* and *meta* C–H bonds with respect to H_0, but too fast for effective dipolar relaxation of the *ortho* and *meta* carbon nuclei.

Table 3.15. Spin-lattice relaxation times T_1 of the ^{13}C atoms in benzene derivatives*).

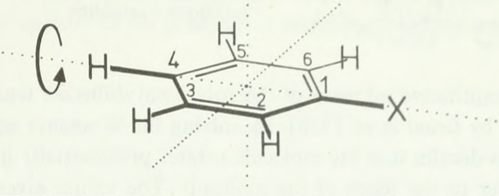

X	C Atom	T_1 [s]	Ref.
H	1−6	29.3 [a]	[125]
CH_2-CH_3	1	36.0	[102]
	2,6	18.0	
	3,5	18.0	
	4	13.0	
	$-CH_2$	13.0	
	$-CH_3$	19.0	
$CH=CH_2$	1	75.0	[125]
	2,6	14.8	
	3,5	13.5	
	4	11.9	
	$-CH=$	17.0	
	$=CH_2$	7.8	
$C\equiv CH$	1	107.0 [a]	[125]
	2,6	14.0	
	3,5	14.0	
	4	8.2	
	$-C\equiv$	132.0	
	$\equiv CH$	9.3	
CH_3	1	58.0	[125]
	2,6	20.0	
	3,5	21.0	
	4	15.0	
	CH_3	16.3	
C_6H_5	1	61.0	[125]
	2,6	5.9	
	3,5	5.9	
	4	3.2	
NO_2	1	56.0	[125]
	2,6	6.9	
	3,5	6.9	
	4	4.8	
OH	1	21.5	[125]
	2,6	4.4	
	3,5	3.9	
	4	2.4	

[a] Degassed.

*) For an additional example see Fig. 2.23.

Preferred rotation is also conceivable in 3-methyl-5,6,7,8-tetrahydroquinoline, *i.e.* about the axis passing through C-7, C-3, and the methyl group [135]. Accordingly, the C-7 methylene group exhibits a smaller T_1 value than all the other CH_2 groups of this molecule.

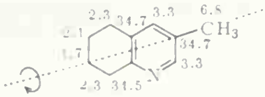

3-Methyl-5,6,7,8-tetrahydroquinoline

The first quantitative estimate of the rotational diffusion tensor for simple molecules was accomplished by *Grant et al.* [136]. By solving the Woessner equations, they were able to show, *e.g.* for *trans*-decalin that the molecule rotates preferentially like a propeller, *i.e.* about the axis perpendicular to the plane of the molecule. The values given as a measure of the rotational frequencies do not correlate with the moments of inertia, but instead with the "ellipticities" of the molecule as defined by *Grant*. They are accessible from the ratios of the interatomic distances perpendicular to the axes of rotation, and can be adopted as a measure of the number of solvent molecules that have to be displaced on rotation about each of the three axes.

The greater the differences between the interatomic distances perpendicular to an axis, the grater will be the ellipticity ε, and the more slowly will the molecule rotate about that axis.

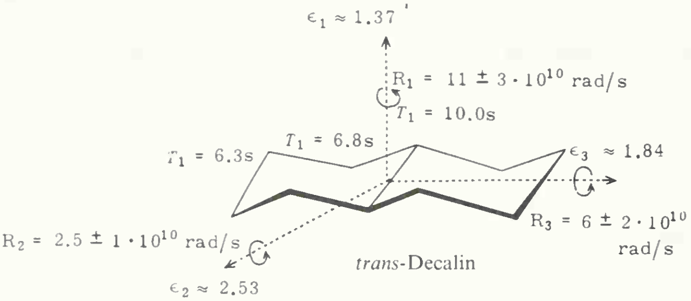
$\epsilon_1 \approx 1.37$
$R_1 = 11 \pm 3 \cdot 10^{10}$ rad/s
$T_1 = 10.0$s
$T_1 = 6.8$s
$T_1 = 6.3$s
$\epsilon_3 \approx 1.84$
$R_3 = 6 \pm 2 \cdot 10^{10}$ rad/s
$R_2 = 2.5 \pm 1 \cdot 10^{10}$ rad/s
$\epsilon_2 \approx 2.53$

trans-Decalin

For less symmetric molecules one has to resort to computer programs [137] to solve the Woessner equations. The orientation of the rotational diffusion tensor is usually defined by assuming that its principal axes coincide with those of the moment of inertia tensor. This assumption is probably a good approximation for molecules of low polarity containing no heavy atoms, since under these conditions the moment of inertia tensor roughly represents the shape of the molecule.

The hitherto most sophisticated application of *Woessner*'s theory has been accomplished for all-*trans*-retinal and its isomers [138]. After determination of the components of the rotational diffusion tensor in retinal for various dihedral angles between the olefinic chain and the cyclohexene ring, the T_1 values could be calculated for each one of these conformations. The best agreement between experimental and calculated ^{13}C T_1 values results when the 5,6–7,8 dihedral angle is 60°, in other words when the cyclohexene ring is bent by 60° towards the plane of the olefinic chain [138]. This is the first example of a conformation being determined by measurement of ^{13}C relaxation times.

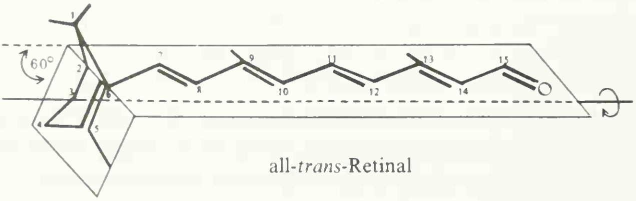

all-*trans*-Retinal

Woessner's equations thus permit prediction of spin-lattice relaxation times for the dipole-dipole mechanism, which can be of help in the assignment of ^{13}C NMR spectra. Moreover, the calculations described can be applied to the problem of internal molecular motion.

3.3.3.4. Internal Molecular Motion

(1) Rotation of Methyl Groups

While the skeleton of large molecules is often relatively rigid, the methyl groups bonded to the backbone are highly mobile. Their rotation is thus much faster than the overall motion of the molecule ($\tau_{C(CH_3)} \ll \tau_{C(skeleton)}$). The methyl groups in proton-decoupled ^{13}C NMR spectra therefore exhibit NOE factors that are smaller than the typical value for pure dipolar relaxation (1.988), *i.e.* the signals are relatively weak. At the same time, the spin-lattice relaxation times of the methyl carbon nuclei are usually much longer than permitted by the ratio expected for the DD mechanism according to eq. (3.21), *i.e.*

$$T_{1(CH)} : T_{1(CH_2)} : T_{1(CH_3)} = 6:3:2$$

The experimental values found for all the methyl carbons in 3-methyl-5,6,7,8-tetrahydroquinoline [135], 8,9,9-trimethyl-5,8-methano-5,6,7,8-tetrahydroquinazoline [135], and cholesteryl chloride [139] may be cited as examples. Lower intensities and longer T_1 values relative to the methylene and methine carbon nuclei thus frequently facilitate detection of methyl resonances in ^{13}C NMR spectra.

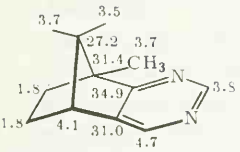

8,9,9-Trimethyl-5,8-methano-5,6,7,8-tetrahydroquinazoline

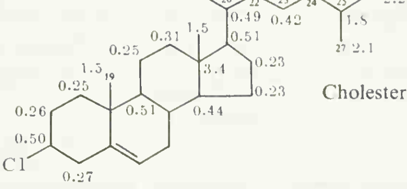

Cholesteryl chloride

(2) Intramolecular Steric Interactions

Steric interactions can hinder the rotation of methyl groups and thus accelerate methyl relaxation. It can be deduced, *e.g.* from the T_1 values of butanone oxime, that the CH_3 group *syn* to the OH group in the more stable *anti* isomer rotates faster ($T_1 = 6.1$ s) than that *anti* to the OH group in the more labile *syn* isomer ($T_1 = 2.8$ s) [140]. As an explanation it is assumed that the van der Waals interactions between the methyl and hydroxyimino groups, and between the methyl and methylene groups are of the same order of magnitude in the *anti* isomer. In contrast, the methyl group in the *syn* isomer adopts an energetically more favorable conformation involving one-sided interaction with the methylene group, with the result that its rotation is hindered [140].

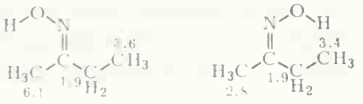

anti Butanone oxime *syn*

The T_1 values of the methyl carbon nucleus in 1-methylnaphthalene and 9-methylanthracene are interpreted accordingly: in 1-methylnaphthalene the *peri* proton forces a preferred conformation of the methyl group and thereby inhibits its rotation. On the other hand, in 9-methylanthracene two energetically equivalent *peri* $H-CH_3$ interactions occur, so that methyl rotation is less hindered because there is no preferred conformation [121].

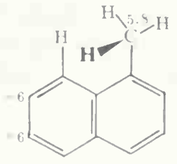

1-Methylnaphthalene

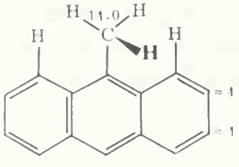

9-Methylanthracene

In the series 6,7-dihydrolinalool, linalool, and 6,7-dehydrolinalool the methyl C atoms of the terminal 1,1-dimethylvinyl group which are located *trans* to the alkyl group show widely differing absolute values of T_1; however, the ratio $T_{1(trans)}:T_{1(cis)}$ is always about 2:1. The rotation of the *trans* methyl groups therefore appears to be less hindered than that of the *cis* methyl groups [102].

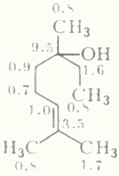

6,7-Dihydro-
linalool

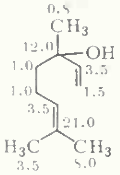

Linalool

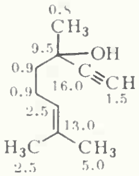

6,7-Dehydro-
linalool

The T_1 values of the methyl carbon atoms of methylated phosphetanes (in s) reveal that the methyl groups attached to C-2 and C-4, as well as to C-3, are subject to greater rotational hindrance than the $P-CH_3$ group [141]. Surprisingly, the pseudoaxial methyl groups sometimes relax more slowly than their pseudoequatorial counterparts, in spite of the stronger van der Waals repulsion expected for the former [141]. Shorter ^{13}C spin-lattice relaxation times thus do not always constitute proof of hindered rotation. Instead, the effects of methyl mobility found from relaxation time measurements must always be considered in relation to the motion of the entire molecule, which can vary markedly during a change of configuration.

A more quantitative interpretation of methyl relaxation requires a knowledge of the motional anisotropy of the entire molecule. Thus the activation energy of methyl rotation can be estimated from T_1 data if the rotational diffusion tensor of the molecule, mentioned in Section 3.3.3.3., is known [137].

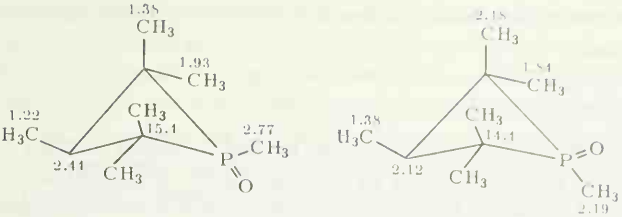

Phosphetanes

In biphenyl derivatives and related compounds, substituents can hinder rotation of the phenyl groups. Since phenyl rotation is anisotropic (Section 3.3.3.3., $T_{1(o,m)} > T_{1(p)}$), the ratio $T_{1(o,m)}:T_{1(p)}$ of the phenyl carbon nuclei will decrease on rotational hindrance. Hence, a smaller ratio, $T_{1(m)}:T_{1(p)}$ is found in 2,2′,6,6′-tetramethylbiphenyl [142] than in biphenyl itself owing to the methyl groups in the *o*- and *o*′-positions (Table 3.15). In 3-bromobiphenyl and phenyl benzoate, the ratio $T_{1(o,m)}:T_{1(p)}$ is significantly larger for the unsubstituted phenyl and phenoxy ring than for the 3-bromophenyl and benzoyl ring [121].

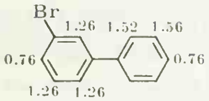

3-Bromobiphenyl

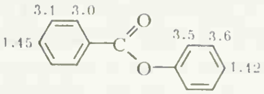

Phenylbenzoate

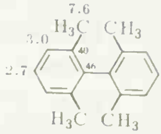

2,2′,6,6′-Tetramethyl-biphenyl

(3) Molecular Flexibility

Differing T_1 values for CH_3, CH_2, and CH carbon nuclei within a molecule can arise not only by methyl rotation or anisotropic molecular motion, but also from the segmental mobility of partial structures, even when the dipolar mechanism predominates. Thus the spin-lattice relaxation times of methylene carbon atoms in long alkane chains pass through a minimum at the middle of the chain. In the presence of heavy nonassociating substituents, the minimum is displaced somewhat towards the heavier end of the molecule, as is apparent for decane [143] and 1-bromodecane [144]. The molecular periphery is accordingly more flexible than the center.

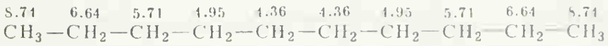

$$\overset{8.71}{CH_3}-\overset{6.64}{CH_2}-\overset{5.71}{CH_2}-\overset{4.95}{CH_2}-\overset{4.36}{CH_2}-\overset{4.36}{CH_2}-\overset{4.95}{CH_2}-\overset{5.71}{CH_2}-\overset{6.64}{CH_2}-\overset{8.71}{CH_3}$$

Decane

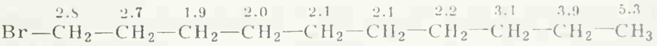

$$Br-\overset{2.8}{CH_2}-\overset{2.7}{CH_2}-\overset{1.9}{CH_2}-\overset{2.0}{CH_2}-\overset{2.1}{CH_2}-\overset{2.1}{CH_2}-\overset{2.2}{CH_2}-\overset{3.1}{CH_2}-\overset{3.9}{CH_2}-\overset{5.3}{CH_3}$$

1-Bromodecane

The same behavior of C atoms having the same number of protons is also observed in the side chain of cholesteryl chloride [139]: the methyl carbon atoms C-26 and C-27 relax more slowly than C-21, the methylene carbon C-24 slower than C-23, and the methine carbon atom C-25 slower than C-20. The mobility of the side chain thus increases with increasing distance from the steroidal skeleton.

In the case of such flexible molecules the correlation time τ_C can be different for each C atom. NT_1 is then no longer a constant as for rigid molecules according to eq. (3.22), but inversely proportional to the correlation time, as can be seen from eq. (3.21) (N is the number of protons bonded to a carbon atom).

$$N T_1 \propto 1/\tau_C \tag{3.25}$$

The product $N T_1$ can therefore be interpreted as an internal molecular mobility parameter, although only qualitatively and with caution, as was apparent for a correlation of carbon-13 T_1 values with diffusion coefficients [143]. The increase in T_1 or $N T_1$ with increasing internal mobility is not only a valuable aid in the signal assignment of carbons having the same degree of substitution, but also offers the possibility of determining the geometry and internal dynamics in the liquid and dissolved states, particularly in the case of large molecules. ^{13}C-T_1 measurements with this aim have been performed on phospholipids, peptides, proteins, and synthetic polymers.

In dipalmitoyllecithin the carbon nuclei relax increasingly slowly going from the central glycerol group to the ends of the two fatty acids, and thence to the tetraalkylammonium end of the choline group [145]. Thus the mobility becomes higher and higher starting from the glycerol skeleton, and proceeding along the fatty acid and choline chains to the molecular periphery. The terminal propyl groups of the fatty acid chains appear to undergo particularly rapid motion. If the fatty acid is shortened or a double bond is introduced, the chain assumes more internal flexibility. This may be seen from a comparison of data for dipalmitoyl-, dioctanoyl-, and dioleoyllecithin*): the "central" methylene carbon atoms in dioctanoyl- and dioleoyllecithin not only relax more slowly than in dipalmitoyllecithin, their T_1 values also differ more significantly [146].

Together with proteins, phospholipids are the most important structural components of biological membranes. Since mobility of the lipid segments favors molecular transport through a membrane

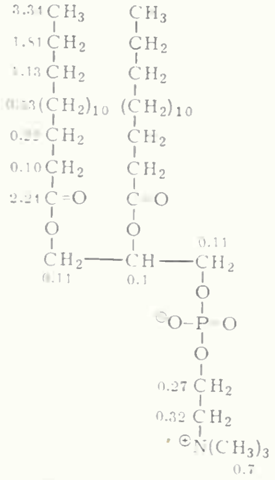

Dipalmitoyl-

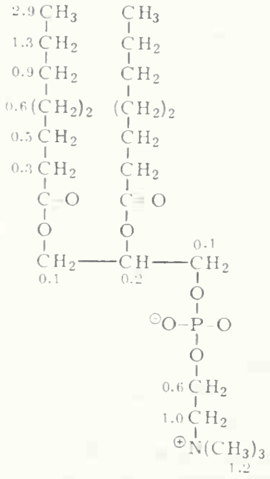

Dioctanoyl-

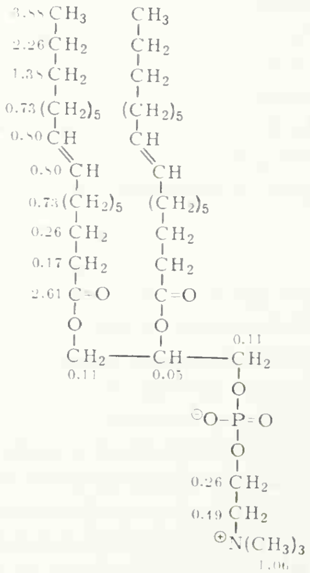

Dioleoyllecithin

---

*) Measured at 52 °C in D_2O solutions that had been treated with ultrasound.

and thereby increases its permeability, a marked increase in T_1 along a lipid-fatty acid chain also reflects a more efficient molecular diffusion through the lipid layer of a membrane [147].

In methanol, all the α carbons of the cyclic decapeptide antibiotic grammicidin S relax at about the same rate ($T_1 \approx$ 135 to 150 ms) [148]. In conclusion, this molecule undergoes approximately isotropic motion in solution, and the motion of the α carbons within the peptide ring is slower than the overall molecular motion itself. The mobility parameters NT_1 increase significantly in the order C-α, C-β, C-γ. Thus the side chains become increasingly mobile with increasing length. It is only in the case of the relatively rigid proline skeleton that all carbon nuclei have similar T_1 values. The phenylalanine side chain displays the anisotropy of rotation ($T_{1(o,m)} > T_{1(p)}$) usually encountered in phenyl derivatives. Since the axis of rotation passes through C-β and C-p, these carbons should show the same NT_1 values. The differences measured in practice ($NT_{1(\beta)} > NT_{1(p)}$) are possibly due to somewhat different C–H bond lengths (C-β: sp^3 C–H bond; C-p: sp^2 C–H bond) [148].

In ribonuclease A ^{13}C spin-lattice relaxation of the carbonyl and α and β carbon atoms is slower in the denatured protein than in the native sample [149]. Apparently, the skeleton of this macromolecule becomes more flexible on denaturation, probably owing to conformational changes. However, the ε carbons of lysine in the native protein exhibit relatively large T_1 values which change only insignificantly on denaturation [149]. This behavior is attributed to a considerable segmental mobility of the lysine side chain (Table 3.16 [149]).

Table 3.16. ^{13}C spin-lattice relaxation times T_1 of ribonuclease A in aqueous solutions (conc. 0.019 M; 45 °C; 15.08 MHz; maximum deviation ±30% [149]).

C Atoms	Native T_1 [s]	Denatured T_1 [s]
Carbonyl	0.416	0.539
α-C	0.042	0.120
β-C (Thr)	0.040	0.099
ε-C (Lys)	0.330	0.306

Indeed, ^{13}C spin-lattice relaxation times can also reflect conformational changes of a protein, *i.e.* helix-random coil transitions. This was demonstrated with models of polyamino acids [150–152], in which definite conformations can be generated, *e.g.* by addition of chemicals or by changes in temperature. Thus effective molecular correlation times τ_C of 24–32 ns/rad were ascertained for the γ carbons of poly(β-benzyl L-glutamate) in the more rigid helical form and about 0.8 ms/rad for the more flexible "random coil" form [152], from spin-lattice relaxation times and the NOE factors.

A certain segmental mobility of the chains can also be deduced from ^{13}C-relaxation measurements on synthetic polymers. For instance, the ratio of the spin-lattice relaxation times for the methine and methylene carbon atoms of polystyrene is $T_{1(CH)} : T_{1(CH_2)} = 2:1$. The NOE factors η_C lie between 0.8 and 1.1, depending upon the solvent. Both parameters T_1 and η_C are independent of tacticity. These results indicate that internuclear dipole-dipole interaction predominates in the ^{13}C relaxation of polystyrene, but that the polymer chain is also relatively flexible [153]. The carbons in amorphous *trans*-polyisoprene relax more slowly and display larger NOE factors than the corresponding atoms of amorphous *cis*-polyisoprene [154]. Apparently, the "frequency" of internal motion of these molecules lies in the region of the minimum of the correlation function (Fig. 3.18): the *trans* chain shows slightly shorter and the *cis* chain slightly longer correlation times τ_C; hence the *trans* isomer is more flexible [154]. If carbon black is added as filler to *cis*-polyisoprene (natural rubber), then no significant decrease in T_1 is observed; however, individual line broadening occurs for each carbon atom. The filler therefore appears to impair the mobility of some carbon atoms in the *cis* chain [154]. A situation can then be reached in which segmental motion in the chain becomes so slow that T_1 increases again while the spin-spin relaxation time T_2 continues to decrease (Fig. 3.18, to right of minimum) so that the signals become broader ($\Delta\nu_{1/2} \propto 1/T_2$).

Natural Rubber

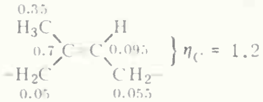

cis

Guttapercha

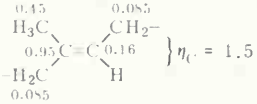

trans

3.3.3.5. Association and Solvation of Molecules and Ions

Strong intermolecular interactions such as hydrogen bonds or ion-dipole pairs restrict the motion of molecules and pertinent molecular segments. These interactions increase the correlation time τ_C and accelerate the ^{13}C spin-lattice relaxation. Shorter ^{13}C relaxation times can therefore also indicate that such interactions are operative. The T_1 values of the C atoms of carboxylic acids, phenols, alcohols, and solvated molecular ions behave in this way.

Table 3.17. T_1 and η_C values of ^{13}C nuclei in formic and acetic acid, and their methyl esters [155].

		T_1 [s] at 15 MHz	T_1 [s] at 25 MHz	η^C
Formic acid	$-CH=O$	10.3 ± 1	10.1 ± 1	2.0 ± 0.15
Methyl formate	$-CH=O$	15.1 ± 2	14.5 ± 1.5	1.55 ± 0.15
	$-OCH_3$	16.8 ± 2	18.0 ± 2	0.8 ± 0.1
Acetic acid	$>C=O$	29.1 ± 2.2	30.0 ± 3.5	1.08 ± 0.04
	$-CH_3$	10.5 ± 0.5	9.8 ± 0.6	1.4 ± 0.13
Methyl acetate	$>C=O$	35.0 ± 5	29.0 ± 5	0.25 ± 0.08
	$-CH_3$	16.3 ± 1.3	17.4 ± 1.5	0.63 ± 0.08
	$-OCH_3$	17.0 ± 1.5	18.3 ± 2.1	0.93 ± 0.04

The ^{13}C nuclei in formic and acetic acid relax faster and show larger nuclear Overhauser enhancements than the ^{13}C nuclei of the methyl esters (Table 3.17) [155]. Hence a methyl ester is more mobile than its parent carboxylic acid, which is dimerized *via* hydrogen bonding. It may also be seen that a pure DD mechanism operates in formic acid, owing to the directly bonded proton ($\eta_C = 2.0$), whereas spin rotation also contributes to ^{13}C relaxation in methyl formate ($\eta_C = 1.55$).

Owing to hydrogen bonding, the ^{13}C nuclei of phenol relax faster than the corresponding nuclei of nonassociating benzenes (Table 3.15). – In decanoic acid [144] and 1-decanol [144, 156], ^{13}C spin-lattice relaxation becomes progressively slower on going from the associating COOH or CH_2OH group to the hydrophobic end of the molecule. Whereas the hydrocarbon part becomes increasingly mobile towards the exterior, the polar end is rooted by hydrogen bonding. This behavior is also observed in branched alcohols and those having shorter chains such as 3,7-dimethyl-1-octanol [102] and 1-butanol [129], although it is less pronounced in such cases. In very small alcohols like methanol [157] relaxation is considerably slower (T_1 = 17.5 s) as a result of the much faster molecular motion.

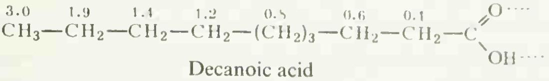
3.0
1.9
1.4
1.2
0.8
0.6
0.4

$CH_3-CH_2-CH_2-CH_2-(CH_2)_3-CH_2-CH_2-C(=O)OH$

Decanoic acid

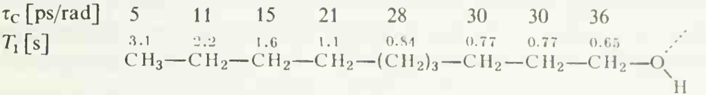
τ_C [ps/rad] 5 11 15 21 28 30 30 36
T_1 [s] 3.1 2.2 1.6 1.1 0.84 0.77 0.77 0.65
H

$CH_3-CH_2-CH_2-CH_2-(CH_2)_3-CH_2-CH_2-CH_2-OH$

Decanol

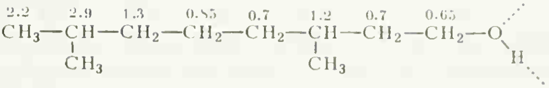
2.2
2.9
1.3
0.85
0.7
1.2
0.7
0.65

$CH_3-CH(CH_3)-CH_2-CH_2-CH_2-CH(CH_3)-CH_2-CH_2-OH$

3,7-Dimethyloctanol

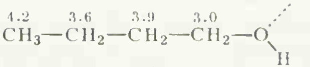

$CH_3-CH_2-CH_2-CH_2-OH$

1-Butanol

In prostaglandin $F_{2\alpha}$, the T_1 values of ^{13}C nuclei in the alkyl side chain increase more significantly towards the periphery than in the associating carboxylic acid chain, thus confirming the assignment of the closely crowded CH_2 signals of the chains in the ^{13}C NMR spectrum [144]. Generally, the increased mobility on going from the associating end of the molecule, and the

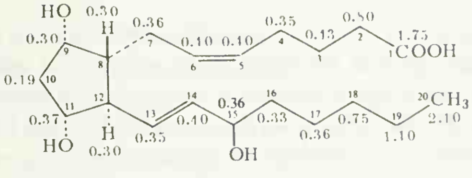
HO 0.30
H
0.30
0.36
0.10 0.10
0.35
0.13
0.80
1.75
COOH
0.19
0.37
H
HO 0.30
0.40
0.35
0.36
OH
0.33
0.36
0.75
1.10
CH3
2.10
1 2 3 4 5 6 7 8 9 10 11 12 13 14 15 16 17 18 19 20

Prostaglandin $F_{2\alpha}$

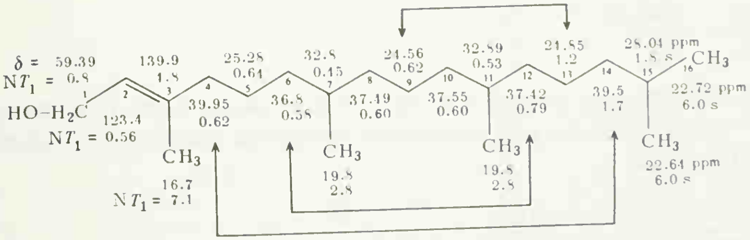
δ = 59.39
NT_1 = 0.8
HO–H2C
123.4
NT_1 = 0.56
139.9
1.8
CH3
16.7
NT_1 = 7.1
39.95
0.62
25.28
0.64
36.8
0.58
32.8
0.45
CH3
19.8
2.8
37.49
0.60
24.56
0.62
37.55
0.60
32.89
0.53
37.42
0.79
CH3
19.8
2.8
24.55
1.2
39.5
1.7
28.04 ppm
1.8 s
CH3
22.72 ppm
6.0 s
CH3
22.64 ppm
6.0 s
1 2 3 4 5 6 7 8 9 10 11 12 13 14 15 16

Phytol

concomitant increase in T_1 or $N\,T_1$ [eq. (3.25)] can be utilized in signal assignment. Thus in phytol, the diterpene alcohol component of chlorophyll, the signals of the carbon atom pairs 4 and 14, 6 and 12, and 9 and 13 defy unequivocal assignment, owing to very similar shifts and equal multiplicities (CH_2 groups). However, the C atoms 12, 13, and 14, which are more removed relative to the associating end of the molecule, undergo faster motion, and the $N\,T_1$ values are therefore larger. Signal assignment then follows readily [158].

Table 3.18. Solvent dependence of spin-lattice relaxation times of the ^{13}C atoms in *n*-butylammonium trifluoroacetate [121].

Solvent	Conc. [wt.-%]	T_1 [s]				
		CH_3—	CH_2—	CH_2—	CH_2—	$\overset{\oplus}{N}H_3\ CF_3COO^{\ominus}$
1,4-Dioxane	20	3.35	1.95	1.54	0.88	
CH_2Cl_2/acetone	24	3.90	2.41	1.67	0.91	
CF_3COOH	15.4	3.98	3.12	2.30	1.54	
	28.2	3.46	2.13	1.50	0.97	
CD_3OD	20	6.00	5.35	4.52	3.10	
D_2O	20	5.00	5.00	4.26	3.75	

In weakly solvating solvents interionic interactions between organic molecular ions can lead to fixation of the ionic end of the molecule. The T_1 values of pertinent and neighboring ^{13}C nuclei become smaller. In contrast, strongly solvating solvents such as water and alcohols inhibit interionic interaction and lead to an enhanced mobility of the ions solvated by ion-dipole interactions, and ^{13}C spin-lattice relaxation is consequently slower in such solvents. Thus the T_1 values of *n*-butylammonium trifluoroacetate increase with the polarity of the solvent, as shown in Table 3.18 [121].

3.3.3.6. Determination of Quadrupole Relaxation Times and Coupling Constants from ^{13}C Spin-Lattice Relaxation Times

While the nuclei ^1H and ^{13}C relax predominantly by the DD mechanism, relaxation of a quadrupole nucleus such as deuterium essentially involves fluctuating fields arising from interaction between the quadrupole moment and the electrical field gradient at the quadrupole nucleus [16]. If the molecular motion is sufficiently fast (decreasing branch of the correlation function, Fig. 3.18), the ^2H spin-lattice relaxation time is inversely proportional to the square of the quadrupole coupling constant $e^2qQ/\hbar$ of deuterium and the effective correlation time [16]:

$$\frac{1}{T_1} = \frac{3}{8}\left(\frac{e^2qQ}{\hbar}\right)^2 \tau_C \qquad (3.26)$$

Since ^{13}C and ^2H relaxation are the consequence of intramolecular interactions, the relaxation times T_1 of ^{13}C and ^2H within a given molecule can be subjected to direct comparison according to eqs. (3.21) and (3.26):

$$\frac{T_1(^{13}C)}{T_1(^2H)} = \frac{3}{8}\,\frac{r^6(e^2qQ/\hbar)^2}{N\hbar^2\gamma_C^2\gamma_H^2} \qquad (3.27)$$

By using the numerical values for the constants (*e.g.* $r_{CH} \approx 0.109$ nm and $e^2qQ/h \approx 170$ kHz for an sp^3 C−H bond) a simple linear relation between the ^{13}C and ^2H relaxation times is obtained:

$$T_1(^{13}C)/T_1(^2H) = 19.9/N \quad (N = 1, 2, 3 \text{ for CD, CD}_2\text{, CD}_3) \tag{3.28}$$

Knowledge of the T_1 values for deuterium thus allows prediction of the ^{13}C relaxation times and *vice versa* [159]. On the other hand, if these data are known the deuterium quadrupole coupling constants can be determined according to eq. (3.27). Agreement between calculated and experimental quadrupole coupling constants is good, any pronounced deviations indicating that alternative relaxation mechanisms are operative. For instance the quadrupole coupling constant calculated for the terminal acetylene deuteron of phenylacetylene according to eq. (3.27) is much too large (calc. 254 kHz; exp. 215 ± 5 kHz). This is explained in terms of the chemical shift anisotropy in phenylacetylene [159].

3.3.4. Medium and Temperature Effects

Any change in the medium, *i.e.* the solvent, the concentration, the pH value, and the temperature will affect the mobility of the molecules and hence also the spin-lattice relaxation. However, few systematic studies have so far been performed on the concentration dependence or on the precise influence of the macroscopic viscosity, the main reason in the case of ^{13}C lying in the need for highly protracted measurements in concentration studies. Moreover, little is known about the pH dependence of ^{13}C relaxation [160]. Nevertheless, the concentration dependence of ^{13}C relaxation is apparent in the case of saccharose (Table 3.19) [139], and intramolecular hydrogen bonds can be detected by measuring the concentration dependence of T_1 [161].

Table 3.19. ^{13}C spin-lattice relaxation times T_1 [s] of saccharose in H_2O and D_2O at 42 °C [139].

Saccharose

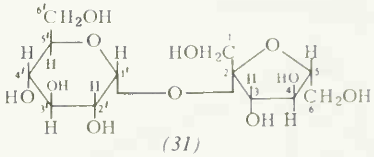

(31)

	C Atom	0.5 M D_2O	0.5 M H_2O	2.0 M H_2O
C	2	6.0	7.8	2.6
CH	1′	0.54	0.69	0.16
	3	0.51	0.64	0.16
	4	0.52	0.49	0.16
	5	0.58	0.61	0.16
	3′	0.61	0.73	0.15
	2′	0.53	0.69	0.17
	5′	0.60	0.70	0.16
	4′	0.59	0.60	0.17
CH_2	1	0.48	0.40	0.12
	6	0.35	0.30	0.15
	6′	0.34	0.37	0.13

Solvating solvents appear to facilitate molecular motion, as has already been shown for *n*-butylammonium trifluoroacetate (Table 3.18) [121].

The ^{13}C nuclei of molecules whose protons undergo exchange relax at different rates in H_2O and D_2O solution. Thus T_1 for the carbonyl carbon of acetamide is 72 s in D_2O, but only 37 s in H_2O [161]. In this context, the influcence of paramagnetic impurities should again be mentioned. Traces of paramagnetic ions (*e.g.* Cu^{2+}) no longer detectable by the usual analytical techniques can drastically lower the ^{13}C relaxation times of complexing substrates (*e.g.* amino acids).

Most previous publications on the temperature dependence of ^{13}C relaxation [162–171] are concerned with simple molecules such as carbon disulfide, iodomethane, and acetonitrile [162–166]. Any interpretation of the temperature dependence of relaxation times requires a knowledge of the relative contributions of dipole-dipole and spin-rotation relaxation, as the former becomes progressively slower and the latter steadily faster with increasing temperature. In special cases, such as that of cyclopropane [172], the effects of both contributions can almost cancel each other.

The temperature dependence of dipole-dipole relaxation is that of the correlation time, which is usually written in the form of an Arrhenius equation (3.29):

$$\tau_C = \tau_{C_0} \times e^{\frac{\Delta E}{RT}} \tag{3.29}$$

Plotting the logarithm of the dipole-dipole relaxation time $T_{1(DD)}$ *versus* the reciprocal temperature therefore gives an activation energy ΔE for molecular reorientation, which is of the order of 8.4 kJ/mole for most of the molecules hitherto studied. In the case of 4,4'-dimethylbiphenyl a value of 16.8 kJ/mole was found from the temperature dependence of T_1 for C-2 and C-3 (Fig. 3.19) [142]. For T_1 of the methyl carbon atom the Arrhenius plot is curved at lower temperatures since the internal rotation of this group is then probably faster than the overall motion of the molecule.

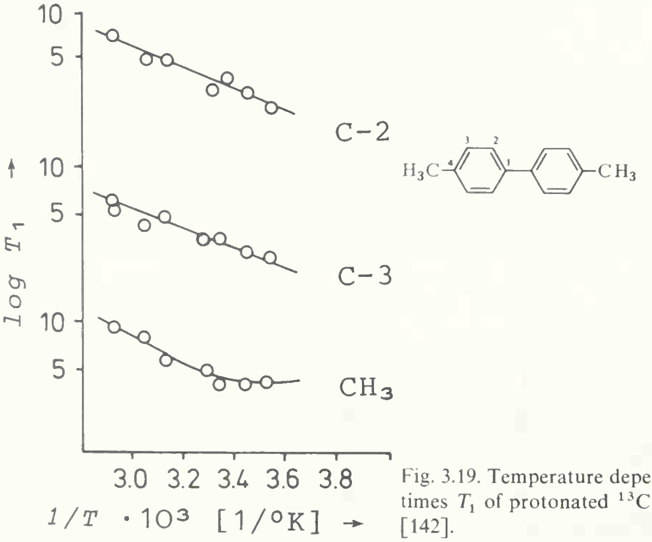

Fig. 3.19. Temperature dependence of spin-lattice relaxation times T_1 of protonated ^{13}C nuclei in 4,4'-dimethylbiphenyl [142].

The temperature dependence of the SR component is more complicated. An Arrhenius relation can again be formulated for the correlation time of spin rotation; however, this function additionally contains a linear temperature term.

3.3.5. Outlook

^{13}C relaxation measurements will assume a firm place in the methodology of nuclear magnetic resonance. The principles of the measuring technique have been established [173] and the specific sources of error recognized [173]. On the other hand, the relevant theory is still in a state of flux [174], particularly with regard to the interpretation of T_1 values in terms of the anisotropy of molecular motion and segmental mobility.

The organic chemist will profit from relaxation time measurements as a tool for assigning ^{13}C NMR spectra whenever decoupling experiments and shift comparisons fail owing to signal overcrowding. The study of events involving intermolecular motion, such as complexation [175] and micelle formation [176] can utilize the ^{13}C spin-lattice relaxation time as a new probe. Temperature dependent measurement of T_1 will certainly also be developed into an additional method for the elucidation of internal dynamic processes of molecules. Finally, such measurements will find wide application in biochemistry, for example in active site determination in biomacromolecules [128], the study of lipid double layers [146], or the determination of peptide conformations [177 – 180].

4. ^{13}C NMR Spectroscopy of Organic Compounds

4.1. Saturated Hydrocarbons

The first ^{13}C chemical shift data of alkanes were reported by Spieseke, Schneider [68a], Grant and Paul [62]. From the values collected in Table 4.1, Grant and Paul [62] deduced their additivity rule for the ^{13}C chemical shifts of alkanes. The signal assignments for the alkanes, also given in Table 4.1, are based on signal intensities, partial proton decoupling, and proton decoupling experiments.

Table 4.1. ^{13}C Chemical Shifts of Alkanes (δ Values in ppm Relative to TMS = 0) [62, 68a].

Compound	C-1	C-2	C-3	C-4	C-5
Methane	− 2.3				
Ethane	5.7				
Propane	15.4	15.9			
n-Butane	13.1	24.9			
n-Pentane	13.7	22.6	34.6		
n-Hexane	13.7	22.8	31.9		
n-Heptane	13.8	22.8	32.2	29.3	
n-Octane	13.9	22.9	32.2	29.5	
n-Nonane	13.9	22.9	32.3	29.7	30.0
n-Decane	14.0	22.8	32.3	29.8	30.1
Isobutane	24.3	25.0			
2-Methylbutane	21.9	29.7	31.7	11.4	
Neopentane	27.4	31.4			
2,2-Dimethylbutane	28.7	30.2	36.5	8.5	
2,3-Dimethylbutane	19.1	33.9			
2-Methylpentane	22.4	27.6	41.6	20.5	14.0
3-Methylpentane	11.1	29.1	36.5	18.4	
3,3-Dimethylpentane	6.6	24.9	35.9	4.2	

^{13}C chemical shift values of *n*-alkanes can be calculated using the additivity relationship given in eq. (4.1) [62]:

$$\delta_c(k) = B + \sum_l A_l n_{kl} + \sum S_{kl} \tag{4.1}$$

$\delta_c(k)$ = chemical shift of the k-th C-atom;
B = a constant given by the ^{13}C chemical shift of methane (-2.3 ppm);
n_{kl} = number of C atoms in position l with respect to C atom k;
A_l = additive shift parameter of C atom l.

The values of A_l given in Table 4.2 were determined for linear alkanes (standard deviation of predicted chemical shifts: ± 0.10 ppm, $B = -2.3$).
Additional parameters S_{kl} are required in order to calculate the chemical shift values of branched chain alkanes (standard deviation of predicted chemical shifts ± 0.3 ppm, $B = -2.3$ ppm) (Table 4.3). The values symbolized by Greek letters indicate the change in chemical shift due to substitution of hydrogen by a methyl group at the α to ε carbon atoms. The remaining 8 correction

parameters account for the effect of branching. The different molecular configurations are denoted by the following symbols:

1°(3°): methyl group adjacent to a tertiary carbon;
1°(4°): methyl group adjacent to a quaternary carbon;
2°(3°): secondary carbon adjacent to a tertiary center;
2°(4°): secondary carbon adjacent to a quaternary carbon;
3°(2°): tertiary carbon bearing a secondary carbon;
3°(3°): tertiary carbon attached to a tertiary carbon;
4°(1°): quaternary carbon adjacent to a methyl group;
4°(2°): quaternary carbon linked to a methylene carbon.

Table 4.2. A_l Parameters of Equation (4.1) (*n*-alkanes).

Carbon position l	A_l in ppm
α	9.1 ± 0.10
β	9.4 ± 0.10
γ	−2.5 ± 0.10
δ	0.3 ± 0.10
ε	0.1 ± 0.10

Table 4.3. Corrective Terms S_{kl} for Equation (4.1) (Branched Chain Alkanes).

	S_{kl} in ppm
1°(3°)	− 1.10 ± 0.20
1°(4°)	− 3.35 ± 0.35
2°(3°)	− 2.50 ± 0.25
2°(4°)	− 7.5
3°(2°)	− 3.65 ± 0.15
3°(3°)	− 9.45
4°(1°)	− 1.50 ± 0.10
4°(2°)	− 8.35

For illustration of the additivity rule, the ^{13}C chemical shift of C-3 in 2-methylhexane is calculated below according to eq. (4.1) using the shift parameters listed in Tables 4.2 and 4.3 [62]:

2-Methylhexane

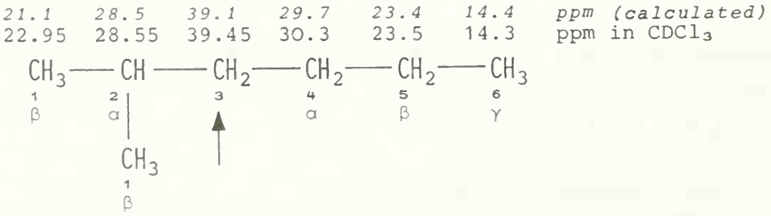
21.1 28.5 39.1 29.7 23.4 14.4 ppm (calculated)
22.95 28.55 39.45 30.3 23.5 14.3 ppm in CDCl3
CH3 — CH — CH2 — CH2 — CH2 — CH3
1 β
2 α
3
4 α
5 β
6 γ
CH3
1 β

$$\delta_3 = B + 2A_\alpha + 3A_\beta + A_\gamma + S_{2°(3°)}$$

$$= -2.3 + 18.2 + 28.2 - 2.5 - 2.5$$

$$= 39.1 \text{ ppm}$$

The calculated shift of C-3 is 39.1 ppm as compared to an observed value of 39.45 ppm. – Prediction of carbon chemical shifts using the Grant-Paul relation (4.1) is a practical aid in assigning the carbon signals of larger alkyl groups, *e.g.* in cholestane derivatives (Chapter 5.2).

Valence-bond calculations of ^{13}C chemical shift parameters of alkanes permit the following general conclusions [181].

(1) The paramagnetic screening term is mainly responsible for ^{13}C chemical shifts [181].
(2) Low-lying excited states cause downfield shifts of the ^{13}C signals [181].
(3) Increasing electron charge density at a carbon atom causes increased shielding and *vice versa*.
(4) Parallel-spin pairing at a carbon atom causes a decrease in the paramagnetic shielding term and, consequently, the carbon resonates at higher field [181].
(5) γ-Substitution effects can be explained in terms of stericly induced polarizations of the electrons of the C−H bond.
(6) Bulky β-substituents force carbons to resonate at lower field due to orbital contraction, which causes an increase in the paramagnetic shielding term [181].

J. Mason [182] pointed out that the diamagnetic shielding term σ_d may show large variations for different compounds. Equations for calculating chemical shifts are of more general applicability if ^{13}C chemical shift values are corrected ($\delta_{corr.}$) for the diamagnetic shielding term σ_d. The values $\delta_{corr.}$ are calculated by eq. (4.2):

$$\delta_{corr.} = \sigma_p + \sigma' = \delta - \sigma_d + 295.3 \qquad (4.2)$$

σ_p = paramagnetic shielding term;
σ' = shielding term due to distant contributions;
δ = chemical shifts relative to methane according to Grant and Paul [62];
σ_d = local diamagnetic shielding term.

The σ_d values of alkanes increase by about 28 ppm per hydrogen-carbon substitution; the numerical values are 295.3 ppm for CH_4, 323.5 ppm for primary, 351.4 ppm for secondary, 379.5 ppm for tertiary and 407.3 ppm for quaternary carbons [182].
The corrected ^{13}C shifts of carbons in alkanes of any kind (normal, branched, cyclic) can be calculated as the sum of shift increments due to each α-(35.4 ppm), β-(8.4 ppm), γ-(−1.5 ppm) and δ-(1.4 ppm) carbon atom and a constant (1.4 ppm) [182]. This relation is of more general

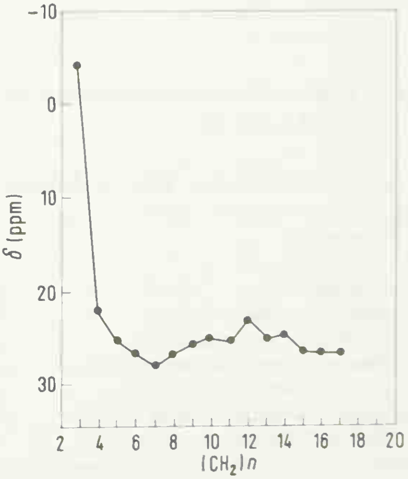

Fig. 4.1. Plot of ^{13}C chemical shifts of cycloalkanes *versus* ring size (δ values (ppm) relative to TMS = 0) [183].

applicability than eq. (4.1) [182]. Similar methods have been used for methylcyclohexanes, alkenes, alkynes, carbenium ions and aromatic carbons [182].

A systematic ^{13}C NMR investigation of cycloalkanes was undertaken by Burke and Lauterbur [183]. The carbons of cyclopropane resonate at remarkably high field (−3.8 ppm). This high shielding of methylene carbons in cyclopropane can be explained satisfactorily by means of a ring-current model [183]. A plot of ^{13}C chemical shifts *versus* ring size shows an oscillating pattern. The carbons of even membered rings are more shielded than carbons of rings having one carbon atom more or less (Fig. 4.1).

Conformational effects have been made responsible for the oscillating behavior of chemical shifts in relation to ring size. The chemical shifts and C−H couplings of 15 cycloalkanes are listed in Table 4.4. The large C−H coupling constant in cyclopropane and − to a lesser amount − in cyclobutane are attributed to a higher s character of the carbon bond orbitals.

Table 4.4. ^{13}C Chemical Shifts and One-Bond Coupling Constants J_{C-H} of Cycloalkanes (δ Values (ppm) Relative to TMS = 0) [183].

Compound	Chemical shift [ppm]	J_{CH} [Hz]
Cyclopropane	−2.80	162 ± 2
Cyclobutane	23.10	136 ± 1
Cyclopentane	26.30	131 ± 2
Cyclohexane	27.60	127 ± 2
Cycloheptane	28.20	126 ± 2
Cyclooctane	26.60	127 ± 2
Cyclononane	25.80	125 ± 2
Cyclodecane	25.00	126 ± 2
Cycloundecane	25.40	126 ± 2
Cyclododecane	23.20	123 ± 3
Cyclotridecane	25.20	127 ± 2
Cyclotetradecane	24.60	126 ± 2
Cyclopentadecane	26.40	126 ± 2
Cyclohexadecane	26.50	126 ± 3
Cycloheptadecane	26.70	126 ± 2

α, β, γ and δ ^{13}C chemical shift substituent effects for a series of methylcyclopentanes are given in Tables 4.5 and 4.6.

Table 4.5. ^{13}C Chemical Shifts of Methylcyclopentanes (δ Values (ppm) Relative to TMS = 0) [184].

Compound	C-1	C-2	C-3	C-4	CH_3
Cyclopentane	25.3				
Methylcyclopentane	34.6	34.6	25.2		20.2
1,1-Dimethylcyclopentane	38.9	41.1	24.7		28.8
trans-1,2-Dimethylcyclopentane	42.5		34.8	23.1	18.5
cis-1,2-Dimethylcyclopentane	37.4		33.0	23.0	14.9
trans-1,3-Dimethylcyclopentane	33.3	42.9		35.0	21.2
cis-1,3-Dimethylcyclopentane	35.2	44.8		34.1	20.9

The following conclusions can be drawn from Table 4.6 [184]:

(1) A methyl group causes the α carbon to resonate 9.1 ± 1.1 ppm towards lower field.
(2) The β-substituent effect of an equatorial methyl group is 9.2 ± 0.9 ppm.

Table 4.6. Methyl Substituent Effects on ^{13}C Chemical Shifts of Cyclopentane and Methylcyclopentane Resonances [184].

Compound	α effect	β effect	γ effect
Methylcyclopentane	9.3	9.3	−0.1
trans-1,2-Dimethylcyclopentane	7.9	7.9	0.2
		9.6	−2.1
cis-1,3-Dimethylcyclopentane	10.0	8.9	0.6
		10.2	−0.5
1.1-Dimethylcyclopentane	4.3	6.5	−0.5
cis-1,2-Dimethylcyclopentane	2.8	2.8	−1.6
		7.8	−2.2
trans-1,3-Dimethylcyclopentane	8.1	8.3	0.4
		9.8	−1.3

Table 4.7. ^{13}C Chemical Shifts of Methylcyclohexanes (δ Values (ppm) Relative to TMS = 0) [64].

Compound	C-1	C-2	C-3	C-4	C-5	C-6	CH_3
Cyclohexane	26.60	26.60	26.60	26.60	26.60	26.60	
Methylcyclohexane	33.10	35.80	26.55	26.40	26.55	35.80	22.75
1,1-Dimethylcyclohexane	30.05	39.85	22.60	26.70	22.60	39.85	28.85
cis-1,2-Dimethylcyclohexane	34.45	34.45	31.55	23.70	23.70	31.55	15.75
trans-1,2-Dimethylcyclohexane	39.55	39.55	36.05	26.85	26.85	36.05	20.25
cis-1,3-Dimethylcyclohexane	32.85	44.70	32.85	35.50	26.45	35.40	22.85
trans-1,3-Dimethylcyclohexane	27.05	41.45	27.05	33.90	20.75	32.90	20.50
cis-1,4-Dimethylcyclohexane	30.15	30.60	30.60	30.15	30.60	30.60	20.10
trans-1,4-Dimethylcyclohexane	32.65	35.65	35.65	32.65	35.65	35.65	22.70
1,1,2-Trimethylcyclohexane	32.90	41.80	31.35	26.80	22.80	41.25	30.55 (e)
							19.15 (a)
							16.35 (2)
1,1,3-Trimethylcyclohexane	30.80	49.35	28.35	35.75	22.65	39.55	33.70 (e)
							24.90 (a)
							23.15 (3)
1-*trans*-2-*cis*-3-Trimethylcyclohexane	39.15	46.25	39.15	36.45	26.45	36.45	20.75 (1.3)
							16.60 (2)
1-*trans*-2-*cis*-4-Trimethylcyclohexane	38.85	33.60	40.75	28.00	31.85	29.50	20.35 (1,2)
							20.05 (1,2)
							19.05 (4)
1-*trans*-2-*trans*-4-Trimethylcyclohexane	39.20	38.90	45.10	32.90	35.95	35.75	20.05 (1,2)
	38.90	39.20			35.75	35.95	20.30 (1,2)
							21.65 (4)
1-*cis*-3-*cis*-5-Trimethylcyclohexane	32.70	44.20	32.70	44.20	32.70	44.20	22.85
1-*cis*-3-*trans*-5-Trimethylcyclohexane	26.45	45.00	26.45	40.95	28.60	40.95	23.05 (1,3)
							18.90 (5)

(3) Replacing a *cis*-2-hydrogen in methylcyclopentane by a methyl group leads to an unusually small β effect at C-1 due to strong sterical hindrance of the methyls.

(4) γ-Effects, caused by axially oriented methyl groups, are much smaller for cyclopentanes than for cyclohexanes. Therefore the 1,3-diaxial interaction must be stronger in six-membered than in five-membered alkane rings.

The ^{13}C chemical shifts of methylcyclohexanes, some of which are presented in Table 4.7, permit the deduction of several general rules [64]:

(1) The signals of the methyl carbons are well separated from those of the ring carbons and occur at highest field.

(2) Isolated equatorial methyl carbons resonate between 22 and 23 ppm [64].

(3) The signals of isolated axial methyl groups are found between 18 to 19 ppm [64].

(4) Methyl substitution parameters for isolated methyl groups are given in Table 4.8:

Table 4.8. Methyl Substituent Parameters for Methylcyclohexanes (in ppm).

α_{eq}	5.65 ± 0.20	α_{ax}	1.10 ± 0.40
β_{eq}	8.90 ± 0.10	β_{ax}	5.15 ± 0.30
γ_{eq}	0.00 ± 0.55	γ_{ax}	-5.40 ± 0.20
δ_{eq}	-0.30 ± 0.15	δ_{ax}	-0.15 ± 0.30

Table 4.9. Differences (ppm) of Sum Totals of ^{13}C Chemical Shifts for *cis-trans* Methylcyclohexanes [130].

Methylcyclohexanes	Δ (ppm)
1,2-*cis*(e,a) – 1,2-*trans*(e,e)	34.6
1,3-*trans*(e,a) – 1,3-*cis*(e,e)	28.1
1,4-*cis*(e,a) – 1,4-*trans*(e,e)	29.1

A consideration of the sum totals of ^{13}C chemical shifts in a series of methylcyclohexanes leads to the following rule [185]: The larger the sum total of the ^{13}C chemical shifts of a methylcyclohexane is, the larger is the number of repulsive interactions in the molecule, and *vice versa*. Subtracting the sum totals of ^{13}C chemical shifts of pairs of *cis-trans* methylcyclohexanes yields values of about 30 ppm, as seen in Table 4.9.

The difference between the interaction energies of the e,a isomer and the e,e isomer is 7.5 kJ/mole for all isomeric pairs of Table 4.9 [185]. From these discussions it is evident that destabilizing effects increase the total shielding of the molecule and *vice versa* [185]. The ^{13}C chemical shifts or norbornane and some related compounds are collected in Table 4.10.

In 2-methylnorbornane, drastic upfield shifts are observed for the signals of C-6 (6.6 ppm) and the methyl carbon (4.9 ppm) when the methyl group changes from *exo* to *endo* configuration. The signal of C-7, however, shifts to lower field (3.9 ppm). These shift differences have been attributed to sterically induced polarizations [186].

Aminoboranes, diborazanes and cycloborazanes may be considered to be analogs of alkanes: carbon-carbon groups are replaced by isoelectronic boron-nitrogen moieties. Plots of ^{13}C chemical shifts of alkanes *versus* ^{11}B chemical shifts of the corresponding inorganic alkane analogs reveal a linear relationship which may be used for the calculation of shifts of ^{11}B in such boron-nitrogen compounds [187].

Table 4.10. ^{13}C Chemical Shifts of Norbornane and Related Compounds (δ Values (ppm) Relative to TMS = 0) [186].

Compound	C-1	C-2	C-3	C-4	C-5	C-6	C-7	CH_3
Quadricyclene	22.9	14.7	14.7	22.9	14.7	14.7	31.9	
Tricylene	9.6	9.6	32.9	29.4	32.9	9.6	32.9	
Norbornane	36.5	29.8	29.8	36.5	29.8	29.8	38.4	
1-Methylnorbornane	43.8	36.8	31.3	37.9	31.3	36.8	45.3	20.7
exo-2-Methylnorbornane	43.2	36.5	39.9	37.0	30.0	28.7	34.7	22.0
endo-2-Methylnorbornane	41.9	34.3	40.4	37.9	30.3	22.1	38.6	17.1
7-Methylnorbornane	40.7	26.9	26.9	40.7	30.7	30.7	44.0	12.4

The superiority of ^{13}C NMR spectroscopy over ^{1}H NMR spectroscopy for investigating conformational problems has been demonstrated by low temperature measurements on methylcyclohexane: The axial form of methylcyclohexane can be observed at −110 °C only by the former method [88].

Pulse Fourier transform ^{13}C NMR spectroscopy thus will be used more and more as a tool for investigating conformational equilibria and supplying data for the calculations of activation enthalpies and rate constants of ring inversions, as has been demonstrated recently for a number of compounds such as 1,1-dimethylcyclohexane, *cis*-1,2-dimethylcyclohexane, *cis*-1,4-dimethylcyclohexane, *trans*-1,3-dimethylcyclohexane, *cis*-decalin and 9-methyl-*cis*-decalin [89, 188].

4.2. Alkenes

Alkene chemical shifts are collected in Table 4.11. Because of the lack of suitable instrumentation in some older references quoted in Table 4.11, often only the shifts of olefinic carbons were reported. Several ^{13}C chemical shift-to-structure relations can be deduced for olefins from the data given in Table 4.11.

(1) Alkene and aromatic carbon resonances have similar shift ranges [5].

(2) Terminal olefinic carbon nuclei ($=CH_2$) resonate about 10–40 ppm at higher field than do alkene carbons bearing alkyl groups [50].

(3) Comparing the chemical shift values of alkene carbons with the corresponding shifts of their parent alkanes demonstrates that the difference is in most cases less than 1 ppm for the β, γ, δ and ε carbons. The Greek letters refer to the carbon positions in the olefins (see formulae below) [190].

(4) Carbon atoms α to the double bond are more shielded in *cis* relative to *trans* alkenes ($\delta_{trans} - \delta_{cis} \approx 5 \pm 0.5$ ppm) due to steric interaction between *cis* alkyl groups [190].

Additive constitutive bond parameters for sp^3 and sp^2 carbons were given by Savitsky et al. [191] for the estimation of ^{13}C chemical shifts in olefins. However, as was shown later, ^{13}C chemical shifts of olefinic carbons can be predicted much more precisely from substituent parameters derived from least squares solutions, using the chemical shift values of Table 4.11 for the calculations [190]. The positions of the carbons are designated as demonstrated for 2-hexene and

Compound	C-1	C-2	C-3	C-4	C-5	C-6	C-7	C-8	Other	Ref.
Ethylene	123.5									[189]
Propene	114.7	135.0								[189]
1-Butene	112.1	139.0								[189]
3,3-Dimethyl-1-butene	108.1	148.1								[68b]
2-Methyl-1-butene	107.4	146.1								[68b]
2-Ethyl-1-butene	105.2	151.4								[68b]
cis-2-Butene	10.9	123.4								[190]
trans-2-Butene	16.4	124.8								[190]
2-Methyl-2-butene		130.1	117.6							[68b]
2,3-Dimethyl-2-butene	17.7	121.6								[68b]
Cyclobutene	136.0		30.2							[190]
Methylenecyclobutane	149.2	31.1	15.8						103.9 (=CH$_2$)	[190]
1,3-Butadiene	116.3	136.9								[190]
2,3-Dimethyl-1,3-butadiene	111,3	142.1								[190]
1-Pentene	113.1	137.3								[68b]
4-Methyl-1-pentene	114.6	137.3								[68b]
3-Methyl-1-pentene	111.7	143.7								[68b]
3-Ethyl-1-pentene	113.8	141.3								[68b]
2-Methyl-1-pentene	108.6	143.3								[68b]
2,4,4-Trimethyl-1-pentene	113.2	142.5	51.0	30.4	29.2				24.2 (2-CH$_3$)	[190]
cis-2-Pentene	11.1	122.0	131.5	19.3	12.8					[190]
trans-2-Pentene		122.5	132.1							[68b]
cis-4-Methyl-2-pentene		120.6	137.6							[68b]
trans-4,4-Dimethyl-2-pentene		118.3	141.7							[68b]
2-Methyl-2-pentene		129.8	125.4							[68b]
cis-3-Methyl-2-pentene		115.7	136.1							[68b]
trans-3-Methyl-2-pentene		117.1	135.4							[68b]
3-Ethyl-2-pentene		115.6	142.6							[68b]
Cyclopentene	129.6		131.6	22.1						[190]
Methylenecyclopentane	151.6	32.1	25.9						103.8 (=CH$_2$)	[190]
1,4-Pentadiene	114.7	136.1								[190]
1-Hexene	113.2	137.5								[68b]
cis-2-Hexene	11.4	122.8	129.7	28.2	21.4	12.5				[190]
cis-3-Hexene			130.0							[68b]
trans-2-Hexene	16.5	123.9	130.6	34.1	22.0	12.5				[190]

Table 4.11. (Continued).

Compound	C-1	C-2	C-3	C-4	C-5	C-6	C-7	C-8	Other	Ref.
trans-3-Hexene			130.1							[68b]
2-Methyl-2-hexene		129.9	125.1							[68b]
cis-3-Methyl-2-hexene	12.0	118.3	134.8	32.7	20.2	12.8			22.1 ($3\text{-}CH_3$)	[190]
trans-3-Methyl-2-hexene	12.0	117.6	134.7	41.2	20.4	12.6			14.2 ($3\text{-}CH_3$)	[190]
2,3-Dimethyl-2-hexene		122.9	126.9							[68b]
Cyclohexene	126.2		24.5	22.1						[190]
Methylenecyclohexane	148.5	35.0	27.7	25.7					105.9 ($=CH_2$)	[190]
1,5-Hexadiene	113.8	137.0								[190]
2,5-Dimethyl-1,5-hexadiene	109.8	144.2								[190]
1-Octene	113.2	138.2	33.2	28.4	28.3	31.2	22.0	13.0		[190]
cis-2-Octene	11.5	122.6	130.0	26.1	28.7	30.9	21.9	13.0		[190]
cis-3-Octene	13.3	19.7	130.6	128.4	26.1	30.8	21.6	12.9		[190]
cis-4-Octene	12.7	22.2	28.6	129.0						[190]
trans-2-Octene	16.7	123.7	130.9	32.0	28.8	30.9	21.9	13.0		[190]
trans-3-Octene	12.9	24.9	131.6	128.6	31.6	31.3	21.5	13.0		[190]
trans-4-Octene	12.6	22.1	32.1	129.6						[190]
cis-Cyclooctene	129.2		24.8	25.8	28.6					[190]
trans-Cyclooctene	132.8		34.3	34.3	28.7					[190]
1.7-Octadiene	113.5	137.9	33.1	27.8						[190]
2,6-*cis,cis*-Octadiene	11.6	123.1	129.5	26.1						[190]
2,6-*cis,trans*-Octadiene	11.6	123.1	129.5	26.3	31.9	130.4	124.1	16.8		[190]
2,6-*trans,trans*-Octadiene	16.8	124.1	130.4	32.1						[190]
3,5-*cis,cis*-Octadiene	13.2	20.0	132.3	122.5						[190]
2-Methyl-1-heptene	109.0	144.6	37.2	26.8	31.0	21.9	13.0		20.9 ($2\text{-}CH_3$)	[190]
2-Methyl-2-heptene	16.4 24.6	129.8	124.3	27.1	31.6	21.7	13.0			[190]
Cycloheptene	131.5		28.4	26.8	31.5					[190]
1,3-Cycloheptadiene	125.6	133.2	133.2	125.6	32.0	25.9	32.0			[50k]
Cycloheptatriene	120.4	126.8	134.1	134.1	126.8	120.4	28.1			[50k]
cis-Cyclododecene	130.7		31.6	25.7	25.1	24.4	24.1			[190]

2,4,4-trimethyl-1-pentene below. The substituent parameters of the corresponding carbons are symbolized by the same letters:

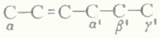

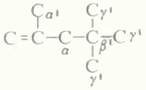

Substituent parameters obtained from least-squares solutions, differ greatly for different kinds of olefins, as is seen in Table 4.12 [190]. The carbon shift of ethylene (123.3 ppm) and the increments listed in Table 4.12 permit a preestimation of olefinic carbon shieldings in alkenes with known constitutions.

Table 4.12. ^{13}C Chemical Shift Parameters for Different Kinds of Alkenes [190] (Relative to Ethylene).

Parameter	Monosubstituted alkenes	Disubstituted alkenes	1,2-Disubstituted alkenes	Trisubstituted alkenes
α	12.63 ± 0.18	8.75 ± 0.43	2.61 ± 0.12 ($\alpha + \alpha'$)	6.35 ± 0.07
β	4.55 ± 0.06	5.90 ± 0.81	6.50 ± 0.05	6.47 ± 0.22
γ	− 1.18 ± 0.07	− 1.10 ± 0.11	− 0.72 ± 0.10	− 0.66 ± 0.29
α'	− 8.03 ± 0.18	− 6.59 ± 0.43	− 2.61 ± 0.12 ($\alpha + \alpha'$)	− 5.14 ± 0.07
β'	− 1.95 ± 0.06	− 1.86 ± 0.81	− 1.82 ± 0.05	− 1.22 ± 0.22
γ'	1.41 ± 0.07	1.99 ± 0.11	0.93 ± 0.10	1.20 ± 0.29
c			0.45 ± 0.08	

In addition to the α, β and γ values, a parameter c, representing the interaction of alkene-alkyl groups in *cis* position, is listed in Table 4.12. The results of the calculations can often be improved considerably by including correction parameters [190].

In an early study on norbornenes [186] olefinic carbons were shown to resonate at δ values similar to those in open chain compounds [186]. Substituent effects of methyl groups at different positions on the bicyclic norbornene ring system are seen in Table 4.13. For instance, steric interactions between methyl groups and π orbitals cause olefinic carbons to resonate at higher field, as must be concluded from a comparison of the ^{13}C chemical shifts of C-2 and C-3 of the stereoisomers *syn*- and *anti*-7-methyl-norbornene [186].

Table 4.13. ^{13}C Chemical Shifts of Norbornenes (δ Values (ppm) Relative to TMS = 0) [186].

Compound	C-1	C-2	C-3	C-4	C-5	C-6	C-7	CH_3
Norbornene	41.9	135.2	135.2	41.9	25.2	25.2	48.5	
1-Methylnorbornene	49.6	139.7	135.5	43.0	27.7	32.3	54.7	17.7
exo-5-Methylnorbornene	42.4	136.9	135.9	48.4	32.7	34.7	44.7	21.4
endo-5-Methylnorbornene	43.3	136.9	132.2	47.5	32.7	33.9	50.2	19.2
syn-7-Methylnorbornene	47.5	132.1	132.1	47.5	25.6	25.6	54.4	12.2
anti-7-Methylnorbornene	45.7	137.5	137.5	45.7	21.5	21.5	53.0	14.1
Norbornadiene	50.6	143.1	143.1	50.6	143.1	143.1	75.1	

4.3. Alkynes and Allenes

^{13}C shifts of alkynes appear to obey patterns similar to those discussed for alkanes in Section 4.1 [5]. Alkyne carbon resonances are found in the narrow range from 63.5 to 88.5 ppm [50a]. The chemical shift positions of alkyne nuclei parallel those known from protons: ^{13}C sp bonded carbons resonate between sp^3 and sp^2 bonded ones [68b]. The shifts of selected acetylenes are tabulated in Table 4.14.

Table 4.14. ^{13}C Chemical Shifts of Alkynes (δ Values (ppm) Relative to TMS).

Compound	C-1	C-2	C-3	C-4	C-5	C-6	C-7	C-8	Ref.
1-Butyne	67.0	84.7							[68b]
2-Butyne		73.6							[68b]
1-Hexyne	67.4	82.8	17.4	29.9	21.2	12.9			[192] [195]
2-Hexyne	1.7	73.7	76.9	19.6	21.6	12.1			[195]
3-Hexyne	14.4	12.0	79.9						[192] [195]
1-Heptyne	67.4	82.9	17.7	28.1	30.7	22.4	14.0		[195]
2-Heptyne	2.3	74.2	77.6	17.7	31.2	21.8	13.5		[192] [195]
3-Heptyne	13.7	12.0	78.3	80.2	20.2	22.5	13.1		[195]
1-Octyne	69.0	84.0	18.4	29.2	29.2	32.0	23.4	14.9	[195]
2-Octyne	2.9	74.8	78.5	18.4	29.5	31.4	22.7	14.5	[195]
3-Octyne	15.1	13.0	79.7	81.0	18.7	31.9	22.8	14.6	[195]
4-Octyne	12.7	21.4	19.2	79.0					[195]
Dodeca-5,7-diyne					66.7	77.4			[192]

Nuclear spin-spin coupling constants have been measured in ^{13}C enriched ethane, ethylene and acetylene [193, 194], and the fractional s character of the C – H bonds has been linearly related to the $^{13}C - {}^{1}H$ one-bond coupling constants [195] (Fig. 3.14, 3.17).

The large ^{13}C shift values of the central *sp* carbons in allenes (200 – 210 ppm) relative to the terminal ones (mostly 72 – 73 ppm, Table 4.15) are attributed to an increased paramagnetic shielding due to two localized π bonds originating from the same carbon.

Table 4.15. ^{13}C Chemical Shifts (δ [ppm]) of Selected Allenes; Data from Ref. [196].

Compound	C-1	C-2	C-3	C-4	C-5	C-6	C-7	C-8
Allene	72.3	211.4						
1,2-Butadiene	72.2	208.2	83.0	12.0				
1,2-Pentadiene	73.5	207.6	90.4	20.4	12.0			
1,2-Hexadiene	73.4	208.3	88.7	29.3	18.1	12.5		
1,2-Heptadiene	72.6	207.8	88.4	29.9	26.4	20.6	12.0	
1,2-Octadiene	73.8	208.2	89.2	30.7	28.3	27.6	22.0	13.4
3-Methyl-1,2-butadiene	69.8	205.7	91.8	17.9	17.9			
2,3-Pentadiene	13.4	83.7	205.3	83.7	13.4			
2-Methyl-2,3-pentadiene	19.5	102.9	202.3	82.3	13.8	13.8		
2,4-Dimethyl-2,3-pentadiene	18.8	90.9	198.8	90.9	18.8	18.8	18.8	

4.4. Haloorganic Compounds

^{13}C chemical shifts of methyl carbons in methane derivatives bearing different atoms of the same group in the periodic table often show a linear relationship if plotted *versus* the Pauling electronegativities of the heteroatoms [197, 198]. Plotting the ^{13}C chemical shifts of a series of methyl compounds CH_3-X *versus* the electronegativities of the heteroatoms X yields a fairly straight line for X = Si, H, C, N, O and F; a straight line, though with a different slope, is also observed for the parameters of the halogen atoms I, Br and Cl (see Fig. 4.2) [68a]. Anisotropy effects of the substituents were assumed responsible for the higher shielding of the carbons in the halo-compounds [68a]. However, it was later pointed out that anisotropy is of only minor influence on the chemical shift of neighboring atoms [199].
A plot of ^{13}C chemical shifts of the methane derivative series CX_4, CHX_3, CH_2X_2, CH_3X (X = Cl, Br, I, CH_3) *versus* the degree of hydrogen substitution is shown in Fig. 4.3. One would expect

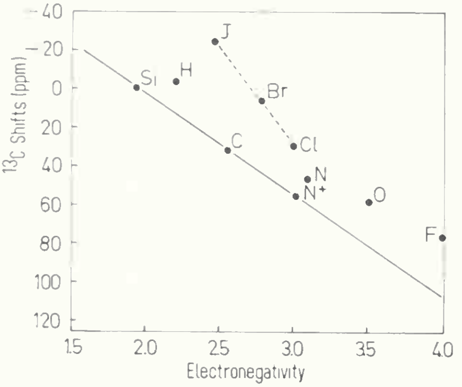

Fig. 4.2. Plot of the electronegativities of the atoms X *versus* the ^{13}C chemical shifts of CH_3X compounds (δ values (ppm) relative to TMS = 0) [68a].

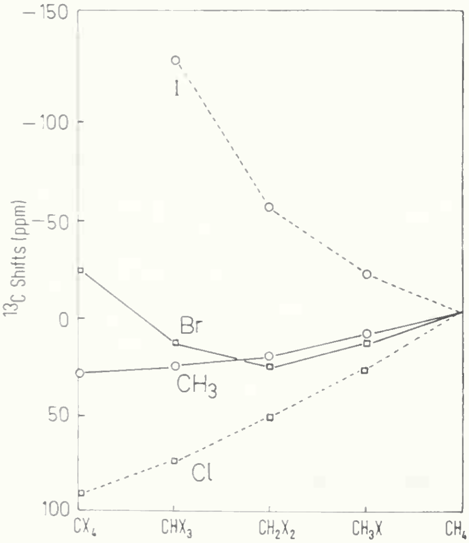

Fig. 4.3. ^{13}C chemical shifts of substituted methanes *versus* the degree of substitution (δ values (ppm) relative to TMS = 0) [68a].
– – –□– – –□ X = Cl;
——□——□ X = Br
– – –○– – –○ X = J;
——○——○ X = CH_3.

that with increasing substitution the carbon signals should shift to lower field. However, this hypothesis holds true only for chlorine, methyl and in part for bromine substitution. The signals of the alkane carbons of the iodo compounds shift to higher field as the number of halogen atoms increases in the methane derivatives [68a].

Charge polarizations, changes in bond lengths caused by steric effects, and deviations from normal electron pairing were shown to be responsible for the ^{13}C chemical shift anomalities of the halomethanes [63]. The following expressions have been developed for the calculation of ^{13}C chemical shifts of halomethanes [63]:

$$\delta_{C^{13}}(CH_4) = \delta_0 \tag{4.3}$$

$$\delta_{C^{13}}(CH_3X) = \delta_0 + \Delta(X) \tag{4.4}$$

$$\delta_{C^{13}}(CH_2XX') = \delta_0 + \Delta(X) + \Delta(X') + \Delta(X-X') \tag{4.5}$$

$$\begin{aligned}\delta_{C^{13}}(CHXX'X'') = {} & \delta_0 + \Delta(X) + \Delta(X') + \Delta(X'') + \Delta(X-X') + \Delta(X-X'') \\ & + \Delta(X'-X'')\end{aligned} \tag{4.6}$$

$$\begin{aligned}\delta_{C^{13}}(CXX'X''X''') = {} & \delta_0 + \Delta(X) + \Delta(X') + \Delta(X'') + \Delta(X''') \\ & + \Delta(X-X') + \Delta(X-X'') + \Delta(X-X''') + \Delta(X'-X'') \\ & + \Delta(X'-X''') + \Delta(X''-X''').\end{aligned} \tag{4.7}$$

The substitution parameters Δ, calculated from a least-squares regression analysis, are collected in Table 4.16. By applying eq. (4.3)–(4.7), the ^{13}C chemical shifts of halomethanes can be calculated with a standard deviation of about 4 ppm.

Table 4.16. Substitution Parameters of Halomethans Obtained from Least-Squares Regression Analysis [63].

Δ(Cl)	33.98 ± 3.04
Δ(Br)	24.18 ± 3.04
Δ(I)	−7.83 ± 4.15
Δ(Cl−Cl)	−5.44 ± 1.87
Δ(Cl−Br)	−11.29 ± 1.52
Δ(Br−Br)	−18.88 ± 1.87
Δ(I−I)	−35.67 ± 3.94

A systematic investigation of chloro substituted ethanes $\overset{1}{C}H_{3-x}Cl_x-\overset{2}{C}H_{3-y}Cl_y$ shows that for y = 0, the C-1 resonance is shifted to lower field by about 30 ppm per hydrogen-chlorine substitution on C-1; with increasing chlorine substitution at C-2 the relative deshielding for C-1 decreases, as can be seen in Fig. 4.4 [200].

As the range of chemical shifts is an order of magnitude larger for ^{13}C than for ^{1}H, cmr is much better suited for investigating stereoisomers. This has been demonstrated by ^{13}C NMR measurements on 2,4-dichloropentane and 2,3-dichlorobutane, which are models for polyvinylchloride [201]. Table 4.17 gives the ^{13}C chemical shift values for *meso-* and *racem-*2,4-dichloropentane and 2,3-dichlorobutane and for polyvinylchloride.

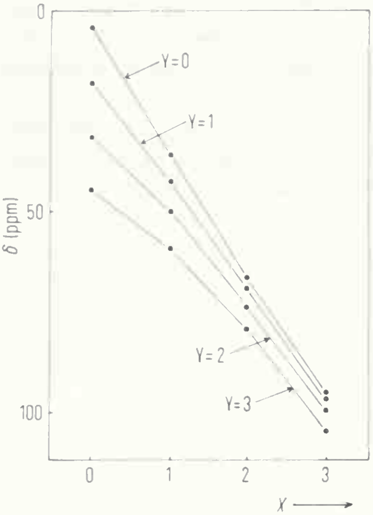

Fig. 4.4. Plot of ^{13}C chemical shifts of chloroethanes $^{*}CH_{3-x}Cl_xCH_{3-y}Cl_y$ *versus* substitution number x [200].

Table 4.17. ^{13}C Chemical Shifts of 2,4-Dichloropentanes, 2,3-Dichlorobutanes and Polyvinylchloride (δ Values (ppm) Relative to TMS = 0) [201].

Compound	CHCl	CHCl (syndio-tactic)	CHCl (hetero-tactic)	CHCl (iso-tactic)	CH_2	CH_3
meso-2,4-Dichloropentane	54.2				50.2	24.4
racem-2,4-Dichloropentane	55.3				50.4	25.2
meso-2,3-Dichlorobutane	61.3					21.8
racem-2,3-Dichlorobutane	60.2					19.7
Polyvinylchloride		56.8	55.7	54.7	46.6	45.6

For example, the most stable conformations of *racem*- and *meso*-2,4-dichloropentane [200] are shown in Fig. 4.5.

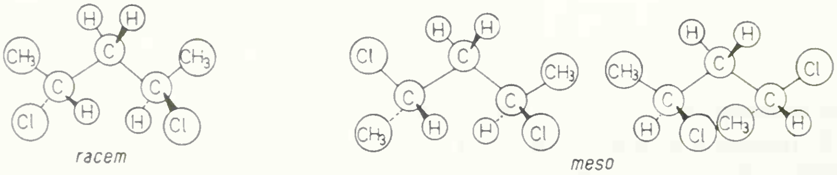

Fig. 4.5. Models for *racem*- and *meso*-2,4-dichloropentane.

In *racem*-2,4-dichloropentane, the methyl groups are in *trans* position to the methine carbons, and in the *meso* isomer, these two groups are partly *cis* and partly *trans* to each other. This different spatial arrangement of groups in the *racem* and *meso* isomers is reflected in a shielding difference of about 1 ppm for the methyl and methine carbons. The ^{13}C chemical shift difference of the methylene carbons of *racem*- and *meso*-2,4-dichloropentane is only 0.2 ppm. Though in both conformations the methylene carbons are not chemically equivalent, their shielding is very similar because no interaction is possible with an alkyl group in *trans* or *gauche* position.

Comparison of the ^{13}C NMR spectrum of commercial polyvinylchloride with the cmr spectra of *racem*- abd *meso*-2,4-dichloropentane leads to the signal identification of the syndiotactic, heterotactic and isotactic methyne carbons of the polymer [201].

Though hydrogen-iodine substitution causes primary carbons of alkanes to resonate at higher field, the signals of secondary and tertiary carbon atoms may be sifted downfield [202]. Strong solvent effects are observed, especially for the ^{13}C resonances of the carbon-iodine groups, as can be seen in Table 4.18 [202].

Table 4.18. ^{13}C Chemical Shifts of Alkyl Iodides in Different Solvents (δ Values (ppm) Relative to TMS = 0) [202].

Compound	C-1	C-2	C-3	C-4	C-5	C-6	C-7	Solvent
1-Iodoethane	−5.6	19.6						Cyclohexane
	−1.4	20.5						Neat Liquid
	−1.2	19.8						Nitromethane
	−0.4	20.3						N,N-Dimethylformamide
1-Iodopentane	3.1	33.1	32.4	21.2	12.8			Cyclohexane
	5.9	33.2	32.5	21.4	13.6			Neat Liquid
	7.0	33.2	32.5	21.3	12.9			Nitromethane
	7.5	33.3	32.5	21.3	13.3			N,N-Dimethylformamide
1-Iodoheptane	3.3	33.5	30.3	28.0	31.5	22.2	13.1	Cyclohexane
	5.8	33.5	30.3	28.0	31.5	22.3	13.7	Neat Liquid
	7.1	33.6	30.3	28.0	31.5	22.3	13.2	Nitromethane
	7.7	33.7		28.0	31.6	22.3	13.5	N,N-Dimethylformamide
2-Iodopropane	30.6	16.9						Cyclohexane
	31.4	20.2						Neat Liquid
	30.5	22.4						Nitromethane
	30.9	22.8						N,N-Dimethylformamide
2-Iodo-2-methyl-propane	39.9	38.3						Cyclohexane
	40.8	41.7						Neat Liquid
	39.9	45.4						Nitromethane

According to a theory by Buckingham [203], which is based on a model from Onsager [204] the ^{13}C solvent chemical shifts for the α-carbons of alkyl iodides should be linearly related to $\left(\frac{\varepsilon - 1}{2\varepsilon + n^2}\right)$ (ε = dielectric constant, n = refractive index). This relationship has been confirmed by experimental data [202].

The ^{13}C chemical shift values of some methyl-2,2-difluoronorbornanes [186] are tabulated in Table 4.19.

The C–F coupling constants proved to be valuable parameters for the signal assignments of the compounds in Table 4.19, as these depend on the number of intervening bonds (see Table 4.20) between the fluorine and carbon atoms [186].

Table 4.19. ^{13}C and ^{19}F Chemical Shifts of Methyl-2,2-difluoronorbornanes [186] (^{13}C Shifts Relative to TMS = 0, ^{19}F Shifts Relative to $CFCl_3$ = 0 in ppm).

Compound	C-1	C-2	C-3	C-4	C-5	C-6	C-7	CH_3	F_{exo}	F_{endo}
2,2-Difluoronorbornane	44.9	131.1	42.7	36.2	27.4	20.8	36.9		86.2	109.3
1-Methyl-2,2-difluoronorbornane	48.7	130.2	43.3	35.3	29.6	28.8	43.0	12.2	94.3	116.7
exo-3-Methyl-2,2-difluoronorbornane	44.9	130.9	46.8	43.6	28.6	21.0	34.2	11.9	104.8	109.6
endo-3-Methyl-2,2-difluoronorbornane	44.0	129.3	45.6	41.2	20.1	20.9	36.0	9.0	84.6	120.6
exo-5-Methyl-2,2-difluoronorbornane	45.6	131.0	43.5	42.5	34.6	30.6	33.4	21.5	86.2	108.0
endo-5-Methyl-2,2-difluoronorbornane	46.0	131.0	35.4	41.3	32.2	29.2	38.5	16.1	83.7	110.1
exo-6-Methyl-2,2-difluoronorbornane	51.4	131.0	41.9	36.5	37.8	27.1	33.4	20.5	85.5	110.0
endo-6-Methyl-2,2-difluoronorbornane	49.5	131.5	43.5	36.1	36.3	32.3	38.7	17.8	74.1	101.8
syn-7-Methyl-2,2-difluoronorbornane	48.8	131.4	40.3	41.1	27.7	22.0	45.2	12.2	81.4	97.8
anti-7-Methyl-2,2-difluoronorbornane	49.1	130.6	44.1	40.1	24.5	17.9	42.1	11.5	86.5	106.5
exo-2-Fluoronorbornane	42.1	95.6	39.8	34.6	28.0	22.3	35.0		158.9	

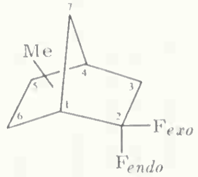

Table 4.20. $^{13}C-^{19}F$ Coupling Constants (in Hz) of Methyl-2,2-Difluoronorbornanes and *exo*-2-Fluoronorbornane [186].

Compound	C-1	C-2	C-3	C-4	C-6	C-7	CH_3
2,2-Difluoronorbornane	24.1; 22.0	253.9; 253.9	24.3; 22.0	5.4; 2.8	5.8; 5.8	4.9	
1-Methyl-2,2-difluoronorbornane	21.9; 21.9	256.5; 256.5	24.7; 22.7	4.5; 2.6	6.3; 4.2	5.3	4.0
exo-3-Methyl-2,2-difluoronorbornane	24.0; 21.8	258.0; 258.0	24.0; 20.3	5.6; 1.2	5.8; 5.8	4.7	14.1; 2.7
endo-3-Methyl-2,2-difluoronorbornane	24.2; 22.4	259.9; 252.6	22.4; 22.1	4.4; 1.9	6.9; 5.9	5.8	1.5; 9.7
exo-5-Methyl-2,2-difluoronorbornane	23.0; 21.8	255.0; 250.2	23.6; 21.6	3.2; 3.2	6.0; 6.0	5.0	<1
endo-5-Methyl-2,2-difluoronorbornane	23.5; 21.3	254.0; 251.6	24.6; 21.8	4.2; 2.2	6.0; 6.0	4.0	<1
exo-6-Methyl-2,2-difluoronorbornane	22.3; 20.9	255.0; 250.2	23.1; 21.1	4.6; 2.0	5.8; 5.8	5.0	≈1
endo-6-Methyl-2,2-difluoronorbornane	22.3; 19.1	257.3; 250.3	21.8; 21.8		3.4; 3.4	5.2	<1; 7.0
syn-7-Methyl-2,2-difluoronorbornane	20.7; 20.7	253.0; 253.0	25.4; 21.6	4.0; 3.0	8.1; 6.8	5.5	4.5; <1
anti-7-Methyl-2,2-difluoronorbornane	22.6; 20.6	254.5; 254.5	24.1; 21.7	3.5; 2.6	5.8; 5.8	4.3	<1
exo-2-Fluoronorbornane	20.2	182.0	20.4	2.3	9.8	<1	

The J_{CF} coupling constants for the α-carbons are about 250 Hz, while those of the β-carbons are on the order of 22 Hz. The three-bond C–F coupling constants vary between 1 and 8 Hz. Measurements on *exo*-2-fluoronorbornane show that only F-2, in *endo* position, couples by through-space interaction with C-7. In most cases no coupling with the fluorine atoms is observed for the C-5 and CH_3 carbons, which are three bonds removed from the halogen atom.

The ^{13}C chemical shifts of ethylenic carbons, bearing iodine atoms, are most influenced (6–8 ppm) by the *cis-trans* position of the substituents [189, 205]; the ^{13}C chemical shift differences of the ethylenic carbons of *cis-trans* isomeric pairs containing bromine are 4–6 ppm; for the chlorine compounds a difference of 1–3 ppm is observed, while the shifts differ less than 2 ppm for olefinic *cis-trans* isomeric pairs containing no halogens [189, 205]. The resonances of the ethylenic carbons in halogen substituted *cis* isomers of unsymmetrically substituted ethylenes have been shown to occur always at lower field than those of the corresponding *trans* compounds. Reduced bond order and greater charge separation in the C=C π bond are reasonable explanations for this effect [189, 205]. Hydrogen-halogen substitution in ethylenes causes a much smaller downfield shift of the signal of the substituted carbon than is observed for alkane carbons. This has been attributed to conjungation between the chlorine and the π bond.

The signal identification of the parent compound and several derivatives could be made unequivocally using the long-range carbon-fluorine coupling constants of 1-fluoro-bicyclo[2,2,2]-octane [206]. The following carbon-fluorine coupling constants for the fluorine compound were reported [206]: $^1J_{CF} = 185.3$ Hz, $^2J_{CF} = 18.4$ Hz, $^3J_{CF} = 9.4$ Hz, $^4J_{CF} = 3.3$ Hz. The shifts of several 1-substituted bicyclo[2,2,2]octanes are listed in Table 4.21.

Table 4.21. ^{13}C Chemical Shifts of 1-Substituted Bicyclo[2,2,2]octanes (δ Values (ppm) Relative to TMS = 0) [206].

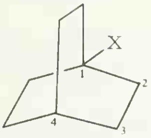

Compound	C-1	C-2	C-3	C-4
Bicyclo[2.2.2]octane	23.55	25.65	25.65	23.55
1-Methoxybicyclo[2.2.2]octane	71.90	28.90	26.50	23.85
1-Fluorobicyclo[2.2.2]octane	92.00	30.85	26.95	23.80
1-Chlorobicyclo[2.2.2]-octane	56.80	35.80	27.80	22.90
1-Bromobicyclo[2.2.2]octane	62.45	37.15	28.70	22.35

Table 4.22. ^{13}C Chemical Shifts and Coupling Constants in Haloorganic Compounds (Derivatives of *n*-Alkanes); δ Values (ppm) Relative to TMS = 0.

Compound	^{13}C Chemical shifts (ppm)	$^1J_{CH}$ [Hz]	$^2J_{CH}$ [Hz]	References	
				Chemical shifts	Coupling constants
CH_3F	74.10	149		[68a]	[196]
CH_3Cl	23.80	150		[63]	[196]
CH_3Br	8.90	152		[63]	[196]
CH_3I	−21.80	151		[63]	[196]
CH_2F_2		185			[208]
CH_2Cl_2	52.85	178		[63]	[196]
CH_2ClBr	38.75			[63]	
CH_2Br_2	20.30			[63]	
CH_2I_2	−55.10	173		[63]	[196]
CHF_3		238			[208]
$CHFCl_2$		220			[208]
CHF_2Cl		231			[208]
$CHCl_3$	77.40	209		[63]	[196]
$CHCl_2Br$	56.05			[63]	
$CHClBr_2$	33.25			[63]	
$CHBr_3$	11.05	206		[63]	[196]
CHI_3	−141.00			[63]	
CCl_4	95.35			[63]	
CCl_3Br	66.50			[63]	
CCl_2Br_2	35.40			[63]	
$CClBr_3$	3.80			[63]	
CBr_4	29.75			[63]	
CH_3-CH_2F	13.30			[68a]	
	78.00				
CH_3-CH_2Cl	17.50	128	2.6	[200]	[200]
	38.70	150	4.2		
CH_3-CH_2Br	18.95			[197]	
	26.95				
CH_3-CH_2I	21.85			[197]	
	−0.25				
CH_3-CHCl_2	31.30	130	< 1.2	[200]	[200]
	68.00	179	5.1		
CH_3-CHBr_2	34.75			[197]	
CH_3-CCl_3	45.10	132		[200]	[200]
	95.00		5.9		
CH_2Cl-CH_2Cl	43.90	155	< 2	[200]	[200]
$CH_2Cl-CHCl_2$	50.40	158	< 2	[200]	[200]
	71.10	181	2.5		
$CH_2Cl-CCl_3$	59.50	158		[200]	[200]
	96.40		3.2		
$CHCl_2-CHCl_2$	74.30	179	< 2	[200]	[200]
$CHCl_2-CCl_3$	80.00	182		[200]	[200]
	99.70		1.5		
CCl_3-CCl_3	104.90			[200]	
$(CH_3)_2CHCl$	26.85			[197]	
	53.75				
$(CH_3)_2CHBr$	28.05			[197]	
	44.05				

Table 4.22. (Continued).

Compound	^{13}C Chemical shifts (ppm)	$^1J_{CH}$ [Hz]	$^2J_{CH}$ [Hz]	References	
				Chemical shifts	Coupling constants
$(CH_3)_2CHI$	31.85			[197]	
	20.95				
$(CH_3)_3CCl$	33.45			[197]	
	165.15				
$(CH_3)_3CBr$	36.35			[197]	
	60.55				
$(CH_3)_3CI$	40.45			[197]	
	41.85				
$CH_2=CHCl$	116.00	198	4.3	[200]	[200]
	124.90	162	9.3; 6.7		
$CH_2=CHBr$	120.80		6.25	[210]	[209]
	114.30		6.75; −8.2		
$CH_2=CHI$	129.20		4.0	[210]	[209]
	84.10		4.15; −7.8		
$CHCl=CHCl$ (*trans*)	119.90	199	<1.8	[200]	[200]
$CHCl=CHCl$ (*cis*)	118.10	198	16.5	[200]	[200]
$CHBr=CHBr$ (*cis*)	115.10			[205]	
$CHBr=CHBr$ (*trans*)	108.10			[205]	
$CHI=CHI$ (*cis*)	95.20			[205]	
$CHI=CHI$ (*trans*)	78.10			[205]	
$CH_2=CCl_2$	112.10	167		[200]	[200]
	125.90		1.3		
$CHCl=CCl_2$	116.40	201		[200]	[200]
	123.90		8.5		
$CCl_2=CCl_2$	120.10			[200]	
$CH_3-CH=CHCl$ (*cis*)	125.40			[189]	
	118.80				
$CH_3-CH=CHCl$ (*trans*)	128.10			[189]	
	116.40				
$CH_3-CH=CHBr$ (*cis*)	129.60			[189]	
	110.10				
$CH_3-CH=CHBr$ (*trans*)	133.40			[189]	
	104.40				
$n\text{-}C_4H_9-CH=CHI$ (*cis*)	140.90			[189]	
	82.90				
$n\text{-}C_4H_9-CH=CHI$ (*trans*)	146.40			[189]	
	75.30				
$C_2H_5-CH=CI-C_2H_5$ (*cis*)	134.70			[189]	
	110.80				
$C_2H_5-CH=CI-C_2H_5$ (*trans*)	141.50			[189]	
	104.80				
$n\text{-}C_4H_9-C\equiv CCl$	67.50			[192]	
	55.40				
$n\text{-}C_4H_9-C\equiv CBr$	78.50			[192]	
	37.10				
$n\text{-}C_4H_9-C\equiv CI$	95.50			[192]	
	−6.60				

Table 4.23. ^{13}C Chemical Shifts of Acyclic Alcohols (δ Values (ppm) Relative to TMS = 0).

Compound	C-1	C-2	C-3	C-4	C-5	C-6	C-7	C-8	C-9	C-10	CH_3	Ref.
Methanol	49.0											[211]
Ethanol	57.0	17.6										[211]
1-Propanol	63.6	25.8	10.0									[211]
1-Butanol	61.4	35.0	19.1	13.6								[211]
1-Pentanol	61.8	32.5	28.2	22.6	13.8							[211]
1-Hexanol	61.9	32.8	25.8	32.0	22.8	14.2						[211]
1-Heptanol	61.9	32.9	26.1	29.4	32.1	22.8	13.9					[211]
1-Octanol	61.9	32.9	26.1	29.7	29.6	32.1	22.8	13.9				[211]
1-Nonanol	62.0	32.9	26.2	29.8	29.9	29.6	32.2	22.9	14.0			[211]
1-Decanol	61.9	32.9	26.1	29.8	29.8	29.9	29.6	32.2	22.8	14.0		[211]
2-Propanol	25.1	63.4										[211]
2-Butanol	22.6	68.7	32.0	9.9								[211]
2-Pentanol	23.3	67.0	41.6	19.1	14.0							[211]
2-Hexanol	23.3	67.2	39.2	28.3	22.9	13.9						[211]
2-Heptanol	23.3	67.2	39.5	25.8	32.3	22.9	13.9					[211]
2-Octanol	23.4	67.2	39.6	26.1	29.7	32.2	22.8	14.0				[211]
2-Decanol	23.4	67.2	39.6	26.2	30.1	30.0	29.6	32.2	22.9	14.0		[211]
3-Pentanol	9.8	29.7	73.8									[211]
3-Hexanol	9.9	30.3	72.3	39.4	19.4	14.0						[211]
3-Heptanol	10.0	29.7	72.6	36.9	28.2	23.0	14.0					[211]
3-Octanol	10.0	30.3	72.6	37.2	25.7	32.3	22.9	13.9				[211]
4-Heptanol	14.1	19.1	40.0	70.6								[211]
4-Octanol	14.0	19.1	40.0	70.9	37.5	28.2	23.0	14.0				[211]
5-Nonanol	14.0	23.0	28.3	37.5	71.1							[211]
2-Methyl-1-propanol	68.9	30.8	18.9									[211]
2-Methyl-2-propanol	31.3	68.4										[211]
2,2-Dimethyl-1-propanol	72.6	32.6	26.3									[211]
2-Methyl-1-butanol	66.9	37.5	25.9	11.1								[211]
			16.0									[211]
3-Methyl-1-butanol	60.2	41.8	24.8	22.5								[211]
3-Methyl-2-butanol	19.7	72.0	35.1	18.1								
4-Methyl-2-pentanol	24.0	65.2	48.9	24.8	22.8							[211]

Table 4.23. (Continued).

Compound	C-1	C-2	C-3	C-4	C-5	C-6	C-7	C-8	C-9	C-10	CH_3	Ref.
4-Methyl-3-pentanol			77.3									[212]
3,3-Dimethyl-1-butanol	58.9	46.4	29.7	29.8								[211]
2,3-Dimethyl-2-butanol	26.3	72.2	38.8	17.5								[211]
3,3-Dimethyl-2-butanol	17.9	74.8	35.0	25.5								[211]
4,4-Dimethyl-3-pentanol			80.9									[212]
2,4-Dimethyl-3-pentanol			80.4									[212]
2,3,3-Trimethyl-2-butanol	25.4	74.1	37.5	25.6								[211]
2,4,4-Trimethyl-3-pentanol			82.8									[212]
2,2,4,4-Tetramethyl-3-pentanol	28.5	36.9	84.7	36.9	28.5							[212]
exo-2-Hydroxynorbornane	44.2	74.1	42.1	35.5	28.5	24.6	34.3					[186]
endo-2-Hydroxynorbornane	42.8	72.2	39.3	37.4	30.0	20.1	37.5					[186]
1-Methyl-2-norbornanol (*endo*)	47.9	76.8	40.8	37.1	31.5	27.1	44.6				18.5	[186]
exo-3-Methyl-2-norbornanol (*endo*)	43.5		45.7	44.1	30.2	19.9	34.3				19.5	[186]
endo-3-Methyl-2-norbornanol (*endo*)	43.9	71.4	37.1	42.6	21.9	19.8	36.8				10.2	[186]
1-Methyl-2-norbornanol (*exo*)	47.6	76.6	43.5	36.1	30.6	33.4	40.3				16.3	[186]
exo-3-Methyl-2-norbornanol (*exo*)	45.1		43.5	43.3	29.4	24.7	31.9				19.6	[186]
endo-3-Methyl-2-norbornanol (*exo*)	45.6		46.4	41.1	21.2	25.2	37.0				14.6	[186]
4-Methyl-3-hydroxy-1-butyne	70.0	88.5										[198]
3-Methyl-3-hydroxy-1-pentyne	71.2	88.0										[198]

Table 4.24. ^{13}C Chemical Shifts of Alicyclic Alcohols (δ Values (ppm) Relative to TMS = 0).

Compound	C-1	C-2	C-3	C-4	C-5	C-6	1-CH_3	2-CH_3	3-CH_3	4-CH_3	Ref.
Cyclopentanol	73.3	35.0	23.4								[184]
trans-2-Methylcyclopentanol	79.8	42.2	33.9	21.5	31.8			18.3			[184]
1-Methylcyclopentanol	79.2	41.2	24.2				28.3				[184]
cis-2-Methylcyclopentanol	75.2	39.8	34.5	22.1	31.0			13.7			[184]
trans-1,2-Dimethylcyclopentanol	79.0	44.3	32.4	21.1	41.3		26.0	12.7			[184]
cis-3-Methylcyclopentanol	73.2	44.1	33.0	32.4	35.4				21.1		[184]
trans-3-Methylcyclopentanol	73.2	44.3	31.9	32.7	35.2				20.7		[184]
1,3-Dimethylcyclopentanol (more abundant isomer)	79.3	50.3	33.8	33.6	42.0		29.6		21.5		[184]
1,3-Dimethylcyclopentanol (less abundant isomer)	79.7	50.7	33.0 33.5	33.0 33.5	41.3		29.3	21.0			[184]
Cyclohexanol	69.5	35.5	24.4	25.9							[211]
trans-2-Methylcyclohexanol	76.6	39.7	34.0	25.8	25.4	35.1		18.8			[211]
cis-3-Methylcyclohexanol	70.5	44.0	31.7	34.8	24.4	34.4			22.5		[211]
trans-4-Methylcyclohexanol	69.7	34.8	33.1	31.4						21.7	[211]
trans-4-Isopropylcyclohexanol	70.7										[213]
trans-4-*t*-Butylcyclohexanol	70.1	35.4	25.4	47.0						27.2 31.8 ($C_{quat.}$)	[211]
1-Methylcyclohexanol	69.0	39.7	22.8	26.0			29.5				[211]
cis-2-Methylcyclohexanol	71.1	35.8	29.3	24.2	21.5	31.8		16.2			[211]
trans-3-Methylcyclohexanol	66.5	41.2	26.6	34.4	20.2	32.8			20.2		[211]
cis-4-Methylcyclohexanol	65.9	31.4	28.7	30.6						20.9	[211]
cis-4-*t*-Butylcyclohexanol	64.7	33.0	20.7	47.9						27.1 32.1 ($C_{quat.}$)	[211]
Cycloheptanol	72.4	37.7	23.3	28.6							[211]
Cyclooctanol	71.9	34.7	23.0	25.5	27.8						[211]

Table 4.25. Substituent Effects of Hydroxyl Groups in Alkylcyclohexanols (in ppm) [211]*).

Compound	C-1	C-2	C-3	C-4	C-5	C-6
Cyclohexanol	42.5	8.5	−2.6	−1.1		
1-Methylcyclohexanol	35.8	3.8	−4.0	−0.7		
cis-2-Methylcyclohexanol	35.2	2.6	−6.6	−2.6	−5.2	5.0
trans-2-Methylcyclohexanol	41.0	6.5	−1.5	−1.0	−1.3	8.3
cis-3-Methylcyclohexanol	43.7	8.1	−1.5	−1.1	−1.4	7.7
trans-3-Methylcyclohexanol	39.7	5.3	−6.6	−1.5	−7.1	6.1
cis-4-Methylcyclohexanol	38.9	4.6	−7.2	−2.6		
trans-4-Methylcyclohexanol	43.0	8.0	−1.1	−1.8		
cis-4-*t*-Butylcyclohexanol	37.8	5.5	−6.8	−0.7		
trans-4-*t*-Butylcyclohexanol	43.2	7.9	−1.1	−1.6		

*) Substituent effect = δ (substituted cyclohexane)-δ (cyclohexane).

4.5. Alcohols

The empirical ^{13}C chemicals shift to structure rules discussed as follows are based on the data collected in Tables 4.23 – 4.25 for acyclic and alicyclic alcohols.

(1) Carbons carrying hydroxyl groups resonate at lowest field due to the electron withdrawing nature of the oxygen atom.

(2) Chemically equivalent carbons give rise to the most intense signals in the cmr spectrum.

(3) The degree of hydrogen substitution is easily determined from the multiplicity of the carbon signals in the proton off-resonance spectra.

(4) Substitution of hydrogen in an alkane by a hydroxyl group causes downfield shifts of 35 to 52 ppm for the α-carbon, 5 to 12 ppm for the β-carbon and 0 to 6 ppm for the γ-carbon. The substitution effects for carbons farther removed from the hydroxyl group are less than 1 ppm.

Table 4.26. ^{13}C Chemical Shifts of Cyclopentanols in the Presence of Varying Concentrations of Eu(DPM)$_3$ in Methylene Chloride (δ Values (ppm) Relative to TMS = 0) [184].

Compound	Molar ratio, complex/ cyclopentanols	C-1	C-2	C-3	C-4	C-5	1-CH$_3$	3-CH$_3$
cis-3-Methylcyclopentanol	0	73.7	44.3	32.9	32.2	35.5		20.9
(equatorial hydroxyl	0.07	76.6	45.0	33.4	33.0	36.2		21.2
group)	0.2	84.1	47.0	34.4	34.4	38.4		21.6
	0.4	96.3	50.7	37.0	37.0	42.3		23.6
trans-3-Methylcyclo-	0	73.7	44.3	31.8	32.4	35.5		20.4
pentanol (axial hydroxyl	0.07	76.6	45.2	32.8	33.0	36.2		20.7
group)	0.2	84.8	47.4	34.4	34.4	38.4		21.6
	0.4	97.7	51.2	37.0	37.0	42.3		22.9
trans-1,3-Dimethylcyclo-	0	79.5	50.0	33.4	33.4	41.9	28.9	21.1
pentanol	0.16	84.5	51.3	34.3	34.3	43.2	30.8	21.6
(more abundant)	0.3	89.5		35.6	35.6	45.2	33.5	22.2
	0.5	96.5	55.8	37.0	37.0	47.7	37.0	22.8
cis-1,3-Dimethylcyclo-	0	79.8	50.3	33.4	42.4	41.1	28.6	20.5
pentanol	0.16	84.6	52.0	34.3	34.3	42.8	30.8	20.9
(less abundant)	0.3	91.4		35.6	35.6	45.2	35.5	22.2
	0.5	99.3	56.8	37.0	37.0	47.7	37.0	22.8

Table 4.27. ^{13}C Chemical Shifts in Acetates (δ Values (ppm) Relative to TMS = 0).

Compound	C-1	C-2	C-3	C-4	C-5	1-CH_3	2-CH_3	3-CH_3	Ac$-CH_3$	Ac$-$CO	Ref.
Methyl acetate	50.7								19.6	170.7	[184]
Ethyl acetate	59.8	13.8							20.0	170.0	[184]
2-Propyl acetate	66.8	20.4							21.4	169.5	[184]
2-Methyl-2-propyl acetate	79.4	27.8							21.7	169.5	[184]
Cyclopentyl acetate	76.5	32.6	23.7						20.5	169.6	[184]
trans-2-Methylcyclopentyl acetate	81.9	40.2	31.4 32.2	22.5	31.4 32.2		18.0		20.5	169.4	[184]
1-Methylcyclopentyl acetate	88.9	39.1	23.7			24.1			21.5	169.4	[184]
cis-2-Methylcyclopentyl acetate	77.9	38.5	31.8 32.0	22.2	31.8 32.0		13.6		20.3	169.4	[184]
trans-1,2-Dimethylcyclopentyl acetate	88.9	45.4	31.8	20.8	36.5	22.0	12.9		21.3	169.4	[184]
cis-3-Methylcyclopentyl acetate	76.3	41.1	33.0	32.5	32.4			20.5	20.4	169.4	[184]
trans-3-Methylcyclopentyl acetate	76.5	41.4	32.6	32.4	32.5			19.9	20.4	169.4	[184]
1,3-Dimethylcyclopentyl acetate (more abundant isomer)	88.6	48.0	33.0	33.0	39.5	25.2		20.7	21.5	169.4	[184]
1,3-Dimethylcyclopentyl acetate (less abundant isomer)	89.4	48.1	33.0	33.0	39.2	24.9		20.3	21.5	169.4	[184]
Vinyl acetate	141.7	96.4							21.0	167.5	[198]

(5) Carbons bearing an axial hydroxy group are more shielded than those with an equatorial one ($\delta_{eq} - \delta_{ax} \approx 5 \pm 1$ ppm). Additionally, an axial hydroxy group at C-1 will shield the C-3,5 carbon pair because of a 1,3-diaxial steric interaction (γ effect, $\delta_{eq} - \delta_{ax} \approx 5.5 \pm 0.5$ ppm).
(6) In the presence of tris(dipivaloylmethanato)europium ($Eu(DMP)_3$) ^{13}C chemical shifts of alcohols are enhanced due to pseudocontact interactions, and often unequivocal signal assignments are made possible, as in the case of the *cis*- and *trans*-1,3-dimethylcyclopentanols. The ^{13}C chemical shift changes are almost linearly proportional to the molar concentration of added contact shift reagent, and the shift changes for the different carbons decrease with the distance from the paramagnetic central ion [184]. Table 4.26 illustrates that carbons bearing axial hydroxyl groups show larger shift changes in the presence of $Eu(DPM)_3$ than comparable carbons bearing equatorial hydroxyl functions.
(7) Acetylation of alcoholic hydroxyl groups causes characteristic downfield α shifts (1.5 to 4 ppm) and upfield β shifts (1 to 5 ppm). Similar β shifts are observed on acetylation of tertiary alcohols. However, the α carbon is shifted to lower field by about 10 ppm in this case. ^{13}C chemical shifts of some representative acetylated alcohols are given in Table 4.27.

4.6. Ethers

In going from the alcohols to the corresponding ethers, the α-carbon signals of primary and secondary alcohols shift downfield by 9 to 10 ppm. The chemical shift values of the α-carbons of ethers are strongly influenced by steric interactions: A reduced downfield shift of 4 ppm is observed in going from *t*-butanol to methyl *t*-butyl ether. This has been attributed to a γ-type interaction for each staggered conformation, which is not possible for ether oxygens bearing only primary and secondary alkyl carbons (see Fig. 4.6). A collection of ^{13}C chemical shifts of selected ethers is given in Table 4.29 [184, 214, 215]. The numbering of the carbon atoms is illustrated in the formulae below (alkyl ethers, 1,4-dioxane and 1,3-dioxanes):

$C_2{-}C_1{-}O{-}CH_3$

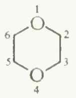

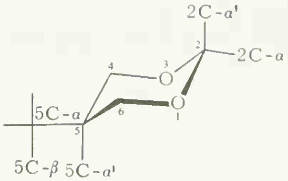

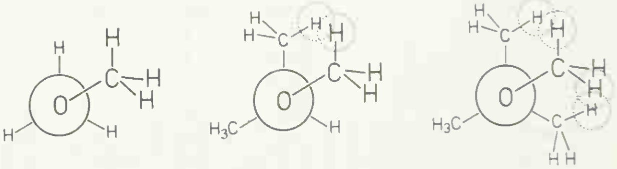

Fig. 4.6. Demonstration of γ-type interactions (--------) in different methyl ethers.

Dimethyl ether Methyl-*i*-propyl ether Methyl-*t*-butyl ether

Interesting information concerning the ^{13}C chemical shift dependence on conformational features is available from measurements on 1,3-dioxanes. The signal assignments of the compounds are based on the signal intensity ratios and multiplicities in the proton coupled spectra as well as on selective proton decoupling. In studying the ^{13}C chemical shifts collected in Table 4.30, several empirical rules become obvious:

(1) Substitution of the equatorial hydrogen at C-2 by a methyl residue causes the corresponding carbon signal to shift downfield by 3 to 5 ppm.
(2) Replacing the axial hydrogen atom at C-2 by a methyl group shifts the signals of C-4 and C-6 about 7 ppm to higher field. This is explained in terms of *syn*-axial 1,3-steric interaction.
(3) The C-5 (α)-carbons resonate at 30.5 to 31.0 and the C-5 (β)-carbons at 27.5 to 27.7 ppm in equatorially oriented *t*-butyl groups at C-5. Equatorial hydrogen-*t*-butyl substitution at C-5 of 1,3-dioxane causes the C-5 signal to shift downfield by 16.3 to 16.7 ppm.
(4) The resonances of C-2 (α) and C-2 (β') with equatorially attached *t*-butyl groups occur at 35.0 to 35.3 and 24.7 to 25.2 ppm, respectively. The signal of C-2 in 1,3-dioxane is shifted 11.0 to 11.6 ppm downfield upon equatorial hydrogen-*t*-butyl substitution.
(5) A comparison of the ^{13}C chemical shifts of *cis*-2,5-di-*t*-butyl-1,3-dioxane (axial *t*-butyl group at C-5) with its *trans* isomer (two equatorial *t*-butyl groups) shows that the largest shift differences are observed for the 5-*t*-butyl group: Its signals occur 2 to 3 ppm at higher field if the 5-*t*-butyl group is changed from axial to equatorial configuration.

Substituent effects have been calculated by least-squares analysis using eq. (4.8) for a series of substituted 1,3-dioxanes [214].

$$\Delta C_{xn} = \Delta C_{xp} + aSE_{x1} + bSE_{x2} \tag{4.8}$$

ΔC_{xn}: Chemical shift of the *x*-th ring carbon in the *n*-th compound;
ΔC_{xp}: Chemical shift of the carbon atom *x* in the corresponding parent compound;
SE_{x1}, SE_{x2} etc.: Substituent effects on the chemical shift of the *x*-th carbon atom;
a, *b* etc.: Number of times a given effect must be accounted for.

Calculated substituent effects for several methylated 1,3-dioxanes are given in Table 4.28 [214].

Table 4.28. Substituent Effects on ^{13}C Chemical Shifts in 1,3-Dioxanes (δ Values (ppm) Relative to the Parent Compound) [214].

Position (s), Substituent (s)	On C-2	On C-4	On C-6	On C-5
C-2, eq. Methyl	5.3	0.1	0.1	−0.8
C-2, ax. Methyl	−1.7	−7.3	−7.3	0.1
C-4, eq. Methyl	0.8	5.7	−0.1	7.3
C-4, ax. Methyl	−9.0	0.6	−5.3	3.7
C-5, eq. Methyl	−0.2	5.8	5.8	3.1
C-5, ax. Methyl	0.4	4.5	4.5	3.1
C-6, eq. Methyl	0.8	−0.1	5.7	7.3
C-6, ax. Methyl	−9.0	−5.3	0.6	3.7
C-4, gem. Dimethyl	2.3	−2.0	1.5	−0.8
C-6, gem. Dimethyl		1.5	−2.0	−0.8
C-5, gem. Dimethyl				−2.3
C-5, gem. Diethyl	0.3	7.7	7.7	8.5
C-4,6, eq. Dimethyl	−1.6			
C-4, eq., C-6, ax. Dimethyl	1.1			
C-4, eq., C-5, eq. Dimethyl		−1.9	1.8	−4.5
C-5, eq., C-6, eq. Dimethyl		1.8	−1.9	−4.5
C-4, ax., C-5, eq. Dimethyl			1.4	3.2
C-5, eq., C-6, ax. Dimethyl		1.4		3.2

Table 4.29. ^{13}C Chemical Shifts of Ethers Including Dioxanes (δ Values (ppm) Relative to TMS = 0).

Compound	C-1	C-2	C-4	C-5	C-6	$O-CH_3$	2C-α	2C-β	5C-α	5C-β or β'	Solvent	Ref.
Dimethyl ether	59.7					59.7					neat liquid	[184]
Ethyl methyl ether	67.7	14.7				57.6					neat liquid	[184]
Methyl 2-propyl ether	72.6	21.4				54.9					neat liquid	[184]
Methyl 2-methyl-2-propyl ether	72.1	26.7				48.6					neat liquid	[184]
1,3-Dioxane		92.8	65.9	26.6	65.9						neat liquid	[214]
2-Methyl-1,3-dioxane		97.8	65.3	24.9	65.3						neat liquid	[214]
4-Methyl-1,3-dioxane		93.6	72.1	33.7	65.8						neat liquid	[214]
5-Methyl-1,3-dioxane		92.7	71.8	28.9	71.8						neat liquid	[214]
2,2-Dimethyl-1,3-dioxane		96.3	58.5	25.5	58.5						neat liquid	[214]
2,4-*cis*-Dimethyl-1,3-dioxane		98.5	71.9	33.3	65.8						neat liquid	[214]
2,5-*cis*-Dimethyl-1,3-dioxane		98.3	70.6	28.9	70.6						neat liquid	[214]
2,5-*trans*-Dimethyl-1,3-dioxane		97.6	71.9	28.9	71.9						neat liquid	[214]
4,4-Dimethyl-1,3-dioxane		86.8	69.3	36.4	61.8						neat liquid	[214]
4,6-*cis*-Dimethyl-1,3-dioxane		92.1	70.8	40.6	70.8						neat liquid	[214]
4,6-*trans*-Dimethyl-1,3-dioxane		85.6	65.9	37.3	65.9						neat liquid	[214]
5,5-Dimethyl-1,3-dioxane		92.3	75.9	30.4	75.9						neat liquid	[214]
2,2,4-Trimethyl-1,3-dioxane		97.2	64.3	33.5	59.6						neat liquid	[214]
2,2,5-Trimethyl-1,3-dioxane		96.3	65.7	28.5	65.7						neat liquid	[214]
2,5,5-Trimethyl-1,3-dioxane		99.1	76.5	29.8	76.5						neat liquid	[214]
2,4,6-*cis*-Trimethyl-1,3-dioxane		97.9	71.6	40.5	71.6						neat liquid	[214]
2,4-*cis*-6-*trans*-Trimethyl-1,3-dioxane		90.8	66.7	37.0	66.7						neat liquid	[214]
4,4,5-Trimethyl-1,3-dioxane		87.5	74.0	39.1	72.1						neat liquid	[214]
4,4,6-Trimethyl-1,3-dioxane		87.2	70.3	43.9	67.8						neat liquid	[214]
4,5,5-Trimethyl-1,3-dioxane		93.7	80.7	32.6	78.3						neat liquid	[214]
4,5-*trans*-6-*cis*-Trimethyl-1,3-dioxane		85.9	70.3	39.1	72.1						neat liquid	[214]
2,2,4,6-*cis*-Tetramethyl-1,3-dioxane		97.0	64.3	40.6	64.3						neat liquid	[214]
2,2-*trans*-4,6-Tetramethyl-1,3-dioxane		99.1	61.8	41.7	61.8						neat liquid	[214]
2,2,5,5-Tetramethyl-1,3-dioxane		96.3	69.1	29.8	69.1						neat liquid	[214]
2,4-*cis*-5-*trans*-6-*cis*-Tetramethyl-1,3-dioxane		90.8	71.8	38.6	71.8						neat liquid	[214]
2,4,4,6-*trans*-Tetramethyl-1,3-dioxane		87.9	70.5	41.3	70.5						neat liquid	[214]
			64.0		64.0							
2,4,4,6-*cis*-Tetramethyl-1,3-dioxane		92.1	70.9	43.7	68.0						neat liquid	[214]

Table 4.29. (Continued).

Compound	C-1	C-2	C-4	C-5	C-6	$O-CH_3$	2C-α	2C-β	5C-α	5C-β or β′	Solvent	Ref.
2,4,5,5-*cis*-Tetramethyl-1,3-dioxane		99.3	79.6	32.3	77.7						neat liquid	[214]
4,4,6,6-Tetramethyl-1,3-dioxane		82.4	69.5	46.3	69.5						neat liquid	[214]
2,2,4,4,6-Pentamethyl-1,3-dioxane		97.2	69.8	43.3	61.4						neat liquid	[214]
2,2-*trans*-4,5-*cis*-6-Pentamethyl-1,3-dioxane		98.9	69.9 63.9	42.1	69.9 63.9						neat liquid	[214]
2,4,4,6,6-Pentamethyl-1,3-dioxane		86.4	69.9	45.9	69.9						neat liquid	[214]
2,2,4,4,6,6-Hexamethyl-1,3-dioxane		97.9	69.5	44.7	69.5						neat liquid	[214]
5,5-Diethyl-1,3-dioxane		93.2	73.4	35.0	73.4						neat liquid	[214]
5,5-Diethyl-2-methyl-1,3-dioxane		98.7	73.7	34.3	73.7						neat liquid	[214]
5,5-Diethyl-2,2-dimethyl-1,3-dioxane		96.3	66.5	34.6	66.5						neat liquid	[214]
5-*t*-Butyl-1,3-dioxane		93.65	68.55	44.40					30.65	27.60	neat liquid	[215]
5-*t*-Butyl-*trans*-2-methyl-1,3-dioxane		99.05	68.60	44.60			21.25		30.55	27.70	neat liquid	[215]
5-*t*-Butyl-*cis*-2-methyl-1,3-dioxane		99.35	67.30	43.60			21.35		32.65 (α′)	29.70	neat liquid	[215]
5-*t*-Butyl-2,2-dimethyl-1,3-dioxane		97.45	60.85	44.25			28.00 20.30 (α′)		30.95	27.55	neat liquid	[215]
2-*t*-Butyl-1,3-dioxane		107.85	66.90	26.35			35.30	25.00			neat liquid	[215]
trans-2-*t*-Butyl-5-methyl-1,3-dioxane		107.70	73.60	29.70			35.25	24.85	12.40		neat liquid	[215]
cis-2-*t*-Butyl-5-methyl-1,3-dioxane		108.10	72.00	29.70			35.30	24.70	15.95		neat liquid	[215]
2-*t*-Butyl-5,5-dimethyl-1,3-dioxane		108.40	77.30	30.15			35.00	25.15	22.20 23.35 (α′)		CS_2	[215]
trans-2,5-Di-*t*-butyl-1,3-dioxane		107.20	68.60	43.70			34.70	24.90	30.00	27.45	CS_2	[215]
cis-2,5-Di-*t*-butyl-1,3-dioxane		108.60	68.00	43.55			35.20	25.05	32.75 (α′)	29.80	CS_2	[215]
cis-2-*t*-Butyl-4-methyl-1,3-dioxane		107.25	72.45	33.70			35.05	24.95			neat liquid	[215]
trans-5-*t*-Butyl-2-phenyl-1,3-dioxane		101.40	69.25	44.00					30.55	27.90	CS_2	[215]
cis-4,6-Dimethyl-2-phenyl-1,3-dioxane		100.85	72.85	40.90							CS_2	[215]
cis-2,4-Dimethyl-1,3-dioxane		98.85	72.45	33.40			21.40				neat liquid	[215]
1,4-Dioxane		66.5	66.5 (C-3)	66.5	66.5						neat liquid	[215]

Substantial deviations between calculated and experimental ^{13}C chemical shift values are observed for compounds such as 2,2,4,4,6-pentamethyl-1,3-dioxane, 2,2-*trans*-4,5-*cis*-6-pentamethyl-1,3-dioxane, 2,2,4,4,6,6-hexamethyl-1,3-dioxane and 2,2-*trans*-4,6-tetramethyl-1,3-dioxane. A plausible suggestion for these discrepancies is that these molecules do not assume chair conformation.

4.7. Carbonyl Compounds

4.7.1. Ketones, Aldehydes

The carbonyl carbons of saturated aliphatic aldehydes are more shielded (202 ± 2 ppm, Table 4.31) than those in comparable alkanones (203 – 217 ppm, Table 4.32).

Increasing alkyl substitution of the hydrogen atoms in acetone shifts the carbonyl resonance monotonically downfield as is demonstrated in Fig. 4.7 and Table 4.32 [212]. This relationship can be explained in terms of inductive effects.

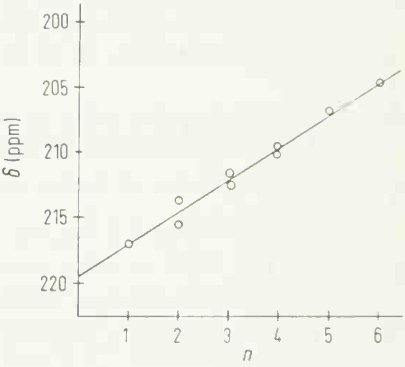

Fig. 4.7. ^{13}C chemical shifts of the C=O resonances in aliphatic acetone derivatives *versus* the number of α-protons (δ values (ppm) relative to TMS = 0) [212].

The carbonyl carbon of di-*t*-butyl ketone, however, resonates at higher field than that of *t*-butyl-isopropyl ketone. A bond angle of 130° compared to 115° in acetone has been assumed responsible for this deviation [212]. The IR and UV spectra of di-*t*-butyl ketone also behave anomalously. The ^{13}C chemical shifts of a series of aliphatic ketones are listed in Table 4.32 [212, 216]. The chemical shift dependence of the carbonyl resonances on ring size in cycloalkanones is particularly remarkable: In the series of cycloalkanones, cyclopentanone is found to have the largest carbonyl shift (213.6 ppm). The CO signals of cyclobutanone and cyclohexanone are both observed at higher field (≈208 ppm). The carbonyl carbons of cyclooctanone and cyclononanone are much more deshielded than those of cyclohexanone, cycloheptanone, cyclodecanone and cycloundecanone. The carbonyl resonances of the twelve to seventeen membered ring ketones occur at similar δ values as those of acyclic ones [216, 217] (see Table 4.32).

The ^{13}C chemical shifts of individual carbon atoms in alkyl cycloalkanones may be predicted with reasonable accuracy by a simple additivity rule [217]: The shift of cyclohexane is subtracted two times from the sum of the ^{13}C chemical shifts of corresponding carbon atoms in the alkyl-cyclohexane and the cyclohexanone. The substituent effects calculated by this procedure are compared with the observed values in Table 4.30:

Table 4.30. Observed and Calculated ^{13}C Chemical Substituent Effects in Alkylcyclohexanones (in ppm) [217].

Compound	C-2		C-3		C-4		C-5		C-6	
	obs.	calc.	obs.	calc.	obs.	calc.	obs.	calc.	obs.	calc.
2-Methylcyclohexanone	17.0	19.6	8.2	8.4	−2.8	−3.4	0.0	−0.6	13.6	13.2
3-Methylcyclohexanone	21.8	22.3	5.7	5.7	5.2	5.7	−2.8	−0.7	12.8	13.3
4-Methylcyclohexanone	12.5	13.2	6.8	8.4	3.1	3.0				
2-*t*-Butylcyclohexanone	33.0	35.0	2.9	0.4	−0.8	−2.7	1.7	−0.6	17.0	13.9
3-*t*-Butylcyclohexanone	16.0	14.3	21.9	21.1	−1.0	−2.3	−0.5	0.0	13.7	13.3
4-*t*-Butylcyclohexanone	14.1	13.9	0.7	0.4	19.8	18.4				
4,4-Dimethylcyclohexanone	10.7	8.9	12.2	12.2	2.9	0.3				
cis-3,4-Dimethylcyclohexanone	22.1	17.8	9.6	6.8	6.4	4.1	3.6	3.9	12.0	10.0
trans-3,4-Dimethylcyclohexanone	19.9	22.3	14.1	11.9	10.7	9.2	7.7	8.4	12.9	13.1
cis-3,5-Dimethylcyclohexanone	22.1	21.7	6.1	5.2	15.7	14.4				
trans-3,5-Dimethylcyclohexanone	21.5	20.2	2.5	−0.6	12.6	11.1				

Table 4.31. ^{13}C Chemical Shifts of Selected Aliphatic Aldehydes (Data from Ref. [50e] and [102]).

Compound	C-1	C-2	C-3	C-4	C-5	C-6	C-7	C-8	C-9	C-10	C-11	C-12
Ethanal	200.5	31.2										
Propanal	202.7	36.7	5.2									
Butanal	201.6	45.7	15.7	13.3								
Pentanal	201.3	43.6	24.3	22.4	13.8							
Heptanal	201.8	45.3	23.6*)	30.1	32.8	23.4*)	15.4					
Nonanal	202.6	44.0	22.2	29.2*)	29.2*)	29.4*)	31.9	22.7	14.1			
2-Methyldecanal	204.3	46.4	30.9	27.2	29.4*)	29.7*)	29.9*)	32.1	22.7	14.2	13.5	
2-Methylundecanal	204.5	46.4	30.9	27.1	29.4*)	29.7*)	29.7*)	29.8*)	32.0	22.7	14.1	13.5
Propenal	193.3	136.0*)	136.4*)									
(*E*)-2-Butenal	193.4	134.8	153.9	18.5								
(*E*)-3-Phenylpropenal	193.5	128.2	152.5	134.1	129.0*) (*o*)	128.5*) (*m*)	131.0 (*p*)					

*) Assignments interchangeable.

In most cases the deviations between theoretical and observed values are less than 2 ppm. Exceptions are 4,4-dimethyl, *cis*-3,4-dimethyl and *trans*-3,5-dimethylcyclohexanone; these compounds all have at least one of their methyl groups axially oriented [217].

It has been demonstrated for a series of cyclic and acyclic ketones that there is a correlation between the ^{13}C chemical shifts of carbonyl groups and their $n \rightarrow \pi^*$ transition energy, as is expressed by eq. (4.9) [218].

$$\delta_{CO} = a\lambda_{max}^{n\rightarrow\pi^*} + b \qquad (4.9)$$

δ_{CO}: ^{13}C chemical shift of the carbonyl group in cyclic ketones;
$\lambda_{max}^{n\rightarrow\pi^*}$: absorption maxima of $n \rightarrow \pi^*$ transitions in cyclic ketones;
a,b: regression coefficients of the least-squares linear fit.

The carbonyl ^{13}C chemical shift of 2-norbornanone is affected by methylation at different positions only to a minor extent (<3 ppm) [186]. Methyl substitution at C-3 causes the largest deshielding of the carbonyl carbon. Steric interactions have been assumed responsible for the upfield shift of the carbonyl resonance upon 6-*endo*-methylation.

Measurements of the cmr spectra (see Table 4.32) of 2-acetoxy-cyclohexanone-1-^{13}C before and after reaction with acetic acid – potassium acetate (218 °C and 22 hours) showed that at elevated temperature the labeled residue is equally distributed among all six carbons of the ring. The cmr spectra thus yielded valuable information concerning the mechanism of the interchange-transfer rearrangement of α-acyloxy ketones [219].

The increased shielding of the carbonyl carbons in ketones with a cyclopropyl ring in α-position to the carbonyl group has been attributed to cyclopropyl conjugation [220].

A systematic investigation of α,β-unsaturated ketones permits the deduction of the following chemical shift rules [221] (see Table 4.34):

(1) The signals of carbonyl groups in conjugated ketones appear at higher field than those in saturated systems. The same trend is observed for aldehydes (Tables 4.31, 4.35).

(2) Alkyl substitution at the β-olefinic carbon shifts the carbonyl resonance 1 to 2 ppm to higher field.

(3) Methyl substitution at the α-olefinic carbon generally causes the carbonyl signal to shift downfield by 1 to 2 ppm.

(4) Dimethyl substitution of the olefinic double bond in α,β-unsaturated ketones decreases the shielding at the carbonyl carbon by 5 to 6 ppm.

(5) The carbonyl carbons in α,β-unsaturated cyclopentenones are much more deshielded than corresponding carbons in cyclohexenones.

(6) The resonances of olefinic carbons in α,β-unsaturated ketones cover the span of 161 to 122 ppm, thus generally appearing at lower field than comparable alkenes.

(7) The β-olefinic carbon resonates at lower field than the α-olefinic carbon; this may be rationalized in terms of a polar resonance formula as discussed in section 3.1.3.6:

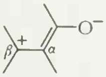

(8) Methyl substitution at olefinic carbons causes the largest deshielding effects at C_α and C_β in cyclopentenones; the effects are smaller in acyclic and six-membered ring α,β-unsaturated ketones.

Table 4.32. ^{13}C Chemical Shifts of Saturated Aliphatic Ketones (δ Values (ppm) Relative to TMS = 0).

Compound	C-1	C-2	C-3	C-4	C-5	C-6	C-7	CH_3	Ref.
$\overset{3}{C}H_3-\overset{1}{C}O-\overset{2}{C}H_3$	206.7	30.7	30.7						[102]
$\overset{4}{C}H_3-\overset{2}{C}H_2-\overset{1}{C}O-\overset{3}{C}H_3$	206.25	35.20	27.50	7.00					[212]
$n\text{-}C_4H_9-\overset{1}{C}O-CH_3$	206.80								[216]
$n\text{-}C_6H_{13}-\overset{1}{C}O-CH_3$	206.50								[216]
$n\text{-}C_7H_{15}-\overset{1}{C}O-CH_3$	206.40								[216]
$(\overset{4}{C}H_3)_2\overset{2}{C}H-\overset{1}{C}O-\overset{3}{C}H_3$	209.30	40.50		17.60					[212]
$(\overset{4}{C}H_3)_3\overset{2}{C}-\overset{1}{C}O-\overset{3}{C}H_3$	210.40	43.40		26.30					[212]
$(CH_3)_2CHCH_2-\overset{1}{C}O-CH_3$	206.00								[216]
$(CH_3)_3CCH_2-\overset{1}{C}O-CH_3$	206.10								[216]
$C_6H_{11}-\overset{1}{C}O-CH_3$	208.20								[216]
$\overset{5}{C}H_3-\overset{3}{C}H_2-\overset{1}{C}O-\overset{2}{C}H_2-\overset{4}{C}H_3$	208.70	35.00	35.00	7.00	7.00				[212]
$\overset{5}{C}H_3-\overset{3}{C}H_2-\overset{1}{C}O-\overset{2}{C}H(\overset{4}{C}H_3)_2$	211.80								[212]
$\overset{5}{C}H_3-\overset{3}{C}H_2-\overset{1}{C}O-\overset{2}{C}(\overset{4}{C}H_3)_3$	213.10	42.40		25.20					[212]
$n\text{-}C_4H_9-\overset{1}{C}O-n\text{-}C_4H_9$	208.30								[216]
$(\overset{5}{C}H_3)_2\overset{3}{C}H-\overset{1}{C}O-\overset{2}{C}H(\overset{4}{C}H_3)_2$	215.10	38.00	38.00	17.80	17.80				[212]
$(\overset{5}{C}H_3)_2\overset{3}{C}H-\overset{1}{C}O-\overset{2}{C}(\overset{4}{C}H_3)_3$	217.05	43.20		24.80					[212]
$(\overset{5}{C}H_3)_3\overset{3}{C}-\overset{1}{C}O-\overset{2}{C}(\overset{4}{C}H_3)_3$	215.15	44.50	44.50	27.80	27.80				[212]
$(CH_3)_2CHCH_2-\overset{1}{C}O-CH_2CH(CH_3)_2$	215.50								[216]
Cyclobutanone	207.90	46.60	8.70						[217]
Cyclopentanone	213.60	36.70	22.00						[217]
Cyclohexanone	208.50	40.40	26.50	23.80					[217]
Cycloheptanone	211.40	42.40	29.40	23.20					[217]
Cyclooctanone	215.60	40.90	26.50	24.80	24.00				[217]
Cyclononanone	214.20								[216]
Cyclodecanone	212.10	41.00	24.30	24.20	22.60	24.40			[217]

Table 4.32. (Continued).

Compound	C-1	C-2	C-3	C-4	C-5	C-6	C-7	CH_3	Ref.
Cycloundecanone	210.80								[216]
Cyclododecanone	208.40	39.20	21.90	24.15	24.05	23.60			[217]
Cyclotridecanone	209.20								[216]
Cyclotetradecanone	207.80								[216]
Cyclopentadecanone	208.60								[216]
Cyclohexadecanone	208.30								[216]
Cycloheptadecanone	208.20								[216]
2-Methylcyclohexanone	210.00	44.00	35.20	24.20	27.00	40.60		13.50	[217]
3-Methylcyclohexanone	208.10	48.80	32.70	32.20	24.20	39.80		20.80	[217]
4-Methylcyclohexanone	208.70	39.50	33.80	30.10				19.90	[217]
2-*t*-Butylcyclohexanone	210.40	59.90	29.90	26.20	28.70	44.00		27.70 31.80 ($C_{quat.}$)	[217]
3-*t*-Butylcyclohexanone	208.70	43.00	48.90	26.50 26.00	26.50 26.00	40.70		27.20 32.30 ($C_{quat.}$)	[217]
4-*t*-Butylcyclohexanone	209.00	41.10	27.70	46.80				27.70 32.50 ($C_{quat.}$)	[217]
trans-3,4-Dimethylcyclohexanone	209.10	46.90	37.70	41.10	34.70	39.90		20.20 18.90	[217]
cis-3,5-Dimethylcyclohexanone	207.90	49.10	33.10	42.70				22.30	[217]
cis-3,4-Dimethylcyclohexanone	209.30	49.10	36.60	33.40	30.60	39.00		16.20 15.90	[217]
trans-3,5-Dimethylcyclohexanone	208.30	48.50	29.50	39.60				20.80	[217]
4,4-Dimethylcyclohexanone	209.10	37.70	39.20	29.90				27.50	[217]

Table 4.32. (Continued).

Compound	C-1	C-2	C-3	C-4	C-5	C-6	C-7	CH_3	Ref.
2-Acetoxycyclohexanone	202.60	76.80	32.90	23.50	26.80	40.30	169.10 (CO, Ac)	20.20	[219]
2-Norbornanone	49.80	215.00	44.90	35.90	27.40	24.00	37.60		[186]
1-Methyl-2-norbornanone	53.30	215.90	45.20	34.40	29.00	31.50	43.90	13.70	[186]
exo-3-Methyl-2-norbornanone	49.30	217.60	47.90	41.60	28.10	23.60	34.10	13.80	[186]
endo-3-Methyl-2-norbornanone	50.10	217.20	48.00	40.60	20.90	25.30	37.00	10.40	[186]
exo-5-Methyl-2-norbornanone	50.40	215.20	45.10	42.00	33.30	34.60	33.90	21.70	[186]
endo-5-Methyl-2-norbornanone	51.10	214.60	38.40	40.60	32.70	33.20	39.00	16.90	[186]
exo-6-Methyl-2-norbornanone	56.40	215.50	43.70	36.10	37.50	31.00	33.90	20.60	[186]
endo-6-Methyl-2-norbornanone	55.80	213.50	45.60	35.80	38.60	32.40	36.00	18.50	[186]
syn-7-Methyl-2-norboranone	54.90	215.60	40.00	39.70	28.80	24.20	43.60	12.60	[186]
anti-7-Methyl-2-norbornanone	54.00	214.80	47.00	39.90	24.60	21.00	42.50	11.80	[186]
Bicyclo[4.1.0]heptan-2-one		206.30							[220]
1-Methylbicyclo[4.1.0]heptan-2-one		207.60							[220]
6-Methylbicyclo[4.1.0]heptan-2-one		205.00							[220]
4,6-Dimethylbicyclo[4.1.0]heptan-2-one		207.00							[220]
1,6-Dimethylbicyclo[4.1.0]heptan-2-one		207.20							[220]
Bicyclo[3.1.0]hexan-2-one		213.40							[220]
1-Methylbicyclo[3.1.0]hexan-2-one		213.40							[220]
5-Methylbicyclo[3.1.0]hexan-2-one		212.10							[220]
1,5-Dimethylbicyclo[3.1.0]hexan-2-one		213.30							[220]
1-Methylspiro[2.5]octan-4-one				207.60					[220]
1,1-Dimethylspiro[2.5]octan-4-one				206.90					[220]
1-Methylspiro[2.4]heptan-4-one				216.40					[220]
1,1-Dimethylspiro[2.4]heptan-4-one				215.10					[220]

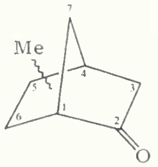

(9) The ^{13}C chemical shifts of α,β-unsaturated ketones allow the differentiation between planar and twisted conjugated systems (Table 4.33) as was outlined in section 3.1.3.8.

Table 4.33. Chemical Shifts of Carbons in α,β-Unsaturated Ketones (Relative to TMS = 0) [221].

Carbon atom	Planar	Nonplanar
Carbonyl	197.5 to 195.0	205.2 to 198.0
C-α	142.5 to 122.5	136.5 to 120.5
C-β	178.5 to 127.5	142.5 to 136.5

Table 4.34. ^{13}C Chemical Shifts of α,β- and β,γ-Unsaturated Ketones (δ Values (ppm) Relative to TMS = 0).

Compound	C=O	C-α	C-β	Ref.
Butenone	198.10	127.70	136.60	[221]
3-Methyl-3-butenone	197.30	124.00	143.30	[221]
3-Penten-2-one	196.20	132.20	142.50	[221]
4-Methyl-3-penten-2-one (mesityl oxide)	195.90	122.70	152.50	[221]
3-Methyl-3-penten-2-one	197.70	138.20	137.70	[221]
3-Ethyl-3-penten-2-one	196.10	143.20	136.20	[221]
3,4-Dimethyl-3-penten-2-one	201.40	130.50	136.20	[221]
3-Hexen-2-one	195.30	129.20	147.50	[221]
3-Methyl-3-hexen-2-one	196.90	135.90	142.00	[221]
3,4-Dimethyl-3-hexen-2-one	201.30	130.00	140.90	[221]
3-Hepten-2-one	195.30	130.60	146.20	[221]
2-Cyclohexenone	196.80	128.10	149.50	[221]
2-Methyl-2-cyclohexenone	197.20	134.60	144.30	[221]
3-Methyl-2-cyclohexenone	196.20	125.30	161.00	[221]
2,3-Dimethyl-2-cyclohexenone	196.10	129.70	153.40	[221]
3,5-Dimethyl-2-cyclohexenone	195.70	124.70	159.70	[221]
3,5,5-Trimethyl-2-cyclohexenone (isophorone)	196.30	124.30	158.20	[221]
3-Methyl-6-isopropyl-2-cyclohexenone (piperitone)	197.60	125.90	159.10	[221]
2-Ethylidenecyclohexanone	197.40	136.90	132.10	[221]
2-Cyclopentenone	207.80	132.60	163.90	[221]
2-Methyl-2-cyclopentenone	207.40	140.60	157.10	[221]
3-Methyl-2-cyclopentenone	207.60	128.90	178.20	[221]
2,3-Dimethyl-2-cyclopentenone	206.00	134.40	167.70	[221]
2-Isopropylidene-2-cyclopentenone	204.30	129.90	144.20	[221]
4-Penten-2-one	204.40			[222]
5-Hexen-3-one	206.40			[222]
3-Methyl-4-penten-2-one	206.40			[222]
4-Hexen-2-one	203.90			[222]
3,3,5-Trimethyl-4-hexen-2-one	209.40			[222]
1-Cyclohexenylacetone	204.10			[222]
3-Cyclopentenone	215.60			[222]
3-Cyclohexenone	207.60			[222]
3,5,5-Trimethyl-3-cyclohexenone	206.60			[222]
Bicyclo[2.2.2]oct-5-en-2-one	212.70			[222]
Bicyclo[2.2.1]hept-5-en-2-one	212.90			[222]
Bicyclo[3.2.1]oct-2-en-8-one	214.50			[222]
Bicyclo[2.2.1]hept-2-en-7-one	203.00			[222]

Table 4.35. ^{13}C Chemical Shifts δ [ppm] of Selected Benzaldehyde Derivatives in Deuteriochloroform as Solvent.

Compound	$-CH=O$	C-1	C-2	C-3	C-4	C-5	C-6	Others	Ref.
Benzaldehyde	192.0	136.7	129.7	129.0	134.3	129.0	129.7		[50k]
, 2-hydroxy-	196.7	120.9	161.6	117.6	136.9	119.9	133.8		[50k]
, 2-nitro-	188.6	131.3	149.5	124.5	134.3*)	134.1*)	129.7		[102]
, 2-amino-	195.2	119.4	151.1	116.7	136.5	116.8	136.0		[102]
, 3-hydroxy-	194.8	139.4	116.5	159.4	123.2	131.4	123.2		[50k]
, 4-hydroxy-	192.0	130.1	133.5	117.4	164.9	117.4	133.5		[50k]
, 4-methoxy-	190.4	130.3	131.9	114.5	164.7	114.5	131.9	55.4 (OCH_3)	[102]
, 4-nitro-	190.4	140.3	130.6	124.4	151.4	124.4	130.6		[50k]
, 4-dimethylamino-	191.0	126.3	133.0	112.5	155.6	112.5	133.0	40.9 ($N(CH_3)_2$)	[50k]
, 4-cyano-	190.8	138.9	129.9	133.0	117.7	133.0	129.9	110.9 (CN)	[50k]
, 4-bromo-	190.9	135.2	130.9	132.4	129.7	132.4	130.9		[50k]
, 4-trimethylsilyl-	192.3	136.6	128.7	133.8	149.0	133.8	128.7	1.4 ($Si(CH_3)_3$)	[50k]
, 2-hydroxy-3-methoxy-	196.6	121.0	148.4	151.4	118.3	119.6	124.6	56.3 (OCH_3)	[50k]
, 4-hydroxy-3-methoxy-	192.4	130.5	110.1	148.4	153.2	115.5	128.3	56.5 (OCH_3)	[50i]
, 3,4-dimethoxy-	190.7	130.3	110.7	149.8	154.6	109.4	126.5	56.0 (OCH_3) 56.1 (OCH_3)	[50k]
, 3,4-methylenedioxy-	190.0	132.1	108.4	148.8	153.2	107.0	128.4	102.2 ($O-CH_2-O$)	[50k]

*) Assignments interchangeable.

Table 4.36. ^{13}C Chemical Shifts of Arylalkylketones (δ Values (ppm) Relative to TMS = 0) [223, 224].

Compound	$R-\underset{\vert}{C}=O$					Aromatic nuclei						Others
	C=O	C–	CH–	CH_2	CH_3	C-1	C-2	C-3	C-4	C-5	C-6	
Acetophenone	195.70				24.60	136.30	128.10	128.10	131.30	128.10	128.10	
p-Methylacetophenone	195.70				25.60	133.40	128.20	128.20	142.70	128.20	128.20	20.90
p-Ethylacetophenone	195.70				25.20	132.90	127.60	127.60	148.60	127.60	127.60	14.60 27.90
p-Isopropylacetophenone	195.90				25.10	135.10	127.80	126.10	153.70	126.10	127.80	22.60 33.50
p-*t*-Butylacetophenone	194.90				25.40	133.00	127.30	124.20	154.70	124.20	127.30	30.10 34.20
p-Methoxyacetophenone	195.40				25.20	129.50	129.80	113.00	162.80	113.00	129.80	54.60
p-Chloroacetophenone	195.50				24.50	134.30	128.80	128.80	137.90	128.80	128.80	
p-Bromoacetophenone	196.30				26.20	134.40	130.50	130.50	126.30	130.50	130.50	
p-Nitroacetophenone	195.80				26.60	140.80	129.00	123.80	150.10	123.80	129.00	
p-N-Dimethylaminoacetophenone	195.10				25.00	124.80	129.90	109.80	152.70	109.80	129.90	39.00
p-Hydroxyacetophenone	197.10				24.80	129.60	130.90	115.20	161.80	115.20	130.90	
m-Methylacetophenone	195.20				24.80	136.60	127.00	136.60	132.20	127.00	124.20	20.20
m-Methoxyacetophenone	195.80				25.20	137.40	111.40	158.50	118.50	128.40	118.50	54.00
m-Chloroacetophenone	195.10				25.50	137.70	128.80	133.80	132.20	128.80	126.50	
m-Bromoacetophenone	195.10				25.80	137.50	129.60	121.30	135.20	129.60	126.50	
m-Nitroacetophenone	195.30											
m-Hydroxyacetophenone	197.40					138.60	113.90	157.40	129.90	119.60		
o-Methylacetophenone	199.00				28.30	136.40	136.40	128.50	130.10	124.80	130.10	20.00
o-Ethylacetophenone	199.40				28.20	135.50	142.70		130.00	123.80	130.00	26.00 14.90
o-Isopropylacetophenone	200.50				28.20	137.40	145.90	124.40	129.50	124.40	126.20	28.10 22.50
o-Phenylacetophenone	202.10				29.50							
o-Methoxyacetophenone	197.50				30.70	127.40	158.20	111.10	132.80	119.40	129.30	54.30
o-Ethoxyacetophenone	198.40				31.60	128.00	158.20	112.30	133.30	119.80	130.30	
o-Chloroacetophenone	198.40				29.20	136.80	131.30	126.20	129.90	126.20	126.20	
o-Bromoacetophenone	199.00				29.40	139.90	122.00	131.50	131.50	127.40	127.40	
o-Iodoacetophenone	200.50				28.70	145.10	90.30	138.10	131.40	128.00	128.00	
o-Nitroacetophenone	198.00				28.10	135.40	144.70	122.50	129.80	133.00	126.30	

Table 4.36. (Continued).

Compound	$\mathrm{R{-}\underset{\vert}{C}{=}O}$					Aromatic nuclei						Others
	C=O	C	CH	CH_2	CH_3	C-1	C-2	C-3	C-4	C-5	C-6	
o-Hydroxyacetophenone	204.10				25.40	118.90	161.50	118.30	135.50	118.30	129.70	
o-Aminoacetophenone	200.00				26.80	117.20	149.80	114.70	133.30	116.80	131.40	
2,3-Dimethylacetophenone	200.30				28.80	139.10	134.00	136.70	131.30	123.90	123.90	19.50 15.30
2,4-Dimethylacetophenone	198.30				27.60	140.50	133.80	129.40	137.30	124.90	129.40	19.50 19.50
2,5-Dimethylacetophenone	198.20				28.10	135.40	133.30	128.30	128.30	133.30	128.30	19.70 19.70
2,4,5-Trimethylacetophenone	198.00				27.80	132.90	134.60	130.70	138.60	134.60	132.30	18.00
2,5-Di-*t*-butylacetophenone	207.80				30.90							35.00 30.90
2,4-Dimethoxyacetophenone	195.30				30.70	119.80	160.20	96.80	163.30	104.50	131.20	54.60 54.60
2,5-Dimethoxyacetophenone	197.00				30.30	127.20	152.40	112.60	118.40	152.40	112.60	54.20 54.20
2,4-Dichloroacetophenone	196.40				29.60	131.70	135.70	129.40	135.70	126.40	129.40	
2,4-Dihydroxyacetophenone	202.60				23.60	113.90	165.10	103.50	165.10	108.60	133.90	
2,6-Dimethylacetophenone	205.40				30.50	141.70	131.50	126.90	126.90	126.90	131.50	17.70
2,4,6-Trimethylacetophenone	205.90				30.80	139.40	131.70	128.10	137.10	128.10	131.70	18.50
2,3,4,6-Tetramethylacetophenone	206.00				30.80	134.60	132.60	140.20	140.20		132.60	18.90 23.20
2,3,5,6-Tetramethylacetophenone	206.70				33.10	144.20	127.70	133.90	131.70	133.90	127.70	16.50 20.40
2,3,4,5,6-Pentamethylacetophenone	206.60				34.40	142.10	127.40	133.30	133.30	133.30	127.40	18.10
4-*t*-Butyl-2,6-dimethylacetophenone	205.80				32.50	140.40	132.00	125.50	150.90	125.50	132.00	34.30 17.80
2,6-Diethylacetophenone	205.50				31.00	141.40	137.70	125.30	128.10	125.30	137.70	25.40 15.10
2,6-Diisopropylacetophenone	206.00				31.70	141.20	143.00	123.20	129.20	123.20	143.00	34.00 25.70
2,4,6-Triisopropylacetophenone	206.30				31.70	138.80	142.70	120.10	148.60	120.10	142.70	32.90 23.60

Table 4.36. (Continued).

Compound	$R-\overset{}{\underset{\vert}{C}}=O$					Aromatic nuclei						Others
	C=O	C	CH	CH_2	CH_3	C-1	C-2	C-3	C-4	C-5	C-6	
2,6-Dimethoxyacetophenone	199.30				31.30	141.20	156.30	104.10	131.10	104.10	156.30	55.20
2,6-Dichloroacetophenone	197.70				29.90	139.40	129.10	128.00	129.80	128.00	129.10	
2,4,6-Tribromoacetophenone	199.70				30.10	142.00	118.50	134.00	123.30	134.00	118.50	
2,6-Dihydroxyacetophenone	204.50				31.90	108.00	161.40	106.50	134.50	106.50	161.40	
2-Hydroxy-6-methoxyacetophenone	204.40				33.20	110.70	164.00	109.90	135.80	100.90	160.80	55.20
2,4,6-Trihydroxyacetophenone	202.90				32.10	104.00	165.10	94.50	165.10	94.50	165.10	
Propiophenone	198.10			30.30	6.70	136.00	126.90	126.90	130.80	126.90	126.90	
4-Methoxypropiophenone	197.20			30.20	7.10	129.20	129.10	112.60	162.30	112.60	129.10	54.40
2-Methylpropiophenone	202.20			33.20	7.40	136.50	136.50	130.60	128.00	125.00	130.60	20.40
2,4,6-Trimethylpropiophenone	207.50			36.30	7.20	138.80	131.00	127.20	136.30	127.20	131.00	18.90 17.10
2,3,5,6-Tetramethylpropiophenone	209.20			38.10		143.30	127.60	133.80	130.60	133.80	127.60	19.10 15.80
2,3,4,5,6-Pentamethylpropiophenone	209.40			37.80		141.40	127.20	133.30	133.30	133.30	127.20	17.40
2,4,6-Triisopropylpropiophenone	208.80			39.40		138.70	143.50	121.20	148.90	121.20	143.50	32.50 24.10 15.70
Isobutyrophenone	202.80		34.60		18.10	135.80	127.90	127.90	132.40	127.90	127.90	
4-Methoxyisobutyrophenone	201.00		34.30		18.80	128.20	129.60	112.90	162.40	112.90	129.60	54.40
2-Methylisobutyrophenone	206.40		37.30		17.90	136.40	136.40	130.70	127.40	125.50	130.70	19.90
2,4,6-Trimethylisobutyrophenone	210.70		41.10		17.60	139.10	132.30	127.80	136.80	127.80	132.30	19.30
2,3,5,6-Tetramethylisobutyrophenone	212.30		44.50		17.50	143.10	129.40	134.90	132.40	134.90	129.40	20.10
2,3,4,5,6-Pentamethylisobutyrophenone	212.60		43.50		18.00	140.20	128.10	132.70	132.70	132.70	128.10	18.00
2,4,6-Triisopropylisobutyrophenone	212.00		42.60		16.80	137.80	144.30	121.10	149.00	121.10	144.30	16.80
Pivalophenone	206.90	43.50			27.90	137.80	127.30	127.30	130.10	127.30	127.30	
4-Methoxypivalophenone	203.50	42.80			27.70	128.90	130.00	112.40	161.00	112.40	130.00	54.30
2-Methylpivalophenone	211.70	43.90			26.50	140.20	133.40	127.20	129.70	124.30	127.20	18.20
5-Methoxy-2-methylpivalophenone	211.70	44.30			27.90	129.90	132.10	127.40	111.20	153.20	111.20	55.80
4-Methoxy-2-methylpivalophenone	211.30	44.10			27.40	139.80	131.80	116.10	155.20	111.90	126.50	54.70
2,4,6-Trimethylpivalophenone	215.50	43.30			27.50	138.60	130.70	127.60	135.80	127.60	130.70	19.30
2,3,4,6-Tetramethylpivalophenone	215.40	43.30			26.80	157.50	128.20	130.30	130.30	127.80	133.30	13.90

Table 4.37. ^{13}C Chemical Shifts of *o*- and *p*-Benzoquinones (δ Values (ppm) Relative to TMS = 0) [226].

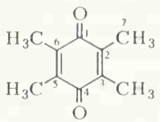
Duroquinone

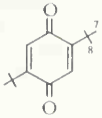
2,5-Di-*t*-butyl-*p*-benzoquinone

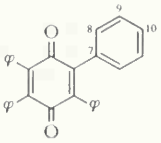
2,3,5,6-Tetraphenyl-*p*-benzoquinone

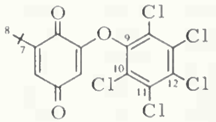
2-Pentachlorophenoxy-6-*t*-butyl-*p*-benzoquinone

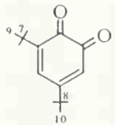
4,6-Di-*t*-butyl-*o*-benzoquinone

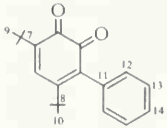
3-Phenyl-4,6-di-*t*-butyl-*o*-benzoquinone

Compound	C-1	C-2	C-3	C-4	C-5	C-6	C-7	C-8	C-9	C-10	Solvent
p-Benzoquinone	187.0	136.4									$CDCl_3$
Duroquinone	187.4	140.4					12.4				$CDCl_3$
2,6-Dimethyl-*p*-benzoquinone	187.6	145.8	133.8	188.3			15.8				$CDCl_3$
2-Methyl-*p*-benzoquinone	187.5	145.9	133.3	187.7	136.6	136.5	15.8				$CDCl_3$
2,6-Di-*t*-butyl-*p*-benzoquinone	187.7	157.7	130.1	188.6			35.5	29.3			$CDCl_3$
2,5-Di-*t*-butyl-*p*-benzoquinone	188.2	154.2	133.5				34.5	29.0			$CDCl_3$
2,6-Diisopropyl-*p*-benzoquinone	186.8	155.3	129.8	188.6			27.0	21.5			$CDCl_3$
2,3,5,6-Tetraphenyl-*p*-benzoquinone	186.9	143.3					132.9	130.9	128.4	127.7	$CDCl_3$
2,6-Diphenyl-*p*-benzoquinone	186.0	146.4	132.5	187.5			133.1	129.9	129.4	128.3	$CDCl_3$
2,5-Diphenyl-*p*-benzoquinone	187.0	145.7	132.6				133.2	129.5	130.1	128.6	$CDCl_3$
2-Chloro-*p*-benzoquinone	179.2	144.1	133.7	184.9	136.8	136.0					$CDCl_3$
2,5-Dichloro-*p*-benzoquinone	176.7	143.8	132.8								C_2H_5OH
2,3,5,6-Tetrachloro-*p*-benzoquinone	169.4	139.4									DMSO-d_6
3,5-Dichloro-2,6-dimethyl-*p*-benzoquinone	182.5	142.7	139.9	172.3			13.4				$CDCl_3$
2,3-Dichloro-5,6-dicyano-*p*-benzoquinone	170.1	142.1	142.1	170.1	132.9	132.9	124.8				CD_3OD
2,6-Diaziridino-*p*-benzoquinone	180.0	154.8	117.2	187.2			27.4				$CDCl_3$
6-*t*-Butyl-2-pentachlorophenoxy-*p*-benzoquinone	179.5	155.0	109.8	186.9	131.9	154.5	35.5	29.1	145.3		$CDCl_3$
o-Benzoquinone	180.2		140.0	130.4							$CDCl_3$
4,6-Di-*t*-butyl-*o*-benzoquinone	179.6	180.6	121.6	149.4	133.1	162.8	35.6	35.6	28.8	27.4	$CDCl_3$
3-Chloro-4,6-di-*t*-butyl-*o*-benzoquinone	178.1	174.8	129.3	147.4	135.9	155.1	37.5	35.5	29.0	28.6	$CDCl_3$
3-Bromo-4,6-di-*t*-butyl-*o*-benzoquinone	178.2	175.0	122.0	147.5	136.3	158.4	38.3	35.5	29.0	28.8	$CDCl_3$
3-Phenyl-4,6-di-*t*-butyl-*o*-benzoquinone	179.0	182.5	135.6	147.9	137.5	155.7	37.5	35.5	29.0	28.6	$CDCl_3$
3-Nitro-4,6-di-*t*-butyl-*o*-benzoquinone	175.3	171.8	143.3	149.6	133.1	150.9	37.6	35.9	28.8	27.2	$CDCl_3$
3,4,5,6-Tetrachloro-*o*-benzoquinone	168.8		143.8	131.9							$CDCl_3$

Homoconjugative interactions in β,γ-unsaturated ketones [222] have been postulated as the reason for the increased shielding of the carbonyl carbons in these systems [222] (see Table 4.34). An aromatic ring in conjugation with a carbonyl group leads to greater shielding of the carbonyl C atom [223, 224]. In arylalkylketones, *ortho* substitution generally causes large downfield shifts for the CO resonance. This deshielding effect has been attributed to a steric hindrance of the coplanarity between the alkylcarbonyl group and the benzene ring [223, 224]. ^{13}C chemical shifts of selected benzaldehyde derivatives and arylalkylketones are listed in Tables 4.35 and 4.36.

4.7.2. Quinones

Systematic PFT ^{13}C NMR investigations on quinones have lead to the following general conclusions [226]:

(1) The carbonyl resonances occur in the ppm range of 170 to 190 ppm.
(2) Substitution of ring protons by chlorine shifts the carbonyl resonances to higher field.
(3) The carbonyl signals of *o*-quinones appear at higher field than those of corresponding *p*-isomers.
(4) A correlation of average shift values $\frac{1}{6}\sum_{i=1}^{6}\delta_i$ with polarographic half-wave potentials and with ^{1}H NMR chemical shifts of quinones demonstrated that most values can be fitted to a linear regression plot. However, for a larger series of quinones larger deviations are observed. The ^{13}C chemical shifts of several selected quinones are listed in Table 4.37.

4.7.3. Carboxylic Acids

The carbonyl carbons of carboxyl groups are usually more shielded than those of ketones and aldehydes (see Tables 4.32 and 4.36). Upon ionization of the carboxyl group, the resonances of COOH and neighbouring carbon atoms shift several ppm downfield. Substitution parameters have been calculated for selected simple aliphatic carboxylic acids and their anions. Subtracting the ^{13}C chemical shift parameters of carbons in alkanes from the corresponding parameters of carboxylic acids yields the increments of Table 4.38 [227].

Table 4.38. ^{13}C Chemical Shift Substitution Parameters of Selected Carboxylic Acids and Carboxylate Groups in ppm [227].

Compound	C-α	C-β	C-γ	C-δ
Acetic acid	23.5			
Propionic acid	22.2	3.4		
Butyric acid	21.0	2.7	−2.0	
Valeric acid	21.2	2.3	−2.7	0.6
Acetate ion	26.3			
Propionate ion	25.7	5.2		
Butyrate ion	24.9	4.1	−1.4	
Valerate ion	25.1	4.0	−2.1	0.8

As can be seen in Table 4.38, the α-, β- and δ carbons of a hydrocarbon chain are deshielded upon substitution by a carboxyl group, while γ carbons are shielded because of steric interactions (γ effect). A similar pattern was observed for alkyl halides (Table 3.2) and will be outlined for many other substituents in section 4.13.

Large solvent effects (up to 2 ppm) are observed for acrylic acid, if the ^{13}C shifts of a neat liquid sample are compared with values obtained from measurements in 50 percent aqueous or dimethyl sulfoxide solution [228].

Table 4.39. Substitution Increments Z_i for Calculation of the Chemical Shifts of α,β-Unsaturated Acids (see eqs. (4.11) and (4.12)) [228].

Substituent R	Z_i^β			Z_i^α		
	gem	*cis*	*trans*	*gem*	*cis*	*trans*
H	0	0	0	0	0	0
Cl	−8	−1	4	2	−6	4
Br	−8	−13	−1	−8	−5	1
I	−9	−39	−35	−38	2	11
CH_3	−6	12	10	7	−6	−4
n-C_2,C_3	−6	21	19	16	−9	−8
α-Branched C_3,C_4	−6	26	24	24	−10	−9
CH_2OH	−4			18		
CH_2Br	6			13		
CHO		22			−4	
COOH		−2	2		2	6

The ^{13}C chemical shift values for the α- and β-carbons in α,β-unsaturated carboxylic acids can be calculated using the eqs. (4.10) and (4.11) [228]:

$$\delta_\alpha = \left(128.5 \quad \sum_i Z_i^\alpha\right) \tag{4.10}$$

$$\delta_\beta = +\left(132.5 + \sum_i Z_i^\beta\right) \tag{4.11}$$

$\sum_i Z_i$ = sum of increments for the substituents R_{gem}, R_{cis} and R_{trans};

Z_i^α, Z_i^β = increments (see Table 4.39);

R_{gem}, R_{cis}, R_{trans} = substituents at the olefinic carbons (configuration relative to the carboxyl group):

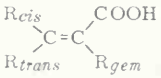

Deviations between calculated and experimental values usually are smaller than 4 ppm [228]. Different shieldings may be attributed partly to different molecular ground states and partly to differences in the excited states of α,β-unsaturated acids [228].

The chemical shifts of selected carboxylic acids and derivates are listed in Tables 4.40 and 4.41.

Table 4.40. ^{13}C Chemical Shifts of Carboxylic Acids (δ Values (ppm) Relative to TMS = 0).

Compound	COOH	α	β	γ	δ	Others	Solvent	Ref.
Formic acid	166.0						H_2O	[227]
Acetic acid	176.9	20.8					H_2O	[227]
Propionic acid	180.1	27.5	8.7				H_2O	[227]
Butyric acid	179.3	36.0	18.2	13.1			H_2O	[227]
Valeric acid	179.4	33.8	26.7	21.7	13.2		H_2O	[227]
Tetramethylammonium formate	171.1						H_2O	[227]
Tetramethylammonium acetate	181.4	23.7					H_2O	[227]
Tetramethylammonium propionate	184.8	31.0	10.5				H_2O	[227]
Tetramethylammonium butyrate	184.0	39.9	19.6	13.6			H_2O	[227]
Tetramethylammonium valerate	184.1	37.7	28.4	22.3	13.4		H_2O	[227]
Acrylic acid	170.4	127.2	131.9				neat	[228]
Methacrylic acid	171.9	135.2	126.3 16.5				neat	[228]
3,3-Dimethylacrylic acid	169.0	115.6	156.9	19.1 26.1			neat	[228]
Tiglic acid	168.9	128.4	136.3 11.5	13.5			neat	[228]
(*Z*)-2-Butenoic acid		120.7	148.0				neat	[228]
(*E*)-2-Butenoic acid		121.7	146.4				neat	[228]
(*Z*)-2-Pentenoic acid	171.5	118.5	154.0	22.30	12.70		neat	[228]
(*E*)-2-Pentenoic acid	171.9	119.5	152.5	24.6	11.1		neat	[228]
(*Z*)-2-Hexenoic acid	171.5	118.7	152.0	30.4	21.5	12.6 (ε)	neat	[228]
(*E*)-2-Hexenoic acid	171.8	120.5	151.3	33.9	20.8	13.0 (ε)	neat	[228]
(*Z*)-4-Methyl-2-pentenoic acid	171.4	116.4	158.3	27.0	21.2		neat	[228]
(*E*)-4-Methyl-2-pentenoic acid	171.6	117.7	157.0	30.4	20.2		neat	[228]
(*Z*)-2-Heptenoic acid	171.5	118.8	152.3	28.3	30.7	21.8 (ε) 13.0 (ζ)	neat	[228]
(*E*)-2-Heptenoic acid	171.7	120.5	151.5				neat	[228]
(*E*)-4,4-Dimethyl-2-pentenoic acid	168.1	117.5	158.2	33.3	28.5		DMSO	[228]
(*Z*)-2-Octenoic acid	173.1	120.1	153.6	29.7	29.7	32.3 (ε) 23.3 (ζ) 14.5 (η)	neat	[228]
(*E*)-2-Nonenoic acid	171.5	120.7	151.1	31.9	27.8	28.5 (ε) 31.5 (ζ) 22.1 (η) 13.4 (θ)	neat	[228]

Table 4.40. (Continued).

Compound	COOH	α	β	γ	δ	Others	Solvent	Ref.
(*E*)-2-Bromo-3-*t*-butylacrylic acid	164.9	114.7	154.0				DMSO	[228]
(*Z*)-3-Chloroacrylic acid	164.7	122.2	131.6				DMSO	[228]
(*E*)-3-Chloroacrylic acid	164.7	125.0	136.3				DMSO	[228]
(*Z*)-3-Bromoacrylic acid	165.1	120.6	124.9				DMSO	[228]
(*E*)-3-Bromoacrylic acid	165.1	130.0	126.4				DMSO	[228]
(*Z*)-3-Iodoacrylic acid	165.7	130.3	95.9				DMSO	[228]
(*E*)-3-Iodoacrylic acid	165.1	137.4	100.9				DMSO	[228]
(*Z*)-2,3-Dichloroacrylic acid	161.5	128.1	131.4				DMSO	[228]
(*Z*)-2,3-Dibromoacrylic acid	161.8	124.2	126.9				DMSO	[228]
(*E*)-2,3-Dibromoacrylic acid	162.7	113.1	110.7				DMSO	[228]
(*E*)-2,3-Diiodoacrylic acid	165.9	89.1	86.5				DMSO	[228]
(*E*)-3-Chloro-2-iodoacrylic acid	164.5	87.4	126.2				DMSO	[228]
(*Z*)-2-Bromo-3-iodoacrylic acid	164.6	134.7	70.2				DMSO	[228]
3,3-Dichloroacrylic acid	163.0	121.5	135.0				DMSO	[228]
3,3-Dibromoacrylic acid	164.0	129.7	103.8				DMSO	[228]
3,3-Dibromomethacrylic acid	167.5	137.7	92.4				DMSO	[228]
			21.6					
3,3-Dibromo-2-ethylacrylic acid	167.4	143.4	90.5				DMSO	[228]
3,3-Dibromo-2-propylacrylic acid	168.4	143.4	91.7				DMSO	[228]
3,3-Dibromo-2-isopropylacrylic acid	167.6	148.6	88.2				DMSO	[228]
3,3-Dibromo-2-hydroxymethylacrylic acid	166.6	142.8	92.2				DMSO	[228]
			63.4					
3,3-Dibromo-2-bromomethylacrylic acid	165.3	137.4	103.0				DMSO	[228]
			32.5					
3,3-Diiodoacrylic acid	165.6	141.5	32.3				DMSO	[228]
2,3,3-Trichloroacrylic acid	161.0	123.1	124.8				DMSO	[228]
2,3,3-Triiodoacrylic acid	168.6	105.6	28.6				DMSO	[228]
(*E*)-3-Chloromethacrylic acid	167.1	131.3	131.3				DMSO	[228]
			12.2					
(*Z*)-3-Bromomethacrylic acid	166.5	133.6	107.5				DMSO	[228]
			19.2					
(*E*)-3-Bromomethacrylic acid	165.6	133.7	121.8				DMSO	[228]
			14.6					
(*E*)-2-Bromocrotonic acid	162.1	114.6	140.6	16.4			DMSO	[228]

Table 4.40. (Continued).

Compound	COOH	α	β	γ	δ	Others	Solvent	Ref.
2-Bromo-3-methylcrotonic acid	165.1	109.7	146.5	22.5 26.6			DMSO	[228]
(*Z*)-3-Chlorocrotonic acid	165.1	117.6	145.1	27.8			DMSO	[228]
(*E*)-3-Chlorocrotonic acid	166.1	119.8	152.0	23.0			DMSO	[228]
(*Z*)-2,3-Dichlorocrotonic acid	162.3	121.0	144.3	23.8			DMSO	[228]
(*E*)-2,3-Dichlorocrotonic acid	162.5	119.6	133.2	24.6			DMSO	[228]
(*Z*)-2,3-Dibromocrotonic acid	163.6	115.3	137.5	27.5			DMSO	[228]
(*E*)-2,3-Dibromocrotonic acid	164.8	109.2	119.8	27.8			DMSO	[228]
(*E*)-2,3-Diiodocrotonic acid	167.2	88.0	95.2	37.8			DMSO	[228]
Maleic acid	167.1 167.1	130.5	130.5					[228]
Fumaric acid	166.6 166.6	134.2	134.2					[228]
Bromocitraconic acid	166.4 164.6	138.2	121.5			20.1		[228]
Bromocitraconic anhydride	163.7 160.8	145.7	125.9			11.1		[228]
Mesaconic acid	168.2 167.0	126.8	142.8			13.7		[228]
Bromomesaconic acid	169.0 164.5	141.3	109.9			18.3		[228]
(*Z*)-Mucochloric acid	163.3	122.2	149.7			97.1		[228]
(*Z*)-Mucobromic acid	164.6	117.0	147.0			99.7		[228]
(*Z*)-Cinnamic acid	172.9	117.5	147.1			134.2 (C-1) 128.5 (C-2,6) 129.0 (C-3,5) 130.8 (C-4)	$CDCl_3$	[50k]

Table 4.41. ^{13}C Chemical Shifts of Substituted Methyl Benzoates (δ Values (ppm) Relative to TMS = 0) [229]

Compound	CH_3O	$\rangle C{=}O$	C-1	C-2	C-3	C-4	C-5	C-6	Solvent
Methyl benzoate	51.0	165.6	129.7	127.9	127.9	131.9	127.9	127.9	neat
Methyl 4-methylbenzoate	50.2	165.0	126.4	128.1	128.1	141.9	128.1	128.1	neat
Methyl 4-methoxybenzoate	50.9	165.3	122.0	130.6	113.1	162.5	113.1	130.6	neat
Methyl 4-dimethylaminobenzoate		166.5	116.1	131.0	110.5	153.1	110.5	131.0	$CHCl_3$
Methyl 4-nitrobenzoate	53.0	164.9	135.8	130.4	123.3	149.9	123.3	130.4	$CHCl_3$
Methyl 3-methylbenzoate	50.4	165.3	129.8	126.9	136.9	130.5	126.9	125.3	neat
Methyl 2-methylbenzoate	50.4	166.0	128.7	135.7	130.5	133.9	124.0	130.5	neat
Methyl 2,3-dimethylbenzoate	50.3	166.8	129.6	136.7	136.7	132.1	126.8	133.9	neat
Methyl 2,6-dimethylbenzoate	50.4	168.9	133.3	133.3	126.5	128.2	126.5	133.3	neat
Methyl 2,4,6-trimethylbenzoate	50.1	168.5	130.4	134.1	127.5	137.8	127.5	134.1	neat
Methyl 2,6-diethylbenzoate	49.9	168.7	133.7	140.2	125.2	128.6	125.2	140.2	neat
Methyl 2-nitrobenzoate	52.0	164.1	125.9	146.8	122.6	131.4	131.4	128.7	neat
Methyl 2-chlorobenzoate	51.5	164.6	129.5	136.1	126.1	130.7	126.1	126.1	neat
Methyl 2-bromobenzoate	51.9	165.1	131.7	121.0	131.4	133.3	126.3	126.3	neat
Methyl 2-iodobenzoate	52.4	165.6	134.5	94.1	141.3	132.1	127.5	130.5	neat
Methyl 2,6-dichlorobenzoate	52.0	163.7	130.8	132.6	126.6	130.2	126.6	132.6	neat
Methyl 2,4,6-tribromobenzoate	53.3	165.3	136.6	120.3	133.4	123.7	133.4	120.3	$CHCl_3$
Methyl 2,4,6-trinitrobenzoate		161.5	129.7	144.9	124.2	144.9	124.2	144.9	Dioxane

4.8. Aliphatic Organonitrogen Compounds

4.8.1. Amines

An amino group deshields at the α and β carbon and shields in γ position while no significant influence is observed for more removed carbons (Table 4.42). The pH dependence of carbon shielding in amines was pointed out in section 3.1.4.3, and the large protonation shift at the β carbon was attributed to the intramolecular field originating from the charged group.
The ^{13}C chemical shifts of aliphatic amines listed in Table 4.43 illustrate that increasing alkylation causes a deshielding α to nitrogen (ca. 7.7 ppm in going from primary to secondary and ca. 4.7 ppm in going from secondary to tertiary amines). The β carbons, however, are shielded upon alkylation (ca. -3.7 ppm from primary to secondary, and ca. -2.7 ppm from secondary to tertiary amines) because of steric polarization of the C–H bonds. Practically no influence (smaller than 0.5 ppm) is found for the carbons γ to nitrogen.

Table 4.42. Substituent Parameters of NH_2 and NH_3^+ Groups in Alkanes [74].

	α	β	γ	δ
NH_2	28.3	11.3	-5.1	≤ 0.5
NH_3^+	26.0	7.5	-4.6	0.0

The largest chemical shift differences between corresponding resonances of *exo*- and *endo*-2-aminonorbornane are observed for the signals of C-6 and C-7. This has been attributed to steric interaction between the amino group and the hydrogen atoms in γ position. Due to larger steric crowding at C-6, this carbon resonates at higher field in *endo*-2-aminonorbornane than in the *exo* isomer. The same effect is presumably responsible for the upfield shift of the resonance of C-7 in 2-aminonorbornanes, observed on changing the configuration of the amino group from *endo* to *exo* [186].

4.8.2. Alkylcyanides, Isocyanides, Isocyanates and Isothiocyanates

A study on representative alkylcyanides, isocyanides, isocyanates and isothiocyanates demonstrates that the carbons of $-CN$, $-NC$, $-NCO$ and $-NCS$ groups resonate in the range of 170 to 110 ppm [54a]. The signals of carbon monoxide, the cyanide ion and alkyl isocyanide groups appear in a relatively small range (181 to 155 ppm); this fact has been explained in terms of closely related resonance hybrids for these different molecules [54a]:

$$ {}^{\ominus}\!:\!C \equiv O\!:^{\oplus} \leftrightarrow {}^{\oplus}\!:\!C - \underset{\cdot\cdot}{\ddot{O}}\!:^{\ominus} \leftrightarrow :C = \ddot{O}: \leftrightarrow :C = \underset{\cdot\cdot}{O}: $$

$$ {}^{\ominus}\!:\!C \equiv N^{\oplus}\!- R \leftrightarrow {}^{\oplus}\!:\!C - \underset{\cdot\cdot}{\ddot{N}}^{\ominus}\!- R \leftrightarrow :C = \ddot{N} - R \leftrightarrow :C = \underset{\cdot\cdot}{N} - R\,. $$

The carbon atoms of carbon dioxide, alkyl cyanide, isocyanate and isothiocyanate groups resonate at much higher field and also in a relatively small range (138 to 116 ppm) which again may be explained by the similar cannonical structures of these molecules [54a]:

Table 4.43. ^{13}C Chemical Shifts δ [ppm] of Aliphatic Amines in Hexadeuteriobenzene as Solvent, Data from Ref. [229] if not otherwise indicated.

-amine	C-1	C-2	C-3	C-4	C-5	C-6	C-7	C-8	C-9	C-10
Methyl-	28.3									
Ethyl-	36.9	19.0								
Propyl-	44.6	27.4	11.5							
Isopropyl-	42.95	26.45								
Butyl-	42.3	36.75	20.45	14.15						
sec-Butyl-	48.8	33.4(2) 23.95(2′)	10.8							
Isobutyl-	50.6	32.05	20.2							
t-Butyl-	47.2	32.85								
Pentyl-	42.65	34.3	29.7	23.1	14.3					
1-Methylbutyl-	46.85	42.8(2) 24.0(2′)	19.85	14.3						
2-Methylbutyl-	48.35	38.5	27.2(3) 17.2(3′)	11.55						
3-Methylbutyl-	40.6	43.7	25.9	22.9						
2,2-Dimethylpropyl-	54.45	32.1	27.0							
Hexyl-	42.65	34.6	27.1	32.35	23.15	14.2				
Heptyl-	42.55	34.45	27.35	29.7	32.35	23.05	14.2			
Octyl-	42.55	34.45	27.4	30.0	29.85	32.35	23.1	14.2		
Nonyl-	42.6	34.55	27.4	30.15	30.15	29.3	32.4	23.1	14.25	
Decyl-	42.6	34.55	27.4	30.1	30.1	30.1	29.8	32.35	23.05	14.25
Diethyl-	44.45	15.7								
Dipropyl-	52.35	23.95	12.0							
Dibutyl-	50.1	33.1	20.9	14.2						
Dipentyl-	50.45	30.6	30.1	23.1	14.25					
Dihexyl-	50.4	30.35	27.55	32.35	23.1	14.2				
Trimethyl-	47.55									
Triethyl-	51.4	12.85								
Tripropyl-	56.75	21.25	12.0							
Tributyl-	54.3	30.3	20.95	14.25						
Tripentyl-	54.5	27.65	30.05	23.0	14.25					
Trihexyl-	54.55	27.95	27.5	32.25	23.05	14.2				
exo-2-Aminonorbornane	45.4	55.1	42.2	36.1	28.6	26.7	34.0			(Ref. [186])
endo-2-Aminonorbornane	43.3	53.1	40.3	37.7	30.4	20.3	38.7			(Ref. [186])

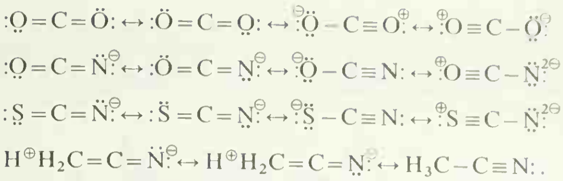

$$:\underset{..}{O}=C=\ddot{O}: \leftrightarrow :\ddot{O}=C=\underset{..}{O}: \leftrightarrow {}^{\ominus}:\underset{..}{\ddot{O}}-C\equiv O:^{\oplus} \leftrightarrow {}^{\oplus}:O\equiv C-\underset{..}{\ddot{O}}:^{\ominus}$$

$$:\underset{..}{O}=C=\ddot{N}:^{\ominus} \leftrightarrow :\ddot{O}=C=\underset{..}{N}:^{\ominus} \leftrightarrow {}^{\ominus}:\underset{..}{\ddot{O}}-C\equiv N: \leftrightarrow {}^{\oplus}:O\equiv C-\underset{..}{\ddot{N}}:^{2\ominus}$$

$$:\underset{..}{S}=C=\ddot{N}:^{\ominus} \leftrightarrow :\ddot{S}=C=\underset{..}{N}:^{\ominus} \leftrightarrow {}^{\ominus}:\underset{..}{\ddot{S}}-C\equiv N: \leftrightarrow {}^{\oplus}:S\equiv C-\underset{..}{\ddot{N}}:^{2\ominus}$$

$$H^{\oplus}H_2C=C=\ddot{N}:^{\ominus} \leftrightarrow H^{\oplus}H_2C=C=\underset{..}{N}:^{\ominus} \leftrightarrow H_3C-C\equiv N:.$$

Table 4.44. $^{13}C-{}^{14}N$ Spin Coupling Constants in $C\equiv N$ Bonds in Hz (Values in Paratheses were Obtained by INDO Calculations) [231]

Molecule	Coupled nuclei	$J_{^{13}C-^{14}N}$
$C^aH_3C^bH_2NC^c$	$^{14}N-{}^{13}C_c$	$\pm 5.2 \pm 0.3$
	$^{13}C_b-{}^{14}N$	$\pm 7.3 \pm 0.3$
	$^{13}C_a-{}^{14}N$	<1
$(C^aH_3)_3C^bNC^c$	$^{14}N-{}^{13}C_c$	$\pm 5.1 \pm 0.3$
	$^{13}C_b-{}^{14}N$	$\pm 6.7 \pm 0.3$
	$^{13}C_a-{}^{14}N$	<1
$C^aH_3NC^b$	$^{13}C_a-{}^{14}N$	$+7.0 \pm 1$ $(+1.55)$
	$^{14}N-{}^{13}C_b$	$\pm 6.5 \pm 0.3$ (-6.02)
$C^aH_3C^bN$	$^{13}C_b-{}^{14}N$	$+12.5$ $(+0.20)$
$C_6H_5C^aH=N-CH_3$	$^{13}C_a-{}^{14}N$	± 4.9

Similar to the central sp carbons of allenes (Table 4.15), the carbodiimide carbons (about 140 ppm) are deshielded relative to nitrile carbons (less than 120 ppm) as can be seen in Table 4.45. Parallel to $J_{^{13}C-^{15}N}$ (Table 3.9), the $^{13}C-{}^{14}N$ spin coupling constants differ substantially between cyanide and isocyanide bonds, as is seen from Table 4.44 [231].

It was stated above that $^{13}C-{}^{14}N$ coupling constants correlate linearly with the products of s characters of the coupling nuclei [111]. However, it appears that this relationship does not apply to isocyanides. The $^{13}C-{}^{14}N$ spin coupling constants, calculated by the INDO SCF–MO method agree only poorly with the experimental data (see Table 4.44).

A ^{13}C NMR study of substituted benzonitriles demonstrated that the ^{13}C chemical shifts of C-1 correlate linearly with their LCAO–MO π electron densities [54b].

The ^{13}C chemical shifts of selected cyanides, isocyanides, isocyanates and isothiocyanates are listed in Table 4.45.

4.8.3. Nitro Compounds and Nitrosamines

The α effect of the nitro group as obtained by comparing the C-1 shieldings in Table 4.46 with those of comparable alkanes (Tables 4.1 and 4.4) is about 60 ppm. Of all substituents investigated so far, only fluorine causes a larger deshielding in α position (Table 3.2).

^{13}C NMR spectroscopy is a sensitive method for investigating *cis* and *trans* isomers of N-nitroso compounds. Chemical shift differences between 5.7 and 10.1 ppm are observed for the α-carbons:

Table 4.45. ^{13}C Chemical Shifts of Cyanides, Isocyanides, Isocyanates, Isothiocyanates, and Carbodiimides (δ Values (ppm) Relative to TMS = 0).

Compound	CN NC NCO NCS $-N=C=N-$	C-1	C-2	C-3	C-4	C-5	C-6	Solvent	Ref
Methyl cyanide	117.7	0.3						neat	[54a]
Ethyl cyanide	120.8							neat	[54a]
Cyclohexyl cyanide	121.4							neat	[54a]
Methyl isocyanide	158.5	29.3						neat	[54a]
Ethyl isocyanide	156.6	36.0	14.4					neat	[231]
Cyclohexyl isocyanide	156.5							neat	[55]
t-Butyl isocyanide	155.0	58.0	9.8					neat	[231]
Methyl isocyanate	121.3	26.1						neat	[54a]
Ethyl isocyanate	122.4							neat	[54a]
Cyclohexyl isocyanate	123.5							neat	[54a]
Methyl isothiocyanate	128.5	29.1						neat	[54a]
Ethyl isothiocyanate	130.6							neat	[54a]
Cyclohexyl isothiocyanate	132.2							neat	[54a]
Diisopropylcarbodiimide	140.2	49.0	24.8					$CDCl_3$	[102]
Dicyclohexylcarbodiimide	139.9	55.7	35.0	24.8	25.5	24.8	35.0	$CDCl_3$	[102]
Benzonitrile	115.9	109.4	129.8	126.9	129.8	126.9	129.8	neat	[54b]
4-Fluorobenzonitrile	113.7	104.5	131.3	112.7	162.9	112.7	131.3	acetone	[54b]
4-Chlorobenzonitrile	114.0	107.0	130.4	126.3	140.8	126.3	130.4	acetone	[54b]
4-Bromobenzonitrile	119.2	109.5	133.4	132.0	160.4	132.0	133.4	DMSO	[54b]
4-Aminobenzonitrile	114.2	90.8	127.3	107.1	146.4	107.1	127.3	acetone	[54b]
4-Dimethylaminobenzonitrile	116.8	92.5	129.7	107.6	150.1	107.6	129.7	acetone	[54b]
4-Methylbenzonitrile	117.0	107.3	130.8	128.5	142.8	128.5	130.8	diethylether	[54b]
4-Nitrobenzonitrile	111.7	116.1	122.6	134.3	149.8	134.3	122.6	DMSO	[54b]
4-Carboxybenzonitrile	117.7	113.9			135.4			DMSO	[54b]
3-Fluorobenzonitrile	113.1	109.5		160.1				acetone	[54b]
3-Chlorobenzonitrile	113.4	109.9		131.4				acetone	[54b]
3-Bromobenzonitrile	118.5	113.1		133.1				acetone	[54b]
3-Aminobenzonitrile	112.8	105.7		142.7				acetone	[54b]
3-Nitrobenzonitrile	109.2	105.9		141.5				nitromethane	[54b]
3-Carboxybenzonitrile	118.0	111.8		132.9				DMSO	[54b]
3,4-Dimethylbenzonitrile	115.6	105.8		135.5	140.1			acetone	[54b]
3,4-Dimethoxybenzonitrile	116.3	99.0		145.7	150.6			acetone	[54b]

Table 4.46. ^{13}Chemical Shifts of Selected Nitroalkanes in ppm Relative to TMS.

Compound	C-1	C-2	C-3	C-4	C-5	C-6	Ref.
Nitromethane	61.4						Table 3.1
Nitroethane	70.4	10.6					[50e]
2-Nitropropane	79.1	19.1					[50e]
2-Nitro-2-methylpropane	85.2	26.9					[50e]
Nitrohexane	75.8	26.2	27.6	31.3	22.5	13.9	[50g]
Nitrocyclohexane	84.6	31.4	24.7	25.5	24.7	31.4	[50g]

the shifts of the β-carbons vary between 1.0 and 4.6 ppm; those of the γ-carbons show differences of 0.2 to 0.6 ppm when going from *cis* to *trans* isomers [232].
One methyl resonance but six signals in the aromatic region are observed for N-methyl-N-nitrosoaniline. In conclusion,

(1) only one isomer is present in solutions of N-methyl-N-nitrosoaniline and
(2) the rotation about the phenyl-nitrogen bond is sterically hindered [232].

The ^{13}C chemical shifts of selected N-nitroso compounds are listed in Table 4.47.

Table 4.47. ^{13}C Chemical Shifts of Carbons in N-Substituents of N-Nitroso Compounds (δ Values (ppm) Relative to TMS = 0) [232].

Compound	Chemical Shifts					
	α		β		γ	
	cis	*trans*	*cis*	*trans*	*cis*	*trans*
N-Nitrosodimethylamine	32.6	40.5				
N-Nitrosodiethylamine	38.4	47.0	11.5	14.5		
N-Nitrosodi-*n*-propylamine	45.2	54.2	20.3	22.5	11.3	11.8
N-Nitrosodiisopropylamine	45.4	51.1	19.1	23.7		
N-Nitrosodi-*n*-butylamine	41.8	51.9	28.9	31.1	20.3	20.9
N-Nitrosodiisobutylamine	50.4	59.9	26.5	27.5	20.1	20.5
N-Methyl-N-nitrosoaniline	30.9					
N-Ethyl-N-nitrosoaniline	38.9		11.8			
N-*n*-Propyl-N-nitrosoaniline	44.9		20.2		11.5	
N-*n*-Butyl-N-nitrosoaniline	43.1		29.0		20.6	
N-Isobutyl-N-nitrosoaniline	52.3	62.0	27.4 (CH_2) 17.7 (CH_3)	28.9 (CH_2) 20.2 (CH_3)	11.0	11.2
N-*t*-Butyl-N-nitrosoaniline		61.8		30.1		

4.9. Aliphatic Organosulfur Compounds

The ^{13}C shift values reported for a selection of organosulfur compounds in Table 4.48 [233] indicate that α and β effects have similar magnitudes and equal signs as described for comparable substituents such as OH and NH_2. Due to the low electronegativity of bivalent sulfur, Table 4.48. ^{13}C Chemical Shifts of Selected Thiols, Sulfides, Sulfoxides, Sulfones and Sulfonic Acids; Data from Ref. [233].

Compound	C-1	C-2	C-3	C-4	C-5	C-6	C-7	C-8	Others (CH_3)	Solvent
1-Propanethiol	26.4	27.6	12.6							CD_3OD
1-Butanethiol	24.6	37.1	22.3	13.9						CD_3OD
1-Octanethiol	24.7	34.2	28.5	29.2*)	29.1*)	31.9	22.7	14.1		$CDCl_3$
Cyclohexanethiol	38.5	38.5	26.8	25.9	26.8	38.5				$CDCl_3$
1-Propanethiolate	27.5	30.2	13.6							CD_3OD
1-Butanethiolate	24.7	38.8	22.5	13.6						CD_3OD
Dimethylsulfide	19.3									$CDCl_3$
Diethylsulfide	25.5	14.8								$CDCl_3$
Dipropylsulfide	34.3	23.2	13.7							$CDCl_3$
Methyloctylsulfide	34.5	29.0*)	29.4*)	29.4*)	29.4*)	31.9	22.8	14.1	15.5	$CDCl_3$
Thiacyclohexane	29.1(α)	27.8(β)	26.6(γ)							$CDCl_3$
Trimethylsulfonium Cation	27.5									D_2O
Dimethylethylsulfonium Cation	38.2	8.3							24.3	D_2O
Dimethylpropylsulfonium Cation	45.4	17.7	12.7						24.8	D_2O
Dimethylbutylsulfonium Cation	43.2	25.7	21.4	13.7					25.3	D_2O
Dimethylsulfoxide	40.9									$CDCl_3$
Diethylsulfoxide	44.9	6.8								$CDCl_3$
Dipropylsulfoxide	54.4	16.3	13.4							$CDCl_3$
Thiacyclohexane-1-oxide	48.2(α)	18.5(β)	24.5(γ)							$CDCl_3$
Dimethylsulfone	42.6									$CDCl_3$
Diethylsulfone	40.4	6.6								$CDCl_3$
Dipropylsulfone	54.5	15.5	13.2							$CDCl_3$
Methylpropylsulfone	56.3	16.3	13.0						40.3	$CDCl_3$
Methylbutylsulfone	54.5	24.4	21.7	13.5					40.4	$CDCl_3$
Thiacyclohexane-1,1-dioxide	52.2(α)	24.3(β)	23.9(γ)							$CDCl_3$
3-Trimethylsilylpropanesulfonic acid, sodium salt	57.2	21.15	17.7						0.0	D_2O

*) Assignments interchangeable.

however, the carbon-sulfur single bonds in thiols are much less polarized, and a smaller α effect (10.5 ± 0.5 ppm) arises for the sulfhydryl group. With increasing alkylation and oxidation state of sulfur, *i.e.* in going from thiol *via* sulfide, sulfoxide, sulfone to sulfonic acid, the α effect increases while γ carbons remain almost unaffected. β Carbons, however, are more shielded in dialkylsulfides, sulfoxides and sulfones when compared to those in thiols, presumably due to steric polarizations of the β C–H bonds.

Thiocarbonyl carbons resonate at much lower fields than comparable carbonyl carbons [50e, i]. This deshielding has been attributed to the lower electronic excitation energy of the thiocarbonyl bond and hence an increased paramagnetic shielding according to eq. (3.4).

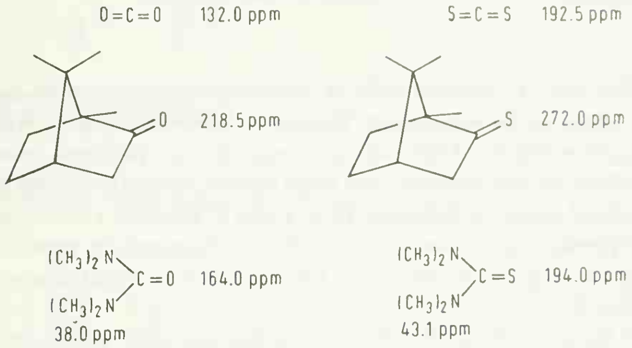

4.10. Aromatic Compounds

4.10.1. Benzene and Derivatives

Substituent shifts of aromatic carbons directly bonded to the substituent are as large as 35 ppm up- or downfield; the signals of carbons in *o*-, *m*- and *p*-position shift only –15 to +15 ppm. The methyl substitution effect in cresols is about 8 ppm, and thus similar to that observed for methyl benzenes (see Table 4.49) [234]. It has been shown for a series of phenols that ring methylation causes shielding of about 2.7 ppm for the *para* carbons; smaller methyl substitution effects are found for ring carbons in *ortho* and *meta* position [234].

The ^{13}C chemical shifts of alkyl substituted benzene carbons depend largely on the branching of the α-carbon atom. In the series toluene, isopropylbenzene, *t*-butylbenzene, the resonance of the substituted aromatic carbon atom shifts from higher to lower field (see Table 4.48 [68b].

The relative ^{13}C chemical shifts of substituted aromatic carbon atoms C–X are mainly influenced by inductive and magnetic anisotropy effects of the substituents X. After corrections accounting for the magnetic anisotropy contribution, a plot of the ^{13}C chemical shifts of C–X carbons *versus* the electronegativities of the X substituents yields a straight line, as is shown in Fig. 4.8 [235]. Resonance effects and paramagnetic terms seem to be of minor influence in the $^{13}C-X$ chemical shifts.

The substituent effects for aromatic carbons in *ortho* position to the introduced residue cannot be explained only by anisotropic shielding contributions. For instance the effects found for iodobenzene were explained in terms of high polarization of the iodine atom [236].

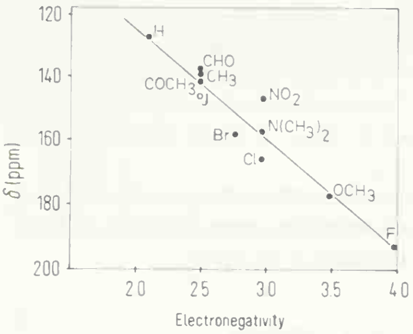

Fig. 4.8. Plot of the electronegativities of substituents X *versus* ^{13}C chemical shifts, corrected for magnetic anisotropy effects of aromatic C–X carbons (δ scale relative to TMS = 0) [235].

Recalling section 3.1.3.6., the ^{13}C chemical shifts of substituted benzenes can be assigned by the mesomeric effects caused by the substituents. Electron withdrawing moijeties will deshield while electron releasing ones will shield the *o* and *p* carbons. In the *o* positions, inductive and magnetic anisotropy effects are also operative but the *p* carbons clearly follow the pattern as described by the cannonical resonance formulae. Thus, a plot of Hammet σ constants *versus p* carbon shifts shows a reasonably good linearity (Fig. 4.9). *m* Carbons remain almost unaffected by all kinds of substituents. They usually resonate at 129 ± 1 ppm in monosubstituted benzenes as can be seen in Table 4.49.

Substitution effects of halogens, alkyl, vinyl, hydroxy, amino and nitro groups on aromatic carbons can be calculated from the δ values of substituted benzene derivatives listed in Table 4.49.

A linear correlation between ^{13}C chemical shifts and local π-electron densities (160 ppm per electron) in aromatic molecules has been reported [240] for the isoelectronic series $C_5H_5^{\ominus}$, C_6H_6, $C_7H_7^{\oplus}$ and $C_8H_8^{2\ominus}$. According to theoretical considerations [76, 77, 241, 242] however, ^{13}C chemical shifts of aromatic compounds depend on σ-electronic contributions, mobile bond orders and magnetic screening anisotropies, in addition to the electron densities.

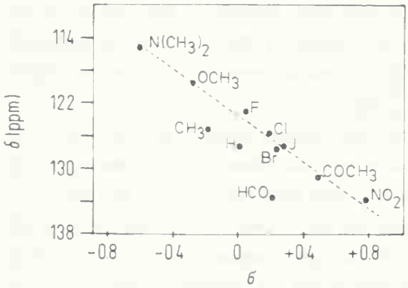

Fig. 4.9. Plot of Hammett σ constants *versus* ^{13}C chemical shifts of *para* carbons in monosubstituted benzenes (δ values relative to TMS = 0) [235].

4.10.2. Fused Aromatic Rings

A ^{13}C NMR study of non-alternant hydrocarbons lead to the conclusion that these systems may be distinguished from alternant ones by larger chemical shift ranges of the carbon signals (14–22 ppm in comparison to values smaller than 10 ppm in alternating systems) [243]. According

Compound	C-1	C-2	C-3	C-4	C-5	C-6	C-α	C-β	C-γ	Others	Solvent	Ref.
Benzene	128.5	128.5	128.5	128.5	128.5	128.5					neat	[233]
Toluene	137.8	128.4	129.2	125.5	129.2	128.4	21.3				$CDCl_3$	[50k]
Ethylbenzene	143.3	127.2	127.8	125.2	127.8	127.2	29.1	15.8			$CDCl_3$	[50k]
Propylbenzene	142.6	128.3	128.6	125.8	128.6	128.3	38.3	24.8	13.8		$CDCl_3$	[50k]
Isopropylbenzene	148.8	126.5	128.4	125.9	128.4	126.5	34.3	24.0			$CDCl_3$	[50k]
sec-Butylbenzene	148.4	127.9	129.3	126.8	129.3	127.9	42.3	31.7 22.2	12.4		$(CD_3)_2CO$	[50i]
t-Butylbenzene	150.3	124.6	127.6	124.9	127.6	124.6	34.4	31.0			$CDCl_3$	[102]
Styrene	137.6	126.1	128.3	127.6	128.3	126.1	137.1	113.3			CCl_4	[50k]
Polystyrene, *atactic*	146.4	128.2	128.2	126.2	128.2	128.2	40.8	43.0	(triade splitting)		$CDCl_3$	[50i]
Polystyrene, *isotactic*	147.0	128.0	128.9	124.4	128.9	128.0	40.7	43.2			$CDCl_3$	[50i]
Ethynylbenzene	122.7	132.4	128.6	128.9	128.6	132.4	84.0	77.8			CCl_4	[50k]
o-Xylene	136.2	136.2	129.7	125.9	125.9	129.7	19.6				$CDCl_3$	[50k]
m-Xylene	137.6	130.0	137.6	126.3	128.3	126.3	21.3				$CDCl_3$	[50k]
p-Xylene	134.6	129.1	129.1	134.6	129.1	129.1	20.9				$CDCl_3$	[50k]
Mesitylene	137.5	127.2	137.5	127.2	137.5	127.2	21.2				$CDCl_3$	[50k]
Durene	132.9	132.9	130.5	132.9	132.9	130.5	18.9				neat	[233]
Hexamethylbenzene	131.7	131.7	131.7	131.7	131.7	131.7	16.9				$CDCl_3$	[50k]
Benzylfluoride	136.6	127.6	128.6	128.7	128.6	127.6	84.5				$CDCl_3$	[50k]
Benzylchloride	137.9	128.8*)	128.9*)	128.7	128.8*)	128.9*)	47.0				CCl_4	[50k]
Benzylbromide	138.2	129.5	129.8	129.1	129.8	129.5	33.7				$CDCl_3$	[102]
Benzylalcohol	141.8	127.7	129.1	128.1	129.1	127.7	65.1				$CDCl_3$	[102]
Dibenzylether	139.0	128.0	129.0	128.0	129.0	128.0	72.5				CCl_4	[50k]
Dibenzylamine	140.4	128.0	128.2	126.8	128.2	128.0	53.1				$CDCl_3$	[50k]
Dibenzylsulfide	139.0	128.8	129.4	127.0	129.4	128.8	37.0				CCl_4	[50k]
Fluorobenzene	163.6	114.2	129.4	124.1	129.4	114.2					neat	[235]
Chlorobenzene	134.9	128.7	129.5	126.5	129.5	128.7					$CDCl_3$	[50k]
Bromobenzene	122.6	131.5	130.0	127.0	130.0	131.5					$CDCl_3$	[50k]
Iodobenzene	96.2	138.4	131.1	128.1	131.1	138.4					neat	[235]
o-Difluorobenzene	150.3	150.3	117.0	124.6	124.6	117.0					neat	[239]
o-Dichlorobenzene	132.6	132.6	130.5	127.7	127.7	130.5					$CDCl_3$	[50k]
o-Dibromobenzene	124.7	124.7	133.5	128.2	128.2	133.5					$CDCl_3$	[50k]
o-Diiodobenzene	108.6	108.6	139.6	129.6	129.6	139.6					neat	[239]
m-Difluorobenzene	163.1	103.3	163.1	110.9	130.7	110.9					neat	[239]
m-Dichlorobenzene	134.9	128.5	134.9	126.9	130.8	126.9					neat	[239]
m-Dibromobenzene	123.1	134.0	123.1	130.4	131.5	130.4					neat	[239]
m-Diiodobenzene	95.8	145.0	95.8	137.0	132.2	137.0					neat	[239]
p-Dichlorobenzene	132.7	130.3	130.3	132.7	130.3	130.3					neat	[102]

Table 4.49. (Continued).

Compound	C-1	C-2	C-3	C-4	C-5	C-6	C-α	C-β	C-γ	Others	Solvent	Ref.
2-Chlorotoluene	136.0	134.5	129.1	127.1	126.6	131.0	19.9				$CDCl_3$	[50k]
3-Chlorotoluene	139.9	129.3*)	134.2	125.7	129.5*)	127.3	21.1				$CDCl_3$	[50k]
4-Chlorotoluene	136.2	130.4	128.5	131.3	128.5	130.4	20.7				$CDCl_3$	[50k]
Phenol	155.1	115.7	130.1	121.4	130.1	115.4					$CHCl_3$	[234]
o-Cresol	153.5	124.0	131.0	121.4	127.7	115.9	16.7				neat	[234]
m-Cresol	154.9	116.1	139.3	122.2	130.3	112.7	20.9				neat	[234]
p-Cresol	152.6	115.3	130.2	130.5	130.2	115.3	20.6				neat	[234]
2,6-Dimethylphenol	152.3	123.6	128.8	120.6	128.8	123.6	15.4				$CHCl_3$	[234]
3,5-Dimethylphenol	154.5	112.8	138.9	121.9	138.9	112.8	20.4				$CHCl_3$	[234]
Brenzcatechine	147.1	147.1	119.3	124.1	124.1	119.3					D_2O	[102]
Resorcinol	159.3	105.3	159.3	110.3	133.3	110.3					D_2O	[102]
Hydroquinone	151.5	118.5	118.5	151.5	118.5	118.5					$(CD_3)_2SO$	[102]
Anisole	159.9	114.1	129.5	120.7	129.5	114.1				54.8 (OCH_3)	$CDCl_3$	[50k]
1,2-Dimethoxybenzene												
1,3-Dimethoxybenzene	161.8	101.0	161.8	106.7	130.4	106.7				55.3 (OCH_3)	$CDCl_3$	[102]
1,4-Dimethoxybenzene	154.1	114.8	114.8	154.1	114.8	114.8				55.4 (OCH_3)	$CDCl_3$	[50k]
Diphenylether	157.7	119.1	129.9	123.2	129.9	119.1					C_6D_6	Fig. 2.23
Thiophenol	130.5	129.1	128.7	125.2	128.7	129.1					$CDCl_3$	[237]
Thioanisol	138.6	126.8	128.8	125.0	128.8	126.8				15.9 (SCH_3)	$CDCl_3$	[237]
Diphenylsulfide	135.8	130.9	129.1	126.9	129.1	130.9					$CDCl_3$	[50k]
Aniline	148.7	114.4	129.1	116.3	129.1	114.4					$(CD_3)_2SO$	[50k, 235]
N-Methylaniline	150.4	112.1	129.1	115.9	129.1	112.1				29.9 ($HNCH_3$)	$(CD_3)_2SO$	[50k]
N,N-Dimethylaniline	150.7	112.7	129.0	116.7	129.0	112.7				40.3 (NCH_3)	$CDCl_3$	[50k, 235]
o-Phenylendiamine	135.0	135.0	117.0	120.5	120.5	117.0					$CDCl_3$	[50k]
m-Phenylendiamine	147.9	102.2	147.9	106.2	130.4	106.2					$CDCl_3$	[50k]
p-Phenylendiamine	138.8	116.9	116.9	138.8	116.9	116.9					$CDCl_3$	[50k]
2-Chloroaniline	143.0	119.1	129.3	118.9	127.6	115.9					$CDCl_3$	[50k]
3-Chloroaniline	148.0	114.8	134.7	118.2	130.4	113.3					$CDCl_3$	[50k]
4-Chloroaniline	144.9	115.9	128.7	128.6	128.7	115.9					$CDCl_3$	[50k]
p-Ethoxyaniline	140.4	116.4	115.9	152.0	115.9	116.4				64.1 (OCH_2) 15.0 (CH_3)	$CDCl_3$	[50k]
p-Ethoxyacetanilide	132.7	121.0	114.5	154.8	114.5	121.0				63.2 (OCH_2) 14.7 (CH_3) 168.2 (CO) 23.8 (CH_3)	$(CD_3)_2SO$	[50i]
Phenylhydrazine	152.3	112.8	129.9	119.9	129.9	112.8					$CDCl_3$	[102]

Table 4.49. (Continued).

Compound	C-1	C-2	C-3	C-4	C-5	C-6	C-α	C-β	C-γ	Others	Solvent	Ref.
Nitrobenzene	149.1	124.2	129.8	134.7	129.8	124.2					$CDCl_3$	[50k]
2-Nitrotoluene	133.4	149.5	124.5	127.1	133.1	132.8	20.1				$CDCl_3$	[50k]
4-Nitrotoluene	146.2	130.0	123.5	146.2	123.5	130.0	21.4				$CDCl_3$	[50k]
2-Nitroaniline	144.5	131.7	125.6	118.5	135.2	116.5					$CDCl_3$	[50k]
3-Nitroaniline	151.4	109.0	150.4	111.7	131.1	121.6					$(CD_3)_2SO$	[50k]
4-Nitroaniline	157.1	114.1	127.8	137.6	127.8	114.1					$(CD_3)_2SO$	[50k]
Azobenzene, *trans*	152.7	123.0	129.7	131.8	129.7	123.0					$(CD_3)_2SO$	[50i]
Benzalaniline	153.0	121.6	129.5	126.6	129.5	121.6	161.0 ($C_6H_5-N=$)				$CDCl_3$	[102]
	137.2	129.9	129.4	132.0	129.4	129.9	161.0 ($C_6H_5-CH=$)					
Phenylcyanate	153.1	115.3	130.7	127.0	130.7	115.3				108.7 (OCN)	$CDCl_3$	[50k]
Phenylisocyanate	133.9	124.8	129.7	125.9	129.7	124.8				120.8 (NCO)	$CDCl_3$	[50k]
Phenylisothiocyanate	145.9	126.3	130.5	128.1	130.5	126.3				131.9 (NCS)	$(CD_3)_2CO$	[102]
Diphenylcarbodiimide	139.3	124.9	130.2	126.3	130.2	124.9				136.0 (NCN)	$CDCl_3$	[102]
Triphenylphosphine	137.8	134.0	128.8	128.5	128.8	134.0					CD_3OD	[102]
Benzenesulfonic acid	145.7	131.8	128.4	134.4	128.4	131.8					D_2O	[102]
Benzenesulfonylchloride	144.3	129.9	126.9	135.5	126.9	129.9					$CDCl_3$	[102]
p-Toluenesulfonic acid	142.5	125.8	129.7	140.0	129.7	125.8	20.9				D_2O	[50k]
p-Toluenesulfonylchloride	142.8	125.5	128.7	139.5	128.7	125.5	20.8				$(CD_3)_2SO$	[50k]
Benzoic acid	131.4	129.8	128.9	133.1	128.9	129.8	168.0 (COOH)				$(CD_3)_2SO$	[102]
Benzoate anion	138.8	131.3	130.7	133.6	130.7	131.3	177.9 (COO^-)				D_2O	[102]
Benzamide	134.3	127.4	128.2	131.2	128.2	127.4	168.2 ($CONH_2$)				$(CD_3)_2SO$	[50k]
Benzoylchloride	133.3	131.4	129.1	135.4	129.1	131.4	167.8 (COCl)				C_6D_6	[50k]
Ethylbenzoate	130.9	129.7	128.4	132.8	128.4	129.7	166.3 (COO)			60.8 (OCH_2) 14.4 (CH_3)	$CDCl_3$	[50k]
o-Toluic acid	129.2	137.7	128.9	130.0	124.3	130.0	21.3			167.0 (COO)	$(CD_3)_2SO$	[50k]
m-Toluic acid	129.5	128.5	136.3	125.2	126.9	131.9	20.7			165.7 (COO)	$(CD_3)_2SO$	[50k]
p-Toluic acid	128.5	129.7*)	129.4*)	143.3	129.4*)	129.7*)	21.4			167.8 (COO)	$(CD_3)_2SO$	[102]
2-Methoxybenzoic acid	119.9	156.3	111.1	131.5	118.7	129.2	165.5			55.0 (OCH_3)	$(CD_3)_2SO$	[50k]
3-Methoxybenzoic acid	133.0	115.6	160.8	120.2	131.0	123.1	168.7			56.6 (OCH_3)	$(CD_3)_2SO$	[50k]
2-Aminobenzoic acid	111.5	152.9	116.4	135.3	118.0	132.8	169.1				$(CD_3)_2SO$	[50k]
4-Aminobenzoic acid	118.7	132.8	114.3	154.6	114.3	132.8	171.3				$(CD_3)_2SO$	[50k]
2-Nitrobenzoic acid	126.1	146.8	122.3	131.5	130.8	128.5	164.0				$(CD_3)_2SO$	[50k]
3-Nitrobenzoic acid	131.0	122.2	146.1	125.7	128.9	133.7	163.6				$(CD_3)_2SO$	[50k]
Benzophenone**)	137.6	130.0	128.3	132.3	128.3	130.0	196.4				$CDCl_3$	[50k]

*) Assignments interchangeable.

**) For benzaldehyde, acetophenone, methyl benzoate and benzonitrile including substituted derivatives see Tables 4.35, 4.36, 4.41 and 4.45.

to this criterion, acepleiadiene and acepleiadylene belong to the class of non-alternant hydrocarbons [244]. A plot of ^{13}C chemical shifts *versus* π or total charge densities derived from CNDO/2-SCF – MO calculations yields a poor correlation for naphthalene, azulene, acenaphalene and acenaphthene [243].

The ^{13}C chemical shifts for the following aromatic hydrocarbons are listed in Table 4.50.

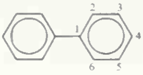

Biphenyl

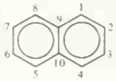
1
2
3
4
5
6
7
8
9
10
Naphthalene

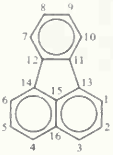
1
2
3
4
5
6
7
8
9
10
11
12
13
14
15
16
Fluoranthene

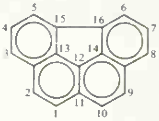
1
2
3
4
5
6
7
8
9
10
11
12
13
14
15
16
Benzo[ghi]fluoranthene

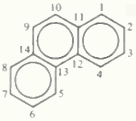
1
2
3
4
5
6
7
8
9
10
11
12
13
14
Phenanthrene

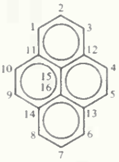
1
2
3
4
5
6
7
8
9
10
11
12
13
14
15
16
Pyrene

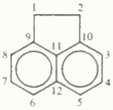
1
2
3
4
5
6
7
8
9
10
11
12
Acenapthene

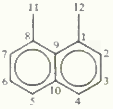
1
2
3
4
5
7
8
9
10
11
12
1,8-Dimethylnaphthalene

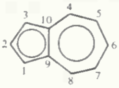
1
2
3
4
5
6
7
8
9
10
Azulene

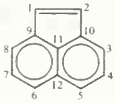
1
2
3
4
5
6
7
8
9
10
11
12
Acenaphthylene

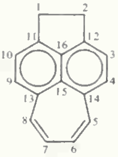
1
2
3
4
5
6
7
8
9
10
11
12
13
14
15
16
Acepleiadiene

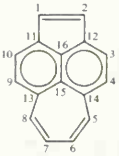
1
2
3
4
5
6
7
8
9
10
11
12
13
14
15
16
Acepleidylene

Table 4.50. ^{13}C Chemical Shifts of Hydrocarbons with More than One Aromatic Ring (δ Values (ppm) Relative to TMS = 0).

	Biphenyl	Naphthalene	Anthracene	Phenanthrene	Pyrene	Azulene	Acenaphthylene
Solvent	CS_2	CS_2	CS_2	CS_2	CS_2	CS_2/Dioxane	CS_2/Dioxane
Reference	[241]	[241]	[241]	[241]	[241]	[243]	[243]
C-Atom							
1	141.50	128.10	130.1	128.90	125.25	119.00	129.70
2	127.40	125.95	125.6	126.75	126.15	137.70	129.70
3	129.00	125.95	125.6	126.75	125.25	119.00	124.30
4	127.50	128.10	130.1	123.05	127.70	136.75	127.85
5	129.00	128.10	130.1	123.05	127.70	123.05	127.35
6	127.40	124.95	125.6	126.75	125.25	137.25	127.35
7		124.95	125.6	126.75	126.15	123.05	127.85
8		128.10	130.1	128.90	125.25	136.75	124.30
9		133.70	132.5	127.30	127.70	140.65	140.00
10		133.70	132.5	127.30	127.70	140.65	140.00
11			132.2	132.30	131.30		128.70
12			132.2	130.50	131.30		128.40
13			132.2	130.50	131.30		
14			132.2	132.30	131.30		
15					124.90		
16					124.90		

Table 4.50. (Continued).

	Fluoranthene	Benzo[ghi]-fluoranthene	Acenaphthene	1,8-Dimethyl-naphthalene	Acepleiadiene	Acepleiadylene
Solvent	CS_2/Dioxane	CS_2/Dioxane	CS_2/Dioxane	CS_2/Dioxane	CS_2/Dioxane	CS_2/Dioxane
Reference	[243]	[243]	[243]	[243]	[244]	[244]
C-Atom						
1	122.90	125.45	30.25	135.60	29.65	126.15
2	128.55	127.05	30.25	128.40	29.65	126.15
3	127.30	126.70	119.45	129.85	120.05	125.80
4	127.30	128.75	128.20	125.35	127.95	127.40
5	128.55	123.65	122.70	125.35	125.95	126.85
6	122.90	123.65	122.70	129.85	138.45	137.00
7	120.70	128.75	128.20	128.40	138.45	137.00
8	128.25	126.70	119.45	135.60	125.95	126.85
9	128.25	127.05	145.90	133.60	127.95	127.40
10	120.70	125.45	145.90	136.35	120.05	125.80
11	140.15	133.40	139.65	26.00	143.85	138.20
12	140.15	126.85	132.10	26.60	143.85	138.20
13	137.65	128.10			135.85	134.85
14	137.65	128.10			135.85	134.85
15	132.95	137.75			136.55	127.20
16	130.70	137.75			142.85	126.60
17		133.70				
18		133.70				

4.10.3. Coupling Constants

In a study on mono-and dihalobenzenes (Table 4.51), all long-range carbon-proton coupling constants and chemical shifts were determined [239]. Substituent effects for the different carbons of monohalobenzenes were determined for ^{13}C chemical shifts and $^{13}C-{}^{1}H$ coupling constants; these parameters could be used for the calculation of the shift values and coupling constants of most dihalobenzene carbons with an accuracy of better than 1 ppm or 0.5 Hz, respectively. As can be seen from Table 4.51, the $^{13}C-{}^{1}H$ three-bond coupling constants are larger than the two-bond coupling values.

$^{13}C-{}^{13}C$ coupling constants were reported recently for a series of ^{13}C-7 labeled monosubstituted benzene derivatives [109]. From the data in Table 4.52, two trends become obvious:

(1) With an increase of the s-character of C-7 the coupling constant $J_{1,7}$ increases;
(2) With decreasing electronegativity of the C-7 substituent smaller values for $J_{1,7}$ are observed.

In a systematic study [245] of carbon-fluorine couplings of substituted fluorobenzenes the following conclusions were arrived at:

(1) Only the data for *para*-substituted fluorobenzenes lead to a linear plot of the one-bond carbon-fluorine coupling constants *vs.* ^{19}F chemical shifts. Thus such couplings are largely influenced by resonance effects.
(2) Calculated carbon-fluorine coupling constants using extended Hückel wave functions agree fairly well with experiments only in the case of one-bond coupling constants.
Carbon-fluorine couplings of selected fluorobenzenes are collected in Table 4.53.

Table 4.51. One-bond and Longer-range $^{13}C-^{1}H$ Coupling Constants [Hz] in Monohalobenzenes [184].

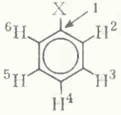

I

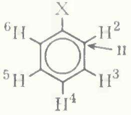

II

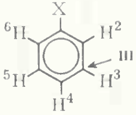

III

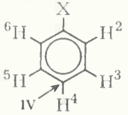

IV

Compound	$^nJ_{1,2}$	$^nJ_{1,3}$	$^nJ_{1,4}$	$^nJ_{1,5}$	$^nJ_{1,6}$	($n = 1-4$)
Benzene	+1.11 (C_IH)	+7.58 (C_IH)	−1.20 (C_IH)	+7.58 (C_IH)	+1.11 (C_IH)	
Chlorobenzene	−3.39 (C_IH)	+11.10 (C_IH)	−2.02 (C_IH)	+11.10 (C_IH)	−3.39 (C_IH)	
Bromobenzene	−3.34 (C_IH)	+11.22 (C_IH)	−1.88 (C_IH)	+11.22 (C_IH)	−3.34 (C_IH)	
Iodobenzene	−2.41 (C_IH)	+10.73 (C_IH)	−1.85 (C_IH)	+10.73 (C_IH)	−2.41 (C_IH)	
Benzene	+158.77 ($C_{II}H$)	+1.11 ($C_{II}H$)	+7.58 ($C_{II}H$)	−1.20 ($C_{II}H$)	+7.58 ($C_{II}H$)	
Fluorobenzene	+163.14 ($C_{II}H$)					
Chlorobenzene	+164.84 ($C_{II}H$)	+1.41 ($C_{II}H$)	+7.85 ($C_{II}H$)	−1.24 ($C_{II}H$)	+4.95 ($C_{II}H$)	
Bromobenzene	+165.77 ($C_{II}H$)	+1.44 ($C_{II}H$)	+7.91 ($C_{II}H$)	−1.24 ($C_{II}H$)	+5.32 ($C_{II}H$)	
Iodobenzene	+165.65 ($C_{II}H$)	+1.55 ($C_{II}H$)	+7.78 ($C_{II}H$)	−1.27 ($C_{II}H$)	+5.98 ($C_{II}H$)	
Benzene	+1.11 ($C_{III}H$)	+158.77 ($C_{III}H$)	+1.11 ($C_{III}H$)	+7.58 ($C_{III}H$)	−1.20 ($C_{III}H$)	
Fluorobenzene		+162.00 ($C_{III}H$)				
Chlorobenzene	+0.29 ($C_{III}H$)	+161.22 ($C_{III}H$)	+1.55 ($C_{III}H$)	+8.18 ($C_{III}H$)	−0.91 ($C_{III}H$)	
Bromobenzene	+0.46 ($C_{III}H$)	+161.90 ($C_{III}H$)	+1.60 ($C_{III}H$)	+8.23 ($C_{III}H$)	−1.05 ($C_{III}H$)	
Iodobenzene	+0.74 ($C_{III}H$)	+161.43 ($C_{III}H$)	+1.44 ($C_{III}H$)	+8.15 ($C_{III}H$)	−1.25 ($C_{III}H$)	
Benzene	+7.58 ($C_{IV}H$)	+1.11 ($C_{IV}H$)	+158.77 ($C_{IV}H$)	+1.11 ($C_{IV}H$)	+7.58 ($C_{IV}H$)	
Fluorobenzene			+162.16 ($C_{IV}H$)			
Chlorobenzene	+7.37 ($C_{IV}H$)	+0.87 ($C_{IV}H$)	+161.30 ($C_{IV}H$)	+0.87 ($C_{IV}H$)	+7.37 ($C_{IV}H$)	
Bromobenzene	+7.39 ($C_{IV}H$)	+0.86 ($C_{IV}H$)	+161.55 ($C_{IV}H$)	+0.86 ($C_{IV}H$)	+7.39 ($C_{IV}H$)	
Iodobenzene	+7.39 ($C_{IV}H$)	+0.82 ($C_{IV}H$)	+160.97 ($C_{IV}H$)	+0.82 ($C_{IV}H$)	+7.39 ($C_{IV}H$)	

Table 4.52. $^{13}C-^{13}C$ One-bond and Longer-range Coupling Constants [Hz] of ^{13}C-7 Labeled Monosubstituted Benzene Derivatives [109]

Compound	$J_{1,7}$	$J_{2,7}$	$J_{3,7}$	$J_{4,7}$	J_{COC}
$C_6H_5-{}^{13}CH_3$	44.19	3.10	3.84	0.86	
$C_6H_5-{}^{13}CH_2OH$	47.72	3.45	3.95	0.73	
$C_6H_5-{}^{13}CH_2Cl$	47.78	3.69	4.23	0.69	
$C_6H_5-{}^{13}CO_2^-Na^+$	65.90	2.23	4.11	0.8	
$C_6H_5-{}^{13}CO_2H$	71.87	2.54	4.53	0.90	
$C_6H_5-{}^{13}CO_2CH_3$	74.79	2.38	4.56	0.90	2.63
$C_6H_5-{}^{13}COCl$	74.35	3.53	5.46	1.18	
$C_6H_5-{}^{13}CN$	80.40	2.61	5.75	1.59	

Table 4.53. Carbon-Fluorine Couplings in Fluorobenzene and Substituted Fluorobenzenes (Hz) [245].

Compound	$-J_{C\text{-}1,F}$	$J_{C\text{-}2,F}$	$J_{C\text{-}3,F}$	$J_{C\text{-}4,F}$	$J_{C\text{-}5,F}$	$J_{C\text{-}6,F}$	Others
Fluorobenzene	245.3	21.0	7.7	3.3	7.7	21.0	
o-Difluorobenzene	248.8	14.1	−3.0	5.2	5.2	20.5	
o-Chloro-fluorobenzene	248.7	17.5	0	4.05	7.2	20.8	
o-Bromo-fluorobenzene	247.0	20.7	0	3.35	7.1	21.95	
o-Iodo-fluorobenzene	245.6	25.2	1.46	3.5	7.2	23.4	
o-Nitro-fluorobenzene	264.4		4.25	2.8	8.7	20.6	
o-Amino-fluorobenzene	237.5	12.7	3.8	3.6	6.7	18.4	
o-Hydroxy-fluorobenzene	238.8	13.7	1.94	3.78	6.6	18.0	
o-Methyl-fluorobenzene	243.9	17.0	4.8	3.7	7.9	22.1	3.8 (CH_3)
o-Fluorobenzaldehyde	257.7	8.2	1.86	3.75	9.1	20.45	6.4 (CHO)
o-Fluoroacetophenone	254.2	12.8	2.54	3.4	9.0	23.7	3.2 (CO) <0.4 (CH_3)
2-Fluoropyridine	236.7		14.7	4.2	7.75	37.4	
m-Difluorobenzene	245.4	25.3	12.1	3.6	9.8	21.2	
m-Chloro-fluorobenzene	249.5	24.6	10.0	3.4	8.9	21.3	
m-Bromo-fluorobenzene	250.4	24.5	9.3	3.4	8.4	21.1	
m-Iodo-fluorobenzene	249.0	23.2	7.8	3.3	8.1	20.8	
m-Nitro-fluorobenzene	250.9	26.5	8.3	3.3	8.2	21.5	
m-Amino-fluorobenzene	241.4	24.6	11.0	2.3	10.2	21.3	
m-Hydroxy-fluorobenzene	244.5	24.8	11.3	3.0	10.2	21.2	
m-Methyl-fluorobenzene	243.6	21.1	7.2	2.2	8.5	21.2	1.75 (CH_3)
m-Fluorobenzaldehyde	248.2	21.7	6.3	2.9	7.8	21.8	2.4 (CHO)
m-Fluoroacetophenone	246.3	22.2	5.9	2.9	7.75	21.6	1.9 (CO) 0.68 (CH_3)
p-Difluorobenzene	242.0	24.3	8.5	3.8	8.5	24.3	
p-Chloro-fluorobenzene	245.5	23.1	8.2	3.1	8.2	23.1	
p-Bromo-fluorobenzene	246.7	23.7	8.0	3.3	8.0	23.7	
p-Iodo-fluorobenzene	247.4	22.2	7.6	3.4	7.6	22.2	
p-Nitro-fluorobenzene	256.6	24.0	10.2		10.2	24.0	
p-Amino-fluorobenzene	233.2	22.4	7.5	1.86	7.5	22.4	
p-Hydroxy-fluorobenzene	237.4	23.0	7.9	2.14	7.9	23.0	
p-Methyl-fluorobenzene	243.5	21.1	7.75	2.9	7.75	21.1	0(CH_3)
p-Fluorobenzaldehyde	255.0	22.4	9.7	2.6	9.7	22.4	0(CHO)

Recalling the relation $^3J_{CH(m)} > {}^2J_{CH(o)} > {}^4J_{CH(p)}$ outlined in section 3.2.2.3., aromatic carbons without hydrogens in any *m* position can mostly be recognized as pure one-bond doublets for unsubstituted carbons and as singlets in the case of substituted ones. A typical example is vanilline (Fig. 4.10), illustrating the assignment of benzenoid carbon signals by means of C–H coupling in a trisubstituted benzene.
The high-field part of a multiplet arising from one-bond and longer-range couplings, frequently differs from the low-field half. This asymmetry of multiplets indicates that the spectrum is second order. To conclude, first-order analysis of single frequency ^{13}C NMR spectra as illustrated in Fig. 4.10 is not generally possible. Even if the proton spectrum of a compound is first-order, the coupled carbon spectrum may be second-order, and a simulation is required for a correct analysis.

The intensities of quaternary carbon signals in proton broad band decoupled ^{13}C NMR spectra of pyrene, acenaphthene, acenaphthylene and fluoranthene may be used for signal identification, as the nuclear Overhauser enhancement is mainly due to r^{-6} dependent carbon hydrogen dipolar interactions. In the spectrum of pyrene for instance, the integral ratios for the signals of C-11 : C-15 are 4 : 1 instead of 2 : 1, and thus allow unequivocal ^{13}C signal assignment of these two quaternary carbon atoms [246].

4.10.4. ^{13}C Enriched Aromatic Compounds, Mechanistic Studies

^{13}C NMR measurements of 6-dimethylamino-6-methylfulvene, synthesized from ^{13}C-7 labeled phenyldiazomethane *via* fulvenallene and ethynylcyclopentadiene, supported the proposed mechanism of the ring contraction of phenylcarbene to fulvenallene. The uniform distribution of ^{13}C in the product fulvenallene may be explained in terms of a "preequilibrium": Before ring contraction, phenylcarbene, a bicyclic intermediate and cycloheptatrienylidene interconvert rapidly [247]:

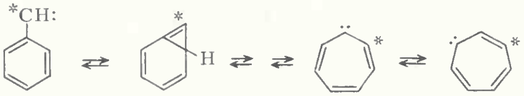

^{13}C NMR spectroscopy on specifically ^{13}C enriched compounds may lead to the unequivocal elucidation of doubtful structures, as was shown recently for the dimer of [α-^{13}C]-triphenylmethyl [248]. According to general chemical shift rules [225], the two resonances at 138.6 and 63.9 ppm are in accordance with the shift ranges of sp^2 and sp^3 carbon atom signals, thus confirming structure I instead of II for the dimer.

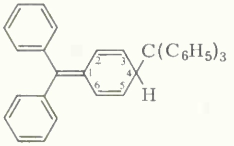

I

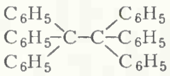

II

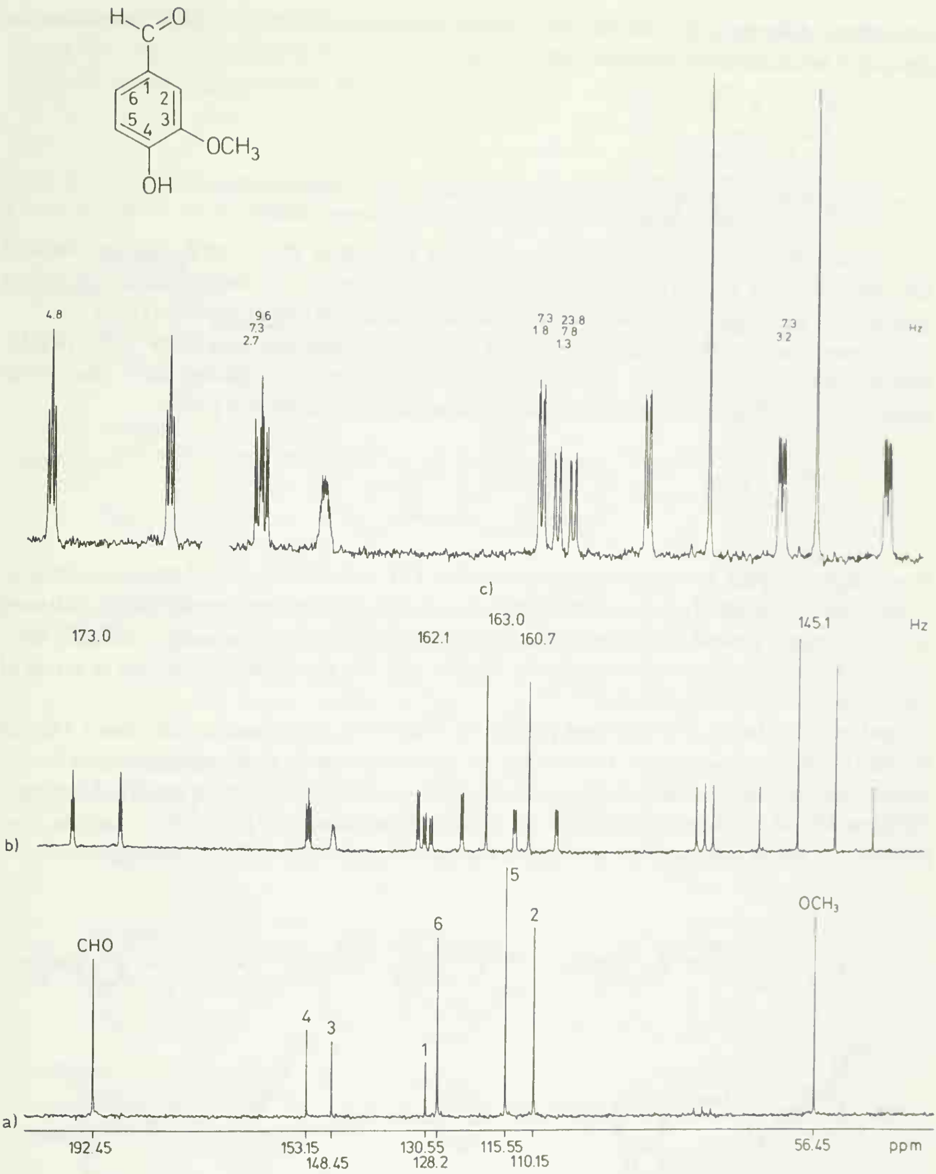

Fig. 4.10. ^{13}C NMR spectrum of vanilline in deuteriochloroform (150 mg/1 ml), 28 °C, 22.63 MHz; (a) proton broad-band decoupled (200 scans); (b) gated decoupled (1600 scans); (c) expaneded output of (b). The CHO carbon splits into a doublet of long-range triplets (4.8 Hz), the latter arising from H-2,6. C-4 shows *m* coupling with H-2 and H-6 (9.6 and 7.3 Hz) and *o* coupling with H-5 (2.7 Hz). C-3 splits into a multiplet due to *m* coupling with H-5, *o* coupling with H-2 and three-bond coupling with the methoxy protons. C-1 couples with the formyl proton (23.8 Hz), with H-5 (7.8 Hz) and with H-2 or H-6 (1.3 Hz). The long-range splittings of C-6 originate from H-2 (7.3 Hz) and CHO (1.8 Hz), those of C-2 from H-6 (7.3 Hz) and CHO (3.2 Hz), while C-5 does not have any hydrogen in a *m* position and does not show any longer-range splitting at all.

The dimer of 9-phenyl-[9-^{13}C]-fluorenyl shows one resonance only at 94.35 ppm, thus indicating a hexaarylethane structure [249]:

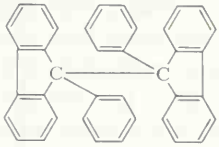

[1-^{13}C]Naphthalene, investigated before and after heating in Al_2O_3 with benzene, showed identical ^{13}C NMR spectra [250]. Thus no automerization (equal ^{13}C enrichment on all carbon positions) of naphthalene occurs under these conditions as was earlier reported [251].

It was determined from temperature dependent ^{13}C NMR measurements on ethyl-7-phenylcycloheptatriene-7-carboxylate and dimethyl-7-phenylcycloheptatriene-7-phosphonate that these molecules must be in equilibrium with the corresponding norcaradienes [252]:

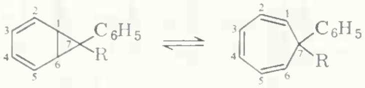

It was demonstrated by spectral comparison that C-1 and C-6 in ethyl-7-phenylcycloheptatriene-7-carboxylate (85.4 ppm) and dimethyl-7-phenyl-cycloheptatriene-7-phosphonate (58.0 ppm) are too strongly shielded to belong to a cycloheptatriene system and too weakly shielded for a norcaradiene system. The anomalous shifts for C-6 and C-1 can be explained only in terms of the above formulated equilibrium.

Instead of ^{13}C labeling, ^{12}C enriched precursors with a ^{13}C abundance of less than 1.1% can be used for mechanistic studies. In this case, the spectra are more easily analyzed as no homonuclear carbon-carbon coupling occurs. An illustrative example is the base catalyzed dehydrohylogenation of 7,7-dichloronorcarene to benzocyclopropene [254]. For this reaction, two pathways A and B have been proposed, mechanism B involving a skeletal rearrangement:

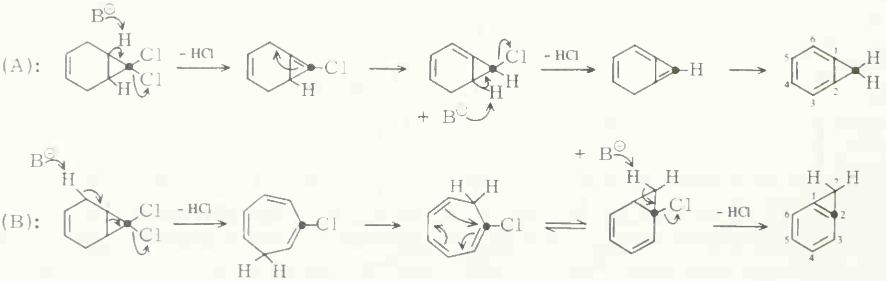

• : ^{12}C labelled carbon

In order to distinguish between both alternatives, [7-^{12}C]-7,7-dichloronorcarene was prepared by reaction of 1,4-cyclohexadiene with [^{12}C]-dichlorocarbene originating from [^{12}C]-deuteriochloroform:

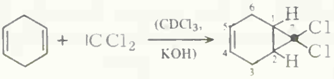

After dehydrohalogenation of the labelled dichloronorcarene, a benzocyclopropene was obtained whose CH_2 signal (denoted as C-7 with 18.4 ppm, Table 4.54) was lost in the noise [254]. As a result, the reaction proceeds *via* mechanism A.

Table 4.54. ^{13}C Chemical Shifts of Benzocycloalkenes [252, 254] and Selected Hydroaromatic Compounds [50e,i] (one-bond C – H coupling constants are given in parentheses if available).

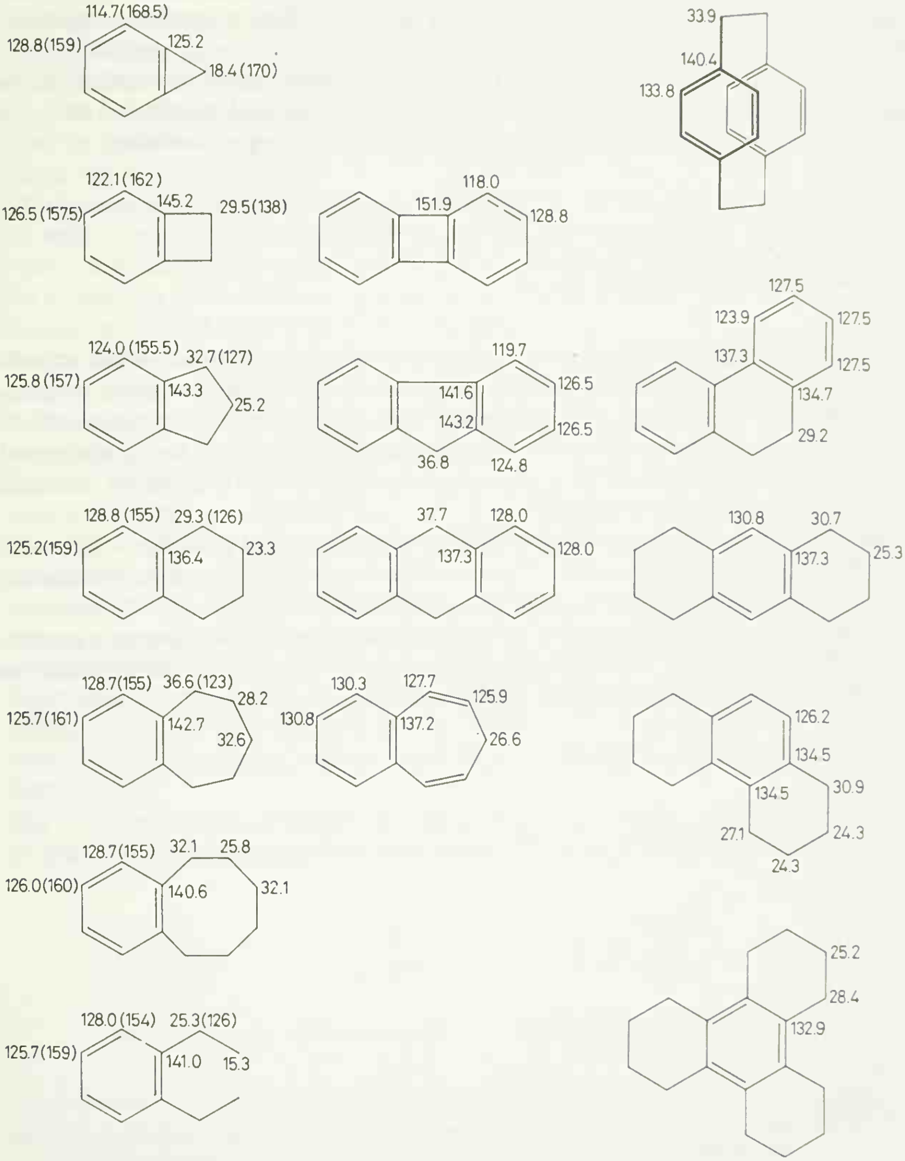
114.7(168.5)
128.8(159)
125.2
18.4(170)
33.9
140.4
133.8
122.1(162)
126.5(157.5)
145.2
29.5(138)
118.0
151.9
128.8
127.5
123.9
127.5
127.5
137.3
134.7
29.2
124.0(155.5)
32.7(127)
125.8(157)
143.3
25.2
119.7
141.6
126.5
143.2
126.5
36.8
124.8
128.8(155)
29.3(126)
125.2(159)
136.4
23.3
37.7
128.0
137.3
128.0
130.8
30.7
137.3
25.3
128.7(155)
36.6(123)
28.2
125.7(161)
142.7
32.6
130.3
127.7
125.9
130.8
137.2
26.6
126.2
134.5
134.5
30.9
27.1
24.3
24.3
128.7(155)
32.1
25.8
126.0(160)
140.6
32.1
25.2
28.4
132.9
128.0(154)
25.3(126)
125.7(159)
141.0
15.3

4.10.5. Hydroaromatic Compounds

The ^{13}C chemical shifts of benzocycloalkenes [252, 253] and other hydroaromatic hydrocarbons [50e] are listed in Table 4.54. Relative to *o*-diethylbenzene as reference compound, small deviations are observed for benzocyclooctene and benzocycloheptene. In going from benzocyclohexene to benzocyclopropene, however, an increasing shielding is measured with increasing ring strain for the carbons *meta* to the bridgeheads while the *ortho* carbons become successively deshielded as the ring strain increases [253]. Additionally, the C–H couplings of the *o* and α carbons increase with a decreasing carbon shielding. A corresponding trend is apparent in the cycloalkane series (Table 4.4).

The ^{13}C shifts of the other hydroaromates (Table 4.54) are closely related to those of tetralin. Angular fusion of the rings usually causes a slight sterically induced shielding of the *o,o′* or α,α′ carbons as can be recognized for the hydrogenated phenanthrene derivatives.

4.11. Heterocyclic Compounds

In pyrimidine, the signal of C-2, which is flanked by two nitrogen atoms, is observed at lowest field of all carbons of free base diazines. The resonances at highest field are caused by carbon atoms bearing no heteroatoms, and intermediate ppm values are found for diazine carbons bearing only one nitrogen atom [76, 199]. This sequence of signals is also to be expected according to general chemical shift rules [225]. However, different patterns are found for the resonances of protonated six-membered heterocyclics.

Pyridine shows the following protonation shifts [71, 76] for the α, β and γ carbons: -7.78, $+5.04$ and $+12.42$, respectively. The signals of the protonated species of pyrimidine, pyrazine and pyridazine can be assigned using these parameters (see Table 4.55) [76].

Plots of mole percent of water *versus* the ^{13}C chemical shifts of the α, β and γ carbons of pyridine-water mixtures yield linear correlations, as can bee seen in Fig. 4.11. This dilution effect has been explained in terms of intermolecular hydrogen bonding between pyridine and water [76].

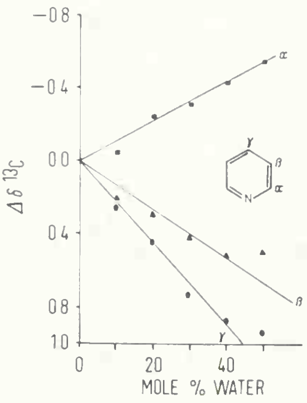

Fig. 4.11. Plot of ^{13}C shift differences of pyridine carbons in pyridine-water mixtures *versus* mole percent water [76].

Several considerations have dealt with correlations of experimental ^{13}C shift values of six membered heterocycles and theoretical terms [76, 242, 255]. A good linear correlation was found between ^{13}C chemical shifts of six π electron heterocyclic carbons and their total electron density [242]. Charge transfer features as well as bond-order parameters influence the shift values of six-membered nitrogen heterocyclic compounds. The ^{13}C protonation shifts observed for carbons in β- and γ-position to nitrogen, have been explained in terms of charge polarization effects. The decrease in bond strength between nitrogen and α-carbon upon protonation leads to a highfield shift of the carbon resonance [76].

Protonation of the pyrrole and imidazole anions causes upfield shifts of the signals of carbons bearing nitrogen atoms. The β-carbons C-3,4 of the pyrrole anion and C-4 of the pyrazole anion are deshielded upon protonation [77].

$\alpha(-9.04)$ and $\beta(+1.59)$ protonation effects similar to those in the six-membered diazines are found for the carbons of the pyrrole, pyrazole, and imidazole anions; these values were obtained from a regression analysis [76].

^{13}C chemical shifts of carbons in five-membered nitrogen heterocycles have been explained on the basis of calculated extended Hückel and self-consistent-field molecular wave functions for σ and π electrons. The β-protonation shifts of the five-membered ring compounds are apparently due to inductive effects, while the protonation effect for the α-carbon atom was attributed to a decrease in the bond order of the $N-C_\alpha$ bonds [77].

The resonances of C-5 in 3-substituted thiophenes and of C-4 in 2-substituted thiophenes are observed within a narrow shift range (5 – 6 ppm); similar electronic features have been postulated for these and the *meta* carbons in monosubstituted benzenes [257]. The substituent effects of several thiophenes [257] and thiazoles [258] can be calculated from the shift values of Table 4.55.

Several ^{13}C NMR investigations have dealt with aza analogs of polycyclic aromatic hydrocarbons [259 – 262]. It was concluded from molecular orbital calculations that the ^{13}C chemical shift variations in these polycyclic heteroaromatic compounds are caused predominantly by resonance and inductive effects [260]. The lone pair electrons of bridgehead nitrogens in 4-azaindenes are considerably delocalized, as was demonstrated by ^{13}C NMR measurements as well as by CNDO – SCF – MO calculations of members of this class of compounds [261].

In a ^{13}C NMR study on all possible methylindoles, the methyl substitution parameters were calculated and were used to predict the ^{13}C chemical shifts in dimethylindoles. In most cases there is a good agreement between experimental and calculated values (closer than 1 ppm) [262].

The ^{13}C chemical shifts of several aza analogs of polycyclic aromatic hydrocarbons are listed in Table 4.56. The numbering of the carbon atoms is seen from the formulae below:

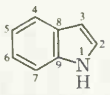

Indole

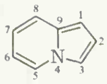

4-Azaindene

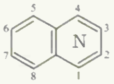

Azanaphthalenes

Using the methyl shift parameters of 4-methyl-, N-methyl- and 2,6-dimethylpiperidine as obtained from Table 4.55 [263, 265], the ^{13}C chemical shifts of higher substituted piperidines can be predicted with fairly good accuracy.

Table 4.55. ^{13}C Chemical Shifts of Selected Heterocycles δ [ppm].

Compound	C-2	C-3	C-4	C-5	C-6	Others	Solvent	Ref
Oxirane	39.5	39.5					neat	[50g]
Oxetane	72.6	22.9	72.6				neat	[50g]
Tetrahydrofuran	68.4	26.5	26.5	68.4			neat	[50g]
Tetrahydropyran	69.5	27.7	24.9	27.7	69.5		neat	[50g]
Thiirane	18.7	18.7					neat	[50g]
Thietane	27.5	29.7	27.5				neat	[50g]
Tetrahydrothiophene	31.7	31.2	31.2	31.7			$CDCl_3$	[233]
Thiacyclohexane	29.1	27.8	26.6	27.8	29.1		$CDCl_3$	[233]
Aziridine	18.2	18.2					$CDCl_3$	[255]
Azetidine	48.1	19.0					$CDCl_3$	[102]
Pyrrolidine	47.1	25.7	25.7	47.1			neat	[50g]
Piperidine	47.9	27.8	25.9	27.8	47.9		neat	[50g]
Piperazine, hexahydrate	47.7	47.7		47.7	47.7		$(CD_3)_2SO$	[50k]
1-Methylaziridine	28.5	28.5				48.6 (NCH_3)	neat	[50g]
1-Methylazetidine	57.7	17.5	57.7			46.4 (NCH_3)	neat	[50g]
1-Methylpyrrolidine	56.7	24.4	24.4	56.7		42.7 (NCH_3)	neat	[50g]
1-Methylpiperidine	57.2	26.4	26.4	26.4	57.2	48.0 (NCH_3)	neat	[50g]
2-Methylpiperidine	52.6	35.0	25.5	26.5	47.4	23.1 (CH_3)	C_6D_6	[50k]
3-Methylpiperidine	53.6	33.7	31.7	26.5	46.4	19.1 (CH_3)	neat	[265]
4-Methylpiperidine	46.5	35.4	31.3	35.4	46.5	22.2 (CH_3)	neat	[265]
1,2-Dimethylpiperidine	58.8	34.4	24.4	25.9	56.6	10.6 (CH_3); 43.4 (NCH_3)	neat	[265]
2,6-Dimethylpiperidine	52.0	33.9	24.7	33.9	52.0	22.8 (CH_3)	neat	[265]
2,2,6,6-Tetramethylpiperidine	48.9	38.1	18.0	38.1	48.9	31.7 (CH_3)	neat	[265]
1-Ethylpiperidine	53.9	25.8	24.4	25.8	53.9	52.5 (NCH_2); 11.9 (CH_3)	neat	[265]
2-Ethylpiperidine	58.3	32.4	25.0	26.5	47.8	30.0 (CH_2); 9.8 (CH_3)	neat	[265]
1-Methylpiperazine	56.0	45.9		45.9	56.0	46.5 (NCH_3)	neat	[265]
2-Methylpiperazine	51.4	53.5		46.0*)	47.0*)	19.6 (CH_3)	neat	[265]
2,5-Dimethylpiperazine	50.7	54.5		50.7	54.5	19.2 (CH_3)	neat	[265]
2,6-Dimethylpiperazine	52.9	51.8		51.8	52.9	19.5 (CH_3)	neat	[265]
1,4-Dimethylpiperazine	54.7	54.7		54.7	54.7	46.5 (NCH_3)	neat	[265]
1,2,4-Trimethylpiperazine	62.5	56.9		55.0*)	55.3*)	45.8 (4-NCH_3); 16.8 (CH_3); 41.9 (1-NCH_3)	neat	[265]
Furan	142.7	109.6	109.6	142.7			neat	[266]
2-Methylfuran	152.2	106.2	110.9	141.2		13.4 (CH_3)	neat	[266]
2,5-Dimethylfuran	149.2	106.2	106.2	149.9		12.9 (CH_3)	neat	[266]
Furan-2-aldehyde	153.2	121.6	112.8	148.4		178.0 (CHO)	$CDCl_3$	[50k]
Furan-2-carboxylic acid	146.6	119.5	113.5	148.5		161.4 (COOH)	$(CD_3)_2CO$	[50i]

Table 4.55. (Continued).

Compound	C-2	C-3	C-4	C-5	C-6	Others	Solvent	Ref.
Thiophene	124.4	126.2	126.2	124.4			neat	[257]
2-Methylthiophene	139.0	124.7	126.4	122.6		15.0 (CH_3)	neat	[257]
3-Methylthiophene	120.1	136.8	128.8	124.7		14.4 (CH_3)	neat	[257]
2-Bromothiophene	112.6	130.0	127.7	127.1			neat	[257]
3-Bromothiophene	126.9	110.4	130.1	123.0			neat	[257]
2-Iodothiophene	74.8	137.7	129.7	132.3			neat	[257]
3-Iodothiophene	128.1	78.7	135.2	129.2			neat	[257]
Thiophene-2-aldehyde	143.3	136.4	128.1	134.6		182.8 (CHO)	neat	[257]
Thiophene-3-aldehyde	137.1	142.6	124.9	127.3		184.7 (CHO)	neat	[257]
Selenophene	130.5	129.2	129.2	130.5			neat	[105]
Pyrrole	116.5	106.5	106.5	116.5			$CDCl_3$	[50k]
Pyrrole, anion	127.0	106.4	106.4	127.0			THF	[77]
1-Methylpyrrole	122.0	108.6	108.6	122.0		35.6 (NCH_3)	neat	[50g]
2-Methylpyrrole	127.5	105.8	108.0	116.9		11.5 (CH_3)	neat	[266]
2,5-Dimethylpyrrole	125.9	106.3	106.3	125.9		12.9 (CH_3)	neat	[266]
1-Methylpyrrole-2-carboxylic acid	121.8	120.0	108.4	130.7		166.6 (COOH); 37.0 (NCH_3)	$CDCl_3$	[102]
1-Methyl-2-acetylpyrrole	145.8	120.6	108.8	132.2		37.5 (NCH_3); 163.8 (CO); 27.0 (CH_3)	$(CD_3)_2CO$	[50i]
Pyrazole		134.5	105.4	134.5			neat	[76]
Pyrazole, anion		138.5	103.4	138.5			H_2O	[76]
Pyrazole, cation		135.0	108.9	135.0			H_2O	[76]
Imidazole	135.4		121.9	121.9			$CDCl_3$	[50k]
Imidazole, anion	145.05		126.7	126.7			H_2O	[77]
Imidazole, cation	134.55		120.0	120.0			H_2O	[77]
1,2,3-Triazole			130.5	130.5			CD_3OD	[102]
1,2,4-Triazole	147.4		147.4				CD_3OD	[102]
Isoxazole		150.0	104.5	158.9			$(CD_3)_2CO$	[258b]
Thiazole	152.2		142.4	118.5			neat	[258a]
2-Methylthiazole	164.0		141.1	118.0		16.9 (CH_3)	neat	[258a]
4-Methylthiazole	151.9		153.0	113.2		16.1 (CH_3)	neat	[258a]
2-Ethylthiazole	170.7		141.4	117.2		25.8 (CH_2); 13.2 (CH_3)	neat	[258a]
4-Ethylthiazole	151.9		159.1	111.7		24.3 (CH_2); 13.1 (CH_3)	neat	[258a]
2,4-Dimethylthiazole	163.3		151.5	111.9		17.4 (2-CH_3); 15.6 (4-CH_3)	neat	[258a]
4,5-Dimethylthiazole	148.1		149.0	125.3		13.3 (4-CH_3); 9.6 (5-CH_3)	neat	[258a]
Isothiazole		157.7	124.1	148.7			$(CD_3)_2CO$	[258b]
3-Methylisothiazole		167.1	124.5	149.1		18.5 (CH_3)	$(CD_3)_2CO$	[258b]
4-Methylisothiazole		159.3	134.8	144.3		11.8 (CH_3)	$(CD_3)_2CO$	[258b]
5-Methylisothiazole		158.3	124.2	163.7		12.7 (CH_3)	$(CD_3)_2CO$	[258b]

Table 4.55. (Continued).

Compound	C-2	C-3	C-4	C-5	C-6	Others	Solvent	Ref.
Pyridine	149.6	124.2	136.2	124.2	149.6		neat	[76]
Pyridine, cation	142.5	129.0	148.4	129.0	148.4		H_2O	[76]
Pyridine-N-oxide	139.1	125.6	126.1	125.6	139.1		$CDCl_3$	[102]
α,α-Dipyridyl	157.4	121.8	137.3	124.3	150.1		C_6D_6	[50i]
2-Methylpyridine	158.4	123.2	136.1	120.7	149.2	24.4 (CH_3)	$CDCl_3$	[50k]
3-Methylpyridine	150.1	132.8	136.1	122.9	146.7	18.3 (CH_3)	$CDCl_3$	[102]
4-Methylpyridine	149.5	124.6	147.0	124.6	149.5	20.8 (CH_3)	$CDCl_3$	[50k]
4-Methylpyridine-N-oxide	138.6	126.9	137.4	126.9	138.6	20.2 (CH_3)	$CDCl_3$	[50k]
2-Aminopyridine	161.4	109.7	138.6	113.6	149.2		$(CD_3)_2SO$	[50i]
3-Aminopyridine	137.7	145.7	122.1	125.2	138.8		$(CD_3)_2SO$	[102]
4-Aminopyridine	150.7	111.7	156.2	111.7	150.7		D_2O	[50k]
2-Bromopyridine	142.1	128.2	138.5	122.7	150.1		$CDCl_3$	[50k]
3-Bromopyridine	151.0	121.6	139.1	125.4	148.7		neat	[102]
4-Bromopyridine	152.5	127.5	133.4	127.5	152.5		neat	[102]
Pyridine-2-aldehyde	153.0	121.6	137.1	127.9	150.3	193.3 (CHO)	$CDCl_3$	[50k]
Pyridine-3-aldehyde	152.3	132.4	136.5	125.1	155.2	192.2 (CHO)	$CDCl_3$	[102]
Pyridine-4-aldehyde	151.5	122.9	141.9	122.9	151.5	192.6 (CHO)	$CDCl_3$	[102]
Pyridine-3-carboxylic acid, methyl ester	149.2	124.7	135.4	121.9	151.6	163.7 (COO); 51.7 (OCH_3)	$CDCl_3$	[50k]
2-Acetylpyridine	154.3	121.5	137.4	127.0	148.5	199.5 (CO); 25.0 (CH_3)	neat	[102]
3-Acetylpyridine	149.8	132.4	135.7	124.0	153.7	197.6 (CO); 26.8 (CH_3)	$(CD_3)_2SO$	[50k]
4-Acetylpyridine	151.2	121.5	143.2	121.5	151.2	198.3 (CO); 26.8 (CH_3)	$(CD_3)_2SO$	[50k]
Phosphabenzene	154.1	133.6	128.8	133.6	154.1		$CDCl_3$	[267]
2-Methylphosphabenzene	166.9	130.7	128.7	134.1	153.9	24.7 (CH_3)	$CDCl_3$	[267]
Arsabenzene	167.7	133.2	128.2	133.2	167.7		$CDCl_3$	[267]
2-Methylarsabenzene	182.9	131.0	129.2	134.4	168.3	26.0 (CH_3)	$CDCl_3$	[267]
Stibabenzene	178.3	134.4	127.4	134.4	178.3		$CDCl_3$/ Diglyme	[267]
Pyridazine		152.8	127.6	127.6	152.8		neat	[76]
Pyridazine, cation		151.7	137.7	137.7	151.7		H_2O	[76]

Table 4.55. (Continued).

Compound	C-2	C-3	C-4	C-5	C-6	Others	Solvent	Ref.
Pyrimidine	158.4		156.4	121.4	156.4		$CDCl_3$	[50i]
Pyrimidine, cation	152.2		158.8	125.1	158.8		H_2O	[76]
Pyrimidine, dication	151.0		159.0	128.1	159.0		H_2O	[76]
2,4,6-Trichloropyrimidine	160.5		163.2	120.3	163.2		C_6D_6	[50i]
2,4,6-Triaminopyrimidine	164.0		165.5	75.5	165.5		$(CD_3)_2SO$	[50i]
4,5,6-Triaminopyrimidine	144.3		149.9	150.4	149.9		$(CD_3)_2SO$	[50i]
Uracil	151.4		164.2	100.3	142.1		$(CD_3)_2SO$	[256]
5-Fluorouracil	150.0		158.3	139.7	126.1		$(CD_3)_2SO$	[256]
5-Chlorouracil	150.0		159.7	106.0	139.6		$(CD_3)_2SO$	[256]
5-Bromouracil	150.2		159.9	94.5	142.0		$(CD_3)_2SO$	[256]
5-Iodouracil	150.7		161.3	67.6	146.9		$(CD_3)_2SO$	[256]
5-Cyanouracil	149.8		160.9	87.0	151.7	114.5 (CN)	$(CD_3)_2SO$	[256]
5-Nitrouracil	150.4		156.2	126.0	148.3		$(CD_3)_2SO$	[256]
5-Aminouracil	149.5		161.4	116.4	121.6		$(CD_3)_2SO$	[256]
5-Hydroxyuracil (Barbituric acid)	149.7		161.1	131.5	120.4		$(CD_3)_2SO$	[256]
5-Methoxyuracil	150.7		160.8	135.9	122.6	58.2 (OCH_3)	$(CD_3)_2SO$	[256]
5-Hydroxymethyluracil	150.9		163.4	112.5	137.8	55.7 (CH_2OH)	$(CD_3)_2SO$	[256]
Pyrazine	145.6	145.6		145.6	145.6		H_2O	[76]
Pyrazine, cation	142.9	142.9		142.9	142.9		H_2O	[76]
Pyrazine, dication	144.0	144.0		144.0	144.0		H_2O	[76]
2,5-Dimethylpyrazine	150.6	143.5		150.6	143.5	20.9 (CH_3)	$CDCl_3$	[50k]
s-Triazine	166.5		166.5		166.5			[255]
s-Tetrazine		160.9		160.9				[255]

*) Assignments interchangeable.

Table 4.56. ^{13}C Chemical Shifts of Aza Analogs of Polycyclic Aromatic Hydrocarbons (δ Values (ppm) Relative to TMS = 0).

	Quinoline	Isoquinoline	Quinoxaline	Phthalazine	Cinnoline	Quinazoline
Solvent	neat	neat	CHCl$_3$	CHCl$_3$	CHCl$_3$	CHCl$_3$
Ref.	[260]	[260]	[260]	[260]	[260]	[260]
C-Atom						
1		153.10		152.00		
2	150.85		145.50			160.50
3	121.55	143.80	145.50		146.10	
4	136.05	120.85		152.00	124.65	155.70
5	128.35	126.80	129.80	126.65	127.90	127.40
6	126.80	130.50	129.90	133.20	132.30	127.95
7	129.75	127.55	129.90	133.20	132.10	134.15
8	130.10	127.85	129.80	126.65	129.50	128.55
9	149.00	129.10	143.20	126.65	151.00	150.15
10	128.70	136.00	143.20	126.65	126.80	125.20
11						
12						
13						
14						
CH$_3$						

Table 4.56. (Continued).

	4-Azaindene	1,4-Diaza-indene	2,4-Diaza-indene	3,4-Diaza-indene	Acridine	Phenazine
Solvent	CHCl$_3$	neat	CHCl$_3$	neat	CHCl$_3$	CHCl$_3$
Ref.	[261]	[261]	[261]	[261]	[261]	[261]
C-Atom						
1	99.45		119.95	96.25	129.55	130.95
2	114.05	134.05		141.30	128.35	130.30
3	113.00	113.40	128.35		125.45	130.30
4					130.30	130.95
5	125.60	126.95	122.80	128.10	130.30	130.95
6	110.45	112.20	112.65	110.85	125.45	130.30
7	117.15	124.60	119.35	112.35	128.35	130.30
8	119.55	117.60	118.15	117.35	129.55	130.95
9	133.35	145.60	130.65	139.50		
10					135.90	
11					126.55	144.00
12					149.15	144.00
13					149.15	144.00
14					126.55	144.00
CH$_3$						

Table 4.56. (Continued).

	1,4,8-Triazaindene	Indole	1-Methylindole	2-Methylindole	3-Methylindole	4-Methylindole
Solvent	DMSO	dioxane	dioxane	dioxane	dioxane	dioxane
Ref.	[261]	[261]	[261]	[261]	[261]	[261]
C-Atom						
1						
2	135.15	124.85	129.00	135.40	122.45	123.90
3	112.65	102.35	101.00	100.10	111.15	100.75
4		120.95	121.00	119.75	119.10	129.90
5	136.05	122.00	121.60	120.80	121.95	121.90
6	109.40	119.95	119.45	119.55	119.30	119.85
7	150.95	111.55	109.50	110.60	111.45	109.00
8		128.45	129.10	129.60	128.90	128.40
9	148.85	135.85	137.25	136.80	137.00	136.25
10						
11						
12						
13						
14						
CH_3			31.80	13.10	9.55	21.30

Table 4.56. (Continued).

	5-Methylindole	6-Methylindole	7-Methylindole	1,2-Dimethylindole	2,3-Dimethylindole	2,7-Dimethylindole	2,3,5-Trimethylindole
Solvent	dioxane	dioxane	dioxane	dioxane	dioxane	dioxane	dioxane
Ref.	[262]	[262]	[262]	[262]	[262]	[262]	[262]
C-Atom							
1							
2	124.70	124.00	124.45	137.75	131.05	134.85	130.90
3	101.80	102.00	102.70	99.70	106.55	100.65	106.00
4	123.45	120.45	118.60	119.70	118.10	117.35	122.20
5	128.50	121.55	122.40	120.40	120.85	121.35	127.50
6	120.50	131.20	120.00	119.30	119.00	119.55	117.85
7	111.45	111.30	120.55	108.90	110.45	119.65	109.90
8	128.85	126.35	128.10	128.55	129.95	129.15	130.15
9	134.95	137.00	136.10	136.75	135.95	136.20	134.30
10							
11							
12							
13							
14							
CH_3	21.20	21.40	16.35	28.35 11.95	10.85 8.20	16.35 13.10	21.25 10.85 8.10

The ^{13}C resonances of selected pyridine, pyrimidine, purine, and isoalloxazine derivatives are reviewed in Section 5.3 and 5.5, respectively.

Typical one bond and longer-range C – H coupling constants of some heterocycles were listed in Tables 3.7 and 3.9. If available, C – H coupling constants are informative in assigning the ^{13}C NMR spectra of differently substituted heterocycles. One simple but representative example is the pair 2,4,6- and 4,5,6-triaminopyrimidine [50i]. In the 2,4,6-isomer, C-5 resonates as a doublet at 75.5 ppm with a one-bond C – H coupling of 167.7 Hz. In the 4,5,6-isomer, however, the larger chemical shift (144.3 ppm) and the stronger coupling (202.5 Hz) of the doublet signal characterize C-2 of the pyrimidine ring.

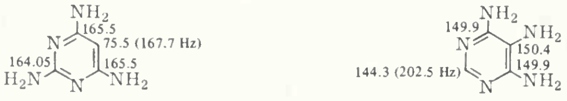

2,4,6- Triaminopyrimidine 4,5,6-

Longer-range C – H couplings are sometimes also useful assignment aids. An example is Fig. 4.12. In the case of 2,3,9,10-tetracyano-6,13-dibutyl-1,8-dihydro-tetraaza[14]annulene, no unequivocal assignment of the nitrile and ethylene carbons (C-2,3,9,10) can be achieved in the wide-band decoupled spectrum because of very similar chemical shifts. The coupled spectrum, however,

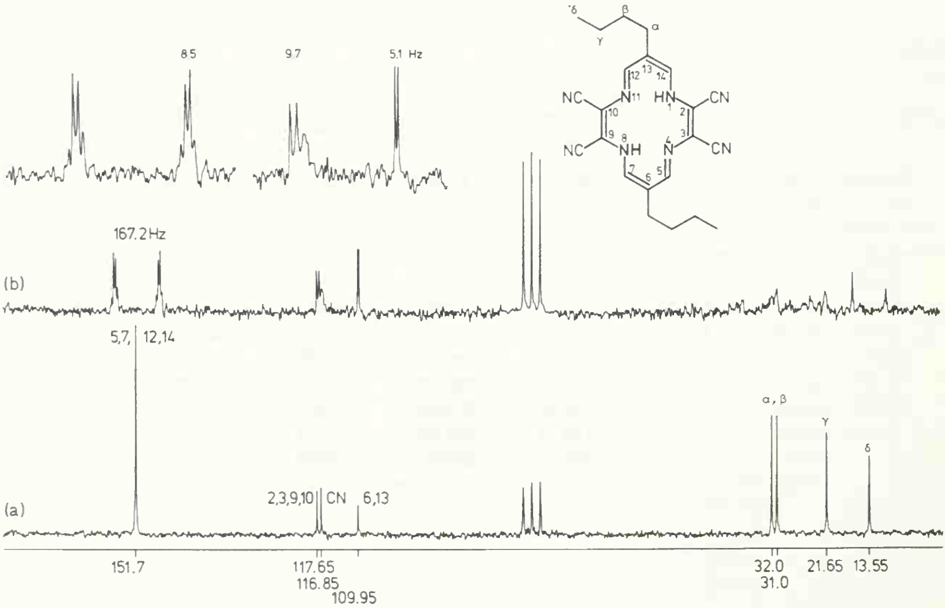

Fig. 4.12. ^{13}C NMR spectrum of 2,3,9,10-tetracyano-6,13-dibutyl-1,8-dihydro-tetraaza[14]annulene, 20 MHz, 25 °C, in deuteriochloroform; (a) proton-broadband decoupled, 2000 scans; (b) gated decoupled, 10000 scans, with expanded partial spectra.

clearly shows a well resolved doublet at 117.65 ppm with $^3J_{CH} \approx 9.7$ Hz which does not collapse upon addition of deuterium oxide, thus indicating a three-bond coupling with the azomethine proton and confirming the assignment as made in Fig. 4.12.

4.12. Carbocations

Due to their positive charge, carbocation carbons are highly deshielded [268]. The *t*-butyl, *t*-amyl and *t*-hexyl cation carbons have similar shifts (327.9 to 331.9 ppm); the alkyl substituent parameters are therefore not additive. Because of larger π electron densities, carbenium ion carbons of hydroxycarbenium moieties are much more shielded than carbons of corresponding aliphatic cations:

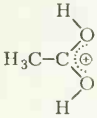

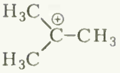

The ^{13}C shifts of carbon atoms attached to halogen in homologous alkyl and alkenyl halides correlate linearly with the electronegativities of the halogens [269]. Due to the back-donation of the halogen atoms the halocarbenium carbon shifts do not obey a similar rule [269]. The ^{13}C chemical shift differences between carbon atoms bearing halogens in halocarbenium ions and corresponding haloolefins may be used for the determination of the degree of halogen back-donation [269].

^{1}H and ^{13}C NMR studies have demonstrated that α,β-unsaturated aldehydes and ketones form hydroxyallyl cations in $HSO_3F-SbF_5-SO_2ClF$ solutions. The positive charge is dispersed between the carbonyl oxygen and the neighboring carbon atoms, with charge density decreasing from C-2 to C-3 to C-1 [271].

If a solution of benzene in SO_2ClF is added to a mixture of $HF-SbF_5$ in SO_2ClF at −78 °C, an average ^{13}C NMR shift value of 144.5 ppm for all six carbons of the benzenonium ion can be recorded by the INDOR technique [272]. Measurements on a series of monoalkylbenzenonium ions demonstrated that a variation of the alkyl residue results in larger shift changes only in the case of the C-4 resonance [272].

A plot of the ^{13}C chemical shifts of the carbenium carbons in homologous series of benzyl cations *versus* the σ^+ constants of Brown yields a straight line [273]. Brown's σ^+ parameters reflect the influence of aromatic substituents on the stability of intermediate substituted benzylic cations relative to the parent ions [274].

The ^{13}C chemical shifts of selected carbenium ions are given in Table 4.57.

4.13. Substituent Increments, Summary and Practical Use

In the following, substituent increments on carbon shielding in basic organic skeletons are summarized. Their practical use according to eq. (4.12) is illustrated by a few representative examples. Most of the tabulated increments are not based on regressional analyses and deviations may be as large as ±0.5 ppm.

Table 4.57. ^{13}C Chemical Shifts of Carbenium Ions (δ Values (ppm) Relative to TMS = 0).

Ion	C-1	C-2	C-3	C-4	C-5	C-6	Solvent	Temp. °C	Ref.
Diethylmethyl-carbenium ion	334.0						$SO_2ClF-SbF_5$	−20	[56]
t-Amyl cation	333.8						$SO_2ClF-SbF_5$	−60	[56]
t-Butyl cation	330.0						$SO_2ClF-SbF_5$	−20	[56]
Isopropyl cation	319.6	61.8					$SO_2ClF-SbF_5$	−20	[56]
Dimethylhydroxy-carbenium ion	250.3						$SO_2-FSO_3H-SbF_5$	−50	[56]
Methylhydroxy-carbenium ion	237.2						$SO_2-FSO_3H-SbF_5$	−50	[56]
Hydroxy-carbenium ion	223.8						$SO_2-FSO_3H-SbF_5$	−50	[56]
Methyldihydroxy-carbenium ion	196.2						$SO_2-FSO_3H-SbF_5$	−30	[56]
Dihydroxy-carbenium ion	177.6						$SO_2-FSO_3H-SbF_5$	−30	[56]
Trihydroxy-carbenium ion	166.6						$SO_2-FSO_3H-SbF_5$	−50	[56]
Methoxydihydroxy-carbenium ion	163.6						$SO_2-FSO_3H-SbF_5$	−30	[56]
Dimethylcyclopropyl-carbenium ion	281.4	29.1 (CH_3)					SO_2-SbF_5	−60	[56]
Dimethylphenyl-carbenium ion	255.7						SO_2-SbF_5	−60	[56]
Diphenyl-carbenium ion	200.2						SO_2-SbF_5	−60	[56]
Triphenyl-carbenium ion	212.7						SO_2-SbF_5	−60	[56]
Dimethylfluoro-carbenium ion	337.3						SbF_5-SO_2	−78	[269]
Dimethylchloro-carbenium ion	314.6						SbF_5-SO_2	−78	[269]
Dimethylbromo-carbenium ion	320.6						SbF_5-SO_2	−78	[269]
Phenylmethylfluoro-carbenium ion	234.1						SbF_5-SO_2	−78	[269]
Phenylmethylchloro-carbenium ion	237.0						SbF_5-SO_2	−78	[269]
Phenylmethylbromo-carbenium ion	240.9						SbF_5-SO_2	−78	[269]
Cyclopentyl cation	97.1						SbF_5-SO_2ClF	−70	[270]
Norbornyl cation	90.7	30.0	36.4				SbF_5-SO_2	−70	[270]
Protonated acrolein	211.5	133.1	176.5				$FSO_3H-SbF_5-SO_2ClF$	−80	[271]
Protonated crotonaldehyde	205.9	130.6	201.1				$FSO_3H-SbF_5-SO_2ClF$	−80	[271]
Protonated tiglaldehyde	205.2	141.0	198.1				$FSO_3H-SbF_5-SO_2ClF$	−80	[271]
Protonated methyl vinyl ketone	225.5	133.2	157.6				$FSO_3H-SbF_5-SO_2ClF$	−80	[271]
Protonated 2-cyclopenten-1-one	230.8	132.9	182.2				$FSO_3H-SbF_5-SO_2ClF$	−80	[271]
Protonated 2-cyclohexen-1-one	224.0	127.5	191.3				$FSO_3H-SbF_5-SO_2ClF$	−80	[271]
Protonated 3,5-dimethyl-2-cyclohexen-1-one	211.6	122.4	177.6				$FSO_3H-SbF_5-SO_2ClF$	−80	[271]

Table 4.57. (Continued).

Ion	C-1	C-2	C-3	C-4	C-5	C-6	Solvent	Temp. °C	Ref.
Benzenonium ion	144.5	144.5	144.5	144.5	144.5	144.5	$HF-SbF_5-SO_2ClF$	−78	[272]
4-Methylbenzenonium ion	47.4	179.1	137.3	199.8	137.3	179.1	$HF-SbF_5-SO_2ClF$	−90	[272]
4-Ethylbenzenonium ion	47.1	179.2	136.3	208.5	136.3	179.2	$HF-SbF_5-SO_2ClF$	−90	[272]
4-Propylbenzenonium ion	47.7	179.4	136.8	203.0	136.8	179.4	$HF-SbF_5-SO_2ClF$	−90	[272]
4-Isopropylbenzenonium ion	46.0	177.8	132.9	210.5	132.9	177.8	$HF-SbF_5-SO_2ClF$	−90	[272]
Mesitylenonium ion	52.1	194.8	133.8	194.8	133.8	194.8	$HF-SbF_5-SO_2ClF$	−90	[272]
p-Methoxybenzyl cation	167.5						$SbF_5-SO_2ClF-FSO_3H$	≈ −80	[273]
α-Phenylethyl cation	232.5						$SbF_5-SO_2ClF-FSO_3H$	≈ −80	[273]
p-Methoxy-α-phenylethyl cation	197.5						$SbF_5-SO_2ClF-FSO_3H$	≈ −80	[273]
p-Methyl-α-phenylethyl cation	220.5						$SbF_5-SO_2ClF-FSO_3H$	≈ −80	[273]
p-Fluoro-α-phenylethyl cation	231.5						$SbF_5-SO_2ClF-FSO_3H$	≈ −80	[273]
p-Trifluoromethyl-α-phenylethyl cation	245.5						$SbF_5-SO_2ClF-FSO_3H$	≈ −80	[273]
Cumyl cation	253.5						$SbF_5-SO_2ClF-FSO_3H$	≈ −80	[273]
p-Methoxycumyl cation	217.5						$SbF_5-SO_2ClF-FSO_3H$	≈ −80	[273]
p-Methylcumyl cation	241.5						$SbF_5-SO_2ClF-FSO_3H$	≈ −80	[273]
p-Fluorocumyl cation	246.5						$SbF_5-SO_2ClF-FSO_3H$	≈ −80	[273]
p-Bromocumyl cation	250.5						$SbF_5-SO_2ClF-FSO_3H$	≈ −80	[273]
m-Fluorocumyl cation	259.5						$SbF_5-SO_2ClF-FSO_3H$	≈ −80	[273]
p-Trifluoromethylcumyl cation	267.5						$SbF_5-SO_2ClF-FSO_3H$	≈ −80	[273]
Phenylmethylethyl-carbenium ion	259.5						$SbF_5-SO_2ClF-FSO_3H$	≈ −80	[273]
p-Methoxyphenylmethylethyl-carbenium ion	222.5						$SbF_5-SO_2ClF-FSO_3H$	≈ −80	[273]
p-Methylphenylmethylethyl-carbenium ion	246.5						$SbF_5-SO_2ClF-FSO_3H$	≈ −80	[273]
p-Trifluoromethylphenylmethylethyl-carbenium ion	274.5						$SbF_5-SO_2ClF-FSO_3H$	≈ −80	[273]
Phenylmethylisopropyl-carbenium ion	264.7						$SbF_5-SO_2ClF-FSO_3H$	≈ −80	[273]
p-Methoxyphenylmethylisopropyl-carbenium ion	225.5						$SbF_5-SO_2ClF-FSO_3H$	≈ −80	[273]
p-Methylphenylmethylisopropyl-carbenium ion	249.5						$SbF_5-SO_2ClF-FSO_3H$	≈ −80	[273]
p-Trifluoromethylphenylmethylisopropyl-carbenium ion	269.5						$SbF_5-SO_2ClF-FSO_3H$	≈ −80	[273]
p-Methoxyphenylmethyl-*t*-butyl-carbenium ion	236.5						$SbF_5-SO_2ClF-FSO_3H$	≈ −80	[273]

$$\delta_k = \delta_{k(RH)} + \sum Z_{ik} (+ \sum S_i) \tag{4.12}$$

δ_k: ^{13}C shift of carbon k to the substituent X;
($k = \alpha, \beta, \gamma, \ldots$ in aliphatic compounds and 1, 2, 3, 4, ... or 1, o m p in heteroaromatic and aromatic compounds);
$\delta_{k(RH)}$: ^{13}C shift of corresponding carbon k in parent hydrocarbon RH;
Z_{ik}: ^{13}C shift increment of the substituent X in position i to the considered carbon k;
S_i: steric correction(s) in *cis*- and *trans*-cyclohexanes and alkenes only;

4.13.1. Substituted Alkanes

It can be seen from Table 4.58 that the α increments can be reasonably rationalized in terms of inductive effects (Pauling electronegativities) while the shielding of carbons γ to the sub-

Table 4.58. Empirical Increments [ppm] of Substituents X Replacing H in Alkanes [50e–k, 275].

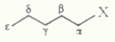

n

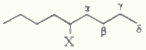

iso

–X	Z_α		Z_β		Z_γ	Z_δ	Z_ε
	n	*iso*	*n*	*iso*			
–F	70	63	8	6	–7	0	0
–Cl	31	32	10	10	–5	–0.5	0
–Br	20	26	10	10	–4	–0.5	0
–I	–7	4	11	12	–1.5	–1	0
–O–	57	51	7	5	–5	–0.5	0
$-OCOCH_3$	52	45	6.5	5	–4	0	0
–OH	49	41	10	8	–6	0	0
$-SCH_3$	20.5	–	6.5	–	–2.5	0	0
–S–	10.5	–	11.5	–	–3.5	–0.5	0
–SH	10.5	11	11.5	11	–3.5	0	0
$-NH_2$	28.5	24	11.5	10	–5	0	0
–NHR	36.5	30	8	7	–4.5	–0.5	–0.5
$-NR_2$	40.5	–	5	–	–4.5	–0.5	0
$-\overset{+}{N}H_3$	26	24	7.5	6	–4.5	0	0
$-\overset{+}{N}R_3$	30.5	–	5.5	–	–7	–0.5	–0.5
$-NO_2$	61.5	57	3	4	–4.5	–1	–0.5
–NC	27.5	–	6.5	–	–4.5	0	0
–CN	3	1	2.5	3	–3	0.5	0
$>$C=NOH *syn*	11.5	–	0.5	–	–2	0	0
$>$C=NOH *anti*	16	–	4.5	–	–1.5	0	0
–CHO	30	–	–0.5	–	–2.5	0	0
$>$CO	23	–	3	–	3	0	0
$-COCH_3$	29	23	3	1	–3.5	0	0
–COCl	33	28	2	2	–3.5	0	0
$-COO^-$	24.5	20	3.5	3	–2.5	0	0
$-COOCH_3$ (and C_2H_5)	22.5	17	2.5	2	–3	0	0
$-CONH_2$	22	–	2.5	–	–3	–0.5	0
–COOH	20	16	2	2	–3	0	0
–Phenyl	23	17	9	7	–2	0	0
$-CH{=}CH_2$	20	–	6	–	–0.5	0	0
$-C{\equiv}CH$	4.5	–	5.5	–	–3.5	0.5	0

stituent is generally attributed to a steric polarization of the γ C – H bond. Inductive and electric field effects contribute to the β increments. As electric fields can be evaluated only in rare cases, no general trend for the β effect has been recognized so far. Frequently, the α and β increments depend on whether a substituent X is terminal (*n*) or central (*iso*). If available, the *iso* increments are also given in Table 4.58.

The increments of Table 4.58 permit a prediction of carbon shifts in substituted alkanes. Thereby, they provide an assignment aid which is particularly useful when proton decoupling experiments (off-resonance, gated, selective) fail because of equal multiplicities ($(-CH_2)_n$ chains) or signal overcrowding in the ^{13}C and ^1H NMR spectra. The practical use of the increments is illustrated for 1,4-dibromopentane and lysine.

1,4-Dibromopentane

			5	4	3	2	1	
reference compound:		pentane	CH_3	CH_2	CH_2	CH_2	CH_3	
		δ [ppm]	13.7	22.6	34.6	22.6	13.7	(Table 4.1)
increments	Z_{nBr}	*[ppm]*	*0*	*−0.5*	*−4*	*10*	*20*	(Table 4.58)
	Z_{isoBr}	*[ppm]*	*10*		*10*	*−4*	*−0.5*	(Table 4.58)
predicted shifts		δ *[ppm]*	*23.7*	*48.1*	*40.6*	*28.6*	*33.1*	
measured shifts		δ [ppm]	26.5	50.0	39.2	30.7	32.8	(in $CDCl_3$)

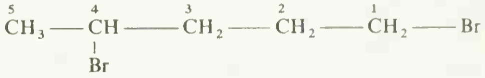
$$\overset{5}{CH_3}-\underset{Br}{\overset{4}{CH}}-\overset{3}{CH_2}-\overset{2}{CH_2}-\overset{1}{CH_2}-Br$$

Lysine (2,6-Diaminohexanedioic acid)

reference compound:		pentane	CH_3	CH_2	CH_2	CH_2	CH_3	
		δ [ppm]	13.7	22.6	34.6	22.6	13.7	(Table 4.1)
increments	Z_{COOH}	*[ppm]*	*0*	*0*	*−3*	*2*	*20*	(Table 4.58)
	Z_{nNH_2}	*[ppm]*	*28.5*	*11.5*	*−5*	*0*	*0*	(Table 4.58)
	Z_{isoNH_2}	*[ppm]*	*0*	*0*	*−5*	*10*	*24*	(Table 4.58)
predicted shifts		δ *[ppm]*	*42.2*	*34.1*	*21.6*	*34.6*	*57.7*	
measured shifts		δ [ppm]	40.0	30.7	22.4	27.2	55.3	(in D_2O)

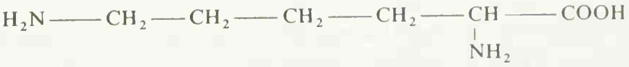
$$H_2N-CH_2-CH_2-CH_2-CH_2-\underset{NH_2}{CH}-COOH$$

Significant differences between predicted and measured ^{13}C chemical shifts as found for some of the lysine carbons indicate that shift increments are not additive when interactions between substituents are involved. Although deviations from increment additivity are frequently observed, the sequence of ^{13}C signals can be qualitively evaluated in many cases.

4.13.2. Substituted Cyclohexanes and Bicyclo[2.2.2]heptanes

Table 4.59 summarizes the increments of some substituents in cyclohexanes. The general scope is similar to that observed for alkyl derivatives (deshielding in α- and β- and shielding in γ position). Additionally, the δ carbons are slightly shielded by substituents. Moreover, axial substituents mostly cause a larger shielding of the carbons in α, β and γ position ($\delta_{eq} > \delta_{ax}$). Concerning the γ effect, the γ *gauche* type shielding (Chapter 3.1.3.8) observed for axial substituents is significantly larger than the γ *trans* effect of equatorial groups (Table 4.59).

Table 4.59. Empirical Increments of Equatorial and Axial Substituents in Cyclohexane [276–278]; Reference Compound: Cyclohexane with δ = 27.6 (±0.5) ppm and Correction terms *S* for 1,1- and 1,2-Dimethylcyclohexanes.

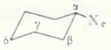

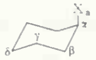

X	$Z_{\alpha a}$	$Z_{\alpha e}$	$Z_{\beta e}$	$Z_{\beta a}$	$Z_{\gamma e}$	$Z_{\gamma a}$	$Z_{\delta e}$	$Z_{\delta a}$
CH_3	6	1.5	9	5.5	0	−6.5	−0.3	0
F	64	61	6	3	−3	−7	−3	−2
Cl	33	33	11	7	0	−6	−2	−1
Br	25	28	12	8	1	−6	−1	−1
I	3	11	13	9	2	−4	−2	−1
CN	1	0	3	−1	−2	−5	−2	−1
NC	25	23	7	4	−3	−7	−2	−2
OH	43	39	8	5	−3	−7	−2	−1
OCH_3	52	47	4	2	−3	−7	−2	−1
$OCOCH_3$	46	42	5	3	−2	−6	−2	0
NH_2	24		10		−2		−1	

Correction terms [ppm]

for 1,1-Dimethylcyclohexane: $Z_{\alpha_a\alpha_e} = -3.8$
$Z_{\beta_a\beta_e} = -1.3$
$Z_{\gamma_a\gamma_e} = 2.0$

for 1,2-Dimethylcyclohexane: $Z_{\alpha_e\beta_a} = -2.9$ (*cis*)
$Z_{\alpha_e\beta_e} = -2.9$ (*trans*)
$Z_{\alpha_a\beta_e} = -3.4$ (*cis*)
$Z_{\beta_e\gamma_a} = -0.8$ (*cis*)
$Z_{\beta_a\gamma_e} = 1.6$ (*cis*)

The application of these increments is illustrated for 1-*trans*-2-*cis*-3-trimethylcyclohexane (data from Table 4.7) and *cis*-3-methylcyclohexanol (data from Table 4.24).

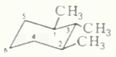

1-*trans*-2-*cis*-3-Trimethylcyclohexane

	C-1,3		C-2		C-4,6		C-5
	27.6		27.6		27.6		27.6
$+ Z_{\alpha e}$	6.0						
$+ Z_{\beta e}$	9.0	$+ Z_{\alpha e}$	6.0	$+ Z_{\beta e}$	9.0	$+ 2Z_{\gamma e}$	0.0
$+ Z_{\gamma e}$	0.0	$+ 2Z_{\beta e}$	18.0	$+ Z_{\gamma e}$	0.0	$+ Z_{\delta e}$	−0.2
$+ Z_{\alpha e\beta e}$	−2.5	$+ 2Z_{\alpha e\beta e}$	5.0	$+ Z_{\delta e}$	−0.2		
calculated δ	*40.1*		*46.6*		*36.4*		*27.4 ppm*
measured δ	39.15		46.25		36.45		26.45 ppm

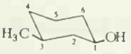

cis-3-Methylcyclohexanol

	predicted [*ppm*]	(measured) [ppm]
$\delta_1 = 27.6 + Z_{\alpha e(OH)} + Z_{\gamma e(CH_3)} = 27.6 + 43 + 0$	$= 70.6$	(70.5)
$\delta_2 = 27.6 + Z_{\beta e(OH)} + Z_{\beta e(CH_3)} = 27.6 + 8 + 9$	$= 44.6$	(44.0)
$\delta_3 = 27.6 + Z_{\gamma e(OH)} + Z_{\alpha e(CH_3)} = 27.6 - 3 + 6$	$= 30.6$	(31.7)
$\delta_4 = 27.6 + Z_{\delta e(OH)} + Z_{\beta e(CH_3)} = 27.6 - 2 + 9$	$= 34.6$	(34.8)
$\delta_5 = 27.6 + Z_{\gamma e(OH)} + Z_{\gamma e(CH_3)} = 27.6 - 3 + 0$	$= 24.6$	(24.4)
$\delta_6 = 27.6 + Z_{\beta e(OH)} + Z_{\delta e(CH_3)} = 27.6 + 8 - 0.3$	$= 35.3$	(34.4)

γ *gauche* and γ *trans* type interactions as discussed for cyclohexanes are also obvious from the shift increments of selected *endo*- and *exo*-substituted norbornanes (Table 4.60). The increased shielding of the γ carbon in the *endo* isomers and the γ'' carbon (C-7) in the *exo* isomers are typical γ *gauche* effects. The shielding differences are useful for configurational assignments in that class of compounds.

Table 4.60. Empirical Increments of 2-*endo* and 2-*exo* Substituents in Norbornanes [50f, 279].

Reference Compound: Norbornane

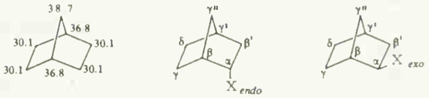

X	Z_α	Z_β	$Z_{\beta'}$	Z_γ	$Z_{\gamma'}$	Z_δ	$Z_{\gamma''}$
endo-CH_3	4.5	5.4	10.6	−7.7	1.4	0.5	0.2
exo-CH_3	6.7	6.7	10.1	−1.1	0.5	0.2	−3.7
endo-CN	0.1	3.4	5.5	−4.9	0.2	−0.7	0.0
exo-CN	1.0	5.5	6.3	−1.6	−0.3	−1.5	−1.3
endo-COOH	16.2	4.2	2.1	−4.8	0.9	−0.6	1.9
exo-COOH	16.7	4.6	4.4	−1.0	−0.2	−0.3	−1.8
endo-$COOCH_3$	15.9	4.0	2.2	−5.0	0.7	−0.7	1.7
exo-$COOCH_3$	16.4	5.1	4.2	−1.4	−0.4	−1.1	−2.1
endo-OH	42.4	6.3	9.5	−9.7	0.9	0.2	−0.9
exo-OH	44.3	7.7	12.3	−5.2	−1.0	−1.3	−4.1
endo-NH_2	23.3	6.8	10.5	−9.5	1.2	0.6	0.3
exo-NH_2	25.3	8.9	12.4	−3.1	−0.4	−1.2	−4.4

4.13.3. Substituted Alkenes

Table 4.61 shows the empirical increments obtained for substituents in position *i* relative to an olefinic carbon denoted as *k*. Correction terms *S* are required for *cis* and *geminal* substituents. As an application of the increments (Table 4.61) the olefinic carbon shifts of (*Z*)-4-Methyl-2-pentenoic acid are predicted:

Table 4.61. (a) Empirical Increments Z [ppm] for Substituents in Position $i\,(i')$ Relative to the Olefinic Carbon k [190].
(b) Correction Terms $S_{ii'}$ [ppm] for Alkyl Groups *cis*, *trans* and *geminal* to each other [190]. The Reference Compound is Ethylene with δ_{RH} = 123.5 ± 0.5 ppm.

(a)	γ' —	β' —	α' —	C=C	— α	— β	— γ
X_i	$Z_{\gamma'}$	$Z_{\beta'}$	$Z_{\alpha'}$	k	Z_α	Z_β	Z_γ
$-\mathrm{C}\lessdot$	1.5	−1.8	−7.9		10.6	7.2	−1.5
$-\mathrm{C_6H_5}$			−11		12		
$-\mathrm{C(CH_3)_3}$			−14		25		
$-\mathrm{Cl}$		2	−6		3	−1	
$-\mathrm{Br}$		2	−1		−8	0	
$-\mathrm{I}$			7		−38		
$-\mathrm{OH}$		−1	—		—	6	
$-\mathrm{OR}$		−1	−39		29	2	
$-\mathrm{OCOCH_3}$			−27		18		
$-\mathrm{CHO}$			13		13		
$-\mathrm{COCH_3}$			6		15		
$-\mathrm{COOH}$			9		4		
$-\mathrm{COOR}$			7		6		
$-\mathrm{CN}$			15		−16		

(b)		
	$S_{\alpha\alpha'(trans)}$:	0.0
	$S_{\alpha\alpha'(cis)}$:	−1.1
	$S_{\alpha\alpha(gem)}$:	−4.8
	$S_{\alpha'\alpha'(gem)}$	2.5
	$S_{\beta\beta}$:	2.3

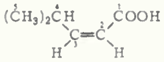

(*Z*)-4-Methyl-2-pentenoic acid

	C-3	C-2	
δ_{RH}	*123.5*	*123.5*	δ_{RH}
$Z_{\alpha' COOH}$	*9*	*4*	$Z_{\alpha COOH}$
$Z_{\alpha C}$	*10.6*	*−7.9*	$Z_{\alpha' C}$
$2Z_{\beta' C}$	*14.4*	*−3.6*	$2Z_{\beta' C}$
$S_{\alpha\alpha'(cis)}$	*−1.1*	*−1.1*	$S_{\alpha\alpha'(cis)}$ *(values for C)*
predicted	*156.4*	*114.9 ppm*	
measured	158.3	116.4 ppm (Table 4.40)	

4.13.4. Substituted Benzenes

Most of the substituent increments presented in Table 4.62 can be derived from ^{13}C shifts of benzenoid carbons in monosubstituted benzenes as listed in Table 4.49. It was pointed out (Section 4.10.1 and 3.1.3.6) that the α effect (Z_1) is predominantly inductive. The *o* increment (Z_o) arises from inductive and mesomeric effects while the mesomeric effect predominates in *p* position (Z_p). Thus, the *p* increments reflect a shielding for +M substituents ($Z_p < 0$) and a deshielding for −M substituents ($Z_p > 0$). This behavior parallels the activation and deactivation of the *p* position towards electrophilic substitution (Fig. 4.9) by those substituents. The *m* carbons are only slightly influenced by substituents ($Z_m < 2$ ppm, mostly $Z_m < 1$ ppm). The practical use of the increments listed in Table 4.62 is illustrated for the benzenoid carbons of 5-chloro-2-nitroaniline, 2-*t*-butyl-4-methoxyphenol and 2,5-dihydroxybenzoic acid. Clearly, prediction of ^{13}C shifts by increment calculations is not accurate if interactions between substituents are involved, *e.g.* hydrogen bonding between OH and COOH in 2,5-dihydroxybenzoic acid.

Table 4.62. Empirical Substituent Increments in Benzene Derivates [50e−k].

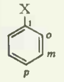

$\delta_{C_6H_6} = 128.5$ ppm

X	Z_1	Z_o	Z_m	Z_p
$-CH_3$	9.3	−0.1	0.7	−3.0
$-CH_2CH_3$	14.9	−1.3	−0.7	−3.3
$-CH_2CH_2CH_3$	14.1	−0.2	0.1	−2.7
$-CH(CH_3)_2$	20.3	−2.0	−0.1	−2.6
$-C(CH_3)_3$	21.8	−3.9	−0.9	−3.6
−Cyclopropyl ($-C_3H_5$)	15.1	−3.3	−0.6	−3.6
$-CH=CH_2$	9.1	−2.4	−0.2	−0.9
−Phenyl ($-C_6H_5$)	13.0	−1.1	0.5	−1.0
$-C\equiv CH$	−5.8	3.9	0.1	0.4
$-CF_3$	−9.0	−2.2	0.3	3.2
$-CH_2F$	8.1	−0.9	0.1	0.2
$-CH_2Cl$	9.4	0.3	0.4	0.2
$-CH_2Br$	9.7	1.0	1.3	0.6
$-CH_2OH$	13.3	−0.8	0.6	−0.4
$-CH_2OCH_2C_6H_5$	10.5	−0.5	0.5	−0.5
$-CH_2NH_2$	15.5	−1.1	0.0	−1.9
$-CH_2NHCH_2C_6H_5$	11.9	−0.5	−0.3	−1.7
$-CH_2SCH_2C_6H_5$	10.5	0.3	0.9	−1.5
$-F$	35.1	−14.4	0.9	−4.4
$-Cl$	6.4	0.2	1.0	−2.0
$-Br$	−5.9	3.0	1.5	−1.5
$-I$	−32.3	9.9	2.6	−0.4
$-OH$	26.6	−12.8	1.6	−7.1
$-OCH_3$	31.4	−14.4	1.0	−7.8
$-OC_6H_5$	29.2	−9.4	1.4	−5.3
$-OCOCH_3$	23.0	−6.4	1.3	−2.3
$-OCN$	24.6	−13.2	2.2	−1.5
$-SH$	2.0	0.6	0.2	−3.3
$-SCH_3$	10.1	−1.7	0.3	−3.5
$-SC_6H_5$	7.3	2.4	0.6	−1.6
$-NH_2$	20.2	−14.1	0.6	−9.6
$-NHCH_3$	21.9	−16.4	0.6	−12.6
$-N(CH_3)_2$	22.2	−15.8	0.5	−11.8
$-NHC_6H_5$	14.7	−10.6	0.8	−7.6
$-N(C_6H_5)_2$	19.0	−4.6	0.9	−5.8

Table 4.62. (Continued).

X	Z_1	Z_o	Z_m	Z_p
$-NHCOCH_3$	11.1	−9.9	0.2	−5.6
$-N=CHC_6H_5$	24.5	−6.9	1.0	−1.9
$-N=C=NC_6H_5$	10.8	−3.6	1.7	−2.2
$-N=C=O$	5.4	−3.7	1.2	−2.6
$-N=C=S$	17.4	−2.2	2.0	−0.4
$-P(C_6H_5)_2$	9.3	5.5	0.3	0.0
$-NO_2$	20.6	−4.3	1.3	6.2
$-N=NC_6H_5$	24.2	−5.5	1.2	3.3
$-N(CH_3)_3^+I^-$	8.8	−8.2	0.2	3.0
$-COCl$	4.8	2.9	0.6	6.9
$-COO^-Na^+$	10.3	2.8	2.2	5.1
$-COOH$	2.9	1.3	0.4	4.6
$-COOCH_3$	2.1	1.2	0.0	4.4
$-COOC_2H_5$	2.4	1.2	−0.1	4.3
$-CONH_2$	5.8	−1.1	−0.3	2.7
$-CHO$	8.2	1.2	0.5	5.8
$-COCH_3$	8.9	0.1	−0.1	4.5
$-COC_6H_5$	9.1	1.5	−0.2	3.8
$-CN$	−15.5	4.1	1.4	5.0

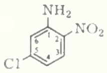

5-Chloro-2-nitroaniline [50k]

	C-1	C-2	C-3	C-4	C-5	C-6
$\delta_{Benzene}$	128.5	128.5	128.5	128.5	128.5	128.5
Z_{NH_2}	*20.2* (Z_1)	*−14.1* (Z_o)	*0.6* (Z_m)	*−9.6* (Z_p)	*0.6* (Z_m)	*−14.4* (Z_o)
Z_{NO_2}	*−4.3* (Z_o)	*20.6* (Z_1)	*−4.3* (Z_o)	*1.3* (Z_m)	*6.2* (Z_p)	*1.3* (Z_m)
Z_{Cl}	*1.0* (Z_m)	*−2.0* (Z_p)	*1.0* (Z_m)	*0.2* (Z_o)	*6.4* (Z_1)	*0.2* (Z_o)
predicted	*145.4*	*133.0*	*125.8*	*120.4*	*141.7*	*115.6* [*ppm*]
measured in $(CD_3)_2SO$	146.5	131.7	125.4	122.6	136.9	120.1 [ppm]

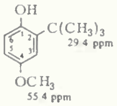

2-*t*-Butyl-4-methoxyphenol[50k]

	C-1	C-2	C-3	C-4	C-5	C-6
$\delta_{Benzene}$	128.5	128.5	128.5	128.5	128.5	128.5
Z_{OH}	*26.6* (Z_1)	*−12.8* (Z_o)	*1.6* (Z_m)	*−7.1* (Z_p)	*1.6* (Z_m)	*−12.8* (Z_o)
$Z_{C(CH_3)_3}$	*−3.9* (Z_o)	*21.8* (Z_1)	*−3.9* (Z_o)	*−0.9* (Z_m)	*−3.6* (Z_p)	*−0.9* (Z_m)
Z_{OCH_3}	*−7.8* (Z_p)	*1.0* (Z_m)	*−14.4* (Z_o)	*31.4* (Z_o)	*−14.4* (Z_o)	*+1.0* (Z_m)
predicted	*143.4*	*138.5*	*111.8*	*151.9*	*112.1*	*115.8* [*ppm*]
measured in $CDCl_3$	147.7	136.9	110.2	152.3	113.5	116.2 [ppm]

Table 4.62. (Continued).

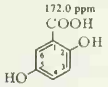

2,5-Dihydroxybenzoic acid [50k]

	C-1	C-2	C-3	C-4	C-5	C-6
$\delta_{Benzene}$	128.5	128.5	128.5	128.5	128.5	128.5
Z_{COOH}	*2.9* (Z_1)	*1.3* (Z_o)	*0.4* (Z_m)	*4.6* (Z_p)	*0.4* (Z_m)	*1.3* (Z_o)
$Z_{2\text{-}OH}$	*−12.8* (Z_o)	*26.6* (Z_1)	*−12.8* (Z_o)	*1.6* (Z_m)	*−7.1* (Z_p)	*1.6* (Z_m)
$Z_{5\text{-}OH}$	*1.6* (Z_m)	*−7.1* (Z_p)	*1.6* (Z_m)	*−12.8* (Z_o)	*26.6* (Z_1)	*−12.8* (Z_o)
predicted	*120.2*	*149.3*	*117.7*	*121.9*	*148.4*	*118.6* [*ppm*]
measured in $(CD_3)_2SO$	112.8	154.5	114.1	123.9	149.5	117.9 [ppm]

4.13.5. Substituted Pyridines

Increments of selected substituents in position 2, 3 and 4 of the pyridine ring are listed in Table 4.63(b). The ^{13}C shifts of C-2,6 (149.7 ppm), C-3,5 (124.2 ppm) and C-4 (136.2 ppm) have been used as references. As can be seen in Table 4.55, N-oxidation causes a significant shielding (−10 ppm) of the carbons α and γ to nitrogen while those in β position are slightly shielded. This parallel to the behavior of pyridine-N-oxide towards electrophilic substitution can be rationalized remembering the known cannonical formulae of this molecule in contrast to pyridine itself.

As is shown for 2-amino-3-methylpyridine in the following, a reasonable prediction of the signal sequence is possible when using the substituent increments presented in Table 4.63.

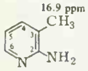

2-Amino-3-methylpyridine [50k]

	C-2	C-3	C-4	C-5	C-6
$\delta_{Pyridine}$	149.7	124.2	136.2	124.2	149.7
Z_{2NH_2}	*11.3*	*−14.7*	*+2.3*	*−10.6*	*−0.9*
Z_{3CH_3}	*1.3*	*9.0*	*0.2*	*−0.8*	*−2.3*
predicted δ [ppm]	*162.3*	*118.5*	*138.7*	*112.8*	*146.5*
measured δ [ppm] in $CDCl_3$	157.9	116.5	137.5	113.8	145.4

4.13.6. Nitrogen Increments in Fused Heterocycles

Based on the carbon shifts of naphthalene as reference, nitrogen increments can be derived for quinoline and isoquinoline as is shown in Table 4.64. These increments are useful aids in assigning the ^{13}C shifts of diazanaphthalenes such as quinazoline (Table 4.64(b) or 2,7-naphthyridine (Table 4.64(c)). Significant deviations between incremental prediction and measurement are found for C-2 and C-4 of quinazoline due to additional interactions between closely attached nitrogens. The values predicted for benzenoid carbons, however, agree well with the experimental data.

Table 4.63. Nitrogen Increments (a) and Substituent Effects of Selected Groups (b) in Pyridine [50].

(a)

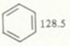

Benzene

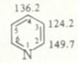

Pyridine

$Z_{2,6} = 149.7 - 128.5 = 21.2$ ppm
$Z_{3,5} = 124.2 - 128.5 = -4.3$ ppm
$Z_{4} = 136.2 - 128.5 = 7.7$ ppm

$\delta_2 = 149.7 + Z_{i2}$
$\delta_3 = 124.2 + Z_{i3}$
$\delta_4 = 136.2 + Z_{i4}$
$\delta_5 = 124.2 + Z_{i5}$
$\delta_6 = 149.7 + Z_{i6}$

(b)

2-Substituent	Z_{22}	Z_{23}	Z_{24}	Z_{25}	Z_{26}
$-CH_3$	9.1	−1.0	−0.1	−3.4	−0.1
$-CH_2-CH_3$	14.0	−2.1	0.1	−3.1	0.2
$-Br$	−6.7	4.8	3.3	−0.5	1.4
$-NH_2$	11.3	−14.7	2.3	−10.6	−0.9
$-CHO$	3.5	−2.6	1.3	4.1	0.7
$-COCH_3$	4.3	−2.8	0.7	3.0	−0.2
$-CN$	−16.1	5.1	1.7	3.7	1.8
3-Substituent	Z_{32}	Z_{33}	Z_{34}	Z_{35}	Z_{36}
$-CH_3$	1.3	9.0	0.2	−0.8	−2.3
$-CH_2-CH_3$	0.3	15.0	−1.5	−0.3	−1.8
$-Br$	2.1	−2.6	2.9	1.2	−0.9
$-NH_2$	−11.9	21.5	−14.2	0.9	−10.8
$-CHO$	2.4	7.9	0.0	0.6	5.4
$-COCH_3$	0.5	−0.3	−3.7	−2.7	4.2
$-CN$	3.6	−14.2	4.6	0.7	4.4
4-Substituent	Z_{42}	Z_{43}	Z_{44}	Z_{45}	Z_{46}
$-CH_3$	0.5	0.8	10.8	0.8	0.5
$-CH_2-CH_3$	0.0	−0.3	15.9	−0.3	0.0
$-Br$	3.0	3.4	−3.0	3.4	3.0
$-NH_2$	0.9	−13.8	19.6	−13.8	0.9
$-CHO$	1.7	−0.6	5.5	−0.6	1.7
$-COCH_3$	1.6	−2.6	6.8	−2.6	1.6
$-CN$	1.7	2.5	−15.3	2.5	1.7

Table 4.64. Nitrogen Increments in Quinoline and Isoquinoline Relative to Naphthalene [50] (a); Application of these Increments to Quinazoline (b) and 2,7-Naphthyridine (c).

(a)

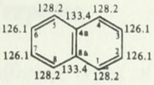
128.2
133.4
128.2
126.1
126.1
126.1
126.1
128.2
133.4
128.2
5
4a
4
6
3
7
8a
2
8
1

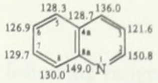
128.3
128.7
136.0
126.9
121.6
129.7
150.8
130.0
149.0
N

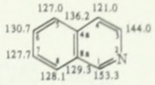
127.0
136.2
121.0
130.7
144.0
127.7
N
128.1
129.5
153.3

Naphthalene (Reference compound)		Quinoline [ppm]	Isoquinoline [ppm]
	Z_1	–	25.1
	Z_2	24.7	–
	Z_3	−4.5	17.9
	Z_4	7.8	−7.2
	Z_5	0.1	−1.2
	Z_6	0.8	4.6
	Z_7	3.6	1.6
	Z_8	1.8	−0.1
	Z_{4a}	−4.7	2.8
	Z_{8a}	15.6	−4.1

(b) Quinazoline

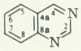
N
N
5
6
7
8
4a
8a
4
2

	calculated [ppm]	measured [ppm]
$\delta_2 = 126.1 + Z_{2q} + Z_{3i} = 126.1 + 24.7 + 17.9 =$	168.7	(160.5)
$\delta_4 = 128.2 + Z_{4q} + Z_{1i} = 128.2 + 7.8 + 25.1 =$	161.1	(155.8)
$\delta_5 = 128.2 + Z_{5q} + Z_{8i} = 128.2 + 0.1 - 0.1 =$	128.2	(127.4)
$\delta_6 = 126.1 + Z_{6q} + Z_{7i} = 126.1 + 0.8 + 1.6 =$	128.5	(127.9)
$\delta_7 = 126.1 + Z_{7q} + Z_{6i} = 126.1 + 3.6 + 4.6 =$	134.3	(134.1)
$\delta_8 = 128.2 + Z_{8q} + Z_{5i} = 128.2 + 1.8 - 1.2 =$	128.8	(128.6)
$\delta_{4a} = 133.4 + Z_{4aq} + Z_{8ai} = 133.4 - 4.7 - 4.1 =$	124.6	(125.2)
$\delta_{8a} = 133.4 + Z_{8aq} + Z_{4ai} = 133.4 + 15.6 + 2.8 =$	151.8	(150.1)

(c) Naphthyridine

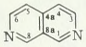
N
N
6
5
4a
4
3
8
8a
1

$\delta_{1,8} = 128.2 + Z_1 + Z_8 = 128.1 + 25.1 - 0.1 =$	153.1	(153.4)
$\delta_{3,6} = 126.1 + Z_3 + Z_6 = 126.1 + 17.9 + 4.6 =$	148.6	(147.2)
$\delta_{4,5} = 128.2 + Z_4 + Z_5 = 128.2 - 7.2 - 1.2 =$	119.8	(119.6)
$\delta_{4a} = 133.9 + 2Z_{4a} = 133.9 + 5.6 =$	139.5	(138.5)
$\delta_{8a} = 133.9 + 2Z_{8a} = 133.9 - 8.1 =$	125.8	(124.3)

5. ^{13}C NMR Spectra of Natural Products

5.1. Terpenes

The different types of terpenoid carbons resonate in the following ranges [280–282].

CH_3 carbons:	10 to 30 ppm
CH_2 carbons:	20 to 45 ppm
CH carbons:	25 to 55 ppm
quaternary carbons:	30 to 55 ppm
olefinic carbons:	105 to 165 ppm
acetylenic carbons:	65 to 95 ppm
alcoholic carbons:	50 to 80 ppm
carbonyl carbons:	180 to 220 ppm.

Electronic and steric effects of neighboring groups cause the relatively strong variation in δ values for the signals of the different kinds of carbon atoms.

The degree of hydrogen substitution can be established for each carbon atom from proton off-resonance experiments, as is demonstrated by the spectra of linalool (Fig. 5.1).

Selective proton decoupling and the spectra of specificly deuterated compounds are sometimes required for the total signal assignments of terpenes.

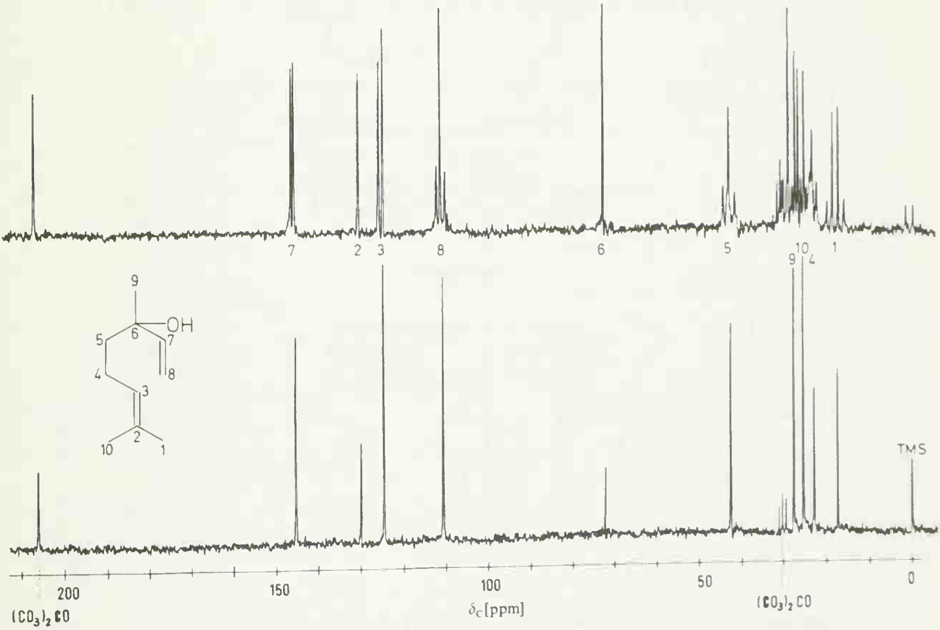

Fig. 5.1. 22.63 MHz PFT $^{13}C\{^1H\}$ NMR spectra of linalool; 75% in hexadeuterioacetone (for field frequency stabilization); 30 °C; pulse width: 10 μs; pulse interval: 0.4 s/4 K interferogram; phase corrected spectra;

(a) proton broad band decoupled; 128 accumulated interferograms;

(b) proton off-resonance decoupled; 1024 accumulated interferograms.

Several rules found for the spectra of a series of camphor derivatives (bicyclo[2,2,1]heptanones) are worthy of mention [280]:

(1) The signals of methylene carbons in the 7-position (the one-carbon bridge) are shifted about 10 ppm to lower field than those of methylene groups in the two-carbon bridges.
(2) Changing the bromine atom in 3-bromo-norbornanones from *endo* to *exo* position causes the signal of C-3 to shift upfield about 6 ppm.
The signal assignments for a series of diterpenes, the pimaradienes [282], were performed as is discussed in detail for the related steroids in the following chapter.
The formulae of several classes of terpenes and the chemical shifts of their carbon atoms are listed below and in Table 5.1.

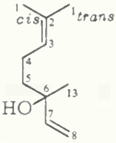

Linalool

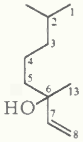

Dihydrolinalool

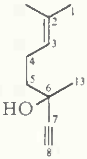

Dehydrolinalool

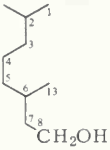

Dimethyloctanol

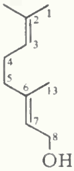

Geraniol

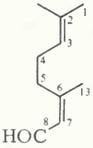

cis-Citral

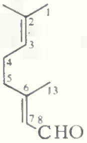

trans-Citral

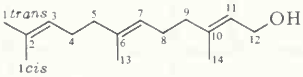

Farnesol

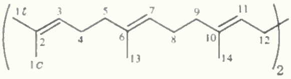

Squalene

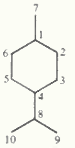

Menthane

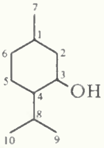

Menthol

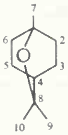

Cineol

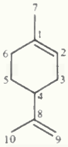

Limonene

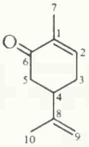

Carvone

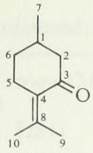

Pulegone

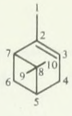

α-Pinene

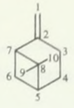

β-Pinene

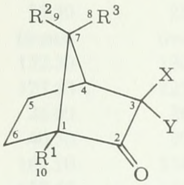

Norbornanone: $R^1 = R^2 = R^3 = X = Y = H$
3-Bromonorbornanone (*endo*): $R^1 = R^2 = R^3 = X = H, Y = Br$
3-Bromonorbornanone (*exo*): $R^1 = R^2 = R^3 = Y = H, X = Br$
3-Methylnorbornanone (*endo*): $R^1 = R^2 = R^3 = X = H, Y = Me$
1-Methylnorbornanone: $R^1 = Me, R^2 = R^3 = X = Y = H$
Camphor: $R^1 = R^2 = R^3 = Me, X = Y = H$
3-Bromocamphor (*endo*): $R^1 = R^2 = R^3 = Me, X = H, Y = Br$
9,3-Dibromocamphor (*endo*): $R^1 = R^3 = Me, R^2 = CH_2Br, X = H, Y = Br$
Fenchone: $R^1 = X = Y = Me, R^2 = R^3 = H$

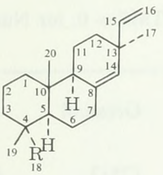

Pimaradiene: R = Me
Pimarol: $R = CH_2OH$
Pimaric acid: R = COOH

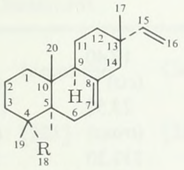

Isopimaradiene: R = Me
Isopimarol: $R = CH_2OH$
Isopimaric acid: R = COOH

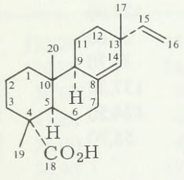

Sandaracopimaric acid

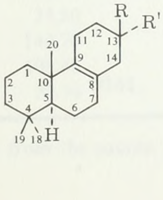

$\Delta^{8(9)}$-Pimaradiene-1: $R = C_2H_3$; $R' = Me$
$\Delta^{8(9)}$-Pimaradiene-2: $R = Me$; $R' = C_2H_3$

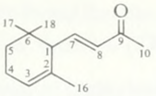
O
17
18
6
1
2
3
4
5
7
8
9
10
16

α-Ionone

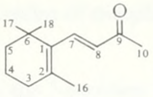
O
17
18
6
1
2
3
4
5
7
8
9
10
16

β-Ionone

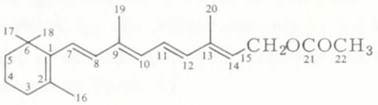
19
20
17
18
6
1
2
3
4
5
7
8
9
10
11
12
13
14
15
CH$_2$OCOCH$_3$
21
22
16

Vitamin A acetate

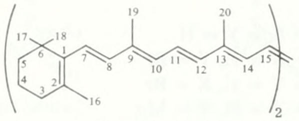
19
20
17
18
6
1
2
3
4
5
7
8
9
10
11
12
13
14
15
16
2

β-Carotene

Table 5.1. ^{13}C Chemical Shifts of Terpenes (δ Values in ppm Relative to TMS = 0; for Numbering See Formulae on Pages 220–222).

	Linalool	Dihydro-linalool	Dehydro-linalool	Dimethyl-octanol	Geraniol	*cis*-Citral
Solvent*)	neat	neat	neat	neat		
Ref.	[102]	[102]	[102]	[102]	[281]	[281]
C-Atom						
1	17.15 (*cis*) 25.25 (*trans*)	22.25	17.25 (*cis*) 25.25 (*trans*)	22.25	17.40 (*cis*) 25.50 (*trans*)	17.40 (*cis*) 25.30 (*trans*)
2	130.25	27.50	130.85	27.60	131.20	132.90
3	124.60	39.15	123.85	39.10	124.90	123.10
4	22.55	21.35	23.20	24.45	26.60	27.20
5	42.20	42.40	43.05	37.30	39.70	32.50
6	72.70	72.60	67.35	29.25	137.30	162.10
7	145.00	145.00	87.60	39.50	124.50	128.70
8	111.25	110.90	71.45	59.55	58.70	189.40
9						
10						
11						
12						
13	27.20	26.95	29.35	19.25	16.00	24.40

*) if known from the source.

Table 5.1. (Continued).

	trans-Citral	Farnesol	Squalene	Menthane	Menthol	Cineol
Solvent*)						
Ref.	[281]	[281]	[281]	[281]	[281]	[281]
C-Atom						
1	17.40	17.40	17.50	35.70	31.90	69.10
	(*cis*)	(*cis*)	(*cis*)			
	25.30	25.40	25.50			
	(*trans*)	(*trans*)	(*trans*)			
2	132.30	130.80	130.60	33.10	45.60	31.70
3	123.50	125.00	124.80	29.90	70.90	23.00
4	26.00	26.90	27.00	44.10	50.40	33.10
5	40.50	39.70	39.90	29.90	23.50	23.00
6	162.10	134.90	134.80	33.10	35.00	31.70
7	127.50	124.30	124.60	22.50	22.30	27.40
8	190.00	25.60	26.90	35.70	25.80	73.00
9		39.80	39.90	19.00	16.00	28.80
10		137.10	134.60	19.00	21.00	28.80
11		124.70	124.60			
12		58.60	28.40			
13	17.00	13.70	15.90			
14		15.90	15.90			

Table 5.1. (Continued).

	Limonene	Carvone	Pulegone	α-Pinene	β-Pinene	Norbornanone
Solvent*)						CCl_4
Ref.	[281]	[281]	[281]	[281]	[281]	[281]
C-Atom						
1	133.20	135.20	31.40	20.80	106.30	49.60
2	120.80	143.80	50.70	144.10	151.30	213.80
3	30.60	31.30	201.10	116.20	23.80	45.00
4	41.20	42.70	131.70	31.50	23.60	35.60
5	28.00	43.10	28.50	41.50	40.80	24.40
6	30.90	197.70	32.90	31.40	27.00	27.70
7	23.80	15.40	21.70	47.30	52.10	37.70
8	149.70	147.20	140.80	38.00	40.80	
9	108.40	110.30	21.80	26.50	25.80	
10	20.50	20.20	22.70	22.80	21.70	

*) if known from the source.

Table 5.1. (Continued).

Solvent Ref. C-Atom	3-Bromo-norbornanone (*endo*) CCl_4 [280]	3-Bromo-norbornanone (*exo*) CCl_4 [280]	3-Methyl-norbornanone (*endo*) CCl_4 [280]	1-Methyl-norbornanone CCl_4 [280]	Camphor CCl_4 [280]	3-Bromo-camphor (*endo*) CCl_4 [280]
1	48.20	49.20	50.00	53.10	57.00	57.10
2	207.80	208.30	216.20	214.80	214.70	209.30
3	55.90	50.10	48.10	45.00	43.20	53.90
4	42.60	44.80	40.70	34.10	43.20	49.80
5	23.10	24.10	21.20	29.00	27.40	22.90
6	25.40	26.60	25.60	31.40	30.10	30.70
7	35.30	35.30	37.20	43.90	46.60	45.80
8			10.70		19.50	20.20
9					20.00	20.20
10				13.80	9.70	10.00

Table 5.1. (Continued).

Solvent Ref. C-Atom	2,3-Dibromo-camphor (*endo*) $CHCl_3$ [280]	Fenchone CCl_4 [280]	Pimaradiene $CHCl_3$ [282]	Pimarol CCl_4 [282]	Pimaric acid $CHCl_3$ [282]	Isopimara-diene CCl_4 [282]
1	58.30	53.80	39.70	38.30	38.60	40.10
2	209.90	219.10	19.40	18.50	18.50	19.00
3	52.40	47.10	42.50	35.50	37.50	42.50
4	47.80	45.50	33.50	37.90	47.60	33.10
5	22.10	25.30	55.20	47.50	49.10	50.50
6	30.40	32.00	22.90	22.50	25.50	23.50
7	50.10	41.80	36.30	35.50	35.80	121.60
8	17.20	21.90 23.60	138.80	138.10	138.50	135.20
9	39.20	23.60 21.90	51.80	51.50	51.90	52.20
10	10.20	15.00	38.80	38.80	38.10	35.60
11			19.10	19.30	19.50	20.30
12			36.30	36.00	36.00	36.40
13			38.80	39.00	39.00	37.00
14			128.10	128.10	128.20	46.30
15			147.70	147.00	147.80	149.90
16			112.90	113.10	113.20	109.50
17			29.80	29.80	29.90	21.80
18			34.50	71.70	185.70	33.90
19			22.50	18.30	17.60	22.60
20			14.90	15.60	15.40	15.20
21						
22						

Table 5.1. (Continued).

	Isopimarol	Isopimaric acid	Sandaracopimaric acid	$\Delta^{8(9)}$-Pimaradiene-1	$\Delta^{8(9)}$-Pimaradiene-2	α-Ionone
Solvent*)	CCl_4	$CHCl_3$	CCl_4	CCl_4	CCl_4	
Ref.	[282]	[282]	[282]	[282]	[282]	[281]
C-Atom						
1	39.60	39.20	38.40	37.00	36.70	54.30
2	18.50	17.90	18.30	19.10	19.00	132.30
3	35.80	37.20	37.10	42.40	42.20	122.50
4	37.60	46.40	47.20	33.50	33.50	23.20
5	43.70	45.40	48.70	52.40	52.00	28.70
6	23.50	25.70	24.90	20.80	21.30	32.40
7	121.50	121.50	35.50	32.70	32.60	132.70
8	135.30	136.00	136.20	124.40	124.40	147.50
9	52.00	52.40	50.70	136.50	134.40	196.00
10	35.40	35.50	37.80	37.60	37.70	27.50
11	20.50	20.50	18.80	19.10	19.00	
12	36.50	36.00	34.60	34.10	35.10	
13	36.90	37.50	37.40	34.90	35.10	
14	46.40	46.50	129.30	42.00	42.00	
15	150.00	150.70	149.00	148.80	146.80	
16	109.50	109.70	110.50	109.80	111.20	31.50
17	21.80	21.90	26.20	23.50	28.20	26.80
18	71.90	183.90	185.30	33.50	33.50	26.80
19	18.50	17.50	16.80	22.00	22.50	
20	15.90	15.70	15.30	19.70	19.70	
21						
22						

*) If known from the source.

5:2. Steroids

^{13}C chemical shifts promise to be informative parameters for solving structural problems in steroid chemistry. As the resonances of most natural steroids cover a range of 200 ppm, signals almost never overlap in the steroid spectra. Therefore, correlations between ^{13}C chemical shifts and configurational changes can be made for individual carbons.

Complete signal assignments have already been achieved for a large number of steroids; the values are collected in Table 5.3.

A series of assignment aids is used for the signal identifications of this complex class of compounds: The resonance of different carbons of steroids are found in the following ranges:

primary alkane carbons: 12 to 24 ppm
secondary alkane carbons: 20 to 41 ppm
tertiary alkane carbons: 35 to 57 ppm
quaternary alkane carbons: 27 to 43 ppm
alcohol carbons: 65 to 91 ppm
olefinic carbons: 119 to 172 ppm
carbonyl carbons: 177 to 220 ppm
carbons bearing fluorine atoms: 88 to 102 ppm.

Table 5.1. (Continued).

	β-Ionone	Vitamin A acetate**)	β-Carotene	15,15′-*cis*-β-carotene	15,15′-Dehydro-β-carotene
Solvent*)			$CDCl_3$	$CDCl_3$	$CDCl_3$
Ref.	[281]	[281]	[281b]	[281b]	[281b]
C-Atom					
1	136.2	138.3	138.0	138.1	138.0
2	134.7	129.3	129.3	129.3	129.5
3	33.3	33.4	33.2	33.2	33.2
4	19.0	19.7	19.4	19.4	19.4
5	39.5	40.0	39.8	39.9	39.9
6	34.0	34.5	34.4	34.4	34.4
7	132.1	126.3	126.7	126.8	127.1
8	141.7	137.7	137.8	137.8	137.6
9	196.2	135.7	136.0	136.1	137.4
10	26.6	130.2	130.8	130.9	130.2
11		125.2	125.1	125.4	127.4
12		135.9	137.3	137.5	135.0
13		125.1	136.4	137.1	146.5
14		137.7	132.4	126.8	110.6
15		61.2	130.0	125.6	98.2
16	21.3	20.5	21.7	21.7	21.7
17	28.6	29.2	29.0	29.1	29.0
18	28.6	29.2	29.0	29.1	29.0
19		12.6	12.8	12.8	12.8
20		12.6	12.8	12.6	15.3
21		169.0			
22		21.8			

*) if known from the source.
**) assignments changed.

Alcohol carbons are identified by spectral comparison of the alcohol with the corresponding acetate: Upon acetylation of cyclohexanols the α-carbons shift about 3 to 4 ppm downfield and the β-carbons move 2–3 ppm upfield. Esterification of axial hydroxyl groups also causes a downfield shift of 1 ppm of the γ-carbons [283].

Replacing hydrogens attached to carbons by deuterium atoms causes spin-spin splitting, quadrupole broadening and – in $^{13}C\{^1H\}$ experiments – reduction of signal : noise due to lack of Overhausers effects. Therefore resonances of specificly deuterated carbons in a proton broad band decoupled ^{13}C NMR spectrum are usually lost in the noise. Recording the spectra before and after specific deuteration allows unequivocal assignment of the corresponding carbon atoms [283]. Proton off-resonance decoupling is used mainly for identifying primary and quaternary carbons of steroids, as the closely spaced $\geqslant$CH and $>CH_2$ carbon resonances often do not split into assignable doublets or triplets in off-resonance experiments [283].

5.2.1. Androstanes, Pregnanes and Estranes

The total signal assignment of a series of androstanes is given in Table 5.3. The formulae of the parent compounds and numbering of the carbon atoms are given below:

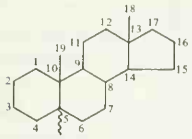
18
12
13
17
19
11
16
1
10
9
15
14
2
8
3
7
5
4
6

5α, β-Androstane

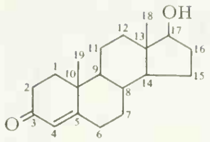
18
OH
12
13
17
19
11
16
1
10
9
15
14
2
8
O
3
5
7
4
6

Testosterone

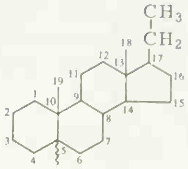
CH3
18
CH2
12
13
17
19
11
16
1
10
9
15
14
2
8
3
7
5
4
6

5α, β-Pregnane

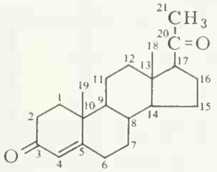
21
CH3
20
18
C=O
12
13
17
19
11
16
1
10
9
15
14
2
8
7
O
3
5
4
6

Progesterone

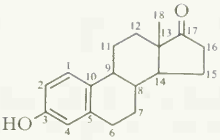
18
O
12
13
17
11
16
1
9
10
15
14
2
8
7
HO
3
5
4
6

Estrone

The coupled, proton broad band and proton off-resonance decoupled ^{13}C NMR spectra of epiandrosterone are shown in Fig. 5.2.

The signal identification were made by applying the general chemical shift rules discussed at the beginning of this chapter, and by comparing the androstane spectra with those of cholestane, cholesterol, 2,2,4,4,16,16-d_6-androstane-3,17-dione and 2,2,15,15,21,21-d_6-16-dehydroprogesterone [283].

If the methyl group attached to C-10 of testosterone is replaced by hydrogen the resonance of C-10 shifts downfield and not upfield as expected. The same was observed for C-10 of the pairs 7α-methyltestosterone, 19-nor-7α-methyltestosterone and androsta-4-ene-3,17-dione, 19-nor-androsta-4-ene-3,17-dione [283].

Replacing the 5α-hydrogen of pregnanes by amino or azido groups causes the signal of C-9 to shift downfield by more than 10 ppm. This was attributed to a 1,3-diaxal interaction between the axial amino or azido group at position 5 and the axial proton attached to C-9. Thus, a downfield shift of the C-9 resonance can be considered as a proof of the axial orientation of the nitrogen containing substituents in these pregnane derivatives [284].

The assignments of the aromatic carbons in ring A of estrone were performed by comparing the ^{13}C spectrum of the steroid hormone with that of its acetate. A correlation with the acetylation shifts of phenol (C-1 (3.7 ppm); C-2 (6.2 ppm); C-3 (0.6 ppm); C-4 (4.4 ppm)) resulted in the signal assignments outlined in Table 5.3 [283].

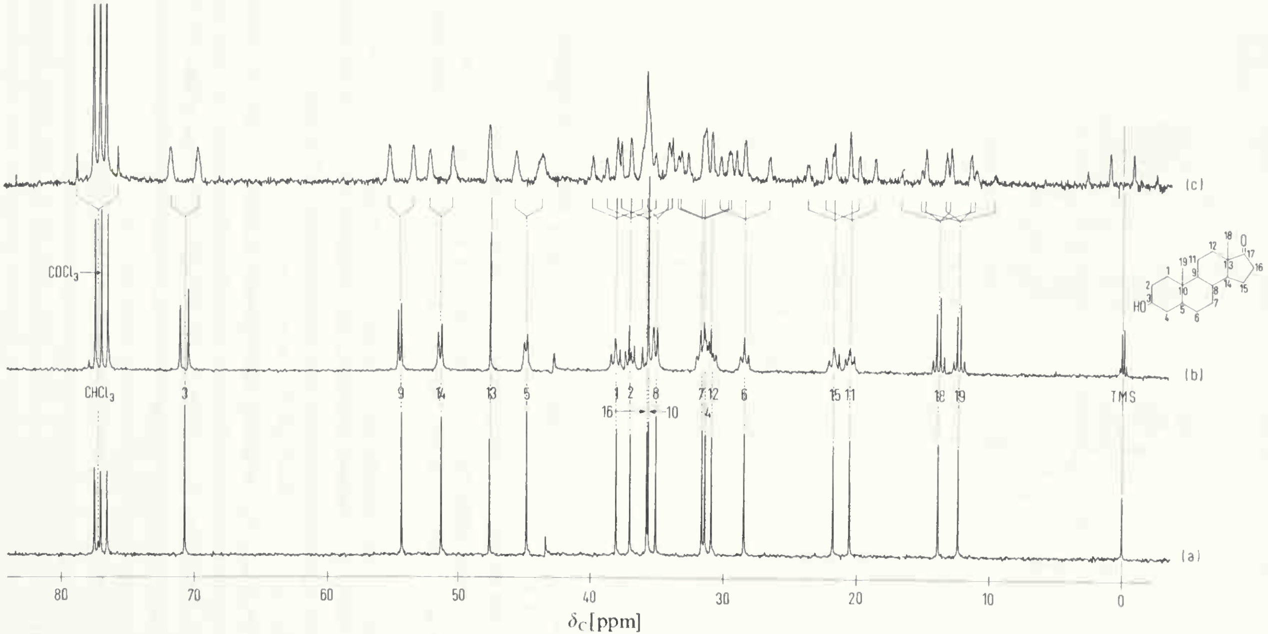

Carbon	*ppm*
1	38.20
2	37.15
3	70.95
4	31.55
5	45.10
6	28.55
7	31.75
8	35.25
9	54.70
10	35.90
11	20.60
12	31.00
13	47.75
14	51.65
15	21.80
16	35.80
17	220.60
18	13.85
19	12.35

Fig. 5.2. High-field 67.88 MHz PFT ${}^{13}C$ NMR spectra*) of epiandrosterone; 100 mg/ml deuteriochloroform; 30 °C; pulse width: 15 μs; pulse interval: 1.28 s; phase corrected partial spectrum (8 K data points);
(a) proton broad-band decoupled; 3 K accumulated pulse interferograms;
(b) proton off-resonance decoupled (1 kHz off-resonance); 16 K accumulated pulse interferograms;
(c) coupled; 64 K accumulated pulse interferograms.

---

*) Recorded by T. Keller, Bruker Physik AG, Karlsruhe-Forchheim, Germany.

The $^{13}C-^{19}F$ coupling constants of fluorinated steroids are helpful for the signal identification of these fluorine derivatives and nonfluorinated analogs. In Table 5.2 the $^{13}C-^{19}F$ coupling constants of four fluorinated steroids are listed [285].

Table 5.2. $^{13}C-^{19}F$ Coupling Constants of Selected Steroids in Hz [285].

	C-1	C-2	C-3	C-5	C-8	C-9	C-10	C-11	C-19
16α-Methyl-11β,21-dihydroxy-9α-fluoropregna-1,4-diene-3,20-dione	–	–	–	–	18.1	174.9	22.6	40.7	4.5
16α-Methyl-11β,17α,21-trihydroxy-9α-fluoropregna-1,4-diene-3,20-dione	–	–	–	–	18.1	174.9	22.6	40.7	4.5
17β-Hydroxy-2α-fluoroandrost-4-en-3-one	34.7	182.5	12.8	–	–	–	4.5	–	–
2-Fluoroestrone	19.6	229.2	19.6	3.8	–	–	3.8	–	–

As can be seen from Table 5.2, the $^{13}C-^{19}F$ coupling constants decrease drastically with the increasing distance of the carbon atoms from the C–F-group in the molecule. With the exception of C-19, fluorine substitution causes the γ-carbon signals to shift upfield (*cf.* resonances of C-1, C-5, C-7, C-12 and C-14 of the compounds in Table 5.2) [285].

A similar 1,3-diaxial shift relationship was found for hydroxyl substitution in cyclohexanols and carbohydrates (*cf.* Sections 4.5 and 5.4).

5.2.2. Cholestanes

All alkane carbons of cholestane are found in the range of 57 to 12 ppm [286]. The signal range of primary, secondary, tertiary and quaternary carbons was outlined at the beginning of this chapter. Due to strong steric interactions of C-11 and C-15 with C-18, C-19 and C-20, the two methylene signals at highest field must be assigned to C-11 and C-15. Substituting hydrogen atoms by double bonds, hydroxyl, carbonyl or fluorine groups causes the above mentioned downfield shifts of the corresponding carbon signals. For the signal identification of cholestanes the ^{13}C NMR spectra of the following compounds were used for correlation: cyclohexane, *trans*-1,2-dimethylcyclohexane, cyclohexene, 2,6-dimethyloctane [283], 2-methyl-2-heptene, $\Delta^{8,9}$-sandaracopimaradiene [286], 2,2,5,6-tetramethyloctane, and 2,5-dihydroxy-2,6-dimethyloctane [287].

The ^{13}C NMR spectrum of 2,6-dimethyloctane can be used for assigning the resonances of the cholestane side chain. Applying the rules proposed by Grant and Paul [62], all signals of the model compound 2,6-dimethyloctane can be identified. The Grant-Paul parameters also helped in identifying the side chain resonances of ergosterol [283].

Inversion of ring A causes significant shifts of the carbon signals of ring A and B in steroids. In 5β-cholestane, the C-19 methyl carbon resonates about 12 ppm towards lower field than in the corresponding 5α-steroid. Conversly, the resonances of C-10, C-9, C-7 and C-5 are shifted 5 to 10 ppm upfield in going from 5α-cholestane to 5β-cholestane (*cf.* Table 5.3) [288]. The numbering of the carbon atoms in the cholestanes of Table 5.4 is shown below.

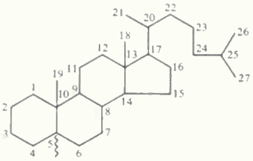

5α, β-Cholestane

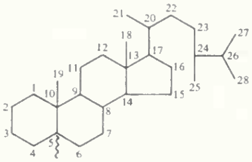

5α, β-Ergostane

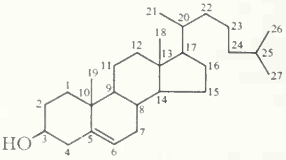

Cholesterol

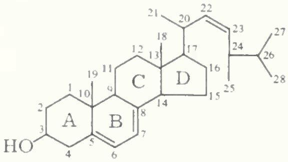

Ergosterol

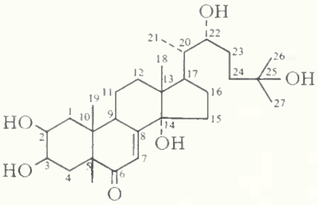

OH
OH
HO
HO
OH
O

α-Ecdysone

5.2.3. Steroid Alkaloids [289, 290]

The signal identifications of steroid alkaloids followed the procedures discussed previously: Again, specificly deuterated compounds such as 17α-d-conanine, 20α-d-conanine, 21-d$_3$-conanine and 8β-d-dihydroconessine were of great help in assigning the signals. The carbon atoms of Table 5.3 are numbered as shown in the following formulae:

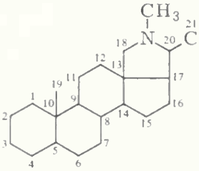

Conanine

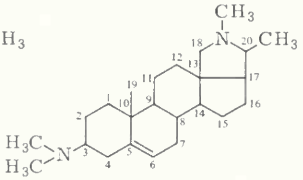

CH3
N
CH3
H3C
N
H3C

Conessine

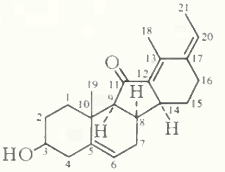

Ethyletiojervatriene-3-ol-11-one

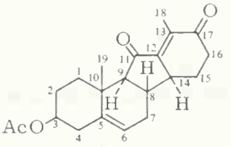

Ethyletiojervadiene-3-ol-11,16-dione acetate

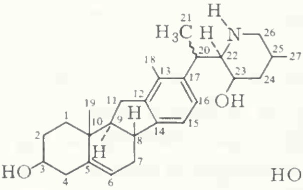

H3C
H
H
N
OH
H
H
HO

Veratramine

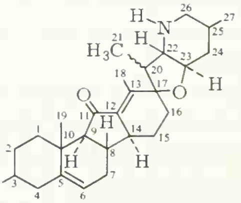

H
N
H3C
H
O
H
O
H
H
H
HO

Jervine

Table 5.3. ^{13}C Chemical Shifts of Steroids (δ Values in ppm Relative to TMS = 0; for Numbering See Formulae on Pages 227, 230).

	5α-Androstane	5β-Androstane	Testosterone	Testosterone acetate	19-Nortestosterone	7α-Methyltestosterone
Solvent	$CDCl_3$	$CDCl_3$	Dioxane/ $CHCl_3$	Dioxane/ $CHCl_3$	Dioxane/ $CHCl_3$	Dioxane/ $CHCl_3$
Ref.	[288]	[288]	[283]	[283]	[283]	[283]
C-Atom						
1	37.6	37.6	35.8	35.8	26.7	36.2
2	22.0	21.2	33.8	33.9	36.3	34.1
3	26.6	26.8	197.7	197.5	198.3	
4	28.9	26.9	123.9	124.0	124.5	
5	46.9	40.3	170.1	170.1	165.9	
6	28.9	26.9	32.5	32.6	35.3	38.9
7	32.3	27.4	31.9	31.7	31.0	31.3
8	35.7	36.1	35.8	35.5	40.7	40.7
9	54.5	43.6	54.3	54.0	48.9	47.2
10	36.1	27.2	38.7	38.6	42.6	38.5
11	20.7	20.7	20.9	20.7	26.3	21.0
12	40.3	40.7	36.8	36.8	36.8	36.8
13	40.6	40.7	42.9	42.6	43.1	43.1
14	54.9	54.5	50.8	50.5	48.6	46.6
15	20.3	20.4	23.5	23.5	23.3	23.0
16	38.8	39.0	30.4	27.6	30.4	30.5
17	25.3	25.4	81.0	82.2	81.1	
18	17.3	18.3	11.0	11.9	11.1	11.0
19	12.0	24.1	17.0	17.3		17.7
20						
21						
22						
23						
24						
25						
26						
27						
28						
CH_3 (acetyl)				20.7		
CO (acetyl)				169.7		
CH_3 (7α)						12.6

Tab. 5.3. (Continued).

	19-Nor-7α-methyl-testosterone	Androstane-3,17-dione	Androst-4-ene-3,17-dione	5-Dehydro-isoandro-sterone	19-Noran-drost-4-ene-3,17-dione	17β-Hy-droxy-2α-fluoroan-drost-4-en-3-one
Solvent	Dioxane/ $CHCl_3$	Dioxane/ $CHCl_3$	Dioxane/ $CHCl_3$	Dioxane/ $CHCl_3$	Dioxane/ $CHCl_3$	DMSO-d_6
Ref.	[283]	[283]	[283]	[283]	[283]	[285]
C-Atom						
1	26.8	38.5	34.7	37.5	26.8	39.3
2	36.5	37.8	33.1	31.8	36.4	88.4
3	197.7	209.0	197.6	71.0	197.7	193.5
4	126.4	44.4	124.0	42.6	124.7	120.7
5	164.0	46.7	169.4	142.1	165.1	171.5
6	43.0	28.8	31.7	120.4	35.3	31.6
7	30.9	31.9	30.9	31.8	31.7	31.3
8	43.1	35.1	34.6	31.8	40.0	34.5
9	43.2	54.3	54.1	50.8	49.8	53.8
10	42.6	35.9	38.0	36.9	42.4	41.1
11	26.8	20.8	20.4	20.6	25.8	20.2
12	36.8	30.7	30.3	30.9	30.2	36.2
13	43.2	47.4	47.2	47.2	47.4	42.4
14	46.8	51.4	50.9	51.9	50.2	49.9
15	22.6	21.8	21.7	21.9	21.6	23.0
16	30.3	35.4	35.1	35.4	35.1	29.8
17	81.0	218.4	218.4	218.7	218.3	79.8
18	11.0	13.5	13.4	13.2	13.5	11.1
19		11.0	17.0	19.2		17.7
20						
21						
22						
23						
24						
25						
26						
27						
28						
CH_3 (7α)	12.6					

Table 5.3. (Continued).

	5α-Amino-pregnane	5β-Amino-pregnane	5α-Azido-pregnane	5β-Azido-pregnane	Pro-gesterone	16-De-hydropro-gesterone
Solvent	$CDCl_3$	$CDCl_3$	$CDCl_3$	$CDCl_3$	Dioxane/ $CHCl_3$	Dioxane/ $CHCl_3$
Ref.	[284]	[284]	[284]	[284]	[283]	[283]
C-Atom						
1	38.0	38.5	32.1	38.3	35.7	34.9
2	23.4	23.2	23.3	23.3	32.6	33.8
3	22.2	21.0	22.3	20.8	197.4	197.3
4	28.6	35.2	28.4	30.9	124.0	124.1
5					169.3	162.4
6	28.6	28.3	28.4	28.3	32.3	32.2
7	33.4	26.5	29.4	27.0	30.7	32.0
8	35.6	35.2	35.3	35.0	33.9	34.1
9	43.4	46.7	43.6	47.0	54.2	54.5
10	40.2	26.5	42.5	30.9	38.6	38.7
11	20.9	20.5	20.4	20.8	21.2	20.9
12	31.8	31.5	32.1	31.8	36.0	35.7
13	42.4	42.6	42.5	42.5	43.7	46.3
14	56.8	56.3	56.4	56.0	56.2	56.0
15	24.9	24.6	24.8	24.6	23.0	32.5
16	38.7	38.5	38.5	38.3	38.8	155.6
17	53.6	53.3	53.4	53.3	63.3	143.2
18	13.5	13.2	13.4	13.4	13.0	15.7
19	17.6	15.6	18.2	15.6	17.0	16.8
20	21.5	21.0	21.1	20.8	197.8	195.4
21	12.6	12.7	12.5	12.7	24.4	26.4
22						
23						
24						
25						
26						
27						
28						

Table 5.3. (Continued).

	11α-Hydroxyprogesterone	11α-Acetoxyprogesterone	3β-Hydroxy-5β-pregn-16-en-20-one	3β-Acetoxy-5β-pregn-16-en-20-one	11β,17α,21-Trihydroxy-pregna-1,4-diene-3,20-dione	16α-Methyl-11β,21-dihydroxy-9α-fluoro-pregna-1,4-diene-3,20-dione
Solvent	Dioxane/ $CDCl_3$	Dioxane/ $CDCl_3$	$CDCl_3$	$CDCl_3$	DMSO-d_6	DMSO-d_6
Ref.	[283]	[283]	[287]	[287]	[285]	[285]
C-Atom						
1	35.1	35.1	33.5	34.5	156.9	152.7
2	33.5	33.2	27.4	24.7	127.3	129.0
3	198.5	197.8	65.8	69.6	185.2	185.3
4	124.4	124.7	34.5	30.3	121.8	124.3
5	170.4	169.5	36.1	36.9	170.6	166.9
6	32.0	32.0	29.4	30.3	31.7	30.4
7	30.6	30.8	26.3	25.9	31.3	27.2
8	34.2	34.0	33.1	33.6	34.2	33.5
9	59.2	55.0	39.8	39.9	55.6	101.2
10	40.1	39.8	26.6	26.7	44.0	48.0
11	68.2	70.6	20.6	20.6	68.7	70.5
12	50.4	45.3	34.8	34.6	39.1	43.0
13	44.0	43.6	45.7	45.8	46.8	44.7
14	55.7	55.7	55.7	55.7	51.3	48.2
15	23.0	23.1	31.7	31.7	23.8	32.9
16	37.7	36.8	153.2	153.2	33.1	30.4
17	63.1	62.9	142.2	141.9	88.6	67.2
18	14.2	13.8	15.7	15.7	17.1	16.1
19	18.0	18.0	23.5	23.5	21.1	22.8
20	207.4	207.1	199.2	199.2	211.6	209.9
21	24.3	24.2	26.0	26.1	66.2	69.2
22						
23						
24						
25						
26						
27						
28						
CH_3 (C-16)						21.8
CH_3 (acetyl)		21.3		21.1		
CO (acetyl)		168.9		167.9		

Table 5.3. (Continued).

	16α-Methyl-11β,17α,21-trihydroxy-9α-fluoro-pregna-1,4-diene-3,20-dione	Estrone	Estrone acetate	2-Fluoro-estrone	5α-Cholestane	5β-Cholestane
Solvent	DMSO-d_6	$CDCl_3$/DMSO-d_6	Dioxane/$CHCl_3$	DMSO-d_6	Dioxane/$CHCl_3$	$CDCl_3$
Ref.	[285]	[102]	[283]	[285]	[283]	[288]
C-Atom						
1	152.9	126.9	126.1	112.8	38.9	37.4
2	129.1	113.4	118.9	149.7	22.3	21.1
3	185.5	155.7	149.2	142.3	27.0	26.4
4	124.1	115.9	121.6	117.5	29.3	26.9
5	167.1	138.2	137.5	130.9	47.3	40.4
6	30.4	39.3	29.4	28.4	29.3	27.1
7	27.4	27.4	26.5	26.2	32.3	28.2
8	33.8	30.2	38.3	37.6	35.8	35.6
9	101.2	44.9	44.4	43.4	55.2	45.6
10	48.3	131.9	131.9	132.2	36.5	27.8
11	70.8	26.4	25.8	25.6	21.1	20.7
12	35.9	32.5	31.9	31.5	28.3	27.8
13	47.7	48.3	47.6	47.5	42.8	42.5
14	43.4	51.1	50.5	49.6	56.9	56.3
15	32.1	22.2	21.5	21.2	24.3	24.1
16	35.1	35.9	35.3	35.5	40.4	40.2
17	90.3	219.9	218.4	219.4	56.8	56.1
18	15.2	13.9	13.4	13.6	12.2	11.9
19	22.9				12.1	24.1
20	211.2				36.0	35.8
21	66.3				18.8	18.5
22					36.4	36.0
23					24.2	23.7
24					39.7	39.4
25					28.1	27.4
26					22.5	22.7
27					22.7	22.3
28						
CH_3 (C-16)	17.6					
CH_3 (acetyl)			20.2			
CO (acetyl)			168.9			

Table 5.3. (Continued).

	5α-Ergostane	Cholestan-3β-ol	Cholestan-3α-yl acetate	Cholestan-3β-yl acetate	Cholesta-3,5-diene	Cholesterol
Solvent	$CDCl_3$	Dioxane/ $CHCl_3$	Dioxane/ $CHCl_3$	Dioxane/ $CHCl_3$	Dioxane/ $CHCl_3$	Dioxane/ $CHCl_3$
Ref.	[288]	[283]	[283]	[283]	[283]	[283]
C-Atom						
1	38.5	37.3	33.1	36.9	34.0	37.5
2	20.3	31.8	26.2	27.6	23.1	31.6
3	26.4	70.4	69.5	73.2	129.6	71.3
4	28.9	38.6	33.1	34.2	124.3	42.4
5	46.9	45.2	40.3	44.8	141.4	141.2
6	28.9	29.0	28.4	28.8	122.9	121.3
7	32.0	32.3	32.1	32.1	31.9	32.0
8	35.3	35.8	35.7	35.7	32.0	160.5
9	54.6	54.8	54.6	54.6	48.6	50.5
10	36.1	35.6	35.8	35.6	35.2	36.5
11	18.6	21.4	21.0	21.4	21.2	21.2
12	28.0	28.3	28.4	28.2	28.3	28.3
13	42.3	42.8	42.7	42.7	42.6	42.4
14	56.3	56.7	56.8	56.7	57.2	56.9
15	24.1	24.3	24.2	24.2	24.2	24.3
16	40.0	40.4	40.3	40.2	40.2	40.0
17	56.0	56.7	56.8	56.7	56.6	56.5
18	12.3	12.1	12.0	12.0	12.0	12.0
19	12.1	12.0	11.2	12.0	18.6	19.4
20	36.1	35.9	36.0	35.9	36.0	35.8
21	14.2	18.6	18.7	18.7	18.8	18.8
22	33.6	36.4	36.4	36.4	36.5	36.4
23	30.6	24.1	24.1	24.1	24.2	24.1
24	39.0	39.7	39.7	39.6	39.8	39.6
25	17.4	28.0	28.0	28.0	28.1	28.0
26	31.2	22.4	22.5	22.4	22.5	22.5
27	21.9	22.6	27.0	22.6	22.7	22.8
28	20.6					
CH_3 (acetyl)			20.7	20.6		
CO (acetyl)			169.3	169.4		

Table 5.3. (Continued).

	Cholesteryl acetate	Cholesteryl methyl ether	7-Dehydro-cholesteryl acetate	Ergosterol	Lanosterol	Dihydro-lanosterol
Solvent	Dioxane/ $CHCl_3$	Dioxane/ $CHCl_3$	Dioxane/ $CHCl_3$	Dioxane/ $CHCl_3$	$CDCl_3$	$CDCl_3$
Ref.	[283]	[283]	[283]	[283]	[286]	[286]
C-Atom						
1	37.3	37.4	38.1	38.6	35.0	35.1
2	28.2	28.3	28.2	32.2	27.4	27.4
3	73.7	80.3	72.6	69.7	78.3	77.9
4	38.4	39.0	36.8	41.1	38.1	38.2
5	139.9	141.0	141.0	140.7	49.8	49.8
6	122.6	121.3	120.4	119.4	20.3	20.5
7	32.2	32.0	116.7	116.7	27.4	27.4
8	32.2	160.5	138.5	140.6	133.9	133.0
9	50.4	50.5	46.2	46.5	133.9	133.0
10	36.7	36.9	37.2	37.2	36.3	36.5
11	21.3	21.2	21.1	21.2	17.6	17.6
12	32.5	28.2	28.2	28.3	25.8	25.8
13	42.5	42.5	43.0	43.0	43.7	43.8
14	57.0	57.0	54.5	54.6	49.1	49.1
15	24.6	24.3	23.0	23.1	30.2	30.3
16	40.1	40.1	39.4	39.4	30.2	30.3
17	56.6	56.6	56.2	56.0	49.8	49.8
18	12.0	11.9	11.8	11.8	15.3	15.2
19	19.3	19.3	16.0	16.0	18.0	18.1
20	36.1	36.0	36.3	40.5	35.1	35.8
21	18.9	18.8	18.9	19.4	18.4	18.5
22	36.7	36.4	36.3	132.2	35.1	35.8
23	24.3	24.1	24.0	136.0	24.2	23.6
24	39.8	39.7	39.6	43.0	124.7	38.9
25	28.2	28.0	28.0	33.2	130.2	27.4
26	22.7	22.5	22.5	19.7	24.9	22.3
27	22.9	22.7	22.7	21.0	16.9	22.0
28				17.4	23.5	23.6
CH_3 (methoxyl)		55.1				
CH_3 (acetyl)	20.9		20.9			
CO (acetyl)	169.6		169.6			
29					27.4	27.4
30					14.8	15.0

Table 5.3. (Continued).

	Cholestan-3-one	Cholesta-3,5-dien-7-one	Cholest-5-en-7-on-3β-yl acetate	2β,3β,14α-Trihydroxy-5β-cholest-7-en-6-one	α-Ecdysone	α-Ecdysone triacetate
Solvent	Dioxane/$CHCl_3$	Dioxane/$CHCl_3$	Dioxane/$CHCl_3$	Pyridine-d_5	Pyridine-d_5	Pyridine-d_5
Ref.	[283]	[283]	[283]	[287]	[287]	[287]
C-Atom						
1	38.6	33.0	36.1	37.2	37.2	33.9
2	37.9	23.5	27.5	66.8		68.2
3	209.1	136.1	72.3	66.8	66.9	66.6
4	44.5	124.4	37.7	31.7	31.7	28.8
5	46.7	160.0	163.2	50.3	50.3	50.7
6	29.1	127.9	126.7	175.7	175.7	175.7
7	31.9	200.4	200.1	119.5	119.5	119.4
8	35.7	46.0	45.3	163.0	162.9	162.9
9	54.1	49.8	49.9	33.9	33.9	33.9
10	35.6	36.2	38.3	37.9	37.9	37.8
11	21.6	21.4	21.3	20.7	20.7	20.9
12	28.3	28.7	28.6	26.9	26.1	25.9
13	42.7	43.6	43.2	46.3	46.7	46.8
14	56.5	50.9	50.2	82.8	82.5	82.4
15	24.3	26.5	26.4	31.2	31.3	31.3
16	40.2	39.2	39.0	30.8	30.8	30.8
17	56.6	55.3	55.2	50.2	47.4	47.3
18	12.0	12.0	11.8	15.6	15.5	15.4
19	11.2	16.5	16.9	24.0	24.0	23.7
20	35.9	35.9	35.9	35.4	41.6	39.1
21	18.7	19.0	18.9	18.9	13.3	13.6
22	36.4	36.4	36.4	36.1	72.8	76.5
23	24.0	24.1	24.1	24.0	25.0	22.5
24	39.6	39.6	39.6	39.1	42.2	40.7
25	28.0	28.0	28.0	27.7	68.6	68.2
26	22.5	22.6	22.4	22.6	29.7	29.7
27	22.7	22.8	22.6	22.3	29.4	29.2
28						
CH_3 (acetyl)			20.5			20.5
CO (acetyl)			169.3			162.9 167.4

Table 5.3. (Continued).

	Conanine	Conessine	Dihydroconessine	Ethyletiojervatrien-3-ol-11-one	Ethyletiojervatrien 3-ol-11-one acetate	Ethyletiojervadien-3-ol-11,16-dione acetate
Solvent	$CDCl_3$	$CDCl_3$	$CDCl_3$	Pyridine	Pyridine	Pyridine
Ref.	[290]	[290]	[290]	[289]	[289]	[289]
C-Atom						
1	39.1	38.5	38.1	36.2	35.7	35.4
2	21.8	25.3	24.9	30.6	26.4	26.6
3	27.0	64.8	64.3	69.7	72.4	72.1
4	29.2	35.6	31.5	41.2	36.6	36.7
5	46.8	141.9	45.9	141.8	140.2	139.5
6	29.2	120.7	29.2	119.4	119.9	120.6
7	32.2	32.2	32.4	37.5	36.6	36.1
8	37.8	33.6	37.8	43.4	43.6	42.9
9	54.7	50.2	54.5	61.6	61.4	61.5
10	36.2	37.0	35.9	36.2	36.2	36.1
11	22.3	22.1	22.3	204.6	205.0	204.9
12	27.6	27.8	27.6	136.4	136.3	
13	50.8	50.2	50.9	140.0	139.9	140.7
14	56.0	56.0	56.0	29.5	29.7	29.1
15	24.8	24.9	24.9	26.0	26.2	26.1
16	39.3	38.9	39.3	24.2	24.4	36.1
17	53.9	53.7	54.0	126.1	126.3	198.4
18	65.1	64.8	65.1	10.8	11.1	8.7
19	12.4	19.6	12.4	17.2	17.2	16.9
20	63.0	62.9	62.9			
21	15.0	15.1	15.1	13.2	13.2	
22						
23						
24						
25						
26						
27						
28						
$N-CH_3$	40.9					
CH_3 (dimethylamino)		41.8	41.8			
CH_3 (methylamino)		41.0	40.9			
CH_3 (acetyl)					20.0	19.7
CO (acetyl)					169.1	168.3

Table 5.3. (Continued).

	Veratramine	Veratramine diformate	Jervine
Solvent	Pyridine	$CHCl_3$	Pyridine
Ref.	[289]	[289]	[289]
C-Atom			
1	37.3	37.7	38.1
2	29.5	26.5	30.5
3	69.8	73.6	70.6
4	41.6	37.7	40.4
5	141.6		145.2
6	120.0		119.9
7	40.2	41.2	38.9
8	44.0	41.8	44.3
9	56.3	56.8	62.2
10	35.9	36.9	36.9
11	29.5	30.3	205.1
12	140.1		135.9
13	131.6		142.0
14	142.6		30.3
15	118.3		24.2
16	125.1		36.9
17	142.6		84.8
18	14.8	15.7	10.5
19	18.0	19.1	18.0
20	31.2	30.3	31.5
21	18.0	18.2	11.8
22	66.9	65.6	66.8
23	69.5	67.7	76.3
24	34.6	30.7	42.0
25	30.8	27.6	31.1
26	53.3	50.9	54.7
27	19.8	19.7	18.0
28			

5.3. Alkaloids

5.3.1. Nicotine

The ^{13}C NMR spectrum of nicotine has two groups of signals: The resonances of the unsaturated carbons appear at lower field and the saturated carbons resonate at higher field [291]. Off-resonance proton decoupling experiments and spectral comparisons with 3-picoline and the methiodide of nicotine led to the total signal assignment of the alkaloid (see Table 5.4).

5.3.2. Gelsemine and Derivatives

Gelsemine was the first alkaloid whose ^{13}C NMR signals could be totally assigned [292]. The signal identifications were made by applying general chemical shift rules [225] and proton off-resonance decoupling and by comparing the spectra of gelsemine with those of 18,19-dihydro-

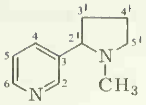

Nicotine

Table 5.4. ^{13}C Chemical Shifts of Nicotine and Analogs (δ Values in ppm Relative to TMS = 0) [291]; see also Fig. 2.21 and 3.1.

Solvent C-Atom	3-Picoline $CHCl_3$	Nicotine $CHCl_3$	Nicotine · 2 MeI DMSO − H_2O
2	149.30	148.80	147.10
3	132.60	138.30	129.80
4	136.10	134.00	146.90
5	122.90	122.60	128.70
6	146.60	147.80	146.70
2'		67.70	74.30
3'		34.40	26.40
4'		21.70	19.30
5'		55.80	67.00
$-NCH_3$		39.20	51.70
			49.70
			46.80

gelsemine, 2-deoxo-2,2,18,19-tetrahydrogelsemine, oxindole, aniline and its derivatives. The ^{13}C chemical shift data of gelsemine and its derivatives are listed in Table 5.5. The numbering of the carbon atoms in the parent alkaloid is used throughout.

5.3.3. Arenaïne

For the structural elucidation of the alkaloid arenaïne, which was isolated recently from the seeds of Plantago arenaria Waldst and Kit., the most valuable information was received from ^{13}C NMR spectroscopy [293]. Proton broad band and off-resonance decoupled spectra provided the following information concerning the structure of this alkaloid: The molecule of arenaïne consists of three quaternary (carbonyl, guanidyl and a $R_3C-N\langle$ group), three methine (olefinic methine, amino methine and a $\geq$CH group), three methylene (olefinic methylene and two $>CH_2$ groups) and two methyl carbons. The chemical shift values relative to TMS = 0 of the carbon atoms of arenaïne (solvent: $CHCl_3$) are denoted in the formula below:

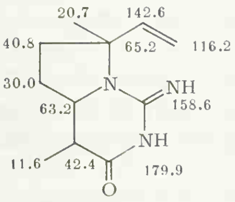

Arenaine

Table 5.5. ^{13}C Chemical Shifts of Gelsemine and Derivatives (δ Values in ppm Relative to TMS = 0, Solvent: $CHCl_3$) [292]

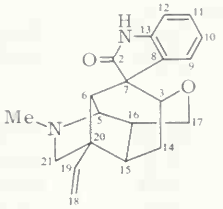

Gelsemine

C-Atom	Gelsemine	18,19-Di-hydrogelsemine	2-Deoxo-2,2,18,19-tetra-hydrogelsemine	Oxindole
C-2	179.40		56.30	178.60
C-3	69.40	69.30	70.80	
C-5	72.00	71.00	70.80	
C-6	40.60	38.60	39.70	
C-7	54.30	54.50	52.40	36.30
C-8	131.80		118.00	125.30
C-9	127.80		127.60	124.40
C-10	121.50		109.00	122.10
C-11	127.80		127.60	127.80
C-12	109.00		98.70	109.80
C-13	140.60		150.50	142.70
C-14	23.10	22.70	23.40	
C-15	38.30	37.20	36.60	
C-16	35.90	35.90	36.30	
C-17	61.50	61.50	61.60	
C-18	112.10	9.50	9.90	
C-19	138.60	21.50	22.20	
C-20	54.30	52.20	52.40	
C-21	66.00	63.40	63.00	
N – Me	50.60	49.60	53.50	

5.3.4. Piperine and Derivatives

The generally applied aids for signal assignment (see Section 5.3.2) resulted only in the unequivocal total resonance identifications of the piperine derivatives 1 and 2 [294].
The assignment of the lines of C-6, C_α, C_β, C_γ and C_δ of piperine could be achieved only by recording the ^{13}C NMR spectra of its $La(dpm)_3$*) and $Eu(dpm)_3$ complexes. As can be seen from Table 5.6, the magnitudes of the chemical shift changes (isotropic shifts) for the resonances of the different carbons upon addition of $Eu(dpm)_3$ or $La(dpm)_3$ depend on the atom's distance from

---

*) dpm = dipivaloylmethanato.

the rare earth metal ion, which is bonded to the amide oxygen. Raising the Eu(dpm)$_3$ concentration to a ratio higher than 1:1 = (Eu:piperine) results in a drastic change of the chemical shifts due to the beginning complexation of the dioxymethylene group.

Table 5.6. ^{13}C Chemical Shifts of Piperine and Dervatives (δ Values in ppm Relative to TMS = 0)[294]

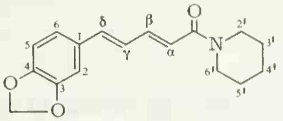

Piperine

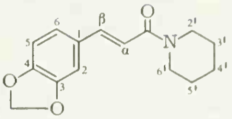

Piperine derivative 1

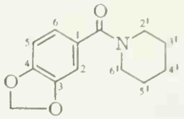

Piperine derivative 2

Solvent C-Atom	Piperine CCl$_4$	Piperine CHCl$_3$	Piperine Eu(dpm)$_3$ complex (1 : 1) CCl$_4$	Piperine La(dpm)$_3$ complex (1 : 1) CCl$_4$	Piperine Derivative 1 CCl$_4$	Piperine Derivative 2 CCl$_4$
C-1	131.10	130.90	130.00	130.60	130.00	130.10
C-2	105.60	105.50	105.30	105.60	106.10	107.50
C-3	147.90	148.00	147.90	147.90	148.40	148.10
C-4	147.90	148.00	147.90	147.90	147.90	148.10
C-5	108.20	108.20	107.80	108.20	108.10	108.00
C-6	121.90	122.30	121.90	122.20	123.20	121.10
α-C	120.10	120.00	136.60	116.60	115.60	
β-C	142.00	142.10	162.30	146.50	141.50	
γ-C	125.50	125.10	126.90	124.60		
δ-C	137.40	137.90	140.30	140.30		
C=O	163.50	165.10	157.50	165.30	163.90	168.30
C-2′	44.70	43.30	58.50	43.60	44.90	45.70
C-3′	26.10	25.80	30.90	25.60	26.10	25.90
C-4′	24.80	24.40	28.10	25.50	24.70	24.60
C-5′	26.10	25.80	30.90	25.60	26.10	25.90
C-6′	44.70	46.30	54.80	46.60	44.90	45.70
CH$_2$	100.80	101.10	100.80	100.80		

5.3.5. Amaryllidaceae Alkaloids

Using the assignment aids discussed previously, a total ^{13}C signal identification of amaryllidaceae alkaloids was achieved [291] as outlined in tables 5.7–5.11.

The assignment of carbon shifts in an alkaloid is illustrated in Fig. 5.3. If the sample is strong enough, proton off-resonance decoupling permits the localization of quaternary, methine, methylene and methyl carbons, respectively, as shown for narcotine in Fig. 5.3(a, b). Using the assigned shifts of β-hydrastine which has one methoxy group less than narcotine [295], a more detailed assignment is possible if the steric and mesomeric effects of the additional methoxy group in narcotine are also taken into account.

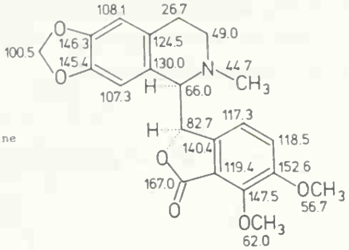
108.1
26.7
100.5
146.3
145.4
124.5
130.0
49.0
44.7
CH3
107.3
H
66.0
H
82.7
117.3
140.4
118.5
O
119.4
152.6
167.0
147.5
OCH3
56.7
O
OCH3
62.0

ß-Hydrastine

If experiments other than proton noise decoupling are not achievable because of weak sample solutions, the nuclear Overhauser enhancement of protonated carbon signals is a minimum assignment aid as illustrated for setoclavine, an alkaloid derived from lysergic acid [296] (Fig. 5.3(c)).

Table 5.7. ^{13}C Chemical Shifts of Tazettine and Derivatives (δ Values in ppm Relative to TMS = 0)[291].

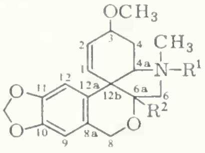
OCH3
CH3
N–R1
R2
O
O
O
1
2
3
4
4a
6
6a
8
8a
9
10
11
12
12a
12b

Tazettine (a) and Derivatives

a: no R^1 group; R^2 = OH
b: no R^1 group; R^2 = H
c: R^1 = H; R^2 = OH
d: R^1 = CH_3; R^2 = OH

	Tazettine			
Solvent C-Atom	a $CHCl_3$	b $CHCl_3$	c $DMSO-H_2O$	d $DMSO-H_2O$
1	130.60	130.80	132.30	131.10
2	128.50	129.50	127.40	127.10
3	72.50	72.70	72.20	73.10
4	26.70	26.10	27.10	24.10
4a	70.00	68.60	66.90	69.90
6	61.80	59.20	63.50	61.90
6a	101.80	81.10	76.30	99.80
8	65.10	65.70	63.80	61.90
8a	127.90	129.10	132.60	124.80
9	103.80	104.30	108.30	104.10
10	146.40	146.40	147.20	147.10
11	146.40	146.00	145.70	146.80
12	109.20	108.80	112.00	108.50
12a	125.50	127.30	132.80	124.10
12b	50.20	48.20	55.30	48.80
$O-CH_2-O$	100.70	100.70	101.00	101.20
$O-CH_3$	55.70	55.60	55.50	55.70
$N-CH_3$	42.00	41.20	40.40	44.10

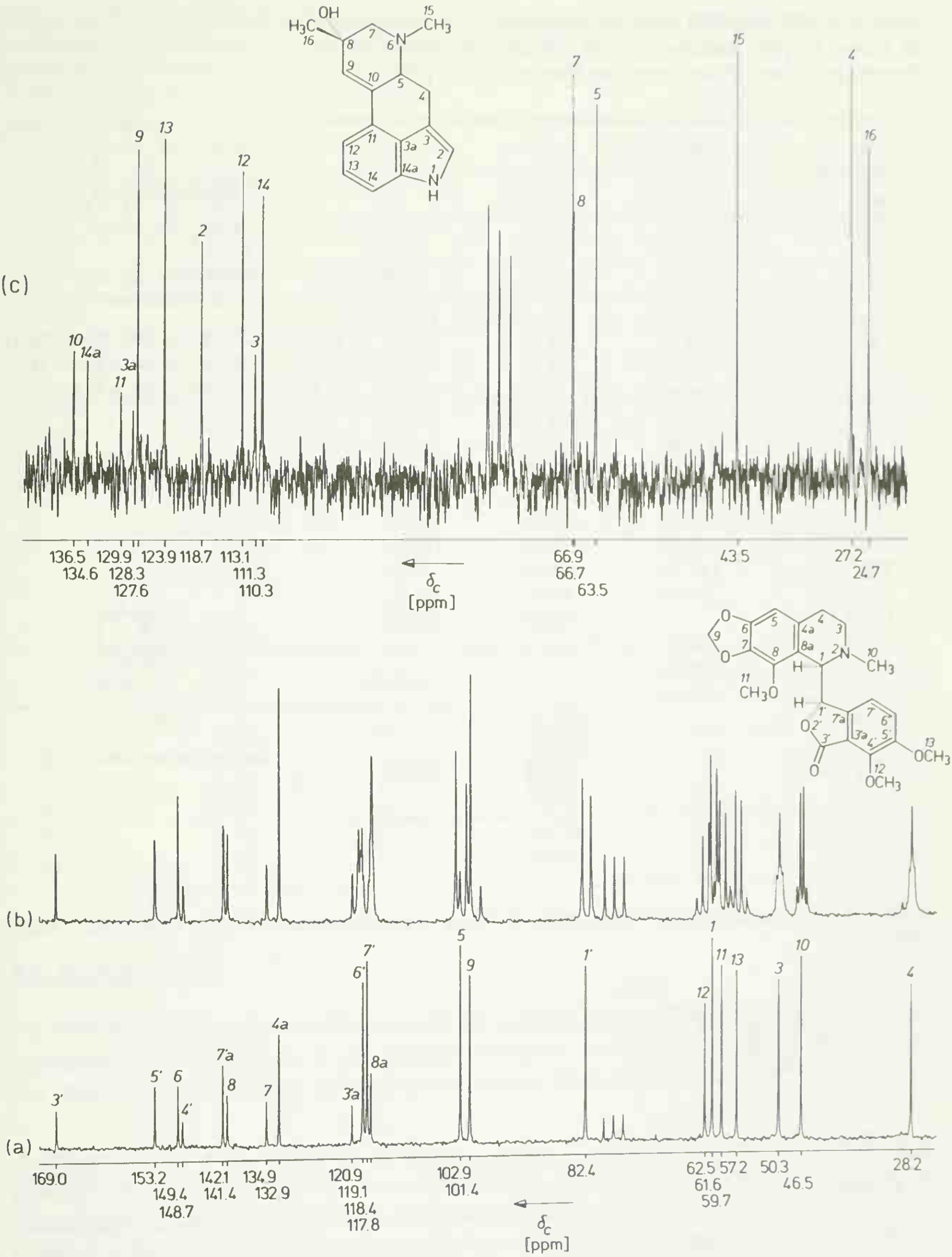

Fig. 5.3. (a,b) PFT ^{13}C NMR spectra of narcotine, 100 mg in 1.5 ml deuteriochloroform; 30 °C; 20 MHz; pulse angle: 45°; (a) proton broad band decoupled, 5000 scans; (b) proton off-resonance decoupled, 10000 scans.
(c) PFT ^{13}C NMR spectrum of setoclavine, 10 mg in 1 ml ^{12}C deuteriochloroform; 30 °C; 20 MHz; pulse angle: 30°; proton broad band decoupled, 30000 scans.

Table 5.8. ^{13}C Chemical Shifts of Galanthine and Derivatives (δ Values in ppm Relative to TMS = 0; Solvent: $CHCl_3$; for Numbering of the Carbon Atoms See Formula above) [291].

C-Atom	Galanthine		
	a	b	c
1	68.20	69.10	66.20
2	80.90	70.50	33.00
3	114.80	113.40	113.70
3a	143.70	145.90	139.30
4	28.30	28.30	28.20
5	53.50	53.10	53.30
7	56.90	56.40	56.60
7a	129.20	129.20	129.30
8	110.90	106.90	106.90
9	147.60	145.90	146.00
10	147.60	145.90	146.00
11	108.20	104.80	104.70
11a	126.70	126.20	127.50
11b	41.30	40.10	43.10
11c	60.70	60.60	60.90
OCH_2O		100.60	100.50
OCH_3	56.30		
	55.90		
	55.70		
C=O		169.30	
		169.00	
CH_3 (acetyl)		20.50	20.70
		20.10	

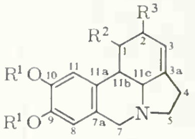
R³
R²
R¹O
R¹O
1
2
3
3a
4
5
N
7
7a
8
9
10
11
11a
11b
11c

Galanthine (a) and Derivatives

a: $R^1 = CH_3$; $R^2 = OH$; $R^3 = OCH_3$
b: $R^1 = CH_2$; $R^2 = OAc$; $R^3 = H$
c: $R^1 = CH_2$; $R^2 = R^3 = OAc$

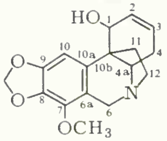
HO
1
2
3
4
10
10a
10b
4a
11
12
9
8
7
6a
6
N
O
O
OCH₃

Buphanamine (table 5.10)

Table 5.9. ^{13}C Chemical Shifts of Montanine (δ Values in ppm Relative to TMS = 0; Solvent: $CHCl_3$) [291].

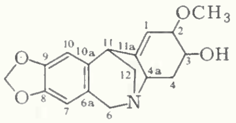
OCH₃
OH
1
2
3
4
4a
10
10a
11
11a
12
9
8
7
6a
6
N
O
O

Montanine

C-Atom		C-Atom		C-Atom	
1	112.80	6a	132.20	11	45.60
2	79.60	7	106.90	11a	153.70
3	68.30	8	146.40	12	57.00
4	32.80	9	145.60	OCH_2O	100.80
4a	60.60	10	106.40	OCH_3	55.10
6	58.40	10a	124.30		

Table 5.10. ^{13}C Chemical Shifts of Buphanamine (δ Values in ppm Relative to TMS = 0; Solvent: $CHCl_3$; for Numbering of the Carbon Atoms See Formula above) [291].

C-Atom		C-Atom		C-Atom	
1	64.30	6a	118.40	10b	48.20
2	128.40	7	140.50	11	39.10
3	125.90	8	137.50	12	51.60
4	28.30	9	148.10	OCH_2O	100.30
4a	59.10	10	98.40	OCH_3	59.10
6	57.20	10a	136.70		

Table 5.11. ^{13}C Chemical Shifts of Lycorenine (δ Values in ppm Relative to TMS = 0; Solvent: $CHCl_3$) [291].

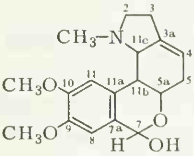

Lycorenine

C-Atom		C-Atom		C-Atom	
2	56.80	7	90.80	11a	126.60
3	28.00	7a	129.60	11b	43.90
3a	139.70	8	112.40	11c	66.50
4	115.00	9	147.70	OCH_3	56.20
5	31.80	10	147.70	OCH_3	56.00
5a	67.40	11	109.50	NCH_3	43.90

5.4. Carbohydrates

^{13}C NMR has proven to be one of the most efficient spectroscopic methods for configurational and conformational investigations in carbohydrate chemistry. The signal assignments of mono-, di- and polysaccharides, inositols and polyols are done on the following basis:

(1) Primary (*e.g.* C-6 of rhamnose), secondary (*e.g.* C-6 of glucose), tertiary (*e.g.* CHOH of a pyranose ring carbon atom) and quaternary carbons (*e.g.* of branched-chain sugars) can be distinguished by proton off-resonance decoupling [66, 297].

(2) Most of the signals are assigned by comparison of the chemical shifts of analogous series of sugars and their derivatives such as glycosides and nucleosides.

(3) The ^{13}C resonances shift downfield with increasing alkyl substitution and increasing number of electron withdrawing substituents A [65, 66, 297–303]

$$\delta_{CCH_3} < \delta_{CCH_2C} < \delta_{CCH_2A} < \delta_{CCHA_2} .$$

(4) Carbons attached to methoxy groups resonate at lower field than corresponding carbon atoms with free hydroxyl groups [65, 66, 297 – 303].

(5) Ring carbon atoms with axially oriented hydroxyl groups generally [245] absorb at higher field than corresponding carbons with equatorially oriented hydroxyl groups [65, 66, 297 – 303].

(6) If an equatorially oriented hydroxyl group on a saturated six membered ring is changed to axial orientation, the γ-carbons with axially oriented hydrogen atoms on the same side of the ring shift to higher field [65, 66, 297a, 299]

(7) Recording ^{13}C NMR spectra before and after the mutarotational equilibration was shown to be a valuable method for assigning signals of anomers (α or β) [297a,b, 301 – 303, 305].

(8) The signals of adjacent carbons bearing hydroxyl groups in *cis* configuration to each other can be identified by a downfield shift observed on addition of boric acid as a complex shift reagent [306].

5.4.1. Aldohexoses and Aldopentoses

The resonances of the aldoses and their derivatives shown in Table 5.12 were assigned according to rules 1 – 8 [65, 66, 297a,b, 299, 302, 303 – 310].

Upon 3-O-methylation of D-galactose the resonance of C-4 shifts about 4.5 ppm upfield. This effect is a general rule: Methylation of pyranose hydroxyl groups causes upfield shifts of the β-carbons with axial hydroxyl groups of about 4.5 ppm [309].

A mutarotational equilibration is demonstrated in Fig. 5.4 by the time dependent ^{13}C NMR spectrum of a solution of D-glucose. Initially, the solution contains almost pure α-D-glucose, but the signals at lower field corresponding to the β-anomer soon appear. At equilibrium, the relative signal intensities indicate that the β-anomer is favored (60% β, 40% α; Fig. 5.4b) [305].

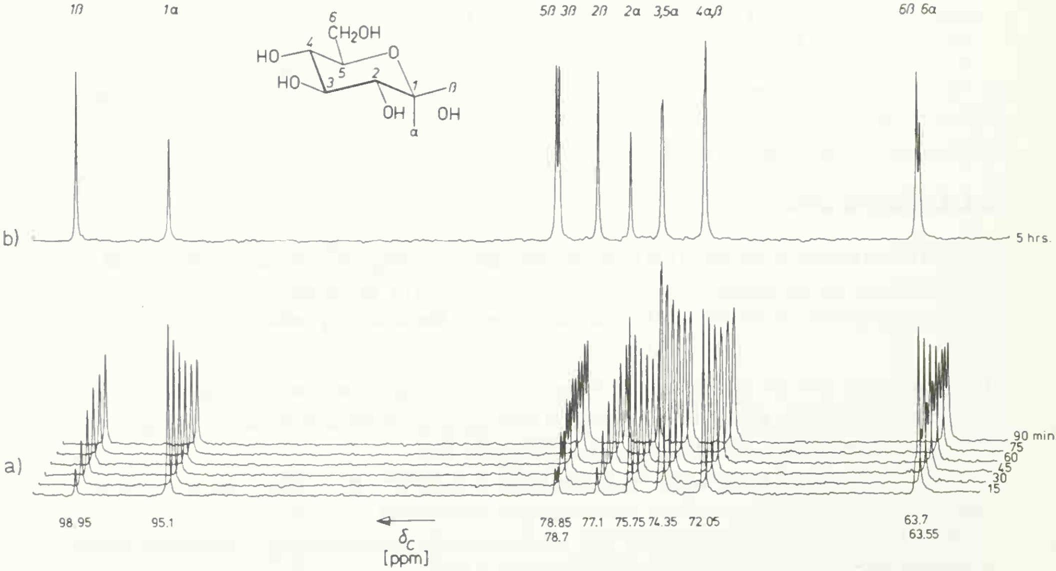

Fig. 5.4. PFT $^{13}C\{^1H\}$ NMR spectrum of D-glucose, 20 MHz, 1 M in D_2O, temperature 30 °C, 90 °C pulses; accumulation of 200 pulse interferograms; (a) series of spectra recorded 15, 30, 45, 60, 75 and 90 min. after sample preparation; (b) spectrum of the same sample, recorded 12 hrs. after sample preparation.

Table 5.12. ^{13}C Chemical Shifts of Aldohexoses, Aldopentoses and Derivatives (δ Values in ppm Relative to TMS = 0; for Numbering See Formulae on Pages 254, 256f.

Compound	C-1	C-2	C-3	C-4	C-5	C-6	OCH_3 *etc.*	Solvent	Ref.
α-D-Glucopyranose	95.10	75.75	74.35	72.05	74.35	63.55		D_2O	Fig. 5.4
β-D-Glucopyranose	98.95	77.10	78.70	72.05	78.85	63.70		D_2O	Fig. 5.4
Methyl-α-D-glucopyranoside	99.60	71.90	73.60	70.10	71.60	61.20	55.30	H_2O	[65]
Methyl-β-D-glucopyranoside	103.40	73.40	75.20	70.00	75.20	61.40	57.50	H_2O	[65]
3-O-Methyl-α-D-glucopyranose	92.10	71.10	82.70	69.10	71.30	60.70	59.90 (OCH_3)	H_2O	[66]
3-O-Methyl-β-D-glucopyranose	96.00	73.70	85.20	68.90	75.70	60.70	59.60 (OCH_3)	H_2O	[66]
α-D-Glucopyranose-pentaacetate	88.60	68.90	69.50	67.70	69.50	61.10	169.80, 169.40, 169.20, 168.80, 168.30 ($C{=}O$); 20.30, 19.80, 19.30 (CH_3)	H_2O	[300]
β-D-Glucopyranose-pentaacetate	91.30	70.00	72.30	67.60	72.30	61.30	169.80, 169.30, 168.90, 168.70, 168.40 ($C{=}O$); 19.90, 19.80 (CH_3)	H_2O	[300]
p-Nitrophenyl-α-D-glucopyranoside	100.45	74.10	76.90	72.50	75.75	63.45	$C_{arom.}$: 119.65, 128.25, 144.35, 164.85	DMSO	[299]
p-Nitrophenyl-β-D-glucopyranoside	102.70	75.95	80.05	72.40	79.30	63.45	$C_{arom.}$: 119.45, 128.50, 144.55, 165.15	DMSO	[299]
m-Nitrophenyl-β-D-glucopyranoside	103.55	76.05	79.95	72.60	79.20	63.55	$C_{arom.}$: 113.90, 119.55, 126.00, 133.45, 151.35, 160.55	DMSO	[299]
o-Nitrophenyl-β-D-glucopyranoside	103.25	75.95	80.05	72.40	79.50	63.45	$C_{arom.}$: 119.85, 124.70, 127.50, 136.90, 143.05, 152.40	DMSO	[299]
Phenyl-β-D-glucopyranoside	103.05	75.80	79.50	72.40	79.30	63.55	$C_{arom.}$: 119.00, 124.60, 132.15, 153.50	DMSO	[299]
Methyl-4,6-O-benzylidene-α-D-glucopyranoside	99.80	72.20	70.40	80.60	61.90	68.40	54.80 (OCH_3); 101.40 (C-7); $C_{arom.}$: 136.80 ($C_{subst.}$); 128.70 (*p*-); 127.80, 125.80 (*o*-, *m*-)	$CDCl_3$: MeOH (4 : 1)	[307]
Methyl-4,6-O-benzylidene-3-amino-3-deoxy-α-D-glucopyranoside	98.40	72.10	52.40	81.00	62.20	68.70	55.00 (OCH_3); 101.50 (C-7); $C_{arom.}$: 136.80 ($C_{subst.}$); 128.70 (*p*-); 127.80, 125.80 (*o*-, *m*-)	$CDCl_3$: MeOH (4 : 1)	[307]
Methyl-4,6-O-benzylidene-β-D-glucopyranoside	103.80	73.90	72.60	80.00	65.70	67.90	56.70 (OCH_3); 101.30 (C-7); $C_{arom.}$: 136.80 ($C_{subst.}$); 128.70 (*p*-); 127.80, 125.80 (*o*-, *m*-)	$CDCl_3$: MeOH (4 : 1)	[307]

Table 5.12. (Continued).

Compound	C-1	C-2	C-3	C-4	C-5	C-6	OCH_3 *etc.*	Solvent	Ref.
Ethyl-4,6-O-benzylidene-1-thio-β-D-glucopyranoside	85.30	74.10	72.90	79.90	69.90	67.90	14.40 (CH_3); 23.90 (CH_2); 101.10 (C-7); $C_{arom.}$: 136.80 ($C_{subst.}$); 128.70 (*p*-); 127.80, 125.80 (*o*-, *m*-)	$CDCl_3$: MeOH (4 : 1)	[307]
Methyl-2-deoxy-4,6-O-benzylidene-3-C-(2-methyl-1,3-dithiane-2-yl)-α-D-glucopyranoside	98.40	36.35	75.65	79.85	59.15	68.85	100.90 (C-7); 58.50 (C-2′); 26.00 (C-4′); 24.15 (C-5′); 26.00 (C-6′); 24.90 (CH_3); 54.70 (OCH_3); $C_{arom.}$: 137.00 ($C_{subst.}$); 128.30 (*p*-); 125.70, 127.55 (*o*-, *m*-)	$CDCl_3$	[308]
Methyl-2-deoxy-4,6-O-benzylidene-3-C-(1,3-dithiane-2-yl)-α-D-glucopyranoside	98.50	35.80	72.85	78.00	59.25	69.05	101.65 (C-7); 53.10 (C-2′); 30.10, 30.65 (C-4′); 25.80 (C-5′); 30.10, 30.65 (C-6′); 55.25 (OCH_3); $C_{arom.}$: 137.25 ($C_{subst.}$); 128.80 (*p*-); 126.15, 127.95 (*o*-, *m*-)	$CDCl_3$	[308]
α-D-Galactopyranose	92.35	69.40	68.40	69.20	70.50	61.25		D_2O	[309]
β-D-Galactopyranose	96.50	71.90	72.85	68.80	75.20	61.05		D_2O	[309]
Methyl-α-D-galactopyranoside	99.50	69.60	68.30	69.30	70.80	61.30	55.15 (OCH_3)	D_2O	[309]
Methyl-β-D-galactopyranoside	103.90	70.80	72.85	68.75	75.20	61.05	57.30 (OCH_3(1))	D_2O	[309]
Methyl-3-O-methyl-β-D-galactopyranoside	103.90	69.80	82.00	64.20	75.10	61.20	56.20 (OCH_3(3)); 57.30 (OCH_3(1))	D_2O	[309]
Methyl-2,6-O-dimethyl-α-D-galactopyranoside	96.80	77.45	68.60	69.50	73.15	71.85	55.05 (OCH_3(1)); 57.70, 58.50 (OCH_3(2,6))	D_2O	[309]
Methyl-2,3,4,6-tetra-O-methyl-β-D-galactopyranoside	103.35	79.75	82.20	73.05	74.90	71.00	57.10 (OCH_3(1)); 57.10, 58.50, 60.20, 60.95 (OCH_3(2,3,4,6))	D_2O	[309]
α-L-Fucopyranose	92.20	69.40	68.20	71.80	66.00	15.60		H_2O	[66]
β-L-Fucopyranose	96.30	71.80	73.00	71.40	70.50	15.60		H_2O	[66]
p-Nitrophenyl-α-D-galactopyranoside	100.75	75.50	71.20	70.45	72.05	63.00	$C_{arom.}$: 119.55, 128.15, 144.15, 165.05	DMSO	[299]
m-Nitrophenyl-β-D-galactopyranoside	104.20	73.25	76.05	71.10	78.65	63.45	$C_{arom.}$: 113.90, 119.55, 126.20, 133.55, 173.05, 160.65	DMSO	[299]

Table 5.12. (Continued).

Compound	C-1	C-2	C-3	C-4	C-5	C-6	OCH_3 *etc.*	Solvent	Ref.
o-Nitrophenyl-β-D-galactopyranoside	104.10	73.15	76.25	71.10	78.65	63.45	$C_{arom.}$: 119.95, 124.70, 127.50, 137.00, 152.55, 143.15	DMSO	[299]
Phenyl-β-D-galactopyranoside	104.00	73.55	76.40	71.30	78.30	63.65	$C_{arom.}$: 119.30, 124.90, 132.50, 160.40	DMSO	[299]
α-D-Mannopyranose	95.20	71.85	71.35	68.05	73.55	62.15		D_2O	[302]
β-D-Mannopyranose	94.85	72.35	74.10	67.75	77.30	62.15		D_2O	[302]
α-L-Rhamnopyranose	95.10	71.90	71.05	73.30	69.40	17.90		D_2O	[302]
β-L-Rhamnopyranose	94.60	72.45	73.85	72.95 73.15	72.95 73.15	17.90		D_2O	[302]
Methyl-α-D-mannopyranoside	101.95	71.70	71.05	67.90	73.70	62.10	55.85 (OCH_3)	D_2O	[302]
Methyl-β-D-mannopyranoside	101.00	70.30	73.00	66.80	76.30	61.10	56.60 (OCH_3)	H_2O	[65]
p-Nitrophenyl-α-D-mannopyranoside	101.50	73.40	72.50	69.45	78.00	63.75	$C_{arom.}$: 119.55, 128.40, 144.45, 164.10	DMSO	[299]
Methyl-4,6-O-benzylidene-α-D-mannopyranoside	101.40	70.40	67.60	78.30	62.70	68.00	101.40 (C-7); 54.10 (OCH_3); $C_{arom.}$: 136.80 ($C_{subst.}$); 128.70 (*p*-); 127.80, 125.80 (*o*-, *m*-)	$CDCl_3$: MeOH (4 : 1)	[307]
Methyl-4,6-O-benzylidene-3-amino-3-deoxy-α-D-mannopyranoside	102.00	70.00	50.30	79.40	63.40	68.60	101.60 (C-7); 54.50 (OCH_3); $C_{arom.}$: 136.80 ($C_{subst.}$); 128.70 (*p*-); 127.80, 125.80 (*o*-, *m*-)	$CDCl_3$: MeOH (4 : 1)	[307]
β-D-Allopyranose	93.50	71.30	71.10	66.90	73.50	61.30		H_2O	[66]
Methyl-4,6-O-benzylidene-α-D-allopyranoside	100.00	67.70	68.70	77.30	56.80	68.70	101.40 (C-7); 55.70 (OCH_3); $C_{arom.}$: 136.80 ($C_{subst.}$); 128.70 (*p*-); 127.80, 125.80 (*o*-, *m*-)	$CDCl_3$: MeOH (4 : 1)	[307]
Methyl-4,6-O-benzylidene-2,3-dideoxy-α-D-erythrohexopyranoside	97.40	28.90	23.40	77.80	64.40	68.90	101.40 (C-7); 54.10 (OCH_3); $C_{arom.}$: 136.80 ($C_{subst.}$); 128.70 (*p*-); 127.80, 125.80 (*o*-, *m*-)	$CDCl_3$: MeOH (4 : 1)	[307]
Methyl-4,6-O-benzylidene-3-amino-3-deoxy-α-D-allopyranoside	100.80	68.90	52.20	78.30	56.70	67.50	101.30 (C-7); 55.60 (OCH_3); $C_{arom.}$: 136.80 ($C_{subst.}$); 128.70 (*p*-); 127.80, 125.80 (*o*-, *m*-)	$CDCl_3$: MeOH (4 : 1)	[307]
1,2,5,6-O-Diisopropylidene-3-C-(1,3-dithiane-2-yl)-allofuranose	104.45	83.20	80.50	80.50	73.05	67.95	25.35, 26.35 (C-7/7′); 50.50 (C-2′); 29.10 (C-4′); 26.75 (C-5′); 29.10 (C-6′); 25.35, 26.36 (CH_3)	$CDCl_3$	[308]
Methyl-α-D-altropyranoside	100.80	69.70	69.70	64.50	69.70	61.00	55.10 (OCH_3)	H_2O	[65]

Table 5.12. (Continued).

Compound	C-1	C-2	C-3	C-4	C-5	C-6	OCH_3 *etc.*	Solvent	Ref.
Methyl-4,6-O-benzylidene-α-D-altropyranoside	101.50	69.30	68.60	75.80	57.60	68.60	101.50 (C-7); 54.80 (OCH_3); $C_{arom.}$: 136.80 ($C_{subst.}$); 128.70 (*p*-); 127.80, 125.80 (*o*-, *m*-)	$CDCl_3$: MeOH (4 : 1)	[307]
Methyl-4,6-O-benzylidene-β-D-altropyranoside	98.90	70.40	68.20	76.00	62.40	68.20	101.40 (C-7); 56.30 (OCH_3); $C_{arom.}$: 136.80 ($C_{subst.}$); 128.70 (*p*-); 127.80, 125.80 (*o*-, *m*-)	$CDCl_3$: MeOH (4 : 1)	[307]
Methyl-4,6-O-benzylidene-3-amino-3-deoxy-α-D-altropyranoside	101.80	69.40	51.30	75.80	57.60	68.70	101.50 (C-7); 54.80 (OCH_3); $C_{arom.}$: 136.80 ($C_{subst.}$); 128.70 (*p*-); 127.80, 125.80 (*o*-, *m*-)	$CDCl_3$: MeOH (4 : 1)	[307]
Methyl-3-O-acetyl-4,6-O-benzylidene-2-deoxy-2-C-(1,3-dithiane-2-yl)-α-D-altropyranoside	102.20	46.10	74.80	69.70	69.50	59.00	55.80 (OCH_3); 99.90 (C-7); 170.50 ($-\mathrm{O}-\underset{\underset{\mathrm{O}}{\Vert}}{\mathrm{C}}-$); 21.40 ($CH_3$); 44.30(C-2′); 27.80(C-4′); 25.30(C-5′); 28.00(C-6′); $C_{arom.}$: 137.60 ($C_{subst.}$); 129.20 (*p*-); 128.20 (*o*-); 126.10 (*m*-)	$CDCl_3$	[310]
Methyl-2-O-acetyl-4,6-O-benzylidene-3-deoxy-3-C-(1,3-dithiane-2-yl)-α-D-altropyranoside	103.10	77.20	45.00	71.50	69.70	59.60	55.70 (OCH_3); 99.50 (C-7); 169.90 ($-\mathrm{O}-\underset{\underset{\mathrm{O}}{\Vert}}{\mathrm{C}}-$); 21.10 ($CH_3$); 44.20(C-2′); 30.20(C-4′); 25.70(C-5′); 30.60 (C-6′)- $C_{arom.}$: 138.00 ($C_{subst.}$); 128.60 (*o*-); 127.00 (*m*-); 129.30 (*p*-)	$CDCl_3$	[310]
Methyl-α-D-idopyranoside	101.20	70.60	71.50	70.00	70.50	59.90	55.50 (OCH_3)	H_2O	[65]
α-D-Talopyranose	94.70	70.70	69.70	65.10	71.20	61.50		H_2O	[303]
β-D-Talopyranose	94.20	68.65	71.55	68.45	75.70	61.25		H_2O	[303]
β-D-Talofuranose	100.95	75.20	81.90	82.50	71.85	62.80		H_2O	[303]
Ascorbic acid	174.00	118.80	156.30	77.10	69.90	63.20		H_2O	[501]
α-D-Arabinopyranose	96.85	71.95	72.55	68.55	66.40			H_2O	[297a]
β-D-Arabinopyranose	92.60	68.70	68.70	68.55	62.55			H_2O	[297a]
α-D-Arabinofuranose	101.15	70.25	70.25	81.50	61.30			H_2O	[297a]
		74.30	74.30	83.05					
		75.75	75.75						
		76.85	76.85						

Table 5.12. (Continued).

Compound	C-1	C-2	C-3	C-4	C-5	C-6	OCH_3 *etc.*	Solvent	Ref.
β-D-Arabinofuranose	95.20	70.25 74.30 75.75 76.85	70.25 74.30 75.75 76.85	81.50 83.05	62.55			H_2O	[297a]
Methyl-α-D-arabinopyranoside	104.05	72.50	70.85	68.35	66.15		57.10 (OCH_3)	H_2O	[297a]
Methyl-β-D-arabinopyranoside	99.95	69.05	69.05	68.35	62.60		55.30 (OCH_3)	H_2O	[297a]
Methyl-4,6-O-benzylidene-3-deoxy-α-D-arabinohexopyranoside	100.40	67.40	31.40	73.40	64.40	68.90	101.70 (C-7); 54.10 (OCH_3); $C_{arom.}$: 136.80 ($C_{subst.}$); 128.70 (*p*-); 127.80, 125.80 (*o*-, *m*-)	$CDCl_3$: MeOH (4 : 1)	[307]
α-D-Ribopyranose	96.25	72.75	71.95	70.00	65.70			D_2O	[107b]
β-D-Ribopyranose	96.55	73.75	71.70	69.95	65.70			D_2O	[107b]
α-D-Ribofuranose	99.00	73.70	72.75	85.75	64.10			D_2O	[107b]
β-D-Ribofuranose	103.65	78.00	73.15	85.20	65.25			D_2O	[107b]
2-Deoxy-α-D-ribopyranose	91.65	35.15	64.65	67.50	62.85			D_2O	[297b]
2-Deoxy-β-D-ribopyranose	93.85	33.80	66.50	67.35	66.00			D_2O	[297b]
2-Deoxy-α-D-ribofuranose	91.65	41.15 41.30	70.95 71.25	85.30 85.85	61.55 62.85			D_2O	[297b]
2-Deoxy-β-D-ribofuranose	98.05	41.15 41.30	70.95 71.25	85.30 85.85	61.55 62.85			D_2O	[297b]
Methyl-β-D-ribopyranoside	103.85	70.40	69.85	72.65	65.55		58.30 (OCH_3)	D_2O	[297b]
Methyl-β-D-ribofuranoside	108.00	74.35	70.85	82.95	62.90		55.30 (OCH_3)	D_2O	[297b]
Methyl-4,6-O-benzylidene-3-deoxy-α-D-ribohexopyranoside	98.90	66.90	32.50	76.00	63.40	68.90	101.20 (C-7); 54.60 (OCH_3); $C_{arom.}$: 136.80 ($C_{subst.}$); 128.70 (*p*-); 127.80, 125.80 (*o*-, *m*-)	$CDCl_3$: MeOH (4 : 1)	[307]
Methyl-3,4-O-isopropylidene-3-C-(1,3-dithiane-2-yl)-β-D-ribopyranoside	99.80	72.05	70.80	72.95	57.30	108.20	25.45 (C-7); 54.70 (C-2'); 29.80, 30.30 (C-4'); 24.80 (C-5'); 29.80, 30.30 (C-6'); 55.45 (OCH_3)	$CDCl_3$	[308]

Table 5.12. (Continued).

Compound	C-1	C-2	C-3	C-4	C-5	C-6	OCH_3 *etc.*	Solvent	Ref.
Methyl-3,4-O-isopropylidene-3-C-(2-methyl-1,3-dithiane-2-yl)-β-D-ribopyranoside	101.40	75.40	71.10	71.55	57.85	108.20	25.55 (C-7); 55.80 (C-2′); 26.55, 26.95 (C-4′); 24.05 (C-5′); 26.55, 26.95 (C-6′); 25.15 (CH_3); 55.05 (OCH_3)	$CDCl_3$	[308]
α-D-Xylopyranose	92.30	71.60	73.00	69.55	61.05			H_2O	[295]
β-D-Xylopyranose	96.70	74.10	75.90	69.35	65.25			H_2O	[295]
Methyl-α-D-xylopyranoside	98.30	71.20	73.20	69.35	60.70		54.60 (OCH_3)	H_2O	[295]
Methyl-β-D-xylopyranoside	103.80	72.70	75.70	69.30	64.70		56.60 (OCH_3)	H_2O	[295]
α-D-Lyxopyranose	94.30	70.40	70.90	67.80	63.10			H_2O	[65]
β-D-Lyxopyranose	94.30	70.40	72.90	67.00	64.20			H_2O	[65]
Methyl-α-D-lyxofuranoside	109.2	77.0	72.2	81.4	61.5		56.9	D_2O	[301]
Methyl-β-D-lyxofuranoside	103.3	73.2	71.0	82.1	62.7		56.7	D_2O	[301]
Methyl-α-D-erythrofuranoside	103.6	72.8	69.9	73.6			56.7	D_2O	[301]
Methyl-β-D-erythrofuranoside	109.6	76.4	71.4	72.6			56.6	D_2O	[301]
Methyl-α-L-threofuranoside	109.4	80.5	76.4	73.7			55.5	D_2O	[301]
Methyl-β-L-threofuranoside	103.8	77.4	75.8	72.0			56.2	D_2O	[301]

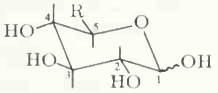
HO
R
O
HO
HO
OH
1
2
3
4
5

D-Glucopyranose: R = CH_2OH

D-Xylopyranose: R = H

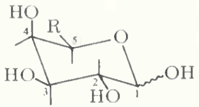
HO
R
O
HO
HO
OH
1
2
3
4
5

D-Galactopyranose: R = CH_2OH

D-Fucose: R = CH_3

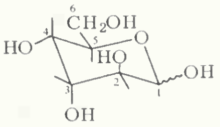
6
CH_2OH
HO
O
HO
OH
OH
1
2
3
4
5

D-Altropyranose

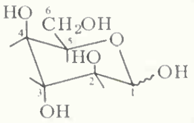
HO
6
CH_2OH
O
HO
OH
OH
1
2
3
4
5

D-Idopyranose

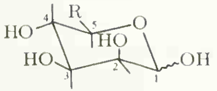
R
HO
O
HO
HO
OH
1
2
3
4
5

D-Mannopyranose: R = CH_2OH

D-Rhamnopyranose: R = CH_3

D-Lyxopyranose: R = H

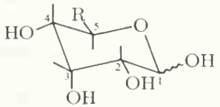
R
HO
O
OH
OH
OH
1
2
3
4
5

D-Allopyranose: R = CH_2OH

D-Ribopyranose: R = H

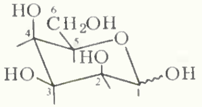
HO
6
CH_2OH
O
HO
HO
OH
1
2
3
4
5

D-Talopyranose

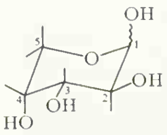
OH
O
OH
OH
HO
1
2
3
4
5

D-Arabinopyranose

Fig. 5.5 illustrates that D-ribose equilibrates in α- and β-pyranoses and furanoses when dissolved in water [107b]. High-field ^{13}C NMR also detected 0.6% α- and 0.3% β-D-mannofuranose in aqueous D-mannose solution [107c].

Hydroxylated furanose ring carbons resonate at lower field than the corresponding pyranose carbons, as is demonstrated by the PFT ^{13}C NMR spectrum of ribose in Fig. 5.5 [297b]

An anomeric carbon with an axial hydroxyl group usually resonates at higher field than the corresponding C-1 with an equatorial hydroxyl group (rule 5). This rule allows to prove, experimentally, that arabinose exists in the 1 C and not in the C 1 conformation, in which most of the sugars occur in solution [65, 304]. However, rule 5 is not valid for the mannose, rhamnose and talose anomers. This was attributed to three closely spaced dipoles (Reeves effect) present in the β-anomeric configuration of these three sugars [302, 303].

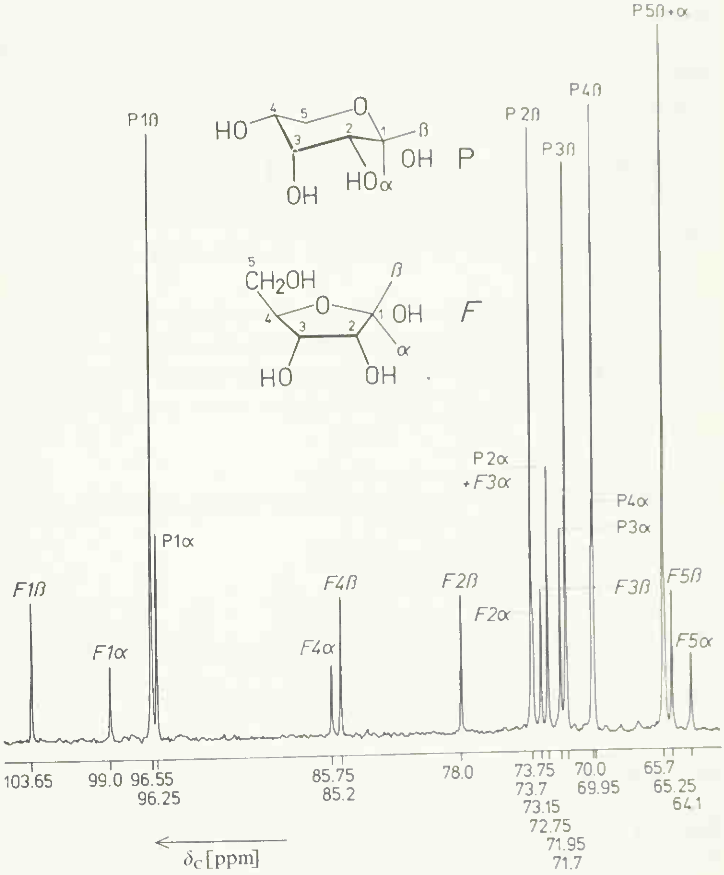

Fig. 5.5. PFT $^{13}\{^1H\}$ NMR spectra of D-ribose, 22.63 MHz, 1 g/2 ml D_2O, temperature 30 °C, accumulation of 2000 pulse interferograms (6 K data points), 90° pulses, pulse interval 6 s, 2500 Hz, the numbers of the signals refer to the numbering of the C-atoms. A quantitative evaluation of the spectrum gave 62% of β-ribopyranose (Pβ), 20.3% of α-ribopyranose (Pα), 11.6% of β-ribofuranose (Fβ) and 6.1% of α-ribofuranose (Fα) [107].

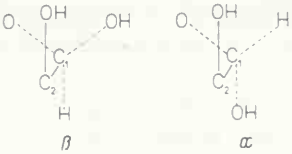

Fig. 5.6. Configuration of α-, and β-C-1,2 of D-talose for the demonstration of the Reeves effect.

Comparing the shifts of the methoxy resonances of anomeric pairs of methyl glycosides is a more reliable method for establishing the pyranose conformations. The methyl carbons of axially oriented methoxy groups in methyl glycosides are found 1.5 to 2 ppm at higher field than those of equatorially oriented anomeric methoxy groups [304]. The ^{13}C resonances of a series of *trans* fused methyl 4,6-O-benzylidene-D-aldohexopyranosides (Table 5.12) were assigned recently by the general chemical shift rules discussed above [307]. The carbons of this series resonate from higher to lower field in the following order: $OCH_3 > C\text{-}5 > C\text{-}6 > C\text{-}2 \approx C\text{-}3 > C\text{-}4 > C\text{-}1$.

^{13}C NMR spectroscopy was successfully used for the structural determination of 1,3-dithiane-2-yl sugars [308, 310], the starting materials of branched-chain carbohydrates. The δ values of the following examples are listed in Table 5.12.

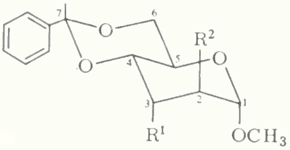

Methyl-2-O-acetyl-4,6-O-benzylidene-3-deoxy-3-C-(1,3-dithiane-2-yl)-α-D-altropyranoside

(R^2 = OAc, R^1 =
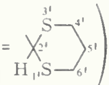

).

Methyl-3-O-acetyl-4,6-O-benzylidene-2-deoxy-2-C-(1,3-dithiane-2-yl)-α-D-altropyranoside

(R^1 = OAc, R^2 =
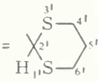

).

Methyl-2-deoxy-4,6-O-benzylidene-3-C-(1,3-dithiane-2-yl)-α-D-glucopyranoside

(R^2 = H, R^1 =
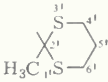

).

Methyl-2-deoxy-4,6-O-benzylidine-3-C-(2-methyl-1,3-dithiane-2-yl)-α-D-glucopyranoside

(R^2 = H, R^1 =
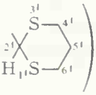

).

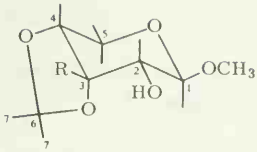

Methyl-3,4-O-isopropylidene-3-C-(1,3-dithiane-2-yl)-β-D-ribopyranoside (R = 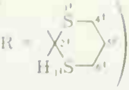).

Methyl-3,4-O-isopropylidene-3-C-(2-methyl-1,3-dithiane-2-yl)-β-D-ribopyranoside (R = 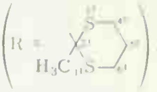).

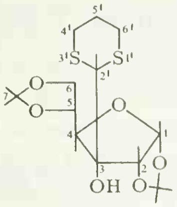

1,2,5,6-O-Diisopropylidene-3-C-(1,3-dithiane-2-yl)-allofuranose.

An almost direct relationship between ^{13}C chemical shifts of glucose and xylose carbons and their electron densities is found for C-1, C-3 and C-5; the shifts of C-2 and C-4, however, deviate substantially. Trans-annular interactions might be responsible for this "excess" shielding of C-2 and C-4 [65].

In reference [65] a relationship between the free energies of sugars and the sums of their chemical shifts was reported. For instance glucose and xylose have, compared to idose or allose, low free energy values, which correspond to low sums of chemical shifts and low values in total shielding for these molecules. Thus for the most stable sugars the lowest values in total shielding are calculated and *vice versa*.

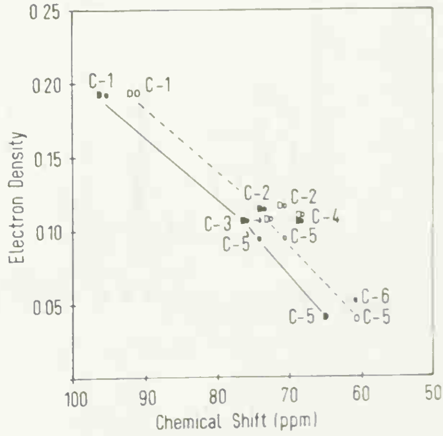

Fig. 5.7. Plot of ^{13}C chemical shift values of xylose and glucose carbons *versus* their calculated electron densities [65].
α-D-glucose ○,
α-D-xylose D,
β-D-glucose ●,
β-D-xylose ◗.

Another discovery [65] merits mention here: Comparing ^{13}C and ^{1}H chemical shift differences of pairs of anomeric carbons or protons shows that ^{13}C and ^{1}H shifts are affected inversely, *i.e.* a low field shift of ^{13}C is accompanied by a high field shift of the corresponding proton.

5.4.2. Di- and Polysaccharides

The signal assignments of di- and polysaccharides [300, 302, 305] are made following the rules discussed at the beginning of Section 5.4; a survey is given in Table 5.13.

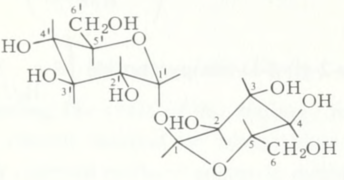

HO
CH₂OH
HO
HO
OH
OH
HO
CH₂OH
O
O
O
1'
2'
3'
4'
5'
6'
1
2
3
4
5
6

Trehalose(α-D-glucopyranosyl-α-D-gluco-pyranoside)

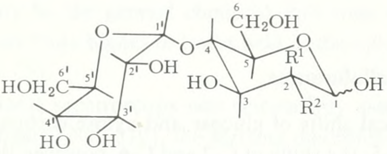

CH₂OH
HOH₂C
OH
HO
HO OH
OH
R¹
R²
O
O
O
1'
2'
3'
4'
5'
6'
1
2
3
4
5
6

Maltose(4-O-α-D-glucopyranosyl-D-glucose):
$R^1 = H, R^2 = OH$.

Epimaltose(4-O-α-D-glucopyranosyl-D-mannose):
$R^1 = OH, R^2 = H$.

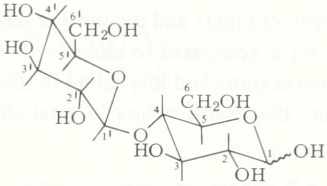

HO
CH₂OH
HO
HO
CH₂OH
HO
OH
OH
O
O
O
1'
2'
3'
4'
5'
6'
1
2
3
4
5
6

Cellobiose(4-O-β-D-glucopyranosyl-D-glucose)

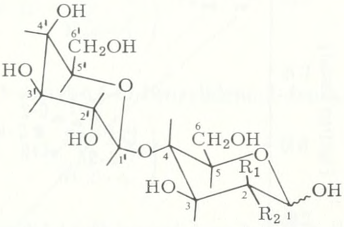

OH
CH₂OH
HO
HO
CH₂OH
HO
R₁
R₂
OH
O
O
O
1'
2'
3'
4'
5'
6'
1
2
3
4
5
6

Lactose(4-O-β-D-galactopyranosyl-D-glucose)
$R^1 = H, R^2 = OH$.

Epilactose(4-O-β-D-galactopyranosyl-D-mannose)
$R^1 = OH, R^2 = H$.

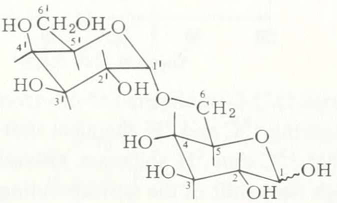

HO CH₂OH
HO
OH
CH₂
HO
HO
OH
OH
O
O
O
1'
2'
3'
4'
5'
6'
1
2
3
4
5
6

Melibiose(6-O-α-D-galactopyranosyl-D-glucose)

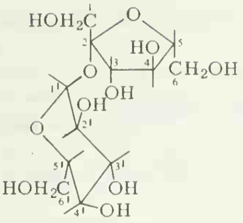

Sucrose(α-D-glucopyranosyl-β-D-fructofuranoside)

Fig. 5.8 shows the PFT ^{13}C NMR spectrum of D-lactose. Before mutarotational equilibration, the resonances of the β-anomeric glucose residue show very low intensities [302]

Peracetylation of carbohydrates usually causes an upfield shift of the carbohydrate resonances (see Table 5.12) with the exception of the C-6 signals [300].

^{13}C NMR investigations of polysaccharides such as amylose, glycogen or cellulose acetate show that no clearcut correlations between chemical shift values of different carbon resonances and conformations can be made so far [300].

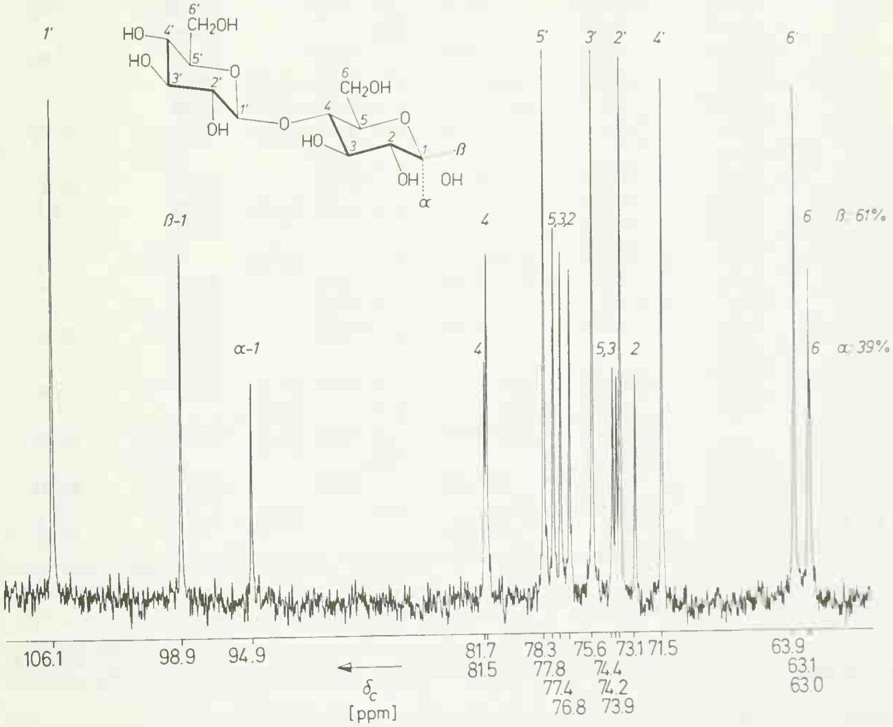

Fig. 5.8. PFT ^{13}C NMR spectrum of D-lactose, 150 mg in 1.5 ml deuterium oxide, 24 hrs. after sample preparation; 30 °C; 20 MHz; proton broad band decoupled, 3000 scans of 90° pulses with a pulse interval of 5 s accounting for spin lattice relaxation times of 1.5 s. The signal intensities indicate that the equilibrium mixture contains 61% β- and 39% (±1%) α-D-lactose. The shift values are measured relative the TMSi signal of internal 3-trimethylsilylpropane-1-sodiumsulfonate.

Table 5.13. ^{13}C Chemical Shifts of Disaccharides and Derivatives (δ Values in ppm Relative to TMS = 0; for Numbering See Formulae on Pages 258, 259).

	Trehalose	Maltose	Methyl-β-maltoside	Epimaltose	Cellobiose	Methyl-β-cellobioside
Solvent	D_2O	D_2O	H_2O	D_2O	D_2O	H_2O
Ref.	[305]	[302]	[300]	[302]	[305]	[300]
C-Atom						
α-1	93.00	91.95		93.85	91.65	
β-1		95.90	102.90	93.65	95.55	103.00
1′		99.60	99.60	99.90	102.40	102.50
α-2	72.35	69.95 71.30 73.25		71.05	71.20	
β-2		74.00	72.60	71.25	73.75	72.80
2′		72.70 72.90	72.90	72.70 72.95	73.00	73.10
α-3	70.85 71.90	69.95 71.30 73.25		70.80	69.90 71.05	
β-3		74.60 76.25	74.50	73.65	74.10 74.60	74.50
3′		72.70 72.90	72.90	72.70 72.95	75.35 75.80	75.80
α-4	69.50	76.95		75.35	78.60	
β-4		76.70	77.20	74.75 74.90	78.50	78.90
4′		69.40	69.40	69.40	69.25	69.50
α-5	70.85 71.90	69.95 71.30 73.25		71.85	69.90 71.05	
β-5		74.60 76.25	76.10	74.75 74.90	74.10 74.60	74.30
5′		71.70	71.70	70.80	75.80 75.35	75.70
α-6	60.35	60.55 60.80		61.05	59.95	
β-6		60.55 60.80	60.50	61.05	59.75	60.20
6′		60.55 60.80	60.70	60.55	60.45	60.70
OCH_3			57.00			57.00

5.4.3. Polyols

Several ^{13}C NMR studies on unsubstituted polyols [297c], O-methylated galactitols [309] and ribitols substituted with isoalloxazine moieties [311, 120] have been reported in the literature. The signals of the unsubstituted polyols were assigned mainly by comparison with the spectra of tetritols, pentitols and hexitols of different configuration [297c]. Specifically methylated polyols, however, allow a more significant signal assignment [309]. 3-O-Methylation of galactitol causes

Table 5.13. (Continued).

Solvent Ref. C-Atom	α-Cellobiose octaacetate[a]) H_2O [300]	β-Cellobiose octaacetate[b]) H_2O [300]	Lactose D_2O [302]	Methyl-β-lactoside D_2O [302]	Epilactose D_2O [302]	Melibiose D_2O [302]	Sucrose H_2O [300]
α-1	88.40		94.9		94.95	94.50	
β-1		91.30	98.9	104.15 104.30	94.85	97.25	62.20
1′	100.40	100.10	106.1	104.15 104.30	104.20	99.40	91.90
α-2	68.80 68.90		73.1		71.35	71.30 72.65 74.20	
β-2		70.00	76.8	74.00	71.80	75.25 75.60 77.15	103.50
2′	72.40	72.40	73.9	72.20	72.15	70.45 70.65	72.20
α-3	68.80 68.90		74.2 74.4		70.20	71.30 72.65 74.20	
β-3		71.70 73.20	77.4 77.8	75.65 76.00	74.90	75.25 75.60	81.30
3′	71.60	71.70	75.6	73.80	73.70	69.70	72.70
α-4	75.50		81.7		77.75	70.45 70.65	
β-4		75.40	81.5	79.75	77.35	70.45 70.65	76.80
4′	67.70	67.70	71.5	69.80	69.75	70.40 70.65	69.30
α-5	70.40		74.2 74.4		72.15	71.30 72.65 74.20	
β-5		71.70 73.20	77.4 77.8	75.65 76.00	76.10	75.25 77.15	74.20
5′	71.10	71.10	78.3	76.55	76.50		71.00
α-6	60.80		63.0		61.55	67.05 67.15	
β-6		61.30	63.1	61.35	61.55	67.05 67.15	61.70
6′	61.20	61.20	63.9	62.25	62.30	62.30	60.40
OCH_3				58.50			

[a]) 169.90, 169.70, 169.50, 169.40, 169.30, 168.90, 168.70, 168.60 (C=O); 19.90 (CH_3).
[b]) 169.80, 169.70, 169.50, 169.20, 168.90, 168.60, 168.30 (C = O); 19.90, 19.60 (CH_3).

a well-known downfield shift for the resonance of C-3 (about 9 ppm). The signals of the neighboring carbons C-2 and C-4 are shifted in the same direction, but only by 0.6 to 0.9 ppm. The lines of the γ-carbons are shifted upfield by 0.3 to 0.5 ppm relative to C-3, C-1 and C-5, and the resonance of C-6 is not influenced by the 3-O-methylation. The same rules can be used for the

Table 5.14. ^{13}C Chemical Shifts of Polyols (δ Values in ppm Relative to TMS = 0).

Compound	$-CH_3$	$-CH_2$	CH_2OH	2-CHOH	3-CHOH	4-CHOH	5-CHOH	OCH_3	Solvent	Ref.
Glycol			67.30						H_2O	[297c]
1,2-Propanediol	22.95		71.60	72.70					H_2O	[297c]
1,3-Butanediol	26.90	44.80	63.20		69.30				H_2O	[297c]
1,4-Butanediol		31.70	65.50						H_2O	[297c]
Glycerol			66.90	76.40					H_2O	[297c]
Erythritol			66.20	75.30	75.30				H_2O	[297c]
Pentaerythritol[a])			64.30						H_2O	[297c]
Ribitol			65.50	75.40	75.60	75.40			H_2O	[297c]
Xylitol			65.90	75.20	73.90	75.20			H_2O	[297c]
D-Arabitol			66.50	73.60	74.00	74.50			H_2O	[297c]
			66.20							
D-Mannitol			76.30	75.30	73.60	73.60	75.30		H_2O	[297c]
D-Sorbitol			65.80	74.50	72.90	74.50	76.10		H_2O	[297c]
			66.10	74.30		74.30				
Galactitol			63.25	69.25	70.15	70.15	69.25		D_2O	[309]
3-O-Methyl-D-galactitol			62.90	70.15	79.40	70.80	68.75	60.20	D_2O	[309]
			63.35							
3,4-Di-O-methyl-D-galactitol			62.90	70.65	78.85	78.85	70.65	60,30	D_2O	[309]

[a]) $C_{quart.}$: 48.3.

signal assignments of 3,4-di-O-methyl-D-galactitol. From the comparison of the galactitol spectra with those of methylated derivatives the signal assignments for the parent compound from higher to lower field are as follows: C-1,6, C-2,5 and C-3,4.

The ^{13}C chemicals shifts of a series of polyols are listed in Table 5.14.

5.4.4. Inositols

The ^{13}C resonances of this class of compounds, which are summarized in Table 5.15 were assigned using the rules discussed in Section 5.4.1.

As the six carbons of *scyllo*-inositol are equivalent, only one signal is observed in the ^{13}C NMR spectrum of this compound [298]. In the spectra of *myo*-, *epi*- and 1,3-di-O-methyl-*myo*-inositol two pairs of carbons always resonate at different δ values for symmetry reasons; these signals can be easily identified by their double intensity [298].

The spectra of D-1-O-methyl-*myo*-inositol and L-2-O-methyl-*chiro*-inositol show that the resonances of β-carbons bearing axial hydroxyl groups shift 4.5 ppm to higher field upon methylation of $C_\alpha-OH$ [298].

Table 5.15. ^{13}C Chemical Shifts of Inositols and O-Methylated Derivatives [298] (δ Values in ppm Relative to TMS = 0).

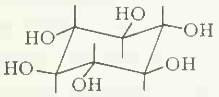

scyllo-Inositol

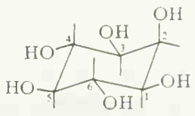

myo-Inositol

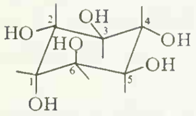

L-*chiro*-Inositol

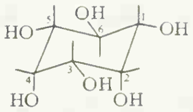

epi-Inositol

Name	C-1	C-2	C-3	C-4	C-5	C-6	CH_3
scyllo-Inositol	73.70	73.70	73.70	73.70	73.70	73.70	
myo-Inositol	72.40	72.20	72.40	71.10	74.30	71.10	
L-*chiro*-Inositol	71.60	70.50	72.80	72.80	70.50	71.60	
epi-Inositol	71.70	74.50	70.10	74.50	71.70	66.80	
D-1-O-Methyl-*myo*-inositol	80.50	68.00	72.30	71.10	74.40	71.60	56.90
1,3-Di-O-Methyl-*myo*-inositol	80.40	63.30	80.40	71.40	74.40	71.40	57.40
1,4-Di-O-Methyl-*myo*-inositol	80.30	67.80	71.70	82.20	73.70	70.50	59.70 (4) 56.70 (1)
1,2-Di-O-Methyl-*myo*-inositol	81.00	78.10	72.60	71.40	74.40	71.80	61.50 (2) 57.40 (1)
L-2-O-Methyl-*chiro*-inositol	67.20	80.10	71.90	72.80	70.40	71.30	56.80
D-3-O-Methyl-*chiro*-inositol	71.70 71.40	69.80	82.50	72.10	70.60	71.70 71.40	59.40

5.5. Nucleosides and Nucleotides

Owing to the great biological importance of this class of compounds, the ^{13}C NMR spectra of a considerable series of nucleosides and nucleotides have been reported in the literature [120, 296, 311–313]. As demonstrated by the spectra of thymidine and flavin adenine dinucleotide (Fig. 5.9, 5.10) the ^{13}C NMR spectra of normal and deoxy nucleosides and nucleotides have two groups of signals:

(1) The pyranose and furanose ring carbon resonances are observed between 40 and 100 ppm.
(2) The resonances of the heterocyclic carbon atoms are found between 90 and 170 ppm.

5.5.1. Assignment of the Purine Resonances

The assignments of the purine resonances of proton broad band decoupled ^{13}C NMR spectra of nucleosides and nucleotides are made using the following aids [312, 314]: Correlation with the signals of the parent bases and analogous nucleosides or nucleotides; comparison of the ^{13}C NMR spectrum with that of a specificly deuterated analog; correlations of the chemical shift values with the π-electron densities [312, 314] and, in addition, proton off-resonance decoupling, which affords the identification of quaternary carbon atoms.
Some of the common purine nucleosides are symbolized by the following formulae:

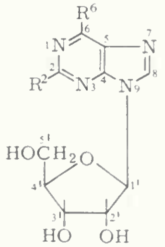

nebularine ($R^2 = R^6 = H$)
adenine ($R^2 = H$; $R^6 = NH_2$)
inosine ($R^2 = H$; $R^6 = OH$)
guanosine ($R^2 = NH_2$; $R^6 = OH$)

Converting purine to the nucleoside nebularine causes considerable shifts of resonances in the spectrum of the parent base (*cf.* Table 5.16).
In contrast, substitution of H-9 of adenine by the ribofuranose moiety causes only very small shifts of the signals of the base. Proton off-resonance decoupling allows the differentiation between the signals of the quaternary carbon atoms C-4, C-5, and C-6 and the tertiary carbons C-2, and C-8. The signal at highest field is assigned to C-5 as this carbon atom is assumed to have the highest π-electron density. The resonance of C-8 is easily identified by comparison with the spectrum of 8-deuterio-adenosine. The second doublet signal in the off-resonance decoupled spectrum is thus attributed to C-2. The resonances due to C-4 and C-6 are assigned by comparison with the spectral data of analogous nucleosides.
C-8 of guanosine is the only tertiary carbon atom and may be easily detected and identified by off-resonance decoupling. Comparing the spectral data of guanosine with those of 6-thioguanosine leads to the assignments of the resonances of C-6 and C-5: Both signals are shifted downfield by 10 to 20 ppm in the spectrum of the thio compound, measured in dimethyl sulfoxide (DMSO). However, oxidation of 6-thioguanosine by this solvent during the measurement cannot be excluded.

Comparison of the spectrum of inosine with that of guanosine leads to the assignments of the signals of C-2 and C-4: both resonances are shifted upfield in inosine by 5.4 ppm because of the lack of an electron withdrawing amino group at C-2.

The signal of the quaternary carbon atom C-4 of inosine can be easily distinguished from that of C-2 by proton off-resonance decoupling. Comparison of the spectrum of inosine with the spectral data of 8-deuterioinosine and 6-thioinosine leads to the unequivocal signal assignment of the base residue of this nucleoside [312] (see Table 5.16).

5.5.2. Assignment of the Pyrimidine Resonances [312]

Some of the common pyrimidine nucleosides are symbolized by the following formulae:

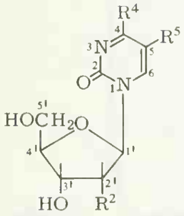

uridine	($R^4, R^{2'} = OH$; $R^5 = H$)
cytidine	($R^4 = NH_2$; $R^5 = H$; $R^{2'} = OH$)
thymidine	($R^4 = OH$; $R^5 = CH_3$; $R^{2'} = H$)

Methods similar to those mentioned above have been used for the signal identification of the pyrimidine resonances.

Comparison of the spectrum of uridine with data of 4-thiouridine, 2,4-dithiouridine, thymidine, 4-thiothymidine, cytidine and 2-thiocytidine allows the assignment of all carbon resonances of these pyrimidine moieties. Further confirmation of these assignments is obtained from the proton off-resonance decoupled ^{13}C spectra of these nucleosides as is shown in Figure 5.9 for thymidine: The pyrimidine CH_3 and CH resonances of the proton broad band decoupled spectrum are split into a quartet and a doublet, respectively, in the proton off-resonance spectrum, and can thus be easily assigned.

5.5.3. Assignment of the Isoalloxazine Resonances [311, 120]

Due to the biological importance of the isoalloxazine moiety in enzyme cofactors, ^{13}C NMR studies of this heterocyclic compound have been reported [311, 320] (Fig. 5.10). The resonances of the methyl groups attached to R 7 and R 8 of the isoalloxazine moiety of riboflavin-5′-monophosphate [120] (*cf.* Fig. 5.10 for FAD) occur at highest field, having shifts corresponding to those of methyl carbons in methyl benzenes and showing quartets in the proton off-resonance decoupled spectra. By proton off-resonance decoupling, the signals of R 6 and R 9 are localized as doublets at higher field than any other isoalloxazine ring carbon. Since R 6 of this ring corresponds to C-8 of acridine (130 ppm) [260], R 6 is less shielded (133.6 ppm) than R 9 (119.9 ppm). The so-far unassigned signals are due to quaternary carbons, as they are singlets in the proton off-resonance decoupled ^{13}C spectra. Of these, the carbonyl carbons R 2 and R 4 occur at lowest field. By comparison with the ^{13}C shifts of xanthosine [312], the signal of R 4 was found to be more deshielded than that of R 2 [311]. The remaining six signals can be assigned only by specificly deuterated or ^{13}C enriched riboflavin derivatives.

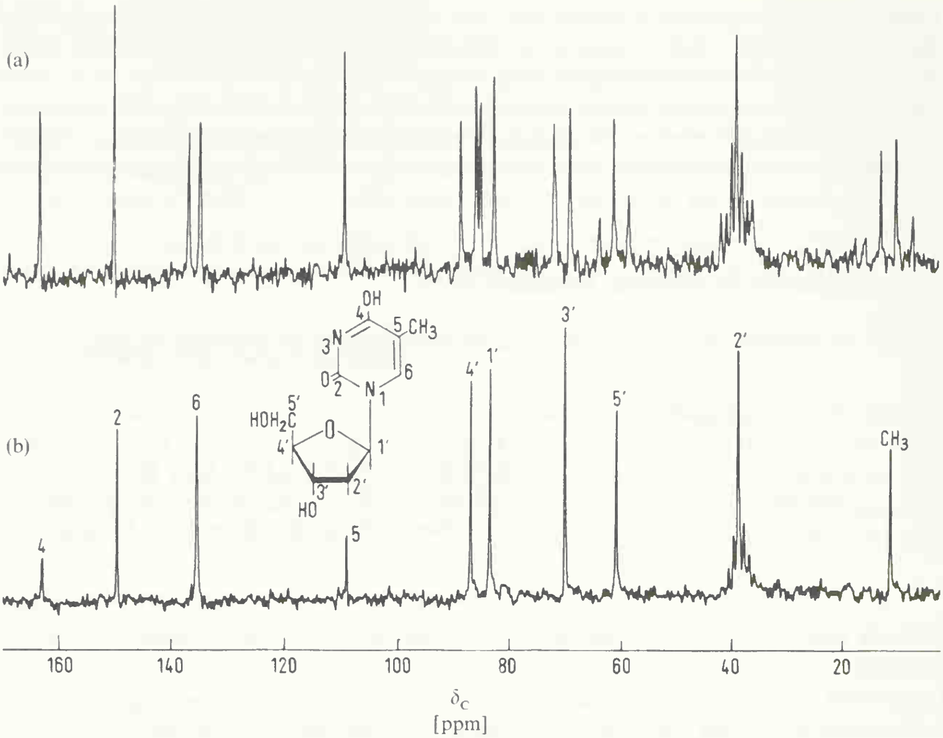

Fig. 5.9. (a) PFT ^{13}C NMR spectrum of thymidine, proton broad band decoupled, 100 mg/ml DMSO-d_6, temperature 30 °C, accumulation of 2048 pulse interferograms (4 K data points); pulse width: 5 µs; pulse interval: 0.4 s; 5000 Hz; the numbers at the signals indicate the numbering of the C-atoms; δ values (ppm) relative to TMS = 0;
(b) as in (a), however proton off-resonance decoupled and 4096 scans.

5.5.4. Assignment of the Sugar and Polyol Carbon Atoms

Most naturally occuring nucleosides and nucleotides contain a ribofuranose moiety. From detailed ^{13}C NMR studies of carbohydrates [65, 66, 299], it is known that primary CH_2OH-groups resonate at higher field than the secondary ring CHOH groups and thus C-5′ of the ribofuranose residue can be easily assigned. Another rule is found for the anomeric carbons C-1′ of the ribofuranose residue which always absorb at lowest field [65, 66, 299]. C-4′ can be assigned by noting the phosphorus-carbon long-range coupling in the proton broad band decoupled ^{13}C NMR spectra of nucleotides [313] as demonstrated in Fig. 5.10. The assignments for C-2′ and C-3′ of the ribofuranose moiety are not yet unequivocal [296]. The resonances C-1′ to C-4′ in the sugar moiety of 2′,3′-O-isopropylidene derivatives of several anhydronucleosides could not be assigned [315].

The ribitol residue of the riboflavin moiety was assigned on the following basis (the same numbering of the C-atoms as in Fig. 5.10 is used here):

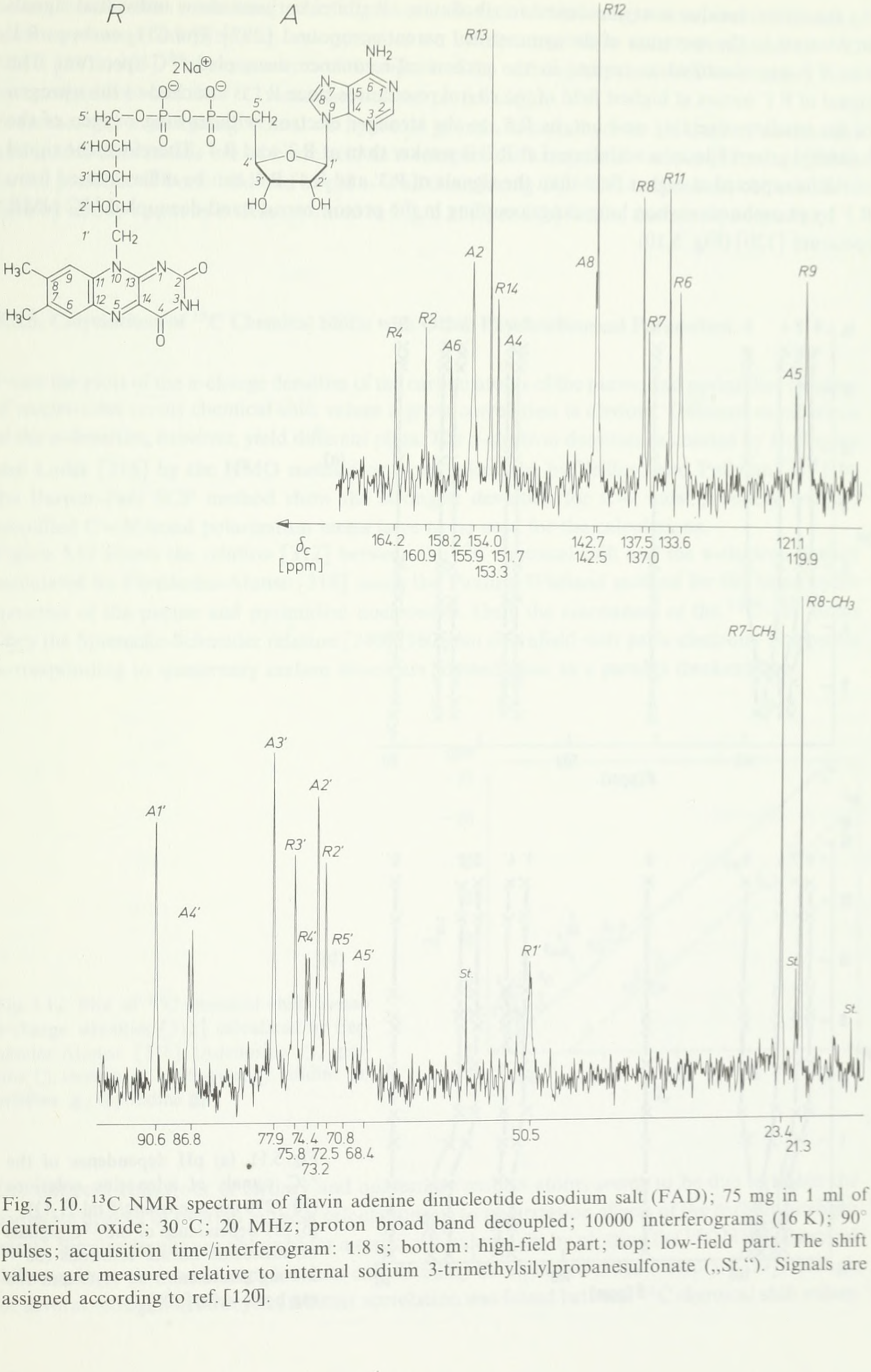

Fig. 5.10. ^{13}C NMR spectrum of flavin adenine dinucleotide disodium salt (FAD); 75 mg in 1 ml of deuterium oxide; 30 °C; 20 MHz; proton broad band decoupled; 10000 interferograms (16 K); 90° pulses; acquisition time/interferogram: 1.8 s; bottom: high-field part; top: low-field part. The shift values are measured relative to internal sodium 3-trimethylsilylpropanesulfonate („St."). Signals are assigned according to ref. [120].

As the ribitol residue is asymmetrical in riboflavin, all ribitol carbons show individual signals in contrast to the spectrum of the symmetrical parent compound [297]. The CH_2 carbons R 1′ and R 5′ are identified as triplets in the proton off-resonance decoupled ^{13}C spectrum. The signal of R 1′ occurs at highest field of the ribitol resonances since R 1 is attached to the nitrogen of the isoalloxazine ring and not, as R 5′, to the stronger electron withdrawing oxygen of the hydroxyl group. Electron withdrawal at R 2′ is weaker than at R 3′ and R 4′. Therefore, the signal of R 2′ is expected at higher field than the signals of R 3′ and R 4′. R 4′ can be differentiated from R 3′ by phosphorus carbon long-range coupling in the proton broad band decoupled ^{13}C NMR spectrum [120] (Fig. 5.10).

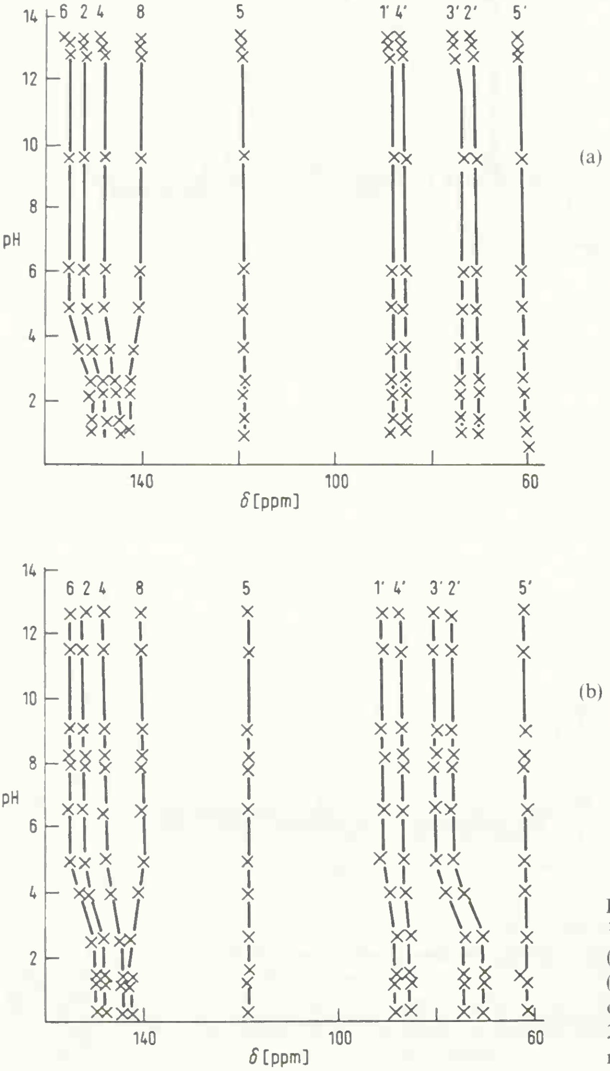

Fig. 5.11. (a) pH dependence of the ^{13}C signals of adenosine solutions (30 – 270 mg adenosine/5 ml H_2O); (b) pH dependence of the ^{13}C signals of adenosine borate solutions (30 – 270 mg adenosine/5 ml H_2O and 100 mg boric acid) [306].

Several nucleosides containing other sugar residues such as arabinopyranose, arabinofuranose, mannopyranose, talopyranose, xylopyranose or xylofuranose have been investigated by ^{13}C NMR [297a, 303]. The assignments of the signals of the carbohydrate moieties were mainly done by comparison with the ^{13}C resonances of the parent sugars.

A further aid in assigning vicinal *cis* hydroxyl groups in carbohydrate residues of nucleosides and nucleotides makes use of boric acid as a complex shift reagent at various pH values [306]. In the presence of boric acid and at pH $>$ 7 all complexing $>$C$-$OH-carbons are shifted downfield by about 6 ppm as is demonstrated in Fig. 5.11(a) and (b) for the nucleoside adenosine.

5.5.5. Correlations of ^{13}C Chemical Shifts with Other Physicochemical Parameters

From the plots of the π-charge densities of the carbon atoms of the purine and pyrimidine residues of nucleosides *versus* chemical shift values a gross correlation is obvious. Different calculations of the π-densities, however, yield different plots. The π-electron densities calculated by Hoffmann and Ladik [316] by the HMO method or those calculated by Veillard and Pullman [317] by the Pariser-Parr SCF method show the strongest deviation for C-4, most probably because amplified C$-$N bond polarization terms have to be used for the calculations.

Figure 5.12 shows the relation [312] between the ^{13}C chemical shift and the π-electron density calculated by Fernández-Alonso [318] using the Pauling-Wheland method for the heterocyclic moieties of the purine and pyrimidine nucleosides. Only the resonances of the ^{13}C$-$H atoms obey the Spiesecke-Schneider relation [240] (160 ppm downfield shift per π-electron). The points corresponding to quaternary carbon atoms are located close to a parallel (broken) line.

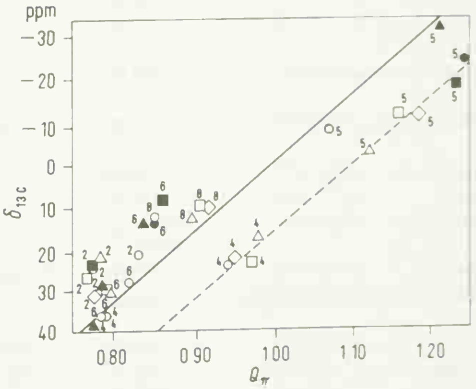

Fig. 5.12. Plot of ^{13}C chemical shifts *versus* π-charge densities [312], calculated by Fernández-Alonso [318]. (Adenosine ○, guasine □, inosine △, xanthosine ◇, uridine ●, cytidine ▲, thymidine ■.)

The different behaviour of tertiary and quaternary carbon atoms seems to be due to either the complete neglect of overlap in these calculations or to polarization effects of the carbon-nitrogen bonds. Similar results are obtained for a series of 5-halouracils by plotting the ^{13}C NMR chemical shifts *versus* π-electron charge densities calculated by the extended Hückel theory [319]. Though for several nitrogen heterocycles a better correlation was found between ^{13}C chemical shift values able 5.16. ^{13}C Chemical Shifts of Purines, Pyrimidines, Nucleosides and Nucleotides.

Compound	C-2	C-4	C-5	C-6	C-8
Cytidine	156.90	166.65	95.65	142.80	
Deoxycytidine	157.00	166.95	95.85	142.45	
2-Thiocytidine	180.85	161.05	98.95	142.65	
6-Methylcytidine	157.30	166.15	96.50	155.35	
Cytidine-5′-monophosphate	157.50	166.20	96.50	141.80	
Deoxycytidine-5′-monophosphate	157.40	166.00	96.50	141.80	
Uridine	152.40	164.70	103.05	142.20	
4-Thiouridine	149.10	191.05	113.65	136.90	
2,4-Dithiouridine	173.75	186.95	118.65	135.50	
5-Hydroxyuridine	150.60	161.70	121.05	133.55	
Uridine-5′-monophosphate	152.90	167.30	103.70	143.20	
2,5′-Anhydro-2,3′-isopropylidene-uridine	157.50	171.10	109.65	143.80	
Thymidine	151.55	164.85	110.50	137.30	
Thymidine-5′-monophosphate	151.50	166.20	111.40	137.40	
4-Thiothymidine	148.70	191.50	118.80	134.15	
1-(2,3-Dideoxy-β-D-glycero)-pent-2-enofuranosylthymine	152.10	165.20	110.30	137.95	
Purine	151.60	154.40	128.10	144.40	147.50
6-Methylpurine	151.60	153.85	145.10	155.45	144.45
6-Chloropurine	151.35	147.80	129.05	154.20	146.10
6-Bromopurine	151.50	146.65	131.85	152.90	146.00
6-Iodopurine	151.80	136.50	120.30	149.95	145.10
6-Methoxypurine	151.50	155.15	118.25	159.35	142.75
6-Dimethylaminopurine	151.80	151.15	118.90	154.30	137.80
6-Methylmercaptopurine	151.60	150.20	129.35	158.60	143.15
Hypoxanthine	150.20	155.50	118.00	158.90	144.80
Adenine	152.45	151.35	117.60	155.35	139.40
6-Cyanopurine	152.25	133.45	127.85	154.95	149.30
Nebularine	151.90	152.95	135.10	148.95	146.35
6-Chloro-9-(β-D-ribofuranosyl)-purine	150.25	152.40	132.15	152.40	146.35
Inosine	149.20	146.95	125.30	157.65	139.90
Deoxyinosine	148.50	146.25	125.20	157.35	139.30
6-Thioinosine	146.10	144.70	136.30	176.70	141.90
Inosine-5′-monophosphate	146.70	148.20	123.10	158.30	139.80
Adenosine	147.40	145.65	118.55	150.50	142.40
2′-Deoxyadenosine	147.50	145.20	118.25	150.10	142.30
9-β-D-Ribopyranosyladenine	148.40	144.90	118.80	150.20	143.15
9-α-D-Arabinopyranosyladenine	148.45	145.00	118.45	150.20	142.85
9-β-D-Arabinopyranosyladenine	147.70	144.70	117.95	150.10	143.30
9-α-D-Arabinofuranosyladenine	148.00	145.00	118.90	150.30	142.85

C-1′	C-2′	C-3′	C-4′	C-5′		Solvent	Ref.
90.10	70.55	75.10	85.25	61.85		DMSO	[312]
86.55	40.60	71.75	88.55	62.60		DMSO	[312]
94.40	69.35	76.00	85.10	60.75		DMSO	[312]
92.90	71.10	71.85	86.15	63.25	20.85 (CH_3)	DMSO	[312]
89.10	69.70	74.30	83.30	63.30		H_2O	[313]
85.60	39.30	70.90	85.90	63.60		H_2O	[313]
89.10	71.10	74.85	85.90	62.20		DMSO	[312]
89.60	70.55	74.90	86.05	61.70		DMSO	[312]
94.30	69.60	75.60	85.65	60.55		DMSO	[312]
88.55	71.30	74.15	85.85	62.35		DMSO	[312]
89.60	71.20	75.10	85.10	64.60		DMSO	[312]
97.60	85.15	84.65	82.00	75.10		DMSO	[312]
85.05	40.40	71.65	88.40	62.35	13.20 (CH_3)	DMSO	[312]
84.80	38.50	71.20	85.90	64.00	11.70 (CH_3)	H_2O	[313]
85.80	39.90	71.15	87.80	62.12	17.85 (CH_3)	DMSO	[312]
88.70	136.05	127.15	90.15	63.65	13.35	DMSO	[312]
						DMSO	[312]
					19.4 (CH_3)	DMSO-d_6	[102]
						DMSO-d_6	[102]
						DMSO-d_6	[102]
						DMSO-d_6	[102]
					53.85 (OCH_3)	DMSO-d_6	[102]
					37.85 (CH_3)	DMSO-d_6	[102]
					11.35 (CH_3)	DMSO-d_6	[102]
						DMSO-d_6	[102]
						DMSO-d_6	[102]
					114.45 (CN)	DMSO-d_6	[102]
89.05	71.40	75.00	86.80	62.25		DMSO-d_6	[312]
89.35	71.00	75.05	86.45	61.70		DMSO	[312]
88.75	71.20	75.15	86.60	62.25		DMSO	[312]
84.35	40.20	71.35	88.70	62.20		DMSO	[312]
88.45	70.85	75.10	86.40	61.95		DMSO	[312]
87.60	70.60	74.80	84.20	63.50		H_2O	[313]
88.45	74.25	70.25	85.55	61.30		0.1 n HCl	[297b]
84.80	39.15	70.90	87.50	61.40		0.1 n HCl	[297b]
81.15	68.60	66.05	70.80	64.95		0.1 n HCl	[297b]
84.15	72.80	69.80 69.50)	69.50 69.80)	68.50		0.1 n HCl	[297a]
80.40	69.80	65.60	69.40	63.35		0.1 n HCl	[297a]
89.20	79.75	74.85	85.25	60.95		0.1 n HCl	[297a]

Table 5.16. (Continued).

Compound	C-2	C-4	C-5	C-6	C-8
9-α-D-Xylopyranosyladenine	147.80	145.10	117.80	150.30	143.50
9-β-D-Xylopyranosyladenine	148.35	144.90	118.70	150.20	143.05
9-β-D-Xylofuranosyladenine	149.20	147.60	118.35	153.10	141.45
Adenosine-5′-monophosphate	152.40	148.40	118.00	155.00	139.90
Adenosine-5′-triphosphate	152.30	148.30	118.00	154.80	139.60
2′-Deoxyadenosine-5′-monophosphate	152.20	148.10	118.10	155.00	139.80
6-N-Methylamino-9-(β-D-ribofuranosyl)-purine	153.60	149.30	120.90	156.25	140.80
2-Amino-9-(β-D-ribofuranosyl)-purine	160.55	154.85	124.75	150.70	142.55
2,6-Diamino-9-(β-D-ribofuranosyl)-purine	161.25	152.55	83.30	157.60	114.95
Guanosine	154.55	152.30	117.50	157.75	136.85
6-Thioguanosine	154.30	148.90	129.40	176.10	139.45
Deoxyguanosine	154.70	152.00	117.65	158.15	136.65
Guanosine-5′-monophosphate	153.60	151.00	115.70	158.30	137.30
Deoxyguanosine-5′-monophosphate	153.80	150.90	115.70	158.50	137.10
2-Chloroadenosine	154.20	151.30	119.30	157.55	141.20
Xanthosine	158.90	152.35	117.25	164.45	137.45
6-Thioxanthosine	158.40	149.00	127.25	182.95	137.45

and total ($\sigma + \pi$) electron charge densities [242], the correlation did not improve in the case of the 5-halouracils. A good correlation exists for the 5-halouracils between the ^{13}C chemical shifts and the substituent electronegativity, E_x [320], as can be seen from Fig. 5.13.
The largest substituent effect was observed for C-5, which is directly attached to the different substituents. Similar results were obtained in an investigation of 6-substituted purines [102].

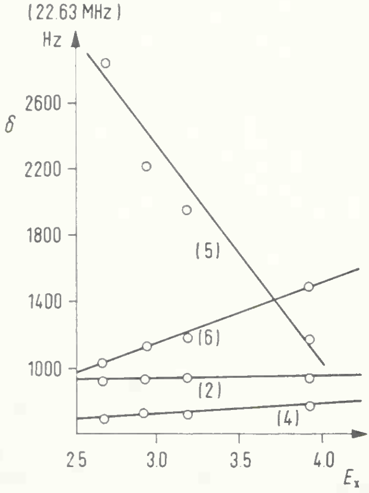

Fig. 5.13. ^{13}C chemical shift values *versus* substituent electronegativity, E_x, for 5-fluoro-, 5-chloro-, 5-bromo- and 5-iodouracil and their different carbon atoms [319].

C-1′	C-2′	C-3′	C-4′	C-5′	Solvent	Ref.
80.70	69.25 (69.60)	67.95 (67.55)	69.60 (69.25)	67.55 (67.95)	0.1 n HCl	[297a]
84.25	71.65	76.40	68.85	68.10	0.1 n HCl	[297a]
89.65	75.20	80.15	82.95	60.00	0.1 n HCl	[297a]
87.00	70.50	74.50	84.20	63.50	H_2O	[313]
86.90	70.10	74.20	83.80	65.20	H_2O	[313]
83.50	39.10	71.40	86.10	63.90	H_2O	[313]
89.40	71.95	74.90	87.10	62.95	DMSO	[312]
88.40	71.35	74.80	86.50	62.25	DMSO	[312]
89.00	72.30	75.00	87.35	63.35	DMSO	[312]
87.25	71.50	74.85	86.35	62.15	DMSO	[312]
87.90	71.40	75.95	86.40	62.40	DMSO	[312]
83.85	40.40	71.80	88.65	62.85	DMSO	[312]
87.00	70.60	74.30	84.10	63.90	H_2O	[313]
83.20	39.10	71.30	86.10	64.00	H_2O	[313]
88.90	71.45	74.80	86.75	62.50	DMSO	[312]
89.85	71.50	74.80	87.25	62.15	DMSO	[312]
89.90	71.65	75.05	87.00	62.15	DMSO	[312]

5.6. Amino Acids

Correlations between the structures of amino acids and peptides and their ^{13}C chemical shifts are of general interest for bio-, enzyme- and peptide chemists since these compounds occur in all cells of living organisms.

5.6.1. ^{13}C Chemical Shifts of Amino Acids

The results of several investigations of amino acids by ^{13}C NMR can be summarized as follows [74, 225, 321–323] (see Fig. 5.14 and Table 5.18):

(1) The ^{13}C signals of carboxyl groups resonate between 168 and 183 ppm.
(2) The ^{13}C resonances of α-carbon atoms absorb in the range of 40 to 65 ppm.
(3) The chemical shift values of the β-carbons spread across the range of 17 to 70 ppm.
(4) The signals of the γ- and δ-carbons are found between 17 and 50 ppm.
(5) The signals of the aromatic and heteroaromatic ring carbons resonate between 110 and 140 ppm.

For the synthesis of peptides, amino acid derivatives with protected amino or carboxyl groups are used as starting materials. The application of ^{13}C NMR spectroscopy for the control of the synthesis of those protected amino acids was reported in the literature [322, 324].

The carbon atoms of some important protecting groups resonate in the following ranges [322, 324] (Fig. 5.14; 5.15; Table 5.18): The carbonyl carbon of the *t*-butyloxycarbonyl groups is found at 150 to 160, the quaternary carbon atom between 77 and 82 and the methyl group at 28 to 30 ppm. The aromatic carbons of benzyloxycarbonyl and benzyl groups absorb at 110 to 140, the CH_2-carbons at 60 to 75 and the carbonyl groups at lowest field (150 to 160 ppm). The signals of acetyl groups occur at 175 to 185 (CO) and at about 25 ppm (CH_3). The resonances of methoxy and methyleneoxy groups of methyl and ethyl ester are found at 55 to 59 and 59 to 63 ppm, respectively. Most of the shifts reported in the literature were measured using dimethyl sulfoxide, D_2O or DCl as solvents (Table 5.18).

Due to their relationship to amino acids, the ^{13}C NMR spectra of derivatives of penicillin [325] are discussed in this chapter. Proton off-resonance decoupling, comparison of the spectra of different analogs and application of the equation derived by Ernst [32] were used as additional aids in signal assignment (Table 5.17).

Table 5.17. ^{13}C Chemical Shift Values of Penicillin Derivatives (δ Values in ppm Relative to TMS = 0) [325].

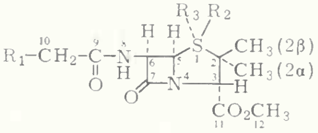

Penicillins

	R^1 = H R^2, R^3 = lone pair	R^1 = H R^2 = O R^3 = lone pair	R^1 = H R^2 = lone pair R^3 = 0	R^1 = OC_6H_5 R^2 = lone pair R^3 = lone pair	R^1 = OC_6H_5 R^2 = O R^3 = lone pair
C-2	63.6	74.1	68.1	64.0	74.9
C-3	69.7	65.1	63.9	70.0	65.8
C-5	67.1	75.5	78.7	67.4	76.0
C-6	58.3	55.5	57.0	58.4	54.8
2β-CH_3	30.0	18.7	23.4	31.0	19.0
2α-CH_3	26.1	17.6	15.3	26.6	18.0
C-12	51.7	52.2	52.2	52.1	52.8
C-10	20.8	22.1	21.6	65.6	67.0
C-7, C-9		168.1	167.3	167.6	167.3
C-9, C-7		169.2	169.5	167.6	167.7
C-11		173.8	170.2	172.6	173.8

Substitution of one of the lone pair electrons (R^2, R^3) by oxygen causes downfield shifts of the signals of C-2 and C-5 due to the expected decrease in electron density at these carbons. Similar downfield shifts are observed for the β-carbon atom upon converting cysteine to cystine and further to cysteic acid [321].

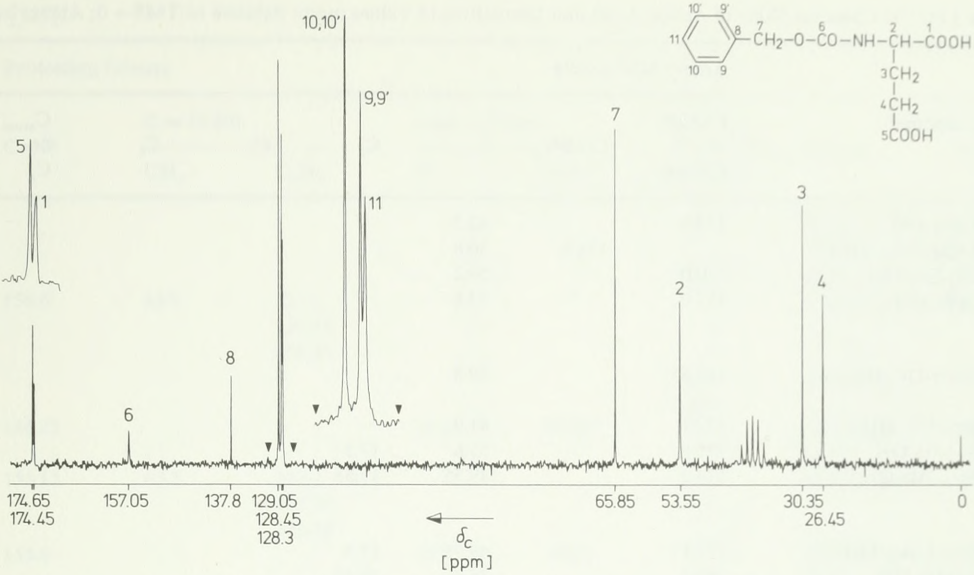

Fig. 5.14. PFT ^{13}C NMR spectrum of benzyloxycarbonyl-L-glutamic acid (Z-L-Glu-OH), 100 mg in 1 ml hexadeuteriodimethylsulfoxide; 30 °C; 20 MHz; pulse angle: 45°; proton broad band decoupled, 1000 scans.

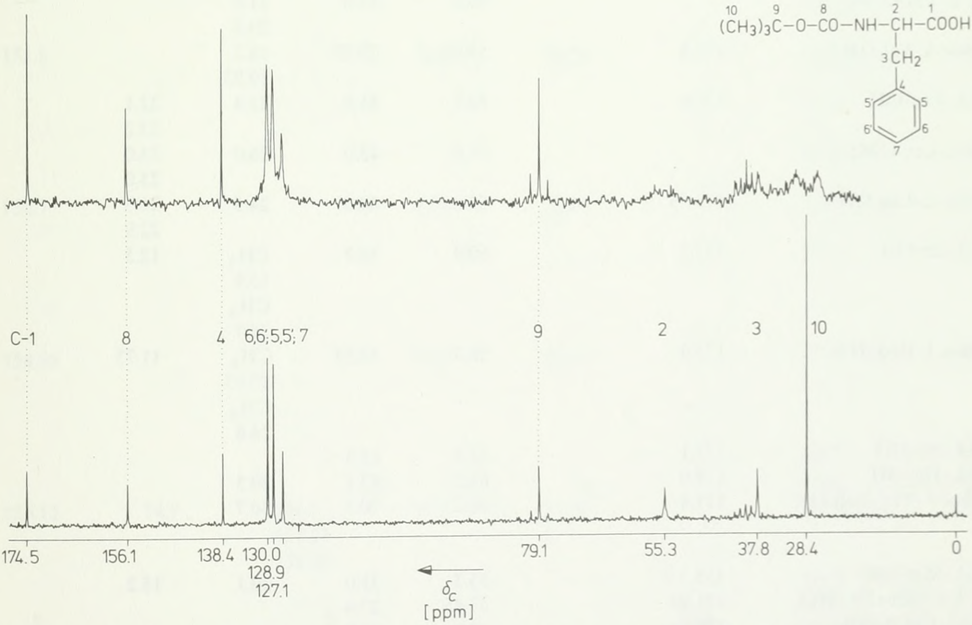

Fig. 5.15. PFT ^{13}C NMR spectra of *t*-butyloxycarbonyl-L-phenylalanine (Boc-L-Phe-OH), 100 mg in deuteriochloroform; 30 °C; 20 MHz; pulse angle: 45°; proton broad band decoupled; 1000 scans; bottom: decoupling with 2 Watt; top: decoupling with 0.05 Watt (low power noise decoupling).

Table 5.18. ^{13}C Chemical Shifts of Amino Acids and Derivatives (δ Values (ppm) Relative to TMS = 0; Abbreviations.

Compound	Amino Acid moiety						
	COOH or COOR	$CONH_2$	C_α	C_β	C_γ	C_δ	$C_{arom.}$ or C_ε
H-Gly-OH	173.5		42.5				
H-Gly-NH_2 · HCl		174.9	50.8				
CH_3-Gly-OH	170.0		50.2				
Z-Gly-OH	171.0		42.6				
H-Gly-OC_2H_5	167.65		39.8				
t-Boc-Gly-OH	172.1		41.9				
H-L-Ala-OH	176.8		51.6	17.3			
Z-DL-Ala-OH	174.0		49.55	17.55			
t-Boc-L-Ala-OH	175.1		48.95	17.3			
H-β-Ala-OH	183.4		35.7	38.45			
H-L-Val-OH	175.3		61.6	30.2	17.9 19.1		
H-L-Val-NH_2 · HBr		168.55	57.25	29.65	17.8 18.6		
Ac-L-Val-OMe			59.3	31.9	21.0 20.5		
t-Boc-L-Val-OH	172.4		58.95	29.85	18.2 19.25		
H-L-Leu-OH	176.6		54.7	41.0	25.4	22.1 23.2	
Ac-L-Leu-OMe			51.9	43.0	26.0	25.0 23.0	
t-Boc-L-Leu-OH	173.55		52.0	40.5	24.5	21.3 22.9	
H-L-Ile-OH	175.2		60.9	39.7	CH_3 15.9 CH_2 25.7	12.5	
t-Boc-L-Ile-OH	173.9		58.3	40.55	CH_3 15.95 CH_2 24.8	11.75	
H-L-Ser-OH	173.1		57.4	61.3			
H-L-Thr-OH	174.0		61.5	67.1	20.5		
t-Boc-L-Thr (Bzl)-OH	171.4		58.2	70.3	16.7		
H-L-Met-OH	175.3		55.3	31.0	30.1	15.2	
H-L-CySH-OH · HCl	171.95		57.45	27.4			
Ac-L-CySH-OH	179.4		57.2	27.3			
$(H\text{-DL-HomocyS-OH})_2$	173.8		54.2	35.3	31.8		
H-L-CySH-OMe · HCl	173.75		57.2	26.5			
H-L-CySH-OMe · HCl	174.2		57.35	25.95			
H-L-$CySO_3H$-OH	175.1		51.7	52.5			

See [327]).

Protecting Groups							
C=O	Z or O-Bzl		*t*-Boc or OBu^t		Ac-, N-, COO–CH$_3$ OC$_2$H$_5$	Solvent	Ref.
	CH$_2$	C$_6$H$_5$	C	CH$_3$			
						D$_2$O	[74]
						D$_2$O	[322]
					78.45	D$_2$O	[322]
156.0	65.8	127.2				DMSO-d$_6$	[322]
		127.95					
		136.65					
					14.25	DMSO-d$_6$	[324]
					61.80		
156.25			78.05	27.95		DMSO-d$_6$	[322]
						D$_2$O	[74]
155.15	65.5	127.2				DMSO-d$_6$	[322]
		127.75					
		136.55					
155.9			78.1	28.05		DMSO-d$_6$	[322]
						D$_2$O	[322]
						D$_2$O	[74]
						D$_2$O	[322]
						DMSO	[326]
151.5			78.0	28.25		DMSO-d$_6$	[322]
						D$_2$O	[74]
						DMSO	[326]
154.7			77.6	28.25		DMSO-d$_6$	[322]
						D$_2$O	[74]
154.95			78.0	28.55		DMSO-d$_6$	[322]
						D$_2$O	[74]
						D$_2$O	[74]
155.15	74.7	126.8	78.3	28.35		DMSO-d$_6$	[322]
		127.55					
		138.05					
						D$_2$O	[74]
						D$_2$O	[322]
178.6					23.75	DMSO-d$_6$	[322]
						DMSO-d$_6$	[322]
					56.1	DMSO-d$_6$	[322]
					56.9	D$_2$O	[322]
						D$_2$O	[322]

Table 5.18. (Continued)

Compound	Amino Acid						
	COOH or COOR	CONH$_2$	C$_\alpha$	C$_\beta$	C$_\gamma$	C$_\delta$	C$_{\text{arom.}}$ or C$_\varepsilon$
(H-L-CyS-OH)$_2$ · 2HCl	175.6		54.7	39.0			
(H-L-CyS-OMe)$_2$ · 2HCl	174.0		53.15	42.85			
(H-L-CyS-OMe)$_2$ · 2HCl	174.55		54.55	38.45			
(t-Boc-L-CyS-OH)$_2$	178.2		55.8	42.75			
(Ac-L-CyS-OH)$_2$	178.85		54.35	41.1			
H-L-Orn-OH · HCl	179.4		56.6	29.2	24.5	41.1	
Ac-L-Orn-OMe			55.7	32.2	26.2	42.2	
H-L-Arg-OH	175.2	157.5	55.1	28.5	24.9	41.5	
t-Boc-L-Arg (NO$_2$) · OH	173.0	158.55	53.3	28.35	25.45	40.25	
H-L-Lys-OH	175.4		55.3	27.2	22.4	30.7	40.0
H-Asp(OH)-OH	α 170.35 171.55		49.20	34.85			
Z-Asp(OH)-OH	α 171.95 173.05		50.80	36.35			
Z-$\overline{\text{Asp-O}}$	α 170.10 172.40		50.70	35.00			
Z-Asp(OH)-OC$_2$H$_5$	α 171.65 171.25		50.80	36.15			
Z-Asp(OBu^t)-OH	α 170.75 174.00		53.05	39.60			
H-Asp(OBu^t)-OH	α 170.35 170.35		50.35	35.85			
t-Boc-Asp(OBu^t)-OH	α 169.50 172.85		50.25	37.55			
t-Boc-Asp(OH)-OH	α 172.50 173.60		50.60	36.70			
t-Boc-L-Asp(OBzl)-OH	α 168.85 171.3		49.85	36.05			
H-L-Asn-OH	174.2	174.45	52.65	36.05			
H-L-Glu-OH	α 175.6 182.3		55.7	28.1	34.5		
t-Boc-L-Glu(OBzl)-OH	α 171.0 172.5		52.65	26.45	30.15		

Protecting Groups							
$C{=}O$	Z or O-Bzl		*t*-Boc- or OBu^t		Ac-, N-, $COO-CH_3$ OC_2H_5	Solvent	Ref.
	CH_2	C_6H_5	C	CH_3			
						D_2O/DCl	[322]
					56.25	DMSO-d_6	[322]
					57.1	D_2O	[322]
160.6			81.75	30.35		DMSO-d_6	[322]
179.3					23.65	D_2O	[322]
						D_2O	[322]
						DMSO	[326]
						D_2O	[74]
154.85			78.0	28.35		DMSO-d_6	[322]
						D_2O	[74]
						DMSO-d_6	[324]
156.20	65.80	127.95 128.70 137.25				DMSO-d_6	[324]
156.10	66.55	128.15 128.70 136.55				DMSO-d_6	[324]
156.00	65.70	127.75 128.50 137.00			14.05 60.95	DMSO-d_6	[324]
155.45	65.15	127.60 128.35 137.45	79.30	27.85		DMSO-d_6	[324]
			82.05	27.95		DMSO-d_6	[324]
155.25			78.30 80.25	27.70 28.30		DMSO-d_6	[324]
155.80			78.85	28.70		DMSO-d_6	[324]
154.1	65.25	126.8 127.0 127.45 135.35	77.8	28.05		DMSO-d_6	[322]
						D_2O/DCl	[322]
						D_2O	[74]
154.4	65.05	126.8 127.0 127.45 135.35	77.6	28.05		DMSO-d_6	[322]

able 5.18. (Continued).

	Amino Acid						
Compound	COOH or COOR	$CONH_2$	C_α	C_β	C_γ	C_δ	$C_{arom.}$ or C_ε
t-Boc-L-Glu(OBu^t)-OH	α 170.35 172.5		52.45	26.45	31.35		
H-L-Gln-OH	179.5	174.45	55.2	28.3	33.0		
Ac-L-Gln-OH	175.55	179.85 179.2	54.6	29.15	33.7		
t-Boc-L-Gln-OH	172.7	172.7	53.05	26.85	31.45		
H-Pyr-OH	180.2		58.35	25.35	29.65		181.2
H-L-Pro-OH	174.6		61.6	29.7	24.4	46.5	
t-Boc-L-Pro-OH (*cis*)	176.3		58.5	30.5	23.3	46.4	
t-Boc-L-Pro-OH (*trans*)	177.0		58.7	29.4	24.0	46.1	
Formyl-L-Pro-OH (*cis*)	175.90		59.40	29.10	22.20	44.00	
Formyl-L-Pro-OH (*trans*)	175.20		56.70	29.10	23.40	47.00	
Ac-L-Pro-OH (*cis*)	173.95		59.55	30.95	22.55	45.95	
Ac-L-Pro-OH (*trans*)	173.60		58.25	29.25	24.50	47.35	
H-L-Phe-OH	175.0		57.3	37.5			129.5 130.7 131.1
Ac-L-Phe-OMe			55.4	38.7			
t-Boc-L-Phe-OH	172.7		55.2	36.9			125.85 127.55 128.6 137.5
H-L-Tyr-OH	175.0		57.3	37.5			117.5 130.5 156.3
t-Boc-L-Tyr(OBzl)-OH	172.4		55.1	35.65			113.65 126.6 126.8 127.45 129.25 136.3
H-L-Try-OH	174.7		56.0	28.2			114.25 120.5 121.8 124.5 127.6 128.9 138.6
t-Boc-L-Try-OH	172.6		54.25	26.85			109.35 110.55 117.5 119.95 135.25
H-L-His-OH	174.9		58.8	29.0			118.2 137.2

Protecting Groups							
C=O	Z or O-Bzl		*t*-Boc or OBu^t		Ac-, N-, COO−CH$_3$ OC$_2$H$_5$	Solvent	Ref.
	CH$_2$	C$_6$H$_5$	C	CH$_3$			
154.5			77.6	28.15	(*t*-Boc)	DMSO-d$_6$	[322]
			79.2	27.7	(O-Bu^t)		
						D$_2$O/DCl	[322]
179.85					24.4	DMSO-d$_6$	[322]
179.2							
154.4			77.6	28.15		DMSO-d$_6$	[322]
						H$_2$O, pH 6.3	[102]
154.8						D$_2$O	[74]
153.8			80.1	27.9		DMSO-d$_6$	[322]
153.05							
175.90						H$_2$O	[323]
175.20						H$_2$O	[323]
168.45					22.25	DMSO-d$_6$	[322]
168.75					22.25	DMSO-d$_6$	[322]
						D$_2$O	[74]
						DMSO	[326]
154.7			78.0	28.35		DMSO-d$_6$	[322]
						D$_2$O	[74]
154.3	68.9	113.65 126.6 126.8 127.45 129.25 136.3	77.6	27.95		DMSO-d$_6$	[322]
						D$_2$O/DCl	[322]
154.1			77.6	28.05		DMSO-d$_6$	[322]
						D$_2$O	[74]

5.6.2. *pH*-Dependence of the ^{13}C Chemical Shift Values of Amino Acids

The first measurements of pH-dependences of ^{13}C spectra of amino acids were done by INDOR spectroscopy [73]. Pulse Fourier transform ^{13}C NMR measurements are less tedious than INDOR experiments and in a series of papers the pH-dependences of ^{13}C chemical shifts of amino acids were reported [61d, 75].

The results may be summarized as follows: Deprotonation of the NH_3^+, SH or COOH functions usually causes downfield shifts of the signals of neighboring carbon atoms. Shifts to lower field may be larger for the signals of vicinal carbons than for α-carbons. Generally, the largest effects are observed on dissociation of the NH_3^+ group. pK and pI values obtained by ^{13}C NMR measurements agree well with the results of electrometric or photometric studies. The pH-dependences of the chemical shifts of the non-equivalent methyl resonances of valine and penicillamine differ from each other. The low field methyl resonance of penicillamine shifts downfield in two steps with increasing hydroxyl concentration, the signal of the more shielded methyl carbon shifts to lower and finally to higher field with decreasing proton concentration.

5.6.3. Prediction of Carbon Shifts and Their Correlation with Other Physicochemical Parameters

According to Grant's additivity rule [62], substitution of a hydrogen atom in alkanes by a methyl group causes downfield shifts of approximately 9 ppm for the α- and β-carbons and an upfield shift of approximately 2.5 ppm for the γ-carbons. If the hydrogen atom is replaced by an amino group the chemical shift parameters are 29.0 (C-α), 11.4 (C-β) and −4.6 (C-γ); for COOH groups values of 21.5 (C-α), 2.0 (C-β) and −2.5 (C-γ) are observed. On the basis of the additivity of these effects, the chemical shift values for the carbons of amino acids were predicted [73] and they are in fairly good agreement with the observed ones.

A semi-empirical molecular orbital method for the correlation of charge distributions with ^{13}C shifts in amino acids was described [72]. Plotting of chemical shift parameters *versus* charge density changes of α-carbon atoms relative to the corresponding atoms in the parent hydrocarbons permits prediction of the chemical shifts of the α-carbons with an accuracy of about 10 %. However, the slope (280 ppm per electron) in Fig. 5.16 is larger than it should be according to the relationship of Spiesecke and Schneider (160 to 200 ppm per electron) [240]. Chemical shift parameters for β-carbons still cannot be explained theoretically, as most probably inductive, field, electron delocalization and steric effects are involved simultaneously.

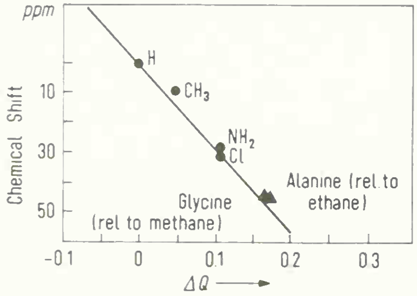

Fig. 5.16. Charge density change (ΔQ) of the α-carbons relative to the corresponding carbon atoms of the parent hydrocarbons *versus* chemical shifts [73].

According to the calculations mentioned above [72] a decrease of the positive charge distribution at the α-carbon and the α-hydrogen should be expected upon dissociation of the ammonium group. In fact, the dissociation leads to an upfield shift only for the α-hydrogen, and a downfield shift for the α-carbon. According to the calculations [72], the strongest charge density changes should occur at the α-carbon upon dissociation of the NH_3^+ group; experimental investigations show, however, that in many cases the chemical shift changes are larger for the *vicinal* carbons [61]. The model of Del Re, therefore, is not accurate enough to describe the dissociation processes in amino acids. Polarization of the C–H-bond by induction through space could be a possible explanation for these dissociation effects [61].

5.7. Peptides

5.7.1. Oligopeptides

The ^{13}C signals of synthetic oligopeptides can be assigned by proton off-resonance decoupling and by comparison with the spectra of the constituent amino acids (see Section 5.6). The signals of the oligopeptides of Table 5.19 and Fig. 5.17 were identified using these assignment aids [75, 321, 322, 324, 328].

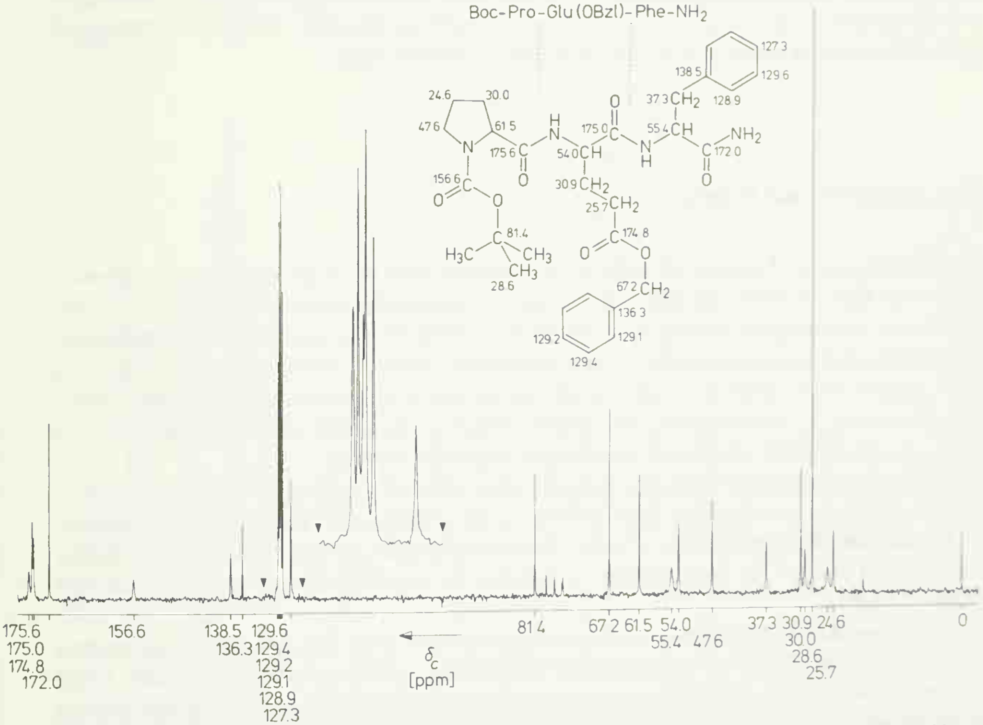

Fig. 5.17. PFT ^{13}C NMR spectrum of the protected tripeptide Boc-Pro-Glu(OBzl)-Phe-NH_2; 200 mg in 2 ml deuteriochloroform; 30 °C; 20 MHz; pulse angle: 45°; proton broad band decoupled; 5000 scans. The assignments made for the signals at 175 ± 0.4 ppm and 129.2 ± 0.4 ppm are interchangeable.

The oxidation state of cysteine in peptides such as glutathione may be easily recognized by the downfield shift of the signal of C_β in the cysteine residue upon oxidation from $-CH_2SH$ to $-CH_2-S-S$ [321]. A ^{13}C NMR study of the series gly$\overset{\alpha}{c}$ine, gly$\overset{\beta}{c}$yl-gly$\overset{\alpha}{c}$ine, gly$\overset{\gamma}{c}$yl-gly$\overset{\beta}{c}$yl-gly$\overset{\alpha}{c}$ine demonstrates the dependence of the chemical shifts of the α-carbon atoms on the chain length (the Greek letters above glycine and the peptides are used for the characterization of the methylene resonances): In glycyl-glycine the signal of the α-methylene group appears 1.5 ppm at lower field, that of the β-methylene group 1.5 ppm at higher field compared to the resonance of the α-carbon of glycine. In triglycine the β-methylene carbon resonates at about the same δ value as that of glycine; the α-methylene resonance appears at lower field and the γ-methylene signal at higher field than the line of the β-carbon. Despite these large shift differences in comparison to ^{1}H NMR, the dependence on neighboring residues does not seem to lead to a useful empirical relationship [73].

Investigations [326] on the decapeptide antibiotic gramicidin demonstrate that the interpretation of ^{13}C NMR spectra of longer chain peptides is more straightforward than that of the corresponding ^{1}H NMR spectra. The ^{13}C NMR spectrum of gramicidin S−A (cyclo(-Phe-Pro-Val-Orn-Leu)$_2$) can be divided into five different groups of signals:

The region of C_γ and methyl carbons (12.5 to 27.5 ppm), the range of the β-carbons (27.5 to 42.5 ppm), at even lower field (52.5 to 62.5 ppm) the lines of the α-carbons, from 122.5 to 142.5 the resonances of aromatic and heteroaromatic carbons and at lowest field (168.5 to 173.5 ppm) the signals of the carbonyl carbons. Only a few of the predicted 28 resonances overlap in the spectrum of the decapeptide gramicidin S−A, and most of them can be assigned by comparison with the spectra of the corresponding amino acids and their N-acetyl methyl ester derivatives [326]. The carbonyl resonances cannot be assigned unequivocally.

5.7.2. Polypeptides and Proteins

A detailed analysis of carbon-13 shifts in polypeptides with up to 20 amino acid residues is achievable. This was shown for several polypeptides, among those alamethicine [329] (Fig. 5.18). The signals were assigned by comparison with the carbon shifts of synthetic partial sequences, by selective proton decoupling and by T_1 measurement using the inversion-recovery technique which permits the localization of some closely spaced signals of non-equivalent α carbons. Moreover, the methyl T_1 values increase with growing length of the amino acid side chain (Leu-C_δ > Val-C_γ > Ala-C_β) [329], reflecting an increased degree of mobility.

While the chemical shifts of the amino acid residues in the rigid α-helical part (Aib^2-Val^8) remain constant within the experimental error, those of carbons belonging to the more flexible portions of the alamethicine sequence are affected by conformational changes when the temperature is elevated up to 100 °C in dimethylsulfoxide solution. To conclude, the α-helix is preserved even at 100 °C [329].

Proton decoupled ^{13}C NMR spectra of several proteins with more than 100 amino acid residues such as lysozyme [330], bovine pancreatic ribonuclease [331] or carboxymyoglobin [225] have been discussed. A complete interpretation of these spectra is usually not possible because of signal overcrowding and slow overall molecular motion so that the motional narrowing condition (section 3.3.2) is only approached for some amino acid side chains with a distinct segmental mobility [149].

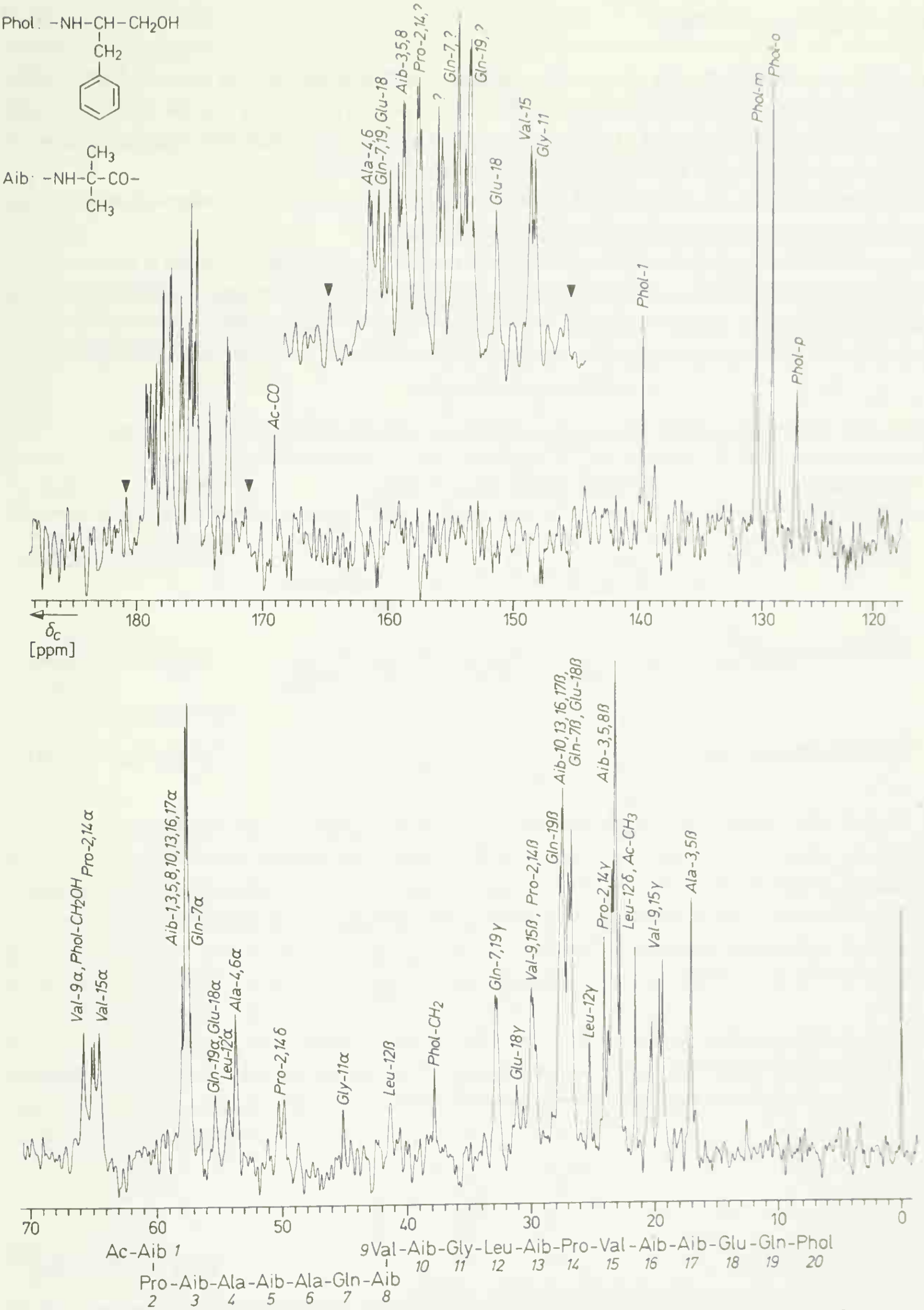

Fig. 5.18. ^{13}C NMR spectrum of alamethicine F 50; 60 mg in 1 ml of deuteriochloroform (^{12}C): tetradeuteriomethanol (^{12}C), 75% : 25% ; 30 °C; 20 MHz; proton broad band decoupled; 30000 interferograms (16 K); 90° pulses; acquisition time/interferogram: 1.8 s; bottom: high-field part; top: low-field part with expanded output for the carbonyl resonances. Signals are assigned according to ref. [329].

5.7.3. Conformational Effects

As the electron charge density of *cis*-proline carbons is different from that of *trans*-proline carbons, these isomers can be differentiated by ^{13}C NMR spectroscopy [332, 333]. On the basis of calculations Tonelli [334] predicted 4 conformations for the dipeptide Boc-Pro-Pro-OBzl, three of which could be detected by ^{13}C NMR spectroscopy [332, 333].

The Larmor frequencies of the α- and amide carbons of the amino acid residues of polypeptides and proteins seem to depend on the peptide conformation:

Converting helical poly-(γ-benzyl-L-glutamate) to a random coil peptide causes a 3 ppm upfield shift for the signal of the α-carbon atom and a 2.7 ppm shift to higher field for the signal of the amide carbon [335]. Similar shifts are observed on the helix coil transition of poly-(N-δ-carbobenzoxy-L-ornithine) for the signals of the backbone carbons of the amino acid units [336].

Table 5.19. ^{13}C Chemical Shift Values (δ [ppm] Relative to TMS) of Oligopeptides [327, 339].

Compound	Formula with δ values in ppm	Solvent	Ref.
Z-Gly-DL-Ala-N_2H_3	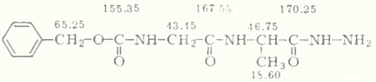 155.35 167.55 170.25 65.25 43.15 46.75 CH₂–O–C–NH–CH₂–C–NH–CH–C–NH–NH₂ O O CH₃ O 15.60	DMSO-d_6	[102]
Z-DL-Ala-Gly-N_2H_3	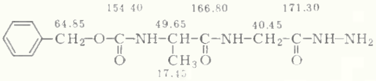 154.40 166.80 171.30 64.85 49.65 40.45 CH₂–O–C–NH–CH–C–NH–CH₂–C–NH–NH₂ O CH₃ O O 17.45	DMSO-d_6	[102]
Z-L-Asp(α-OEt)-Gly-OEt	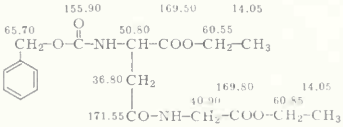 155.90 169.50 14.05 65.70 O 50.80 60.55 CH₂–O–C–NH–CH–COO–CH₂–CH₃ 36.80 CH₂ 169.80 14.05 40.90 60.85 171.55 CO–NH–CH₂–COO–CH₂–CH₃	DMSO-d_6	[324]
Boc-L-Val^2-OH	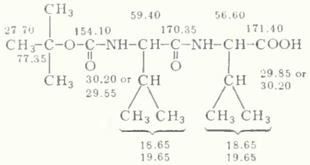 CH₃ 59.40 56.60 27.70 154.10 170.35 171.40 CH₃–C–O–C–NH–CH–C–NH–CH–COOH 77.35 O O CH₃ 30.20 or CH 29.55 CH 29.85 or 30.20 CH₃ CH₃ CH₃ CH₃ 16.65 19.65 18.65 19.65	DMSO-d_6	[322]
H-DL-Leu-DL-Leu-OH · · HCl	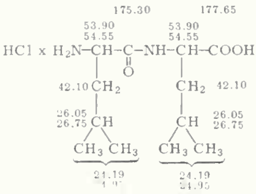 175.30 177.65 53.90 54.55 53.90 54.55 HCl x H₂N–CH–C–NH–CH–COOH O 42.10 CH₂ CH₂ 42.10 26.05 26.75 CH CH 26.05 26.75 CH₃ CH₃ CH₃ CH₃ 24.19 24.95 24.19 24.95	D_2O	[322]
β-Ala-His (Carnosin)	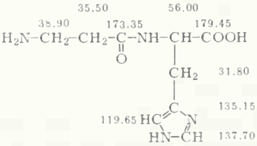 35.50 56.00 38.90 173.35 179.45 H₂N–CH₂–CH₂–C–NH–CH–COOH O CH₂ 31.80 C 135.15 119.65 HC N HN–CH 137.70	D_2O	[328]

Table 5.19. (Continued).

Compound	Formula with δ values	Solvent	Ref
Z-L-Cys(Bzl)-Gly-OEt	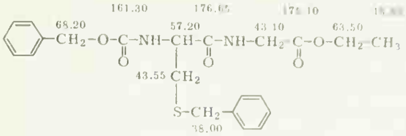 161.30 176.65 175.10 68.20 57.20 43.10 63.50 43.55 38.00	DMSO-d_6	[322]
Z-L-Asp(α-OH)-L-Cys(Bzl)-Gly-OH (protected Asparthione)	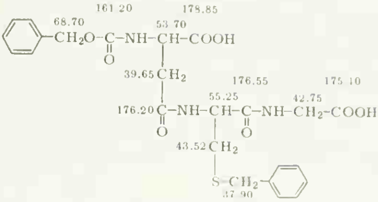 161.20 178.85 68.70 53.70 39.65 176.55 175.10 55.25 42.75 176.20 43.52 37.90	DMSO-d_6	[322]
L-Glu(α-OH)-L-Cys-Gly-OH (Glutathione)	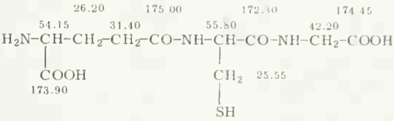 26.20 175.00 172.30 174.45 54.15 31.40 55.80 42.20 173.90 25.55 $H_2N{-}CH(COOH){-}CH_2{-}CH_2{-}CO{-}NH{-}CH(CH_2{-}SH){-}CO{-}NH{-}CH_2{-}COOH$	H_2O (pH 3.52)	[75]
L-Glu(α-OH)-L-Cys(Glutathionyl)-Gly-OH (Glutathione oxidized)	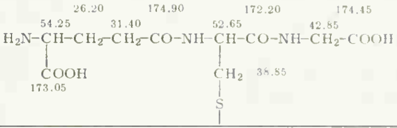 26.20 174.90 172.20 174.45 54.25 31.40 52.65 42.85 173.05 38.85 $H_2N{-}CH(COOH){-}CH_2{-}CH_2{-}CO{-}NH{-}CH(CH_2{-}S{-}){-}CO{-}NH{-}CH_2{-}COOH$	H_2O (pH 3.52)	[75]

Measurements of spin-lattice relaxation times (T_1) for different carbon atoms will become a fruitful method for investigating conformational changes of peptides and proteins [41, 337]. The T_1 value of the α-carbon band of native ribonuclease at pH 6.55 is 35 ms. The T_1 values of the same carbon atoms in denatured ribonuclease (pH 2.12) are 60 ms on the average. The lysine side chain carbons of this protein relax significantly slower and remain practically unaffected on denaturation. This has been attributed to an enlarged segmental mobility of the lysine side chain in ribonuclease [149].

Another study [338] on amino acids bound to macromolecular cationic exchange resins reported strongly shortened spin-lattice relaxation times, especially for the quaternary carbon atoms of the amino acid moieties. This effect can be used to detect and distinguish these quaternary carbons from CH groups.

5.8. Porphyrins

To date only partial signal assignments of various porphyrins have been reported in the literature [340]. Total signal identifications for these biologically and theoretically important molecules should be possible, however, from the study of additional model compounds, specificly deuterated and ^{13}C enriched porphyrins.

Table 5.20. ^{13}C Chemical Shifts of Porphyrins (δ Values in ppm Relative to TMS = 0; Solvent: $CHCl_3$) [340]

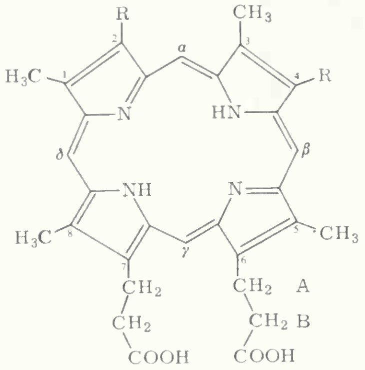

Deuterioporphyrin: R = ^{2}H
Mesoporphyrin: R = $^{2',4'}CH_2$-CH_3
Protoporphyrin: R = $^{2',4'}CH$=CH_2

C-Atom	Deuterio-porphyrin dimethyl ester	Deuterio-porphyrin diethyl ester	2,4-Di-acetyl-deuterio-porphyrin dimethyl ester	2,4-Di-propionyl-deuterio-porphyrin dimethyl ester	Meso-porphyrin dimethyl ester	Proto-porphyrin diethyl ester
1,3-CH_3	13.60	13.60	13.60	13.80	17.80	12.50
C-2,4	128.60	128.80				
C-2′,4′			197.80		19.90	130.40
5,8-CH_3	11.60	11.50	11.50	11.30	11.60	11.80
C-6A, 7A	21.90	21.90	21.50	21.30	22.10	22.00
C-6B,7B	37.40	37.00	36.60	38.00 36.20	37.50	37.40
meso carbons	100.20 99.40 97.00 96.00	100.00 99.20 96.90 95.90	101.90 99.70 96.80 95.30	101.70 99.80 96.80 95.10	96.30	96.90
CO (ester)	173.50 to 173.20	173.50 to 173.20	173.50 to 173.20	173.50 to 173.20	173.50 to 173.20	173.50 to 173.20
C_{quat} (pyrrole)	147.50 to 135.50	147.50 to 135.50	147.50 to 135.50	147.50 to 135.50	147.50 to 135.50	147.50 to 135.50
CH_3 (methyl ester)	51.80 to 51.60		51.80 to 51.60	51.80 to 51.60	51.80 to 51.60	
CH_3 (ethyl ester)		14.40				14.40
CH_2 (ethyl ester)		60.80				60.80
CH_3 (acetyl)			33.10 to 32.80			
CH_2 (propionyl)				38.00 36.20		
CH_3 (propionyl)				9.10		
CH_3 (ethyl)					11.60	
CH_2 (vinyl)						120.10

The signal assignments in Table 5.20 were made mainly by correlation of the ^{13}C NMR spectra of different analogs and by proton off-resonance decoupling.

The quaternary carbons of the pyrrole rings resonate within a range of 147.5 to 135.5 ppm; though all their resonances can be resolved in the spectrum, individual assignments are not yet possible. Furthermore, no unequivocal signal identifications can be made of the four resonances of the *meso* carbons. Though C-2, C-4 and the *meso* carbons of deuterioporphyrin dimethyl ester are in *β*-positions relative to the nitrogens, only the former carbons absorb in the olefinic range. This efficient shielding of the *meso* carbons can be explained in terms of cyclic conjugation in the 16-membered porphyrin ring [340].

The carbon shifts of the phytyl residue in chlorophyll a have been assigned on the basis of substituent increments and T_1 measurements as was outlined in section 3.3.3.5 [158]. While the side chain carbons of the chlorine macrocycle could be recognized mainly by proton-off-resonance decoupling, all non-protonated pyrrole ring carbons remained unassigned [158]. Reasonably, the larger shift values belong to the carbons α to nitrogen.

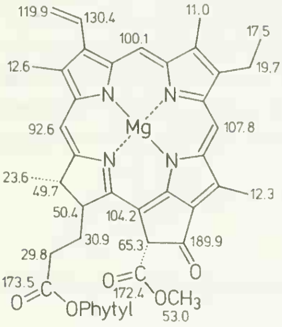

Chlorophyll a: Pyrrole Ring Carbon Shifts [ppm]

168.7	146.2
161.9	144.5
155.5	139.3
155.1	135.7
152.7	134.6
148.6	134.0
147.6	129.8

[158]

5.9. Elucidation of Biosynthetic Pathways

The examination of biosynthetic pathways will become an important application of ^{13}C NMR spectroscopy in biochemistry. This is demonstrated by several examples reported in the literature and summarized in this section. By adding ^{13}C enriched precursors to culture media, specificly labelled biosynthetic materials can be isolated. ^{13}C enriched positions are easy to identify as they cause large signal intensities in the ^{13}C NMR spectrum.

5.9.1. Radicinin

The ^{13}C NMR spectrum of radicinin, isolated from cultures of Stenphylium radicinum, containing sodium [2-^{13}C]-acetate, showed strong signals for the carbons C-3, -5, -9, -11, -12 and -14 only. Stenphylium radicinum cultures grown in media containing sodium [1-^{13}C]-acetate yielded a radicinin giving intense resonances for C-2, -4, -6, -8, -10 and -13 only [341]. These ^{13}C NMR experiments prove that only acetate is needed for the biosynthesis of radicinin, as is demonstrated by the following scheme:

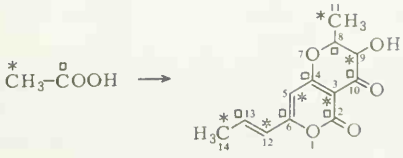

Radicinin

5.9.2. Asperlin

In a similar manner the pentaacetyl origin of the antibiotic asperlin could be proved experimentally. The ^{13}C NMR spectrum of the antibiotic lactone isolated from Apergillus nidulans, grown in a culture medium supplemented with sodium [2-^{13}C]-acetate shows resonances of increased intensity for the carbons 2, 4, 6, 8 and 10 [342]. The origin of the different carbon atoms is demonstrated from the following scheme:

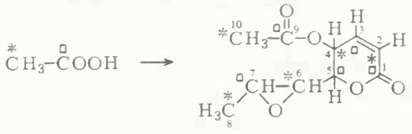

Asperlin

5.9.3. Sterigmatocystin

One biogenetic hypothesis postulates a nonaacetyl naphthacene endoperoxide as the precursor of sterigmatocystin. This hypothesis could be confirmed by recording the ^{13}C NMR spectra of the biosynthetic sterigmatocystins derived from [1-^{13}C]-acetate and [2-^{13}C]-acetate, respectively [343]. The carbons originating from [1-^{13}C]-acetate are marked with asterisks in the formula.

The partial signal assignment of sterigmatocystin is listed in Table 5.21.

Table 5.21. ^{13}C Chemical Shifts of Sterigmatocystin (δ Values in ppm Relative to TMS = 0; Solvent: Dioxane) [343].

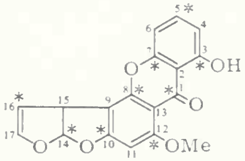

Sterigmatocystin

C-Atom		C-Atom		C-Atom	
C-1	181	C-7	154 to 164	C-13	104 112
C-2	104 to 112	C-8	154 to 164	C-14	103
C-3	154 to 164	C-9	104 to 112	C-15	49
C-4	104 to 112	C-10	154 to 164	C-16	115
C-5	135	C-11	91	C-17	146
C-6	104 to 112	C-12	154 to 112		

5.9.4. Virescenosides

The theory of terpene biosynthesis was confirmed by ^{13}C NMR measurements on derivatives of the diterpenic compounds virescenoside A and B isolated from cultures of the mushroom Oospora virescens (Link) Wallr., inoculated with [1-^{13}C]-acetate and [2-^{13}C]-acetate [344].

Measurements on these ^{13}C enriched compounds and the application of common assignment aids [50] led to the total signal identification of the following diterpenes; the ^{13}C shifts are outlined in Table 5.22.

Table 5.22. ^{13}C Chemical Shifts of Diterpenes (δ Values in ppm Relative to TMS = 0; Solvent: $CHCl_3$) [344].

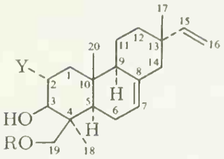
17
15
16
20
11
12
13
9
14
8
Y
1
2
10
H
3
5
7
4
6
HO
H
RO
19
18

Aglycone of virescenoside A: R = H; Y = OH
Aglycone of virescenoside B: R = Y = H

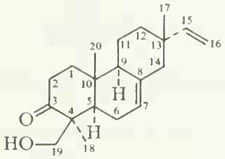
17
15
16
20
11
12
13
9
14
8
1
2
10
H
3
5
7
4
6
O
H
HO
19
18

Aglycone of virescenoside C

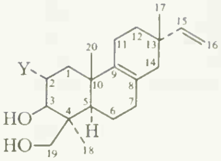
17
15
16
20
11
12
13
14
Y
1
9
2
10
8
3
5
7
4
6
HO
H
HO
19
18

Isovirescenol A: Y = OH
Isovirescenol B: Y = H

C-Atom	Aglycone of Virescenoside A	Aglycone of Virescenoside B	Aglycone of Virescenoside C	Isovirescenol A	Isovirescenol B
C-1	43.3	38.0	36.8	42.6	35.4
C-2	69.1	28.0	35.5	69.6	29.2
C-3	85.8	81.4	217.6	85.4	81.0
C-4	43.3	42.1	52.9	43.2	43.0
C-5	51.8	51.4	53.3	51.9	52.1
C-6	23.6	23.2	24.2	21.6	21.6
C-7	121.8	121.7	121.7	32.8	33.1
C-8	135.9	136.0	136.2	125.0	125.1
C-9	52.5	52.1	50.8	134.9	136.7
C-10	37.4	35.2	35.5	38.4	37.4
C-11	21.2	20.6	21.1	19.6	19.1
C-12	36.7	36.3	36.5	35.0	34.9
C-13	37.0	37.0	37.2	35.3	35.1
C-14	46.4	46.1	46.3	42.0	42.0
C-15	150.6	150.6	150.3	146.1	146.2
C-16	110.2	109.7	109.9	111.3	111.1
C-17	22.2	21.7	21.9	28.1	28.3
C-18	24.0	23.0	22.5	23.3	22.9
C-19	66.0	64.8	66.4	65.5	64.7
C-20	17.8	16.4	16.0	21.6	20.6

5.9.5. Methyl Palmitoleate

The ^{13}C NMR spectrum of specificly ^{13}C labeled methyl palmitoleate isolated from Saccharomyces cerevisiae was a great aid for the total ^{13}C signal assignment of this lipid [345]. The shifts relative to TMS = 0 are listed in the following table.

Table 5.23. ^{13}C Chemical Shifts of Methyl Palmitoleate (δ Values in ppm Relative to TMS = 0; Solvent: $CDCl_3$) [345].

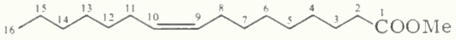

Methyl palmitoleate

C-Atom		C-Atom		C-Atom	
1	173.90	7	28.80	13	29.40
2	33.70	8	29.40	14	31.50
3	24.70	9	129.60	15	22.40
4	26.90	10	129.60	16	13.70
5	28.80	11	29.40	OMe	51.10
6	28.80	12	28.80		

5.9.6. Sepedonin

The biosynthetic incorporation of [1-^{13}C]-acetate, [2-^{13}C]-acetate and [^{13}C]-formate into the molecule of the fungal tropolone sepedonin was investigated recently by ^{13}C NMR spectroscopy [346]. These measurements demonstrate that carbon atom 8 is the only one originating from the formate precursor, as is seen in the scheme in Table 5.24.

Table 5.24. ^{13}C Chemical Shifts of Sepedonin (δ Values in ppm Relative to TMS = 0; Solvent: Pyridine) [346].

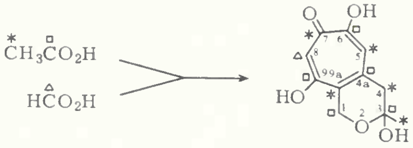

C-Atom		C-Atom		C-Atom	
C-1	60.6	C-6	161.6	C-9	161.6
C-3	93.6		166.0		166.0
C-4	44.0	C-7	174.3	C-9a	128.4
C-4a	140.6	C-8	113.5	CH_3	29.0
C-5	115.6				

Moreover, these investigations led to a total signal assignment of this natural tropolone. The shifts are listed in Table 5.24.

5.9.7. Antibiotic X-537 A

The ^{13}C NMR spectrum of the antibiotic X-537 A, isolated from fermentations containing [1-^{13}C]-butyrate had three signals of very strong intensity caused by the carbons 13, 17 and 21. These ^{13}C NMR experiments demonstrated that all ethyl residues stem from butyrate units [347]. The ^{13}C chemical shift values of the antibiotic X-537 A are listed in Table 5.25.

Table 5.25. ^{13}C Chemical Shifts of the Antibiotic X-537 A (δ Values in ppm Relative to TMS = 0; Solvent: $CHCl_3$) [347].

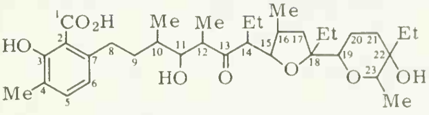

Antibiotic X-537 A

C-Atom		C-Atom		C-Atom	
C-1	177.0	C-8	49.0	C-18	87.7
C-2	118.7	C-9	37.8	C-19	68.7
C-3	166.0	C-11	70.7	C-21	38.5
C-4	123.2	C-12	56.0	C-22	71.3
C-5	131.3	C-13	218.4	C-23	77.3
C-6	119.8	C-15	83.4		
C-7	143.3	C-17	29.5		

Further signals were found at: 34.5, 34.0, 33.5, 31.2, 19.7, 16.2, 15.8, 15.5, 13.6, 13.3, 12.7, 12.1, 9.4 and 7.0 ppm.

5.9.8. Cephalosporin

Part of the biogenesis of cephalosporins was confirmed recently by isolating ^{13}C labeled compounds [348]. Adding [2-^{13}C]-acetate to cultures of Cephalosporium acremonium yielded an antibiotic labeled at C-11, -12, -13, -14 and -19 (marked with asterisks in the formula); [1-^{13}C]-acetate, on the other hand, yielded a compound labeled at positions 10, 15 and 18 (symbolized by □ in the formula).
The specificly ^{13}C enriched compounds were useful for the signal identification of the ^{13}C NMR spectrum of this microbial product. Spectral comparison of cephalosporin C with α-amino-adipic acid-N-ethylamide, cephalexin, 3-methyl-7(2-phenoxyacetamido)-3-cepham and 7-amino cephalosporanic acid led to the total signal identification of this antibiotic. The shifts are listed in Table 5.26.

Table 5.26. ^{13}C Chemical Shifts of Cephalosporin and Derivatives (δ Values in ppm Relative to TMS = 0) [348].

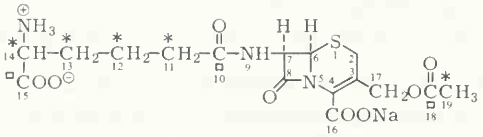

Cephalosporin C

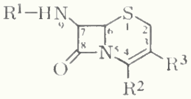

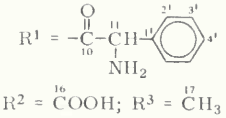

Cephalexin

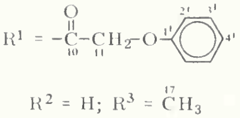

3-Methyl-7(2-phenoxy-acetamido)-3-cepham

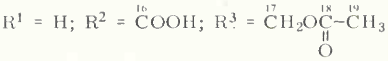

$R^1 = H;\ R^2 = \overset{16}{C}OOH;\ R^3 = \overset{17}{C}H_2O\overset{18}{C}-\overset{19}{C}H_3$ (with =O on C-18)

7-Amino cephalosporanic acid

Solvent C-Atom	Cephalo-sporin C H_2O	D-1α-Amino-adipic acid-N-ethylamide H_2O	Cephalexin H_2O	3-Methyl-7-(2-phenoxy-acetamido)-3-cepham $CHCl_3$	7-Amino-cephalo-sporanic acid 3% $NaHCO_3$
2	24.70		28.00	27.80	25.50
3	134.00		142.60	116.70	132.10
4	118.00		124.10	122.70	116.70
6	57.30		57.10	56.40	62.50
7	59.30		58.60	58.20	58.80
8	168.20		167.40	163.60	163.50
10	180.50	181.50	179.60	169.60	
11	34.40	29.50	58.60	67.10	
12	19.90	17.40			
13	29.40	24.70			
14	54.60	56.70			
15	178.40	177.90			
16	171.90		173.00		168.50
17	64.70		17.70	20.60	64.50
18	177.90				174.90
19	19.30				20.50
1′		34.80 } N-C_2H_5	128.90	158.00	
2′		10.60	131.20	115.10	
3′			128.90	130.20	
4′			130.40	118.60	

5.9.9. Prodigiosin

In a similar manner, the biosynthetic incorporation of acetate into prodigiosin was investigated by isolating the pyrrole derivative from cultures of the bacterium Serratia marcescens growing on media containing sodium [1-^{13}C]- or [2-^{13}C]-acetate [349]. The ^{13}C NMR spectra of the different ^{13}C labeled prodigiosins clearly show that carbons B3, C3, C5, 2′ and 4′ originate from the carboxyl part in contrast to the carbons B4, C4, 1′, 3′ and 5′, which originate from the methyl part of the acetate precursor (Table 5.27):

Table 5.27. ^{13}C Chemical Shifts of Prodigiosin Hydrochloride (δ Values in ppm Relative to TMS = 0; Solvent: $CHCl_3$) [349].

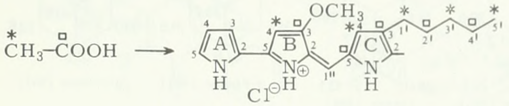

Prodigiosin

C-Atom		C-Atom		C-Atom	
A-2	122.20	B-5	147.75	C-5	128.25
A-3	117.25	Methoxyl	58.80	C-2-methyl	12.30
A-4	111.75	Bridge-head (1″)	115.75	1′	25.30
A-5	126.55			2′	29.70
B-2	146.30	C-2	120.80	3′	31.50
B-3	165.80	C-3	125.15	4′	22.50
B-4	93.05	C-4	128.25	5′	14.00

5.10. Appendix

The following table contains the carbon-13 shifts of some hydrocarbon parent skeletons often required for the assignments of terpene and steroid carbons. It also includes a selection of natural products with biological and pharmacological importance as well as useful reference compounds. Sources are given in brackets. The assignments of carbons with equal off-resonance multiplicities and (or) small shift differences (less than 1 ppm) may be reversed.

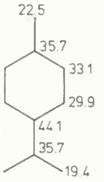
22.5
35.7
33.1
29.9
44.1
35.7
19.4
Menthane [50j]

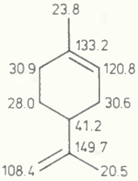
23.8
133.2
30.9
120.8
28.0
30.6
41.2
149.7
108.4
20.5
Limonene [50j]

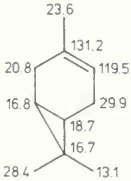
23.6
131.2
20.8
119.5
16.8
29.9
18.7
16.7
28.4
13.1
Carene [50l]

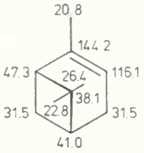
20.8
144.2
47.3
26.4
116.1
38.1
31.5
22.8
31.5
41.0
α-Pinene [50l]

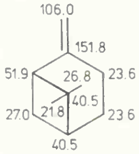
106.0
151.8
51.9
26.8
23.6
40.5
27.0
21.8
23.6
40.5
β-Pinene [50l]

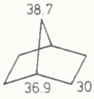

Norbornane [50e,f]

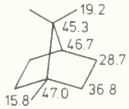
19.2
45.3
46.7
28.7
15.8
47.0
36.8
Bornane [50e]

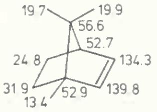
19.7
19.9
56.6
52.7
24.8
134.3
31.9
52.9
139.8
13.4
Bornylene [50e]

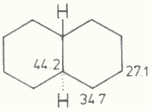
H
44.2
27.1
H
34.7
trans-Decalin [350]

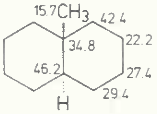
15.7 CH3
42.4
34.8
22.2
46.2
27.4
29.4
H
trans-9-Methyldecalin [350]

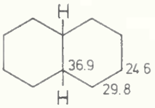
H
36.9
24.6
29.8
H
cis-Decalin [350]

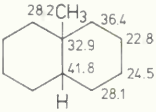
28.2 CH3
36.4
32.9
22.8
41.8
24.5
28.1
H
cis-9-Methyldecalin [350]

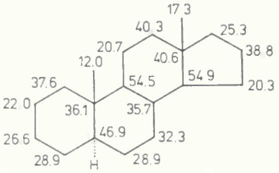
17.3
40.3
25.3
20.7
40.6
38.8
12.0
54.9
37.6
54.5
20.3
22.0
36.1
35.7
46.9
26.6
32.3
28.9
H
28.9
5β-Androstane [288]

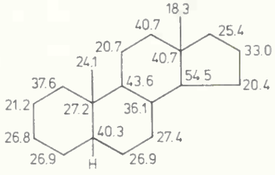
18.3
40.7
25.4
20.7
33.0
24.1
40.7
54.5
37.6
43.6
20.4
21.2
27.2
36.1
40.3
26.8
27.4
26.9
H
26.9
5α-Androstane [288]

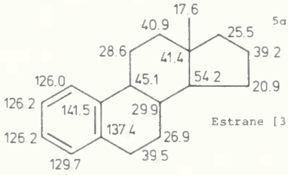
17.6
40.9
25.5
28.6
41.4
39.2
45.1
54.2
126.0
20.9
126.2
141.5
29.9
137.4
126.2
26.9
39.5
129.7
Estrane [351]

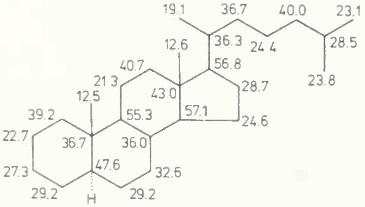
19.1
36.7
40.0
23.1
12.6
36.3
24.4
28.5
40.7
56.8
21.3
23.8
12.5
43.0
28.7
39.2
55.3
57.1
24.6
22.7
36.7
36.0
47.6
27.3
32.6
29.2
H
29.2
Cholestane [352]

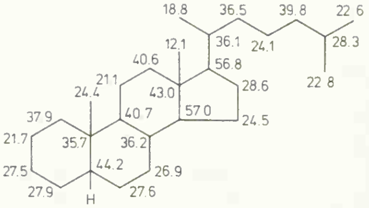
18.8
36.5
39.8
22.6
12.1
36.1
24.1
28.3
40.6
56.8
21.1
24.4
43.0
28.6
22.8
37.9
40.7
57.0
24.5
21.7
35.7
36.2
44.2
27.5
26.9
27.9
H
27.6
Coprostane [352]

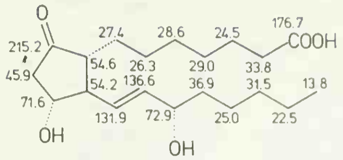
O
215.2
45.9
71.6
OH
27.4
54.6
54.2
26.3
136.6
131.9
28.6
29.0
36.9
72.9
OH
24.5
33.8
31.5
25.0
176.7
COOH
13.8
22.5

Prostaglandin E1 [353,354]

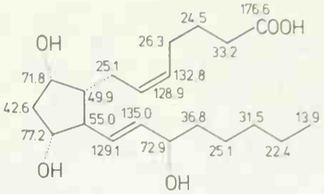
OH
71.8
42.6
77.2
OH
25.1
49.9
55.0
135.0
129.1
72.9
OH
26.3
132.8
128.9
24.5
33.2
176.6
COOH
36.8
25.1
31.5
22.4
13.9

Prostaglandin F2α [353]

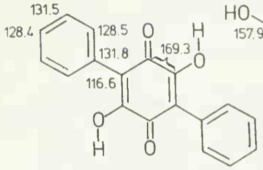
131.5
128.4
128.5
131.8
116.6
O
169.3
H
O
O
H
O

Polyporic acid [355]

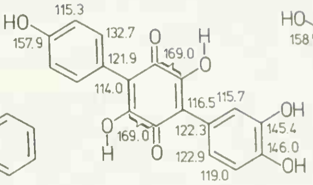
115.3
HO
157.9
132.7
121.9
114.0
O
169.0
H
O
116.5
115.7
OH
145.4
146.0
OH
122.3
122.9
119.0
O
H
169.0
O

Leucomelon [355]

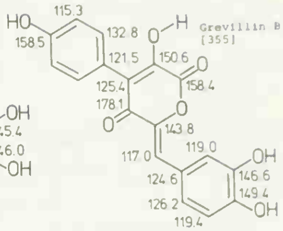
HO
115.3
158.5
132.8
121.5
O
H
150.6
O
125.4
158.4
178.1
O
O
143.8
117.0
119.0
OH
124.6
146.6
149.4
126.2
OH
119.4

Grevillin B [355]

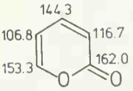
144.3
106.8
116.7
153.3
162.0
O
O

α-Pyrone [356]

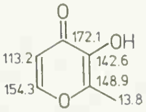
O
172.1
OH
113.2
142.6
154.3
148.9
O
13.8

Maltol [357]

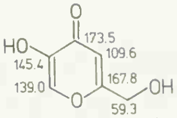
O
HO
173.5
109.6
145.4
139.0
167.8
O
OH
59.3

Kojic acid [357]

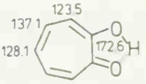
123.5
137.1
128.1
O
172.6
H
O

Tropolone [358]

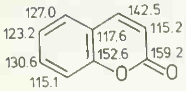
127.0
142.5
123.2
117.6
115.2
152.6
159.2
130.6
O
O
115.1

Coumarin [359]

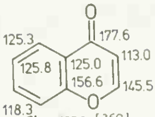
O
177.6
125.3
113.0
125.8
125.0
156.6
145.5
118.3
O

Chromone [360]

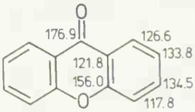
O
176.9
126.6
133.8
121.8
156.0
134.5
O
117.8

Xanthone [361]

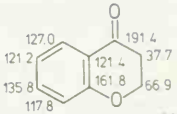
O
127.0
191.4
121.2
121.4
37.7
135.8
161.8
66.9
117.8
O

Chroman-4-one [360]

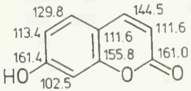
129.8
144.5
113.4
111.6
111.6
161.4
155.8
161.0
HO
102.5
O
O

7-Hydroxycoumarin [359]

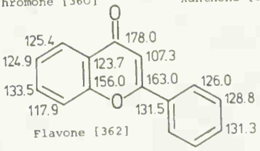
O
178.0
125.4
124.9
123.7
107.3
156.0
163.0
126.0
133.5
128.8
117.9
O
131.5
131.3

Flavone [362]

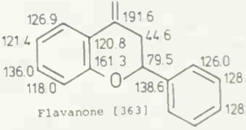
O
126.9
191.6
121.4
120.8
44.6
161.3
79.5
126.0
136.0
128.7
118.0
O
138.6
128.7

Flavanone [363]

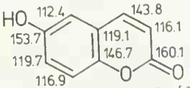
HO
112.4
143.8
153.7
119.1
116.1
146.7
160.1
119.7
O
O
116.9

6-Hydroxycoumarin [359]

7-Methoxyisoflavone [362]

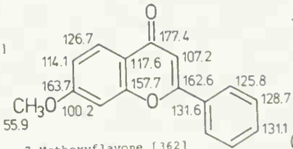
O
126.7
177.4
114.1
117.6
107.2
163.7
157.7
162.6
125.8
CH3O
100.2
O
128.7
55.9
131.6
131.1

7-Methoxyflavone [362]

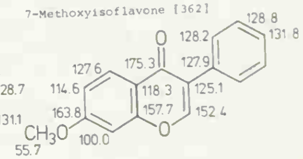
128.8
O
128.2
131.8
127.6
175.3
127.9
114.6
118.3
125.1
163.8
157.7
152.4
CH3O
100.0
O
55.7

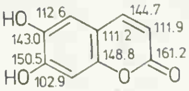
HO
112.6
144.7
143.0
111.2
111.9
150.5
148.8
161.2
HO
102.9
O
O

6,7-Dihydroxycoumarin [359]

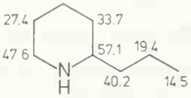
25.7
27.4
33.7
47.6
57.1
19.4
N
H
40.2
14.5

Coniine [364]

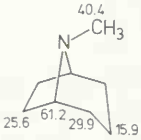
40.4
N
CH3
25.6
61.2
29.9
15.9

Tropine [364]

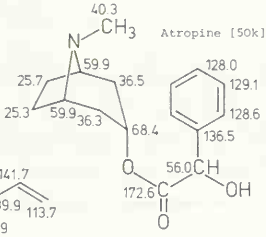
40.3
N
CH3
59.9
25.7
36.5
25.3
59.9
36.3
68.4
128.0
129.1
128.6
136.5
O
56.0
CH
OH
172.6
C
O

Atropine [50k]

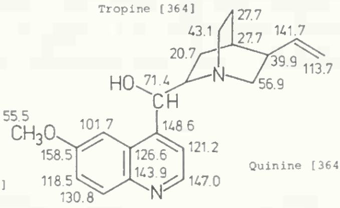
27.7
43.1
27.7
141.7
20.7
39.9
113.7
N
56.9
HO
71.4
CH
55.5
CH3O
101.7
148.6
158.5
126.6
121.2
143.9
118.5
147.0
130.8
N

Quinine [364]

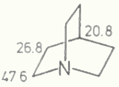
20.8
26.8
N
47.6

Quinuclidine [364]

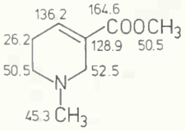
136.2
164.6
COOCH3
26.2
128.9
50.5
50.5
52.5
N
45.3 CH3

Arecoline [364]

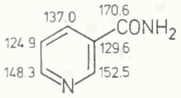
137.0
170.6
CONH2
124.9
129.6
148.3
152.5
N

Nicotinamide [501]

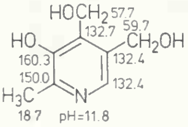
HOCH2 57.7
132.7
59.7
HO
CH2OH
160.3
132.4
150.0
132.4
H3C
N
18.7
pH=11.8

Pyridoxine [365]

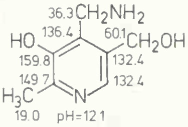
36.3 CH2NH2
136.4
60.1
HO
CH2OH
159.8
132.4
149.7
132.4
H3C
N
19.0
pH=12.1

Pyridoxamine [365]

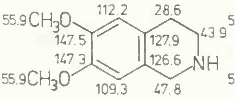
55.9 CH3O
112.2
28.6
147.5
127.9
43.9
147.3
126.6
NH
55.9 CH3O
109.3
47.8

6,7-Dimethoxy-1,2,3,4-tetrahydroisoquinoline [295]

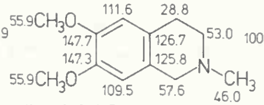
55.9 CH3O
111.6
28.8
147.7
126.7
53.0
147.3
125.8
N
CH3
55.9 CH3O
109.5
57.6
46.0

N-Methyl-6,7-dimethoxy-1,2,3,4-tetrahydroisoquinoline [295]

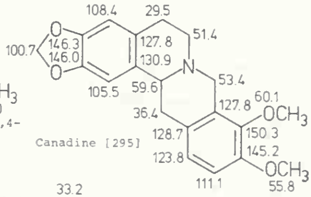
108.4
29.5
O
146.3
127.8
51.4
100.7
146.0
130.9
N
O
105.5
59.6
53.4
36.4
127.8
60.1
OCH3
128.7
150.3
123.8
145.2
OCH3
111.1
55.8

Canadine [295]

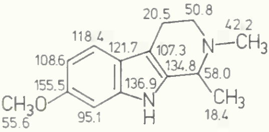
20.5
50.8
42.2
118.4
121.7
107.3
N
CH3
108.6
134.8
58.0
155.5
136.9
CH3
CH3O
95.1
N
H
18.4
55.6

N-Methyltetrahydroharmine [364]

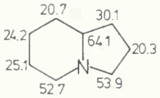
20.7
30.1
24.2
64.1
20.3
25.1
N
52.7
53.9

Indolizidine [364]

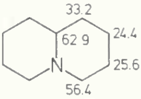
33.2
62.9
24.4
N
25.6
56.4

Quinolizidine [364]

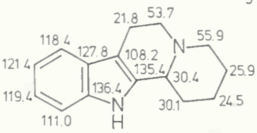
21.8
53.7
118.4
127.8
108.2
N
55.9
121.4
135.4
30.4
25.9
119.4
136.4
N
H
30.1
24.5
111.0

Indolo[2,3-a]quinolizine [364]

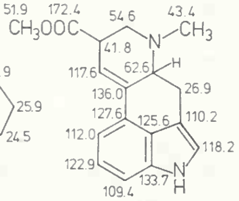
51.9
172.4
54.6
43.4
CH3OOC
41.8
N
CH3
117.6
62.6
H
136.0
26.9
127.6
125.6
110.2
112.0
118.2
122.9
NH
109.4
133.7

Lysergic acid methyl ester [296]

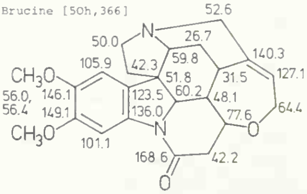
52.6
50.0
N
26.7
140.3
105.9
42.3
59.8
127.1
CH3O
51.8
31.5
56.0,
146.1
123.5
60.2
48.1
64.4
56.4
149.1
136.0
77.6
CH3O
N
O
101.1
168.6
42.2
O

Brucine [50h,366]

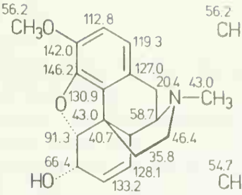
56.2
CH3O
112.8
119.3
142.0
146.2
127.0
20.4
43.0
N—CH3
O
130.9
43.0
58.7
91.3
40.7
46.4
35.8
66.4
128.1
HO
133.2

Codeine [367]

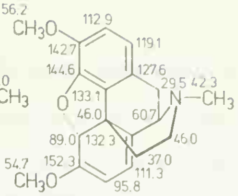
56.2
CH3O
112.9
119.1
142.7
144.6
127.6
29.5
42.3
N—CH3
O
133.1
46.0
60.7
89.0
132.3
46.0
54.7
152.3
37.0
111.3
CH3O
95.8

Thebain [367]

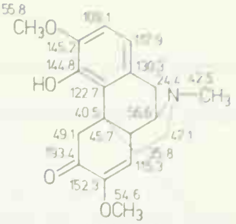
55.8
CH3O
145.2
144.8
HO
122.7
130.3
24.4
47.5
N—CH3
40.5
49.1
45.7
47.1
35.8
O
152.3
54.6
OCH3

Sinomenine [367]

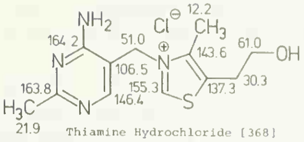
NH2
Cl⊖
12.2
CH3
164.2
51.0
⊕
N
143.6
61.0
OH
N
106.5
155.3
30.3
163.8
137.3
H3C
N
146.4
S
21.9

Thiamine Hydrochloride [368]

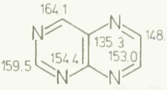
164.1
N
N
148.4
135.3
154.4
153.0
159.5
N
N

Pteridine [369]

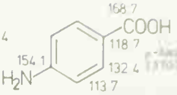
168.7
COOH
118.7
154.1
132.4
H2N
113.7

p-Aminobenzoic acid [370]

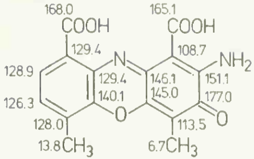
168.0
COOH
165.1
COOH
129.4
N
108.7
NH2
128.9
129.4
146.1
151.1
140.1
145.0
177.0
126.3
O
O
128.0
113.5
13.8CH3
6.7CH3

Actinocin [371]

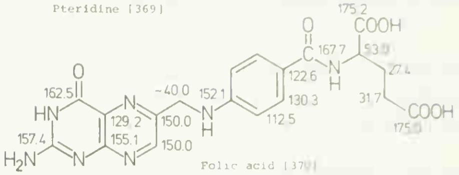
175.2
O
COOH
C
167.7
N
53.0
H
O
122.6
27.4
162.5
~40.0
152.1
130.3
31.7
HN
N
N
H
COOH
129.2
150.0
112.5
175.0
157.4
155.1
150.0
H2N
N
N

Folic acid [370]

Tetracycline Hydrochloride [501]

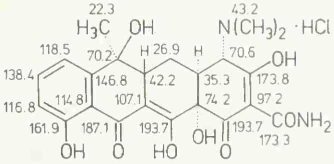
22.3
H3C
OH
43.2
N(CH3)2 ·HCl
118.5
70.2
H 26.9
H
70.6
OH
138.4
146.8
42.2
35.3
173.8
114.8
107.1
74.2
97.2
116.8
CONH2
161.9
187.1
193.7
193.7
173.3
OH
O
HO
OH
O

Nonactine [372]

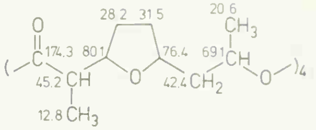
28.2
31.5
20.6
O
CH3
174.3
80.1
76.4
69.1
CH
45.2
CH
O
42.4CH2
O
)4
12.8CH3

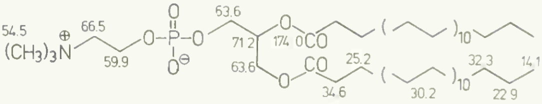
O
63.6
54.5
66.5
O
(CH3)3N
O-P-O
71.2
174.0CO
)10
59.9
O⊖
63.6
CO
25.2
32.3
14.1
O
34.6
30.2
)10
22.9

Dipalmitoyllecithin [373]

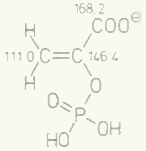
168.2
COO⊖
H
111.0
C=C
146.4
H
O
O
P
OH
HO

Phosphoenolpyruvate [501]

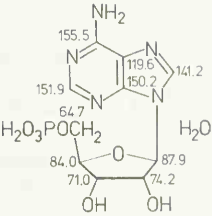
NH2
155.5
N
N
119.6
141.2
151.9
150.2
N
N
64.7
H2O3POCH2
84.0
O
87.9
71.0
74.2
OH
OH

Adenosine monophosphate [50i]

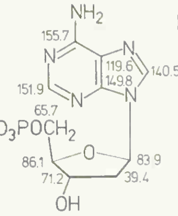
NH2
155.7
N
N
119.6
140.5
151.9
149.8
N
N
65.7
H2O3POCH2
86.1
O
83.9
71.2
39.4
OH

Deoxyadenosine monophosphate [102]

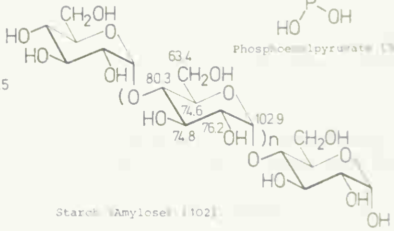
CH2OH
HO
O
HO
OH
63.4
80.3
CH2OH
(O
O
HO
74.6
102.9
74.8
76.2
OH
)n
CH2OH
O
O
HO
OH
OH

Starch (Amylose) [102]

References

[1] J. A. Pople, W. G. Schneider, and H. J. Bernstein: High Resolution Nuclear Magnetic Resonance. McGraw-Hill, New York 1959.

[2] H. Suhr: Anwendungen der Kernmagnetischen Resonanz in der Organischen Chemie. Springer, Berlin-Heidelberg-New York 1965.

[3] E. D. Becker: High Resolution NMR. Academic Press, New York 1969.

[4] F. A. Bovey: Nuclear Magnetic Resonance Spectroscopy. Academic Press, New York 1969.

[5] J. W. Emsley, J. Feeney, and L. H. Sutcliffe: High Resolution Nuclear Magnetic Resonance Spectroscopy, Vols. 1 and 2. Pergamon Press, Oxford 1965, p. 166.

[6] F. Bloch: Phys. Rev. *70*, 460 (1946); F. Bloch, W. W. Hansen, and M. Packard: Phys. Rev. *70*, 474 (1946).

[7] T. C. Farrar and E. D. Becker: Pulse and Fourier Transform NMR, Introduction to Theory and Methods. Academic Press, New York 1971.

[8] W. Finkelnburg: Einführung in die Atomphysik, 7th and 8th Ed. Springer, Berlin-Göttingen-Heidelberg-New York 1962, S. 251.

[9] W. E. Lamb: Phys. Rev. *60*, 817 (1941).

[10] N. F. Ramsey and E. M. Purcell: Phys. Rev. *85*, 143 (1952); N. F. Ramsey: Phys. Rev. *91*, 303 (1953).

[11] P. Diehl, H. Kellerhals, and E. Lustig: NMR, Basic Principles and Progress, Vol. 6, Computer Assistance in the Analysis of High-Resolution NMR Spectra. Springer, Berlin-Heidelberg-New York 1972.

[12] E. G. Hoffmann, W. Stempfle, G. Schroth, B. Weimann, E. Ziegler, and J. Brandt: Angew. Chem. *84*, 400 (1972) and Internat. Edit. *11*, 375 (1972).

[13] N. Boden: Pulsed NMR Methods in: F. C. Nachod and J. J. Zuckerman, Ed., Determination of Organic Structures by Physical Methods, Vol. 4. Academic Press, New York-London 1971, Chapter 2.

[14] H. Margenau and G. M. Murphy: The Mathematics of Physics and Chemistry. Van Nostrand, Princeton, N.J. 1943, Chapter 8.

[15] I. J. Lowe and R. E. Norberg: Phys. Rev. *107*, 46 (1957).

[16] A. Abragam: The Principles of Nuclear Magnetism. Clarendon Press, Oxford 1951, pp. 32, 114.

[17] R. R. Ernst and W. A. Anderson: Rev. Sci. Instr. *37*, 93 (1966); R. R. Ernst: Chimia *26*, 53 (1972).

[18] R. B. Blackman and J. W. Tukey: The Measurement of Power Spectra. Dover, New York 1958; S. Goldman: Information Theory. Prentice Hall, Englewood Cliffs, N.J. 1953.

[19] J. W. Cooley and J. W. Tukey: Math. Comput. *19*, 296 (1965).

[20] R. Klahn and R. R. Shively: Electronics *124* (1968).

[21] R. R. Ernst: Adv. Magn. Res. *2*, 1 (1966).

[22] J. S. Waugh: J. Mol. Spectrosc. *35*, 298 (1970).

[23] R. L. Streever and H. Y. Carr: Phys. Rev. *121*, 20 (1961).

[24] E. D. Becker, J. A. Ferretti, and T. C. Farrar: J. Amer. Chem. Soc. *91*, 7784 (1969).

[25] A. Allerhand and D. W. Cochran: J. Amer. Chem. Soc. *92*, 4482 (1970).

[26] P. Fellgett: Thesis. University of Cambridge 1951.

[27] P. L. Richards in: D. H. Martin, Ed., Spectroscopic Techniques. North Holland Publishers, Amsterdam 1967.

[28] W. A. Anderson: Phys. Rev. *102*, 151 (1956).

[29] W. McFarlane: Nuclear Magnetic Double Resonance in: F. C. Nachod and J. J. Zuckerman, Ed., Determination of Organic Structures by Physical Methods, Vol. 4. Academic Press, New York, London 1971, Chapter 3.

[30] W. v. Philipsborn: Angew. Chem. *83*, 470 (1971) and Internat. Edit. *10*, 472 (1971).

[31] W. A. Anderson and F. A. Nelson: J. Chem. Phys. *39*, 183 (1963).

[32] R. R. Ernst: J. Chem. Phys. *45*, 3845 (1966); J. Mol. Phys. *16*, 241 (1969).

[33] K. F. Kuhlmann and D. M. Grant: J. Amer. Chem. Soc. *90*, 7355 (1968).

[34] J. H. Noggle and R. E. Schirmer: The Nuclear Overhauser Effect, Chemical Applications. Academic Press, New York, London 1971.

[35] R. Freeman: J. Chem. Phys. *53*, 457 (1970).

[36] O. A. Gansow and W. Schittenhelm: J. Amer. Chem. Soc. *93*, 4294 (1971).

[37] G. N. La Mar: J. Amer. Chem. Soc. *93*, 1040 (1971); R. Freeman, K. G. R. Pachler, and G. N. La Mar: J. Chem. Phys. *55*, 4586 (1971).

[38] S. Barcza and N. Engstrom: J. Amer. Chem. Soc. *94*, 1762 (1972).

[39] R. L. Vold, J. S. Waugh, M. P. Klein, and D. E. Phelps: J. Chem. Phys. *48*, 3831 (1968).

[40] R. Freeman and R. C. Jones: J. Chem. Phys. *52*, 465 (1970); R. Freeman and H. D. W. Hill: J. Chem. Phys. *53*, 4103 (1971).

[41] A. Allerhand, D. Doddrell, V. Gluschko, D. W. Cochran, E. Wenkert, P. J. Lawson, and F. R. N. Gurd: J. Amer. Chem. Soc. *93*, 544 (1971).

[42] see also W. Bremser, H. D. W. Hill, and R. Freeman: Meßtechnik *78*, 14 (1971).

[43a] R. Freeman and H. D. W. Hill: J. Chem. Phys. *54*, 3367 (1971).

[43b] J. L. Markley, W. J. Horsley, and M. P. Klein: J. Chem. Phys. *55*, 3604 (1971).

[43c] G. C. McDonald and J. S. Leigh: J. Magn. Res. *9*, 358 (1973).

[44] E. L. Hahn: Phys. Rev. *80*, 580 (1950).

[45] H. Y. Carr and E. M. Purcell: Phys. Rev. *94*, 630 (1954).

[46] S. Meiboom and D. Gill: Rev. Sci. Instr. *29*, 688 (1958).

[47] R. Freeman and H. D. W. Hill: J. Chem. Phys. *55*, 1985 (1971).

[48] see for example P. C. Jurs: Anal. Chem. *43*, 364 (1971); P. C. Jurs, B. R. Kowalski, and T. L. Isenhour: Anal. Chem. *41*, 21 (1969); L. E. Wangen, N. M. Frew, and T. L. Isenhour: Anal. Chem. *43*, 845 (1971); T. L. Isenhour and P. C. Jurs: Anal. Chem. *43*, 20A (1971).

[49] J. I. Kaplan: J. Chem. Phys. *27*, 1426 (1957).

[50a] J. B. Stothers: Quat. Rev. Chem. Soc. [London] *19*, 144 (1965).

[50b] P. S. Pregosin and E. W. Randall: ^{13}C Nuclear Magnetic Resonance in: F. C. Nachod and J. J. Zuckerman, Ed., Determination of Organic Structures by Physical Methods. Vol. 4. Academic Press, New York, London 1971, Chapter 6.

[50c] H. Günther: Chem. Unserer Zeit *8*, 45 (1974).

[50d] E. Breitmaier and G. Bauer: Pharm. unserer Zeit *5*, 113 (1976).

[50e] J. B. Stothers: Carbon-13 NMR Spectroscopy. Academic Press, New York, London 1972.

[50f] G. C. Levy and G. L. Nelson: Carbon-13 Nuclear Magnetic Resonance for Organic Chemists. Wiley Interscience, New York, London, Sidney, Toronto 1972.

[50g] J. T. Clerc, E. Pretsch, and S. Sternhell: ^{13}C-Kernresonanzspektroskopie. Akademische Verlagsgesellschaft, Frankfurt am Main 1973.

[50h] F. W. Wehrli and T. Wirthlin: Interpretation of Carbon-13 NMR Spectra. Heyden & Son Ltd. London, New York, Rheine 1976.

[50i] E. Breitmaier and G. Bauer: ^{13}C-NMR-Spektroskopie, eine Arbeitsanleitung mit Übungen. Georg Thieme Verlag, Stuttgart 1977.

[50j] E. Breitmaier, G. Haas, and W. Voelter: Atlas of Carbon-13 NMR Data. Vol. 1. Heyden & Son Ltd., London, New York 1975.

[50k] V. Formacek, L. Desnoyer, H. P. Kellerhals, and J. T. Clerc: ^{13}C Data Bank. Vol. 1. Copyright Bruker-Physik, Karlsruhe 1976.

[50l] L. F. Johnson and W. C. Jankowski: Carbon-13 NMR Spectra (Collection), John Wiley and Sons, New York (1972).

[51] D. Ziessow and M. Carrol: Ber. Bunsenges. Phys. Chem. *76*, 61 (1972).

[52] M. Karplus and J. A. Pople: J. Chem. Phys. *38*, 2803 (1963).

[53] H. Spiesecke and W. G. Schneider: Tetrahedron Lett. 468 (1961).

[54a] G. E. Maciel and D. A. Beatty: J. Phys. Chem. *69*, 3920 (1965).

[54b] F. W. Wehrli, J. W. de Haan, A. I. Keulemans, D. Exner, and W. Simon: Helv. Chim. Acta *52*, 103 (1969).

[55] R. B. Bates, S. Brenner, C. M. Cole, E. W. Davidson, G. D. Forsythe, D. A. Mc Combs, and A. S. Roth. J. Amer. Chem. Soc. *95*, 926 (1973).

[56] G. A. Olah and A. M. White: J. Amer. Chem. Soc. *91*, 5801 (1969); see also G. A. Olah: Angew. Chem. *85*, 183 (1973); Internat. Edit. *12*, 173 (1973).

[57a] C. G. Kreiter and V. Formáček: Angew. Chem. *84*, 155 (1972); Internat. Ed. *11*, 141 (1972).

[57b] H. L. Retcotsky, E. N. Frankel, and H. S. Gutowsky: J. Amer. Chem. Soc. *88*, 271 (1966).

[58] J. Firl, W. Runge, and W. Hartmann: Angew. Chem. *86*, 274 (1974); Internat. Ed. *13*, 270 (1974).

[59] D. M. Grant and V. B. Cheney: J. Amer. Chem. Soc. *89*, 5315 (1967).

[60] R. H. Levin and J. D. Roberts: Tetrahedron Lett. 135 (1973).

[61a] J. G. Batchelor, J. H. Prestgard, R. J. Cushley, and S. R. Lipsky: J. Amer. Chem. Soc. *95*, 6358 (1973).

[61b] J. G. Batchelor, J. Feeney, and G. C. K. Roberts: J. Magn. Res. *20*, 19 (1975).

[61c] J. G. Batchelor, J. Amer. Chem. Soc. *97*, 3410 (1975).

[61d] L. Flohé, E. Breitmaier, W. A. Günzler, W. Voelter, and G. Jung: Hoppe-Seyler's Z. Physiol Chem. *353*, 1159 (1972).

[62] E. G. Paul and D. M. Grant: J. Amer. Chem. Soc. *85*, 1701 (1963); D. M. Grant and E. G. Paul: J. Amer. Chem. Soc. *86*, 2984 (1964).

[63] W. M. Litchman and D. M. Grant: J. Amer. Chem. Soc. *90*, 1400 (1968).

[64] D. K. Dalling and D. M. Grant: J. Amer. Chem. Soc. *89*, 6612 (1967).

[65] A. S. Perlin, B. Casu, and H. J. Koch: Canad. J. Chem. *48*, 2599 (1970).

[66] D. E. Dorman and J. D. Roberts: J. Amer. Chem. Soc. *92*, 1355 (1970).

[67] R. A. Friedel and H. L. Retcotsky: J. Amer. Chem. Soc. *85*, 1300 (1963).

[68a] H. Spiesecke and W. G. Schneider: J. Chem. Phys. *35*, 722 (1961).

[68b] J. K. Becconsall and P. Hampson: J. Mol. Phys. *10*, 21 (1965).

[69] R. L. Lichter and J. D. Roberts: J. Chem. Phys. *74*, 912 (1970).

[70] G. L. Nelson, G. C. Levy, and J. D. Cargioli: J. Amer. Chem. Soc. *94*, 3089 (1972).

[71] E. Breitmaier and K. H. Spohn: Tetrahedron [London] *29*, 1145 (1973).

[72] G. Del Re, B. Pullman, and T. Yonezawa: Biochem. Biophys. Acta *75*, 153 (1963).

[73] W. J. Horsley and H. Sternlicht: J. Amer. Chem. Soc. *90*, 3738 (1968).

[74] W. J. Horsley, H. Sternlicht, and J. S. Cohen: J. Amer. Chem. Soc. *92*, 680 (1970).

[75] G. Jung, E. Breitmaier, and W. Voelter: Eur. J. Biochem. *24*, 438 (1972).

[76] R. J. Pugmire and D. M. Grant: J. Amer. Chem. Soc. *90*, 697 (1968).

[77] R. J. Pugmire and D. M. Grant: J. Amer. Chem. Soc. *90*, 4232 (1968).

[78] J. S. Cohen, R. I. Shrager, M. McNeel, and A. N. Schechter: Nature *228*, 642 (1970).

[79] E. G. Finer: Macromolecules and Solids, in: R. K. Harris, Ed., Nuclear Magnetic Resonance, Vol. 1. The Chemical Society, London 1972, p. 281.

[80] R. v. Ammon and R. D. Fischer: Angew. Chem. *84*, 737 (1972); Internat. Edit. *11*, 675 (1972) and 168 references cited therin.

[81] B. Birdsall, J. Feeney, J. A. Glasel, R. J. P. Williams, and A. V. Xavier: Chem. Commun. [London] *1971*, 1473.

[82] O. A. Gansow, M. R. Willcott, and R. E. Lenkinski: J. Amer. Chem. Soc. *93*, 4295 (1971).

[83] K. Beyer: Thesis, Tübingen 1973.

[84] F. A. L. Anet and R. Anet: Configuration and Conformation by NMR, in: F. C. Nachod and J. J. Zuckerman, Ed., Determination of Organic Structures by Physical Methods, Vol. 3. Academic Press, New York, London 1971, Chapter 7 and other references cited therin.

[85] H. Kessler: Angew. Chem. *82*, 237 (1970); Internat. Edit. *9*, 219 (1970) and other references cited therin.

[86] O. A. Gansow, J. Killough, and A. R. Burke: J. Amer. Chem. Soc. *93*, 4297 (1971).

[87] F. A. L. Anet and J. J. Wagner: J. Amer. Chem. Soc. *93*, 5266 (1971).

[88] F. A. L. Anet, C. H. Bradley, and G. W. Buchanan: J. Amer. Chem. Soc. *93*, 258 (1971).

[89] H. J. Schneider, R. Price, and T. Keller: Angew. Chem. *83*, 759 (1971); Internat. Edit. *10*, 730 (1971).

[90] L. F. Johnson: private communication cited in ref. [84].

[91] O. A. Gansow, A. R. Burke, and W. D. Vernon: J. Amer. Chem. Soc. *94*, 2552 (1972).

[92] G. E. Maciel, J. W. McIver, Jr., N. S. Ostlund, and J. A. Pople: J. Amer. Chem. Soc. *92*, 1 and 11 (1970) and other references cited therin.

[93] D. M. Grant and W. M. Litchman: J. Amer. Chem. Soc. *87*, 3994 (1965).

[94] N. Cyr and T. J. Cyr: J. Chem. Phys. *47*, 3082 (1967).

[95] E. R. Malinowski: J. Amer. Chem. Soc. *83*, 4479 (1961).

[96] A. W. Douglass: J. Chem. Phys. *40*, 2413 (1964).

[97] G. S. Handler and J. H. Anderson: Tetrahedron [London] *2*, 345 (1958); J. J. Burke and P. C. Lauterbur: J. Amer. Chem. Soc. *86*, 1870 (1964).

[98] G. L. Gloss: Proc. Chem. Soc. [London] *1962*, 152.

[99] E. Lippert and H. Prigge: Ber. Bunsenges. Phys. Chem. *67*, 415 (1963).

[100] T. Yonezawa and I. Morishima: J. Mol. Spectrosc. *27*, 210 (1968); V. M. S. Gil and A. C. P. Alves: J. Mol. Phys. *16*, 527 (1969).

[101] C. H. Yoder, R. H. Tuck, and R. E. Hess: J. Amer. Chem. Soc. *91*, 539 (1969).

[102] E. Breitmaier: unpublished results (1972–1977).

[103] E. F. Mooney and P. H. Winson, in: E. F. Mooney, Ed., Annual Review of NMR Spectroscopy, Vol. 2. Academic Press, New York, London 1969, p. 153.

[104] G. A. Olah and A. M. White: J. Amer. Chem. Soc. *89*, 7072 (1967).

[105] F. J. Weigert and J. D. Roberts: J. Amer. Chem. Soc. *90*, 3543 (1968); *91*, 4940 (1969).

[106] G. M. Whitesides and G. Maglio: J. Amer. Chem. Soc. *91*, 4980 (1969).

[107a] E. Breitmaier: Chimia *28*, 120 (1974).

[107b] E. Breitmaier and U. Hollstein: Org. Magn. Res. *8*, 573 (1976).

[107c] D. J. Wilbur, C. Williams, and A. Allerhand: J. Amer. Chem. Soc. *99*, 5450 (1977).

[108] A. S. Perlin and B. Casu: Tetrahedron Letters [London] *1969*, 2921.

[109] (a) F. J. Weigert and J. D. Roberts: J. Amer. Chem. Soc. *94*, 6021 (1972).
(b) A. M. Ihrig and J. L. Marshall: J. Amer. Chem. Soc. *94*, 1756 (1972).

[110] P. R. Wells: NMR Spectra of the Heavier Elements, in: F. C. Nachod and J. J. Zuckerman, Ed., Determination of Organic Structures by Physical Methods, Vol. 4. Academic Press, New York, London 1971, Chapter 5 and other references cited therin.

[111] G. Binsch, J. B. Lambert, B. W. Roberts, and J. D. Roberts: J. Amer. Chem. Soc. *86*, 5564 (1964).

[112] E. Bullock, D. G. Tuck, and E. Woodhouse: J. Chem. Phys. *38*, 2318 (1963).

[113] R. L. Lichter: ^{15}N Nuclear Magnetic Resonance, in: F. C. Nachod and J. J. Zuckerman, Ed., Determination of Organic Structures by Physical Methods, Vol. 4. Academic Press, New York, London 1971, Chapter 4 and other references cited therin.

[114] W. M. McFarlane: Mol. Phys. *10*, 603 (1966).

[115] D. M. Jerina, D. R. Boyd, L. Paolillo, and E. D. Becker: Tetrahedron Letters [London] *1970*, 1484.

[116] F. R. Jerome and K. L. Servis: J. Amer. Chem. Soc. *94*, 5896 (1972).

[117] G. A. Gray: J. Amer. Chem. Soc. *93*, 2132 (1971).

[118] G. A. Gray and S. E. Cremer: Chem. Commun. Chem. Soc. [London] *7*, 367 (1972); Tetrahedron Letters [London] *1971*, 3061.

[119] P. D. Lapper, H. H. Mantsch, and J. C. P. Smith: J. Amer. Chem. Soc. *94*, 6243 (1972).

[120] E. Breitmaier and W. Voelter: Eur. J. Biochem. *31*, 234 (1972).

[121] G. C. Levy: Accounts Chem. Res. *6*, 161 (1973).

[122] J. R. Lyerla, Jr. and D. M. Grant: Int. Rev. Sci. Phys. Chem. Ser. *1*, 4, 155 (1972).

[123] T. D. Alger and D. M. Grant: J. Phys. Chem. *75*, 2538 (1971).

[124] G. C. Levy, J. D. Cargioli, and F. A. L. Anet: J. Amer. Chem. Soc. *95*, 1527 (1973).

[125] G. C. Levy: J. C. S. Chem. Comm. *1972*, 47.

[126] Determination of $T_{1(DD)}$ and $T_{1(SR)}$ of the C atoms of camphor: J. Grandjean, P. Laszlo, and R. Price: Mol. Phys. *25*, 695 (1973).

[127] R. Freeman, K. G. R. Pachler, and G. N. La Mar: J. Chem. Phys. *55*, 4586 (1971).

[128] C. F. Brewer, H. Sternlicht, D. M. Marcus, and A. P. Grollmann, Biochemistry *12*, 4448 (1973).

[129] D. Doddrell, V. Gluschko, and A. Allerhand: J. Chem. Phys. *56*, 3683 (1972).

[130] W. T. Huntress, Jr.: J. Chem. Phys. *48*, 3524 (1968).

[131] D. E. Woessner: J. Chem. Phys. *42*, 1855 (1965); *36*, 1 (1962).

[132] K. F. Kuhlmann, D. M. Grant, and R. K. Harris: J. Chem. Phys. *52*, 3439 (1970).

[133] S. Berger, F. R. Kreissl, and J. D. Roberts: J. Amer. Chem. Soc. *96*, 4348 (1974).

[134] D. E. Woessner, J. Chem. Phys. *37*, 647 (1962).

[135] K. H. Spohn: Dissertation, Universität Tübingen 1974.

[136] D. M. Grant, R. J. Pugmire, E. P. Black, and K. A. Christensen, J. Amer. Chem. Soc. *95*, 8465 (1973).

[137] S. Berger, F. R. Kreissl, D. M. Grant, and J. D. Roberts: J. Amer. Chem. Soc. *97*, 1805 (1975).

[138] R. S. Becker, S. Berger, D. K. Dalling, D. M. Grant, and R. J. Pugmire: J. Amer. Chem. Soc. *96*, 7008 (1974).

[139] A. Allerhand, D. Doddrell, and R. Komoroski: J. Chem. Phys. *55*, 189 (1971).

[140] G. C. Levy and G. L. Nelson: J. Amer. Chem. Soc. *94*, 4897 (1972).

[141] G. A. Gray and S. E. Cremer: J. Magn. Resonance *12*, 5 (1973).

[142] M. Imanari, M. Ohuchi, and K. Ishizu, J. Magn. Resonance *14*, 374 (1974).

[143] N. J. M. Birdsall, A. G. Lee, Y. K. Levine, J. C. Metcalfe, P. Partington, and G. C. K. Roberts: J. C. S. Chem. Comm. *1973*, 757.

[144] C. Chachaty, Z. Wolkowski, F. Piriou, and G. Lukacs: J. C. S. Chem. Comm. *1973*, 951.

[145] J. C. Metcalfe, N. J. M. Birdsall, J. Feeney, A. G. Lee, Y. K. Levine, and P. Partington, Nature *233*, 199 (1971).

[146] Y. K. Levine, N. J. M. Birdsall, A. G. Lee, and J. C. Metcalfe: Biochemistry *11*, 1416 (1972).

[147] A. G. Lee, N. J. M. Birdsall, and J. C. Metcalfe: Chem. Brit. *9*, 116 (1973).

[148] A. Allerhand and R. A. Komoroski, J. Amer. Chem. Soc. *95*, 8228 (1973).

[149] A. Allerhand, D. Doddrell, V. Gluschko, D. W. Cochran, E. Wenkert, P. J. Lawson, and F. R. N. Gurd: J. Amer. Chem. Soc. *93*, 544 (1971).

[150] L. Paolillo, T. Tancredi, P. A. Temussi, E. Trivellone, E. M. Bradbury, and C. Crane-Robinson J. C. S. Chem. Comm. *1972*, 335.

[151] S. Tadorko, S. Fujiwara, and Y. Ichihara: Chem. Lett. *1973*, 849.

[152] A. Allerhand and E. Oldfield: Biochemistry *12*, 3428 (1973).

[153] J. Schaefer and D. F. S. Natusch: Macromolecules *5*, 416 (1972).

[154] J. Schaefer, Macromolecules *5*, 427 (1972).

[155] T. D. Alger, D. M. Grant, and J. R. Lyerla: J. Phys. Chem. *75*, 2539 (1971).

[156] D. Doddrell and A. Allerhand: J. Amer. Chem. Soc. *93*, 1558 (1971).

[157] T. C. Farrar, S. J. Druck, R. R. Shoup, and E. D. Becker: J. Amer. Chem. Soc. *94*, 699 (1972).

[158] R. A. Goodman, E. Oldfield, and A. Allerhand: J. Amer. Chem. Soc. *95*, 7553 (1973).

[159] H. Saito, H. H. Mantsch, and J. C. P. Smith: J. Amer. Chem. Soc. *95*, 8453 (1973).

[160] I. M. Armitage, H. Huber, H. Pearson, and J. D. Roberts: Proc. Nat. Acad. Sci. USA *71*, 2096 (1974).

[161] D. D. Gianini, I. M. Armitage, H. Pearson, D. M. Grant, and J. D. Roberts: J. Amer. Chem. Soc. *97*, 3416 (1975).

[162] J. R. Lyerla, Jr., D. M. Grant, and R. B. Bertrand: J. Phys. Chem. *75*, 3967 (1971).

[163] K. T. Gillen, M. Schwartz, and J. H. Noggle: Mol. Phys. *20*, 899 (1971).

[164] H. W. Spiess, D. Schweitzer, U. Haeberlein, and K. H. Hausser: J. Magn. Resonance *5*, 101 (1971).

[165] A. Olivson and E. Lippmaa: Chem. Phys. Lett. *11*, 241 (1971).

[166] T. C. Farrar, S. J. Druck, R. R. Shoup, and E. D. Becker: J. Amer. Chem. Soc. *94*, 699 (1972).

[167] H. W. Spiess, D. Schweitzer, and U. Haeberlein, J. Magn. Resonance *9*, 444 (1973).

[168] L. J. Burnett and S. B. Roeder: J. Chem. Phys. *60*, 2420 (1974).

[169] E. Goldammer, H. D. Luedemann, and A. Mueller: J. Chem. Phys. *60*, 4590 (1974).

[170] T. K. Leipert, J. H. Noggle, and K. T. Gillen, J. Magn. Resonance *13*, 158 (1974).

[171] E. Goldammer, H. D. Luedemann, and O. Roeder: Chem. Phys. Lett. *26*, 387 (1974).

[172] S. Berger, F. R. Kreissl, D. M. Grant, and J. D. Roberts: to be published.

[173] I. M. Armitage, H. Huber, D. H. Live, H. Pearson, and J. D. Roberts: J. Magn. Resonance *15*, 142 (1974).

[174] Y. K. Levine, N. J. M. Birdsall, A. G. Lee, J. C. Metcalfe, P. Partington, and G. C. K. Roberts: J. Chem. Phys. *60*, 2890 (1974).

[175] M. C. Fedarko: J. Magn. Resonance *12*, 1985 (1973).

[176] R. T. Roberts and C. Chachaty, Chem. Phys. Lett. *22*, 348 (1973).

[177] D. G. Gianini, I. M. Armitage, H. Pearson, and J. D. Roberts: Proc. Nat. Acad. Sci. USA *71*, 4221 (1974).

[178] R. Deslauriers, I. P. C. Smith, and R. Walter: J. Amer. Chem. Soc. *96*, 2289 (1974).

[179] R. Deslauriers, C. Garrigou-Lagrange, A. Bellocq, and I. P. C. Smith: FEBS Lett. *31*, 59 (1973).

[180] R. B. Moon and J. H. Richards: Proc. Nat. Akad. Sci. USA *69*, 2983 (1972).

[181] B. V. Cheney and D. M. Grant: J. Amer. Chem. Soc. *89*, 5319 (1967).

[182] J. Mason: J. Chem. Soc. *A*, *1971*, 1038.

[183] J. J. Burke and P. C. Lauterbur: J. Amer. Chem. Soc. *86*, 1870 (1964).

[184] M. Christl, H. J. Reich, and J. D. Roberts: J. Amer. Chem. Soc. *93*, 3463 (1971).

[185] A. S. Perlin and H. J. Koch: Canad. J. Chem. *48*, 2639 (1970).

[186] J. B. Grutzner, M. Jautelat, J. B. Dence, R. A. Smith, and J. D. Roberts: J. Amer. Chem. Soc. *92*, 7107 (1970).

[187] B. F. Spielvogel and J. M. Purser: J. Amer. Chem. Soc. *89*, 5294 (1967).

[188] D. K. Dalling, D. M. Grant, and L. F. Johnson: J. Amer. Chem. Soc. *93*, 3678 (1971).

[189] G. B. Savitsky, P. D. Ellis, K. Namikawa, and G. E. Maciel: J. Chem. Phys. *49*, 2395 (1968).

[190] D. E. Dorman, M. Jautelat, and J. D. Roberts: J. Org. Chem. *36*, 2757 (1971).

[191] G. B. Savitsky and K. Namikawa: J. Phys. Chem. *68*, 1956 (1964).

[192] D. D. Traficante and G. E. Maciel: J. Phys. Chem. *69*, 1348 (1965).

[193] D. M. Graham and C. E. Holloway: Canad. J. Chem. *41*, 2114 (1963).

[194] R. M. Lynden-Bell and N. Sheppard: Proc. Roy. Soc., *Ser. A 269*, 385 (1962).

[195] S. Rang, T. Pehk, E. Lippma, and O. Eisen: Eesti NSV Tead. Akad. Toim. Keem. Geol. *16*, 346 (1967) and *17*, 294 (1968), and N. Müller and D. E. Pritchard: J. Chem. Phys. *31*, 768 and 1471 (1959).

[196] J. K. Crandall and S. A. Sojka: J. Amer. Chem. Soc. *94*, 5084 (1972).

[197] P. C. Lauterbur: Ann. New York Acad. Sci. *70*, 841 (1958).

[198] P. C. Lauterbur, in: F. C. Nachod and W. D. Phillips, Ed.: Determination of Organic Structures by Physical Methods, Vol. 2, Chapter 7. Academic Press, New York, London 1962.

[199] E. Pitcher, A. D. Buckingham, and F. G. A. Stone: J. Chem. Phys. *36*, 124 (1962).

[200] G. Miyajima and K. Takahashi: J. Phys. Chem. *75*, 331 (1971).

[201] C. J. Carman, A. R. Tarpley, and J. H. Goldstein: J. Amer. Chem. Soc. *93*, 2864 (1971).

[202] A. Marker, D. Doddrell, and N. V. Riggs: Chem. Commun. *1972*, 724.

[203] A. D. Buckingham: Canad. J. Chem. *38*, 300 (1960).

[204] L. Onsager: J. Amer. Chem. Soc. *58*, 1486 (1936).

[205] G. B. Savitsky and K. Namikawa: J. Phys. Chem. *67*, 2754 (1963).

[206] G. E. Maciel and H. C. Dorn: J. Amer. Chem. Soc. *93*, 1268 (1971).

[207] D. T. Carr: Thesis, Purdue University, 1962.

[208] N. Muller and P. I. Rose: J. Amer. Chem. Soc. *84*, 3973 (1962).

[209] K. M. Crecely, R. W. Crecely, and J. H. Goldstein: J. Mol. Spectrosc. *37*, 252 (1971).

[210] G. E. Maciel: J. Phys. Chem. *69*, 1947 (1965).

[211] J. D. Roberts, F. J. Weigert, J. I. Kroschwitz, and H. J. Reich: J. Amer. Chem. Soc. *92*, 1338 (1970).

[212] L. M. Jackman and D. P. Kelly: J. Chem. Soc. *B 1970*, 102.

[213] G. W. Buchanan, D. A. Ross, and J. B. Stothers: J. Amer. Chem. Soc. *88*, 4301 (1966).

[214] G. M. Kellie and F. G. Riddell: J. Chem. Soc. *B 1971*, 1030.

[215] A. J. Jones, E. L. Eliel, D. M. Grant, M. C. Knoeber, and W. F. Bailey: J. Amer. Chem. Soc. *93*, 4772 (1971).

[216] J. B. Stothers and P. C. Lauterbur: Canad. J. Chem. *42*, 1563 (1964).

[217] F. J. Weigert and J. D. Roberts: J. Amer. Chem. Soc. *92*, 1347 (1970).

[218] G. B. Savitsky, K. Namikawa, and G. Zweifel: J. Phys. Chem. *69*, 3105 (1965).

[219] J. B. Stothers, I. S. Y. Wang, D. Ouchi, and E. Warnhoff: J. Amer. Chem. Soc. *93*, 6702 (1971).

[220] D. H. Marr and J. B. Stothers: Canad. J. Chem. *45*, 225 (1967).

[221] D. H. Marr and J. B. Stothers: Canad. J. Chem. *43*, 596 (1965).

[222] Gurudata and J. B. Stothers: Canad. J. Chem. *47*, 3601 (1969).

[223] K. S. Dhami and J. B. Stothers: Canad. J. Chem. *43*, 479 (1965).

[224] K. S. Dhami and J. B. Stothers: Canad. J. Chem. *43*, 498 (1965).

[225] E. Breitmaier, G. Jung, and W. Voelter: Angew. Chem. *83*, 659 (1971); Angew. Chem. Internat. Edit. *10*, 673 (1971).

[226] S. Berger and A. Rieker: Tetrahedron *28*, 3123 (1972).

[227] R. Hagen and J. D. Roberts: J. Amer. Chem. Soc. *91*, 4504 (1969).

[228] E. Lippmaa, T. Pehk, K. Andersson, and C. Rappe: Org. Magn. Resonance *2*, 109 (1970).

[229] H. Eggert and C. Djerassi: J. Amer. Chem. Soc. *95*, 3710 (1973).

[230] K. S. Dhami and J. B. Stothers: Canad. J. Chem. *45*, 233 (1967).

[231] I. Morishima, A. Mizuno, and T. Yonezawa: Chem. Commun. *1970*, 1321.

[232] P. S. Pregosin and E. Randall: Chem. Commun. *1971*, 399.

[233] G. Barbarella, P. Dembech, A. Garbesi, and A. Fava: Org. Magn. Res. *8*, 108 (1976).

[234] P. C. Lauterbur: J. Amer. Chem. Soc. *83*, 1846 (1961).

[235] H. Spiesecke and W. G. Schneider: J. Chem. Phys. *35*, 731 (1961).

[236] P. C. Lauterbur: J. Chem. Phys. *38*, 1406 (1963).

[237a] C. V. Senoff and J. E. H. Ward: Inorg. Chem. *14*, 278 (1975).

[237b] G. W. Buchanan, C. R. Zamora, and D. E. Clarke: Can. J. Chem. *52*, 3895 (1974).

[238] D. Lauer, E. L. Motell, D. D. Traficante, and G. E. Maciel: J. Amer. Chem. Soc. *94*, 5335 (1972).

[239] A. R. Tarpley and J. H. Goldstein: J. Amer. Chem. Soc. *76*, 515 (1972).

[240] H. Spiesecke and W. G. Schneider: Tetrahedron Lett. *1961*, 468.

[241] T. D. Alger, D. M. Grant, and E. G. Paul: J. Amer. Chem. Soc. *88*, 5397 (1966).

[242] W. Adam, A. Grimison, and G. Rodriguez: Tetrahedron *23*, 2513 (1967).

[243] A. J. Jones, T. D. Alger, D. M. Grant, and W. M. Litchman: J. Amer. Chem. Soc. *92*, 2386 (1970).

[244] A. J. Jones, P. D. Gardner, D. M. Grant, W. M. Litchman, and V. Boekelheide: J. Amer. Chem. Soc. *92*, 2395 (1970).

[245] F. J. Weigert and J. D. Roberts: J. Amer. Chem. Soc. *93*, 2361 (1971).

[246] A. J. Jones, D. M. Grant, and K. F. Kuhlmann: J. Amer. Chem. Soc. *91*, 5013 (1969).

[247] W. D. Crow and M. N. Paddon-Row: J. Amer. Chem. Soc. *94*, 4746 (1972).

[248] H. A. Staab, H. Brettschneider, and H. Brunner: Chem. Ber. *103*, 1101 (1970).

[249] H. A. Staab, K. Sudarsana Rao, and H. Brunner: Chem. Ber. *104*, 2634 (1971).

[250] H. A. Staab and M. Haenel: Chem. Ber. *103*, 1095 (1970).

[251] A. T. Balaban and D. Fărcaşiu: J. Amer. Chem. Soc. *89*, 1958 (1967).

[252] H. Günther, B. D. Tunggal, M. Regitz, H. Scherer, and T. Keller: Angew. Chem. *83*, 585 (1971); Angew. Chem. Internat. Edit. *10*, 563 (1971).

[253] J. Prestien and H. Günther: Angew. Chem. *86*, 278 (1974); Angew. Chem. Internat. Edit. *13*, 276 (1974).

[254] H. Günther, G. Jikeli, H. Schmickler, and J. Prestien: Angew. Chem. *85*, 826 (1973); Angew. Chem. Internat. Edit. *12*, 762 (1973).

[255] T. Tokuhiro and G. Fraenkel: J. Amer. Chem. Soc. *91*, 5005 (1969).

[256] P. D. Ellis, R. B. Dunlap, A. L. Pollard, K. Seidman, and A. D. Cardin: J. Amer. Chem. Soc. *95*, 4398 (1973).

[257] K. Takahashi, T. Sone, and K. Fujieda: J. phys. Chem. *74*, 2765 (1970).

[258] R. Garnier, R. Faure, A. Babadjamian, and E.-J. Vincent: Bull. Soc. Chim. Fr. *3*, 1040 (1972).

[259] I. Morishima, K. Okada, and T. Yonezawa: J. Amer. Chem. Soc. *94*, 1425 (1972).

[260] R. J. Pugmire, D. M. Grant, M. J. Robins, and R. K. Robins: J. Amer. Chem. Soc. *91*, 6381 (1969).

[261] R. J. Pugmire, M. J. Robins, D. M. Grant, and R. K. Robins: J. Amer. Chem. Soc. *93*, 1887 (1971).

[262] R. G. Parker and J. D. Roberts: J. Org. Chem. *35*, 996 (1970).

[263] I. Morishima, K. Okada, T. Yonezawa, and K. Goto: J. Amer. Chem. Soc. *93*, 3922 (1971).

[264] D. Wendisch: Coll. Spectroscopicum Intern. XVI, Vol. *1*, 75 (1971).

[265] G. Ellis and R. G. Jones: J. Chem. Soc., Perkin Transactions II *1972*, 437.

[266] T. F. Page, T. Alger, and D. M. Grant: J. Amer. Chem. Soc. *87*, 5333 (1965).

[267] A. J. Ashe, R. R. Sharp, and J. W. Tolan: J. Amer. Chem. Soc. *98*, 5451 (1976).

[268a] G. A. Olah and A. M. White: J. Amer. Chem. Soc. *90*, 1884 (1968).

[268b] R. Ditchfield and D. P. Miller: J. Amer. Chem. Soc. *93*, 5287 (1971).

[269] G. A. Olah, Y. K. Mo, and Y. Halpern: J. Amer. Chem. Soc. *94*, 3551 (1972).

[270] G. A. Olah and A. M. White: J. Amer. Chem. Soc. *91*, 3954 (1969).

[271] G. A. Olah, Y. Halpern, Y. K. Mo, and G. Liang: J. Amer. Chem. Soc. *94*, 3554 (1972).

[272] G. A. Olah, R. H. Schlosberg, R. D. Porter, Y. K. Mo, D. P. Kelly, and G. D. Mateescu: J. Amer. Chem. Soc. *94*, 2034 (1972).

[273] G. A. Olah, R. D. Porter, C. L. Jeuell, and A. M. White: J. Amer. Chem. Soc. *94*, 2044 (1972).

[274] L. M. Stock and H. C. Brown: Advan. Phys. Org. Chem. *1*, 35 (1963).

[275] T. Pehk and E. Lippma: Org. Magn. Res. *3*, 679 (1971).

[276] D. K. Dalling and D. M. Grant: J. Amer. Chem. Soc. *94*, 5318 (1972).

[277] H. J. Schneider and V. Hoppen: Tetrahedron Letters *1974*, 579.

[278] O. A. Subbotin and N. M. Sergejev: J. Amer. Chem. Soc. *97*, 1080 (1975).

[279] J. B. Stothers, C. T. Tan, and K. C. Teo: Canad. J. Chem. *54*, 1211 (1976).

[280] E. Wenkert, A. O. Clouse, D. W. Cochran, and D. Doddrell: Chem. Commun. *1969*, 1433.

[281a] M. Jautelat, J. B. Grutzner, and J. D. Roberts: Proc. Nat. Acad. Sci. *65*, 288 (1970).

[281b] G. Englert, Helv. Chim. Acta *58*, 2367 (1975).

[282] E. Wenkert and B. L. Buckwalter: J. Amer. Chem. Soc. *94*, 4367 (1972).

[283] H. J. Reich, M. Jautelat, M. T. Messe, F. J. Weigert, and J. D. Roberts: J. Amer. Chem. Soc. *91*, 7445 (1969).

[284] Q. Khuong-Huu, G. Lukacs, A. Pancrazi, and G. Goutarel: Tetrahedron Lett. *1972*, 3579.

[285] G. Lukacs, X. Lusinchi, E. W. Hagaman, B. L. Buckwalter, F. M. Schell, and E. Wenkert: C. R. Acad. Sci., *Ser. C 274*, 1458 (1972).

[286] G. Lukacs, F. Khuong-Huu, C. R. Bennett, B. L. Buckwalter, and E. Wenkert: Tetrahedron Lett. *1972*, 3515.

[287] G. Lukacs and C. R. Bennett: Bull. Soc. Chim. France *1972*, 3996.

[288] B. Balogh, D. M. Wilson, and A. L. Burlingame: Nature *233*, 261 (1971).

[289] P. W. Sprague, D. Doddrell, and J. D. Roberts: Tetrahedron *27*, 4857 (1971).

[290] G. Lukacs, A. Picot, X. Lusinchi, H. J. Koch, and A. S. Perlin: C. R. Acad. Sci., *Ser. C 272*, 2171 (1971).

[291] W. O. Crain, W. C. Wildman, and J. D. Roberts: J. Amer. Chem. Soc. *93*, 990 (1971).

[292] E. Wenkert, C.-J. Chang, A. O. Clouse, and D. W. Cochran: Chem. Commun. *1970*, 961.

[293] A. Rabaron, M. Koch, M. Plat, J. Peyroux, E. Wenkert, and D. W. Cochran: J. Amer. Chem. Soc. *93*, 6270 (1971).

[294] E. Wenkert, D. W. Cochran, E. W. Hagaman, R. B. Lewis, and F. M. Schell: J. Amer. Chem. Soc. *93*, 6271 (1971).

[295] D. W. Hughes, H. L. Holland, and D. B. Mac Lean: Cand. J. Chem. *54*, 2252 (1976).

[296] N. J. Bach, H. E. Boaz, E. C. Cornfeld, C. J. Chang, H. G. Floss, E. W. Hagaman, and E. Wenkert: J. Org. Chem. *39*, 1272 (1974).

[297a] E. Breitmaier and W. Voelter: Tetrahedron *29*, 227 (1973).

[297b] E. Breitmaier, G. Jung, and W. Voelter: Chimia *26*, 136 (1972).

[297c] W. Voelter, E. Breitmaier, G. Jung, T. Keller, and D. Hiss: Angew. Chem. *82*, 812 (1970); Angew. Chem. Internat. Edit. *9*, 803 (1970).

[298] D. E. Dorman, S. J. Angyal, and J. D. Roberts: J. Amer. Chem. Soc. *92*, 1351 (1970).

[299] E. Breitmaier, W. Voelter, G. Jung, and C. Tänzer: Chem. Ber. *104*, 1147 (1971).

[300] D. E. Dorman and J. D. Roberts: J. Amer. Chem. Soc. *93*, 4463 (1971).

[301] R. G. S. Ritchie, N. Cyr, B. Korsch, H. J. Koch, and A. S. Perlin: Canad. J. Chem. *53*, 1424 1975).

[302] W. Voelter, V. Bilík, and E. Breitmaier: Collect. Czech. Chem. Commun. *38*, 2054 (1973).

[303] W. Voelter and E. Breitmaier: Org. Magn. Resonance *5*, 311 (1973).

[304] W. Voelter, E. Breitmaier, R. Price, and G. Jung: Chimia *25*, 168 (1971).

[305] W. Voelter, E. Breitmaier, and G. Jung: Angew. Chem. *83*, 1011 (1971); Angew. Chem. Internat. Edit. *10*, 935 (1971).

[306] W. Voelter, C. Bürvenich, and E. Breitmaier: Angew. Chem. *84*, 589 (1972); Angew. Chem. Internat. Edit. *11*, 539 (1972).

[307] E. Conway, R. D. Guthrie, S. D. Gero, G. Lukacs, A. M. Sepulchre, E. W. Hagaman, and E. Wenkert: Tetrahedron Lett. *1972*, 4879.

[308] G. Lukacs, A. M. Sepulchre, A. Gateau-Olesker, G. Vass, S. D. Gero, R. D. Guthrie, W. Voelter, and E. Breitmaier: Tetrahedron Lett. *1972*, 5163.

[309] E. Breitmaier, W. Voelter, E. B. Rathbone, and E. M. Stephen: Tetrahedron *29*, 3845 (1973).

[310] A. M. Sepulchre, G. Lukacs, G. Vass, and S. D. Gero: Angew. Chem. *84*, 111 (1972); Angew. Chem. Internat. Edit. *11*, 148 (1972).

[311] W. Voelter, G. Jung, E. Breitmaier, and R. Price: Hoppe-Seyler's Z. Physiol. Chem. *352*, 1034 (1971).

[312] A. J. Jones, D. M. Grant, M. W. Winkley, and R. K. Robins: J. Amer. Chem. Soc. *92*, 4079 (1970).

[313] D. E. Dorman and J. D. Roberts: Proc. Nat. Acad. Sci. *65*, 19 (1970).

[314] R. J. Pugmire, D. M. Grant, R. K. Robins, and G. W. Rhodes: J. Amer. Chem. Soc. *87*, 2225 (1965).

[315] A. J. Jones, M. W. Winkley, and D. M. Grant: Tetrahedron Lett. *1969*, 5197.

[316] T. A. Hoffmann and J. Ladik: Advan. Chem. Phys. *7*, 94 (1969).

[317] A. Veillard and B. Pullman: J. Theor. Biol. *4*, 37 (1963).

[318] J. I. Fernández-Alonso: Advan. Chem. Phys. *7*, 1 (1964).

[319] A. R. Tarpley and J. H. Goldstein: J. Amer. Chem. Soc. *93*, 3573 (1971).

[320] B. P. Dailey and J. N. Shoolery: J. Amer. Chem. Soc. *77*, 3977 (1955).

[321] G. Jung, E. Breitmaier, W. Voelter, T. Keller, and C. Tänzer: Angew. Chem. *82*, 882 (1970); Angew. Chem. Internat. Edit. *9*, 894 (1970).

[322a] W. Voelter, G. Jung, E. Breitmaier, and E. Bayer: Z. Naturforsch. *26b*, 213 (1971).

[322b] W. Voelter, S. Fuchs, R. H. Seuffer, and K. Zech: Monatsh. Chem. *105*, 1110 (1974).

[323] D. E. Dorman, and F. A. Bovey: J. Org. Chem. *38*, 2379 (1973).

[324] W. Voelter, K. Zech, W. Grimminger, E. Breitmaier, and G. Jung: Chem. Ber. *105*, 3650 (1972)

[325] R. A. Archer, R. D. G. Cooper, P. V. Demarco, and L. R. F. Johnson: Chem. Commun. *1970*, 1291.

[326] W. A. Gibbons, J. A. Sogn, A. Stern, L. C. Craig, and L. F. Johnson: Nature *227*, 840 (1970).

[327] Abbreviations according to IUPAC, Europ. J. Biochem. *1*, 375 (1967).

[328] G. Jung, E. Breitmaier, and W. Voelter: Hoppe-Seyler's Z. Physiol. Chem. *352*, 16 (1971).

[329] G. Jung, N. Dubischar, and D. Leibfritz: Eur. J. Biochem. *54*, 395 (1975); G. Irmscher, and G. Jung: Eur. J. Biochem. *80*, 165 (1977).

[330] P. C. Lauterbur: Appl. Spectrosc. *24*, 450 (1970).
[331] A. Allerhand, D. W. Cochran, and D. Doddrell: Proc. Nat. Acad. Sci. *67*, 1093 (1970).
[332] W. Voelter and O. Oster: Z. Naturforsch. *28b*, 370 (1973).
[333] O. Oster and W. Voelter in T. Axenrod and G. A. Webb (Edit.): NMR of Elements Other than Hydrogen. Wiley-Interscience, New York, 1974.
[334] A. E. Tonelli: J. Amer. Chem. Soc. *92*, 6187 (1970).
[335] L. Paolillo, T. Tancredi, P. A. Temussi, E. Trivellone, E. M. Bradbury, and C. Crane-Robinson: Chem. Commun. *1972*, 335.
[336] G. Boccalon, A. S. Verdini, and G. Giacometti: J. Amer. Chem. Soc. *94*, 3639 (1972).
[337] V. Glushko, P. J. Lawson, and F. R. N. Gurd: J. Biol. Chem. *247*, 3176 (1962).
[338] H. Sternlicht, G. L. Kenyon, E. L. Packer, and J. Sinclair: J. Amer. Chem. Soc. *93*, 199 (1971).
[339] Abbreviations according to IUPAC, Europ. J. Biochem. *17*, 193 (1970).
[340] D. Doddrell and W. S. Caughey: J. Amer. Chem. Soc. *94*, 2510 (1972).
[341] M. Tanabe, H. Seto, and L. Johnson: J. Amer. Chem. Soc. *92*, 2157 (1970).
[342] M. Tanabe, T. Hamasaki, D. Thomas, and L. Johnson: J. Amer. Chem. Soc. *93*, 273 (1971).
[343] M. Tanabe, T. Hamasaki, and H. Seto: Chem. Commun. *1970*, 1539.
[344] J. Polonsky, Z. Baskevitch, N. Cagnoli-Bellavita, P. Ceccherelli, B. L. Buckwalter, and E. Wenkert: J. Amer. Chem. Soc. *94*, 4369 (1972).
[345] A. L. Burlingame, B. Balogh, J. Welch, S. Lewis, and D. Wilson: Chem. Commun. *1972*, 318.
[346] A. G. McInnes, D. G. Smith, L. C. Vining, and L. Johnson: Chem. Commun. *1971*, 325.
[347] J. W. Westley, D. L. Pruess, and R. G. Pitcher: Chem. Commun. *1972*, 161.
[348] N. Neuss, C. N. Nash, P. A. Lemke, and J. B. Grutzner: J. Amer. Chem. Soc. *93*, 2337 (1971).
[349] R. J. Cushley, D. R. Anderson, S. R. Lipsky, R. J. Sykes, and H. H. Wasserman: J. Amer. Chem. Soc. *93*, 6284 (1971).
[350] D. K. Dalling and D. M. Grant: J. Amer. Chem. Soc. *96*, 1827 (1974).
[351] T. A. Wittstruck and K. I. H. Williams: J. Org. Chem. *38*, 1582 (1973).
[352] D. Leibfritz and J. D. Roberts: J. Amer. Chem. Soc. *95*, 4996 (1973).
[353] G. Lukacs, F. Piriou, S. D. Gero, D. A. v. Dorp, E. W. Hagaman, and E. Wenkert: Tetrahedron Letters 515 (1973).
[354] D. M. Rackham, S. E. Cowdry, N. J. A. Gutteridge, and D. J. Osborne: Org. Magn. Res. *9*, 160 (1977).
[355] H. J. Lohrisch: Thesis, Univ. of Bonn, 1977.
[356] W. V. Turner and W. H. Pirkle: J. Org. Chem. *39*, 1935 (1974).
[357] C. A. Kingsbury, M. Clifton, and J. H. Looker: J. Org. Chem. *41*, 2777 (1976).
[358] L. Weiler: Canad. J. Chem. *50*, 1975 (1972).
[359] N. J. Cussans and T. N. Huckerby: Tetrahedron *31*, 2719 (1975).
[360] M. S. Chauhan and I. W. J. Still: Canad. J. Chem. *53*, 2880 (1975).
[361] P. W. Westerman, S. P. Gunasekera, M. Uvais, S. Sultanbawa, and R. Kazlauskas: Org. Magn Res. *9*, 631 (1977).
[362] C. A. Kingsbury and J. H. Looker: J. Org. Chem. *40*, 1120 (1975).
[363] A. Pelter, R. S. Ward, and T. I. Gray: J. Chem. Soc. (Perkin Trans. I) *23*, 2475 (1976).
[364] E. Wenkert, J. S. Bindra, C. J. Chang, D. W. Cochran, and F. M. Schell: Acc. Chem. Res. *7*, 46 (1974).
[365] R. C. Haruff and W. T. Jenkins: Org. Magn. Res. *8*, 548 (1976).
[366] R. Verpoorte, P. J. Hylands, and N. G. Bisset: Org. Magn. Res. *9*, 567 (1977).
[367] Y. Terui, K. Tori, S. Maeda, and Y. K. Sawa: Tetrahedron Letters 2853 (1975).
[368] R. E. Echols and G. C. Levy: J. Org. Chem. *39*, 1321 (1974).
[369] J. P. Geerts, A. Nagel, and H. C. v. d. Plas: Org. Magn. Res. *8*, 607 (1976).
[370] U. Ewers, H. Günther, and L. Jaenicke: Chem. Ber. *106*, 3951 (1973).
[371] U. Hollstein, E. Breitmaier, and G. Jung: J. Amer. Chem. Soc. *96*, 8036 (1974).
[372] E. Pretsch, M. Vasak, and W. Simon: Helv. Chim. Acta *55*, 1098 (1972).
[373] N. J. M. Birdsall, J. Feeney, Y. K. Levine, and J. C. Metcalfe: J. Chem. Soc. (Perkin Trans. I) 1441 (1972).

Subject Index

Absorption-mode spectra 12
  example 29
Absorption signal 4
Accumulation of spectra 19
Acetates 154
Acetophenones 167f.
Acetylenes 141
Additivity relationships 131ff., 172f., 208ff.
Alcohols 150ff.
Aldehydes 159f., 166
Aldohexoses 249f.
Aldopentoses 252f.
Alkaloids 240ff., 298f.
Alkanes
  ^{13}C shifts 131ff.
  CH couplings 93ff.
  CC couplings 105
Alkenes
  ^{13}C shifts 137ff., 211f.
  CH couplings 97
  CC couplings 105f.
Alkyl halides (haloorganic compounds)
  ^{13}C shifts 142ff., 209
  CH couplings 95f., 148f.
Alkynes
  ^{13}C shifts 141
  CH couplings 98
  CC couplings 105f.
Allenes 141
Alternately pulsed $^{13}C\{^1H\}$ NMR 43
Amines 177f.
Amino acids 276ff.
Androstanes 231f.
Angular momentum 1
Anisotropic rotation, effect on T_1 116
Applied magnetic field H_0 2
Aromatic compounds
  ^{13}C shifts 185f.
  CH couplings 99, 101
  CC couplings 106
Arrhenius equation 88
Axial configuration 75, 91, 210

Benzene derivatives 183ff.
Benzoates (esters) 176
Benzocycloalkenes 195f.
Biopolymers 258, 284, 299
Biosynthetic pathways 289ff.
Bloch equations 7ff.
Boltzmann distribution of spins 4f.
Boron-nitrogen compounds 136
Bulk susceptibilities 15

Carbocations 205ff.
Calibration of NMR spectra 14f.
Carbanions 72
Carbenium ions 72, 205ff.
Carbodiimides 179f.
Carbohydrates 247ff.
Carbon-13 chemical shifts
  correlation with UV absorption 70, 161
  influence of
    carbon hybridization 71
    configuration 75
    conjugation 73f.
    crowded substituents 71
    dilution 77
    electron deficiency 72
    electronegativity 71
    heavy atoms 76
    hydrogen bonding 76f.
    intramolecular fields 75, 76
    isotopic substitution 76
    pH 80f.
    resonance 72f.
    solvents 77, 78f.
    steric interactions 74f.
    unshared electron pairs 72
  survey 70ff.
Carbon-13 coupling constants 79, 92ff.
  carbon-boron 107
  carbon-cadmium 107
  carbon-carbon 102ff., 191
    one-bond 105f.
    longer-range 106
  carbon-deuterium 69, 100
  carbon-fluorine 109, 189f., 229
    one-bond 109, 146
    longer-range 109, 146, 191
  carbon-lead 107
  carbon-mercury 107
  carbon-nitrogen 107f., 179
  carbon-phosphorus 107
  carbon-proton 92ff.
    one-bond 92ff., 195
    two-bond 98, 100
    longer-range 98, 101, 193
  carbon-selenium 107
  carbon-silicon 107
  carbon-tellurium 107
  carbon-tin 107
  influence of
    carbon hybridization 93
    dihedral angle 98
    electron withdrawing 92, 93
Carbon-13 enriched compounds 102ff., 192f.
Carbon-13 satellites 102
Carbonyl compounds 159ff.

Carboxylic acids 171 ff.
Carr-Purell-Meiboom-Gill spin echo (CPMGSE) experiments 55, 57 f.
CAT-method 19
Charge densities *vs.* ^{13}C shifts 70 (fig.), 269 (fig.), 282 (fig.)
Chemical shift(s) 13 f.; see also carbon-13 chemical shifts
  ^{1}H *versus* ^{13}C 67, 76
Chemical shifts anisotropy relaxation 110
Chemical shift ranges 78
Cholestanes 235 ff.
Cis configuration 75, 137
cis-trans isomerism
  in alkenes 75, 137, 212
  in cyclic compounds 75, 210 f.
  in N-nitroso compounds 181
Coalescence temperature 88
Complexation shifts 268 (fig.)
Computer simulation of lineshapes 89
Configuration
  effects on ^{13}C shifts 74, 136, 137, 152 f, 210 f.
Conjugation effects 73 f., 161
Continuous wave (CW) NMR 19
  sensitivity relative to PFT 35
Conversion of ^{13}C shifts 68
Correlation function 113
Correlation time 113
  versus T_1, T_2 113 (fig.)
Coupling constants (see carbon-13 coupling constants)
Cyanides 180
Cycloalkanes
  ^{13}C shifts 134 f.
  CH couplings 99
  CC couplings 105
Cycloalkanols 152 ff.
Cycloalkanones 160, 162 ff.

Decoupling 36 ff.
DEFT technique 33 f.
Degree of alkylation
  influence on T_1 115
Degree of Substitution *vs.* CH coupling constants 94 f.
Deshielding 15
Diamagnetic shielding term 68
Digital filtering 30
Digitization 24
Dilution shifts 77
Dipeptides 286 f.
Dipole-dipole relaxation mechanism 39, 111
Disaccharides 258 ff.
Dispersion spectrum 12
  example 29
Dissociation effects 80

Double resonance techniques in ^{13}C NMR 36 ff.
Dwell time 25

Electron deficiency effects 72
Electronegativity 71, 208
  vs. ^{13}C shifts 272
Electron density *vs.* ^{13}C shifts 70, 269, 282
Electron withdrawing
  effect on ^{13}C shifts 72, 208
  effect on ^{13}C coupling constants 92, 93
Energy of activation 88
Equatorial configuration 75, 91, 210
Esters 154, 176
Estranes 235, 296
Ethers 155 ff.
Exponential multiplication 30
External lock 66
External reference 15, 66
Eyring equation 86

Fermi-contact shift 82
Field-frequency lock 63
Filtering of frequencies 25
Folding back 25, 26
Formyl compounds
  ^{13}C shifts 160, 166
  CH couplings 97
Fourier series 24
Fourier transform 23 f.
Fourier transformation 27
Free enthalpy of activation 86
Free-induction decay 20 ff., expls.: 21, 23, 31
Fused aromatic compounds 188

Gated decoupling 43
Gibbs-Helmholtz equation 88
Gyromagnetic ratio 2, 39

H_0 homogeneity control 63
H_1 radiofrequency 3, 63
H_2 decoupling radiofrequency 65
Half-maximum intensity width 4
Hammet σ constants *vs.* ^{13}C shifts 184 (fig.)
Haloalkanes, ^{13}C shifts 142 ff., 209
Heisenberg uncertainty relation 5
Henderson-Hasselbach equation 81
Heteroalicyclics ^{13}C shifts 198
  CH couplings 99
Heteroaromatics ^{13}C shifts 196, 199 ff.
  CH couplings 99, 101
  CC couplings 106, 204
High-field ^{13}C spectra
  examples 103, 228
Hindered rotation 86
Heteronuclear couplings 106 ff.
Homonuclear couplings 102

Hybridization effects
  on ^{13}C shifts 71
  on ^{13}C coupling constants 93ff.
Hydroaromatic compounds 195f.
Hydrocarbon shieldings 131ff.
Hydrogen bonding 76
  effect on T_1 124

Imaginary spectra 29
Indoles 203
INDOR 282
Inositols 263
Intermolecular interaction, effect on T_1 124
Internal reference 15
Intramolecular mobility 85
  effect on ^{13}C shifts 89ff.
  effect on T_1 119ff.
Inversion of rings 86, 90f.
Inversion recovery techniques 48ff.
Ionic species 72, 97, 107f., 182, 199ff., 205ff.
Isocyanates 180
Isocyanides 179f.
Isothiocyanates 180
Isotope effect on ^{13}C shifts 69, 76
Isotropic shifts 82ff., 243

Ketenes 73
Ketones 159ff.

Lanthanoid shift reagents 82ff., 153, 243
Larmor equation 3, 10
Larmor frequencies of nuclei (fig.) 63
Larmor frequency 2
Larmor precession 2
Line broadening 6
Line shape simulation 89
Line width 5
Lock signals 64
Longitudinal magnetization 7
Longitudinal relaxation time 7
Long-range couplings
  examples CH: 100, 101, CC: 106, CN: 108
Lorentzian line shape 12, 24
Low power noise decoupling 38

Magnetic moment 1
Magnetic susceptibility corrections 15
Magnetization 6
  equilibrium 6
  partially relaxed 51
  steady state 55
Magnetization vector 6
Magnetogyric ratio (see gyromagnetic ratio)
Magnitude spectrum 13, 30
  example 29
Measurement of ^{13}C parameters 19ff.
Mechanisms
  of coupling 16, 92
  of spin-lattice relaxation 110f.
Medium shifts 77ff.
Mesomeric effects
  on carbon shifts 72
Methane derivatives
  ^{13}C shifts 143, 148
  CH couplings 148
Methyl carbon shieldings 131f.
Methyl substituent effects 131f., 207ff.
Modulation
  of frequencies 38
  of pulse interferograms 22
Molecular mobility
  and spin-lattice relaxation 113ff.
Motional narrowing 114
Multiple resonance 36ff.
Multiplet line intensities 18
Multiplicity 18
Multipulse experiments 33, 48ff.
Mutarotation 248 (fig.), 255, 259

Nitriles 180
Nitro compounds 75, 99, 181
Nitroso compounds 181
NMR 3
NMR detection 11
NMR instrumentation 59ff.
NMR spectrometer, schematic diagram 62
NMR theory 1ff.
Noise decoupling 38
Noise modulation 38
Nuclear induction 11
Nonbonded (through-space) interactions in carbon-fluorine coupling 109
Norbornyl derivatives 137, 146, 151, 178
Nuclear Overhauser effect (NOE) 39f.
  NOE enhancement 39, 111
  quenching of 40
Nuclear properties 1
Nuclear shielding 13
Nuclear spin 1
Nucleosides and nucleotides 264ff.

Off-resonance decoupling 42
Olefins (see alkenes)
Oligopeptides 283
One-bond coupling 93ff.
Overhauser effect (see nuclear Overhauser effect)
Oxygen
  influence on T_1 113, 128

Paramagnetic additives 40, 113
Paramagnetic compounds
  influence on T_1 112f.

  shift reagents 82f.
Paramagnetic shielding term 70
Partially relaxed Fourier transform spectra 48ff.
Peptides 283ff.
Phase correction 28ff.
Phase memory time 7
pH shifts 80f., 282
Phosphorus compounds
  coupling constants 107, 267 (fig.)
pK Determination 82, 282
Polycyclic hydrocarbons ^{13}C shifts 137
Polycyclic (fused) nitrogen heterocycles 202
Polymers 144, 185
Polyols 260, 262
Polypeptides 284
Polysaccharides 259, 299
Porphyrins 287f.
Power spectra 29f.
Pregnanes 233f.
Progressive saturation 53ff.
Proteins 284
Proton decoupling techniques
  gated decoupling 43
  inverse gated decoupling 43
  low-power noise decoupling 38
  noise decoupling
    (broad-band decoupling) 38
  off-resonance decoupling
    (single frequency off-resonance decoupling) 42
  pulsed decoupling 43
    for determination of nuclear Overhauser enhancements 46
  selectice decoupling 48
Pseudo-contact shift 82
Pulsed NMR 20ff.
Pulse Fourier Transform NMR 22ff.
Pulse frequency 26
Pulse interferograms 22
  examples 21, 23
Pulse interval 25
Pulse sequences 33, 48ff.
Pulse width 20, 27
  adjustment 27 (fig.)
Purines 270ff.
Pyridines
  ^{13}C shifts 200, 215f.
  CH couplings 99
  CC couplings 106
  CN couplings 108
Pyrimidines 201, 204, 270ff.

Quadrature detection
  (digital quadrature detection) 26
Quantum number 1
Quinones 170f.

Rate constant *vs.* shift difference 87 (fig.)
Reaction mechanisms 179
Real spectra 30
Referencing of ^{13}C shifts 15, 68
Relaxation 11, 48ff., 110ff.
Relaxation mechanisms 110f.
Relaxation times 5
Resolution in PFT NMR 30ff.
Resonance effects on ^{13}C shifts 72f., 212f.
Restricted rotation 86
Rf field 3, 64
Ring inversion 86, 90f.
Ring size
  influence on ^{13}C shift 134
Rotating frame of reference 9ff.
Rotations 86

Saturation 6
Saturation-recovery method 52f.
Scalar (spin-spin) relaxation 110
s-Character of carbon
  influence on coupling constants 93 (fig.), 134
Segmental mobility
  effect on T_1 121ff.
Sensitivity (signal: noise), enhancement in ^{13}C NMR 19
  for protonated carbons 39ff.
  for slowly relaxing carbons 33, 113
Shielding constant 13, 68, 70
Shielding of nuclei 13, 15
Shift reagents 82ff., 153, 243
Shift references in ^{13}C NMR 68
Signal intensities 43
Signal to noise ratio 19
Single frequency proton decoupling
  (off-resonance decoupling) 42
Solvent shifts 77ff.
Solvent effects on carbon-proton coupling 79
sp Carbon shifts 71, 72, 141
  coupling constants 98, 105
sp^2 Carbon shifts 71, 72, 138ff., 185ff.
  coupling constants 97, 99, 105
sp^3 Carbon shifts 71, 72, 131ff.
  coupling constants 96, 99, 105
Spin 1
Spin alignments 2, 3
Spin-decoupling 36ff.
Spin-echo techniques 33, 55ff.
Spin-lattice relaxation 110ff.
  influence on signal: noise 33
  mechanisms 110f.
Spin-lattice relaxation time (T_1) 110ff.
  correlation with mobility and constitution 113ff.
  definition 5
  influence on signal intensity 33
  methods of measurement 48ff.

  versus T_2 5, 113
Spin-locking FT experiments 57
Spin-quantum number 1
Spin-rotation relaxation 111
Spin-spin coupling 15ff.
  mechanism 16f., 92f.
Spin-spin relaxation 5
Spin-spin-relaxation time (T_2)
  definition 5
  influence on line-width 5
  measurement 55, 57f.
  versus T_1 5, 57f., 113
Steric effect on ^{13}C shifts 74f., 132, 155, 208ff.
Steroid alkaloids 230, 239
Steroids 225ff.
Substituent effects (increments) 77, 208ff.
  of alkyl groups 132, 136, 208ff.
  of amino groups 177, 208ff.
  of carboxyl groups 171, 208ff.
  of halogens 71, 143, 208ff.
  of hydroxyl groups 153
  on aromatic ring carbons 183f., 213f.
Sulfides 182
Sulfones 182
Sulfonic acids 182
  (and salts)
Sulfonium ions 182
Sulfoxides 182
Sugars 247ff.
Superconducting solenoids 19

Tacticity 145, 185
Temperature dependence of ^{13}C NMR 89f.
Temperature effects on T_1 128
Terpenes 219ff.
Thermodynamic data of interconversion 88f.
Thiocyanates 180
Thioketones 183
Thiols (mercaptans) 182
Thiophenes 199
Thioureas 183
Tracer techniques 192, 194, 289
Trans configuration 75, 137
Transverse magnetization 7, 20
Transverse relaxation time 7
Tripeptides 283, 286

U-mode 14
Uracils 201
Ureas 183

V-mode 14
Variable temperature studies 89f.
Vinyl halides 149
Viscosity effects on T_1 127

Width of NMR lines
  influence of T_2 5
  influence of rate constants and temperature 87

Compound Index

Individual Compounds are collected in this index if the text includes

specific shift values [no comment before page number(s)];
coupling constants [(J) before page number(s)];
spin-lattice relaxation times [(T_1) before page number(s)];
spectra or diagrams with such data [(fig.) before page number(s)].

The precision of all collected data is not better than

±0.1 ppm for chemical shifts,
±0.3 Hz for coupling constants, and
±10% for spin-lattice relaxation times.

Acenaphthene 189
Acenaphthylene 188
Acepleiadiene 189
Acepleiadylene 189
Acetaldehyde (J) 97, 100, 105
Acetaldoxime (J) 97
Acetamide (J) 108
Acetanilide (J) 108
Acetate anion (aq.) (J) 105
Acetic acid 69, 173; (J) 69, 96, 105; (T_1) 124
Acetone 69, 162; (J) 69, 100, 105; (fig.) 14
Acetonitrile 69, 72; (J) 69, 96, 105, 108, 179
Acetophenone 74, 75, 167; (J) 105
2-Acetoxycyclohexanone 164
3β-Acetoxy-5β-pregn-16-en-20-one 234
11α-Acetoxyprogesterone 234
Acetylacetone (fig.) 45
Acetylene (J) 93, 98, 100, 106
Acetylfluoride (J) 109
Acetyl-L-cysteine 276
Acetyl-L-cystine 278
Acetyl-L-glutamine 280
Acetyl-L-leucine methyl ester 276
Acetyl-L-ornithine methyl ester 278
Acetyl-L-phenylalanine methyl ester 280
Acetyl-L-proline, *cis*- and *trans*- 280
2-Acetylpyridine 200
3-Acetylpyridine 200
4-Acetylpyridine 200
Acetyl-L-valine methyl ester 276
Acridine 202
Acrolein (J) 100
Acrylic acid 173; (J) 105
Acrylonitrile (J) 105
Actinocin 299
Adamantane (fig.) 54; (T_1) 115
Adenine 270
Adenosine 270
Adenosine-5′-monophosphate 272, 299
Adenosine-5′-triphosphate 272
Alamethicine (fig.) 285
β-Alanine 276
DL-Alanine (J) 108
L-Alanine 276
Alanylglycine, protected 286
β-Alanylhistidine, protected 286
Allene 141; (J) 97
β-D-Allopyranose 251
o-Aminoacetophenone 168
3-Aminoacrolein (J) 100
D-1α-Aminoadipic acid-N-ethylamide 294
2-Aminobenzaldehyde 166
2-Aminobenzoic acid 187
4-Aminobenzoic acid 187, 299
3-Aminobenzonitrile 180
4-Aminobenzonitrile 180
7-Aminocephalosporanic acid 294
m-Aminofluorobenzene (J) 191
o-Aminofluorobenzene (J) 191
p-Aminofluorobenzene (J) 191
2-Amino-3-methylpyridine 215
endo-2-Aminonorbornane 178
exo-2-Aminonorbornane 178
5α-Aminopregnane 233
5β-Aminopregnane 233
2-Aminopyridine 200
3-Aminopyridine 200
4-Aminopyridine 200
2-Amino-9-(β-D-ribofuranosyl)-purine 272
5-Aminouracil 201
t-Amyl cation 206
5α-Androstane 231, 296
5β-Androstane 231, 296
Androstane-3,17-dione 232
Androst-4-ene-3,17-dione 232
2,5′-Anhydro-2,3′-isopropylideneuridine 270
Aniline 73, 186; (J) 106
Anisole 186; (J) 106
Anthracene 188
Antibiotic X-537 A 293

α-D-Arabinofuranose 252
β-D-Arabinofuranose 253
9-α-D-Arabinofuranosyladenine 270
α-D-Arabinopyranose 252
β-D-Arabinopyranose 252
9-α-D-Arabinopyranosyladenine 270
9-β-D-Arabinopyranosyladenine 270
D-Arabitol 262
Arecoline 298
L-Arginine 278
Arsabenzene 200
Ascorbic acid 252
L-Asparagine 278
Asparaginylglycine, protected 286
Asparthione, protected 287
L-Aspartic acid 278
L-Aspartic acid *t*-butyl ester 278
Atropine 298
4-Azaindene 202
Azetidine 198
5α-Azidopregnane 233
5β-Azidopregnane 233
Aziridine 198
Azobenzene, *trans* 187
Azulene 188

Benzalaniline 187
Benzaldehyde 74, 166
Benzamide 187
Benzene 69, 185, 216; (*J*) 69, 99, 101, 102, 106, 107, 190; (T_1) 112, 117
Benzenesulfonic acid 187
Benzenesulfonylchloride 187
Benzenonium ion 207
Benzoate anion 187; (*J*) 191
Benzocyclobutene 195; (*J*) 195
Benzocycloheptatriene 195
Benzocycloheptene 195; (*J*) 195
Benzocyclooctene 195; (*J*) 195
Benzocyclopentene 195; (*J*) 195
Benzocyclopropene 195; (*J*) 195
Benzo[g.h.i]fluoranthene 189
Benzoic acid 187; (*J*) 191
Benzonitrile 73, 180; (*J*) 99, 106, 191
Benzophenone 187
o-Benzoquinone 170
p-Benzoquinone 170
Benzoylchloride 187; (*J*) 191
Benzylalcohol 185; (*J*) 191
Benzylbromide 185
Benzylchloride 185; (*J*) 191
Benzylfluoride 185; (*J*) 109
Benzyloxycarbonyl-L-alanine 276
Benzyloxycarbonyl-L-aspartic acid 278
Benzyloxycarbonyl-L-aspartic acid anhydride 278
Benzyloxycarbonyl-L-aspartic acid *t*-butyl ester 278
Benzyloxycarbonyl-L-aspartic acid ethyl ester 278
Benzyloxycarbonyl-L-glutamic acid (fig.) 275
Benzyloxycarbonylglycine 276
Bicyclo[4.1.0]heptan-2-one 164
Bicyclo[2.2.1]hept-2-en-7-one 165
Bicyclo[2.2.1]hept-5-en-2-one 165
Bicyclo[3.1.0]hexan-2-one 164
Bicyclo[2.2.2]octane 147
Bicyclo[2.2.2]oct-5-en-2-one 165
Bicyclo[3.2.1]oct-2-en-8-one 165
Biphenyl 188; (T_1) 117
Biphenylene 195; (*J*) 195
Bornane 296
Bornylene 296
Brenzcatechine 186
m-Bromoacetophenone 167
o-Bromoacetophenone 167
p-Bromoacetophenone 167
(*E*)-3-Bromoacrylic acid 174
(*Z*)-3-Bromoacrylic acid 174
4-Bromobenzaldehyde 166
Bromobenzene 185; (*J*) 99, 190
3-Bromobenzonitrile 180
4-Bromobenzonitrile 180
1-Bromobicyclo[2.2.2]octane 147
3-Bromobiphenyl (T_1) 121
(*E*)-2-Bromo-3-*t*-butylacrylic acid 174
3-Bromocamphor (*endo*) 224
Bromochloromethane 148
Bromocitraconic acid 175
Bromocitraconic anhydride 175
(*E*)-2-Bromocrotonic acid 174
p-Bromocumyl cation 207
1-Bromodecane (T_1) 121
3-Bromo-4,6-di-*t*-butyl-*o*-benzoquinone 170
Bromodichloromethane 148
Bromoethane 148
Bromoethene (Vinylbromide) 149; (*J*) 149
m-Bromofluorobenzene (*J*) 191
o-Bromofluorobenzene (*J*) 191
p-Bromofluorobenzene (*J*) 191
Bromoform 69, 148; (*J*) 69, 148; (T_1) 111
1-Bromohexane 71
1-Bromohexyne 149
(*Z*)-2-Bromo-3-iodoacrylic acid 174
Bromomesaconic acid 175
(*E*)-3-Bromomethacrylic acid 174
(*Z*)-3-Bromomethacrylic acid 174
Bromomethane 148; (*J*) 148
2-Bromo-3-methylcrotonic acid 175
2-Bromo-2-methylpropane (*t*-Butylbromide) 149
3-Bromonorbornanone (*endo*) 224
3-Bromonorbornanone (*exo*) 224
2-Bromopropane 148

cis-1-Bromopropene 149
trans-1-Bromopropene 149
6-Bromopurine 270
2-Bromopyridine 200
3-Bromopyridine 200
4-Bromopyridine 200
2-Bromothiophene 199
3-Bromothiophene 199
Bromotrichloromethane 148
5-Bromouracil 201
Brucine 298
Buphanamine 247
1,2-Butadiene 141
1,3-Butadiene 73, 138
Butanal 160
n-Butane 131
1,3-Butanediol 262
1,4-Butanediol 262
t-Butane (*J*) 96
1-Butanethiol 182
1-Butanethiolate 182
1-Butanol 150; (T_1) 125
2-Butanol 150
t-Butanol (*J*) 105
Butanone 74, 162
2-Butanone (*J*) 105, 106
anti-Butanone oxime (T_1) 120
syn-Butanone oxime (T_1) 120
(*E*)-2-Butenal 160
1-Butene 73, 138
cis-2-Butene 138
trans-2-Butene 138
(*E*)-2-Butenoic acid 173
(*Z*)-2-Butenoic acid 173
Butenone 74, 165
p-*t*-Butylacetophenone 167
Butylamine 178
sec-Butylamine 178
t-Butylamine 178; (*J*) 105
n-Butylammonium trifluoroacetate (T_1) 126
sec-Butylbenzene 185
t-Butylbenzene 185
t-Butylcarbenium ion 72
t-Butyl cation 206
t-Butyl cyanide (*J*) 105, 108
cis-4-*t*-Butylcyclohexanol 152, 153
trans-4-*t*-Butylcyclohexanol 152, 153
2-*t*-Butylcyclohexanone 160, 163
3-*t*-Butylcyclohexanone 160, 163
4-*t*-Butylcyclohexanone 160, 163
4-*t*-Butyl-2,6-dimethylacetophenone 168
2-*t*-Butyl-5,5-dimethyl-1,3-dioxane 158
5-*t*-Butyl-2,2-dimethyl-1,3-dioxane 158
2-*t*-Butyl-1,3-dioxane 158
5-*t*-Butyl-1,3-dioxane 258
t-Butyl fluoride (*J*) 109
t-Butyl isocyanide 180; (*J*) 179
2-*t*-Butyl-4-methoxyphenol 214
cis-2-*t*-Butyl-4-methyl-1,3-dioxane 158
cis-2-*t*-Butyl-5-methyl-1,3-dioxane 158
trans-2-*t*-Butyl-5-methyl-1,3-dioxane 158
cis-5-*t*-Butyl-2-methyl-1,3-dioxane 158
trans-5-*t*-Butyl-2-methyl-1,3-dioxane 158
N-*n*-Butyl-N-nitrosoaniline 181
N-*t*-Butyl-N-nitrosoaniline 181
t-Butyloxycarbonyl-L-alanine 276
t-Butyloxycarbonyl-L-aspartic acid 278
t-Butyloxycarbonyl-L-aspartic acid benzyl ester 278
t-Butyloxycarbonyl-L-aspartic acid *t*-butyl ester 278
t-Butyloxycarbonyl-O-benzyl-L-threonine 276
t-Butyloxycarbonyl-L-cystine 278
t-Butyloxycarbonyl-L-glutamic acid benzyl ester 278
t-Butyloxycarbonyl-L-glutamic acid *t*-butyl ester 280
t-Butyloxycarbonyl-L-glutamine 280
t-Butyloxycarbonylglycine 276
t-Butyloxycarbonyl-L-isoleucine 276
t-Butyloxycarbonyl-L-leucine 276
t-Butyloxycarbonyl-L-nitroarginine 278
t-Butyloxycarbonyl-L-phenylalanine 280
t-Butyloxycarbonyl-L-phenylalanine (fig.) 275
t-Butyloxycarbonyl-L-proline, *cis*- and *trans*- 280
t-Butyloxycarbonyl-L-tryptophane 280
t-Butyloxycarbonyl-L-tyrosine benzyl ester 280
t-Butyloxycarbonyl-L-valine 276
6-*t*-Butyl-2-pentachloro-*p*-benzoquinone 170
trans-5-*t*-Butyl-2-phenyl-1,3-dioxane 158
1-Butyne 141
2-Butyne 141
Butyric acid 173

Camphor 183, 224; (fig.) 84
Canadine 298
Carbenium ion, diethylmethyl 206
Carbenium ion, dihydroxy 206
Carbenium ion, dimethylbromo 206
Carbenium ion, dimethylchloro 206
Carbenium ion, dimethylcyclopropyl 206
Carbenium ion, dimethylfluoro 206
Carbenium ion, dimethylhydroxy 206
Carbenium ion, dimethylphenyl 206
Carbenium ion, diphenyl 206
Carbenium ion, hydroxy 206
Carbenium ion, methoxydihydroxy 206
Carbenium ion, *p*-methoxyphenylmethyl-*t*-butyl 207
Carbenium ion, *p*-methoxyphenyl-methylethyl 207
Carbenium ion, *p*-methoxyphenylmethylisopropyl 207

Carbenium ion, methyldihydroxy 206
Carbenium ion, methylhydroxy 206
Carbenium ion, *p*-methylphenylmethylethyl
Carbenium ion, *p*-methylphenylmethylisopropyl
Carbenium ion, phenylmethylbromo 206
Carbenium ion, phenylmethylchloro 206
Carbenium ion, phenylmethylethyl 207
Carbenium ion, phenylmethylfluoro 206
Carbenium ion, phenylmethylisopropyl 207
Carbenium ion, *p*-trifluoromethylphenylmethylethyl 207
Carbenium ion, *p*-trifluoromethylphenylmethylisopropyl 207
Carbenium ion, trihydroxy 206
Carbenium ion, triphenyl 206
Carbon dioxide 72, 183
Carbon disulfide 68, 183
Carbon monoxide 72
Carbon tetrabromide 148
Carbon tetrachloride 71, 148; (fig.) 34, 50, 61; (T_1) 115
3-Carboxybenzonitrile 180
4-Carboxybenzonitrile 180
Carene 296
β-Carotene 226
15,15′-*cis*-β-Carotene 226
Carvone 223
Cellobiose 260
α-Cellobiose octaacetate 261
β-Cellobiose octaacetate 261
Cephalexin 294
Cephalosporin C 294
Chloroacetaldehyde (*J*) 100
m-Chloroacetophenone 167
o-Chloroacetophenone 167
p-Chloroacetophenone 167
(*E*)-3-Chloroacrylic acid 174
(*Z*)-3-Chloroacrylic acid 174
2-Chloroadenosine 272
2-Chloroaniline 186
3-Chloroaniline 186
4-Chloroaniline 186
Chlorobenzene 185; (*J*) 190
3-Chlorobenzonitrile 180
4-Chlorobenzonitrile 180
2-Chloro-*p*-benzoquinone 170
1-Chlorobicyclo[2.2.2]octane 147
(*E*)-3-Chlorocrotonic acid 175
(*Z*)-3-Chlorocrotonic acid 175
3-Chloro-4,6-di-*t*-butyl-*o*-benzoquinone 170
Chlorodifluoromethane (*J*) 148
Chloroethane 148; (*J*) 148
Chloroethene (Vinylchloride) 149; (*J*) 149
m-Chlorofluorobenzene (*J*) 191
o-Chlorofluorobenzene (*J*) 191
p-Chlorofluorobenzene (*J*) 191
Chloroform 69, 71, 79, 148; (*J*) 69, 79, 94, 96, 148; (T_1) 111
1-Chlorohexane 71
1-Chlorohexyne 149
(*E*)-3-Chloro-2-iodoacrylic acid 174
(*E*)-3-Chloromethacrylic acid 174
Chloromethane 71, 148; (*J*) 94, 148
2-Chloro-2-methylpropane (*t*-Butylchloride) 149
5-Chloro-2-nitroaniline 214
6-Chloro-9-(β-D-ribofuranosyl)-purine 270
Chlorophyll a 289
2-Chloropropane 148
cis-1-Chloropropene 149
trans-1-Chloropropene 149
6-Chloropurine 270
2-Chlorotoluene 186
3-Chlorotoluene 186
4-Chlorotoluene 186
Chlorotribromomethane 148
5-Chlorouracil 201
Cholesta-3,5-diene 236
Cholesta-3,5-dien-7-one 238
Cholestane 296
5α-Cholestane 235
5β-Cholestane 235
Cholestan-3β-ol 236
Cholestan-3-one 238
Cholestan-3α-yl acetate 236
Cholestan-3β-yl acetate 236
Cholest-5-en-7-on-3β-yl acetate 238
Cholesterol 236
Cholesteryl acetate 237
Cholesteryl chloride (T_1) 119
Cholesteryl methyl ether 237
Chroman-4-one 297
Chromone 297
Cineol 223
(*Z*)-Cinnamic acid 175
Cinnoline 202
cis-Citral 222
trans-Citral 223
Codeine 299
Colchicine (fig.) 38
Conanine 239
Conessine 239
Coniine 298
Coprostane 296
Coumarin 297
m-Cresol 186
o-Cresol 186
p-Cresol 186
Cumyl cation 207
Cyanide anion 72; (*J*) 108
4-Cyanobenzaldehyde 166
6-Cyanopurine 270

5-Cyanouracil 201
Cyclobutane 134; (J) 99, 134; (T_1) 116
Cyclobutanone 162; (J) 106
Cyclobutene 138
Cyclobutyl bromide (J) 106
Cyclodecane 134; (J) 134; (T_1) 116
Cyclodecanone 162
Cyclododecane 134; (J) 134
Cyclododecanone 163
cis-Cyclododecene 139
Cycloheptadecane 134; (J) 134
Cycloheptadecanone 163
1,3-Cycloheptadiene 139
Cycloheptane 134; (J) 134; (T_1) 116
Cycloheptanol 152
Cycloheptanone 162
Cycloheptatriene 139
Cycloheptene 139
Cyclohexadecane 134; (J) 134
Cyclohexadecanone 163
Cyclohexane 69, 134, 135, 210; (J) 69, 99, 134; (T_1) 116
Cyclohexanethiol 182
Cyclohexanol 152, 153
Cyclohexanone 162
Cyclohexene 139
2-Cyclohexenone 73, 165
3-Cyclohexenone 165
1-Cyclohexenylacetone 165
Cyclohexyl cyanide 180
Cyclohexyl isocyanate 180
Cyclohexyl isocyanide 180
Cyclohexyl isothiocyanate 180
Cyclononane 134; (J) 134; (fig.) 90
Cyclononanone 162
Cyclooctane 134; (J) 134; (T_1) 116
Cyclooctanol 152
Cyclooctanone 162
cis-Cyclooctene 139
trans-Cyclooctene 139
Cyclopentadecane 76, 134; (J) 134
Cyclopentadecanone 163
Cyclopentane 134; (J) 99, 134; (T_1) 116
Cyclopentanol 152
Cyclopentanone 162
Cyclopentene 138
2-Cyclopentenone 165
3-Cyclopentenone 165
Cyclopentyl acetate 124
Cyclopentyl cation 206
Cyclopropanecarboxylic acid (J) 105
Cyclopropane 134; (J) 99, 134; (T_1) 116
Cyclopropene (J) 99
Cyclopropyl bromide (J) 105
Cyclopropyl chloride (J) 105
Cyclopropyl cyanide (J) 105
Cyclopropyl iodide (J) 105
Cyclotetradecane 134; (J) 134
Cyclotetradecanone 163
Cyclotridecane 134; (J) 134
Cyclotridecanone 162
Cycloundecane 134; (J) 134
Cycloundecanone 163
L-Cysteic acid 276
L-Cysteine hydrochloride 276
L-Cysteine methyl ester hydrochloride 276
Cysteinylglycine, protected 287
L-Cystine dihydrochloride 278
L-Cystine methyl ester dihydrochloride 278
Cytidine 270
Cytidine-5′-monophosphate 270

Decadeuteriodiethylether 69; (J) 69
cis-Decalin 296
trans-Decalin 296; (T_1) 118
n-Decane 131; (T_1) 121
Decanoic acid (T_1) 125
1-Decanol 150; (T_1) 125
2-Decanol 150
Decylamine 178
15,15′-Dehydro-β-carotene 226
7-Dehydrocholesteryl acetate 237
5-Dehydroisoandrosterone 232
6,7-Dehydrolinalool 222; (T_1) 120
16-Dehydroprogesterone 233
2′-Deoxyadenosine 270
2′-Deoxyadenosine-5′-monophosphate 272
Deoxyadenosine monophosphate 299
Deoxycytidine 270
Deoxycytidine-5′-monophosphate 270
Deoxyguanosine 272
Deoxyguanosine-5′-monophosphate 272
Deoxyinosine 270
2-Deoxy-α-D-ribofuranose 253
2-Deoxy-β-D-ribofuranose 253
2-Deoxy-α-D-ribopyranose 253
2-Deoxy-β-D-ribopyranose 253
2-Deoxy-2,2,18,19-tetrahydrogelsemine 242
Deuteriobromoform 69; (J) 69
Deuteriochloroform 69; (J) 69
Deuterioporphyrin diethyl ester 288
Deuterioporphyrin dimethyl ester 288
2,4-Diacetyldeuterioporphyrin dimethyl ester 288
2,6-Diamino-9-(β-D-ribofuranosyl)-purine 272
1,4-Diazaindene 202
2,4-Diazaindene 202
3,4-Diazaindene 202
cis-Diazastilbene (*cis*-Di-α-pyridylethylene) (J) 97
trans-Diazastilbene (*trans*-Di-α-pyridylethylene) (J) 97
2,6-Diaziridino-*p*-benzophenone 170
Diazomethane 73

Dibenzylamine 185
Dibenzylether 185
Dibenzylsulfide 185
3,3-Dibromoacrylic acid 174
(*E*)-2,3-Dibromoacrylic acid 174
(*Z*)-2,3-Dibromoacrylic acid 174
m-Dibromobenzene 185
o-Dibromobenzene 185
3,3-Dibromo-2-bromomethylacrylic acid 174
2,3-Dibromocamphor (*endo*) 224
Dibromochloromethane 148
(*E*)-2,3-Dibromocrotonic acid 175
(*Z*)-2,3-Dibromocrotonic acid 175
Dibromodichloromethane 148
1,1-Dibromoethane 148
cis-1,2-Dibromoethene 149
trans-1,2-Dibromoethene 149
3,3-Dibromo-2-ethylacrylic acid 174
3,3-Dibromo-2-hydroxymethylacrylic acid 174
3,3-Dibromo-2-isopropylacrylic acid 174
3,3-Dibromomethacrylic acid 174
Dibromomethane 148
1,4-Dibromopentane 209
3,3-Dibromo-2-propylacrylic acid 174
2,5-Di-*t*-butylacetophenone 168
Dibutylamine 178
4,6-Di-*t*-butyl-*o*-benzoquinone 170
2,5-Di-*t*-butyl-*p*-benzoquinone 170
2,6-Di-*t*-butyl-*p*-benzoquinone 170
cis-2,5-Di-*t*-butyl-1,3-dioxane 158
trans-2,5-Di-*t*-butyl-1,3-dioxane 158
1,1-Di-*t*-butylethylene (*J*) 97
4,6-Di-*t*-butyl-3-nitro-*o*-benzoquinone 170
4,6-Di-*t*-butyl-3-phenyl-*o*-benzoquinone 170
Dichloroacetaldehyde (*J*) 100
2,4-Dichloroacetophenone 168
2,6-Dichloroacetophenone 169
(*Z*)-2,3-Dichloroacrylic acid 174
3,3-Dichloroacrylic acid 174
m-Dichlorobenzene 185
o-Dichlorobenzene 185; (fig.) 61
p-Dichlorobenzene 185
2,5-Dichloro-*p*-benzoquinone 170
meso-2,3-Dichlorobutane 144
racem-2,3-Dichlorobutane 144
(*E*)-2,3-Dichlorocrotonic acid 175
(*Z*)-2,3-Dichlorocrotonic acid 175
2,3-Dichloro-5,6-dicyano-*p*-benzoquinone 170
3,5-Dichloro-2,6-dimethyl-*p*-benzoquinone 170
1,1-Dichloroethane 148; (*J*) 148
1,2-Dichloroethane 148; (*J*) 100, 148
1,1-Dichloroethene 149; (*J*) 149
cis-1,2-Dichloroethene 149; (*J*) 149
trans-1,2-Dichloroethene 149; (*J*) 149
cis-1,2-Dichloroethylene (*J*) 100
trans-1,2-Dichloroethylene (*J*) 100
Dichlorofluoromethane (*J*) 148
Dichloromethane 71, 148; (*J*) 94, 96, 148
meso-2,4-Dichloropentane 144
racem-2,4-Dichloropentane 144
Dicyclohexylcarbodiimide 180
Dicyclopropylketone (*J*) 105
1-(2,3-Dideoxy-β-D-glycero)-pent-2-enofuranosylthymine 270
Dideuteriomethylenchloride 69; (*J*) 69
2,6-Diethylacetophenone 168
Diethylamine 178
o-Diethylbenzene 195; (*J*) 195
5,5-Diethyl-2,2-dimethyl-1,3-dioxane 158
5,5-Diethyl-1,3-dioxane 158
Diethylether 69; (*J*) 69
5,5-Diethyl-2-methyl-1,3-dioxane 158
Diethylsulfide 182
Diethylsulfone 182
Diethylsulfoxide 182
Difluoroacetonitril (*J*) 96
m-Difluorobenzene 185; (*J*) 191
o-Difluorobenzene 185; (*J*) 191
p-Difluorobenzene (*J*) 191
2,2-Difluoroethanol (*J*) 109
1,1-Difluoroethylene (*J*) 109
Difluoromethane (*J*) 94, 96, 109, 148
2,2-Difluoronorbornane 146; (*J*) 146
Dihexylamine 178
9,10-Dihydroanthracene 195
Dihydroconessine 239
18,19-Dihydrogelsemine 242
Dihydrolanosterol 237
6,7-Dihydrolinalool 222; (T_1) 120
9,10-Dihydrophenanthrene 195
2,4-Dihydroxyacetophenone 168
2,6-Dihydroxyacetophenone 169
2,5-Dihydroxybenzoic acid 215
6,7-Dihydroxycoumarin 297
3,3-Diiodoacrylic acid 174
(*E*)-2,3-Diiodoacrylic acid 174
m-Diiodobenzene 185
o-Diiodobenzene 185
(*E*)-2,3-Diiodocrotonic acid 175
cis-1,2-Diiodoethene 149
trans-1,2-Diiodoethene 149
Diiodomethane 148; (*J*) 148
2,6-Diisopropylacetophenone 168
2,6-Diisopropyl-*p*-benzoquinone 170
Diisopropylcarbodiimide 180
1,2,5,6-O-Diisopropylidene-3-C-(1,3-dithiane-2-yl)-allofuranose 251
2,4-Dimethoxyacetophenone 168
2,5-Dimethoxyacetophenone 168
2,6-Dimethoxyacetophenone 169
3,4-Dimethoxybenzaldehyde 166
1,2-Dimethoxybenzene 186

1,3-Dimethoxybenzene 186
1,4-Dimethoxybenzene 186
3,4-Dimethoxybenzonitrile 180
1,2-Dimethoxyethane (fig.) 41
6,7-Dimethoxy-1,2,3,4-tetrahydroisoquinoline 298
N,N-Dimethylacetamide (*J*) 105
2,3-Dimethylacetophenone 168
2,4-Dimethylacetophenone 168
2,5-Dimethylacetophenone 168
2,6-Dimethylacetophenone 75, 168
3,3-Dimethylacrylic acid 173
1,1-Dimethylallene (*J*) 106
p-N-Dimethylaminoacetophenone 167
4-Dimethylaminobenzaldehyde 166
4-Dimethylaminobenzonitrile 180
6-Dimethylaminopurine 270
N,N-Dimethylaniline 186
3,4-Dimethylbenzonitrile 180
2,6-Dimethyl-*p*-benzoquinone 170
1,6-Dimethylbicyclo[4.1.0]heptan-2-one 164
4,6-Dimethylbicyclo[4.1.0]heptan-2-one 164
1,5-Dimethylbicyclo[3.1.0]hexan-2-one 164
4,4′-Dimethylbiphenyl (T_1) 128
2,3-Dimethyl-1,3-butadiene 138
2,2-Dimethylbutane 131
2,3-Dimethylbutane 131
2,3-Dimethyl-2-butanol 151
3,3-Dimethyl-2-butanol 151
3,3-Dimethyl-1-butanol 151
3,3-Dimethylbutanone 162
3,3-Dimethyl-1-butene 138
2,3-Dimethyl-2-butene 138
Dimethylbutylsulfonium cation 182
Dimethyl cadmium (*J*) 107
1,1-Dimethylcyclohexane 135
cis-1,2-Dimethylcyclohexane 135; (fig.) 91
trans-1,2-Dimethylcyclohexane 135
cis-1,3-Dimethylcyclohexane 135
trans-1,3-Dimethylcyclohexane 135
cis-1,4-Dimethylcyclohexane 75, 135
trans-1,4-Dimethylcyclohexane 75, 135
4,4-Dimethylcyclohexanone 160, 163
cis-3,4-Dimethylcyclohexanone 160, 163
trans-3,4-Dimethylcyclohexanone 160, 163
cis-3,5-Dimethylcyclohexanone 160, 163
trans-3,5-Dimethylcyclohexanone 160, 163
2,3-Dimethyl-2-cyclohexenone 165
3,5-Dimethyl-2-cyclohexenone 165
1,1-Dimethylcyclopentane 134
cis-1,2-Dimethylcyclopentane 134
trans-1,2-Dimethylcyclopentane 134
cis-1,3-Dimethylcyclopentane 134
trans-1,3-Dimethylcyclopentane 134
trans-1,2-Dimethylcyclopentanol 152
cis-1,3-Dimethylcyclopentanol 152, 153
trans-1,3-Dimethylcyclopentanol 152, 153
2,3-Dimethyl-2-cyclopentenone 165
trans-1,2-Dimethylcyclopentyl acetate 154
1,3-Dimethylcyclopentyl acetate (less abundant isomer) 154
1,3-Dimethylcyclopentyl acetate (more abundant isomer) 154
2,2-Dimethyl-1,3-dioxane 157
4,4-Dimethyl-1,3-dioxane 157
5,5-Dimethyl-1,3-dioxane 157
cis-2,4-Dimethyl-1,3-dioxane 157, 158
cis-2,5-Dimethyl-1,3-dioxane 157
trans-2,5-Dimethyl-1,3-dioxane 157
cis-4,6-Dimethyl-1,3-dioxane 157
trans-4,6-Dimethyl-1,3-dioxane 157
Dimethyl ether 157; (*J*) 94, 96
Dimethylethylsulfonium cation 182
N,N-Dimethylformamide 69; (*J*) 69, 97, 108
2,5-Dimethylfuran 198
3,4-Di-O-methyl-D-galactitol 262
2,6-Dimethyl-3-heptanone 162
2,5-Dimethyl-1,5-hexadiene 139
2,3-Dimethyl-2-hexene 139
3,4-Dimethyl-3-hexen-2-one 165
1,1-Dimethylhydrazine (*J*) 108
Dimethylhydroxycarbenium ion 72
1,2-Dimethylindole 203
2,3-Dimethylindole 203
2,7-Dimethylindole 203
1,2-Di-O-methyl-*myo*-inositol 263
1,3-Di-O-methyl-*myo*-inositol 263
1,4-Di-O-methyl-*myo*-inositol 263
Dimethyllead (*J*) 107
Dimethylmercury (*J*) 107
1,8-Dimethylnaphthalene 189
Dimethylnitrosamine (*J*) 108
Dimethyloctanol 222
3,7-Dimethyloctanol (T_1) 125
2,4-Dimethyl-2,3-pentadiene 141
3,3-Dimethylpentane 131
2,4-Dimethyl-3-pentanol 151
4,4-Dimethyl-3-pentanol 151
2,4-Dimethyl-3-pentanone 162
4,4-Dimethyl-2-pentanone 162
4,4-Dimethyl-3-pentanone 162
trans-4,4-Dimethyl-2-pentene 138
(*E*)-4,4-Dimethyl-2-pentenoic acid 173
3,4-Dimethyl-3-penten-2-one 165
2,6-Dimethylphenol 186
3,5-Dimethylphenol 186
Dimethylphenylcarbenium ion 72
cis-4,6-Dimethyl-2-phenyl-1,3-dioxane 158
1,4-Dimethylpiperazine 198
2,5-Dimethylpiperazine 198
2,6-Dimethylpiperazine 198
1,2-Dimethylpiperidine 198
2,6-Dimethylpiperidine 198

2,2-Dimethylpropane 71; (J) 107
2,2-Dimethyl-1-propanol 150
2,2-Dimethylpropylamine 178
Dimethylpropylsulfonium cation 182
2,5-Dimethylpyrazine 201
2,5-Dimethylpyrrole 199
Dimethylselenide (J) 107
1,1-Dimethylspiro[2.4]heptan-4-one 164
1,1-Dimethylspiro[2.5]octan-4-one 164
Dimethylsulfide 182
Dimethylsulfone 182
Dimethylsulfoxide 69, 182; (J) 69
Dimethyltellur (J) 107
2,4-Dimethylthiazole 199
4,5-Dimethylthiazole 199
N,N-Dimethyltrichloroacetamide (fig.) 89
Dinitromethane (J) 96
Dioctanoyllecithin (T_1) 122
Dioleoyllecithin (T_1) 122
1,3-Dioxane 157
1,4-Dioxane 68, 69, 158; (J) 69, 99
Dipalmitoyllecithin 299; (T_1) 122
Dipentylamine 178
2,5-Diphenyl-*p*-benzoquinone 170
2,6-Diphenyl-*p*-benzoquinone 170
Diphenylcarbodiimide 187
Diphenylether 186; (fig.) 52
Diphenylmercury (J) 107
Diphenylsulfide 186
2,4-Dipropionyldeuterioporphyrin dimethyl ester 288
Dipropylamine 178
Dipropylsulfide 182
Dipropylsulfone 182
Dipropylsulfoxide 182
α,α′-Dipyridyl 200
2,4-Dithiouridine 270
Dodecadeuteriocyclohexane 69; (J) 69
Dodeca-5,7-diyne 141
1,2,3,4,5,6,7,8,9,10,11,12-Dodecahydrotriphenylene 195
1,4-Dodecamethylene benzene 76
Durene 185
Duroquinone 170

α-Ecdysone 238
α-Ecdysone triacetate 238
endo-5-Methyl-2-norbornanone 164
Epiandrosterone (fig.) 228
Epilactose 261
Epimaltose 260
5α-Ergostane 236
Ergosterol 237
Erythritol 262
Estrane 296
Estrone 235
Estrone acetate 235
Ethanal 160
Ethane 71, 131; (J) 93, 96, 100, 105
Ethanol 69, 150; (J) 69, 96, 105
p-Ethoxyacetanilide 186
o-Ethoxyacetophenone 167
p-Ethoxyaniline 186
Ethyl acetate 154; (J) 105
o-Ethylacetophenone 167
p-Ethylacetophenone 167
Ethylamine 178
Ethylbenzene 185; (J) 105; (fig.) 26; (T_1) 117
4-Ethylbenzenonium ion 207
Ethylbenzoate 187
Ethyl-4,6-O-benzylidene-1-thio-β-D-glucopyranoside 250
2-Ethyl-1-butene 138
2-Ethylbutyraldehyde (J) 100
Ethyl cyanide 180
Ethylene 138; (J) 93, 97, 100, 105
Ethyletiojervadien-3-ol-11,16-dione acetate 239
Ethyletiojervatrien-3-ol-11-one 239
Ethyletiojervatrien-3-ol-11-one acetate 239
2-Ethylidenecyclohexanone 165
Ethyl isocyanate 180
Ethyl isocyanide 180; (J) 197
Ethyl isothiocyanate 180
Ethyl methyl ether 157
N-Ethyl-N-nitrosoaniline 181
3-Ethyl-1-pentene 138
3-Ethyl-2-pentene 138
2-Ethyl-3-penten-2-one 165
1-Ethylpiperidine 198
2-Ethylpiperidine 198
2-Ethylthiazole 199
4-Ethylthiazole 199
Ethynylbenzene 185

Farnesol 223
Fenchone 224
Flavanone 297
Flavin adenine dinucleotide disodium salt (FAD) (fig.) 267
Flavone 297
Fluoranthene 189
Fluorene 195
Fluoroacetonitrile (J) 96
m-Fluoroacetophenone (J) 191
o-Fluoroacetophenone (J) 191
p-Fluoroacetophenone (J) 109
p-Fluoroanisole (J) 109
m-Fluorobenzaldehyde (J) 191
o-Fluorobenzaldehyde (J) 191
p-Fluorobenzaldehyde (J) 191
Fluorobenzene 185; (J) 99, 107, 109, 190, 191
3-Fluorobenzonitrile 180

4-Fluorobenzonitrile 180
1-Fluorobicyclo[2.2.2]octane 147; (*J*) 147
m-Fluorocumyl cation 207
p-Fluorocumyl cation 207
2-Fluoroestrone 235; (*J*) 229
Fluoroethane 148
2-Fluoroethanol (*J*) 109
1-Fluorohexane 71
m-Fluorohydroxybenzene (*J*) 191
o-Fluorohydroxybenzene (*J*) 191
p-Fluorohydroxybenzene (*J*) 191
m-Fluoroiodobenzene (*J*) 191
o-Fluoroiodobenzene (*J*) 191
p-Fluoroiodobenzene (*J*) 191
Fluoromethane 148; (*J*) 94, 107, 109, 148
m-Fluoromethylbenzene (*J*) 191
o-Fluoromethylbenzene (*J*) 191
p-Fluoromethylbenzene (*J*) 191
m-Fluoronitrobenzene (*J*) 191
o-Fluoronitrobenzene (*J*) 191
p-Fluoronitrobenzene (*J*) 191
exo-2-Fluoronorbornane 146; (*J*) 146
p-Fluoro-α-phenylethyl cation 207
Fluorophosgene (*J*) 109
2-Fluoropyridine (*J*) 191
p-Fluorotoluene (*J*) 109
5-Fluorouracil 201
Folic acid 299
Formaldehyde (*J*) 97
Formaldehyde dimethylacetal (*J*) 94, 96
Formaldimine (*J*) 93
Formamide (*J*) 97
Formate anion in aq. sol. (*J*) 97
Formic acid 173; (*J*) 97; (fig.) 39; (T_1) 124
Formyl fluoride (*J*) 97, 109
Formyl-L-proline, *cis*- and *trans*- 280
α-L-Fucopyranose 250
β-L-Fucopyranose 250
Fumaric acid 175
Furan 198; (*J*) 101, 106
Furan-2-aldehyde 198
Furan-2-carboxylic acid 198

Galacitol 262
α-D-Galactopyranose 250
β-D-Galactopyranose 250
D-Galactose (fig.) 32
Galanthine 246
Gelsemine 242
Geraniol 222
α-D-Glucopyranose 249
β-D-Glucopyranose 249
α-D-Glucopyranose pentaacetate 249
β-D-Glucopyranose pentaacetate 249
1-^{13}C-D-Glucose (fig.) 23
D-Glucose (fig.) 103, 248
L-Glutamic acid 278
L-Glutamine 280
Glutathione 287
Glutathione, oxidized 287
Glycerol 262
Glycine 276; (*J*) 108
Glycine ethyl ester 276
Glycine hydrochloride 276
Glycol 262
Glycylalanine (fig.) 85
Glycylalanine, protected 286
Grammicidin S (T_1) 123
Grevillin B 297
Guanosine 272
Guanosine-5′-monophosphate 272
Guttapercha (T_1) 124

Heptadeuteriodimethylformamide 69; (*J*) 69
1,2-Heptadiene 141
Heptanal 160
n-Heptane 131
1-Heptanol 150
2-Heptanol 150
3-Heptanol 150
4-Heptanol 150
(*E*)-2-Heptenoic acid 173
(*Z*)-2-Heptenoic acid 173
3-Hepten-2-one 165
Heptylamine 178
1-Heptyne 141
2-Heptyne 141
3-Heptyne 141
Hexachloroethane 148
Hexadeuterioacetone 69; (*J*) 69
Hexadeuteriobenzene 69; (*J*) 69
Hexadeuteriodimethylsulfoxide 69; (*J*) 69; (fig.) 21
Hexadeuterioethanol 69; (*J*) 69
1,2-Hexadiene 141
1,5-Hexadiene 139
Hexafluoroacetone hydrate (*J*) 109
Hexafluorodiethyl ether (*J*) 109
Hexamethylbenzene 185
2,2,4,4,6,6-Hexamethyl-1,3-dioxane 158
Hexamethylphosphoramide 69; (*J*) 69; (fig.) 31
n-Hexane 71, 131
1-Hexanol 150
2-Hexanol 150
3-Hexanol 150
2-Hexanone 160
1-Hexene 138
cis-2-Hexene 75, 138
trans-2-Hexene 75, 138
cis-3-Hexene 138
trans-3-Hexene 139
(*E*)-2-Hexene (see *trans*-2-Hexene)

(*Z*)-2-Hexene (see *cis*-2-Hexene)
(*E*)-2-Hexenoic acid 173
(*Z*)-2-Hexenoic acid 173
3-Hexen-2-one 165
4-Hexen-2-one 165
5-Hexen-3-one 165
Hexylamine 178
1-Hexyne 141
2-Hexyne 141
3-Hexyne 141
L-Histidine 280
DL-Homocystine 276
β-Hydrastine 244
Hydrogen cyanide (*J*) 93, 98
Hydroquinone 186
m-Hydroxyacetophenone 167
o-Hydroxyacetophenone 77, 168
p-Hydroxyacetophenone 167
2-Hydroxybenzaldehyde 166
3-Hydroxybenzaldehyde 166
4-Hydroxybenzaldehyde 166
6-Hydroxycoumarin 297
7-Hydroxycoumarin 297
17*β*-Hydroxy-2*α*-fluoroandrost-4-en-3-one 232; (*J*) 229
2-Hydroxy-6-methoxyacetophenone 169
2-Hydroxy-3-methoxybenzaldehyde 166
4-Hydroxy-3-methoxybenzaldehyde 166
5-Hydroxymethyluracil 201
endo-2-Hydroxynorbornane 151
exo-2-Hydroxynorbornane 151
3*β*-Hydroxy-5*β*-pregn-16-en-20-one 234
11*α*-Hydroxyprogesterone 234
5-Hydroxyuracil (Barbituric acid) 201
5-Hydroxyuridine 270
Hypoxanthine 270

Imidazole 199; (*J*) 99, 101
Imidazole anion 199
Imidazole cation 199
Indole 203
Indolizidine 298
Indolo[2,3-a]quinolizine 298
Inosine 270
Inosine-5′-monophosphate 270
L-*chiro*-Inositol 263
epi-Inositol 263
myo-Inositol 263
scyllo-Inositol 263
o-Iodoacetophenone 167
(*E*)-3-Iodoacrylic acid 174
(*Z*)-3-Iodoacrylic acid 174
Iodobenzene 185; (*J*) 106, 190
Iodoethane 145, 148
Iodoethene (Vinyliodide) 149; (*J*) 149
Iodoform 148
1-Iodoheptane 145
1-Iodohexane 71
cis-1-Iodohexene 149
trans-1-Iodohexene 149
cis-3-Iodohex-3-ene 149
trans-3-Iodohex-3-ene 149
1-Iodohexyne 149
Iodomethane 148; (*J*) 148
2-Iodo-2-methylpropane (*t*-Butyliodide) 145, 149
1-Iodopentane 145
2-Iodopropane 145, 149
6-Iodopurine 270
2-Iodothiophene 199
3-Iodothiophene 199
5-Iodouracil 201
α-Ionone 225
β-Ionone 226
Isoborneol (fig.) 84
Isobutane 131
Isobutylamine 178
N-Isobutyl-N-nitrosoaniline 181
Isobutyrophenone 169
L-Isoleucine 276
Isopimaradiene 224
Isopimaric acid 225
Isopimarol 225
o-Isopropylacetophenone 167
p-Isopropylacetophenone 167
Isopropylamine 178
Isopropylbenzene 185
4-Isopropylbenzenonium ion 207
Isopropyl cation 206
trans-4-Isopropylcyclohexanol 152
2-Isopropylidene-2-cyclopentenone 165
Isoquinoline 202, 217
Isothiazole 199
Isovirescenol A 291
Isovirescenol B 291
Isoxazole 199

Jervine 240

Ketene 73
Kojic acid 297

D-Lactose 261; (fig.) 259
Lanosterol 237
L-Leucine 276
Leucomelon 297
Leucylleucine, protected 286
Limonene 223, 296
Linalool 222; (fig.) 219; (T_1) 120
Lycorenine 247
Lysergic acid methyl ester 298
L-Lysine 209, 278

α-D-Lyxopyranose 254
β-D-Lyxopyranose 254

Maleic acid 175
Malodinitril (J) 96
Malonic acid (J) 96
Maltol 297
Maltose 260
D-Mannitol 262
α-D-Mannopyranose 251
β-D-Mannopyranose 251
Meliobiose 261
Menthane 223, 296
Menthol 223; (fig.) 46
Mesaconic acid 175
Mesitylene 185; (J) 99
Mesitylenonium ion 207
Mesoporphyrin dimethyl ester 288
Methacrylic acid 173
Methane 71, 131; (J) 69, 107
Methanol 69, 150; (J) 69, 96; (fig.) 27
L-Methionine 276
m-Methoxyacetophenone 167
o-Methoxyacetophenone 167
p-Methoxyacetophenone 167
4-Methoxybenzaldehyde 166
2-Methoxybenzoic acid 187
3-Methoxybenzoic acid 187
p-Methoxybenzyl cation 207
1-Methoxybicyclo[2.2.2]octane 147
p-Methoxycumyl cation 207
7-Methoxyflavone 297
4-Methoxyisobutyrophenone 169
7-Methoxyisoflavone 297
4-Methoxy-2-methylpivalophenone 169
5-Methoxy-2-methylpivalophenone 169
p-Methoxy-α-phenylethyl cation 207
4-Methoxypivalophenone 169
4-Methoxypropiophenone 169
6-Methoxypurine 270
6-Methoxy-α-tetralone (fig.) 47
5-Methoxyuracil 201
Methyl acetate 154; (fig.) 28; (T_1) 124
2-Methylacetophenone (see *o*-Methylacetophenone
m-Methylacetophenone 167
o-Methylacetophenone 75, 167
p-Methylacetophenone 167
Methyl-2-O-acetyl-4,6-O-benzylidene-3-deoxy-3-O-(1,3-dithiane-2-yl)-α-D-altropyranoside 252
Methyl-3-O-acetyl-4,6-O-benzylidene-2-deoxy-2-O-(1,3-dithiane-2-yl)-α-D-altropyranoside 252
1-Methyl-2-acetylpyrrole 199
Methyl-α-D-altropyranoside 251
Methylamine 178; (J) 93, 96, 108
6-N-Methylamino-9-(β-D-ribofuranosyl)-purine 272
Methylammonium ion (J) 108
N-Methylaniline 186
9-Methylanthracene (T_1) 120
Methyl-α-D-arabinopyranoside 253
Methyl-β-D-arabinopyranoside 253
2-Methylarsabenzene 200
1-Methylazetidine 198
1-Methylaziridine 198
trans-N-Methylbenzaldimine (J) 108
N-Methylbenzaldimine (J) 179
4-Methylbenzenonium ion 207
Methyl benzoate 176; (J) 191
4-Methylbenzonitrile 180
2-Methyl-*p*-benzoquinone 170
Methyl-4,6-O-benzylidene-α-D-allopyranoside 251
Methyl-4,6-O-benzylidene-α-D-altropyranoside 252
Methyl-4,6-O-benzylidene-β-D-altropyranoside 252
Methyl-4,6-O-benzylidene-3-amino-3-deoxy-α-D-allopyranoside 251
Methyl-4,6-O-benzylidene-3-amino-3-deoxy-α-D-altropyranoside 252
Methyl-4,6-O-benzylidene-3-amino-3-deoxy-α-D-glucopyranoside 249
Methyl-4,6-O-benzylidene-3-amino-3-deoxy-α-D-mannopyranoside 251
Methyl-4,6-O-benzylidene-3-deoxy-α-D-arabino-hexopyranoside 253
Methyl-4,6-O-benzylidene-3-deoxy-α-D-ribo-hexopyranoside 253
Methyl-4,6-D-benzylidene-2,3-dideoxy-α-D-erythrohexopyranoside 251
Methyl-4,6-O-benzylidene-α-D-glucopyranoside 249
Methyl-4,6-O-benzylidene-β-D-glucopyranoside 249
Methyl-4,6-O-benzylidene-α-D-mannopyranoside 251
1-Methylbicyclo[4.1.0]heptan-2-one 164
6-Methylbicyclo[4.1.0]heptan-2-one 164
1-Methylbicyclo[3.1.0]hexan-2-one 164
5-Methylbicyclo[3.1.0]hexan-2-one 164
Methyl bromide (J) 96
Methyl 2-bromobenzoate 176
3-Methyl-1,2-butadiene 141
2-Methylbutane 131
2-Methyl-1-butanol 150
3-Methyl-1-butanol 150
3-Methyl-2-butanol 150
3-Methylbutanone 162
2-Methyl-1-butene 138
2-Methyl-2-butene 138
3-Methyl-2-butenone 165
1-Methylbutylamine 178

2-Methylbutylamine 178
3-Methylbutylamine 178
Methylbutylsulfone 182
Methyl-β-cellobioside 260
Methyl chloride (*J*) 96
Methyl 2-chlorobenzoate 176
p-Methylcumyl cation 207
Methyl cyanide 180
Methylcyclohexane 135
1-Methylcyclohexanol 152, 153
cis-2-Methylcyclohexanol 152, 153
trans-2-Methylcyclohexanol 152, 153
cis-3-Methylcyclohexanol 152, 153, 211
trans-3-Methylcyclohexanol 152, 153
cis-4-Methylcyclohexanol 152, 153
trans-4-Methylcyclohexanol 152, 153
2-Methylcyclohexanone 160, 163
3-Methylcyclohexanone 160, 163
4-Methylcyclohexanone 160, 163
Methylcyclohexene 76
2-Methyl-2-cyclohexenone 165
3-Methyl-2-cyclohexenone 165
Methyl cyclohexyl ketone 162
Methylcyclopentane 134
1-Methylcyclopentanol 152
cis-2-Methylcyclopentanol 152
trans-2-Methylcyclopentanol 152
cis-3-Methylcyclopentanol 152, 153
trans-3-Methylcyclopentanol 152, 153
2-Methyl-2-cyclopentenone 165
3-Methyl-2-cyclopentenone 165
1-Methylcyclopentyl acetate 154
cis-2-Methylcyclopentyl acetate 154
trans-2-Methylcyclopentyl acetate 154
cis-3-Methylcyclopentyl acetate 154
trans-3-Methylcyclopentyl acetate 154
Methylcyclopropane (*J*) 105
6-Methylcytidine 270
cis-9-Methyldecalin 296
trans-9-Methyldecalin 296
2-Methyldecanal 160
Methyl-2-deoxy-4,6-O-benzylidene-3-C-(1,3-dithiane-2-yl)-α-D-glucopyranoside 250
Methyl-2-deoxy-4,6-O-benzylidene-3-C-(2-methyl-1,3-dithiane-2-yl)-α-D-glucopyranoside 250
Methyl 2,6-dichlorobenzoate 176
Methyl 2,6-diethylbenzoate 176
1-Methyl-2,2-difluoronorbornane 146; (*J*) 146
endo-3-Methyl-2,2-difluoronorbornane 146; (*J*) 146
exo-3-Methyl-2,2-difluoronorbornane 146; (*J*) 146
endo-5-Methyl-2,2-difluoronorbornane 146; (*J*) 146
exo-5-Methyl-2,2-difluoronorbornane 146; (*J*) 146
endo-6-Methyl-2,2-difluoronorbornane 146; (*J*) 146
exo-6-Methyl-2,2-difluoronorbornane 146, (*J*) 146
anti-7-Methyl-2,2-difluoronorbornane 146; (*J*) 146
syn-7-Methyl-2,2-difluoronorbornane 146; (*J*) 146
16α-Methyl-11β,21-dihydroxy-9α-fluoropregna-1,4-diene-3,20-dione 234; (*J*) 229
N-Methyl-6,7-dimethoxy-1,2,3,4-tetrahydroisoquinoline 298
Methyl 4-dimethylaminobenzoate 176
Methyl 2,3-dimethylbenzoate 176
Methyl 2,6-dimethylbenzoate 176
Methyl-2,6-O-dimethyl-α-D-galactopyranoside 250
2-Methyl-1,3-dioxane 157
4-Methyl-1,3-dioxane 157
5-Methyl-1,3-dioxane 157
Methylenchloride 69; (*J*) 69
Methylenecyclobutane 138; (*J*) 97
Methylenecycloheptane (*J*) 97, 100
Methylenecyclohexane 139; (*J*) 97, 100
Methylenecyclopentane 138; (*J*) 97, 100
3,4-Methylenedioxybenzaldehyde 166
Methyl-α-D-erythrofuranoside 254
Methyl-β-D-erythrofuranoside 254
Methyl fluoride (*J*) 96
Methyl formate (*J*) 97; (T_1) 124
2-Methylfuran 198
3-O-Methyl-D-galacitol 262
Methyl-α-D-galactopyranoside 250
Methyl-β-D-galactopyranoside 250
3-O-Methyl-α-D-glucopyranose 249
3-O-Methyl-β-D-glucopyranose 249
Methyl-α-D-glucopyranoside 249
Methyl-β-D-glucopyranoside 249
2-Methyl-1-heptene 139
2-Methyl-2-heptene 139
2-Methylhexane 132
2-Methyl-2-hexene 139
cis-3-Methyl-2-hexene 139
trans-3-Methyl-2-hexene 139
3-Methyl-3-hexen-2-one 165
4-Methyl-3-hydroxy-1-butyne 151
3-Methyl-3-hydroxy-1-pentyne 151
Methyl-α-D-idopyranoside 252
1-Methylindole 203
2-Methylindole 203
3-Methylindole 203
4-Methylindole 203
5-Methylindole 203
6-Methylindole 203
7-Methylindole 203
D-3-O-Methyl-*chiro*-inositol 263

L-2-O-Methyl-*chiro*-inositol 263
D-1-O-Methyl-*myo*-inositol 263
Methyl iodide (*J*) 96
Methyl 2-iodobenzoate 176
2-Methylisobutyrophenone 169
Methyl isocyanate 180
Methyl isocyanide 72, 180; (*J*) 179
3-Methyl-6-isopropyl-2-cyclohexenone (piperitone) 165
Methyl-3,4-O-isopropylidene-3-C-(1,3-dithiane-2-yl)-β-D-ribopyranoside 253
Methyl-3,4-O-isopropylidene-3-C-(2-methyl-1,3-dithiane-2-yl)-β-D-ribopyranoside 254
3-Methylisothiazole 199
4-Methylisothiazole 199
5-Methylisothiazole 199
Methyl isothiocyanate 180; (*J*) 108
Methyl-β-lactoside 261
Methyl-α-D-lyxofuranoside 254
Methyl-β-D-lyxofuranoside 254
Methyl-β-maltoside 260
Methyl-α-D-mannopyranoside 251
Methyl-β-D-mannopyranoside 251
6-Methylmercaptopurine 270
Methyl 4-methoxybenzoate 176
Methyl 2-methylbenzoate 176
Methyl 3-methylbenzoate 176
Methyl 4-methylbenzoate 176
Methyl-3-O-methyl-β-D-galactopyranoside 250
Methyl 2-methyl-2-propyl ether 157
1-Methylnaphthalene (T_1) 120
Methyl 2-nitrobenzoate 176
Methyl 4-nitrobenzoate 176
2-Methyl-2-nitropropane 181
N-Methyl-N-nitrosoaniline 181
1-Methylnorbornane 137
7-Methylnorbornane 137
endo-2-Methylnorbornane 75, 137
exo-2-Methylnorbornane 75, 137
1-Methyl-2-norbornanol (*endo*) 151
1-Methyl-2-norbornanol (*exo*) 151
endo-3-Methyl-2-norbornanol (*endo*) 151
endo-3-Methyl-2-norbornanol (*exo*) 151
exo-3-Methyl-2-norbornanol (*endo*) 151
exo-3-Methyl-2-norbornanol (*exo*) 151
1-Methyl-2-norbornanone 164, 224
endo-3-Methyl-2-norbornanone 164, 224
exo-3-Methyl-2-norbornanone 164
exo-5-Methyl-2-norbornanone 164
endo-6-Methyl-2-norbornanone 164
exo-6-Methyl-2-norbornanone 164
anti-7-Methyl-2-norbornanone 164
syn-7-Methyl-2-norbornanone 164
1-Methylnorbornene 140
endo-5-Methylnorbornene 140
exo-5-Methylnorbornene 140
anti-7-Methylnorbornene 140
syn-7-Methylnorbornene 140
Methyloctylsulfide 182
Methyl orthoformate (*J*) 94, 96
Methyl palmitoleate 292
2-Methyl-2,3-pentadiene 141
3-Methylpentadienyl anion 72
2-Methylpentane 131
3-Methylpentane 131
4-Methyl-2-pentanol 150
4-Methyl-3-pentanol 151
4-Methyl-2-pentanone 162
4-Methyl-3-pentanone 162
2-Methyl-1-pentene 138
2-Methyl-2-pentene 138
3-Methyl-1-pentene 138
4-Methyl-1-pentene 138
cis-3-Methyl-2-pentene 138
trans-3-Methyl-2-pentene 138
cis-4-Methyl-2-pentene 138
(*E*)-4-Methyl-2-pentenoic acid 173
(*Z*)-4-Methyl-2-pentenoic acid 173, 212
3-Methyl-3-penten-2-one 165
3-Methyl-4-penten-2-one 165
4-Methyl-3-penten-2-one (mesityl oxide) 165
3-Methyl-7-(2-phenoxyacetamido)-3-cepham 294
p-Methyl-α-phenylethyl cation 207
2-Methylphosphabenzene 200
1-Methylpiperazine 198
2-Methylpiperazine 198
1-Methylpiperidine 198
2-Methylpiperidine 198
3-Methylpiperidine 198
4-Methylpiperidine 198
2-Methylpivalophenone 169
2-Methylpropane 71; (*J*) 105
2-Methyl-1-propanol 150
2-Methyl-2-propanol 150
2-Methylpropiophenone 169
2-Methyl-2-propyl acetate 154
Methyl 2-propyl ether 157
Methylpropylsulfone 182
6-Methylpurine 270
2-Methylpyridine 200
3-Methylpyridine 200
4-Methylpyridine 200
4-Methylpyridine N-oxide 200
1-Methylpyrrole 199
2-Methylpyrrole 199
1-Methylpyrrole-2-carboxylic acid 199
1-Methylpyrrolidine 198
Methyl-α-D-ribofuranoside 253
Methyl-β-D-ribopyranoside 253
1-Methylspiro[2.4]heptan-4-one 164
1-Methylspiro[2.5]octan-4-one 164

7α-Methyltestosterone 231
N-Methyltetrahydroharmine 298
3-Methyl-5,6,7,8-tetrahydroquinoline (fig.) 29; (T_1) 118
Methyl-2,3,4,6-tetra-O-methyl-β-D-galactopyranoside 250
2-Methylthiazole 199
4-Methylthiazole 199
2-Methylthiophene 199
3-Methylthiophene 199
Methyl-α-L-threofuranoside 254
Methyl-β-L-threofuranoside 254
Methyl 2,4,6-tribromobenzoate 176
16α-Methyl-11β,17α,21-trihydroxy-9α-fluoropregna-1,4-diene-3,20-dione 235; (*J*) 229
Methyl 2,4,6-trimethylbenzoate 176
Methyl 2,4,6-trinitrobenzoate 176
2-Methylundecanal 160
Methyl-α-D-xylopyranoside 254
Methyl-β-D-xylopyranoside 254
Monofluoroacetic acid (*J*) 109
Montanine 246
(*Z*)-Mucobromic acid 175
(*Z*)-Mucochloric acid 175

Naphthalene 188, 217
Naphthyridine 217
Narcotine (fig.) 245
Natural rubber (T_1) 124
Nebularine 270
Neopentane 131
Nicotinamide 298
Nicotine 241; (fig.) 47, 67
Nicotine methiodide 241
m-Nitroacetophenone 167
o-Nitroacetophenone 167
p-Nitroacetophenone 167
2-Nitroaniline 187
3-Nitroaniline 187
4-Nitroaniline 187
2-Nitrobenzaldehyde 166
4-Nitrobenzaldehyde 166
Nitrobenzene 187; (*J*) 99, 106; (T_1) 117
2-Nitrobenzoic acid 187
3-Nitrobenzoic acid 187
3-Nitrobenzonitrile 180
4-Nitrobenzonitrile 180
Nitrocyclohexane 181
Nitroethane 181
p-Nitrofluorobenzene (*J*) 109
Nitrohexane 181
Nitromethane 69, 181; (*J*) 69, 96
m-Nitrophenyl-β-D-galactopyranoside 250
o-Nitrophenyl-β-D-galactopyranoside 251
p-Nitrophenyl-α-D-galactopyranoside 250
m-Nitrophenyl-β-D-glucopyranoside 249
o-Nitrophenyl-β-D-glucopyranoside 249
p-Nitrophenyl-α-D-glucopyranoside 249
p-Nitrophenyl-β-D-glucopyranoside 249
p-Nitrophenyl-α-D-mannopyranoside 251
2-Nitropropane 181
N-Nitrosodi-*n*-butylamine 181
N-Nitrosodiethylamine 181
N-Nitrosodiisobutylamine 181
N-Nitrosodiisopropylamine 181
N-Nitrosodimethylamine 181
N-Nitrosodi-*n*-propylamine 181
2-Nitrotoluene 187
4-Nitrotoluene 187
5-Nitrouracil 201
Nonactine 299
Nonanal 160
n-Nonane 131
1-Nonanol 150
5-Nonanol 150
2-Nonanone 162
5-Nonanone 162
(*E*)-2-Nonenoic acid 173
Nonylamine 178
19-Norandrost-4-ene-3,17-dione 232
Norbornadiene 140
Norbornane 137, 211, 296
2-Norbornanone 164, 223
Norbornene 140
Norbornyl cation 206
19-Nor-7α-methyltestosterone 232
19-Nortestosterone 231

Octadecadeuteriohexamethylphosphoramide 69; (*J*) 69
Octadeuterio-1,4-dioxane 69; (*J*) 69
Octadeuteriotetrahydrofuran 69; (*J*) 69
1,2-Octadiene 141
1,7-Octadiene 139
cis,cis-2,6-Octadiene 139
cis-trans-2,6-Octadiene 139
trans,trans-2,6-Octadiene 139
cis,cis-3,5-Octadiene 73, 139
1,2,3,4,5,6,7,8-Octahydroanthracene 195
1,2,3,4,5,6,7,8-Octahydrophenanthrene 195
n-Octane 131
1-Octanethiol 182
1-Octanol 150
2-Octanol 150
3-Octanol 150
4-Octanol 150
2-Octanone 162
1-Octene 139
cis-2-Octene 139
trans-2-Octene 139
cis-3-Octene 73, 139
trans-3-Octene 139

cis-4-Octene 139
trans-4-Octene 139
(*Z*)-2-Octenoic acid 173
Octylamine 178
1-Octyne 141
2-Octyne 141
3-Octyne 141
4-Octyne 141
L-Ornithine hydrochloride 278
Oxetane 198
Oxindole 242
Oxirane 198

Paracyclophane 195
Penicillin Derivates 274
Pentachloroethane 148; (*J*) 148
Pentadeuteriopyridine 69; (*J*) 69
1,2-Pentadiene 141
1,4-Pentadiene 138
2,3-Pentadiene 141
Pentadienyl anion 72
Pentaerythritol 262
2,3,4,5,6-Pentamethylacetophenone 168
2,2,4,4,6-Pentamethyl-1,3-dioxane 158
2,4,4,6,6-Pentamethyl-1,3-dioxane 158
2,2-*trans*-4,5-*cis*-6-Pentamethyl-1,3-dioxane 158
2,3,4,5,6-Pentamethylisobutyrophenone 169
2,3,4,5,6-Pentamethylpropiophenone 169
Pentanal 160
n-Pentane 131
1-Pentanol 150
2-Pentanol 150
3-Pentanol 150
3-Pentanone 162; (*J*) 105
1-Pentene 138
cis-2-Pentene 138
trans-2-Pentene 138
(*E*)-2-Pentenoic acid 173
(*Z*)-2-Pentenoic acid 173
3-Penten-2-one 165
4-Penten-2-one 165
Pentylamine 178
Phenanthrene 188
Phenazine 202
Phenol 186; (T_1) 117
Phenoxyacetylene (*J*) 100
1-Phenoxy-1-propyne (*J*) 100
o-Phenylacetophenone 167
Phenylacetylene (*J*) 98, 106; (T_1) 113, 117
Phenylalanine 280
Phenylbenzoate (T_1) 121
Phenylcyanate 187
m-Phenylendiamine 186
o-Phenylendiamine 186
p-Phenylendiamine 186
α-Phenylethyl cation 207
Phenylethynyl cyanide (*J*) 106
9-Phenyl-[9-^{13}C]-fluorenyl, dimer 194
Phenyl-β-D-galactopyranoside 251
Phenyl-β-D-glucopyranoside 249
Phenylhydrazine 186
Phenylisocyanate 187
Phenylisothiocyanate 187
(*E*)-3-Phenylpropenal 160
Phosphabenzene 200
Phosphetanes (T_1) 121
Phosphoenolpyruvate 299
Phthalazine 202
Phytol 125; (T_1) 125
3-Picoline 241
Pimaradiene 224
$\Delta^{8(9)}$-Pimaradiene-1 225
$\Delta^{8(9)}$-Pimaradiene-2 225
Pimaric acid 224
Pimarol 224
α-Pinene 223, 296
β-Pinene 223, 296
Piperazine hexahydrate 198
Piperidine 198
Piperine 243
Pivalophenone 169
Poly(β-benzyl L-glutamate) (T_1) 123
Polyporic acid 297
Polystyrene, *atactic* 185
Polystyrene, *isotactic* 185
Polyvinylchloride 144
Prodigiosin 295
Progesterone 233
L-Pro-L-Glu-Phe-NH_2, protected tripeptide (fig.) 283
L-Proline 280
Propanal 74, 160
Propane 71, 131; (*J*) 96
1,2-Propanediol 262
1-Propanethiol 182
1-Propanethiolate 182
Propanoic acid 74
1-Propanol 150; (*J*) 105
2-Propanol 150; (*J*) 96, 105
Propenal 74, 160
Propene 138; (*J*) 96
Propenoic acid 74
Propionic acid 173
Propionitrile (*J*) 105, 108
Propiophenone 169
2-Propyl acetate 154
Propylamine 178
Propylbenzene 185
4-Propylbenzenonium ion 207
iso-Propyl cyanide (*J*) 105
N-*n*-Propyl-N-nitrosoaniline 181
Propynal (*J*) 100

Propyne (*J*) 96, 98, 105, 106
Propynol (*J*) 98; (fig.) 57
Prostaglandin E1 297
Prostaglandin F2α 297; (T_1) 125
Protonated acrolein 206
Protonated crotonaldehyde 206
Protonated 2-cyclohexen-1-one 206
Protonated 2-cyclopenten-1-one 206
Protonated 3,5-dimethyl-2-cyclohexen-1-one 206
Protonated methyl vinyl ketone 206
Protonated tiglaldehyde 206
Protoporphyrin diethyl ester 288
Pteridine 299
Pulegone 223
Purine 270
Pyrazine 201
Pyrazine cation 201
Pyrazine dication 201
Pyrazole 199; (*J*) 99, 101
Pyrazole anion 199
Pyrazole cation 199
Pyrene 188
Pyridazine 200
Pyridazine cation 200
Pyridine 69, 200, 210; (*J*) 69, 99, 101, 106, 108; (fig.) 196
Pyridine-2-aldehyde 200
Pyridine-3-aldehyde 200
Pyridine-4-aldehyde 200
Pyridine-3-carboxylic acid methyl ester 200
Pyridine cation 200
Pyridine N-oxide 200
Pyridinium ion (*J*) 108
Pyridoxamine 298
Pyridoxine 298
Pyrimidine 201
Pyrimidine cation 201
Pyrimidine dication 201
Pyroglutamic acid 280
α-Pyrone 297
Pyrrole 199; (*J*) 99, 101, 106
Pyrrole anion 199
Pyrrolidine 198

Quadricyclene 137
Quinazoline 202, 217
Quinine 298
Quinoline 202, 217; (fig.) 36, 79, 81, 82
Quinolizidine 298
Quinoxaline 202
Quinuclidine 298

Resorcinol 186
α-L-Rhamnopyranose 251
β-L-Rhamnopyranose 251
Ribitol 262
α-D-Ribofuranose 253
β-D-Ribofuranose 253
Ribonuclease A (T_1) 123
α-D-Ribopyranose 253
β-D-Ribopyranose 253
9-β-D-Ribopyranosyladenine 270
D-Ribose (fig.) 255

Saccharose 261; (T_1) 127
Salicylaldehyde 77
Salicylic acid 74
Sandaracopimaric acid 225
Sarcosine 276
Selenophene 199; (*J*) 101
Sepedonin 292
L-Serine 276
Setoclavine (fig.) 245
Sinomenine 299
D-Sorbitol 262
Squalene 223
Starch (Amylose) 299
Sterigmatocystin 290
Stibabenzene 200
cis-Stilbene (*J*) 97
trans-Stilbene (*J*) 97
Styrene 185; (*J*) 105; (T_1) 117
Sucrose (see saccharose)

β-D-Talofuranose 252
α-D-Talopyranose 252
β-D-Talopyranose 252
Tazettine 244
Testosterone 231
Testosterone acetate 231
3,4,5,6-Tetrachloro-*o*-benzoquinone 170
2,3,5,6-Tetrachloro-*p*-benzoquinone 170
1,1,1,2-Tetrachloroethane 148; (*J*) 148
1,1,2,2-Tetrachloroethane 148; (*J*) 100, 148
Tetrachloroethane 149
2,3,9,10-Tetracyano-6,13-dibutyl-1,8-dihydrotetraaza[14]annulene (fig.) 204
Tetracyclin hydrochloride 299
Tetradeuterioacetic acid 69; (*J*) 69
Tetradeuteriomethanol 69; (*J*) 69; (fig.) 31
1,1,3,3-Tetraethoxypropane (fig.) 41
Tetraethylammonium ion (*J*) 108
Tetrafluoromethane (*J*) 109
Tetrahydrofuran 69, 198; (*J*) 69, 99
Tetrahydropyran 198
Tetrahydrothiophene 198
Tetralin 195; (*J*) 195
2,3,4,6-Tetramethylacetophenone 168
2,3,5,6-Tetramethylacetophenone 168
Tetramethylammonium acetate 173
Tetramethylammonium butyrate 173
Tetramethylammonium formate 173

Tetramethylammonium ion (*J*) 107, 108
Tetramethylammonium propionate 173
Tetramethylammonium valerate 173
2,2′,6,6′-Tetramethylbiphenyl (T_1) 121
Tetramethylborate anion (*J*) 107
2,2,5,5-Tetramethyl-1,3-dioxane 157
4,4,6,6-Tetramethyl-1,3-dioxane 158
2,2,4,6-*cis*-Tetramethyl-1,3-dioxane 157
2,4,4,6-*cis*-Tetramethyl-1,3-dioxane 157
2,4,4,6-*trans*-Tetramethyl-1,3-dioxane 157
2,4,5,5-*cis*-Tetramethyl-1,3-dioxane 158
2,4-*cis*-5-*trans*-6-*cis*-Tetramethyl-1,3-dioxane 157
2,2-*trans*-4,6-Tetramethyl-1,3-dioxane 157
2,3,5,6-Tetramethylisobutyrophenone 169
2,2,4,4-Tetramethyl-3-pentanol 151
2,2,4,4-Tetramethyl-3-pentanone 162
Tetramethylphosphonium ion (*J*) 107
2,2,6,6-Tetramethylpiperidine 198
2,3,4,6-Tetramethylpivalophenone 169
2,3,5,6-Tetramethylpropiophenone 169
Tetramethylsilane (*J*) 107
Tetramethylstannane (*J*) 107
Tetramethylthiourea 183
Tetramethylurea 183
2,3,5,6-Tetraphenyl-*p*-benzoquinone 170
s-Tetrazine 201
Tetrazole (*J*) 99
Thebain 299
Thiacyclohexane 182, 198
Thiacyclohexane-1,1-dioxide 182
Thiacyclohexane-1-oxide 182
Thiamine hydrochloride 299
Thiazole 199
Thietane 198
Thiirane 198
Thioanisol 186
Thiocamphor 183
2-Thiocytidine 270
6-Thioguanosine 272
6-Thioinosine 270
Thiophene 190; (*J*) 101, 106
Thiophene-2-aldehyde 199
Thiophene-3-aldehyde 199
Thiophenol 186
4-Thiothymidine 270
4-Thiouridine 270
6-Thioxanthosine 272
L-Threonine 276
Thymidine 270; (fig.) 266
Thymidine-5′-monophosphate 270
Tiglic acid 173
Toluene 76, 185; (*J*) 96, 191; (T_1) 117
p-Toluenesulfonic acid 187
p-Toluenesulfonylchloride 187
m-Toluic acid 187
o-Toluic acid 187
p-Toluic acid 187
Trehalose 260
2,4,6-Triaminopyrimidine 201, 204; (*J*) 204
4,5,6-Triaminopyrimidine 201, 204; (*J*) 204
1,4,8-Triazaindene 203
s-Triazine 201
1,2,3-Triazole 199; (*J*) 99
1,2,4-Triazole 199; (*J*) 99, 101
2,4,6-Tribromoacetophenone 169
Tributylamine 178
Tri-*t*-butylethylene (*J*) 97
Trichloroacetaldehyde (*J*) 100
2,3,3-Trichloroacrylic acid 174
1,1,1-Trichloroethane 148; (*J*) 148
1,1,2-Trichloroethane 148; (*J*) 148
Trichloroethene 149; (*J*) 149
2,4,6-Trichloropyrimidine 201; (fig.) 44
Tricyclene 137
Trideuterioacetonitrile 69; (*J*) 69
Trideuterionitromethane 69; (*J*) 69
Triethylamine 178
Trifluoroacetic acid (*J*) 109
Trifluoroacetone (*J*) 109
1,1,1-Trifluoroethane (*J*) 109
2,2,2-Trifluoroethanol (*J*) 109
Trifluoromethane (*J*) 94, 96, 109, 148
p-Trifluoromethylcumyl cation 207
p-Trifluoromethylfluorobenzene (*J*) 109
p-Trifluoromethyl-α-phenylethyl cation 207
Trihexylamine 178
2,4,6-Trihydroxyacetophenone 169
2β,3β,14 α-Trihydroxy-5β-cholest-7-en-6-one 238
11β,17α,21-Trihydroxypregna-1,4-diene-3,20-dione 234
2,3,3-Triiodoacrylic acid 174
2,4,6-Triisopropylacetophenone 168
2,4,6-Triisopropylisobutyrophenone 169
2,4,6-Triisopropylpropiophenone 169
2,4,5-Trimethylacetophenone 168
2,4,6-Trimethylacetophenone 168
Trimethylamine 178
2,3,3-Trimethyl-2-butanol 151
1,1,2-Trimethylcyclohexane 135
1,1,3-Trimethylcyclohexane 135
1-*cis*-3-*cis*-5-Trimethylcyclohexane 135
1-*cis*-3-*trans*-5-Trimethylcyclohexane 135, 210
1-*trans*-2-*cis*-3-Trimethylcyclohexane 135
1-*trans*-2-*cis*-4-Trimethylcyclohexane 135
1-*trans*-2-*trans*-4-Trimethylcyclohexane 135
3,5,5-Trimethyl-2-cyclohexenone (isophorone) 165
3,3,5-Trimethyl-3-cyclohexenone 165
2,2,4-Trimethyl-1,3-dioxane 157
2,2,5-Trimethyl-1,3-dioxane 157
2,5,5-Trimethyl-1,3-dioxane 157
4,4,5-Trimethyl-1,3-dioxane 157

4,4,6-Trimethyl-1,3-dioxane 157
4,5,5-Trimethyl-1,3-dioxane 157
2,4,6-*cis*-Trimethyl-1,3-dioxane 157
2,4-*cis*-6-*trans*-Trimethyl-1,3-dioxane 157
4,5-*trans*-6-*cis*-Trimethyl-1,3-dioxane 157
Trimethylethylene (J) 97
3,3,5-Trimethyl-4-hexen-2-one 165
2,3,5-Trimethylindole 203
2,4,6-Trimethylisobutyrophenone 169
8,9,9-Trimethyl-5,8-methano-5,6,7,8-tetrahydroquinazoline (T_1) 119
2,4,4-Trimethyl-3-pentanol 151
2,2,4-Trimethyl-3-pentanone 162
2,4,4-Trimethyl-1-pentene 138
Trimethylphosphine (J) 107
1,2,4-Trimethylpiperazine 198
2,4,6-Trimethylpivalophenone 169
2,4,6-Trimethylpropiophenone 169
2,4,6-Trimethylpyridine (J) 99
Trimethylselenium ion (J) 107
4-Trimethylsilylbenzaldehyde 166
3-Trimethylsilylpropanesulfonic acid sodium salt 182
Trimethylsulfonium cation 182
Tripentylamine 178
Triphenylmethyl, dimer 192
Triphenylphosphine 187
Tripropylamine 178
Tropine 298
Tropolone 297
L-Tryptophane 280
L-Tyrosine 280

Uracil 201
Uridine 270
Uridine-5′-monophosphate 270

Valeric acid 173
L-Valinamide hydrobromide 276
L-Valine 276
Valylvaline, protected 286
Vanilline (fig.) 193
Veratramine 240
Veratramine diformate 240
Vinyl acetate 154
Vinyl fluoride (J) 97
Virescenoside A, aglycone 291
Virescenoside B, aglycone 291
Virescenoside C, aglycone 291
Vitamin A acetate 226

Xanthone 297
Xanthosine 272
m-Xylene 185
o-Xylene 185
p-Xylene 185
Xylitol 262
9-β-D-Xylofuranosyladenine 272
α-D-Xylopyranose 254
β-D-Xylopyranose 254
9-α-D-Xylopyranosyladenine 272
9-β-D-Xylopyranosyladenine 272

Author Index

The reference numbers are given in brackets. Numbers in italics refer to the pages on which the complete references are listed. All other numbers indicate the pages on which an author's work is cited.

Abragam, A. [16] *301*; 24, 126
Adam, W. [242] *306*; 184, 197, 272
Alger, T. D. [123] *304*; 112
Alger, T. D. [155] *305*; 124
Alger, T. D. [243] *306*; 184, 188, 189
Alger, T. D. [241] *306*; 184, 188
Alger, T. D. [266] *307*; 198, 199
Allerhand, A. [25] *301*; 33
Allerhand, A. [41] *302*; 48, 287
Allerhand, A. [107c] *304*; 101, 255
Allerhand, A. [129] *304*; 113, 114, 125, 129
Allerhand, A. [139] *304*; 119, 121
Allerhand, A. [152] *305*; 123
Allerhand, A. [148] *305*; 123
Allerhand, A. [149] *305*; 123, 284
Allerhand, A. [156] *305*; 124
Allerhand, A. [158] *305*; 126, 289
Allerhand, A. [331] *309*; 284
Alves, A. C. P. [100] *303*; 95
Ammon, R. v. [80] *303*; 82, 83, 84
Anderson, D. R. [349] *309*; 295
Anderson, J. H. [97] *303*; 95, 99
Anderson, W. A. [17] *301*; 24, 33
Anderson, W. A. [28] *301*; 37
Anderson, W. A. [31] *301*; 38
Andersson, K. [228] *306*; 172, 173, 174, 175
Anet, F. A. L. [84] *303*; 86, 88
Anet, F. A. L. [87] *303*; 89, 90
Anet, F. A. L. [88] *303*; 89, 90, 137
Anet, F. A. L. [124] *304*; 112
Anet, R. [84] *303*; 86, 88
Angyal, S. J. [298] *308*; 247, 248, 263
Archer, R. A. [325] *308*; 274
Armitage, I. M. [160] *305*; 127
Armitage, I. M. [161] *305*; 127, 128
Armitage, I. M. [173] *305*; 129
Armitage, I. M. [177] *305*; 129
Ashe, A. J. [267] *307*; 200

Babadjamian, A. [258] *307*; 197, 199
Bach, N. J. [296] *308*; 244, 264, 266, 271, 299
Bailey, W. F. [215] *306*; 155, 158
Balaban, A. T. [251] *307*; 194
Balogh, B. [288] *307*; 230, 231, 236, 296
Balogh, B. [345] *309*; 292
Barbarella, G. [233] *306*; 181, 182, 185, 198
Barcza, S. [38] *302*; 40
Baskevitch, Z. [344] *309*; 290, 291
Batchelor, J. G. [61a] *302*; 75, 80, 81, 282, 283
Batchelor, J. G. [61c] *303*; 75, 80, 81, 283
Batchelor, J. G. [61b] *303*; 75, 80, 81, 283
Bates, R. B. [55] *302*; 72, 180
Bauer, G. [50i] *302*; 68, 71, 73, 74, 75, 76, 98, 137, 166, 183, 185, 186, 187, 195, 198, 199, 200, 201, 204, 208, 213, 291, 298
Bauer, G. [50d] *302*; 68, 71, 73, 74, 75, 76, 98, 137, 291
Bayer, E. [322a] *308*; 273, 277, 279, 281, 283, 286, 287
Beatty, D. A. [54a] *302*; 72, 177, 180
Becconsall, J. K. [68b] *303*; 77, 138, 139, 141, 183
Becker, E. D. [24] *301*; 33
Becker, E. D. [7] *301*; 9, 21, 22, 33, 48, 55, 56, 110, 113
Becker, E. D. [3] *301*; 1, 19, 59, 64, 77
Becker, E. D. [115] *304*; 107, 108
Becker, E. D. [166] *305*; 128
Becker, E. D. [157] *305*; 125
Becker, R. S. [138] *304*; 118
Bellocq, A. [179] *305*; 129
Bennett, C. R. [287] *307*; 229, 234, 237, 238
Bennett, C. R. [286] *307*; 226, 229, 237
Berger, S. [137] *304*; 118, 120
Berger, S. [138] *304*; 118
Berger, S. [133] *304*; 115, 116
Berger, S. [172] *305*; 128
Berger, S. [226] *306*; 170, 171
Bernstein, H. J. [1] *301*; 1, 19, 59, 64
Bertrand, R. B. [162] *305*; 128
Beyer, K. [83] *303*; 83, 85
Bilik, V. [302] *308*; 247, 248, 251, 255, 258, 259, 260, 261
Bindra, J. S. [364] *309*; 299
Binsch, G. [111] *304*; 107, 108, 179
Birdsall, B. [81] *303*; 83
Birdsall, N. J. M. [143] *304*; 121, 122
Birdsall, N. J. M. [143] *304*; 121, 122
Birdsall, N. J. M. [174] *305*; 129
Birdsall, N. J. M. [147] *305*; 123
Birdsall, N. J. M. [146] *305*; 122, 129
Birdsall, N. J. M. [373] *309*; 298
Bisset, N. G. [366] *309*; 299
Black, E. P. [136] *304*; 118
Blackman, R. B. [18] *301*; 25
Bloch, F. [6] *301*; 7
Boaz, H. E. [296] *308*; 244, 264, 266, 271, 299
Boccalon, G. [336] *309*; 286
Boden, N. [13] *301*; 22, 48
Boekelheide, V. [244] *307*; 188, 189

Bovey, F. A. [4] *301*; 1, 59, 64, 77
Bovey, F. A. [323] *308*; 273, 281, 287
Boyd, D. R. [115] *304*; 107, 108
Brandt, J. [12] *301*; 18
Bradbury, E. M. [150] *305*; 123
Bradbury, E. M. [335] *309*; 286
Bradley, C. H. [88] *303*; 89, 90, 137
Breitmaier, E. [50j] *302*; 68, 71, 73, 74, 75, 76, 137, 208, 213, 291, 296
Breitmaier, E. [50i] *302*; 68, 71, 73, 74, 75, 76, 98, 137, 166, 183, 185, 186, 187, 195, 198, 199, 200, 201, 204, 208, 213, 291, 298
Breitmaier, E. [50d] *302*; 68, 71, 73, 74, 75, 76, 98, 137, 291
Breitmaier, E. [61d] *303*; 75, 80, 81, 283
Breitmaier, E. [71] *303*; 79, 80, 81, 196
Breitmaier, E. [75] *303*; 80, 81, 282, 283, 287
Breitmaier, E. [102] *303*; 98, 99, 100, 107, 109, 117, 120, 125, 160, 162, 166, 180, 185, 186, 187, 198, 199, 200, 222, 235, 271, 272, 281, 298
Breitmaier, E. [107b] *304*; 101, 253, 155
Breitmaier, E. [120] *304*; 110, 260, 264, 265, 267, 268
Breitmaier, E. [225] *306*; 192, 196, 240, 273, 284
Breitmaier, E. [299] *308*; 247, 248, 249, 250, 251, 266
Breitmaier, E. [297c] *308*; 247, 248, 260, 262, 268
Breitmaier, E. [297b] *308*; 247, 248, 253, 255, 260, 262, 268
Breitmaier, E. [297a] *308*; 247, 248, 252, 253, 260, 262, 268
Breitmaier, E. [321] *308*; 273, 274, 283, 284
Breitmaier, E. [322a] *308*; 273, 277, 279, 281, 283, 286, 287
Breitmaier, E. [324] *308*; 273, 277, 279, 283, 286
Breitmaier, E. [328] *308*, 283, 286
Breitmaier, E. [311] *308*; 260, 264, 265
Breitmaier, E. [309] *308*; 248, 250, 260, 262
Breitmaier, E. [308] *308*; 248, 250, 251, 253, 254, 256
Breitmaier, E. [306] *308*; 248, 268, 269
Breitmaier, E. [304] *308*; 248, 255, 256
Breitmaier, E. [305] *308*; 248, 258, 260
Breitmaier, E. [303] *308*; 247, 248, 255, 269
Breitmaier, E. [302] *308*; 247, 248, 251, 255, 258, 259, 260, 261
Breitmaier, E. [371] *309*; 298
Brenner, S. [55] *302*; 72, 180
Brettschneider, H. [248] *307*; 192
Brewer, C. F. [128] *304*; 113, 129
Brown, H. C. [274] *307*; 205
Brunner, H. [248] *307*; 192
Brunner, H. [249] *307*; 194
Buchanan, G. W. [88] *303*; 89, 90, 137
Buchanan, G. W. [213] *306*; 152
Buchanan, G. W. [237b] *306*; 186
Buckingham, A. D. [199] *306*; 142, 196
Buckingham, A. D. [203] *306*; 145
Buckwalter, B. L. [282] *307*; 219, 220, 224, 225
Buckwalter, B. L. [286] *307*; 226, 229, 237
Buckwalter, B. L. [285] *307*; 229, 232, 234, 235
Buckwalter, B. L. [344] *309*; 290, 291
Bürvenich, C. [306] *308*; 248, 268, 269
Bullock, E. [112] *304*; 107, 108
Burke, A. R. [86] *303*; 89, 91
Burke, A. R. [91] *303*; 92
Burke, J. J. [97] *303*; 95, 99
Burke, J. J. [183] *305*; 133, 134
Burlingame, A. L. [288] *307*; 230, 231, 236, 296
Burlingame, A. L. [345] *309*; 292
Burnett, L. J. [168] *305*; 128

Cagnoli-Bellavita, N. [344] *309*; 290, 291
Cardin, A. D. [256] *307*; 201
Cargioli, J. D. [70] *303*; 77, 80
Cargioli, J. D. [124] *304*; 112
Carman, C. J. [201] *306*; 143, 144, 145
Carr, H. Y. [23] *301*; 33
Carr, H. Y. [45] *302*; 55, 56
Carrol, M. [51] *302*; 68
Casu, B. [65] *303*; 74, 247, 248, 249, 251, 252, 254, 255, 257, 266
Casu, B. [108] *304*; 102
Caughey, W. S. [340] *309*; 287, 288, 289
Ceccherelli, P. [344] *309*; 290, 291
Chachaty, C. [144] *304*; 121, 124, 125
Chachaty, C. [176] *305*; 129
Chang, C. J. [296] *308*; 244, 264, 266, 271, 299
Chang, C. J. [292] *308*; 240, 242
Chang, C. J. [364] *309*; 299
Chauhan, M. S. [360] *309*; 297
Cheney, B. V. [59] *302*; 74
Cheney, B. V. [181] *305*; 133
Christensen, K. A. [136] *304*; 118
Christl, M. [184] *305*; 134, 135, 152, 153, 154, 155, 157, 190
Clarke, D. E. [237b] *306*; 186
Clerc, J. T. [50g] *302*; 68, 71, 73, 74, 75, 76, 137, 181, 198, 199, 208, 213, 291
Clerc, J. T. [50k] *302*; 68, 71, 73, 74, 75, 76, 137, 139, 166, 172, 185, 186, 187, 198, 199, 200, 201, 208, 213, 214, 215, 291
Clifton, M. [357] *309*; 297
Clouse, A. O. [280] *307*; 219, 220, 224
Clouse, A. O. [292] *308*; 240, 242
Cochran, D. W. [25] *301*; 33
Cochran, D. W. [41] *302*; 48, 287
Cochran, D. W. [149] *305*; 123, 284
Cochran, D. W. [280] *307*; 219, 220, 224
Cochran, D. W. [294] *308*; 242, 243
Cochran, D. W. [293] *308*; 241
Cochran, D. W. [292] *308*; 240, 242

Cochran, D. W. [364] *309*; 299
Cochran, D. W. [331] *309*; 284
Cohen, J. S. [78] *303*; 81
Cohen, J. S. [74] *303*; 80, 177, 273, 277, 279, 281
Cole, C. M. [55] *302*; 72, 180
Conway, E. [307] *308*; 248, 249, 250, 252, 253, 256
Cooley, J. W. [19] *301*; 27
Cooper, R. D. G. [325] *308*; 274
Cornfeld, E. C. [296] *308*; 244, 264, 266, 271, 299
Cowdry, S. E. [354] *309*; 297
Craig, L. C. [326] *308*; 277, 279, 281, 284
Crain, W. O. [291] *308*; 240, 243, 244, 246, 247
Crandall, J. K. [196] *306*; 141, 148
Crane-Robinson, C. [335] *309*; 286
Crecely, K. M. [209] *306*; 149
Crecely, R. W. [209] *306*; 149
Cremer, S. E. [141] *304*; 120
Cremer, S. E. [118] *304*; 110
Crow, W. D. [247] *307*; 192
Cussans, N. J. [359] *309*; 297
Cushley, R. J. [61a] *302*; 75, 80, 81, 282, 283
Cushley, R. J. [349] *309*; 295
Cyr, N. [94] *303*; 92
Cyr, N. [301] *308*; 247, 248, 254
Cyr, T. J. [94] *303*; 92

Dailey, B. P. [320] *308*; 272
Dalling, D. K. [64] *303*; 74, 135, 136
Dalling, D. K. [138] *304*; 118
Dalling, D. K. [188] *305*; 137
Dalling, D. K. [276] *307*; 210
Dalling, D. K. [350] *309*; 296
Davidson, E. W. [55] *302*; 72, 180
Del Re, G. [72] *303*; 80, 282, 283
Demarco, P. V. [325] *308*; 274
Dembech, P. [233] *306*; 181, 182, 185, 198
Dence, J. B. [186] *305*; 136, 137, 140, 145, 146, 151, 161, 164, 177, 178
Deslauriers, R. [178] *305*; 129
Deslauriers, R. [179] *305*; 129
Desnoyer, L. [50k] *302*; 68, 71, 73, 74, 75, 76, 137, 139, 166, 172, 185, 186, 187, 198, 199, 200, 201, 208, 213, 214, 215, 291
Dhami, K. S. [224] *306*; 167, 171
Dhami, K. S. [223] *306*; 167, 171
Ditchfield, R. [268b] *307*; 205
Djerassi, C. [229] *306*; 176, 178
Doddrell, D. [41] *302*; 48, 287
Doddrell, D. [139] *304*; 119, 121
Doddrell, D. [129] *304*; 113, 114, 125, 128
Doddrell, D. [156] *305*; 124
Doddrell, D. [149] *305*; 123, 284
Doddrell, D. [202] *306*; 145
Doddrell, D. [280] *307*; 219, 220, 224
Doddrell, D. [289] *308*; 230, 239, 240
Doddrell, D. [331] *309*; 284
Doddrell, D. [340] *309*; 287, 288, 289
McDonald, G. C. [43c] *302*; 52, 53, 55
Dop, D. A. v. [353] *309*; 297
Dorman, D. E. [66] *303*; 74, 247, 248, 249, 250, 251, 266
Dorman, D. E. [190] *305*; 137, 138, 139, 140, 212
Dorman, D. E. [313] *308*; 264, 266, 271, 273
Dorman, D. E. [298] *308*; 247, 248, 263
Dorman, D. E. [323] *308*; 273, 281
Dorn, H. C. [206] *306*; 147
Douglass, A. W. [96] *303*; 95
Druck, S. J. [157] *305*; 125
Druck, S. J. [166] *305*; 128
Dubischar, N. [329] *308*; 283, 284, 285, 286
Dunlap, R. B. [256] *307*; 201

Echols, R. E. [368] *309*; 298
Eggert, H. [229] *306*; 176, 178
Eisen, O. [195] *306*; 141
Eliel, E. L. [215] *306*; 155, 158
Ellis, P. D. [256] *307*; 201
Ellis, G. [265] *307*; 197, 198
Emsley, J. W. [5] *301*; 1, 11, 17, 18, 59, 64, 77, 88, 100, 137, 141
Englert, G. [281b] *307*; 219, 222, 223, 225, 226
Engstrom, N. [38] *302*; 40
Ernst, R. R. [32] *301*; 38, 274
Ernst, R. R. [21] *301*; 30
Ernst, R. R. [17] *301*; 24, 33
Ewers, U. [370] *309*; 298
Exner, D. [54b] *302*; 72, 179, 180

Fărcaşiu, D. [251] *307*; 194
Farrar, T. C. [24] *301*; 33
Farrar, T. C. [7] *301*; 9, 21, 22, 33, 48, 55, 56, 110, 113
Farrar, T. C. [166] *305*; 128
Farrar, T. C. [157] *305*; 125
Faure, R. [258] *307*; 197, 199
Fava, A. [233] *306*; 181, 182, 185, 198
Fedarko, M. C. [175] *305*; 129
Feeney, J. [5] *301*; 1, 11, 17, 18, 59, 64, 77, 88, 100, 137, 141
Feeney, J. [81] *303*; 83
Feeney, J. [61b] *303*; 75, 80, 81, 283
Feeney, J. [145] *304*; 122
Feeney, J. [373] *309*; 298
Fellgett, P. [26] *301*; 35
Fernández-Alonso, J. I. [318] *308*; 269
Ferretti, J. A. [24] *301*; 33
Finer, E. G. [79] *303*; 81
Finkelnburg, W. [8] *301*; 11
Firl, J. [58] *302*; 73

Fischer, R. D. [80] *303*; 82, 83, 84
Flohé, L. [61d] *303*; 75, 80, 81, 283
Floss, H. G. [296] *308*; 244, 264, 266, 271, 299
Formáček, V. [57a] *302*; 72
Formáček, V. [50k] *302*; 68, 71, 73, 74, 75, 76, 137, 139, 166, 172, 185, 186, 187, 198, 199, 200, 201, 208, 213, 214, 215, 291
Forsythe, G. D. [55] *302*; 72, 180
Fraenkel, G. [255] *307*; 197, 198, 201
Frankel, E. N. [57b] *302*; 72
Freeman, R. [37] *301*; 40
Freeman, R. [35] *301*; 43
Freeman, R. [40] *302*; 48
Freeman, R. [40] *302*; 48
Freeman, R. [43a] *302*; 52, 53, 55
Freeman, R. [47] *302*; 59
Freeman, R. [127] *304*; 113
Frew, N. M. [48] *302*; 65
Friedel, R. A. [67] *303*; 75
Fuchs, S. [322b] *308*; 273, 277, 279, 281, 283, 286, 287
Fujieda, K. [257] *307*; 197, 199
Fujiwara, S. [151] *305*; 123

Gansow, O. A. [36] *301*; 43
Gansow, O. A. [91] *303*; 92
Gansow, O. A. [86] *303*; 89, 91
Gansow, O. A. [82] *303*; 83, 84
Garbesi, A. [233] *306*; 181, 182, 185, 198
Gardner, P. D. [244] *307*; 188, 189
Garnier, R. [258] *307*; 197, 199
Garrigou-Lagrange, C. [179] *305*; 129
Gateau-Olesker, A. [308] *308*; 248, 250, 251, 253, 254, 256
Geerts, J. P. [369] *309*; 298
Gero, S. D. [308] *308*; 248, 250, 251, 253, 254, 256
Gero, S. D. [310] *308*; 248, 252, 256
Gero, S. D. [307] *308*; 248, 249, 250, 252, 253, 256
Gero, S. D. [353] *309*; 297
Giacometti, G. [336] *309*; 286
Gianini, D. D. [161] *305*; 127, 128
Gianini, D. G. [177] *305*; 129
Gibbons, W. A. [326] *308*; 277, 279, 281, 284
Gil, V. M. S. [100] *303*; 95
Gill, D. [46] *302*; 55, 56
Gillen, K. T. [163] *305*; 128
Gillen, K. T. [170] *305*; 128
Glasel, J. A. [81] *303*; 83
Gloss, G. L. [98] *303*; 95, 99
Gluschko, V. [41] *302*; 48, 287
Gluschko, V. [129] *304*; 113, 114, 125, 128
Gluschko, V. [149] *305*; 123, 284
Gluschko, V. [337] *309*; 287
Goldammer, E. [171] *305*; 128
Goldammer, E. [169] *305*; 128
Goldman, S. [18] *301*; 25
Goldstein, J. H. [209] *306*; 149
Goldstein, J. H. [239] *306*; 185, 189
Goldstein, J. H. [201] *306*; 143, 144, 145
Goldstein, J. H. [319] *308*; 269, 272
Goodman, R. A. [158] *305*; 126, 289
Goto, K. [263] *307*; 197
Goutarel, G. [284] *307*; 227, 233
Graham, D. M. [193] *305*; 141
Grandjean, J. [126] *304*; 112
Grant, D. M. [33] *301*; 39, 40, 111
Grant, D. M. [59] *302*; 74
Grant, D. M. [62] *303*; 131, 132, 133, 229, 282
Grant, D. M. [63] *303*; 71, 143, 148
Grant, D. M. [77] *303*; 81, 184, 197, 199
Grant, D. M. [76] *303*; 81, 184, 196, 197, 200, 201
Grant, D. M. [93] *303*; 92
Grant, D. M. [64] *303*; 74, 135, 136
Grant, D. M. [123] *304*; 112
Grant, D. M. [122] *304*; 113, 114
Grant, D. M. [132] *304*; 115
Grant, D. M. [136] *304*; 118
Grant, D. M. [137] *304*; 118, 120
Grant, D. M. [138] *304*; 118
Grant, D. M. [172] *305*; 128
Grant, D. M. [162] *305*; 128
Grant, D. M. [181] *305*; 133
Grant, D. M. [188] *305*; 137
Grant, D. M. [161] *305*; 127, 128
Grant, D. M. [155] *305*; 124
Grant, D. M. [241] *306*; 184, 188
Grant, D. M. [243] *306*; 184, 188, 189
Grant, D. M. [215] *306*; 155, 158
Grant, D. M. [276] *307*; 210
Grant, D. M. [266] *307*; 198, 199
Grant, D. M. [260] *307*; 197, 202, 265
Grant, D. M. [261] *307*; 197, 202, 203
Grant, D. M. [246] *307*; 192
Grant, D. M. [244] *307*; 188, 189
Grant, D. M. [312] *308*; 264, 265, 269, 271, 273
Grant, D. M. [314] *308*; 264
Grant, D. M. [315] *308*; 266
Grant, D. M. [350] *309*; 296
Gray, G. A. [141] *304*; 120
Gray, G. A. [118] *304*; 110
Gray, G. A. [117] *304*; 109
Gray, T. I. [363] *309*; 297
Grimison, A. [242] *306*; 184, 197, 272
Grimminger, W. [324] *308*; 273, 277, 279, 283, 286
Grollmann, A. P. [128] *304*; 113, 129
Grutzner, J. B. [186] *305*; 136, 137, 140, 145, 146, 151, 161, 164, 177, 178
Grutzner, J. B. [281a] *307*; 219, 222, 223, 225, 226

Grutzner, J. B. [347] *309*; 293
Günther, H. [50c] *302*; 68, 71, 73, 74, 75, 76, 137, 291
Günther, H. [253] *307*; 196
Günther, H. [254] *307*; 194, 195
Günther, H. [252] *307*; 194, 195, 196
Günther, H. [370] *309*; 298
Günzler, W. A. [61d] *303*; 75, 80, 81, 283
Gunasekera, S. P. [361] *309*; 297
Gurd, F. R. N. [41] *302*; 48, 287
Gurd, F. R. N. [149] *305*; 123, 284
Gurd, F. R. N. [337] *309*; 287
Gurudata [222] *306*; 165
Guthrie, R. D. [308] *308*; 248, 250, 251, 253, 254, 256
Guthrie, R. D. [307] *308*; 248, 249, 250,252, 253, 256
Gutowsky, H. S. [57b] *302*; 72
Gutteridge, N. J. A. [354] *309*; 297

Haan, J. W. de [54b] *302*; 52, 179, 180
Haas, G. [50j] *302*; 68, 71, 73, 74, 75, 76, 137, 208, 213, 291, 296
Haeberlein, U. [164] *305*; 128
Haeberlein, U. [167] *305*; 128
Haenel, M. [250] *307*; 194
Hagaman, E. W. [285] *307*; 229, 232, 234, 235
Hagaman, E. W. [296] *308*; 244, 264, 266, 271, 299
Hagaman, E. W. [294] *308*; 242, 243
Hagaman, E. W. [307] *308*; 248, 249, 250, 252, 253, 256
Hagaman, E. W. [353] *309*; 297
Hagen, R. [227] *306*; 171, 173
Hahn, E. L. [44] *302*; 55
Halpern, Y. [271] *307*; 205, 206
Halpern, Y. [269] *307*; 205, 206
Hamasaki, T. [343] *309*; 290
Hamasaki, T. [342] *309*; 290
Hampson, P. [68b] *303*; 77, 138, 139, 141, 183
Handler, G. S. [97] *303*; 95, 99
Hansen, W. W. [6] *301*; 7
Harris, R. K. [79] *303*; 81
Harris, R. K. [132] *304*; 115
Hartmann, W. [58] *302*; 73
Haruff, R. C. [365] *309*; 299
Hausser, K. H. [164] *305*; 128
Hess, R. E. [101] *303*; 95, 100
Hill, H. D. W. [47] *302*; 59
Hill, H. D. W. [43a] *302*; 52, 53, 55
Hill, H. D. W. [40] *302*; 48
Hiss, D. [297c] *308*; 247, 248, 260, 262, 268
Hoffmann, E. G. [12] *301*; 18
Hoffmann, T. A. [316] *308*; 269
Holland, H. L. [295] *308*; 243, 254, 271, 273, 299
Holloway, C. E. [193] *305*; 141
Hollstein, U. [107b] *304*; 101, 253, 255
Hollstein, U. [371] *309*; 298
Hoppen, V. [277] *307*; 210
Horsley, W. J. [43b] *302*; 52, 53, 55
Horsley, W. J. [73] *303*; 80, 282, 284
Horsley, W. J. [74] *303*; 80, 177, 273, 277, 279, 281
Huber, H. [173] *305*; 129
Huber, H. [160] *305*; 127
Huckerby, T. N. [359] *309*; 297
Hughes, D. W. [295] *308*; 243, 254, 271, 273, 299
Huntress, W. T. [130] *304*; 113, 114, 136
Hylands, P. J. [366] *309*; 299

Ichihara, Y. [151] *305*; 123
Imanari, M. [142] *304*; 121, 128
Isenhour, T. L. [48] *302*; 65
Isenhour, T. L. [48] *302*; 65
Ishizu, K. [142] *304*; 121, 128

Jackman, L. M. [212] *306*; 151, 159, 162
Jaenicke, L. [370] *309*; 298
Jankowski, W. C. [50l] *302*; 71, 73, 74, 75, 76, 137, 252, 291, 296, 298, 299
Jautelat, M. [186] *305*; 136, 137, 140, 146, 151, 161, 164, 177, 178
Jautelat, M. [190] *305*; 137, 138, 139, 140
Jautelat, M. [281a] *307*; 219, 222, 223, 225, 226
Jautelat, M. [283] *307*; 226, 227, 229, 231, 232, 233, 234, 235, 236, 237, 238
Jenkins, W. T. [365] *309*; 299
Jerina, D. M. [115] *304*; 107, 108
Jerome, F. R. [116] *304*; 109
Jeuell, C. [273] *307*; 205
Jikeli, G. [254] *307*; 194, 195, 196
Johnson, [341] *309*; 289
Johnson, [342] *309*; 290
Johnson, [346] *309*; 292
Johnson, [50l] *302*; 71, 73, 74, 75, 76, 137, 252, 291, 296, 298, 299
Johnson, L. F. [90] *303*; 89, 90
Johnson, L. F. [188] *305*; 137
Johnson, L. F. [326] *308*; 277, 279, 281, 284
Johnson, L. R. F. [325] *308*; 274
Jones, A. J. [215] *306*; 155, 158
Jones, A. J. [243] *306*; 184, 188, 189
Jones, A. J. [246] *307*; 192
Jones, A. J. [244] *307*; 188, 189
Jones, A. J. [312] *308*; 264, 265, 269, 271, 273
Jones, A. J. [315] *308*; 266
Jones, R. C. [40] *302*; 48
Jones, R. G. [265] *307*; 197, 198
Jung, G. [102] *303*; 98, 99, 100, 107, 109, 117, 120, 125, 160, 162, 166, 180, 185, 186, 187, 198, 199, 200, 222, 235, 271, 272, 281, 298
Jung, G. [75] *303*; 80, 81, 282, 283, 287

Jung, G. [61d] *303*; 75, 80, 81, 283
Jung, G. [225] *306*; 192, 196, 240, 273, 284
Jung, G. [297c] *308*; 247, 248, 260, 262, 268
Jung, G. [299] *308*; 247, 248, 249, 250, 251, 266
Jung, G. [297b] *308*; 247, 248, 253, 255, 260, 262, 268
Jung, G. [328] *308*; 283, 286
Jung, G. [329] *308*; 283, 284, 285, 286
Jung, G. [324] *308*; 273, 277, 279, 283, 286
Jung, G. [322a] *308*; 273, 277, 279, 281, 283, 286, 287
Jung, G. [321] *308*; 273, 274, 283, 284
Jung, G. [311] *308*; 260, 264, 265
Jung, G. [305] *308*; 248, 258, 260
Jung, G. [304] *308*; 248, 255, 256
Jung, G. [371] *309*; 298
Jurs, P. C. [48] *302*; 65

Kaplan, J. I. [49] *302*; 65
Karplus, M. [52] *302*; 70, 95
Kazlauskas, R. [361] *309*; 297
Keller, T. [89] *303*; 89, 90, 91, 137
Keller, T. [252] *307*; 194, 195, 196
Keller, T. [297c] *308*; 247, 248, 260, 262, 268
Keller, T. [321] *308*; 273, 274, 283, 284
Kellerhals, H. P. [50k] *302*; 68, 71, 73, 74, 75, 76, 137, 139, 166, 172, 185, 186, 187, 198, 199, 200, 201, 208, 213, 214, 215, 291
Kellie, G. M. [214] *306*; 155, 156, 157, 158
Kelly, D. P. [212] *306*; 151, 159, 162
Kelly, D. P. [272] *307*; 205, 207
Kenyon, G. L. [338] *309*; 287
Kessler, H. [85] *303*; 86, 88, 91
Keulemans, A. I. [54b] *302*; 72, 180
Khuong-Huu. F. [286] *307*; 226, 229, 237
Khuong-Huu, F. [284] *307*; 227, 233
Killough, J. [86] *303*; 86, 88, 91
Kingsbury, C. A. [357] *309*; 297
Kingsbury, C. A. [362] *309*; 297
Klahn, R. [20] *301*; 27
Klein, M. P. [39] *302*; 48
Klein, M. P. [43b] *302*; 52, 53, 55
Knoeber, M. C. [215] *306*; 155, 158
Koch, H. J. [65] *303*; 74, 247, 248, 249, 251, 252, 254, 255, 257, 266
Koch, H. J. [185] *305*; 136
Koch, H. J. [290] *308*; 230, 239
Koch, H. J. [301] *308*; 247, 248, 251
Koch, M. [293] *308*; 241
Komoroski, R. [139] *304*; 119, 121
Komoroski, R. A. [148] *305*; 123
Korsch, B. [301] *308*; 247, 248, 254
Kowalski, B. R. [48] *302*; 65
Kreissl, F. R. [133] *304*; 115, 116
Kreissl, F. R. [137] *304*; 118, 120
Kreissl, F. R. [172] *305*; 128
Kreiter, C. G. [57a] *302*; 72
Kroschwitz, J. I. [211] *306*; 150, 151, 152, 153
Kuhlmann, K. F. [33] *301*; 39, 40, 111
Kuhlmann, K. F. [132] *304*; 115
Kuhlmann, K. F. [246] *307*; 192

Ladik, J. [316] *308*; 269
La Mar, G. N. [37] *301*; 40
La Mar, G. N. [37] *301*; 40
La Mar, G. N. [127] *304*; 113
Lamb, W. E. [9] *301*; 13, 68
Lambert, J. B. [111] *304*; 107, 108, 179
Lapper, P. D. [119] *304*; 110
Laszlo, P. [126] *304*; 112
Lauterbur, P. C. [97] *303*; 95, 99
Lauterbur, P. C. [183] *305*; 133, 134
Lauterbur, P. C. [236] *306*; 183
Lauterbur, P. C. [234] *306*; 186, 193
Lauterbur, P. C. [198] *306*; 142, 151, 154
Lauterbur, P. C. [197] *306*; 142, 148, 149
Lauterbur, P. C. [216] *306*; 159, 162, 163
Lauterbur, P. C. [330] *309*; 284
Lawson, P. J. [41] *302*; 48, 287
Lawson, P. J. [149] *305*; 123, 284
Lawson, P. J. [337[*309*; 287
Lee, A. G. [145] *304*; 122
Lee, A. G. [143] *304*; 121, 122
Lee, A. G. [174] *305*; 129
Lee, A. G. [146] *305*; 122, 129
Lee, A. G. [147] *305*; 123
Leibfritz, D. [329] *308*; 283, 284, 285, 286
Leibfritz, D. [352] *309*; 296
Leigh, J. S. [43c] *302*; 52, 53, 55
Leipert, T. K. [170] *305*; 128
Lemke, P. A. [348] *309*; 293, 294
Lenkinski, R. E. [82] *303*; 83, 84
Levin, R. H. [60] *302*; 76
Levine, Y. K. [145] *304*; 122
Levine, Y. K. [143] *304*; 121, 122
Levine, Y. K. [174] *305*; 129
Levine, Y. K. [146] *305*; 122, 129
Levine, Y. K. [373] *309*; 298
Levy, G. C. [50f] *302*; 68, 71, 73, 74, 75, 76, 137, 208, 211, 213, 291, 296
Levy, G. C. [70] *303*; 77, 80
Levy, G. C. [140] *304*; 119
Levy, G. C. [125] *304*; 112, 113, 116, 117
Levy, G. C. [124] *304*; 112
Levy, G. C. [121] *304*; 110, 111, 120, 121, 126, 128
Levy, G. C. [368] *309*; 298
Lewis, R. B. [294] *308*; 242, 243
Lewis, S. [345] *309*; 292
Liang, G. [271] *307*; 205, 206
Lichter, R. L. [69] *303*; 77, 78, 79, 80, 96
Lichter, R. L. [113] *304*; 107, 108, 110

Lippert, E. [99] *303*; 95, 102

Lippmaa, E. [165] *305*; 128

Lippmaa, E. [195] *306*; 141

Lippmaa, E. [228] *306*; 172, 173, 174, 175

Lippmaa, E. [275] *307*; 208

Lipsky, S. R. [61a] *302*; 75, 80, 81, 282, 283

Lipsky, S. R. [349] *309*; 295

Litchman, W. M. [93] *303*; 92

Litchman, W. M. [63] *303*; 71, 143, 148

Litchman, W. M. [243] *306*; 184, 188, 189

Litchman, W. M. [244] *307*; 188, 189

Live, D. H. [173] *305*; 129

Lohrisch, H. J. [355] *309*; 297

Looker, J. H. [357] *309*; 297

Looker, J. H. [362] *309*; 297

Lowe, I. J. [15] *301*; 24

Luedemann, H. D. [171] *305*; 128

Luedemann, H. D. [169] *305*; 128

Lukacs, G. [144] *304*; 121, 124, 125

Lukacs, G. [287] *307*; 229, 234, 237, 238

Lukacs, G. [285] *307*; 229, 232, 234, 235

Lukacs, G. [284] *307*; 227, 233

Lukacs, G. [286] *307*; 226, 229, 237

Lukacs, G. [307] *308*; 248, 249, 250, 252, 253, 256

Lukacs, G. [308] *308*; 248, 250, 251, 253, 254, 256

Lukacs, G. [310] *308*; 248, 252, 256

Lukacs, G. [290] *308*; 230, 239

Lukacs, G. [353] *309*; 297

Lusinchi, X. [285] *307*; 229, 232, 234, 235

Lusinchi, X. [290] *308*; 230, 239

Lyerla, Jr., J. R. [122] *304*; 113, 114

Lyerla, J. R. [155] *305*; 124

Lyerla, Jr., J. R. [162] *305*; 128

Lynden-Bell, R. M. [194] *305*; 141

Maciel, G. E. [54a] *302*; 72, 177, 180

Maciel, G. E. [92] *303*; 92, 93, 96, 99, 102, 106, 107, 108, 109

Maciel, G. E. [192] *305*; 141, 149

Maciel, G. E. [188] *305*; 147

Maciel, G. E. [210] *306*; 149

Maciel, G. E. [206] *306*; 147

Mac Lean, D. B. [295] *308*; 243, 254, 271, 273, 299

Maeda, S. [367] *309*; 298

Maglio, G. [106] *304*; 98

Malinowski, E. R. [95] *303*; 95

Mantsch, H. H. [119] *304*; 110

Mantsch, H. H. [159] *305*; 127

Marcus, D. M. [128] *304*; 113, 129

Margenau, H. [14] *301*; 24, 33, 204

Marker, A. [202] *306*; 145

Markley, J. L. [43b] *302*; 52, 53, 55

Marr, D. H. [220] *306*; 161, 164

Marr, D. H. [221] *306*; 161, 165

Martin, D. H. [27] *301*; 35

Mason, J. [182] *305*; 133, 134

Mateescu, G. D. [272] *307*; 205, 207

Mc Combs, D. A. [55] *302*; 72, 180

McFarlane, W. [29] *301*; 37

McFarlane, W. M. [114] *304*; 107, 108

McInnes, A. G. [346] *309*; 292

McIver, J. W. [92] *303*; 92, 93, 96, 99, 102, 106, 107, 108, 109

McNeel, M. [78] *303*; 81

Meiboom, S. [46] *302*; 55, 56

Metcalfe, J. C. [145] *304*; 122

Metcalfe, J. C. [143] *304*; 121, 122

Metcalfe, J. C. [174] *305*; 129

Metcalfe, J. C. [147] *305*; 123

Metcalfe, J. C. [146] *305*; 122, 129

Metcalfe, J. C. [373] *309*; 298

Messe, M. T. [283] *307*; 226, 227, 229, 231, 232, 233, 234, 235, 236, 237, 238

Miller, D. P. [268b] *307*; 205

Miyajima, G. [200] *306*; 143, 144, 148, 149

Mizuno, A. [231] *306*; 179

Mo, Y. K. [272] *307*; 205, 207

Mo, Y. K. [271] *307*; 205, 206

Mo, Y. K. [269] *307*; 205, 206

Moon, R. B. [180] *305*; 129

Mooney, E. F. [103] *304*; 95, 98, 100

Morishima, I. [100] *303*; 95

Morishima, I. [231] *306*; 179

Morishima, I. [259] *307*; 197

Morishima, I. [263] *307*; 197

Muller, N. [208] *306*; 148

Mueller, A. [169] *305*; 128

Müller, N. [195] *306*; 141

Murphy, G. M. [14] *301*; 24, 33, 204

Nachod, F. C. [29] *301*; 37

Nachod, F. C. [13] *301*; 22, 48

Nachod, F. C. [50b] *302*; 68, 71, 73, 74, 75, 76, 137, 291

Nachod, F. C. [84] *303*; 86, 88

Nachod, F. C. [110] *304*; 107

Nachod, F. C. [113] *304*; 107, 108, 110

Nachod, F. C. [198] *306*; 142, 151, 154

Nagel, A. [369] *309*; 298

Namikawa, K. [191] *305*; 137

Namikawa, K. [189] *305*; 138, 147, 149

Namikawa, K. [218] *306*; 161

Namikawa, K. [205] *306*; 147, 149

Nash, C. N. [348] *309*; 293, 294

Natusch, D. F. S. [153] *305*; 123

Nelson, F. A. [31] *301*; 38

Nelson, G. L. [50f] *302*; 68, 71, 73, 74, 75, 76, 137, 208, 211, 213, 291, 296

Nelson, G. L. [70] *303*; 77, 80
Nelson, G. L. [140] *304*; 119
Neuss, N. [348] *309*; 293, 294
Noggle, J. H. [34] *301*; 39, 40, 111
Noggle, J. H. [163] *305*; 128
Noggle, J. H. [170] *305*; 128
Norberg, R. E. [15] *301*; 24

Ohuchi, M. [142] *304*; 121, 128
Okada, K. [263] *307*; 197
Okada, K. [259] *307*; 197
Olah, G. A. [56] *302*; 72, 206
Olah, G. A. [104] *304*; 100
Olah, G. A. [273] *307*; 205
Olah, G. A. [272] *307*; 205, 207
Olah, G. A. [271] *307*; 205, 206
Olah, G. A. [270] *307*; 206
Olah, G. A. [269] *307*; 205, 206
Olah, G. A. [268a] *307*; 205
Oldfield, E. [152] *305*; 123
Oldfield, E. [158] *305*; 126, 289
Olivson, A. [165] *305*; 128
Onsager, L. [204] *306*; 145
Osborne, D. J. [354] *309*; 297
Oster, O. [332] *309*; 286
Oster, O. [333] *309*; 286
Ostlund, N. S. [92] *303*; 92, 93, 96, 99, 102, 106, 107, 108, 109
Ouchi, D. [219] *306*; 161, 164

Pachler, K. G. R. [37] *301*; 40
Pachler, K. G. R. [127] *304*; 113
Packard, M. [6] *301*; 7
Packer, E. L. [338] *309*; 287
Paddon-Row, M. N. [247] *307*; 192
Page, T. F. [266] *307*; 198, 199
Pancrazi, A. [284] *307*; 227, 233
Paolillo, L. [115] *304*; 107, 108
Paolillo, L. [150] *305*; 123
Paolillo, L. [335] *309*; 286
Parker, R. G. [262] *307*; 197, 203
Partington, P. [145] *304*; 122
Partington, P. [143] *304*; 121, 122
Partington, P. [174] *305*; 129
Paul, E. G. [62] *303*; 131, 132, 133, 229, 282
Paul, E. G. [241] *306*; 184, 188
Pearson, H. [173] *305*; 129
Pearson, H. [161] *305*; 127, 128
Pearson, H. [160] *305*; 127
Pearson, H. [177] *305*; 129
Pehk, T. [228] *306*; 172, 173, 174, 175
Pehk, T. [195] *306*; 141
Pehk, T. [275] *307*; 208
Pelter, A. [363] *309*; 297
Perlin, A. S. [65] *303*; 74, 247, 248, 249, 251, 252, 254, 255, 257, 266
Perlin, A. S. [108] *304*; 102
Perlin, A. S. [185] *305*; 136
Perlin, A. S. [300] *308*; 247, 248, 258, 259, 260, 261
Perlin, A. S. [290] *308*; 230, 239
Peyroux, J. [293] *308*; 241
Phelps, D. E. [39] *302*; 48
Philipsborn, W. v. [30] *301*; 37
Phillips, W. D. [198] *306*; 142, 151, 154
Picot, A. [290] *308*; 230, 239
Piriou, F. [144] *304*; 121, 124, 125
Piriou, F. [353] *309*; 297
Pirkle, W. H. [356] *309*; 297
Pitcher, E. [199] *306*; 142, 196
Pitcher, R. G. [347] *309*; 293
Plas, H.C. v. d. [369] *309*; 298
Plat, M. [293] *308*; 241
Pollard, A. L. [256] *307*; 201
Polonsky, J. [344] *309*; 290, 291
Pople, J. A. [1] *301*; 1, 19, 59, 64
Pople, J. A. [52] *302*; 70, 95
Pople, J. A. [92] *303*; 92, 93, 96, 99, 102, 106, 107, 108, 109
Porter, R. D. [272] *307*; 205, 207
Porter, R. D. [273] *307*; 205
Pregosin, P. S. [50b] *302*; 68, 71, 73, 74, 75, 76, 137, 291
Pregosin, P. S. [232] *306*; 181
Prestgard, J. H. [61a] *302*; 75, 80, 81, 282, 283
Prestien, J. [254] *307*; 194, 195
Pretsch, E. [50g] *302*; 68, 71, 73, 74, 75, 76, 137, 181, 198, 199, 208, 213, 291
Pretsch, E. [372] *309*; 298
Price, R. [89] *303*; 89, 90, 91, 137
Price, R. [126] *304*; 112
Price, R. [311] *308*; 260, 264, 265
Price, R. [304] *308*; 248, 256
Prigge, H. [99] *303*; 95, 102
Pritchard, D. E. [195] *306*; 141
Pruess, D. L. [347] *309*; 293
Pugmire, R. J. [77] *303*; 81, 184, 197, 199
Pugmire, R. J. [76] *303*; 81, 184, 196, 197, 200, 201
Pugmire, R. J. [138] *304*; 118
Pugmire, R. J. [136] *304*; 118
Pugmire, R. J. [261] *307*; 197, 202, 203
Pugmire, R. J. [260] *307*; 197, 202, 265
Pugmire, R. J. [314] *308*; 264
Pullman, B. [72] *303*; 80, 282, 283
Pullman, B. [317] *308*; 269
Purcell, E. M. [10] *301*; 16, 100
Purcell, E. M. [45] *302*; 55, 56
Purser, J. M. [187] *305*; 136

Rabaron, A. [293] *308*; 241
Rackham, D. M. [354] *309*; 297

Ramsey, N. F. [10] *301*; 16
Randall, E. [50b] *302*; 68, 71, 73, 74, 75, 76, 137, 291
Randall, E. [232] *306*; 181
Rang, S. [195] *306*; 141
Rappe, C. [228] *306*; 172, 173, 174, 175
Rathbone, E. B. [309] *308*; 248, 250, 260, 262
Regitz, M. [252] *307*; 194, 195, 196
Reich, H. J. [184] *305*; 134, 135, 152, 153, 154, 155, 157, 190
Reich, H. J. [211] *306*; 150, 151, 152, 153
Reich, H. J. [283] *307*; 226, 227, 229, 231, 232, 233, 234, 235, 236, 237, 238
Retcotsky, H. L. [67] *303*; 75
Rhodes, G. W. [314] *308*; 264
Richards, J. H. [180] *305*; 129
Richards, P. L. [27] *301*; 35
Riddell, F. G. [214] *306*; 155, 156, 157, 158
Rieker, A. [226] *306*; 170, 171
Riggs, N. V. [202] *306*; 145
Ritchie, R. G. S. [301] *308*; 247, 248, 254
Roberts, B. W. [111] *304*; 107, 108, 179
Roberts, G. C. K. [61b] *303*; 75, 80, 81, 283
Roberts, G. C. K. [143] *304*; 121, 122
Roberts, G. C. K. [174] *305*; 129
Roberts, J. D. [60] *302*; 76
Roberts, J. D. [66] *303*; 74, 247, 248, 249, 250, 251, 266
Roberts, J. D. [69] *303*; 77, 78, 79, 80, 96
Roberts, J. D. [109] *304*; 102, 106, 107, 189, 191
Roberts, J. D. [105] *304*; 98, 99, 101, 199
Roberts, J. D. [137] *304*; 118, 120
Roberts, J. D. [133] *304*; 115, 116
Roberts, J. D. [111] *304*; 107, 108, 179
Roberts, J. D. [190] *305*; 137, 138, 139, 140, 212
Roberts, J. D. [186] *305*; 136, 137, 140, 145, 146, 151, 161, 164, 177, 178
Roberts, J. D. [177] *305*; 129
Roberts, J. D. [184] *305*; 134, 135, 152, 153, 154, 155, 157, 190
Roberts, J. D. [173] *305*; 129
Roberts, J. D. [172] *305*; 128
Roberts, J. D. [160] *305*; 127
Roberts, J. D. [161] *305*; 127, 128
Roberts, J. D. [217] *306*; 159, 160, 161, 162, 163
Roberts, J. D. [227] *306*; 171, 173
Roberts, J. D. [211] *306*; 150, 151, 152, 153
Roberts, J. D. [283] *307*; 226, 227, 229, 231, 232, 233, 234, 235, 236, 237, 238
Roberts, J. D. [281a] *307*; 219, 222, 223, 225, 226
Roberts, J. D. [262] *307*; 197, 203
Roberts, J. D. [245] *307*; 189, 191, 248
Roberts, J. D. [298] *308*; 247, 248, 263
Roberts, J. D. [291] *308*; 240, 243, 244, 246, 247
Roberts, J. D. [289] *308*; 230, 239, 240
Roberts, J. D. [313] *308*; 264, 266, 271, 273
Roberts, J. D. [300] *308*; 247, 248, 258, 259, 260, 261
Roberts, J. D. [352] *309*; 296
Robins, M. J. [260] *307*; 197, 202, 265
Robins, M. J. [261] *307*; 197, 202, 203
Robins, R. K. [261] *307*; 197, 202, 203
Robins, R. K. [260] *307*; 197, 202, 265
Robins, R. K. [312] *308*; 264, 265, 269, 271, 273
Robins, R. K. [314] *308*; 264
Rodriguez, G. [242] *306*; 184, 197, 272
Roeder, O. [171] *305*; 128
Roeder, S. B. [168] *305*; 128
Rose, P. I. [208] *306*; 148
Ross, D. A. [213] *306*; 152
Roth, A. S. [55] *302*; 72, 180
Runge, W. [58] *302*; 73

Saito, H. [159] *305*; 127
Savitsky, G. B. [189] *305*; 138, 147, 149
Savitsky, G. B. [191] *305*; 137
Savitsky, G. B. [218] *306*; 161
Savitsky, G. B. [205] *306*; 147, 149
Sawa, Y. K. [367] *309*; 298
Schaefer, J. [154] *305*; 123, 124
Schaefer, J. [153] *305*; 123
Schechter, A. N. [78] *303*; 81
Schell, F. M. [285] *307*; 229, 232, 234, 235
Schell, F. M. [294] *308*; 242, 243
Schell, F. M. [364] *309*; 299
Scherer, H. [252] *307*; 194, 195, 196
Schirmer, R. E. [34] *301*; 39, 40, 111
Schittenheim, W. [36] *301*; 43
Schlosberg, R. H. [272] *307*; 205, 207
Schmickler, H. [254] *307*; 194, 195
Schneider, H. J. [89] *303*; 89, 90, 91, 137
Schneider, H. J. [277] *307*; 210
Schneider, W. G. [1] *301*; 1, 19, 59, 64
Schneider, W. G. [53] *302*; 70
Schneider, W. G. [68a] *303*; 77, 131, 142, 143, 148
Schneider, W. G. [240] *306*; 184, 269, 282
Schneider, W. G. [235] *306*; 183, 184, 185, 186
Schroth, G. [12] *301*; 18
Schwartz, M. [163] *305*; 128
Schweitzer, D. [167] *305*; 128
Schweitzer, D. [164] *305*; 128
Seidman, K. [256] *307*; 201
Senoff, C. V. [237a] *306*; 186
Sepulchre, A. M. [307] *308*; 248, 249, 250, 252, 253, 256
Sepulchre, A. M. [308] *308*; 248, 250, 251, 253, 254, 256
Sepulchre, A. M. [310] *308*; 248, 252, 256
Sergejev, N. M. [278] *307*; 210

Servis, K. L. [116] *304*; 109
Seto, H. [341] *309*; 289
Seto, H. [343] *309*; 290
Seuffer, R. H. [322b] *308*; 273, 277, 279, 281, 283, 286, 287
Sharp, R. R. [267] *307*; 200
Sheppard, N. [194] *305*; 141
Shively, R. R. [20] *301*; 27
Shoolery, J. N. [320] *308*; 272
Shoup, R. R. [157] *305*; 125
Shoup, R. R. [166] *305*; 128
Shrager, R. I. [78] *303*; 81
Simon, W. [54b] *302*; 72, 179, 180
Simon, W. [372] *309*; 298
Sinclair, J. [338] *309*; 287
Smith, D. G. [346] *309*; 292
Smith, I. P. C. [179] *305*; 129
Smith, I. P. C. [178] *305*; 129
Smith, J. C. P. [159] *305*; 127
Smith, J. C. P. [119] *304*; 110
Smith, R. A. [186] *305*; 136, 137, 140, 145, 146, 151, 161, 164, 177, 178
Sogn, J. A. [326] *308*; 277, 279, 281, 284
Sojka, S. A. [196] *306*; 141, 148
Sone, T. [257] *307*; 197, 199
Spielvogel, B. F. [187] *305*; 136
Spiesecke, H. [53] *302*; 70
Spiesecke, H. [68a] *303*; 77, 131, 142, 143, 148
Spiesecke, H. [240] *306*; 184, 269, 282
Spiesecke, H. [235] *306*; 183, 184, 185, 186
Spiess, H. W. [167] *305*; 128
Spiess, H. W. [164] *305*; 128
Spohn, K. H. [71] *303*; 79, 80, 81, 196
Spohn, K. H. [135] *304*; 117, 119
Sprague, P. W. [289] *308*; 230, 239, 240
Staab, H. A. [250] *307*; 194
Staab, H. A. [249] *307*; 194
Staab, H. A. [248] *307*; 192
Stempfle, W. [12] *301*; 18
Stephen, E. M. [309] *308*; 248, 250, 260, 262
Stern, A. [326] *308*; 277, 279, 281, 284
Sternhell, S. [50g] *302*; 68, 71, 73, 74, 75, 76, 137, 181, 198, 199, 208, 213, 291
Sternlicht, H. [74] *303*; 80, 177, 273, 277, 279, 281
Sternlicht, H. [73] *303*; 80, 282, 284
Sternlicht, H. [128] *304*; 113, 129
Sternlicht, H. [338] *309*; 287
Still, I. W. J. [360] *309*; 297
Stock, L. M. [274] *307*; 205
Stone, F. G. A. [199] *306*; 142, 196
Stothers, J. B. [50e] *302*; 68, 71, 73, 74, 75, 76, 137, 160, 181, 183, 195, 196, 208, 213, 291, 296
Stothers, J. B. [50a] *302*; 68, 71, 73, 74, 75, 76, 137, 141, 291
Stothers, J. B. [216] *306*; 159, 162, 163
Stothers, J. B. [220] *306*; 161, 164
Stothers, J. B. [213] *306*; 152
Stothers, J. B. [219] *306*; *161*, 164
Stothers, J. B. [221] *306*; 161, 165
Stothers, J. B. [222] *306*; 165
Stothers, J. B. [223] *306*; 167, 171
Stothers, J. B. [224] *306*; 167, 171
Stothers, J. B. [279] *307*; 211
Streever, R. L. [23] *301*; 33
Subbotin, O. A. [278] *307*; 210
Sudarsana Rao, K. [249] *307*; 194
Suhr, H. [2] *301*; 1, 19, 59, 64, 66, 77, 95
Sultanbawa, S. [361] *309*; 297
Sutcliffe, L. H. [5] *301*; 1, 11, 17, 18, 59, 64, 77, 88, 100, 137, 141
Sykes, R. J. [349] *309*; 295

Tadorko, S. [151] *305*; 123
Tänzer, C. [299] *308*; 247, 248, 249, 250, 251, 266
Tänzer, C. [321] *308*; 273, 274, 283, 284
Takahashi, K. [200] *306*; 143, 144, 148, 149
Takahashi, K. [257] *307*; 197, 199
Tan, C. T. [279] *307*; 211
Tanabe, M. [341] *309*; 289
Tanabe, M. [342] *309*; 290
Tanabe, M. [343] *309*; 290
Tancredi, T. [150] *305*; 123
Tancredi, T. [335] *309*; 286
Tarpley, A. R. [239] *306*; 185, 189
Tarpley, A. R. [201] *306*; 143, 144, 145
Tarpley, A. R. [319] *308*; 269, 272
Temussi, P. A. [150] *305*; 123
Temussi, P. A. [335] *309*; 286
Teo, K. C. [279] *307*; 211
Terui, Y. [367] *309*; 298
Thomas, D. [342] *309*; 290
Tokuhiro, T. [255] *307*; 197, 198, 201
Tolan, J. W. [267] *307*; 200
Tonelli, A. E. [334] *309*; 286
Tori, K. [367] *309*; 298
Traficante, D. D. [192] *305*; 141, 149
Trivellone, E. [150] *305*; 123
Trivellone, E. [335] *309*; 286
Tuck, D. G. [112] *304*; 107, 108
Tuck, R. H. [101] *303*; 95, 100
Tukey, J. W. [19] *301*; 27
Tukey, J. W. [18] *301*; 25
Tunggal, B. D. [252] *307*; 194, 195, 196
Turner, W. V. [356] *309*; 297

Uvais, M. [361] *309*; 297

Vasak, M. [372] *309*; 298
Vass, G. [308] *308*; 248, 250, 251, 253, 254, 256
Vass, G. [310] *308*; 248, 252, 256
Veillard, A. [317] *308*; 269
Verdini, A. S. [336] *309*; 286

Vernon, W. D. [91] *303*; 92
Verpoorte, R. [366] *309*; 299
Vincent, E.-J. [258] *307*; 197, 199
Vining, L. C. [346] *309*; 292
Voelter, W. [50j] *302*; 68, 71, 73, 74, 75, 76, 137, 208, 213, 291, 296
Voelter, W. [61d] *303*; 75, 80, 81, 283
Voelter, W. [102] *303*; 98, 99, 100, 107, 109, 117, 120, 125, 160, 162, 166, 180, 185, 186, 187, 198, 199, 200, 222, 235, 271, 272, 281, 298
Voelter, W. [75] *303*; 80, 81, 282, 283, 287
Voelter, W. [120] *304*; 110, 260, 264, 265, 267, 268
Voelter, W. [225] *306*; 192, 196, 240, 273, 284
Voelter, W. [302] *308*; 247, 248, 251, 255, 258, 259, 260, 261
Voelter, W. [303] *308*; 247, 248, 255, 269
Voelter, W. [304] *308*; 248, 255, 256
Voelter, W. [305] *308*; 248, 258, 260
Voelter, W. [306] *308*; 248, 268, 269
Voelter, W. [308] *308*; 248, 250, 251, 253, 254, 256
Voelter, W. [309] *308*; 248, 250, 260, 262
Voelter, W. [311] *308*; 260, 264, 265
Voelter, W. [320] *308*; 272
Voelter, W. [322a] *308*; 273, 277, 279, 281, 283, 286, 287
Voelter, W. [322b] *308*; 273, 277, 279, 281, 283, 286, 287
Voelter, W. [324] *308*; 273, 277, 279, 283, 286
Voelter, W. [328] *308*; 283, 286
Voelter, W. [297b] *308*; 247, 248, 253, 255, 260, 262, 268
Voelter, W. [297a] *308*; 247, 248, 252, 253, 260, 262, 268
Voelter, W. [297c] *308*; 247, 248, 260, 262, 268
Voelter, W. [299] *308*; 247, 248, 249, 250, 251, 266
Voelter, W. [332] *309*; 286
Voelter, W. [333] *309*; 286
Vold, R. L. [39] *302*; 48

Wagner, J. J. [87] *303*; 89, 90
Walter, R. [178] *305*; 129
Wang, I. S. Y. [219] *306*; 161, 164
Wangen, L. E. [48] *302*; 65
Ward, J. E. H. [237a] *306*; 186
Ward, R. S. [363] *309*; 297
Warnhoff, E. [219] *306*; 161, 164
Wasserman, H. H. [348] *309*; 293, 294
Waugh, J. S. [22] *301*; 33, 54
Waugh, J. S. [39] *302*; 48
Wehrli, F. W. [54b] *302*; 72, 179, 180
Wehrli, F. W. [50h] *302*; 68, 71, 73, 74, 75, 76, 98, 137, 208, 213, 291
Weigert, F. J. [109] *304*; 102, 106, 107, 189, 191
Weigert, F. J. [105] *304*; 98, 99, 101, 198
Weigert, F. J. [217] *306*; 159, 160, 161, 162, 163
Weigert, F. J. [211] *306*; 150, 151, 152, 153
Weigert, F. J. [283] *307*; 226, 227, 229, 231, 232, 233, 234, 235, 236, 237, 238
Weigert, F. J. [245] *307*; 189, 191, 248
Weiler, L. [358] *309*; 297
Weimann, B. [12] *301*; 18
Welch, J. [345] *309*; 292
Wells, P. R. [110] *304*; 107
Wenkert, E. [41] *302*; 48, 287
Wenkert, E. [149] *305*; 123, 284
Wenkert, E. [285] *307*; 229, 232, 234, 235
Wenkert, E. [286] *307*; 226, 229, 237
Wenkert, E. [282] *307*; 219, 220, 224, 225
Wenkert, E. [280] *307*; 219, 220, 224
Wenkert, E. [296] *308*; 244, 264, 266, 271, 299
Wenkert, E. [294] *308*; 242, 243
Wenkert, E. [293] *308*; 241
Wenkert, E. [292] *308*; 240, 242
Wenkert, E. [307] *308*; 248, 249, 250, 252, 253, 256
Wenkert, E. [364] *309*; 299
Wenkert, E. [353] *309*; 297
Wenkert, E. [344] *309*; 290, 291
Westerman, P. W. [361] *309*; 297
Westley, J. W. [347] *309*; 293
White, A. M. [56] *302*; 72, 206
White, A. M. [104] *304*; 100
White, A. M. [268a] *307*; 205
White, A. M. [270] *307*; 206
White, A. M. [273] *307*; 205
Whitesides, G. M. [106] *304*; 98
Wilbur, D. J. [107c] *304*; 101, 255
Wildman, W. C. [291] *308*; 240, 243, 244, 246, 247
Willcott, M. R. [82] *303*; 83, 84
Williams, C. [107c] *304*; 101, 255
Williams, K. I. H. [351] *309*; 296
Williams, R. J. P. [81] *303*; 83
Wilson, D. M. [288] *307*; 230, 231, 236, 296
Wilson, D. [345] *309*; 292
Winkley, M. W. [312] *308*; 264, 265, 269, 271, 273
Winkley, M. W. [315] *308*; 266
Winson, P. H. [103] *304*; 95, 98, 100
Wirthlin, T. [50h] *302*; 68, 71, 73, 74, 75, 76, 98, 137, 208, 213, 291
Wittstruck, T. A. [351] *309*; 296
Woessner, D. E. [131] *304*; 113, 114
Woessner, D. E. [134] *304*; 116
Wolkowski, Z. [144] *304*; 121, 124, 125
Woodhouse, E. [112] *304*; 107, 108

Xavier, A. V. [81] *303*; 83

Yoder, C. H. [101] *303*; 95, 100
Yonezawa, T. [72] *303*; 80, 282, 283
Yonezawa, T. [100] *303*; 95
Yonezawa, T. [231] *306*; 179
Yonezawa, T. [259] *307*; 197
Yonezawa, T. [263] *307*; 197

Zamora, C. R. [237b] *306*; 186
Zech, K. [324] *308*; 273, 277, 279, 283, 286
Zech, K. [322b] *308*; 273, 277, 279, 281, 283, 286, 287
Ziegler, E. [12] *301*; 18
Ziessow, D. [51] *302*; 68
Zuckerman, J. J. [13] *301*; 22, 48
Zuckerman, J. J. [29] *301*; 37
Zuckerman, J. J. [50b] *302*; 68, 71, 73, 74, 75, 76, 137, 291
Zuckerman, J. J. [84] *303*; 86, 88
Zuckerman, J. J. [113] *304*; 107, 108, 110
Zuckerman, J. J. [110] *304*; 107
Zweifel, G. [218] *306*; 161

3-527-25780-2

0-89573-004-9